NASA Contractor Report 4706

# Structural Damage Prediction and Analysis for Hypervelocity Impacts – Handbook

*N.C. Elfer*

Contract NAS8–38856
Prepared for Marshall Space Flight Center

February 1996

NASA Contractor Report 4706

# Structural Damage Prediction and Analysis for Hypervelocity Impacts – Handbook

*N.C. Elfer*
*Lockheed Martin Marietta Manned Space Systems*

National Aeronautics and Space Administration
Marshall Space Flight Center • MSFC, Alabama 35812

Prepared for Marshall Space Flight Center
under Contract NAS8–38856

February 1996

# FOREWORD

This handbook was prepared under contract NAS8-38856 from NASA Marshall Space Flight Center. The study contract title was "Structural Damage Prediction and Analysis for Hypervelocity Impacts." The Technical Monitors were Dr. Joel Williamsen, Greg Olsen, and Jennifer Robinson. The work was performed between October, 1989, and September, 1995.

In the area of ballistic limits and fracture mechanics, there are often several different philosophies in the technical community. The author has his own opinions which are reflected in this work. The author's opinions are based on his interpretation of test and analysis data, which may be different than others in the scientific community. Furthermore, the reader is urged to consult the references quoted in this work, other literature, and investigators currently active in the field to ensure the accuracy and relevance of the equations and trends quoted here.

# TABLE OF CONTENTS

Foreword ..... ii

Table of Contents ..... v

Appendices ..... vi

Figures ..... vii

**1 INTRODUCTION ..... 1-1**

**2 ENVIRONMENT ..... 2-1**

2.1 Meteoroids ..... 2-1

2.2 Space Debris ..... 2-1

**3 PENETRATION MECHANISMS ..... 3-1**

3.1 Penetration Definitions ..... 3-1

3.2 Single Wall Damage Mechanisms ..... 3-1

3.3 Double Wall Penetration Mechanisms ..... 3-2

3.3.1 Fragment Penetration ..... 3-2

3.3.2.1 Projectile Shape Effects ..... 3-4

3.3.2 Momentum Failure ..... 3-4

3.3.2.1 Wilkinson Model ..... 3-4

3.3.2.2 Modifications to the Wilkinson Model ..... 3-5

3.3.2.3 Grove's Model ..... 3-5

3.3.2.4 Housen and Schmidt's Scaled Velocity Model ..... 3-5

3.3.3 Spall Failure ..... 3-6

3.3.4 Oblique Impact Effects ..... 3-7

3.3.5 Christiansen's High Velocity Extrapolation ..... 3-8

3.3.6 Comparison of High Velocity Predictions ..... 3-8

**4 PROBABILITY ANALYSIS ..... 4-1**

4.1 Probability of No Impact ..... 4-1

4.2 Probability of No Penetration ..... 4-1

4.3 Probability of No Critical Damage ..... 4-2

4.4 Probability Analysis Codes ..... 4-3

5 ADVANCED SHIELD CONCEPTS ..... 5-1
5.1 Bumper Material Selection ..... 5-1
5.2 Multiple Bumpers ..... 5-2
5.3 Intermediate Catcher Shields ..... 5-3
5.3.1 Catcher materials ..... 5-3
5.3.2 Impregnated Catcher materials ..... 5-4
5.3.3 Catcher Location ..... 5-4
5.4 Analysis of Advanced Shield Designs ..... 5-5
5.5 Geometric Bumper Shapes ..... 5-5
6 DEFORMATION ANALYSIS ..... 6-1
6.1 Bulge Deformation Analysis ..... 6-1
6.1.1 Deformation ..... 6-2
6.2 Hole Size ..... 6-3
6.2.1 Effect of wall thickness on hole size ..... 6-4
6.2.2 Effect of projectile size ..... 6-4
6.2.3 Tearing of petal ends ..... 6-5
7 DAMAGE TOLERANCE ..... 7-1
7.1 Initial Crack Length ..... 7-1
7.1.1 Crack Propagation Energy Balance ..... 7-1
7.2 Structural Failure ..... 7-2
7.2.1 Material Properties for Fracture Analysis ..... 7-2
7.2.2 Cylinder Effect ..... 7-4
7.2.3 Hole Effect ..... 7-5
7.2.4 Influence Function for a Cylinder ..... 7-5
7.2.5 Cylinder with integrally machined stiffeners ..... 7-6

## APPENDICES

A. Equations
B. Bibliography
C. Hypervelocity Test Databases
- Martin Marietta IRAD M01S Test Database (Tests performed at UDRI)
- MSFC Test Database (July 1991)
- JSC Space Station Test Database (July 1991)

D. Modeling the Response of a Thin Sheet Due to a Hypervelocity Debris Cloud Impact

# FIGURES


Fig. 1-1 Rupture of a pre-loaded 2219-T851 panel due to a hypervelocity impact with a 3 gram projectile at 6.4 km/s....1-3

Fig. 1-2 Bumper and Kevlar 29 cloth in front of rear wall in Fig. 1-1 after the impact....1-4

Fig. 1-3 Front of the fractured rear wall in Fig. 1-1. Integrally machined stiffeners could not stop the crack....1-5

Fig. 2-1 Impact flux for space debris or meteoroids of diameter shown and larger. Flux is defined for a randomly tumbling surface. [as published in Williamsen94]....2-3

Fig. 2-2 Impact flux for space debris of diameter shown and larger, with and without 100% effective collision avoidance....2-4

Fig. 2-3 Angular and velocity distribution of debris flux....2-5

Fig. 3-1. Multi-layer penetration mechanisms....3-9

Fig. 3-2. Typical ballistic limit as a function of impact velocity and obliquity for a multi-layer design....3-10

Fig. 3-3 Typical Whipple bumper fragment damage....3-11

Fig. 3-4. Post impact debris cloud radiographs from a spherical projectiles. [UDRI shot in Rajendran89]....3-12

Fig. 3-5 Post impact debris cloud radiographs from a cylindrical projectile. [UDRI shot in Rajendran89]....3-13

Fig. 3-6 Rear wall damage from a cylindrical projectile that impacted the bumper without yaw. (UDRI shot 4-0411)....3-14

Fig. 3-7 Front of rear wall from Fig. 3.6. Note central crater probably from the tip of the bumper debris cloud....3-15

Fig. 3-8 Rear of rear wall from Fig. 3.6 showing wide area spall....3-16

Fig. 3-9 Rear wall damage due to a cylindrical projectile that had yaw. (UDRI shot 4-0436)....3-17

Fig. 3-10 Front of rear wall from Fig. 3.9....3-18

Fig. 3-11 Rear of rear wall from Fig. 3.9. Penetration and spall from aligned projectile fragments, and spall probably from the tip of the bumper debris cloud....3-19

Fig. 3-12 Wilkinson type momentum bulge and failure with Kevlar intermediate shields to prevent fragment damage....3-20

Fig. 3-13 Ballistic limit determined from aluminum rear wall with cadmium projectile and bumper tests, scaled to equivalent all aluminum test. [Schmidt94]. ..... 3-21
Fig. 3-14 Oblique impact schematic ..... 3-22
Fig. 3-15 Oblique impact bumper damage. (UDRI shot 4-0657) ..... 3-23
Fig. 3-16 Oblique impact ricochet damage. (same as Fig 3-14) ..... 3-24
Fig. 3-17 Oblique impact rear wall damage (back side) due to a fragment normal to the bumper. The fragment was likely bumper material. (same as Fig 3-14) ..... 3-25
Fig. 3-18 Comparison of high velocity penetration equations. [Hayashida95] ..... 3-26
Fig. 4-1 Flux times the exposed area times the exposure time versus velocity and obliquity from SD_SURF. ..... 4-4
Fig. 5-1 Multi-shock aluminum bumper compared to Whipple bumper (Fig. 3-3). MSFC tests. [Elfer88] ..... 5-6
Fig. 5-2 Double bumper (equal weight) test results. MSFC tests. [Elfer88] ..... 5-7
Fig. 5-3 Kevlar cloth intermediate shield (catcher) UDRI tests. Same designs as Fig. 1-1, with (no penetration) and without Kevlar 29 cloth (penetration) for a 1 gram projectile. [Elfer88] ..... 5-8
Fig. 5-4 Multiple layers of aluminum bumper and Kevlar cloth can prevent penetration for the same conditions as Fig. 1-1. (UDRI 4-0675)[Elfer88] ..... 5-9
Fig. 6-1 Rear wall deformation (same design as Fig. 1-1) 1 gram projectile 6.4 km/s. (UDRI 4-0508) [Elfer] ..... 6-6
Fig. 6-2 Rear wall deformation (same design as Fig. 1-1 except -T62 rear wall) 1.3 gram projectile 6.4 km/s. (UDRI 4-0508) [Elfer] ..... 6-7
Fig. 6-3 Projectile mass for no penetration (or rupture) is proportional to $S^2$ for adequate bumpers and catchers. ..... 6-8
Fig. 6-4 Comparison of debris spray dispersion angle between HULL results and Wilkinson's vaporization equation. ..... 6-9
Fig. 6-5 STEALTH models of rear wall deformation. ..... 6-10
Fig. 6-6 Measured thinning of rear wall. Maximum thinning may occur at the centerline or in a circle away from the centerline. ..... 6-11
Fig. 6-7 Measured thinning of rear wall compared to a HULL analysis. ..... 6-12
Fig. 6-8 Comparison of measured permanent deformation, HULL analyses and simple NASTRAN sheet element analyses. ..... 6-13

Fig. 6-9 Correlation between maximum effective rear wall strain as predicted by EPIC simulation and Grove's dimensionless design parameter. ..... 6-14
Fig. 6-10 Summary of pre-stressed panel test results. Large panels similar to Fig. 1-1. [Elfer] ..... 6-15
Fig. 6-11 Same as Fig.1-1 except for 5456 rear wall material and impact occurred on a stiffener. ..... 6-16
Fig. 6-12 Same as Fig. 6-10 except that stiffener was removed prior to impact ..... 6-17
Fig. 6-13 Same as Fig. 6.11 except sheet was used instead of machining plate down to same 1/8 inch thickness ..... 6-18
Fig. 6-14 Same as Fig. 6.12 except thinner sheet. ..... 6-19
Fig. 6-15 Same as Fig. 6.12 and 6-13 except thinner sheet ..... 6-20
Fig. 6-16 Same as Fig. 6-10 and 1.1 except 6061-T6 material used. ..... 6-21
Fig. 6-17 Reverse of Fig. 6-12, showing torn petals, catcher cloth, and bumper. ..... 6-22
Fig. 6-18 The petals were bent back in on the rear wall shown in Fig. 6-13. Note that the impact area is approximately one third the diameter of the final hole size. ..... 6-23
Fig. 7-1. An illustration of the energy balance for rear wall crack propagation. ..... 7-7
Fig. 7-2. Tear Resistance of 0.063 in. thick aluminum sheet. [Kaufman and Hunsicker] ..... 7-8
Fig. 7-3. Unit propagation energy of some aluminum alloys at various temperatures. [Kaufman and Hunsicker] ..... 7-9
Fig. 7-4. Failure stress versus flaw size in 61 cm wide sheet of 2219 and 5456. [Elfer 88] ..... 7-10
Fig. 7-5. R-curve versus physical flaw size a 61 cm wide sheet of 2219-T87 and 5456-H116. [Elfer 88] A flaw length was not necessarily measured at max stress. ..... 7-11
Fig. 7-6 Stress intensity magnification factor for a cylinder relative to a flat plate ..... 7-12
Fig. 7-7 Influence function for a flat plate. ..... 7-13
Fig. 7-8 Effect of a Hole (modeled as depressurized zone) on the Stress Intensity in a Cylinder. [Rajendran in Elfer88] ..... 7-14
Fig. 7-9 NASTRAN 1/4 cylinder symmetric model ..... 7-15

Fig. 7-10 Effect of mesh size on the calculated stress intensity for a cylinder (using NASTRAN crack tip element). ..... 7-16
Fig. 7-11 Influence function for a crack in a cylinder. ..... 7-17

# 1 INTRODUCTION

This handbook provides a reference for the prediction and analysis of structural damage due to hypervelocity impact. It is applicable to Space Station habitable module walls and other similar spacecraft . Hypervelocity impact includes both meteoroid and space debris impacts. The emphasis of the discussion is stretching, petaling, and tearing of a module wall by either meteoroid or debris impacts.

The analyses and comments are general design guidelines and not necessarily applicable to final Space Station designs since several configuration and detail design changes were being made during the course of this contract. Rather, the analyses and comments may indicate either a point-in-time concept analysis, available test data, or desirable protection goals, not hindered by the design and operation constraints faced by Space Station designers. The baseline design for debris protection was nominally:

- bumper of 0.13 cm (0.050 inch) 6061-T6 aluminum
- 30 layers of 1.3 μm (0.0005 inch) thick Multi-Layer Insulation (MLI)
- standoff of 10.2 cm (four inch) and
- rear wall of 0.32 cm (0.125 inch) age-formed 2219-T87 aluminum.

However, this does not reflect the final space station design and is a point of reference only.

Selected equations are included in appendix A. A Bibliography for the report and appendix A is included as Appendix B. Appendix C contains several light gas gun hypervelocity test databases.

The typical space vehicle design requirement is to meet a specified probability of no penetration or failure in the design lifetime. Large area and long duration spacecraft require a substantial weight of protective shielding. For example, an object the size of the Space Station Freedom, will require on the order of 10 kg/m$^2$ or more for meteoroid and space debris protection. Part of the problem in determining a shield to meet a given reliability is understanding the threat. Rather than having a unique threat size and velocity which must be defeated, there is a spectrum of sizes, velocities, and obliquities, and consequently a variety of penetration mechanisms which must be considered.

To design these shields accurate analysis of the probability of penetration must consider the flux, velocity and angular distributions of debris, as well as the debris shape and density distributions, the spacecraft geometry, and the penetration resistance of the structure. Each has a high level of uncertainty. Penetration resistance is analyzed with a combination

of light gas gun simulation testing, and computer models. Routine testing is possible up to 7 km/s which encompasses a portion of the possible debris impact velocities. A three stage light gas gun has been developed at Sandia National Laboratory, as well as an inhibited shaped charge launcher at Southwest Research Institute (SWRI), to achieve 10 km/s, but in each case the state of the projectile at impact needs to be better characterized. The average space debris impact velocity is 10 km/s but impacts can occur at up to 16 km/s. Meteoroid impact velocities can be up to 72 km/s.

Damage tolerance in manned systems is essential to provide fail-safe vehicles. A goal is to have pressure vessels leak, but not burst in the event of an impact beyond the design considerations. However, this is not practically achievable for all situations. "No-burst" analysis for a hypervelocity penetration must consider a damage zone on the order of 25 cm, which is much larger than the typical flaw size analyzed in aerospace structures.

Figure 1-1 shows the catastrophic results possible for an impact beyond a design's capability. This was tested at the University of Dayton Research Institute (UDRI) as a Martin Marietta IR&D project. [Elfer88]* The projectile was a 12.7 mm (0.5 inch) sphere of 2017 aluminum, weighing 3 grams and fired at 6.4 km/s. The rear wall was 2219-T851, nominally 3.2 mm (0.125 inch) thick, pre-loaded with Bellville washers to a stress of 130 MPa (19 ksi). The wall had an 2 mm (0.080 inch) 6061 bumper held 114 mm (4.5 inches) in front of the wall, with 4 layers of style 710 Kevlar 29 cloth held 38 mm (1.5 inch) from the wall. The Kevlar cloth was essential to this type of failure, as will be discussed in Sec. 6. Figure 2 shows the bumper and Kevlar cloth after the impact. Figure 3 shows the front of the rear wall. Integrally machined stiffeners, 3.2 mm (0.125 inch) thick and 32 mm high, could not stop the crack from running.

---

* References in the Bibliography, Appendix B, are shown in square brackets. A number refers to the year of publication of the referenced author's document.

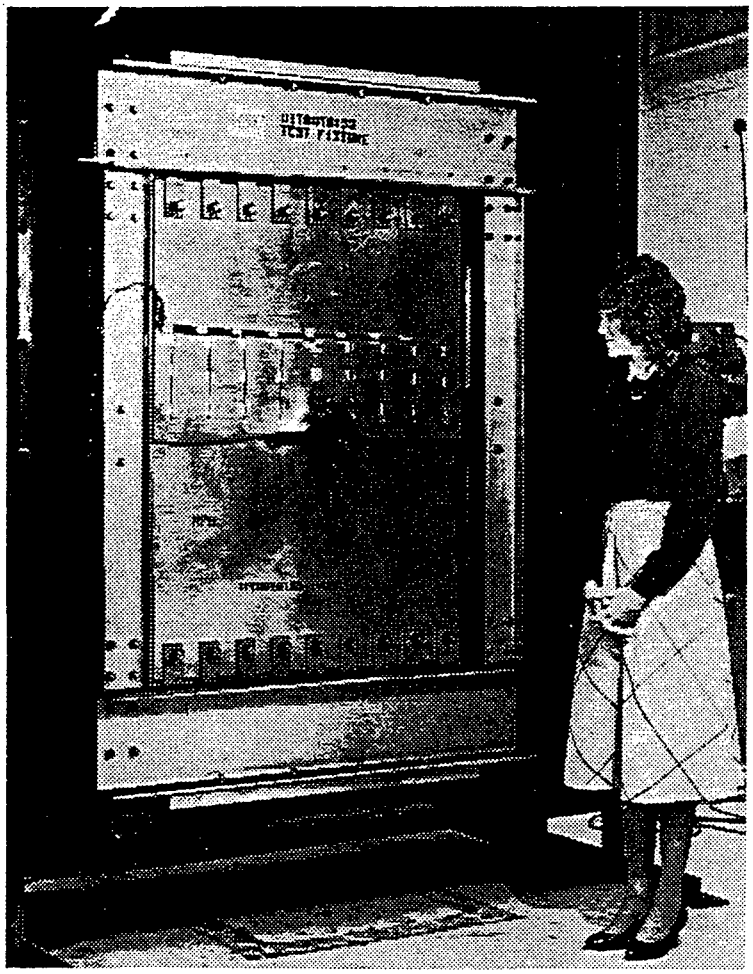

Fig. 1-1 Rupture of a pre-loaded 2219-T851 panel due to a hypervelocity impact with a 3 gram projectile at 6.4 km/s.

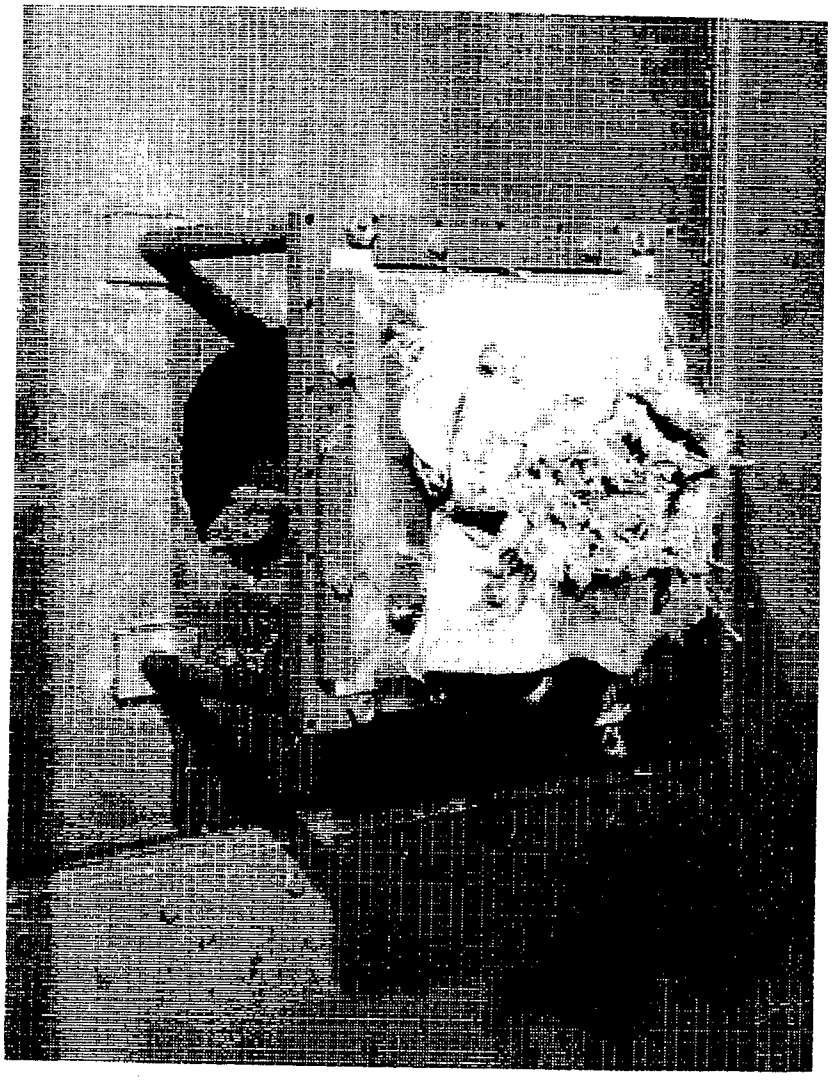

Fig. 1-2 Bumper and Kevlar 29 cloth in front of rear wall in Fig. 1-1 after the impact.

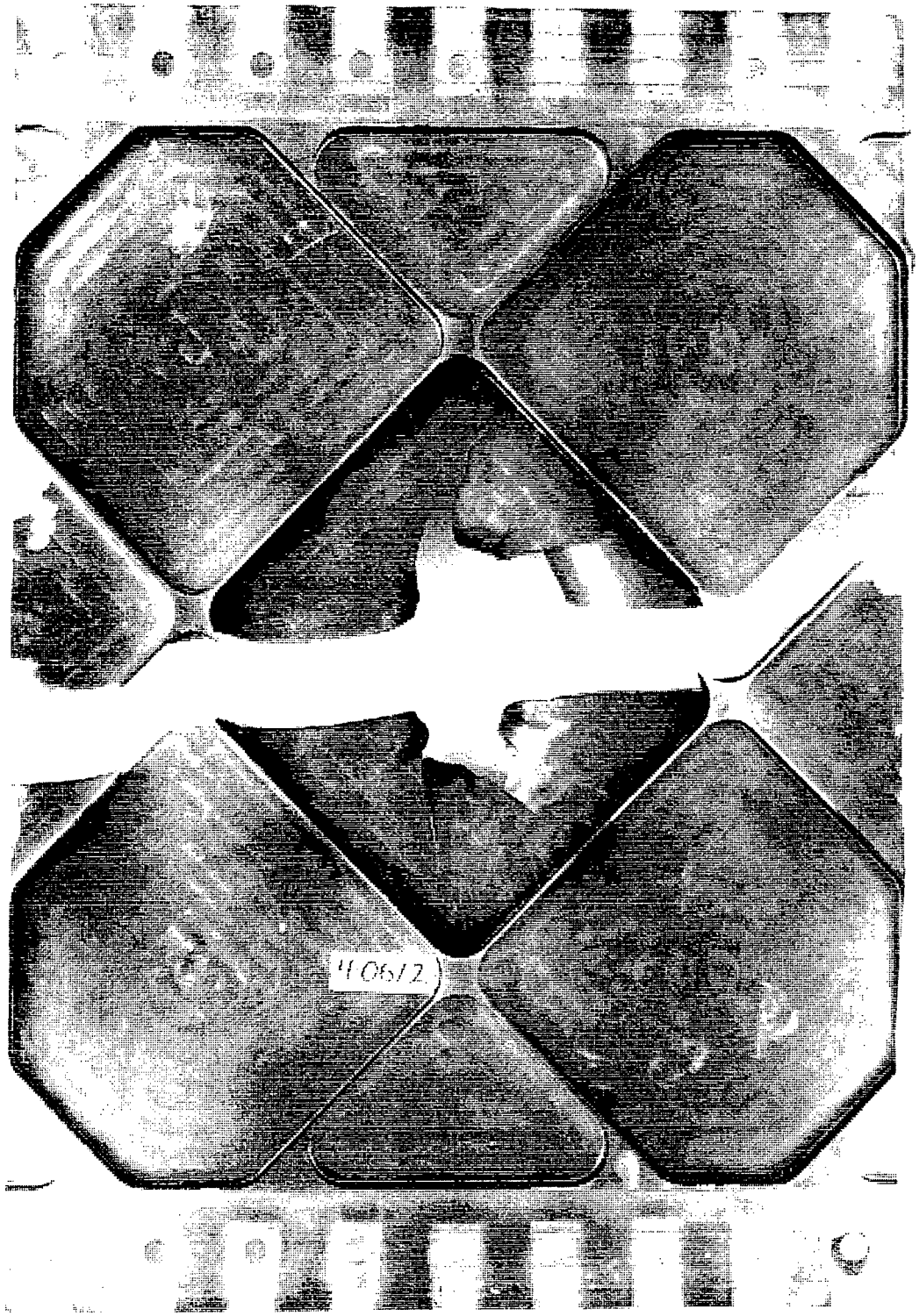


Fig. 1-3 Front of the fractured rear wall in Fig. 1-1. Integrally machined stiffeners could not stop the crack.

# 2 ENVIRONMENT

Equations for the meteoroid and debris flux are given in NASA SSP 30425 (Rev. A with change A1) "Space Station Program Natural Environment Definition." and are built into the BUMPERII analysis code. [Graves; Coronado] Figure 2-1 shows the meteoroid and debris flux. The definition of the flux is for the diameter shown *and larger*. The diameter shown is the minimum diameter with that flux. Fig. 2-2 shows that if trackable debris, 10 cm and larger, can be completely avoided then there is a significant impact on the flux of particles in the 1 cm to 10 cm *and larger* sizes. Note that the graphs in Fig. 2-1 and 2-2 are for specific years, inclinations, altitudes and solar activity. The EnviroNET computer system is a convenient method of checking the currently accepted definition of the orbital environment. [The EnviroNET user guide is available from Dr. Michael Lauriente, Code 400.1, Goddard Space Flight Center, Greenbelt MD 20771, phone (301)-286-5690.]

## 2.1 Meteoroids

The meteoroid environment is dominated by low density (0.5 to 2 g/cm$^3$) loosely packed ice rather than the more dense iron-nickel meteoroids. However, the loosely packed ice can be very damaging at the high impact velocities. The meteoroid environment is better seen in relationship to the Earth rather than the spacecraft. The earth regularly moves through streams (densely populated orbits) which produce meteoroid showers. There is also a random "sporadic" flux. The earth also tends to focus the meteoroids due to gravitational attraction. The spacecraft then moves through this changing environment, shadowed by the Earth, accumulating most impacts on the forward and then the skyward facing surfaces.

## 2.2 Space Debris

For a large-area, long-duration spacecraft the debris flux will by more significant, as shown in Fig. 2-1. Much of the environment definition has been driven by D. Kessler at NASA-JSC and it is continually subject to updates because significant break-up events, or possibly the lack thereof. Users of this document will either have a contractual requirement, or they should consult EnviroNET as mentioned at the start of this section.

The debris environment is predominantly aluminum particles, although a variety of other materials are present, including paint, electronic components, composites, titanium, and steel.

Space debris is very directional. For low earth orbit (LEO) debris may be described by the intersection of circular orbits. Besides the dominant polar, 60°(e.g.. Baikonur, Tyuratam) and 28° (Cape Canaveral, Fl) inclinations, precession of orbits can result in high impact velocities from orbits with the same inclination. Figure 2-2 shows the fraction of the total flux coming from angles relative to the direction of flight in 5° increments. The relative impact velocity for the intersection of 500 km orbits is also labeled on the plot. The relative impact velocity in LEO is determined by the orbital velocity and the intersection angle of the two orbits.

If the spacecraft is not fixed relative to the earth then it can be treated as randomly tumbling. There will be a spectrum of relative impact velocities and obliquities which must be considered in the penetration analysis with the different penetration mechanisms which will be discussed later.

When the spacecraft attitude is fixed relative to the earth, each facet of the surface will have its own distribution of probable obliquity angles and velocities. While no debris overtakes from the rear, a rear facing facet can be impacted by debris which appears to come from the side (an orbit with a shallow intersection angle). Debris cannot intercept a LEO spacecraft from more than 10° above or below a plane tangent to the local Earth normal, since the debris would otherwise enter the Earth's atmosphere and be removed as a threat. The typical angle is only 3° for a 500 km orbit being crossed by trackable debris.

It must be noted that the definition of flux used is the flux, F, on a randomly rotating object. This means that the area will spend half of its time with no exposure to a given stream. However, when a stream from a particular direction is used with the projected area in that direction, then the flux, J, is given by

$$J = 4\,F$$

The simplest derivation of this is that the projected area of a sphere, $\pi r^2$, is one fourth of the surface area of a sphere, $4\pi r^2$. While each will receive the same number of impacts from a stream perpendicular to the disk, the impacts per square meter are four times higher for the disk. An alternative definition is

$$j = F/\pi = J/(4\pi)$$

where $j$ is the flux in terms of impacts per square meter per year per steradian.

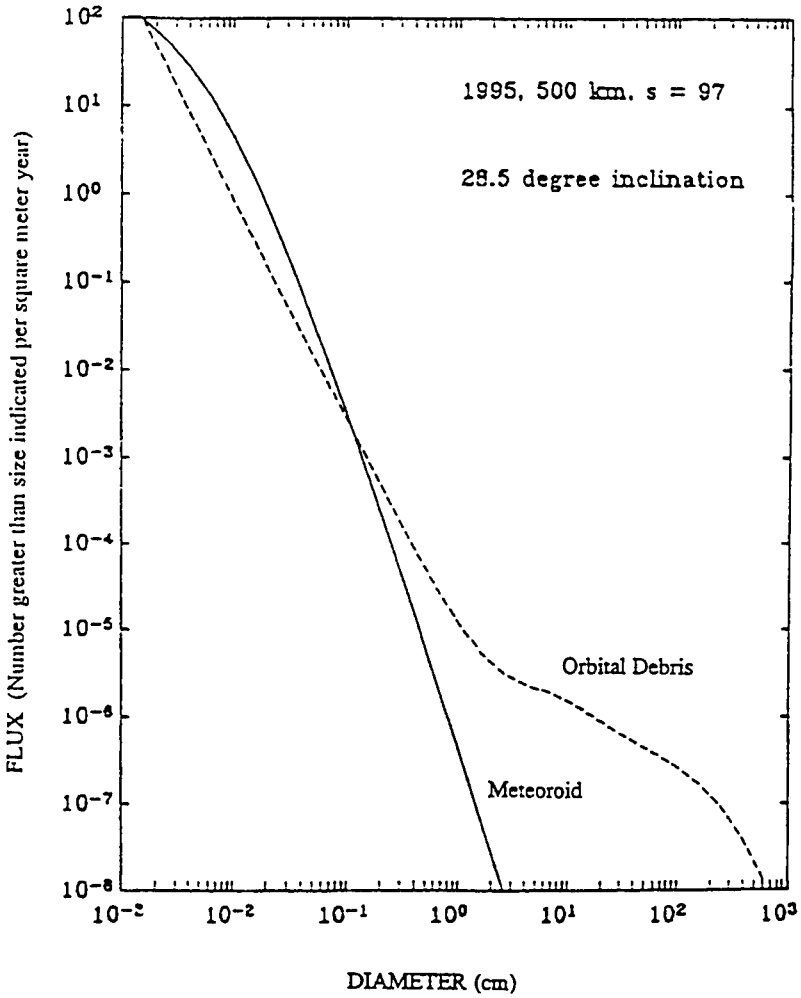


Fig. 2-1 Impact flux for space debris or meteoroids of diameter shown and larger. Flux is defined for a randomly tumbling surface. [as published in Williamsen94]

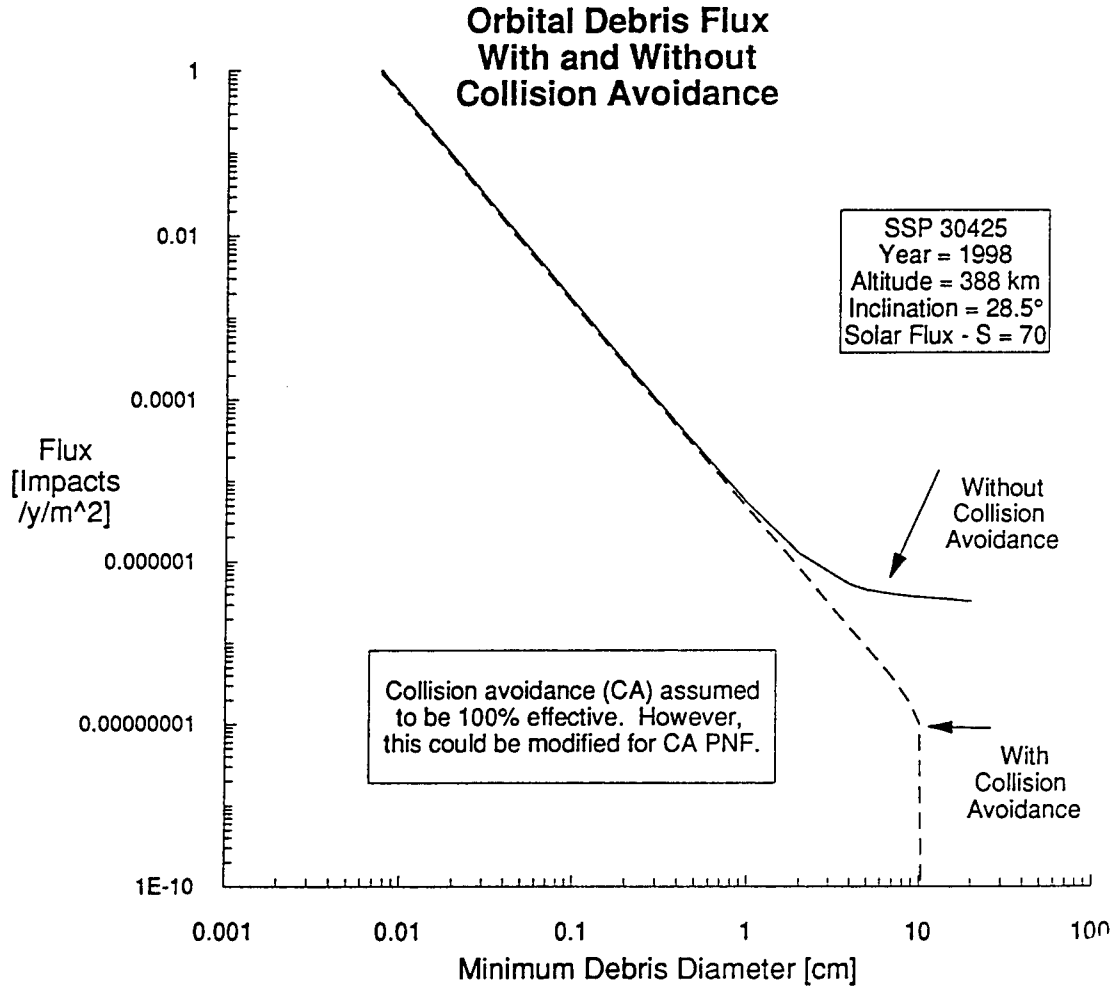


Fig. 2-2 Impact flux for space debris of diameter shown and larger, with and without 100% effective collision avoidance.

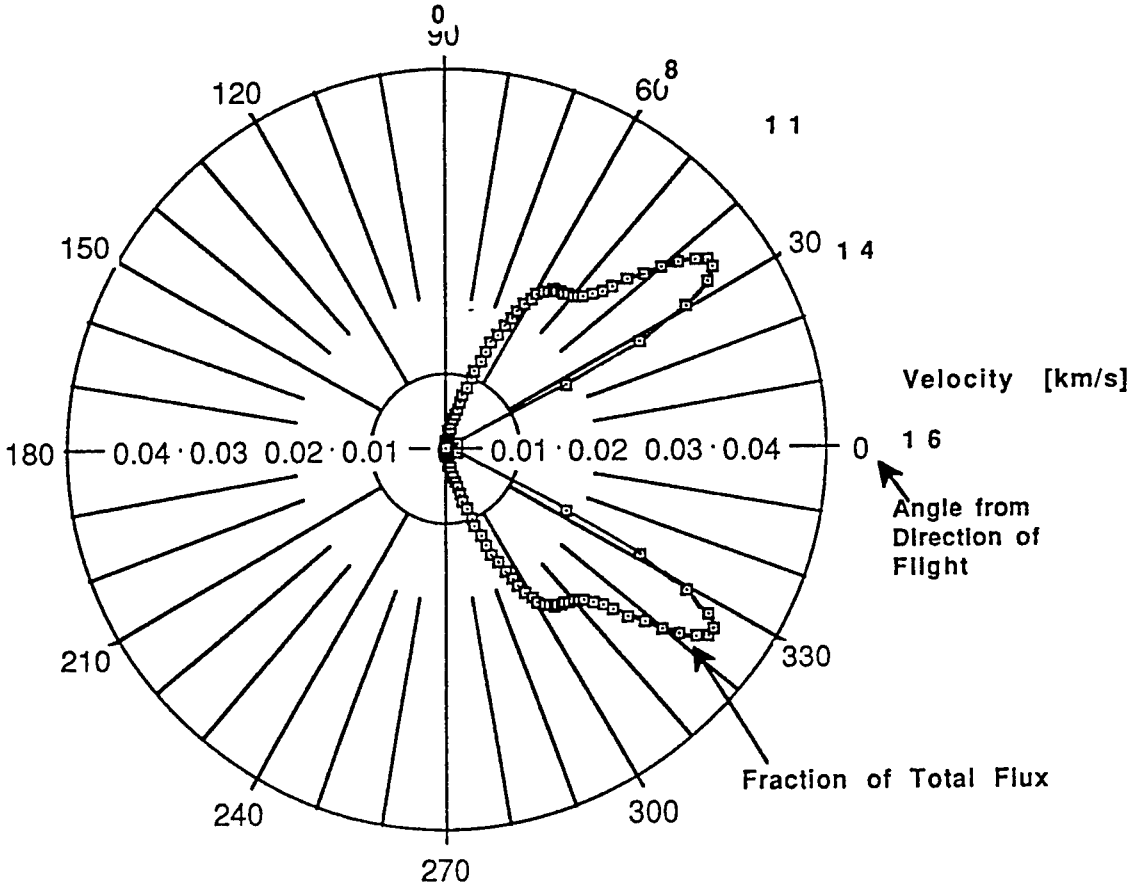


Fig. 2-3 Angular and velocity distribution of debris flux.

# 3 PENETRATION MECHANISMS

There are a variety of penetration mechanisms that work in unison or compete with each other to cause a failure. Penetration predictions based on one penetration mechanism may lead to a gross error when extrapolated to conditions for which another penetration mechanism is occurring. Appendix C contains hypervelocity impact test data from NASA-MSFC, NASA-JSC and Martin Marietta IR&D M-01S.

Debris cloud analysis characterization was reviewed by Piekutowski. [Piekutowski 95]

## 3.1 Penetration Definitions

The definition of penetration used in most recently in hypervelocity testing for the Space Station, is no detached spall or no visible hole through the thickness. Leaking helium, or penetration of a witness sheet behind the rear wall are alternate definitions of penetration that have been used on other programs. (Note that while detached spall is considered a failure, it does not appear to make a significant difference compared to the no-visible-hole definition, at least for Space Station shields up to 7 km/s. )

## 3.2 Single Wall Damage Mechanisms

A single wall can be very vulnerable to hypervelocity impact. At low velocities, the depth of the crater is controlled by erosion of the projectile. However, as velocity increases, the crater becomes hemispherical and the volume of material removed is roughly proportional to the energy of the impacting particle. Tests indicate oblique impacts should use only the normal component of the impact velocity to calculate energy and crater volume.[Summers59] As the obliquity angle becomes large, greater than 45°, the crater becomes elongated, and at greater than 65° from the normal, the projectile primarily ricochets from the surface (as small fragments).

For a finite thickness sheet, the threshold of penetration is reached when the bottom of the crater links up with spall from the back of the sheet. Spall occurs when the compressive shock wave accelerates the rear of the sheet and reflects as a tensile wave above the ultimate strength of the material.

Five single wall penetration equations were reviewed by Hayashida and Robinson. The Fish-Summers and JSC (Modified Cour-Palais) are given in Appendix A. Both found to adequately fit recent test data. The Schmidt-Holsapple equation was found to predict significantly higher diameters to

cause penetration, and it significantly overestimate the penetration threshold on at least one test.

## 3.3 Double Wall Penetration Mechanisms

At different impact velocities and obliquities, multi-wall designs may be penetrated by projectile or bumper shield fragments, spall, melting, or by a late time momentum failure of the final wall. Intermediate shields are useful in further breaking up projectile fragments and reducing spall in a rear wall. At very high velocities the bumper and projectile will melt or even vaporize. If the final wall is not penetrated by fragments it must still absorb the momentum of the initial projectile.

The ballistic limit is dictated by the operative penetration mechanism. The reaction of a multiwall shield to a projectile impact is shown schematically in Fig. 3-1. With increasing shock pressures the original projectile will first fragment into smaller and smaller sizes, then melt and even vaporize. Subsequent layers must stop the fragments from the initial impact, resist spall, and also absorb the momentum. Tests at the University of Dayton Research Institute (UDRI) and at Marshall Space Flight Center (NASA-MSFC) have demonstrated that an intermediate layer of thermal insulation material can be very effective in preventing cratering and spallation of the rear wall, but the momentum of the initial impact must still be absorbed by the rear wall. Even if the original particle is fragmented and "ricochets" from the bumper, bumper fragments may still penetrate the rear wall.

The ballistic limit for a given shield can be plotted as a function of impact velocity and obliquity as shown in Fig. 3-2. This will be called the ballistic limit surface, the shape of which will change radically for changes in shield design. For example, a change in spacing will strongly influence momentum failure, have a mild influence on fragment penetration, and almost no effect on single particle, or ricochet penetration. It is interesting to note that in the valley, or "bucket" of the surface, an oblique impact can be more penetrating than a normal impact because the projectile is not as effectively fragmented.

### 3.3.1 Fragment Penetration

For penetrations less than 1.5 km/s, there will typically be a single hole in the bumper and the rear wall. As impact velocity increases the projectile begins to fragment into smaller and smaller pieces. Figure 3-3 shows typical rear wall damage that may result from normal incidence hypervelocity impact. There may be one or many rear wall holes.

Individual holes may be due to single particles, multiple craters occurring at the same location, or then interaction of rear wall momentum and a weakened and cratered rear wall. Piekutowski showed that for thin bumpers (relative to the projectile diameter) a single large, and lethal, fragment may remain at the center of the post impact fragment debris cloud.

As a rule of thumb, to be effective at 6 km/s impacts the bumper should be 0.15 to 0.25 times the projectile diameter, although much lighter bumpers can work well at these high velocities if the standoff is large. [Christiansen91,92]

There have been several attempts at empirically determining the ballistic limit for fragment penetration. Projectile break-up is analyzed with a combination of experimental data, scaling, hydrocodes, and phenomenological models. The test databases in Appendix C contain a wealth of information, but much of it remains anecdotal in terms of different shield parameters. Jolly and Williamsen [93] performed a curve fit to the data for 0.125 inch rear walls, but even this was difficult due to the go/no-go nature of penetration tests and the results contained both conservative and non-conservative predictions.

The ballistic limit diameter for normal impact reaches a low, on the order of the total shield thickness, at approximately 3 km/s, and goes up to almost twice the total shield thickness for standoffs of 30 times the projectile diameter.

The available penetration equations in BUMPERII appear to be adequate in the regime less than 7 km/s. Christiansen's equations in Appendix A have a simple expression for the ballistic limit below 3 km/s and use linear interpolation between there and the transition to the high velocity penetration mechanism at 6 to 7 km/s, depending on the shield. The THOR equations in BUMPERII were not included in Appendix A due to their complexity, but they are more general and can be used for different materials besides aluminum-on-aluminum. The Burch equations, also included in Appendix A, are particularly useful for prediction of penetration through multiple plates. Although Jolly and Williamsen note they may not reflect oblique impact results accurately. Only the Burch aluminum-on-aluminum equations were included in appendix A, but the original paper has steel-on-aluminum as well.

For the initial baseline design, the fragment penetration equations do not have a strong influence on the probability of no penetration [Elfer92a] as will be discussed in Sec. 4.

#### 3.3.2.1 Projectile Shape Effects

Cylinders with a length to diameter ratio of 1 (L/D = 1) have been found to be much less penetrating than equivalent mass spheres at low velocities, 3 km/s, but the ranking reversed at 6+ km/s.[Morrison72, Elfer 88] This was because the cylinder shatters more easily than the sphere at 3 km/s. At 6+ km/s, in normal impacts the cylinder creates a debris cloud with a spike, of which the tip is the most lethal. The tip appears to be a spall fragment from the bumper, normal to the flat of the cylinder, that can penetrate the rear wall. This is illustrated in Fig. 3-4 and 3-5. Morrison described this: "for cylindrical projectiles, the shock [in the rear surface of the bumper} near the axis is planar, whereas for the sphere the shock is more hemispherical."

Schmidt et al [1992] showed that a disk with a small L/D could be very penetrating even for a cadmium on cadmium impact. A flat fragment, including all or part of the bumper, tended to continue in the line of flight with very little dispersion. This easily penetrated the rear wall.

The fragments from a yawed cylinder (as opposed to the bumper) can tend to line up and penetrate the rear wall, rather than being spread over a large area like the sphere fragments. A typical penetration is shown in Fig. 3-6 through Fig. 3-11.

### 3.3.2 Momentum Failure

If the wall is not penetrated by fragments then it must absorb the debris cloud momentum. The failure of the rear wall from this blast loading can be very sensitive to the momentum distribution, the rate of loading, momentum multiplication due to rebound and/or cratering, and damage to the surface from early time cratering. Generally, the failure models have either relied on an assumed momentum distribution in the rear wall, or a critical momentum intensity. This will be discussed briefly in the following sections and in greater detail in Section 6. This failure mode can be achieved in typical light gas gun tests only with intermediate shields or by the use of cadmium projectiles and cadmium bumpers (Cd-on-Cd) to simulate vaporization. [Schmidt92] Figure 3-12 shows a momentum bulge and failure in specimens with a Kevlar intermediate shield to prevent fragment damage. The specimen that failed was impact by the same size projectile with slightly higher velocity.

#### 3.3.2.1 Wilkinson Model

The Wilkinson model for momentum failure was based on McMillan's hydrocode models of impacts at velocities sufficient to cause complete vaporization of the projectile and bumper. The dispersion of the debris

cloud momentum intensity on the rear wall is given in Appendix 1. Note that the dispersion angle corresponds to one standard deviation on a Gausian momentum distribution. A significant amount of momentum was assumed to be outside of the dispersion angle.

The rear wall failure criterion was determined by Wilkinson from two dimensional analyses of a strip bulging under a Gausian momentum intensity distribution.

**3.3.2.2 Modifications to the Wilkinson Model**

Elfer [88] modified the Wilkinson dispersion angle for aluminum impacts based on two reasons. The first reason was to select a constant to fit the equation to observed failures in Whipple bumpers with Kevlar cloth intermediate shields. The second reason was that the dispersion angle observed from HULL hydrocode analyses, as well as observed rear wall damage rings, was smaller than the dispersion angle that Wilkinson used. This is simply a manifestation of the fact that Wilkinson's analysis was for aluminum vaporization at meteoroid impact velocities while complete vaporization does not occur for aluminum except over 12 km/s impact speeds. For a t/d ratio of 0.252, Wilkinson's equation predicted a dispersion angle of 16 degrees. Note that Wilkinson's angle is for one standard deviation, approximately 1/3 of the mass was at higher dispersion angles. Hull hydrocode results were closer to 11 degrees at 7 to 13 km/s. Piekutowski's analysis [95] of post-impact radiographs shows the dispersion angle of the outer bubble can be up to 18 degrees, but the momentum distribution may not be consistent with Wilkinson's assumed Gausian distribution.

Bjorkman [91] also suggested modifying the Wilkinson equation to 80% of the original value, similar to Elfer. However, this was based on the potential for elastic rebound which could double the momentum, rather than due to a dispersion angle effect.

**3.3.2.3 Grove's Model**

Grove and Rajendran modeled rear wall bulge, and necking, with varying the input parameters. [Appendix D] Their equation summarizing rear wall thinning is also given in Appendix B. The analyses were for Gausian momentum distribution, so that using either the Wilkinson or a modified Wilkinson equation, failure can be predicted for a wide variety of rear wall material characteristics.

**3.3.2.4 Housen and Schmidt's Scaled Velocity Model**

Schmidt et al [94] performed tests with cadmium bumpers and projectiles with a standoff from aluminum rear walls. The cadmium bumper and projectile were assumed to produce the same damage in the

aluminum rear wall as for an aluminum bumper and projectile (Al-on-Al) at 3.1 times higher velocity. The 3.1 scales both the energy of melting and vaporization of the debris cloud, as well as the cloud's momentum, due to the density ratio of cadmium to aluminum. [Holsapple93]

Figure 3-13 shows the experimental scaled ballistic limit based on Cd-on-Cd, and a comparison to Christiansen's Whipple shield equation. The remarkable feature is that the ballistic limit increases from 12 to 18 km/s (Cd-on-Cd test velocities 3.9 to 5.8 km/s). This is probably due a transition from liquid to all vapor as the impact velocity increases. In terms of the previous models, the there would be a transition from a modified Wilkinson model to an un-modified Wilkinson equation, although even that would not account for the increase in penetration diameter observed in the test. And the reason for the transition is not clear. The tests at UDRI [Schmidt94] show the shape of the cloud is similar for both velocities. This means that either there is a different mass distribution in the cloud which affects the rate of loading of the rear wall, or there is less rebound and momentum multiplication for the higher velocity test. Both of these benefits could actually be changed or even negated by intermediate shields.

There is still a question of whether cadmium-on-cadmium can adequately simulate rear wall damage for aluminum-on-aluminum impacts at a higher scaled velocity. While the state and momentum of the debris cloud is adequately reproduced by the scaled tests, the rate of load application on the rear wall is not simulated. Without an intermediate shield, the debris cloud impulse will have 3.1 times longer duration for Cd-on-Cd surrogate tests. For that case, shear waves can extend from the initial impact location before the remainder of the debris cloud can impact the rear wall. This can over-estimate the penetration resistance, but is probably the worst case for tearing.

This is certainly one of the most revealing means of analyzing 10 to 18 km/s impacts. However, surrogate material tests are also potentially misleading if intermediate shield and rear wall loading rates are not considered.

### 3.3.3 Spall Failure

Spall of a large area is possible due to an impulse from the liquid or gaseous debris cloud. Wide area spall of a 0.64 cm thick sheet is shown in Fig. 3-8. It has also be observed in 0.32 cm thick 2219. Spall failure should extrapolate with projectile energy rather than momentum. (The peak pressure would vary linearly with impact velocity for the same momentum.) This is not favorable for PNP predictions, but should decrease

the chance of critical damage if more of the momentum passes through the wall.

Without an intermediate shield, the debris cloud momentum is transferred over a short time span. Even without fragments in the debris cloud, gas and droplets can generate pressures which exceed the spall strength of the rear wall. This failure mode can be difficult to achieve in light gas gun testing. Fragment penetration is usually observed for shields of interest, and similitude testing does not typically address this failure mode. Most hydrocode models do not consider this failure mode.

The debris cloud model by Piekutowski was used by Rajendran [89] to predict that spall will be associated with the initial bumper material in the cloud. A typical spall strength for aluminum is on the order of 800 to 1200 MPa (110 to 170 ksi). At 6.5 km/s, with out an intermediate catcher, the cloud model produced pressures of 6000 MPa.

Schmitt et al [94] noted that spall occurred for aluminum-on-aluminum impacts but not for Cd-on-Cd for the same dimensionless impact speed. This shows that Cd-on-Cd scaled velocity tests may adequately model the physical state and momentum of the debris cloud, the tests do not properly scale rear wall effects.

As impact velocity increases, the threshold mass to cause penetration should scale with projectile velocity squared, modified for debris cloud dispersion angles. The time duration of the momentum transfer is inversely proportional to the velocity of the leading edge of the debris cloud. To maintain the same peak pressure at high velocity, the total momentum must by smaller.

Spall has been observed even with intermediate shields. A rigid intermediate shield, if it is uniformly accelerated, can act as a flyer plate and cause spall.

### 3.3.4 Oblique Impact Effects

Above 60° obliquity, the projectile tends to ricochet off the bumper as illustrated in Fig. 3-14. Fragments of the projectile or bumper can still cause penetrating craters in the rear wall. Figures 3-15 to 3-17 show a ricochet test result.

Tests at 30 to 55 degrees obliquity and 5 to 7 km/s show that a much smaller particle can penetrate a given design than would be possible for an impact at normal obliquity.[Gehring, Brewer, Coronado, Elfer, Christiansen, Jolly, and others]

Increased penetration for oblique impacts appears to be contrary to normal logic for penetration when the projectile does not fragment. The

reason is that the projectile does not fragment (and possibly disperse) as well as for a normal incidence impact. Just as cratering volume is related to the normal component of velocity of the projectile relative to the target, shatter of the projectile appears to be related to the normal component of velocity relative to the bumper.

The initial contact point of an oblique impact is on the side of a spherical projectile. Release waves reduce the stress compared to a normal incidence impact. Furthermore, the bumper material along the centerline of the projectile is imparted a velocity before projectile material would even hit it. Hydrocode analysis shows the material along the bumper centerline has a significant component of velocity radial to the shotline after impact.

### 3.3.5 Christiansen's High Velocity Extrapolation

Christiansen has high velocity penetration equations for several different shield designs. [Appendix A contains several of the equations.] In general they extrapolate from 6 to 7 km/s, the maximum test velocity or an observed transition to a different failure mode, using either constant energy or constant momentum. Considering the uncertainties in fragment penetration, spall, and load rate effects on the rear wall, constant energy extrapolation may be somewhat conservative but it is warranted for simple Whipple shields.

### 3.3.6 Comparison of High Velocity Predictions

Hayashida [95] plotted ballistic limits for several penetration equations as shown in Fig. 3-18. The new Cour-Palais equation is from a modification with Christiansen. The Housen-Schmidt equation, shown on Fig. 3-13, has a larger diameter to penetrate than the un-modified Wilkinson equation at the high velocity range. The author of this handbook has an opinion on which equations are most appropriate, but he also recommends the use of each in a PNP analysis [Section 4] to estimate design sensitivity. Without an intermediate shield [Section 5] constant energy extrapolation is probably appropriate due to the potential for spall, bumper fragment penetration, or a "trap door" failure mode rather than a Wilkinson type momentum failure [see Sec. 6]. When an intermediate shield is used, the modified Wilkinson equation will probably be appropriate. There may be a transition to an un-modified Wilkinson equation around 10 to 12 km/s, based on Housen-Schmidt results, but how the intermediate shield interacts with the cloud and the rear wall is not known and cannot be relied on with existing data.

# Impact Process

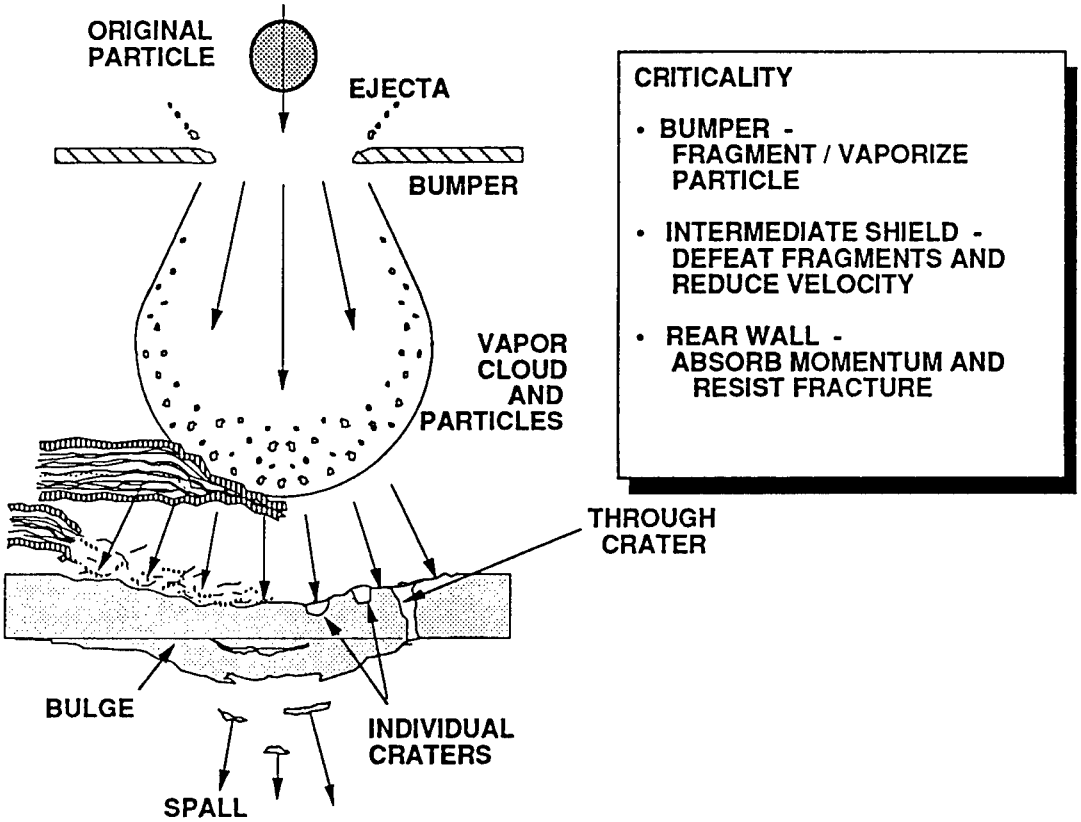


Fig. 3-1. Multi-layer penetration mechanisms.

*The Ballistic Limit Surface Separates Penetration (All Points Above the Surface) from No Penetration (Below the Surface).*

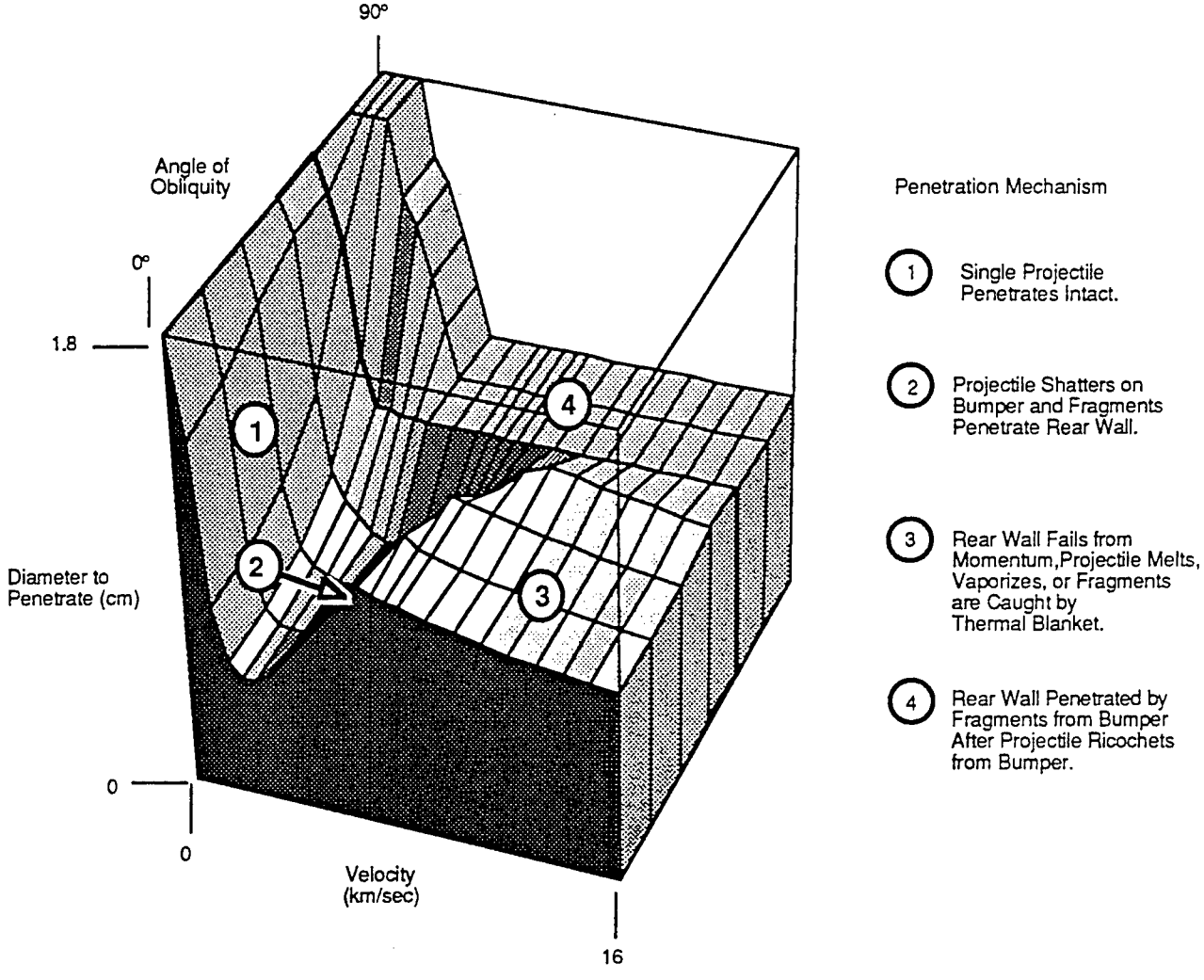


Fig. 3-2. Typical ballistic limit as a function of impact velocity and obliquity for a multi-layer design.

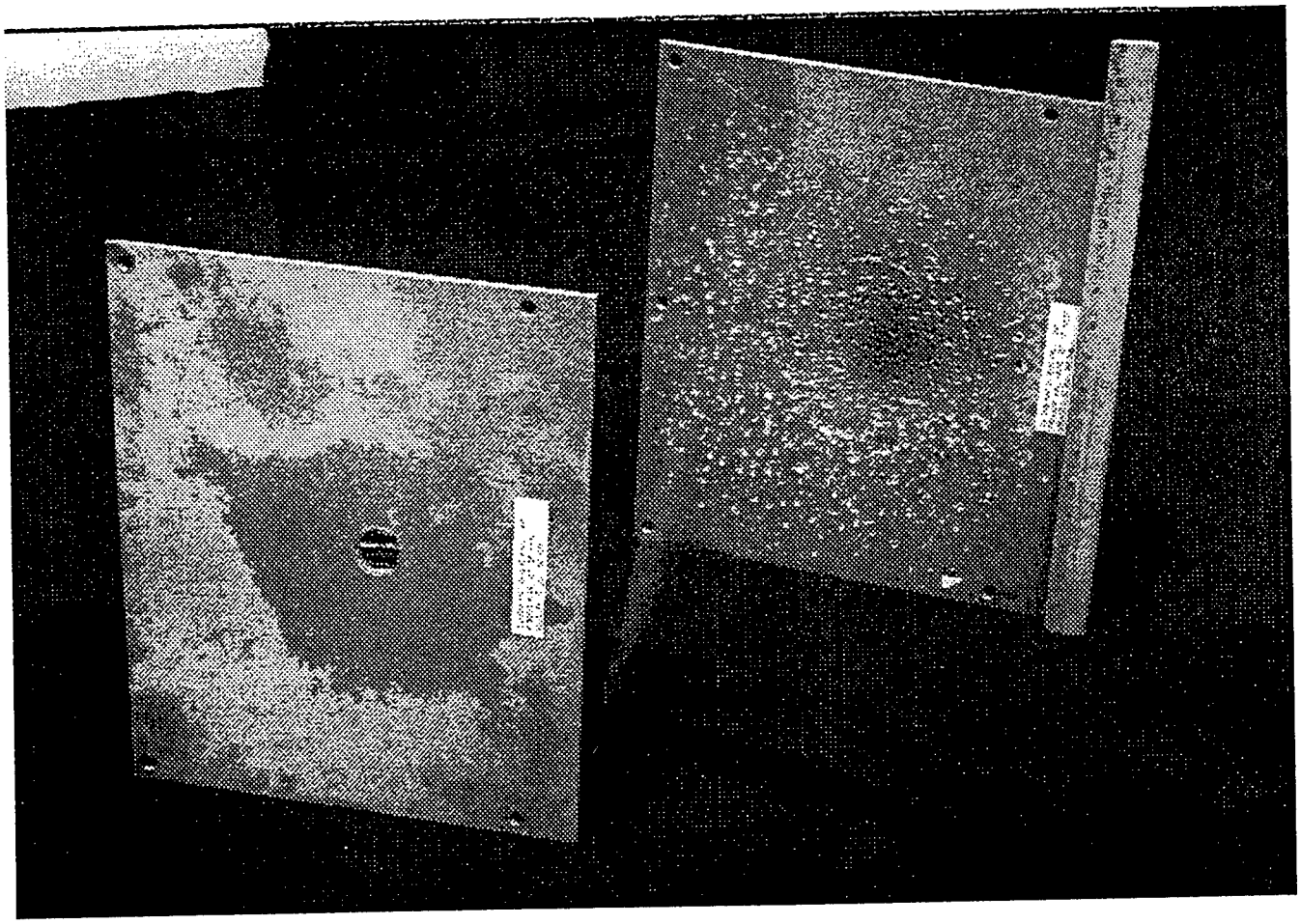

Fig. 3-3 Typical Whipple bumper fragment damage. (305 mm (12 inch) standoff.) (MSFC shot.)

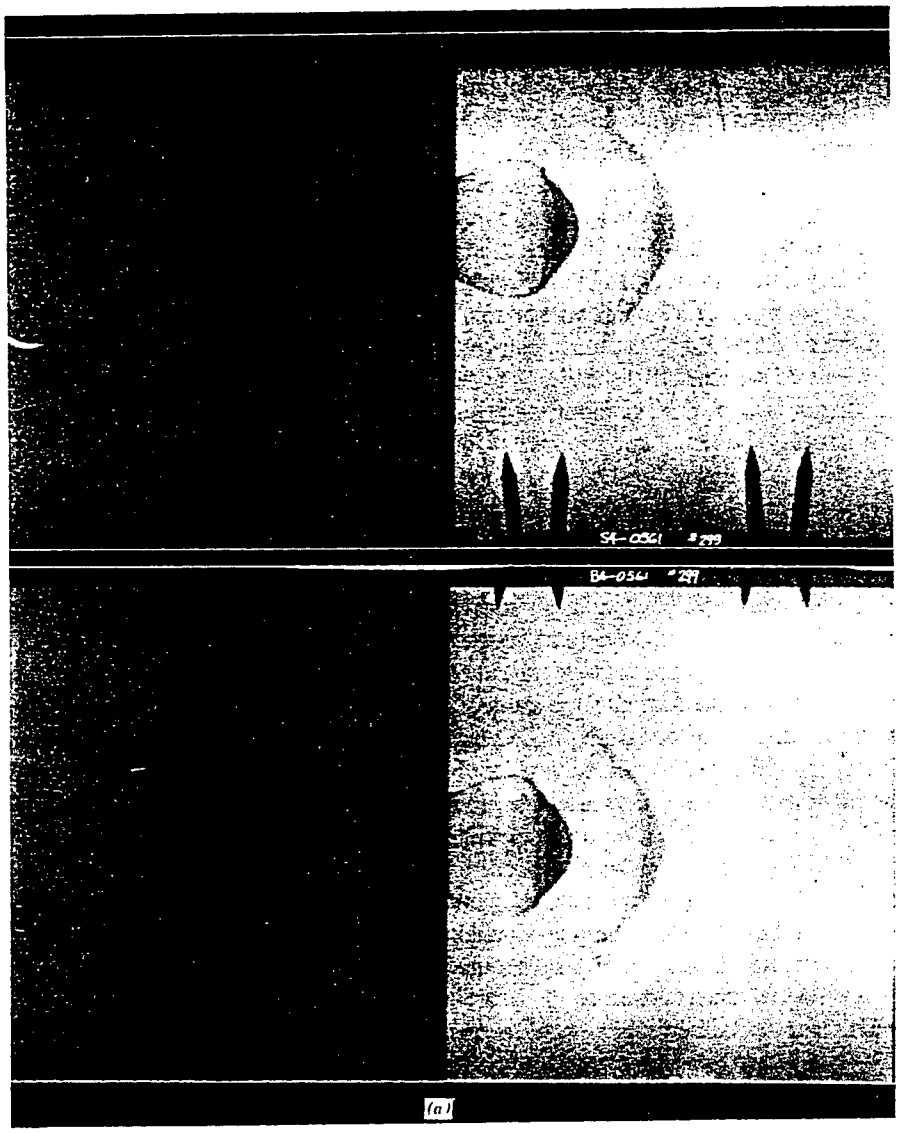


Fig. 3-4. Post impact debris cloud radiographs from a spherical projectiles. [UDRI shot in Rajendran89]

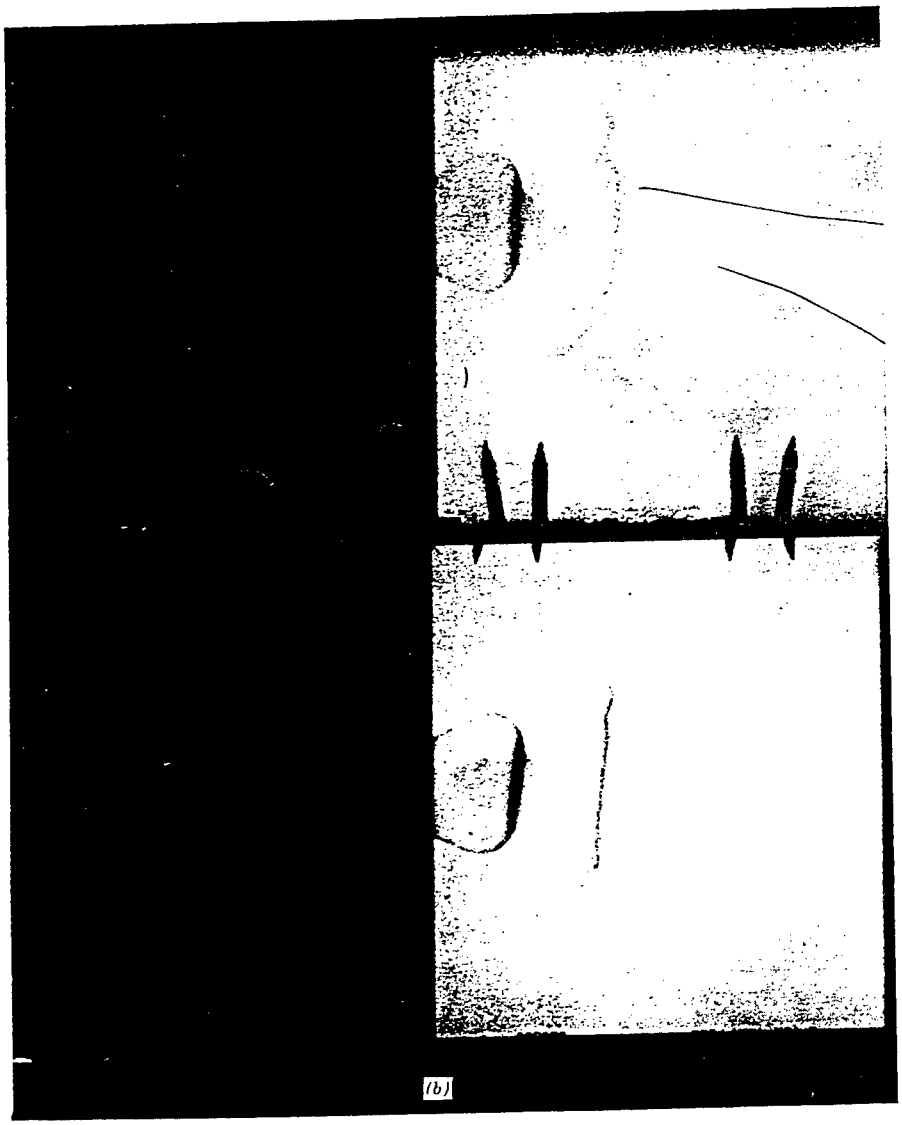


Fig. 3-5 Post impact debris cloud radiographs from a cylindrical projectile. [UDRI shot in Rajendran89]

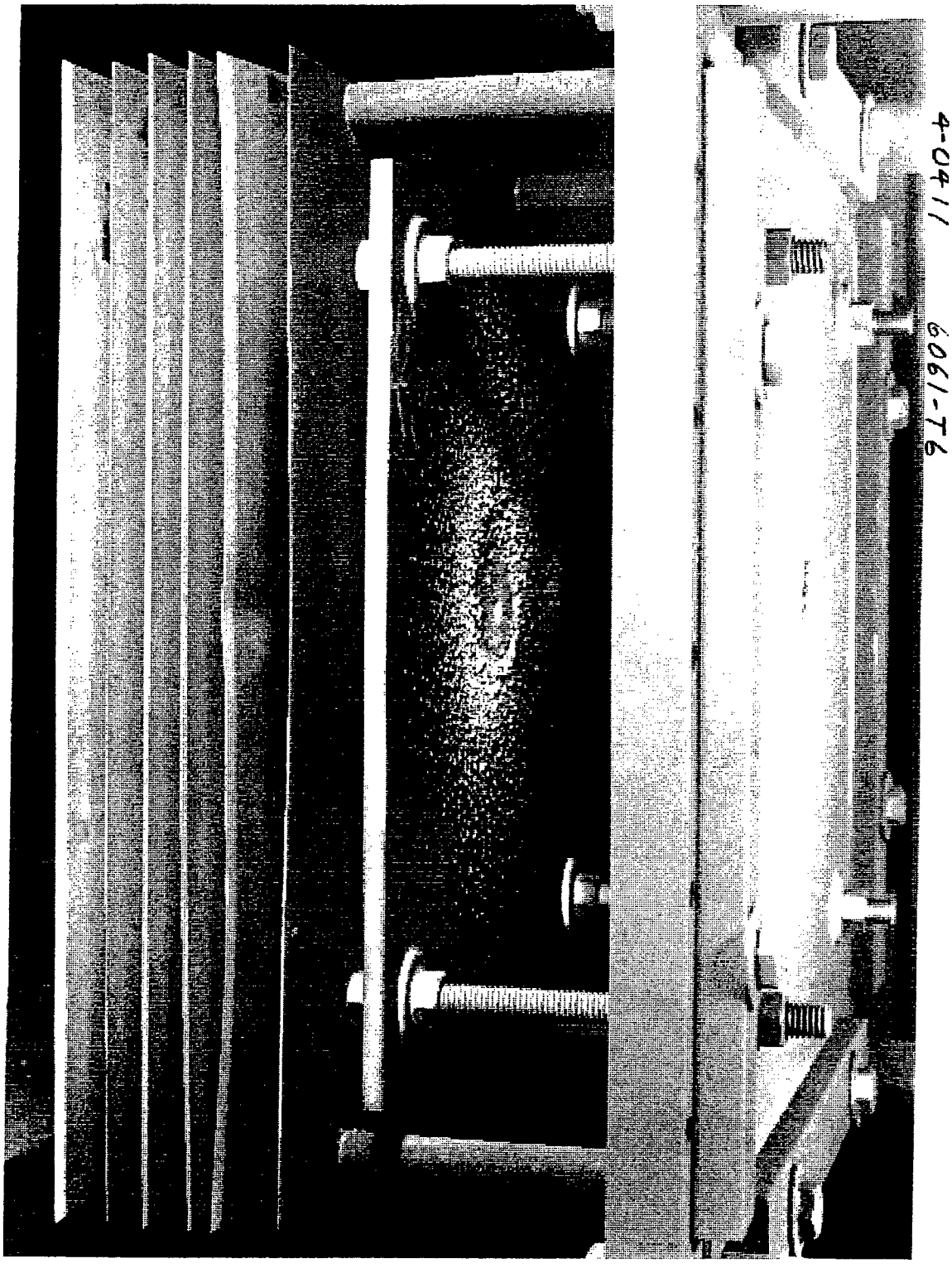


Fig. 3-6 Rear wall damage from a cylindrical projectile that impacted the bumper without yaw. (UDRI shot 4-0411)

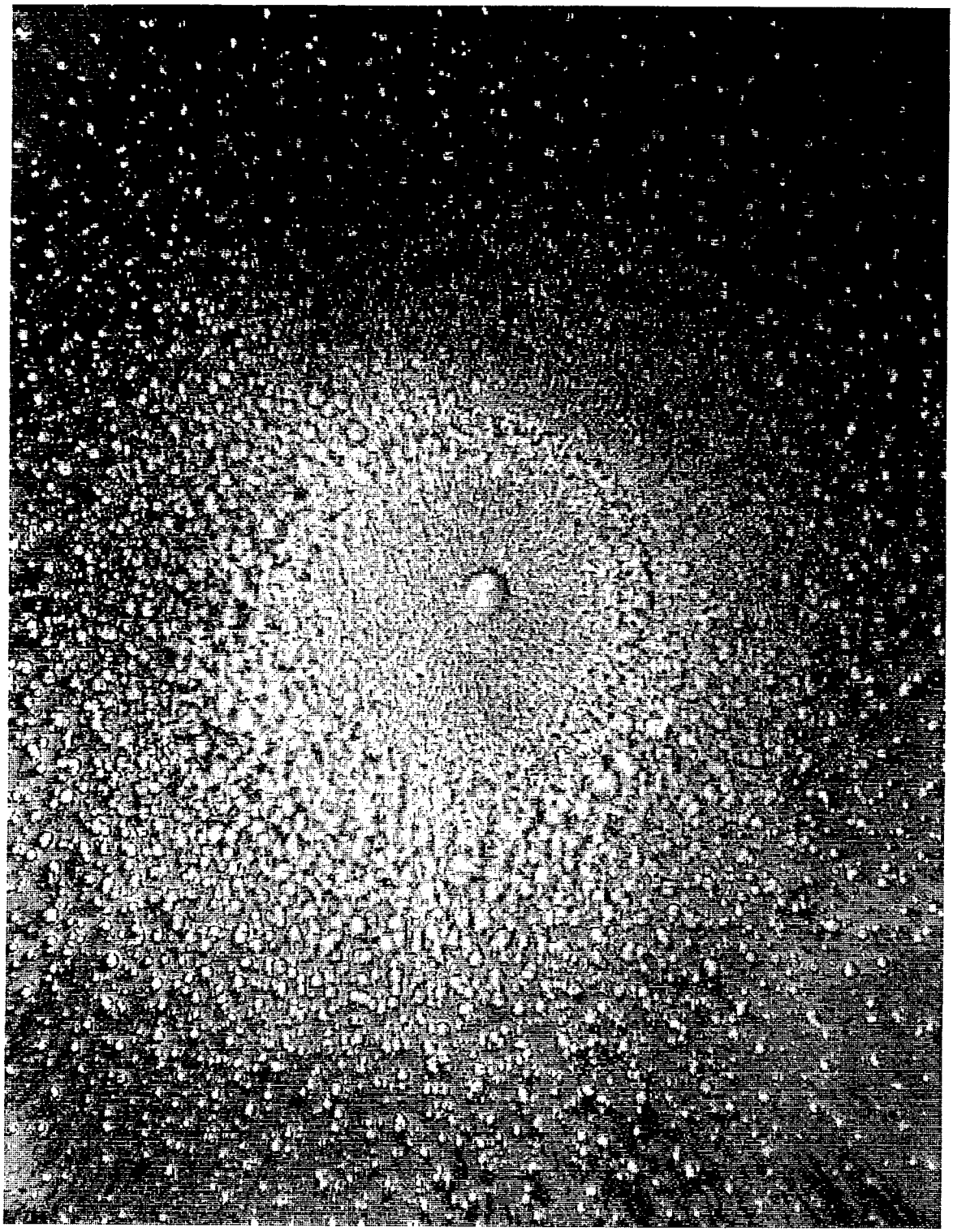

Fig. 3-7 Front of rear wall from Fig. 3.6. Note central crater probably from the tip of the bumper debris cloud.

Fig. 3-8 Rear of rear wall from Fig. 3.6 showing wide area spall.

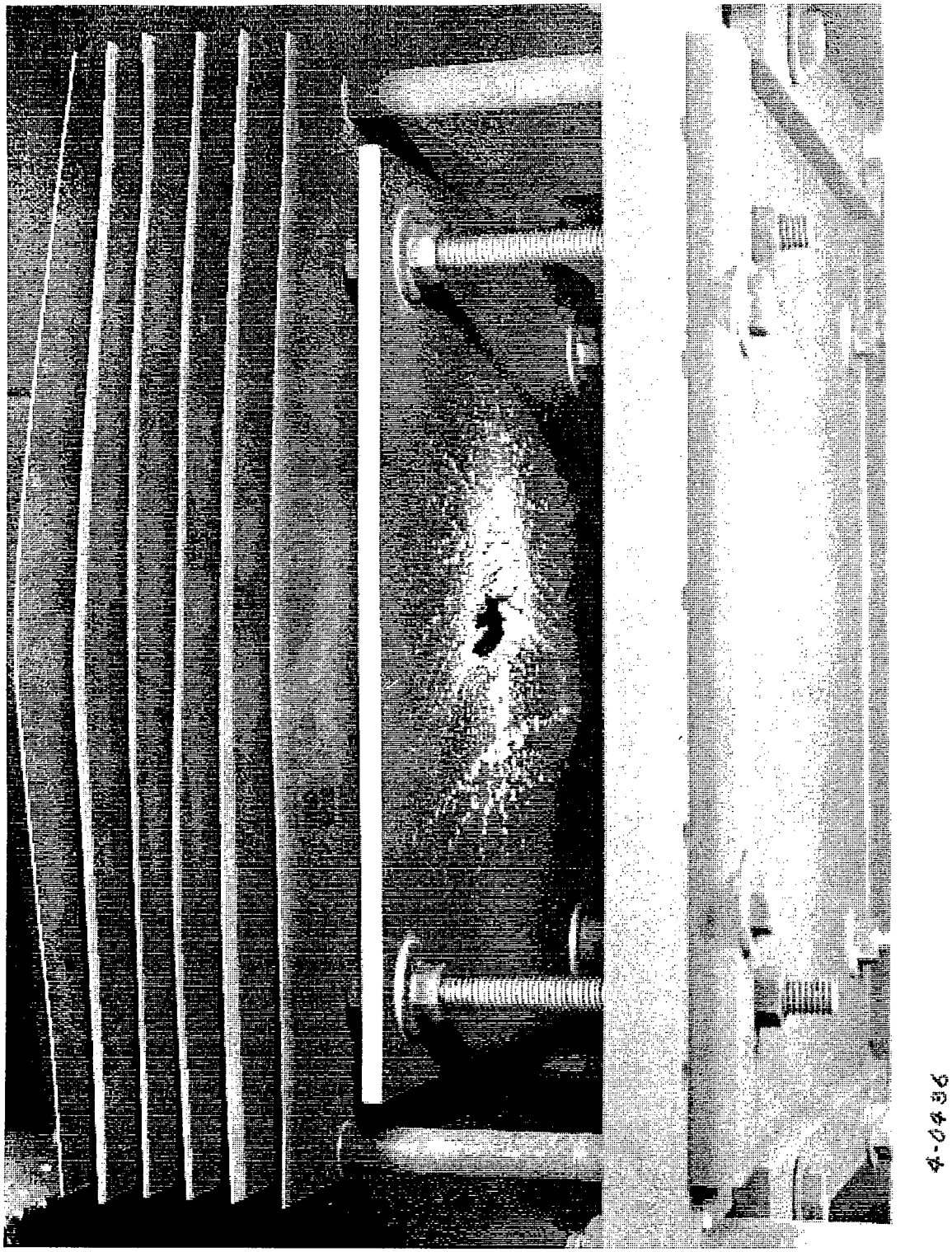


Fig. 3-9 Rear wall damage due to a cylindrical projectile that had yaw. (UDRI shot 4-0436)

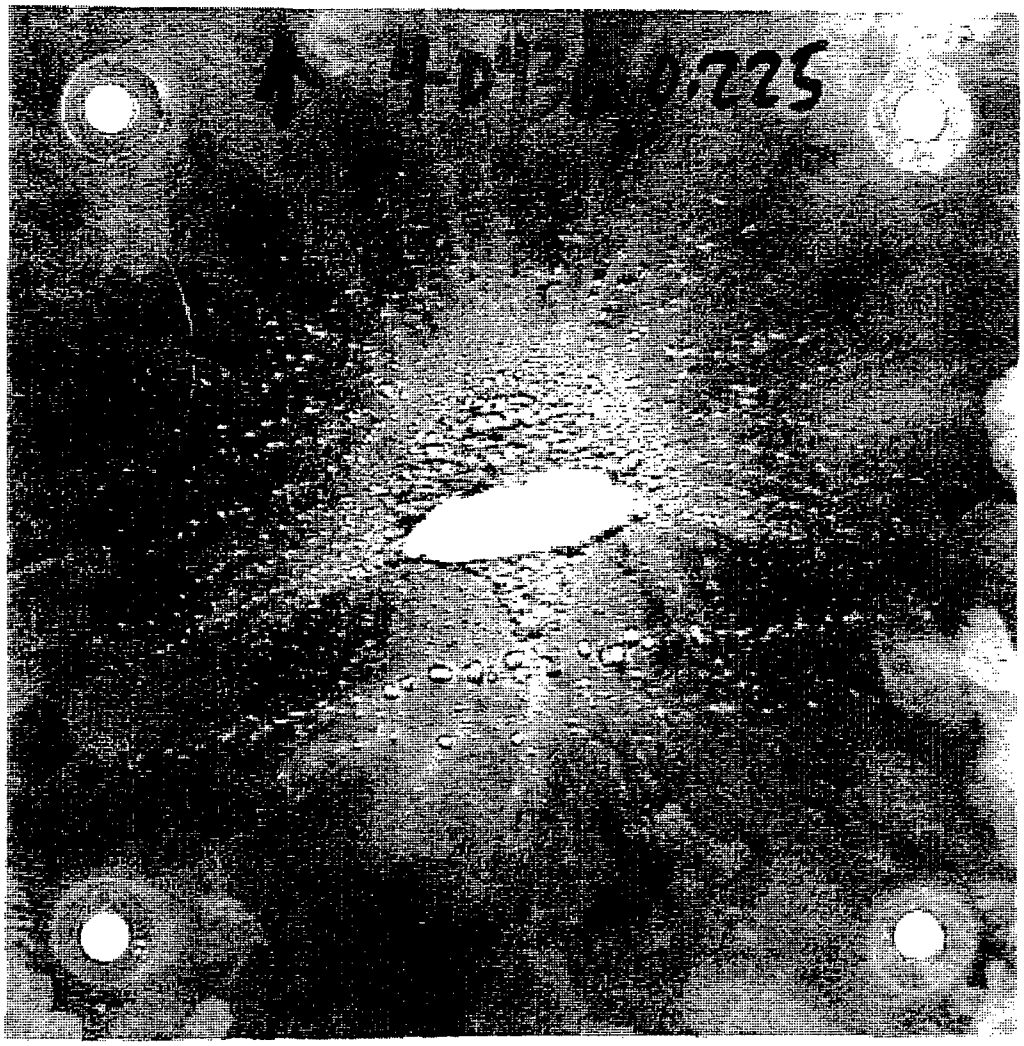

Fig. 3-10 Front of rear wall from Fig. 3.9.

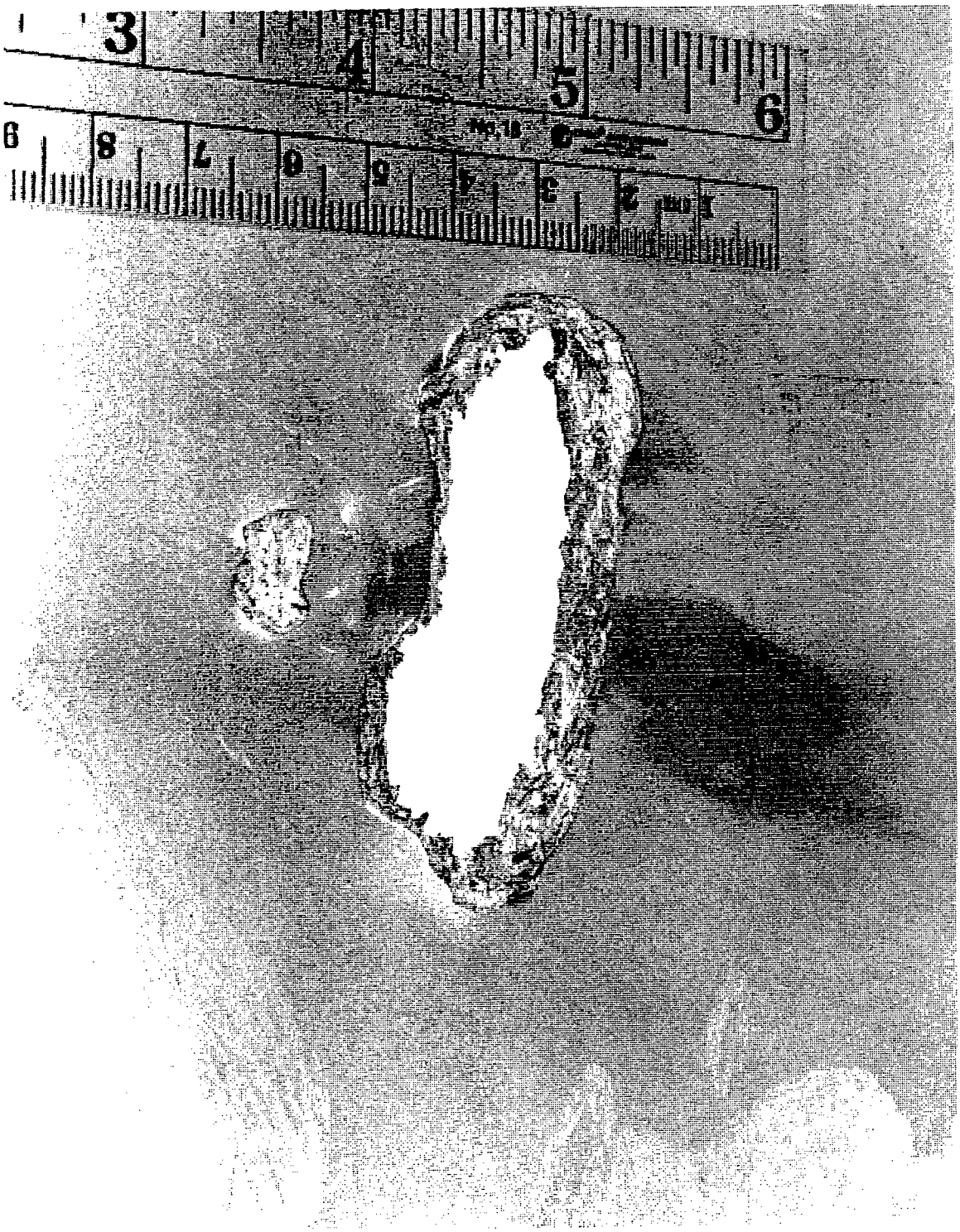

Fig. 3-11 Rear of rear wall from Fig. 3.9. Penetration and spall from aligned projectile fragments, and spall probably from the tip of the bumper debris cloud.

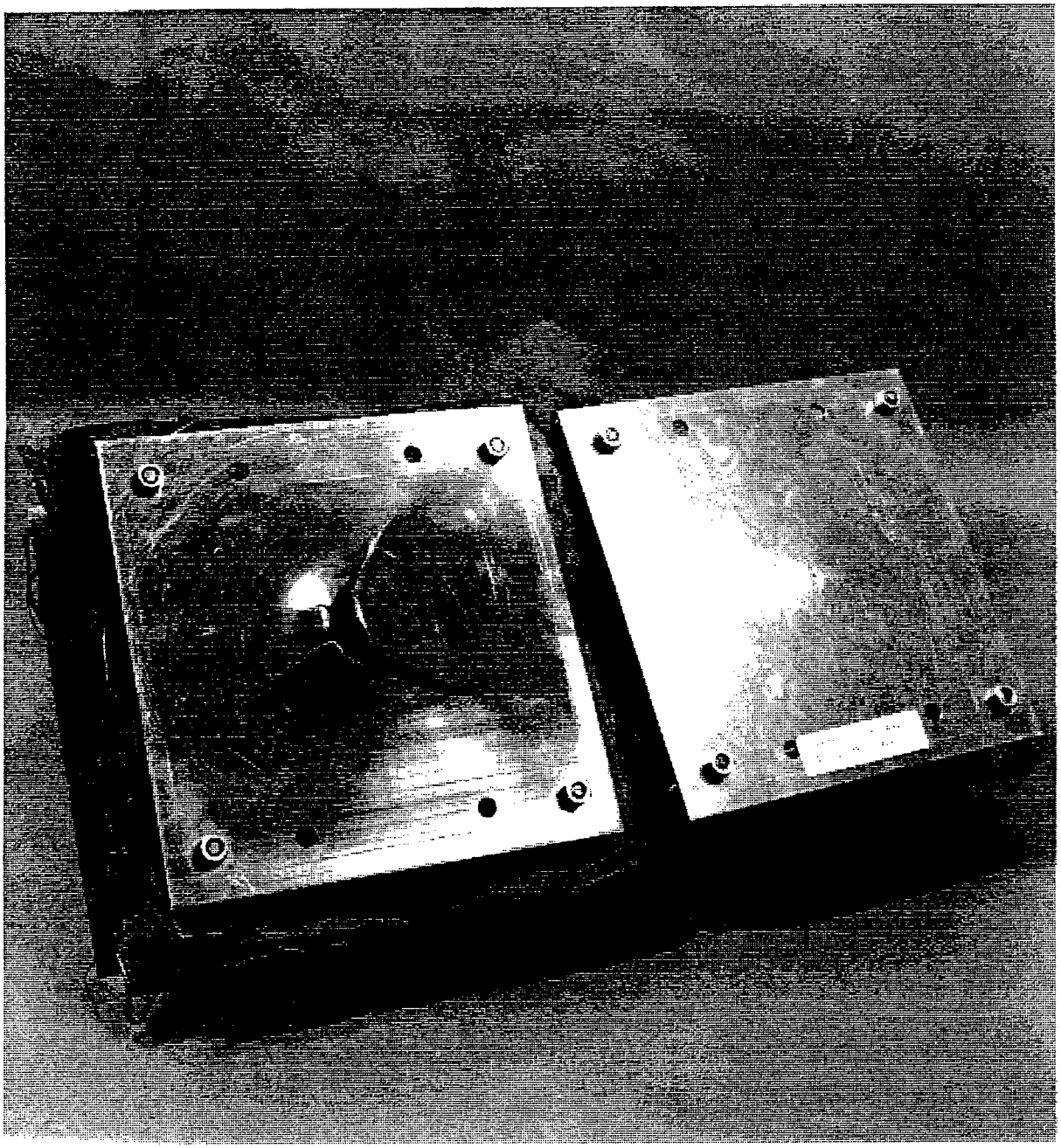

Fig. 3-12 Wilkinson type momentum bulge and failure with Kevlar intermediate shields to prevent fragment damage.

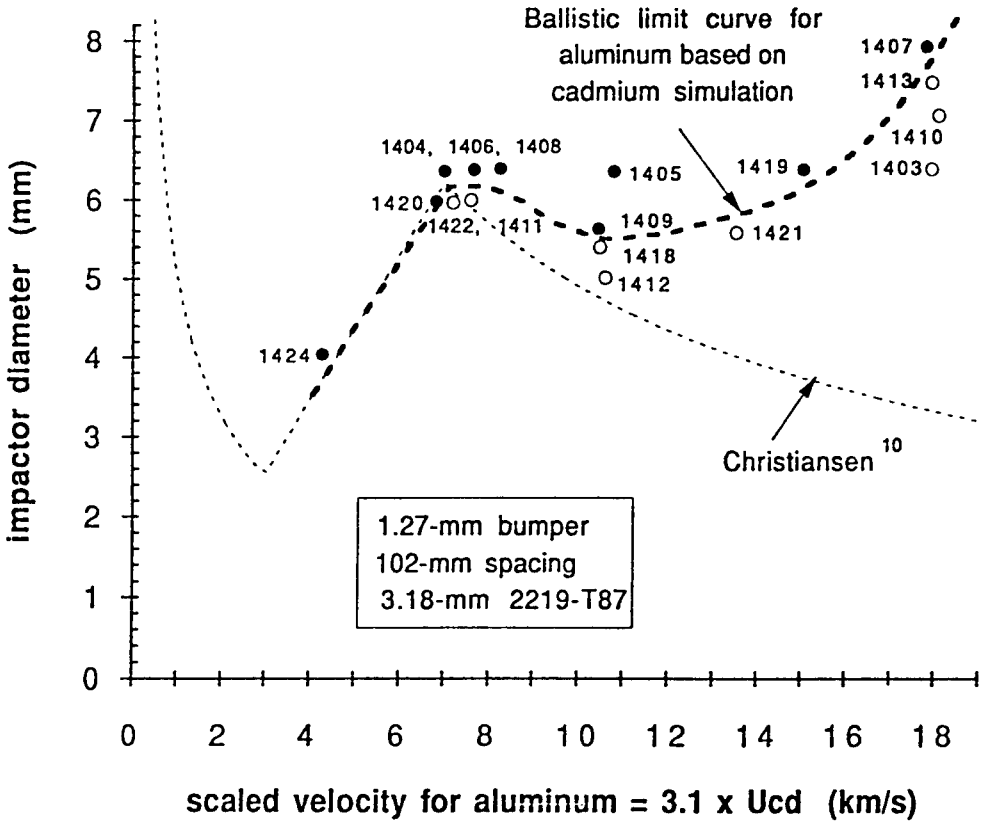


Fig. 3-13 Ballistic limit determined from aluminum rear wall with cadmium projectile and bumper tests, scaled to equivalent all aluminum test. [Schmidt94]

# Ricochet

- Above 65° projectiles will ricochet off the bumper
- Projectile fragments come off in streams
- Bumper fragments (spall) may penetrate the pressure wall

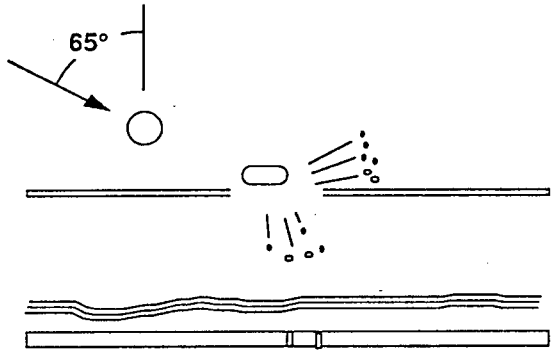


- BAC approach for ricochet stream PNP seems conservative
- Analysis of multiple impacts in same location maybe needed.
  - Depends on operations (removeable log modules vs permanent hangar)

Fig. 3-14 Oblique impact schematic.

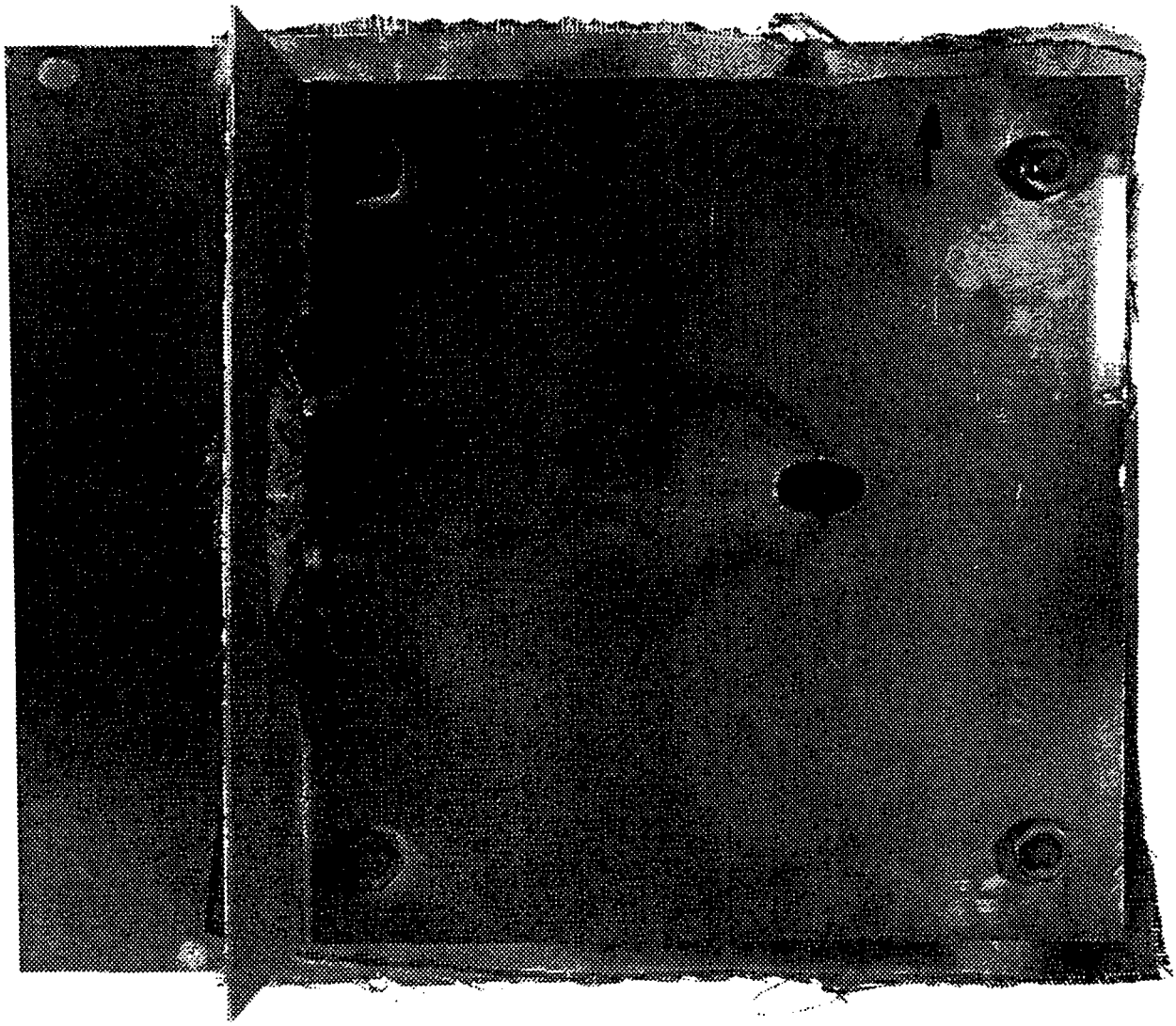

Fig. 3-15 Oblique impact bumper damage. (UDRI shot 4-0657)

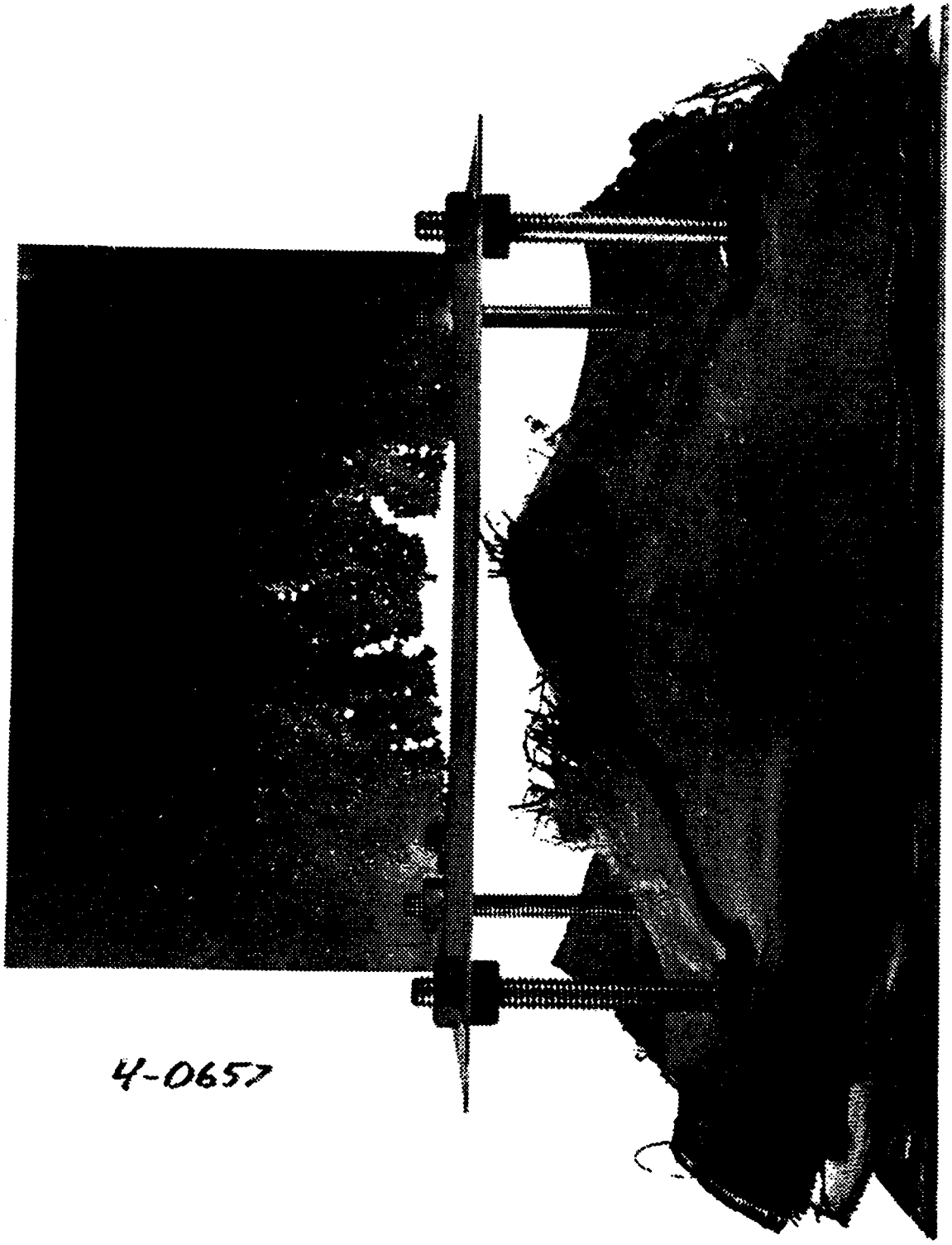


Fig. 3-16 Oblique impact ricochet damage. (same as Fig 3-15)

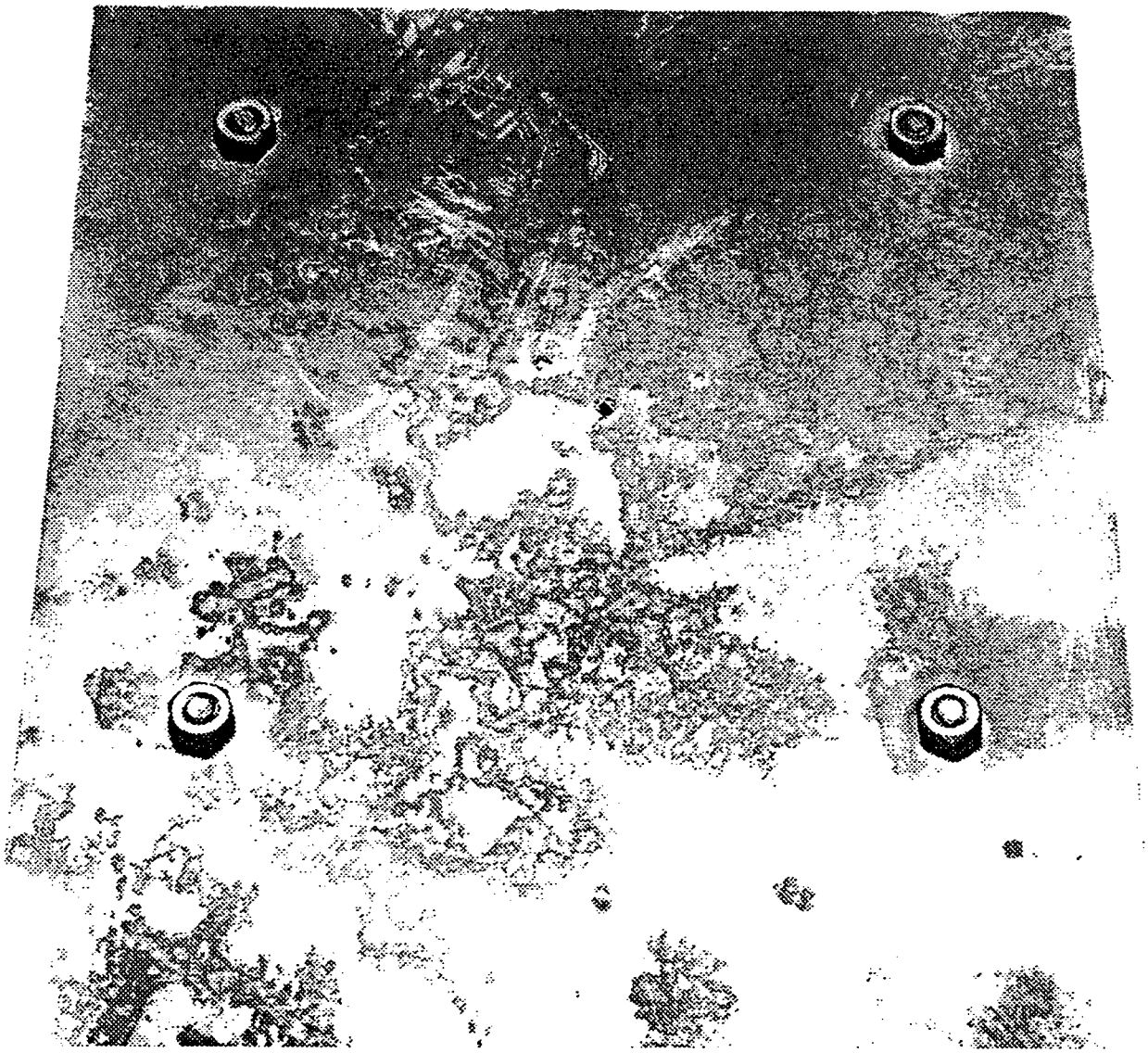

Fig. 3-17 Oblique impact rear wall damage (back side) due to a fragment normal to the bumper. The fragment was likely bumper material. (same as Fig 3-15)

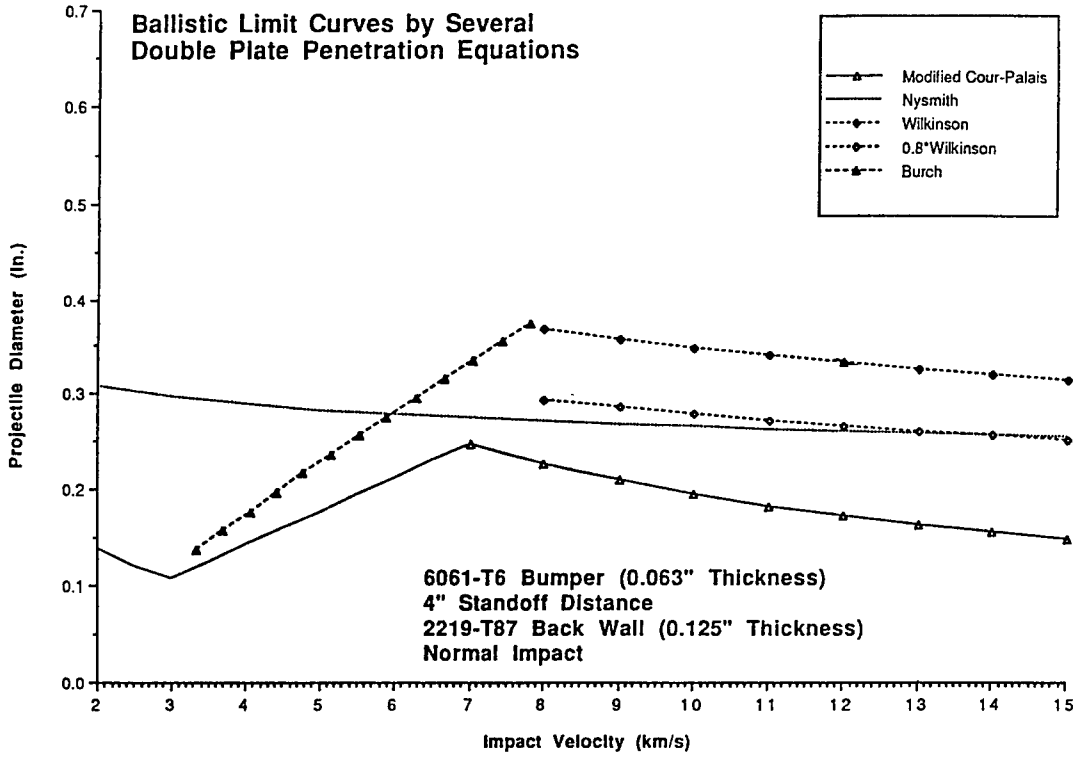


Fig. 3-18 Comparison of high velocity penetration equations. [Hayashida95]

# 4 PROBABILITY ANALYSIS

The probability analysis approach is based on the use of the BUMPERII [Graves] and SD_SURF [Elfer 92] computer codes. These computer code integrate the probability of no penetration (PNP) on a faceted spacecraft model. The programs work with an earth oriented spacecraft in low earth orbit . The codes do the bookkeeping on the spacecraft geometry, ballistic limit and meteoroid and debris flux. A separate analysis of the environment and impact probabilities was developed by Klindrad and Jehn.[92]*

These codes are very useful in doing sensitivity analyses for assumed variations in the ballistic limit surface, spacecraft design or operation, or the environment definition. The particulars of many parts of the analysis are subject to debate, and it is important to understand the effect on the overall PNP to put their significance into perspective.

## 4.1 Probability of No Impact

The traditional analysis is based on a the Poisson distribution for a probability, P, of zero impacts:

$$P = (F \times A \times T)n \quad \times \exp(- F \times A \times T) / n!$$

where F is the flux, A is the exposure area, n is the number of impacts, and t is time, all in consistent units. The simplest approach is to use the total surface area of the space craft, or the area of a simple shape which envelopes the spacecraft. Given the area, the design lifetime, and the required reliability, a flux can be determined and from that a particle size can be determined which has that probability of no impact. If this size can be stopped by the basic structure at all velocities and obliquities, then the requirement has been met.

## 4.2 Probability of No Penetration

If the design is driven by the penetration resistance, then a proper weighting of probable velocities and obliquities must be done. For a spacecraft with a fixed orientation relative to the earth, a more accurate calculation is possible. The space debris and meteoroid threats can be broken down into streams of flux from different directions, *i*, at specific velocities. The diameter to penetrate every area on the spacecraft is determined for each stream element (reference the ballistic limit surface in

Fig. 3-2). The flux for each diameter is determined from the $N_r$ relationship shown in Fig. 2-1 or 2-2 and then multiplied by the fraction of the flux, $f_i$, in each stream as adapted from Fig.2-3.

The probability of no penetration (PNP) from each direction and for each element is based on the Poisson distribution for zero events:

$$PNP_{el} = \exp\left(- \sum_{i=1}^{nthreats} (N_i \cdot A_i) \cdot t\right)$$

where (with consistent units)

$N_i$ = flux which penetrates from each threat direction, $i$.
= $4 \cdot f_i \cdot N_r(d_i)$

$N_r$ = flux on a randomly tumbling plate of diameter $d_i$ or larger. (As defined in the specifications.)

$d_i$ = diameter to penetrate at the velocity and obliquity of the $i$th threat.

$f_i$ = fraction of flux from threat direction

$A_i$ = projected area of the facet in the flux direction.

$t$ = exposure time.

The total PNP is determined by the product of the PNP for each element.

$$PNP_{total} = \prod_{j=1}^{nelements} PNP_j$$

## 4.3 Probability of No Critical Damage

The probability on no critical damage (PNCD) is determined in the same way as PNP, except that the projectile diameter to cause critical damage is used instead of the diameter to penetrate. Williamsen has performed a complete analysis for crew loss due to debris impact. [Williamsen94] Critical damage to a module can result from:

- a hole size that leads to too rapid depressurization of a module.
- a crack that will propagate due to structural loads (catastrophic rupture of a module) as shown in Fig. 1-1.
- damage to a critical system.

For these definitions, the particle to cause this damage will generally be larger than the ballistic limit. For some other design considerations, critical damage could occur for a non-penetrating particle. This could

include deformation, cratering or spall on a critical component before penetration occurs.

## 4.4 Probability Analysis Codes

The BUMPERII computer code may be used alone or in combination with SD_SURF to analyze a spacecraft's PNP (or PNCD). [Graves91, Elfer 92] BUMPERII can show threat contours on the spacecraft geometry model. The threat contours can be generated by BUMPERII to show which areas of the spacecraft are most responsible for reducing the PNP. SD_SURF works alone or with BUMPERII to calculate PNP and to show which impact velocities and obliquities are most responsible for reducing the PNP. Figure 4-1 shows the results of a SD_SURF analysis.

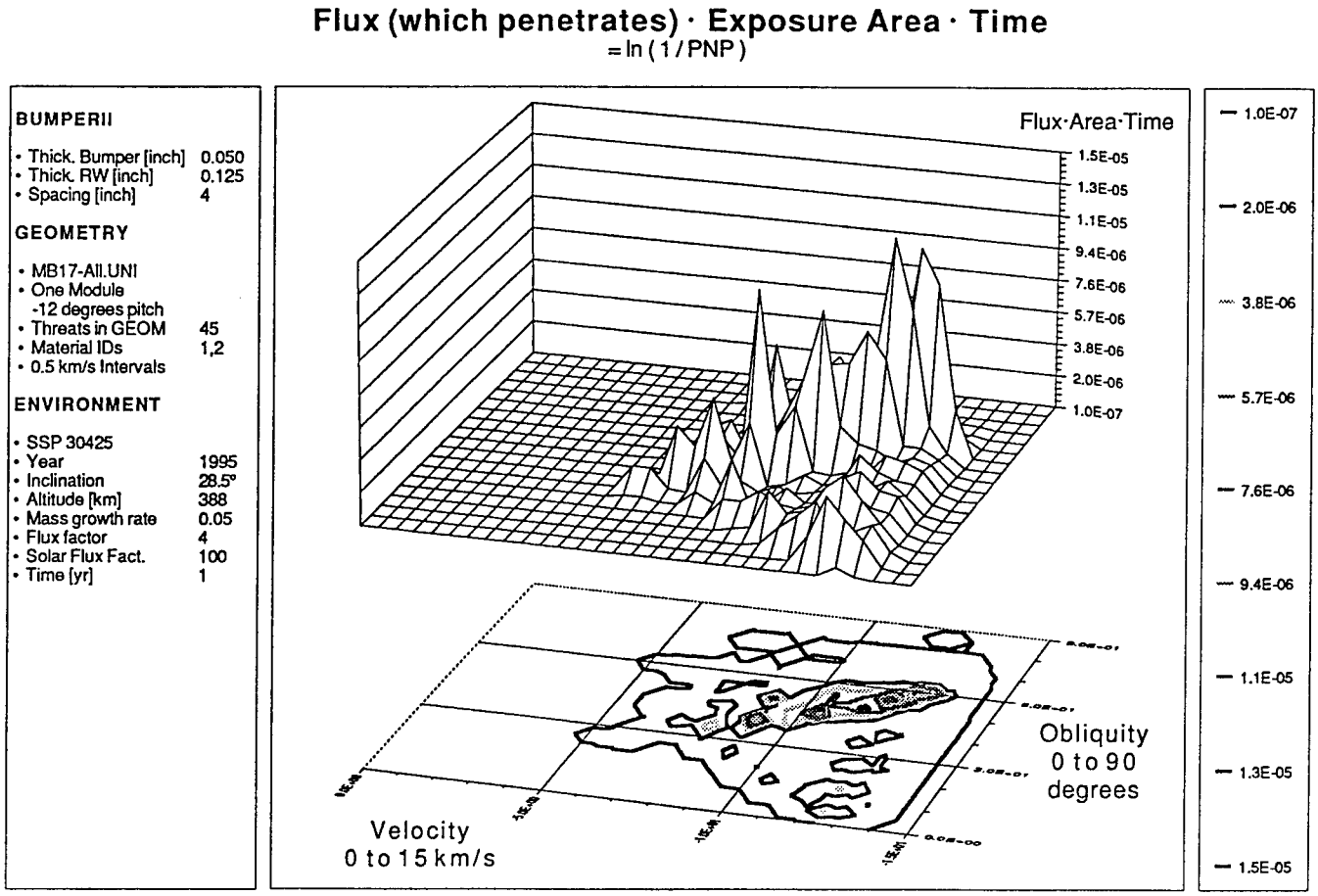


Flux of Penetrating Debris vs. Impact Velocity and Obliquity

Fig. 4-1 Flux times the exposed area times the exposure time versus velocity and obliquity from SD_SURF.

# 5 ADVANCED SHIELD CONCEPTS

Advanced shields have been designed using a variety of intermediate shields and customized geometries. Intermediate shields have several important roles:

- Shock fragments.
- Catch fragments.
- Reduce debris cloud velocity by adding mass.
- Reduce debris cloud momentum (depending on support structure).
- Reduce momentum multiplication (rebound or cratering) on the rear wall.

## 5.1 Bumper Material Selection

Swift [70, 82] came to the conclusion that the bumper material should have the same density as the projectile to be shattered. Lower density was not sufficient, and higher densities (especially with higher melting temperatures) tended to cause rear wall failure from bumper fragments.

It is of interest to compare the ballistic limit of single sheets of aluminum and steel. For the same impacting projectile the volume of material removed is much larger in aluminum. However, the lower density is an advantage in preventing perforation. If equal weights of steel and aluminum are equally effective bumpers for a large design projectile, then aluminum is the better choice for a bumper for spacecraft applications, because it will not be penetrated as frequently as the steel bumper. Hence the thermal insulation layers beneath the bumper and the rear wall will suffer less degradation from micrometeoroids which will certainly impact the spacecraft.

Low density fiber resin composites have been shown to be less effective in fragmenting aluminum projectile than aluminum bumpers. [Christiansen87, Elfer87, ESA] However, the fiber composites do not create fragments that can penetrate the rear wall. This feature makes them extremely attractive for protection against icy meteoroids, which would be expected to vaporize. Also, if composites could deflect debris projectiles at high obliquities, then composites would be better than monolithic aluminum bumpers which generate penetrating fragments.

Ceramic plates can be effective bumpers, but multi-impact capability is limited and they need to be supported to avoid completely shattering.

Christiansen [87] showed that an equal weight of an alumina-boro-silica ceramic cloth (tradename Nextel) should shock the projectile to higher

pressures and temperatures than an aluminum bumper. However, a cloth can have a lower apparent density and is best used as an intermediate shield in an advanced shield system.

Metal matrix and ceramic matrix composites appear to be marginally better than monolithic aluminum bumpers as debris bumpers [McGill92] but a more complete analysis is necessary to quantify the benefit. Again, the effects on numerous non-critical meteoroid impacts needs to be evaluated.

## 5.2 Multiple Bumpers

Intermediate shields may further shock the fragments, thereby increasing fragment temperature, reducing fragment size, and increasing the debris cloud dispersion angle. This is similar to the performance of the bumper as discussed previously.

The use of multiple bumpers can significantly improve penetration resistance compared to a single bumper with the same total weight as shown in Fig. 5-1. The repeated impacts do a better job by fragmenting and raising the temperature of the initial impact fragments.[Richardson, Cour-Palais89,-91] Figure 5-1 shows that for an overall 12 inch spacing, and 0.125" 2219-T87 rear wall, a 0.5" diameter 6061 projectile was stopped by 3 bumpers of 0.040" Al, each 4 inches apart. The rear wall was coated with molten aluminum. However, in a similar test, penetration occurred both for a single 0.125" bumper, and for six 0.020" bumper with 2" spacing between the sheets.

Multiple bumpers can be more effective at shattering the projectile, but they do not tend to spread the momentum over as large an area as a thicker single bumper with the same areal density. Therefore a larger standoff distance is required to resist momentum failure. Christiansen's equations for the mesh double bumper versus multi-shock bumpers tend to bear this out.

Figure 5-2 shows the results at MSFC for two equal weight bumpers. The total spacing was restricted in this example. The second bumper performed best when close to the front bumper to provide a better dispersion of fragments on the rear wall. However, the Richardson multiple bumper was more effective when the second bumper was about 20% of the thickness of the first bumper and places just above the rear wall.

Multiple bumpers appear to be very effective means of building up the performance of a spacecraft on orbit. An initial low weigh configuration can be flown, and as the environment increases, successive layers, with greater standoff can be added.

## 5.3 Intermediate Catcher Shields

Intermediate shields may catch fragments. While the net momentum that impinges on the rear wall is not decreased, the mass is increased and the velocity is decreased. The benefit is illustrated in Fig. 5-3.

The intermediate shield will also affect rebound and momentum multiplication on the rear wall. If fragments impact the rear wall, cratering may occur that causes momentum multiplication. Cratering can eject more momentum than the momentum of the initial fragment. Even if cratering does not occur, elastic rebound from the rear wall can double the momentum transferred to the rear wall.

The impact of the cloth intermediate shield on the rear wall will not increase the momentum of the rear wall significantly over the initial projectile momentum. The bumper was often bulged out away from the intermediate shield after impact. The bulge was not as significant as rear wall bulges, even though the bumper was always thinner. The bulge may be due to impact of the debris cloud with the intermediate shield or rebound of the intermediate shield from the rear wall. Whatever the cause, limited bumper deformation is evidence of a contribution of some small fraction of the initial momentum to the rear wall. Momentum doubling at the rear wall does not occur.

### 5.3.1 Catcher materials

As an intermediate debris cloud catcher, Kevlar cloth was found to be very weight efficient in preventing cratering of the rear wall from impact velocities at 5 to 7 km/s.[Elfer 88] This is illustrated in Fig. 5-3. In one test program, Spectra 900 cloth was not as effective as Kevlar cloth.[Elfer 88] This is probably due to differences in the thermal properties of the materials. Other test programs have shown Spectra to be as effective as Kevlar even though melting of the fibers was obvious.[Christensen92] This emphasizes the need for accurate material properties as well as penetration models for extrapolation beyond test velocity.

Considering its outstanding performance in multi-shock shields, Nextel is expected to be as good or better than Kevlar as an intermediate shield catcher material. However, Christiansen's sizing equations (Appendix A) for Mesh Double-Bumpers indicate that up to 50% higher areal density is required for Nextel catcher layers, compared to Spectra or Kevlar catcher layers. Nextel also has a design advantage in that it is more stable than Kevlar or Spectra, which will degrade from exposure to either atomic oxygen or UV.

### 5.3.2 Impregnated Catcher materials

It should be noted that there are potential contamination issues associated with Nextel fibers breaking off. This may be true of any blanket material. Impregnation may control fiber loss. Impregnation materials should not be too stiff and have relatively weak interfacial bonds with the fibers so as not to affect ballistic performance.

Elfer found that in nominally identical tests, a monolithic Kevlar-Epoxy intermediate shield allowed rear wall failure while an equivalent weight of Kevlar cloth did not cause rear wall failure. In normal ballistic testing dry Kevlar fabric can outperform due to ability of fibers to slip and stretch. However, there was no apparent difference in cratering of the rear wall, and it was suspected that the difference in elastic rebound from the rear wall caused a different momentum multiplication.

Another problem with epoxy composites is that if the catcher is stiff, then the acoustic environment of launch must be considered. This can present severe design constraints that are not applicable to a flexible cloth catcher.

Teflon impregnated beta cloth may also have an added benefit beyond just mechanically catching projectile fragments. The Teflon can chemically react with the fragments to promote further reduction in fragment size. It is not known whether this is a significant contribution to penetration resistance but it warrants further investigation as a possible means of enhancing penetration resistance.

### 5.3.3 Catcher Location

The location of the cloth was shown to be critical to effective performance. If the cloth was against the bumper, fragments would overwhelm the cloth; too close to the rear wall and the momentum could not be transferred to the cloth. The momentum transfer to the cloth is necessary for higher mass and lower velocity than the initial debris cloud so that the rear wall will not spall. Christiansen suggested that the catcher be four projectile diameters from the rear wall.

Momentum absorption by the cloth was negligible due to tearing of the cloth. A six inch square of material was just as effective as a 12 inch square fixed on the edges. After the impact the cloth was shredded but remained fluffed up in the same location. The shreds of the cloth could be a significant enhancement for multi-hit capability.

## 5.4 Analysis of Advanced Shield Designs

Determination of the ballistic limit surface of advanced shield designs has depended more on empirical data and less on modeling capability. Momentum failure is discussed in greater detail in Sec. 6.

Test data is the best method of anchoring the Wilkinson momentum failure analysis. If tests cannot generate a momentum failure it would be conservative to use just the outer bumper and the total standoff to predict the dispersion angle for failure. This assumes that the intermediate layers only reduce fragment penetration and do not contribute to dispersing the momentum. An alternative approach was used by Elfer: an effective bumper was assumed to be equal to the total thickness of the two bumpers and at a standoff two thirds of the distance from the front bumper to the second bumper. The areal density is expected to be conservative, and the reduced standoff (rather than just using the standoff distance to the front bumper) was an estimate believed to be adequate to describe the reduce area of the spray.

Figure 5-4 shows the benefit of adding multiple bumpers and catchers. The bumper and catcher configuration used in Fig. 1-1 was repeated 3 times and was able to prevent penetration for the same projectile as used in Fig. 1-1.

## 5.5 Geometric Bumper Shapes

Christiansen [92] noted that mesh bumpers are effective in breaking up projectiles at 3 to 5 km/s. However, it was only effective in combination with a second bumper plate to further shock the fragments. Along a similar vein, a geometric disrupter was developed by Martin Marietta, the University of Dayton Research Institute (UDRI), and Kaman Sciences. UDRI succeeded in rolling a plate into a hexagonal ribbed configuration, similar to side-by-side wires. An oblique impact at greater than six km/s did not show it to be significantly different than a homogeneous bumper sheet in preventing rear wall penetration and no further testing was performed.

A faceted or corrugated bumper may be useful in turning an oblique impact into a locally normal impact. The facets should probably be on the order of one-half to one times the anticipated projectile diameter. While this increases the surface area of the bumper, the bumper may be so much more effective that the overall weight requirement could be reduced. However, to effectively use this concept, the relationship of the facets to debris would have to be thoroughly modeled for all spacecraft orientations.

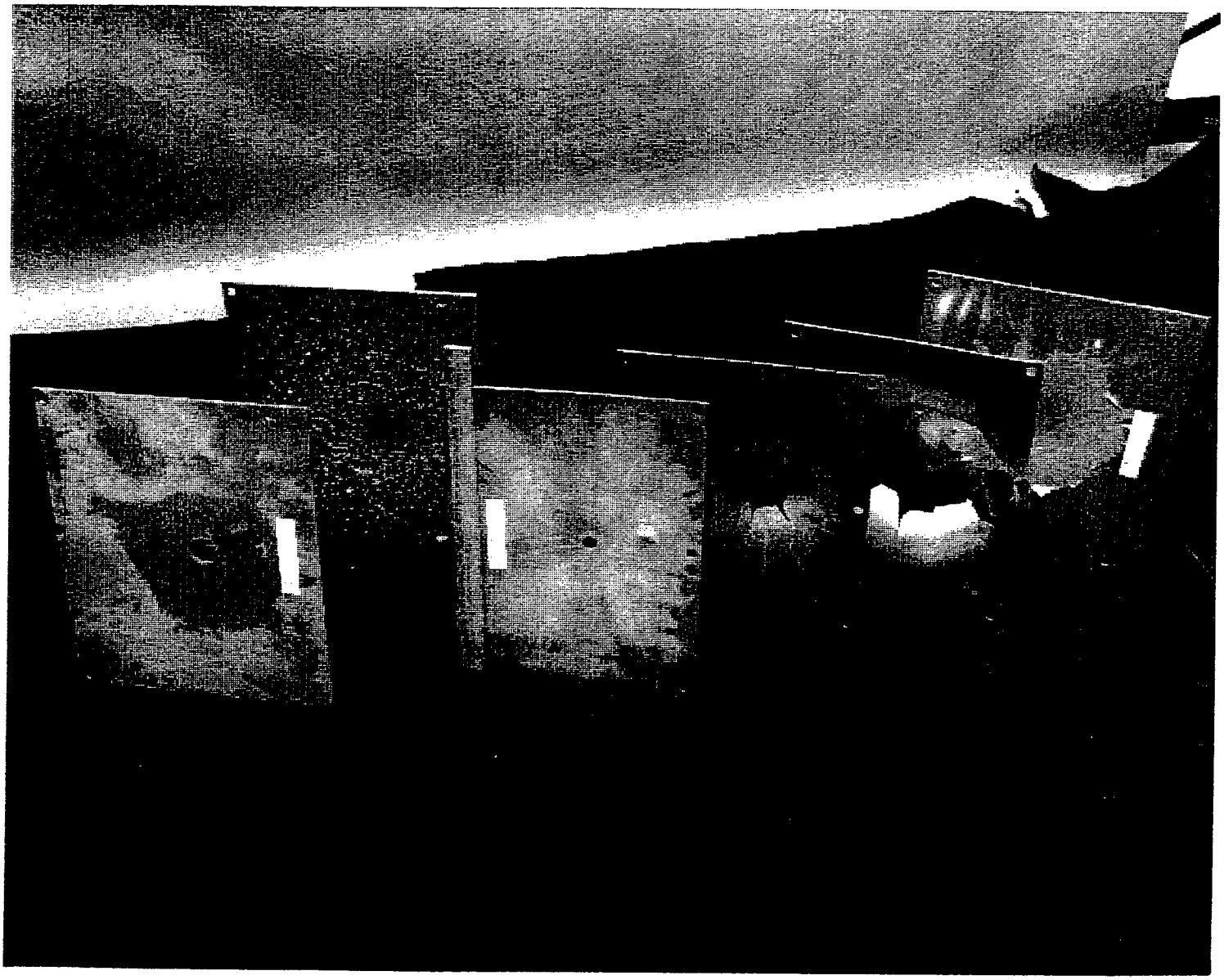

Fig. 5-1 Multi-shock aluminum bumper compared to Whipple bumper (Fig. 3-3). MSFC tests. [Elfer88]

# Double Bumper System

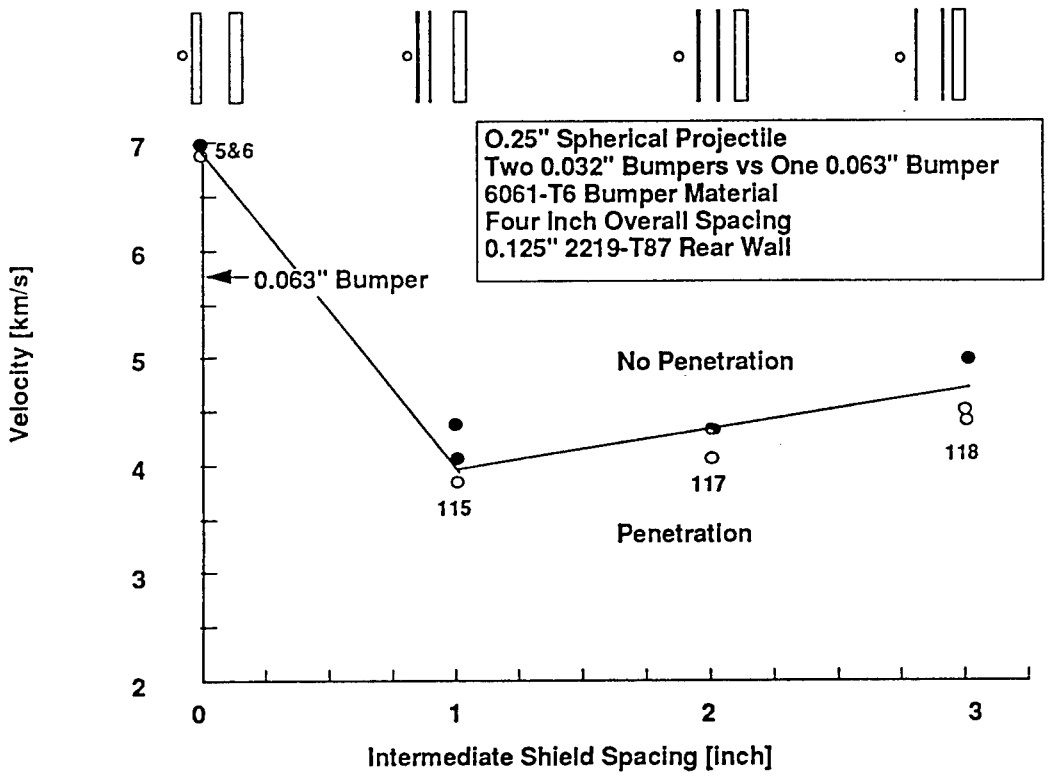


Fig. 5-2 Double bumper (equal weight) test results. MSFC tests. [Elfer88]

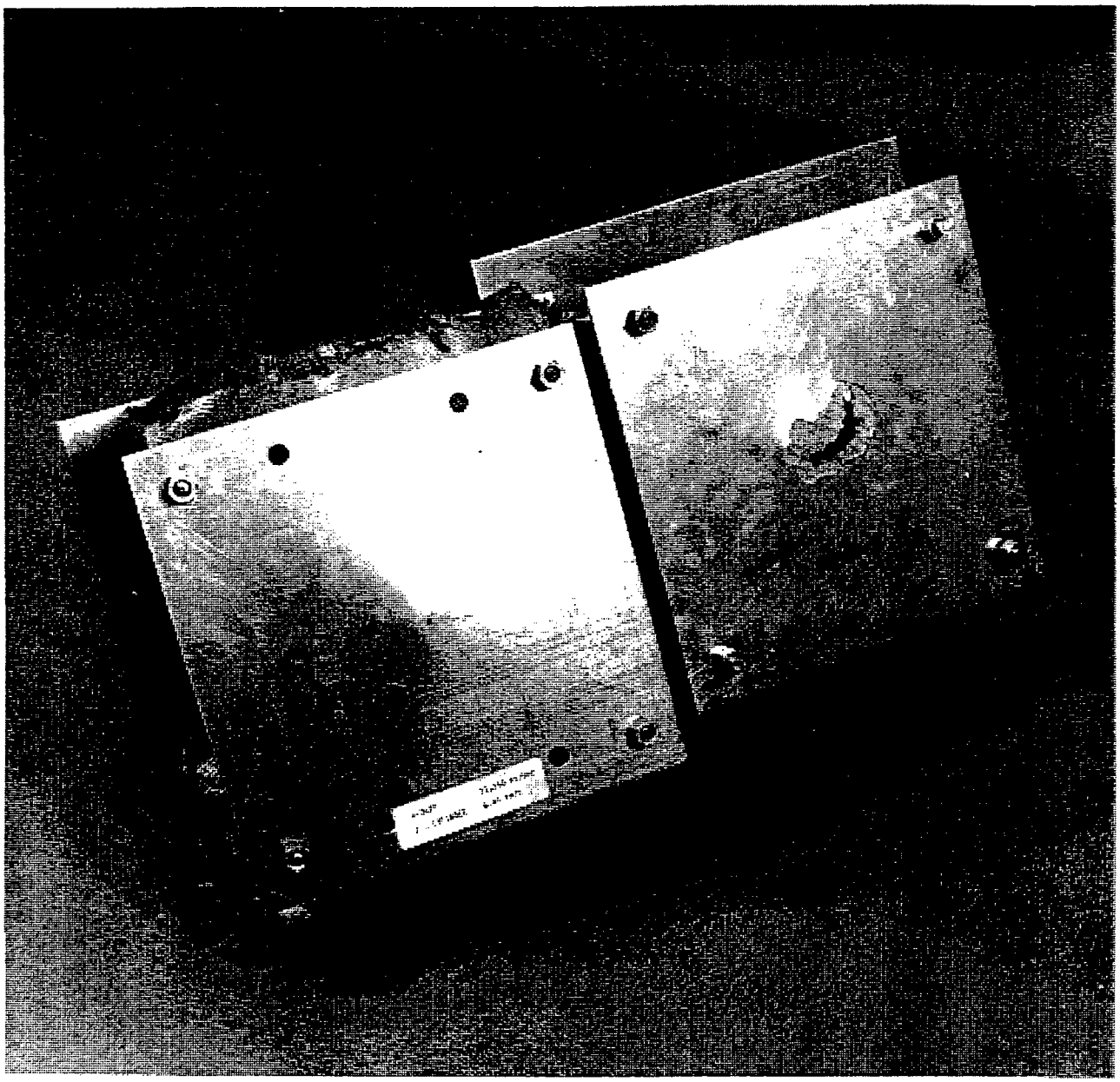

Fig. 5-3 Kevlar cloth intermediate shield (catcher) UDRI tests. Same designs as Fig. 1-1, with (no penetration) and without Kevlar 29 cloth (penetration) for a 1 gram projectile. [Elfer88]

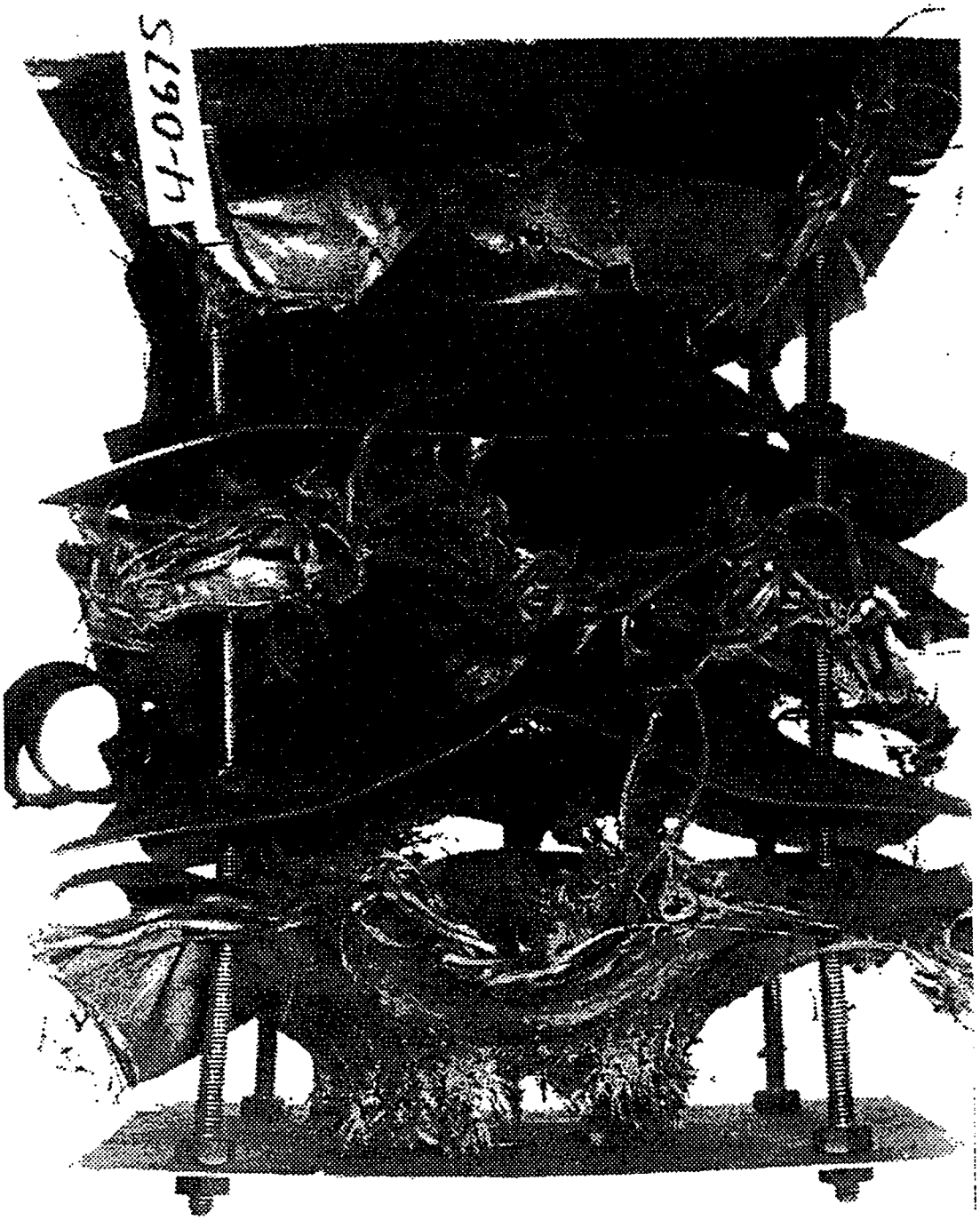


Fig. 5-4 Multiple layers of aluminum bumper and Kevlar cloth can prevent penetration for the same conditions as Fig. 1-1. (UDRI 4-0675)[Elfer88]

# 6 DEFORMATION ANALYSIS

## 6.1 Bulge Deformation Analysis

Figures 6-1 and 6-2 show rear wall bulge for 2219-T87 and 2219-T62 for 1 g and 1.27 g projectiles respectively, at 6.4+ km/s.

The starting point of the analysis is an assumed distribution of momentum on the rear wall. The assumed distribution in both time and position can have a large influence on rear wall failure.

The Christiansen equations for multi-shock shields and mesh-double-bumpers (Appendix A) assume that for velocities greater than 6 km/s, the rear wall will fail for constant projectile momentum normal to the wall. The equation assumes that the allowable momentum is proportional to $1/S^2$. Note that oblique effects are only assumed in the normal component of velocity, while any beneficial effect on the effective spacing, S, is conservatively ignored. The equation also includes a yield strength term to account for different rear wall materials, but tests and analysis, in the following sections, show that rear wall ductility have a larger influence, and should be included in a general penetration equation.

For velocities greater than 6 km/s, the Wilkinson equation for momentum failure has been used successfully for shields with intermediate catchers. (See Fig. 6-2 with next paragraph) This is slightly less conservative than a constant momentum approach, since for a larger t/d ratio there will be a larger dispersion angle. A larger t/d ratio occurs for constant momentum at higher impact velocities.

However, Elfer used Wilkinson's equation with a modified dispersion angle from the original Wilkinson equation. The dispersion angle used was 25% lower than Wilkinson proposed. because the lower angle agrees with rear wall damage, with HULL analysis, (Fig. 6-3) and it also predicts the observed momentum failure in specimens. The lower angle was likely a result of melting of the aluminum particle in the 6 to 8 km/s range, while Wilkinson's analysis was for vaporization at higher impact velocities.

Momentum multiplication occurs in both elastic collisions and cratering events. McMillan assumed elastic rebound of vaporized gas and that the rear wall momentum was twice that of the original projectile. If the debris "sticks" to the rear wall, then the rear wall will be approximately equal to the original projectile. However, if ablation or cratering of the rear wall occur, then the momentum can be up to five times that of the original projectile. Although bumper debris may be spread over too large an area to significantly affect the rear wall loading, the uncertainty associated with

momentum multiplication can mean a factor of two difference in the rear wall thickness to resist penetration.

A general test observation is that the bumper is not deformed as much as the rear wall, even though the bumper is much thinner. See Figures 6-1 and 6-2. Therefore, the momentum in the rear wall probably does not approach the upper limits theoretically possible for even the rebound case. This lends credibility to just using the initial projectile momentum as the starting assumption for rear wall models.

A curve fit to Lagrangian rear wall deformation predictions was generated by Grove and Rajendran to provide an alternate analysis method provided the original Gausian distribution of momentum can be applied. The curve fit is included in Appendix A.

### 6.1.1 Deformation

This type of failure mode leads to large petaled holes, potentially more dangerous than the relatively clean holes produced by fragment penetration.

The analysis of bulging is different than the initial impact analysis. The use of an Lagrangian model is best for late time momentum failure to accurately track deformations and strain. The deformation usually occurs over about 50 to 100 microseconds after the initial impact of the debris cloud on the rear wall. It is impractical to run the Lagrangian models from Eulerian hydrocode input because computer memory and time requirements. This is true for two dimensional calculations much less for three dimensional calculations. Furthermore, the pressure distribution from hydrocode analyses tends to be too jagged, resulting in failure.

Most models of rear wall deformation derive the loading from either simple models of vaporized clouds or assume that the momentum intensity is deposited either uniformly or with a Gausian distribution over some area on the rear wall.

STEALTH and EPIC calculations of rear wall deformation were done at the University of Dayton. [Rajendran] When models of the debris cloud were used to drive the calculation, the stresses exceeded the spall strength by several times. When an intermediate shield is used, the extra mass involved can slow down the impact sufficiently so that spall should not be predicted.

Figure 6-5 shows rear wall deformation models. Thinning can occur at the centerline or also away from the centerline depending on the starting momentum distribution. Figure 6-6 shows measured thinning on two different specimens and it can be seen that the maximum strain can occur

either on or away from the centerline. Figure 6-7 shows Roberts' HULL predicted thinning versus measured thinning. While the absolute agreement is not good, the relative shape of the two curves was judged acceptable. The HULL standard properties for aluminum were used which were low relative to the measured strength of the alloys of interest, and this accounts for the discrepancy. HULL uses a strength of approximately 300 MPa while Rajendran measured a flow stress of 480 MPa for 2219 and 5456 using a split Hopkinson bar tensile test. While the dynamic strength was similar for the two materials, 5456 had 30% elongation compared to 12% for 2219.[Elfer88] The effects of strength and strain were included in Grove's parametric analyses to give a general solution.

Figure 6-8 shows rear wall deformation on two specimens as well as HULL and NASTRAN analyses performed by Roberts. (The 5456 specimen deformation was measured before and after sectioning. There were no residual stress effects.) The HULL analyses again gave the correct qualitative shape, although more analyses would be required to completely match the correct momentum (with rebound), momentum distribution, and material properties. The NASTRAN 3D sheet elements appeared to accentuate the thinning and deformation at the center of the specimen. This was true for 10.16 and 30.48 cm radius pie slices. While the simpler model would be useful for petaling type of analysis, this may be inadequate for accurate simulations.

Groves performed parametric analyses of rear wall deformation using EPIC (similar to the HULL analyses) and fit the results to a dimensionless parameter to predict failure (Appendix A) Figure 6-9 shows the correlation between Groves dimensionless parameter and calculated rear wall strain. [Analysis in Final Report Attachment 7]

## 6.2 Hole Size

The hole size depends on the penetration mechanism that forms the hole and the amount of momentum that remains in the rear wall after the initial penetration. Hole sizes are related to:

- single fragments crater damage (with sizes as little as a crack to leak gas)
- debris cloud diameter, with a hole formed immediately after impact (multiple fragments, spall enhanced penetration, or a shear plug)
- petaled holes larger than the debris cloud diameter. Theses are formed 10s of milliseconds after the wall is penetrated.

There is no lower limit on hole size. A front wall crater may be linked by a minute crack to allow a gas leak. If the hole is created by a fragment,

then bumper holes size equations are appropriate. Larger size holes may be estimated from the debris cloud diameter.

The larger holes, associated with a petaled hole, are the greatest concern for critical damage to a manned module. Notwithstanding, most tests have been designed for penetration resistance testing rather than hole size characterization.

### 6.2.1 Effect of wall thickness on hole size

There appears to be an upper limit on hole size for a given wall design and a given impact velocity. Figure 6-10 shows how petaled hole size varied with rear wall thickness for a series of specimens. Several of the specimens are shown in Fig. 6-10 to 6-17. The specimens were each impacted by a 1.27 cm aluminum projectile with a nominal velocity of 6.4 km/s. Each rear wall was protected by a 0.2 cm thick 6061 aluminum bumper at 11.4 cm and 4 layers of style 710 Kevlar 29 cloth at 5.7 cm.

The exact amount of momentum absorbed by the rear wall is not known. The bumper and Kevlar cloth probably allowed a large central particle to penetrate the rear wall. The remainder of the debris cloud (including Kevlar cloth) imparted some of its momentum to the rear wall. After tearing the rear wall, and giving it an initial momentum, the rest of the debris cloud continued along the shot direction.

The initial velocity was higher for the thinner rear walls, due to their lower mass. Also thinner rear walls, will absorb less momentum from the debris cloud. If the rear wall mass is small relative to the debris cloud mass, the rear wall will attain cloud velocity as it is pushed out of the way.

Figure 6-18 show the rear wall in Fig. 6-13 with the petals bent back in. Note that the impact area is approximately one third the diameter of the final hole size. This would be a good estimate for maximum petaled hole size. Also note that the petals overlap. It is obvious that cracks or tears that make the petals form after the bulging is complete, which is a relatively late time effect.

Measurements of thinning were made on some of the petaled holes to try and compare to the data in Fig. 6-6 and 6-7. However, due to difficulties with craters raising or lowering the thickness measurement, it can only be said the data appeared to be similar. The strain at failure was approximately 11 percent.

### 6.2.2 Effect of increasing the projectile size

Once the hole is "fully developed," further increases in projectile size are not expected to significantly increase the hole size. Most of the additional projectile momentum will go into the central fragments. Any additional

momentum in the cloud will have a smaller effect on rear wall velocity. For the 2219 and 5456 walls described in the previous section, the "fully developed" hole size is approximately 22 centimeters.

### 6.2.3 Tearing of petal ends

Examination of the petals (described in Sec 6.2.1) showed that the tips were torn off some petals. The tip was torn approximately two to five centimeters behind the initial fragment penetration hole. See Fig. 6-17 for a partial tear. The petals with torn tips did not open up as much as the other petals. Some of the momentum to open the petal was lost to the tip. It is not known whether the torn petal tips were related to initial crater damage, to a neck generated early during the initial deformation (before the petal formed), or whether it is a natural consequence of having so much momentum that the tip tears off the end of the petal. If the latter is the case, then this is a mechanism to limit the maximum momentum transferred to the rear wall.

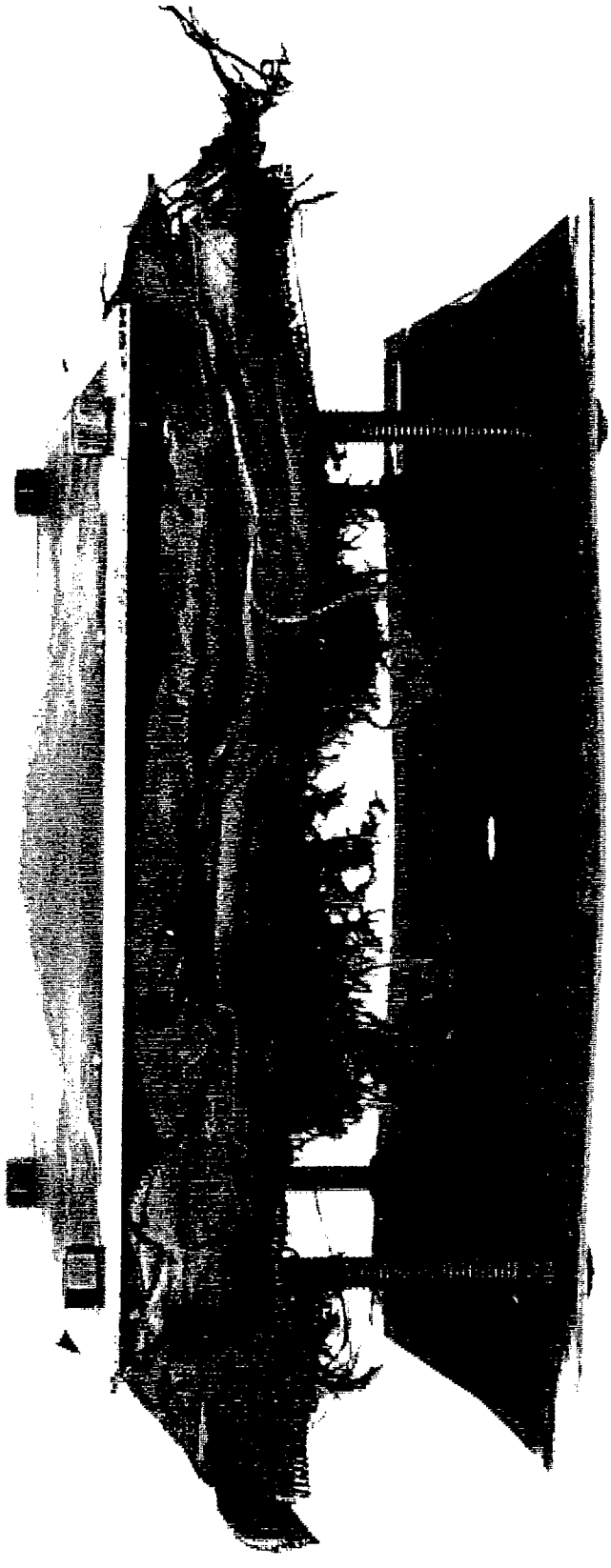

4-0508

Fig. 6-1 Rear wall deformation (same design as Fig. 1-1) 1 gram projectile 6.4 km/s. (UDRI 4-0508) [Elfer]

Fig. 6-2 Rear wall deformation (same design as Fig. 1-1 except -T62 rear wall) 1.3 gram projectile 6.4 km/s. (UDRI 4-0508) [Elfer]

# Standoff Distance with Kevlar

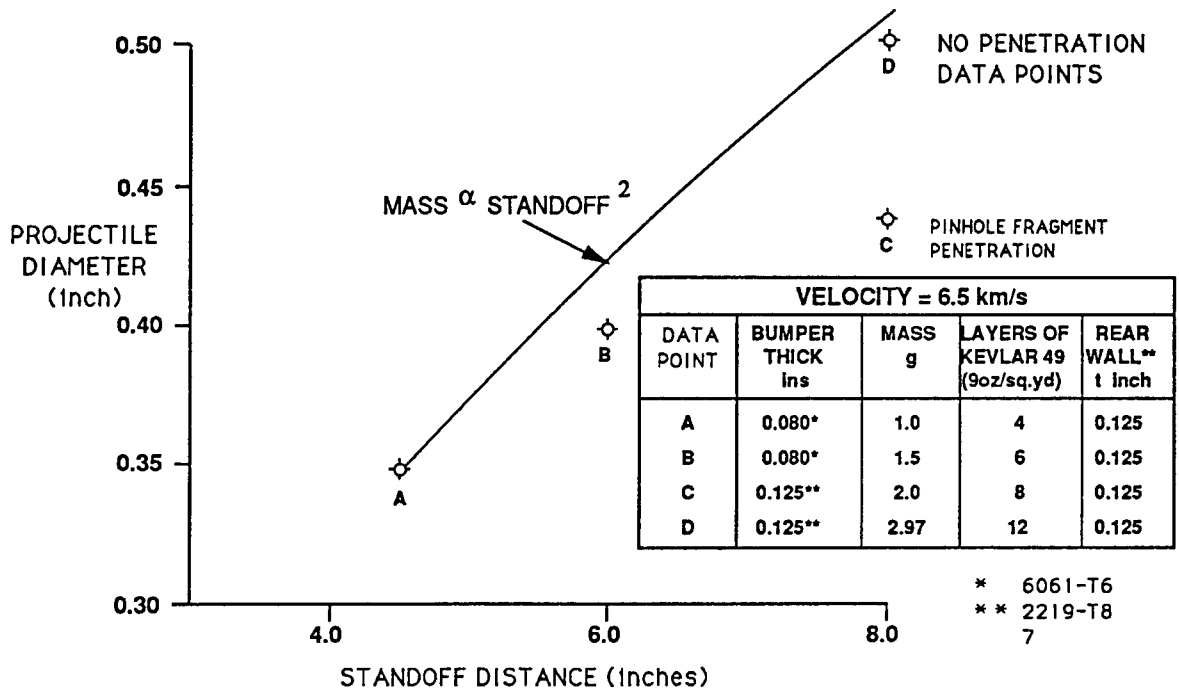


| VELOCITY = 6.5 km/s | | | | |
|---|---|---|---|---|
| DATA POINT | BUMPER THICK ins | MASS g | LAYERS OF KEVLAR 49 (9oz/sq.yd) | REAR WALL** t inch |
| A | 0.080* | 1.0 | 4 | 0.125 |
| B | 0.080* | 1.5 | 6 | 0.125 |
| C | 0.125** | 2.0 | 8 | 0.125 |
| D | 0.125** | 2.97 | 12 | 0.125 |

* 6061-T6
** 2219-T87

Fig. 6-3 Projectile mass for no penetration (or rupture) is proportional to $S^2$ for adequate bumpers and catchers.

# Spray Angle

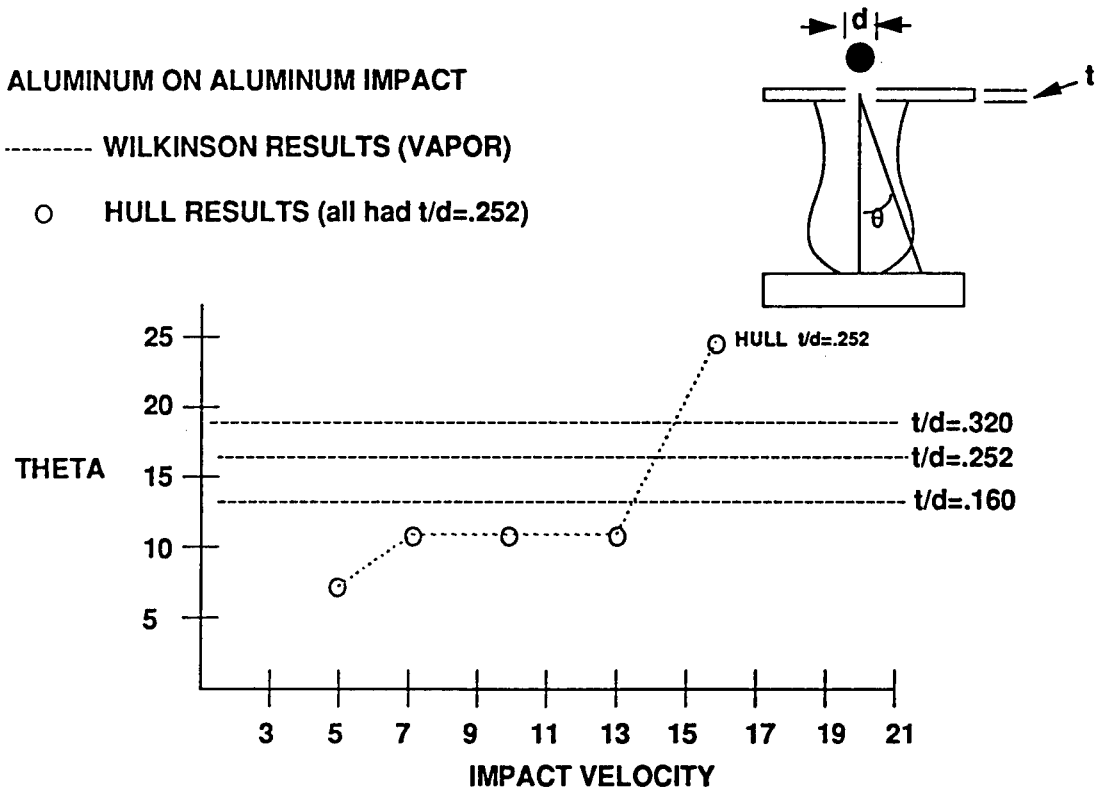


Fig. 6-4 Comparison of debris spray dispersion angle between HULL results and Wilkinson's vaporization equation. Note that HULL results are outer diameter of spray while Wilkinson's dispersion angle is one standard deviation on a Gausian distribution.

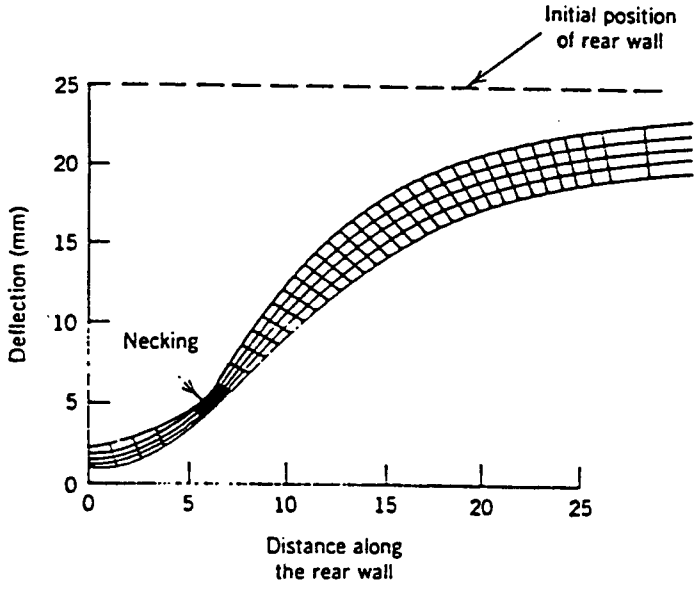


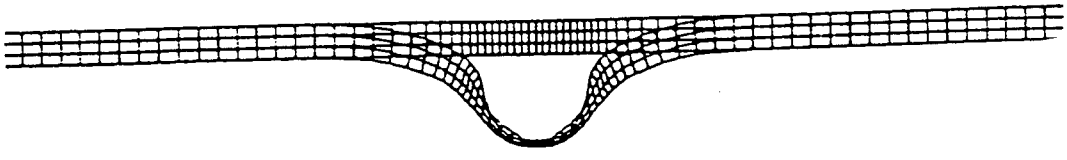

Fig. 6-5 STEALTH models of rear wall deformation.

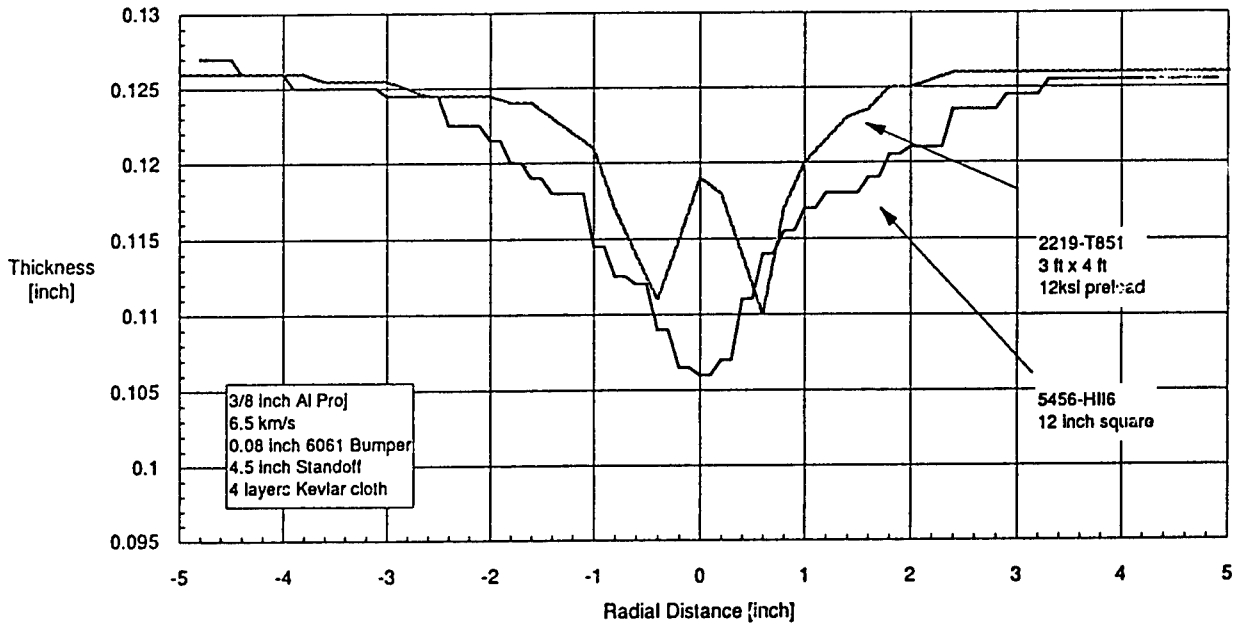


Fig. 6-6 Measured thinning of rear wall. Maximum thinning may occur at the centerline or in a circle away from the centerline.

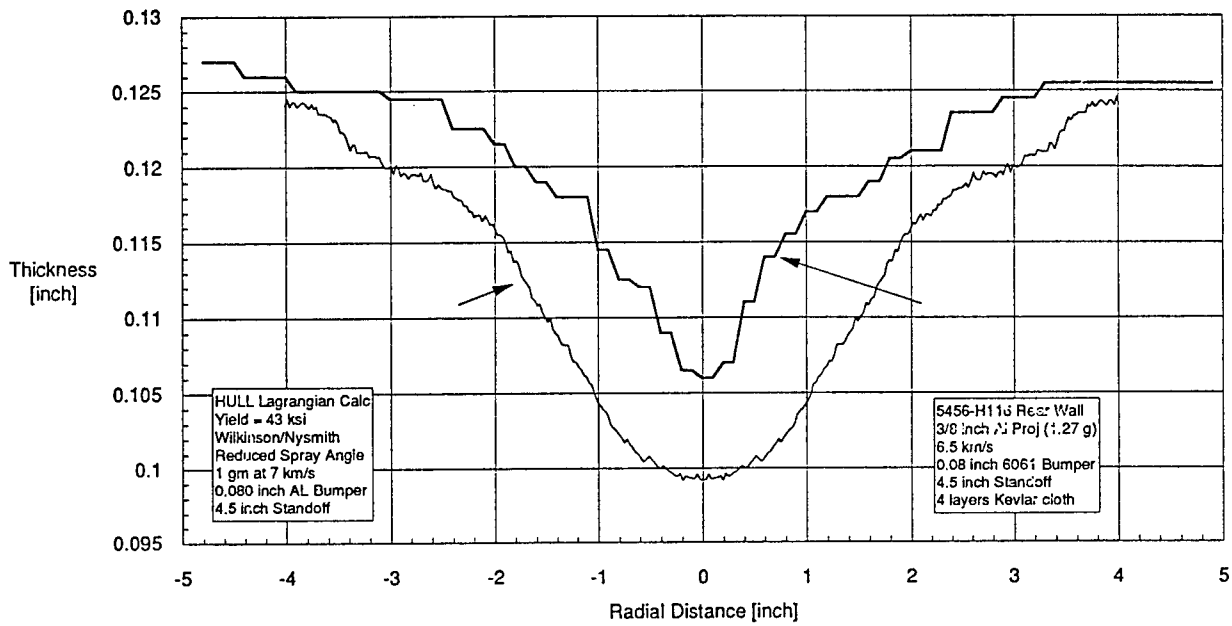


Fig. 6-7 Measured thinning of rear wall compared to a HULL analysis. The low strength in the HULL model ended with more thinning than the test, but the relative shape of the curves was in agreement.

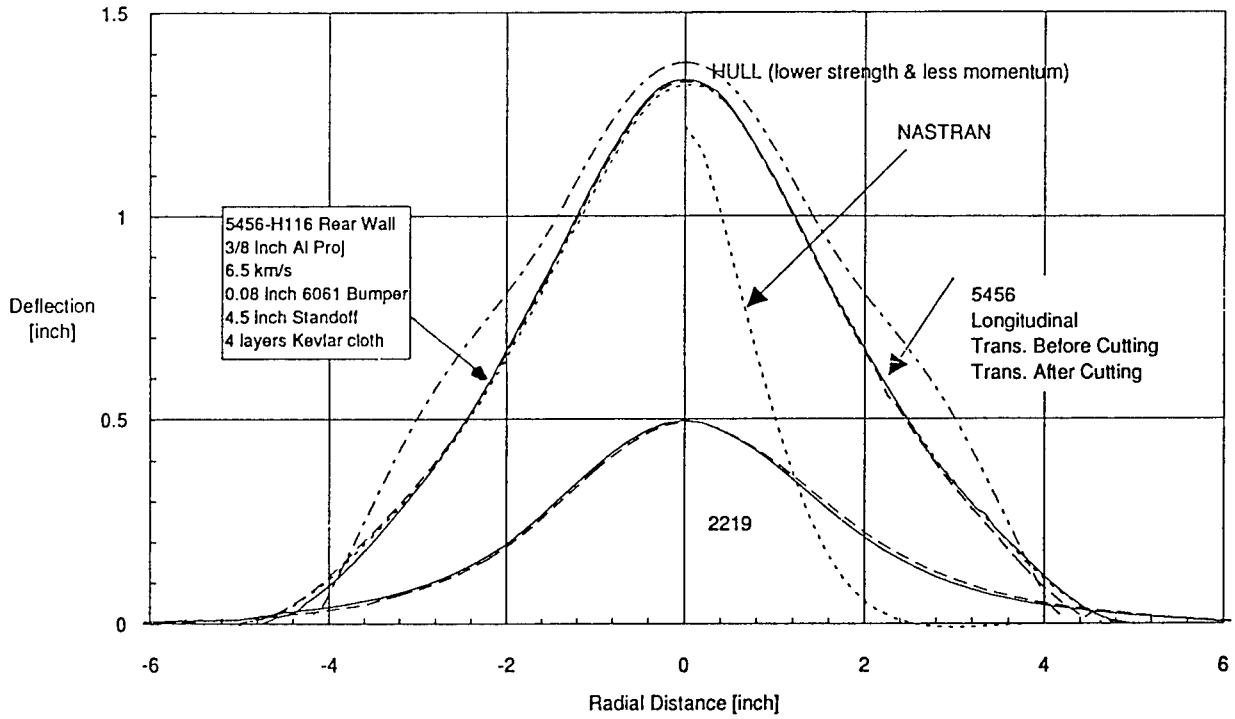


Fig. 6-8 Comparison of measured permanent deformation, HULL analyses and simple NASTRAN sheet element analyses.

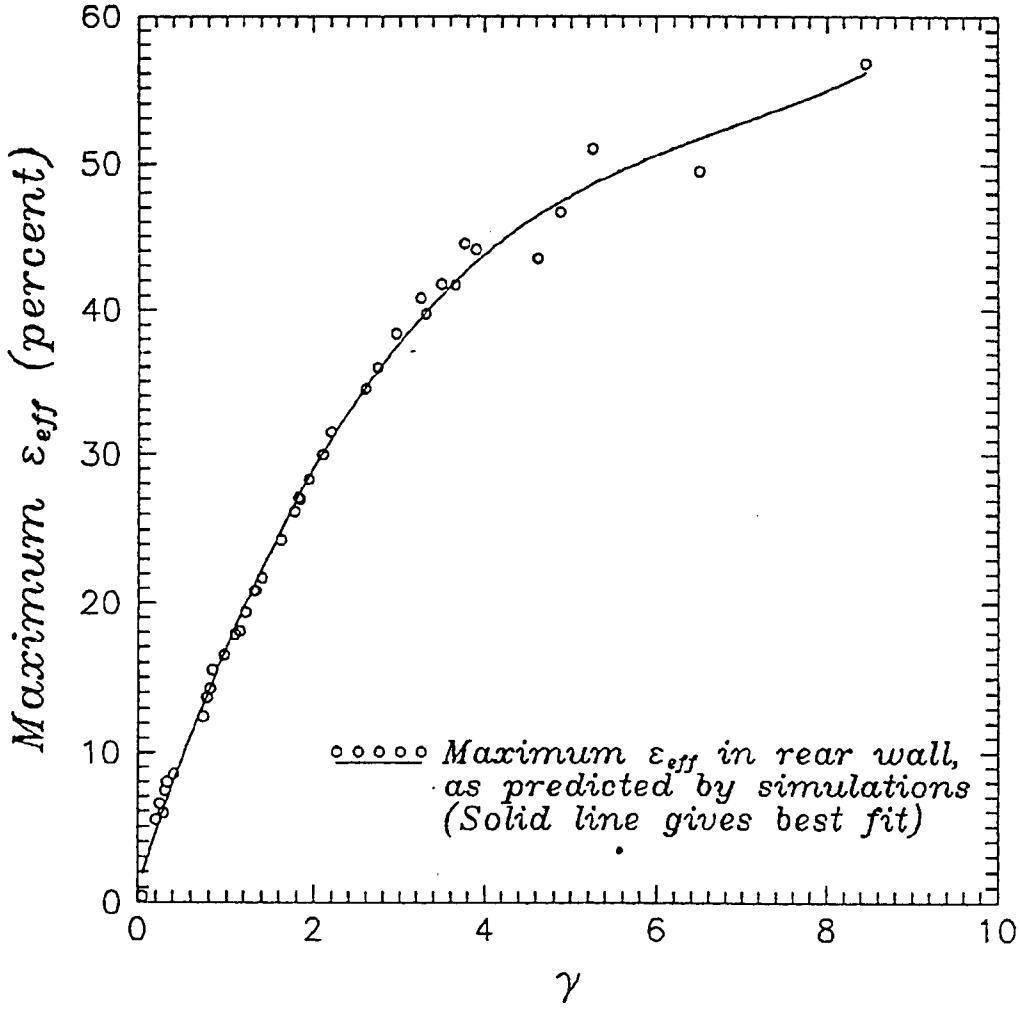


Fig. 6-9 Correlation between maximum effective rear wall strain as predicted by EPIC simulation and Groves dimensionless design parameter.

# STRESSED PANEL DEBRIS TESTS

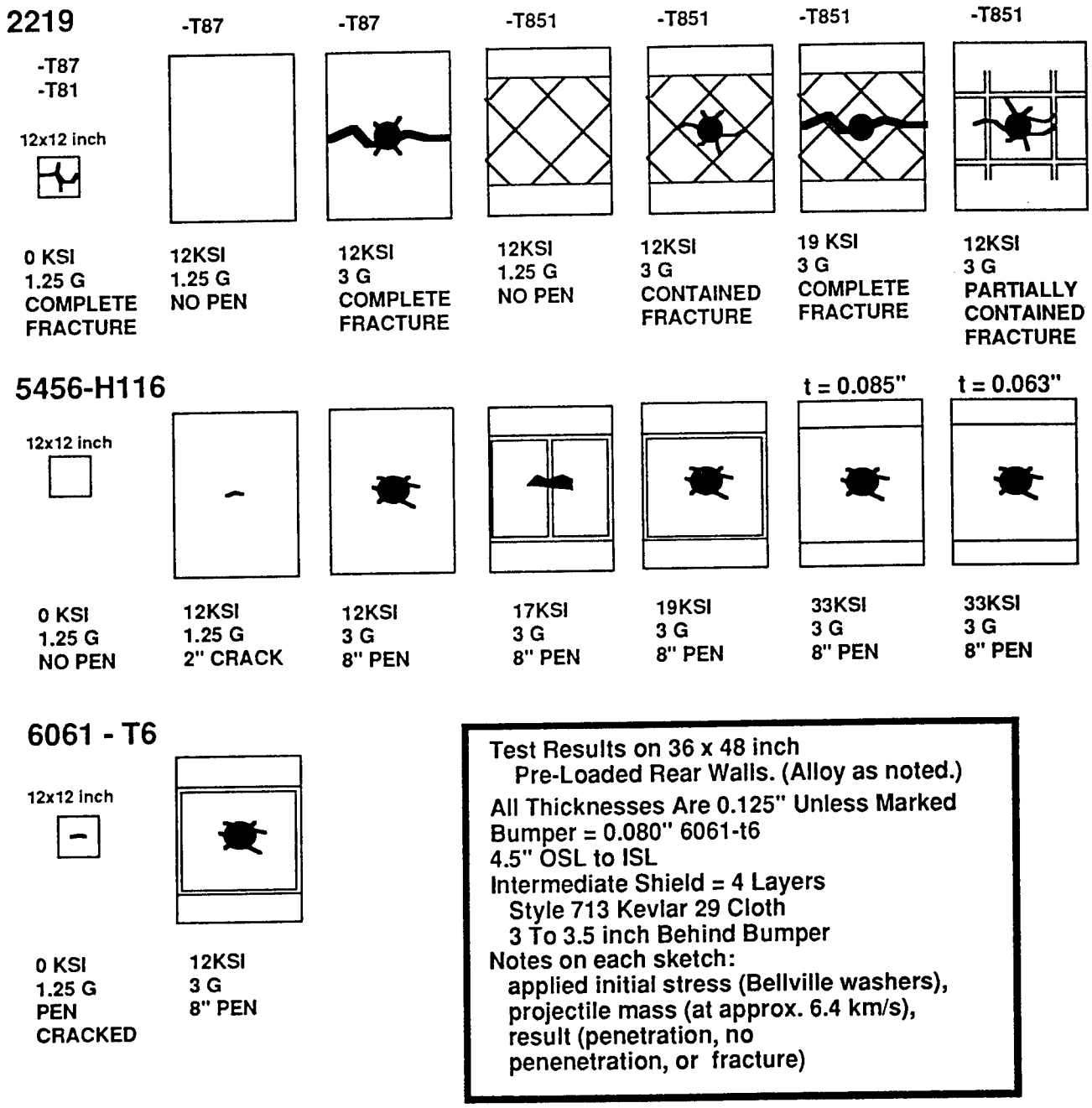


Fig. 6-10 Summary of pre-stressed panel test results. Large panels similar to Fig. 1-1. [Elfer]

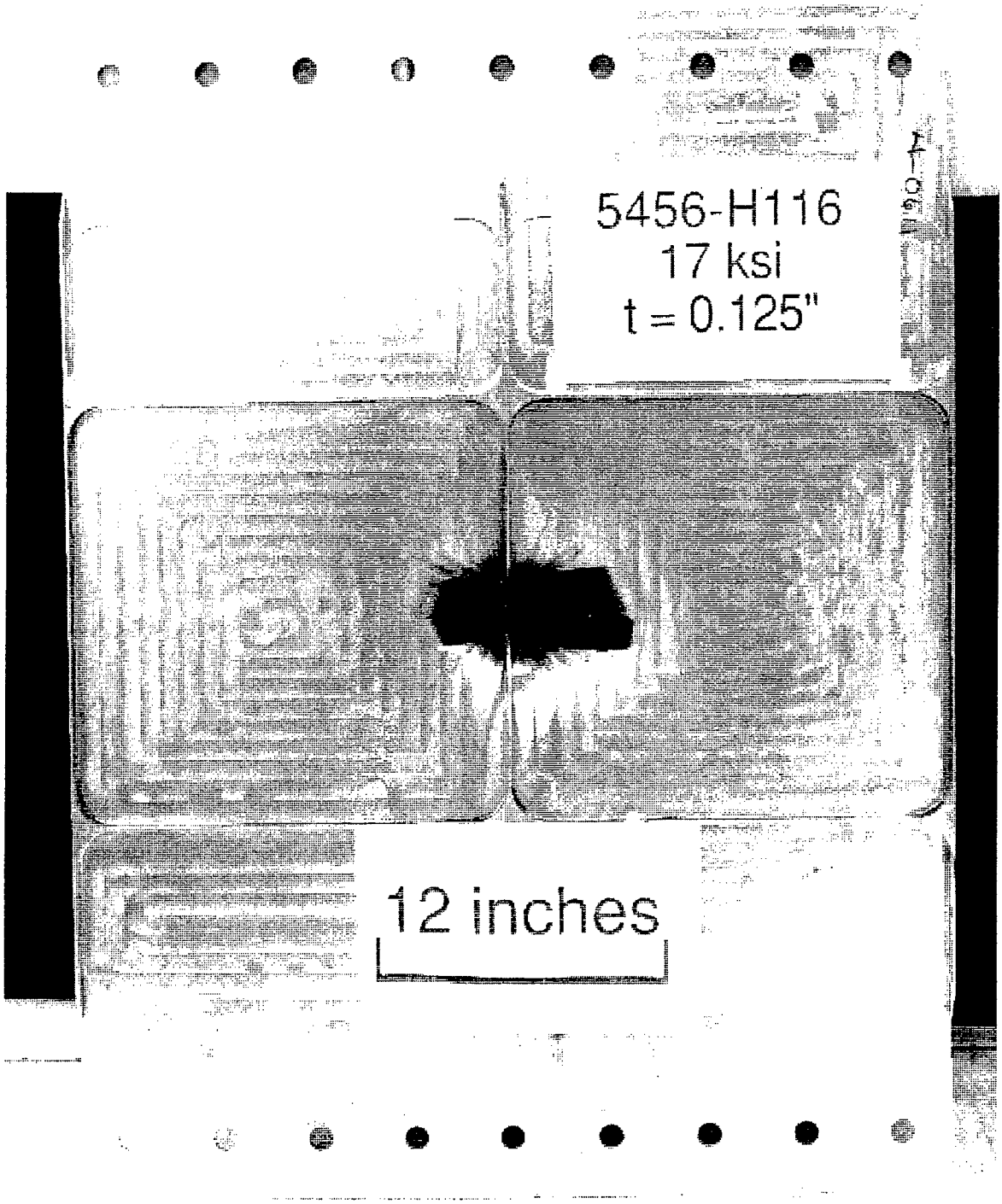


Fig. 6-11 Same as Fig.1-1 except for 5456 rear wall material and impact occurred on a stiffener.

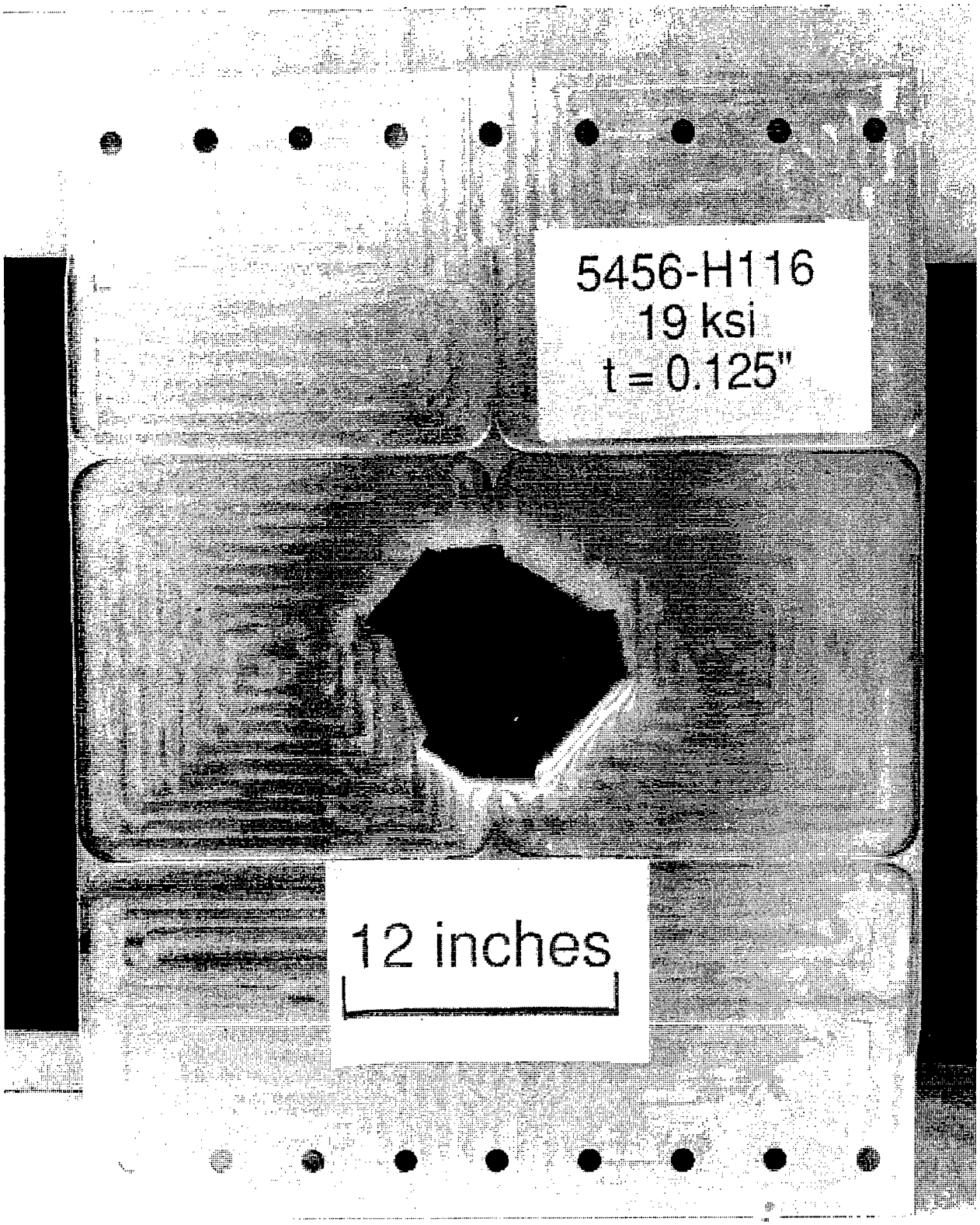


Fig. 6-12 Same as Fig. 6-10 except that stiffener was removed prior to impact.

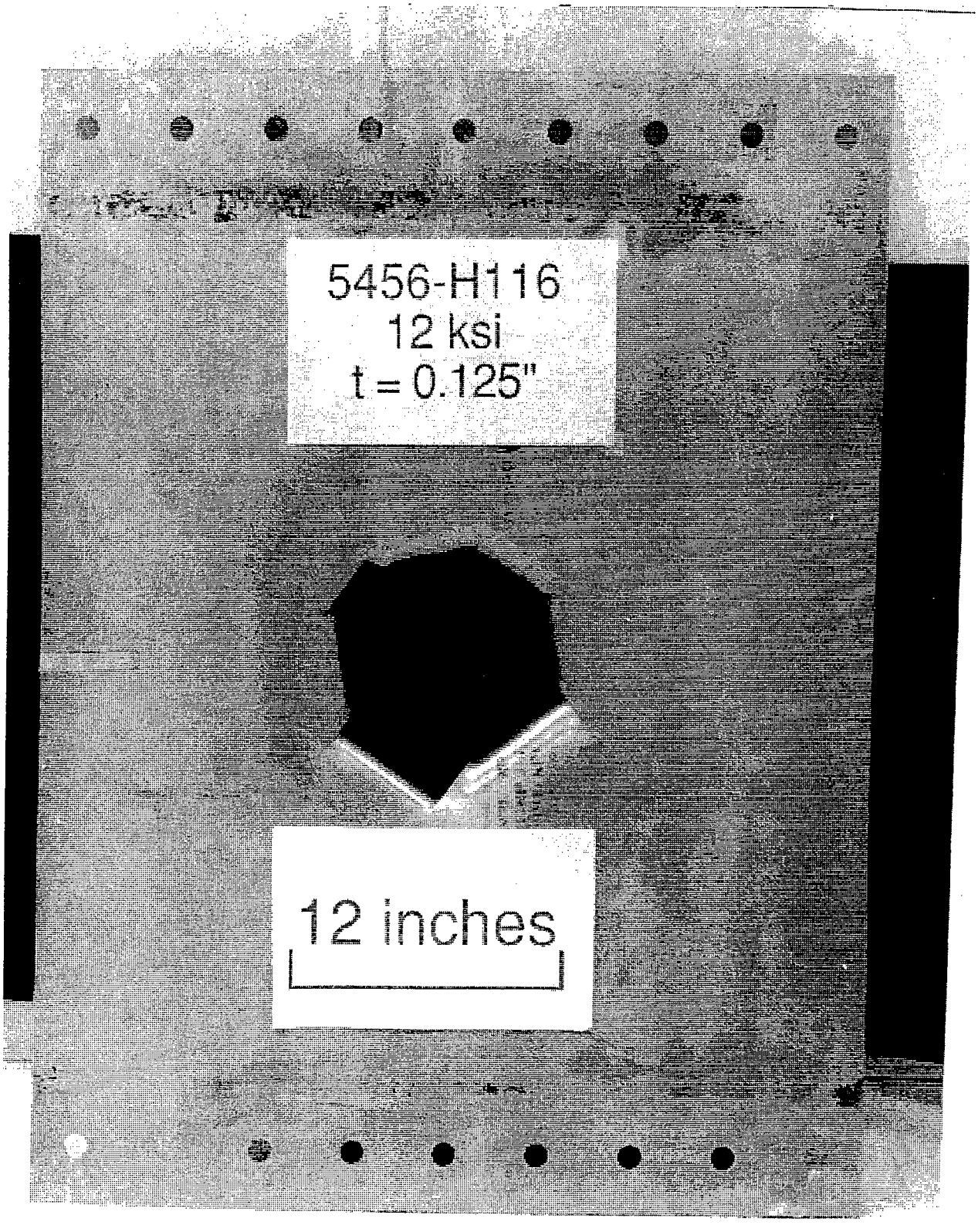


Fig. 6-13 Same as Fig. 6.11 except sheet was used instead of machining plate down to same 1/8 inch thickness.

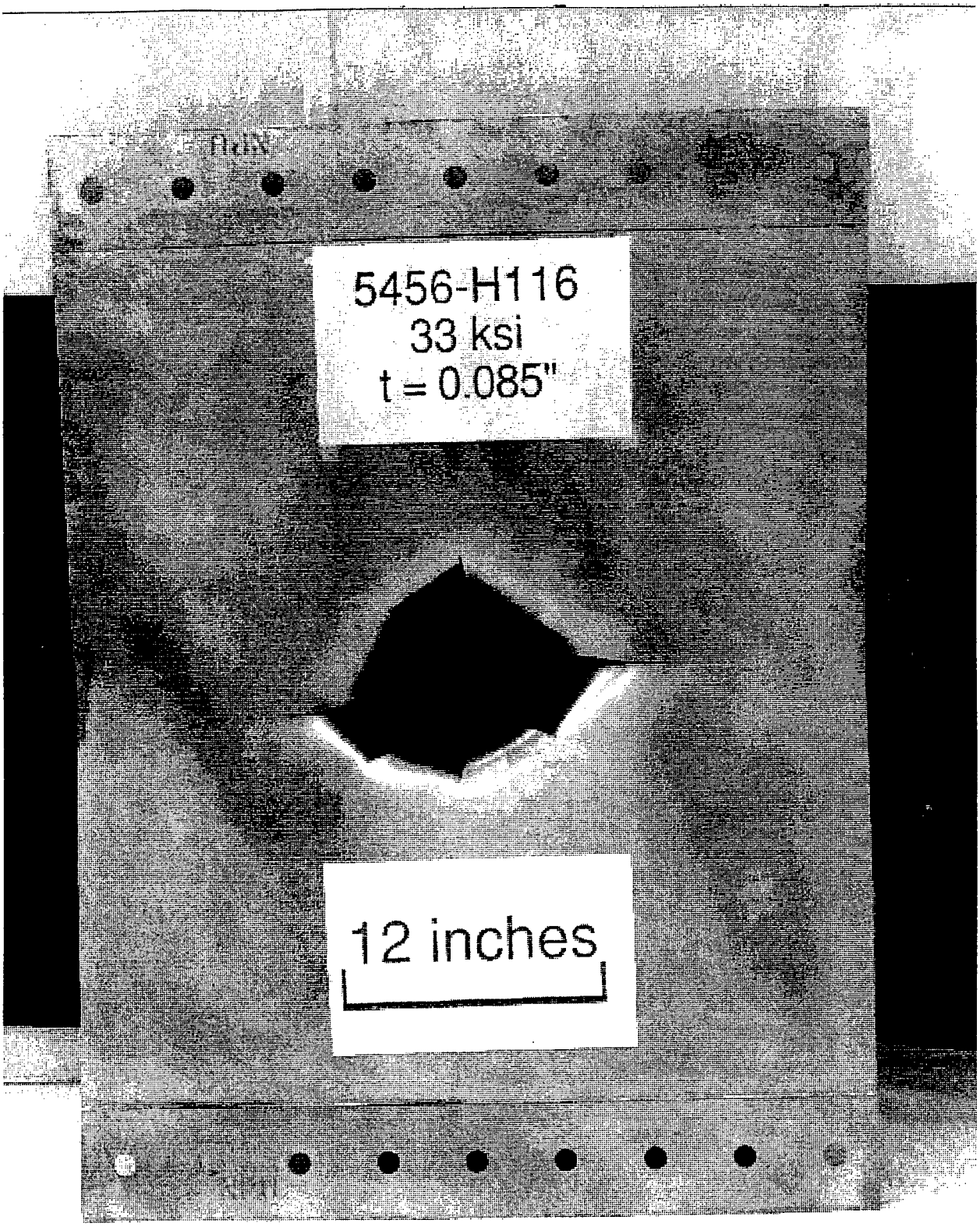


Fig. 6-14 Same as Fig. 6.12 except thinner sheet.

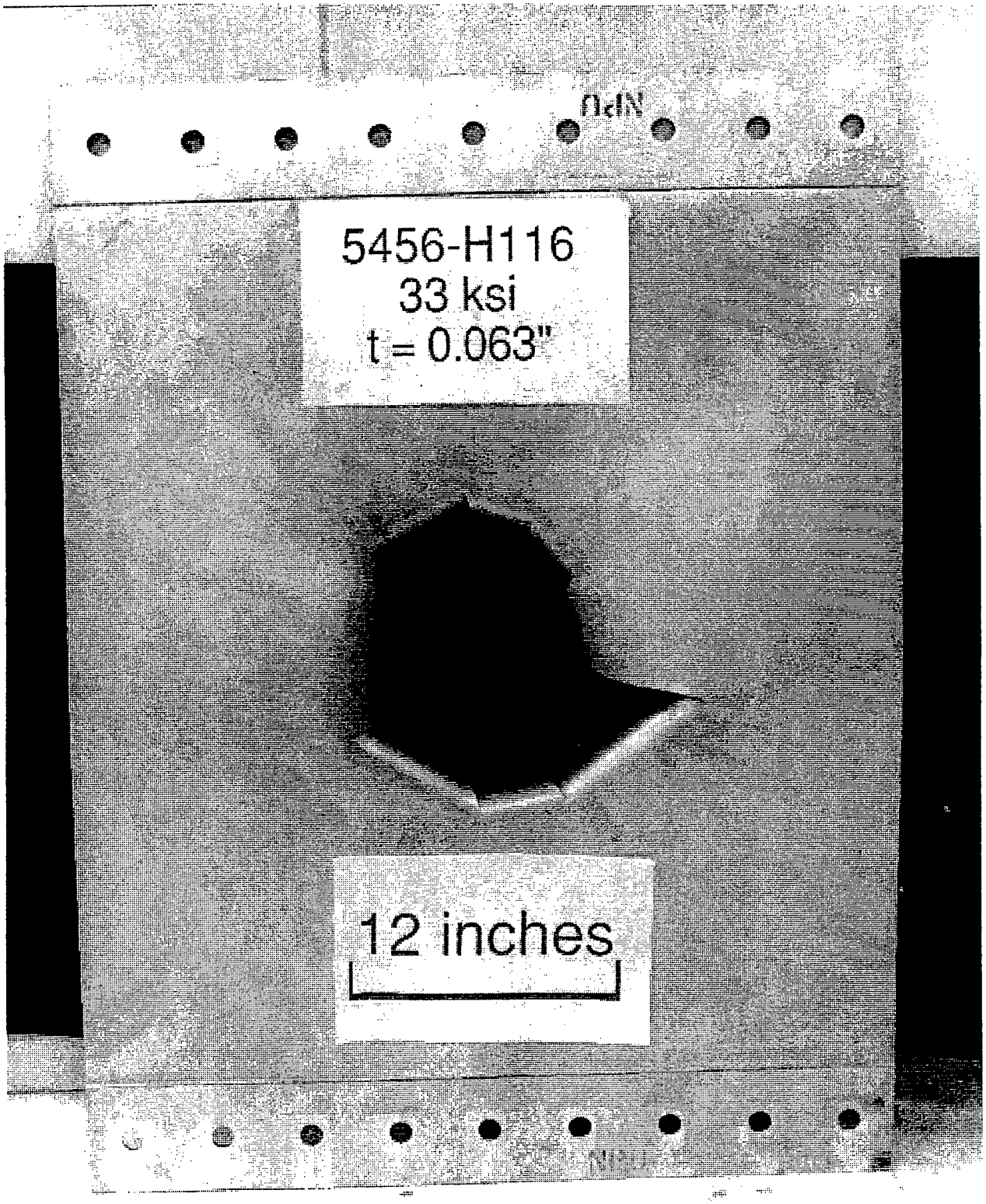


Fig. 6-15 Same as Fig. 6.12 and 6-13 except thinner sheet.

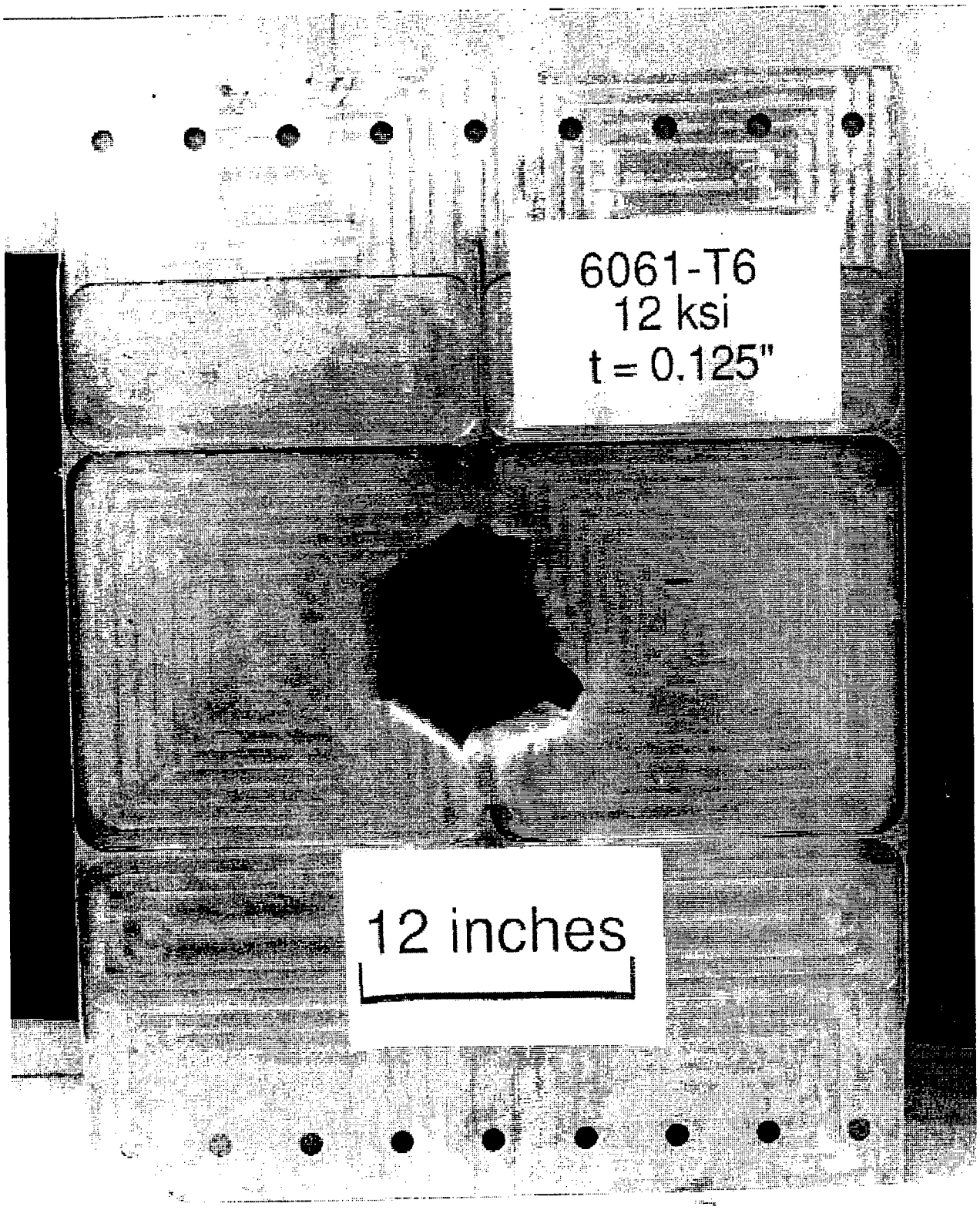


Fig. 6-16 Same as Fig. 6-10 and 1.1 except 6061-T6 material used.

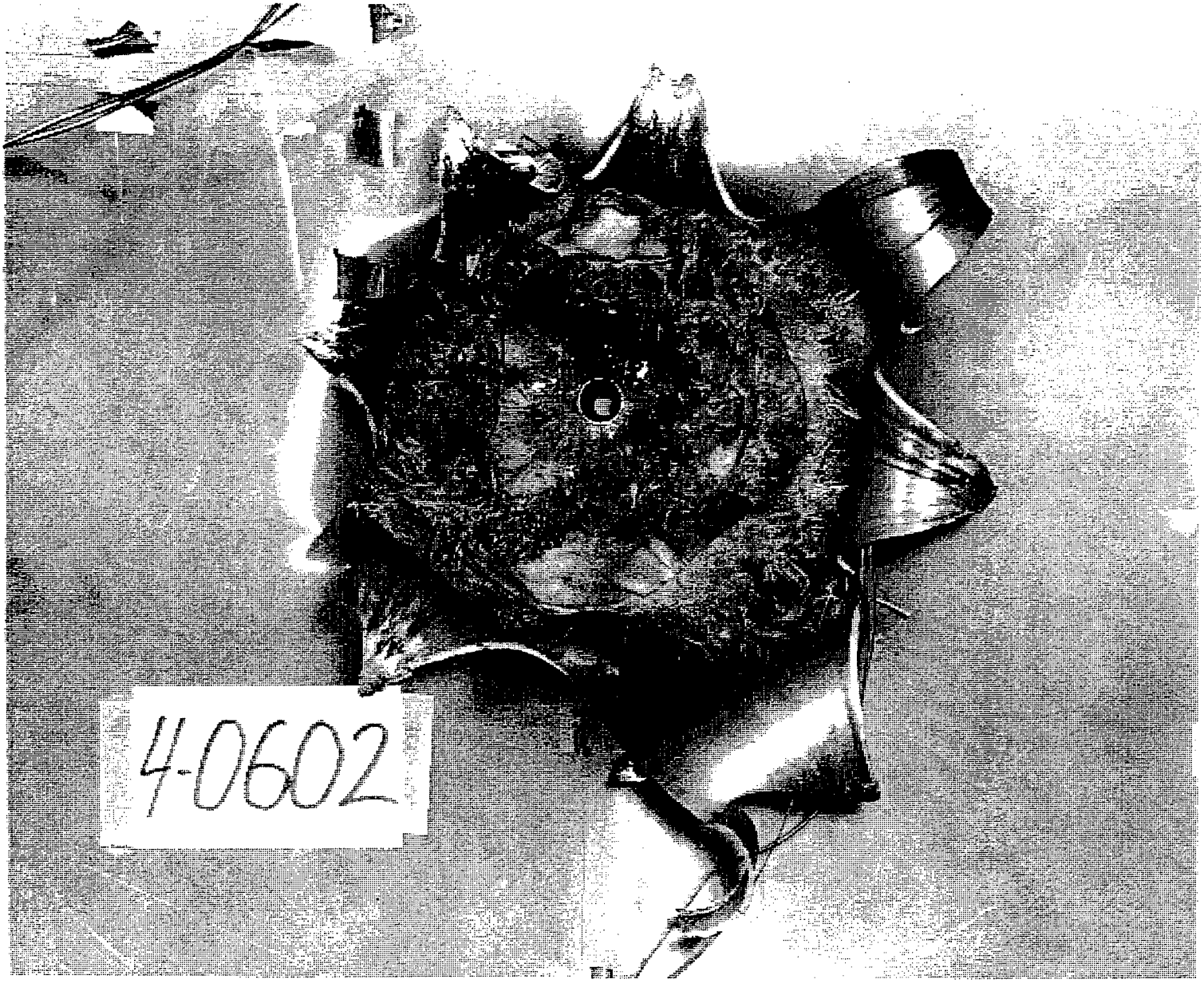


Fig. 6-17 Reverse of Fig. 6-12, showing torn petals, catcher cloth, and bumper.

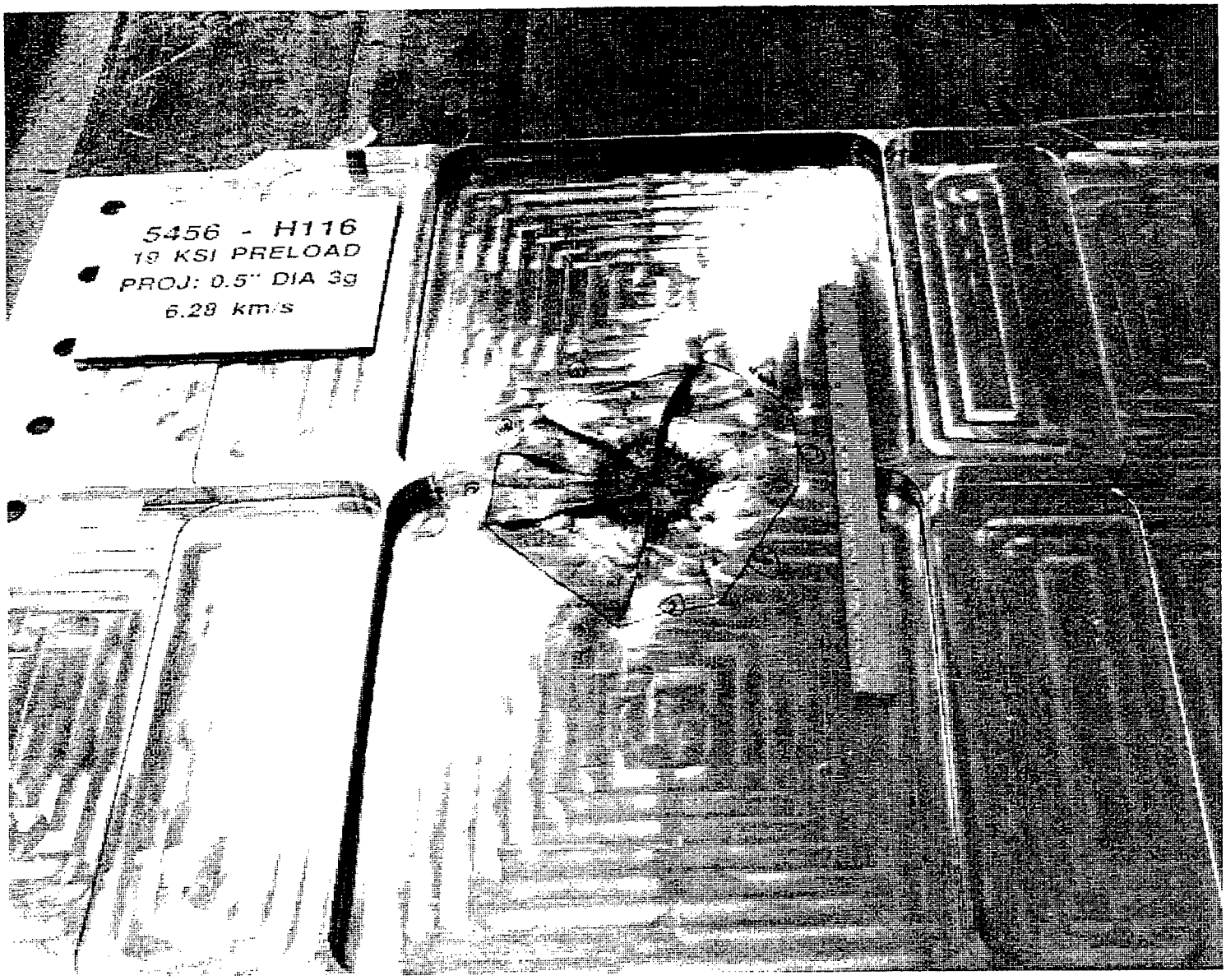


Fig. 6-18 The petals were bent back in on the rear wall shown in Fig. 6-13. Note that the impact area is approximately one third the diameter of the final hole size.

# 7 DAMAGE TOLERANCE

The section addresses the potential for a meteoroid or debris impact to create a large crack which will propagate to complete fracture of a module. The first step in this process is a penetration which forms petals or cracks. This occurs due to the inward bulging that occurs as projectile momentum is absorbed. The crack driving force due to impact decrease as the crack gets longer. The next step in the process is to determine whether internal loads will cause catastrophic crack growth. As will be discussed, the separation of these processes is appropriate. The impact bends the metal inward, whereas the internal pressure is the prime structural load, and it bends the petals back out. (The hoop stress is constant but it has less than one half of the crack driving force.)

## 7.1 Initial Crack Length

Prediction of crack length after penetration is very difficult. One must know the residual momentum distribution left in the specimen and how this affects crack length.

For a given shield design, there may be a maximum rear wall crack length generated regardless of impact projectile size. As momentum increases beyond the penetration threshold, more petals are formed up to an experimentally observed limiting number of eight to twelve. As projectile size increases further, most of the momentum just continues along the shot line, rather than being deposited in the rear wall. This is illustrated in the first block in Fig. 7-1.

### 7.1.1 Crack Propagation Energy Balance

The following approach to predicting fracture is based on an energy balance. The Wilkinson equation provides a starting estimate of the rear wall momentum distribution. The momentum deposited in the rear wall is used to determine the initial kinetic energy. This is much different than the initial kinetic energy of the projectile since the total mass is much higher and the velocity is lower. Furthermore, a significant fraction of the initial momentum may propagate through the wall.

K.E.(rear wall) = Work of deformation + Fracture Energy + K.E.(torn fragments)

where

Fracture Energy = No. of petals x length of tear x energy of fracture per unit length

It is assumed that the elastic energy absorbed by the rear wall is negligible. Assume that the kinetic energy is absorbed initially by plastic deformation (bulging) of the rear wall, and when radial cracks initiate, the remainder of the energy is consumed by crack propagation.

The crack propagation energy is dependent on the number of cracks formed. Assume that the maximum number of cracks/petals is eight. Although more petals may form (as many as twelve), this is a conservative upper limit. (It is conservative to estimate fewer petals, since the cracks must be longer to account for the same amount of energy.) The actual number of petals to be used in the analysis depends on the amount of kinetic energy available beyond that required to fail the rear wall by bulging.

Figure 7-1 schematically shows the processes that will occur for increasing momentum. A key assumption is that the rear wall was optimized to the bumper shield system to allow momentum failure before fragment penetration could occur. However, if the rear wall always fails by fragment pentration, spall, or plug failure, before bulging and momentum failure can occur, then significant crack propagation will not occur.

Figure 7-2 shows Kaufman and Hunsicker's results on crack propagation energy per unit length. The numbers are not actual material properties. The resistance to crack propagation is dependent on specimen geometry and increases as the crack gets longer (R-Curve effect), but the chart shows relative rankings of several alloys. Figure 7-3 shows crack propagation energy per unit length for three alloys as a function of temperature. These charts help explain why the 5456 and 6061 aluminum rear walls did not have as much crack growth as the 2219 rear walls (which will be similar to 2014).

## 7.2 Structural Failure

One simplifying approach to predicting failure, is the separation of the initial flaw size from the analysis of the structure of with a crack. This is supported by the tests on pre-loaded specimens as shown in Fig. 6-10 through 6-17. [Elfer87] In those tests the crack growth perpendicular to the tensile load was not significantly larger than the crack growth in the same direction as the principal stress. This section reviews the damage tolerance analysis after the initial impact induced damage.

### 7.2.1 Material Properties for Fracture Analysis

Figure 7-4 shows the fracture stress for different initial flaw lengths in a 61 cm wide sheets of 2219-T87 and 5456-H116. [Elfer88] For 2219, there is only a small R-curve effect, and linear elastic fracture mechanics with a

toughness of 60 ksi·√in appears to adequately model the failure. Measured R-curves versus physical flaw size are shown in Fig. 7-5. [Elfer88] This is in contrast to the values reported in the Air Force Damage Tolerant Design Handbook. There values in excess of 100 ksi·√in were reported for wide specimens of 0.100 inch material. Those specimens exhibited a definite R-curve effect, longer flaws failed at higher toughness values. Both test programs used anti-buckling restraints on the specimens.

One possible cause for the difference in the toughness between the two test programs, was that values from the Damage Tolerant Design Handbook were from a 1962 report by Eichenberger[62]. However, in 1963 the aging heat treatment for 2219-T87 was changed from 14 to 24 hours at 325°F to prevent the possibility of stress corrosion cracking. The specimens with the shorter aging time, especially at lower aging temperatures, could have higher ductility, and hence higher toughness, than the current heat treatment. Kaufman and Hunsicker showed that for 2014 alloy the peak aged condition has the lowest unit propagation energy, and that for equal stregths, the underaged condition is much tougher than the overaged condition.

Pfluger[64] also reported through flaw toughness for 2219-T87. The toughness (~60 ksi√in) appear to be consistent with Elfer's results based on maximum load and initial flaw size. However, the toughness was reported as approximately 100 ksi√in based on maximum load and the flaw size at onset of rapid crack growth. This is not a typical way of quoting the R-curve. The load level typically drops before unstable crack growth, although Pfluger may not have been able to measure the load drop.

For 2219 aluminum considerations, the lower values reported by Elfer are more representative, but specimens actually matching the heat treatment would be preferred. For example, age-forming can use higher temperatures and relatively longer times to reduce spring-back. The age-forming practice could further reduce strength and/or ductility compared to the standard heat treat, so it is important to test the actual heat treat conditions.

One issue is whether an impact induced crack length should be evaluated using the K from the initial flaw size or from the final flaw size. The tearing associated with the impact has already moved the crack tip up the R-curve. It is conservative to start the R-curve at the final flaw size from the impact (assume the crack will continue to grow at low R-curve levels). However, it may be more realistic to use the peak value on the R-curve (K-max). This simplifies the analysis to a simple linear elastic fracture mechanics analysis.

Dynamic fracture toughness, $K_{Id}$, should be considered for impact induced flaws. For several materials $K_{Id}$ is lower than the static $K_{Ic}$. However, for 2219-T87, like several other aluminum alloys, the dynamic toughness is always greater than the static toughness. This may be inferred for the increase in toughness under cryogenic conditions, and this was confirmed by dynamic toughness measurements. [Kanninen93] While the higher dynamic toughness is of interest in trying to predict the crack growth during impact, the lower static toughness is what should be used to analyze whether the structure is stable due to internal pressure.

### 7.2.2 Cylinder Effect

A cylinder with internal pressure, and a longitudinal crack, has a much higher stress intensity than would be predicted in a flat plate with a similar hoop stress. Several solutions are given in Appendix A and Newman's solution in NASA-FLAGRO is preferred. Fig. 7-6 shows a magnification factor for a cylinder relative to a flat plate.

It has been shown that biaxial loads can cause a significant increase in toughness, but this does not appear to be significant to large cracks in manned modules. Tests by Erdogan and Ratwani [1972] showed a large (30%) improvement in toughness in 6061-T6 aluminum for a biaxial load equal to half of the opening load. This appears to be due to biaxial effects on the crack tip strain response (provided adequate anti-buckling restraints were used in uni-axial testing). While Erdogan's test showed a significant effect, the flaw was relatively small (1.3 inch) and the biaxial load was large. For larger flaws, of concern to a manned module, the hoop stress is small and so is the biaxial stress (on the order of 5 ksi for a 0.125 inch thick manned module). At the crack tip, the opening stresses will be above yield, but the biaxial stress will still be small, and there will be a negligible effect. This says that the magnitude of the stress parallel to the crack is much more important than the biaxial stress ratio. R-curve calculations by Nied [93] verified that a biaxial stress had a negligible effect on the R-curve of the 24 inch wide specimens tested by Elfer [section 7.2.1].

A possible conservatism in the analysis is the fact that some of the stress intensity is due to through-the-thickness bending. However, bending is not generally as detrimental as pure tension. The material may exhibit a higher toughness for a bending induced stress intensity. This effect has been observed in 2219-T87 surface flaws [Elfer92] and may be related to loss of constraint. However, considering Zahoor's fit of Erdogan's data (Appendix A) the bending contribution is less than 10% of the total stress intensity in the flaw sizes of interest to Space Station.

It is worth noting that the bending induced by the internal pressure is opposite to the bending induced by the initial impact. This substantiates the approach of separating the initial impact from the structural effects.

### 7.2.3 Hole Effect

A crack emanating from the edge of hole in a cylinder is more representative of a petaled hole than a simple crack in a cylinder. This significantly reduces the stress intensity at the crack tip since internal pressure would not work over a large area. To analyze these effects Rajendran and Grove modeled a cylinder with a depressurized area at the center of the crack.[in Elfer88] This is shown in Fig. 7-7. A generalized curve fit to their results is given in Appendix A. The curve fit is based on simple modification to the Folias equation (also in Appendix A) and used to ratio the Newman solution. As the radius of the area without pressure approached the half crack length, the closer the results came to the solution for a flat plate.

There is one caution in using the hole size directly in the analysis. Due to the petals bending inward, there will still be a bending moment on the petal. A somewhat smaller hole size should probably used to account for this.

Solutions for a star crack in a flat plate are included in Appendix A. While this looks like petals and should be applicable to a flat plate, this is probably not an accurate modification for a crack in a cylinder. Nevertheless, the petals are expected to reduce the stress intensity compared to a single longitudinal crack in a cylinder.

### 7.2.4 Influence Function for a Cylinder

Influence functions provide a means of analyzing a crack in an arbitrary stress field. This is illustrated for a flat plate in Fig. 7-8.

Influence functions were calculated for a longitudinal crack in a cylinder using a NASTRAN model with a crack tip element as shown in Appendix A. The geometry is shown in Fig. 7-9. Even though NASTRAN has special crack tip elements available, the analysis only converged on the FLAGRO solution for 3D brick elements when the mesh size was 0.25 inch square or twice the wall thickness, as shown in Fig. 7-10. The influence funtion was developed by applying point loads along the crack length. Since the model was only a quarter of the cylinder the influence funtion is for symmetric loads about the center of the crack. The analysis results for a particular flaw are shown in Fig. 7-11. An equation for the influence funtion is in Appendix A. The typical influence funtion for a center cracked plate, Green' function, is also included. The cylinder equation includes

components for Green's function in a flat plate and a cylindrical component so that the whole equation will integrate to Newman's solution for a uniform load. It is obvious that the cylinder is much more sensitive to loads at the center of the crack, compared to the flat plate. The influence function does converge to the flat plate solution close to the crack tip.

### 7.2.5 Cylinder with integrally machined stiffeners

Most manned modules require stiffeners for launch. There is a natural desire to determine if these stiffeners can prevent catastrophic rupture due to the large cracks that can be generated by debris impacts. In general, analysis of aircraft structures has shown that mechanically attached stiffeners, which can bridge a crack, are better than integrally machined stiffeners to slow fatigue crack growth and provide damage tolerance.

The integrally machined stiffeners originally planned for manned modules were in a 45° diamond pattern with 20.95 inches on diagonal. The stiffeners were 0.090 inches thick on a cylinder with a 0.125 inch membrane. An analysis by Eidinoff showed that the stiffeners have a significant influence on the stress intensity of centrally located crack in the membrane of cylinder.[Eidinoff93] This was based on a 3D analysis with 2D elements. On the other hand, separate 2D hoop stress analyses by Rajendran [in Elfer88] and Nied[93] did not predict as significant a reduction in the stress intensity except at the stiffener, and for that large a crack the stress intensity was so large that the crack would continue to propagate. The stress intensity away from the stiffener could be estimated on the smeared thickness. The influence funtion by Elfer (section 7.2.4) shows that pressure loads at the center of the crack to have a large influence on the stress intensity. If there are no stiffeners at the center of the crack, then the stiffener effects should not be significant.

The stiffeners do appear to have a significant effect on the impact induced crack growth. Impacts centered on the stiffener may not fracture the stiffener and, even when the stiffener failed, rear wall petaling was significantly reduced. Compare Fig. 6-11 and 6-12.

A conservative approach is to assume that the impact induced crack length will be limited by the stiffener spacing and then determine if the resultant crack is critical without including the stiffener influence on stress intensity.

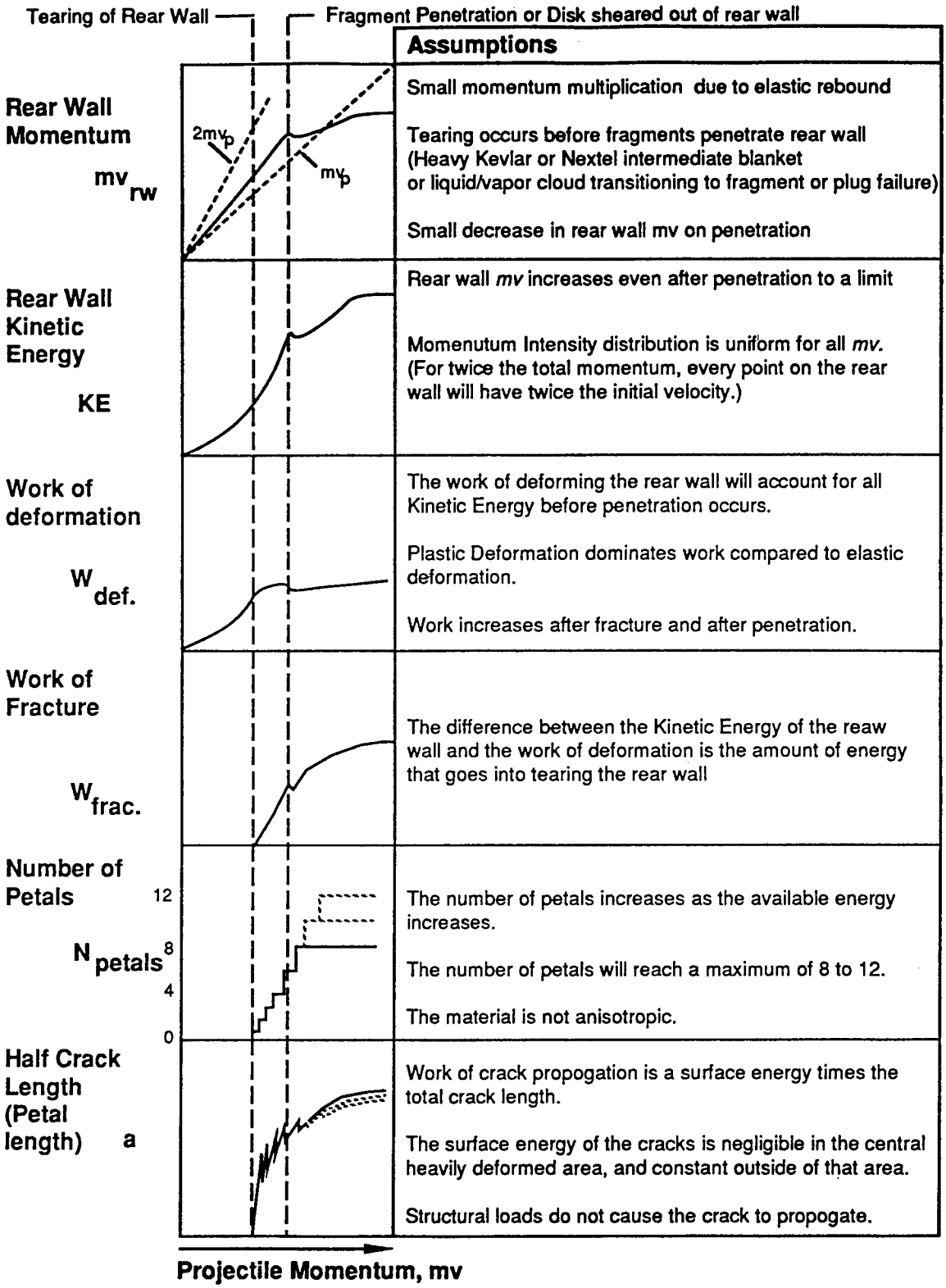


Fig. 7-1. An illustration of the energy balance for rear wall crack propagation.

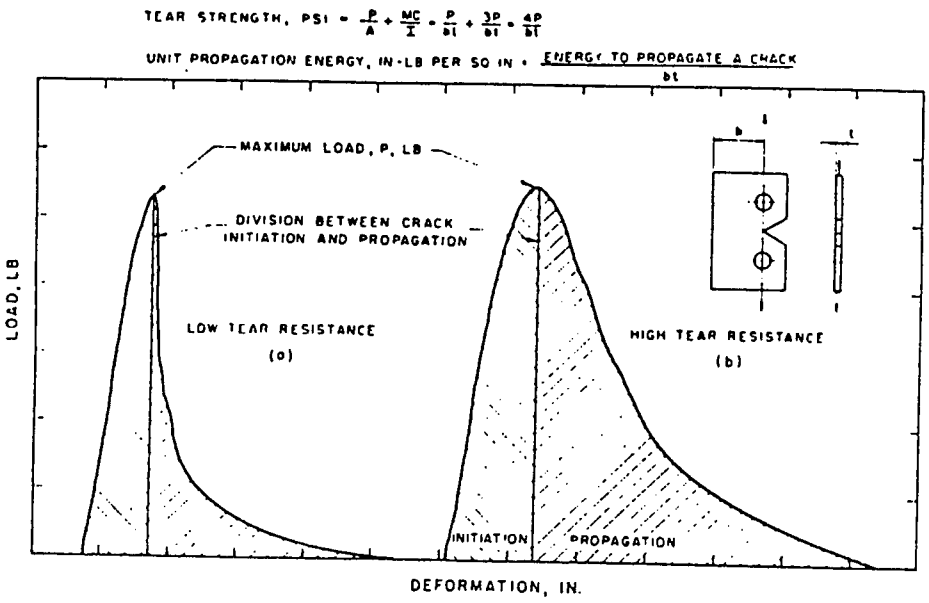


FRACTURE TOUGHNESS TESTING

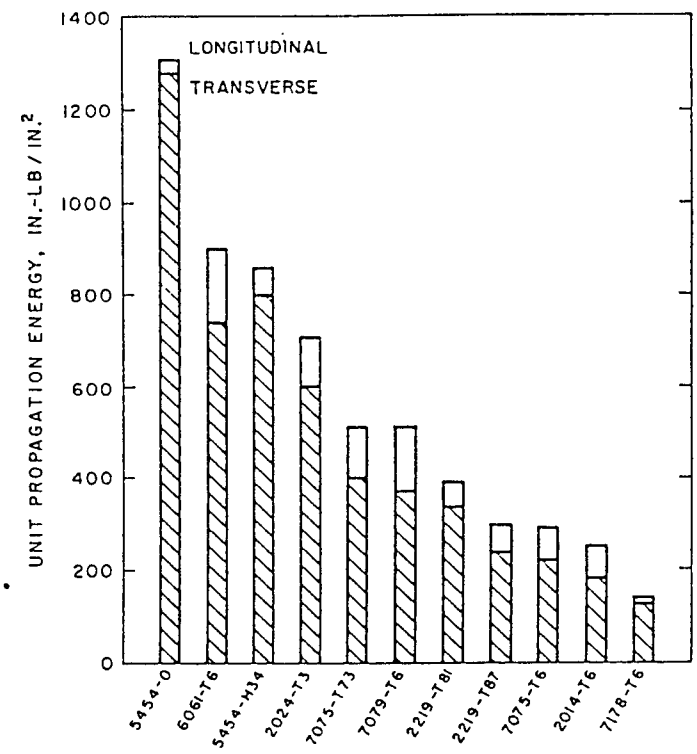


Fig. 7-2. Tear Resistance of 0.063 in. thick aluminum sheet. [Kaufman and Hunsicker]

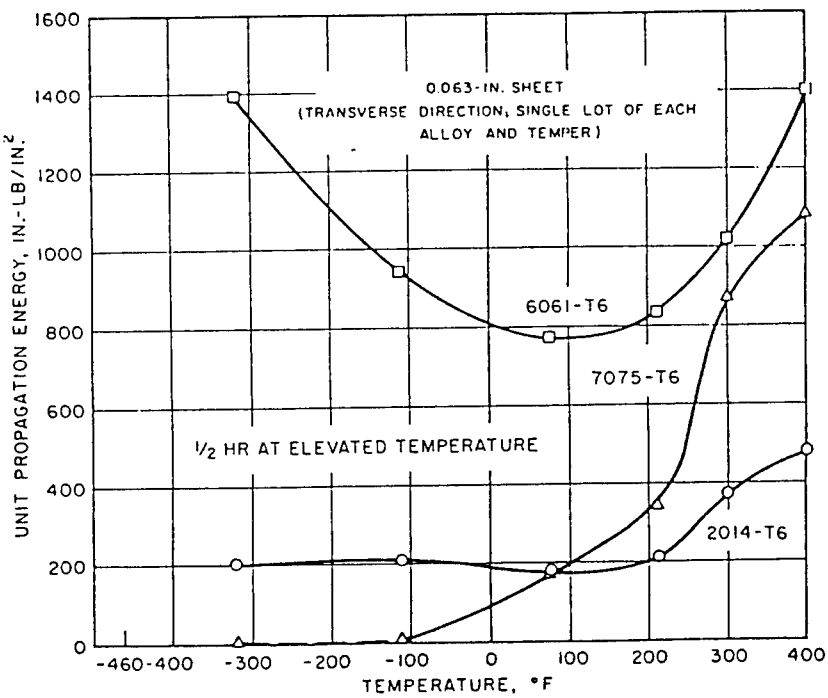


Fig. 7-3. Unit propagation energy of some aluminum alloys at various temperatures. [Kaufman and Hunsicker]

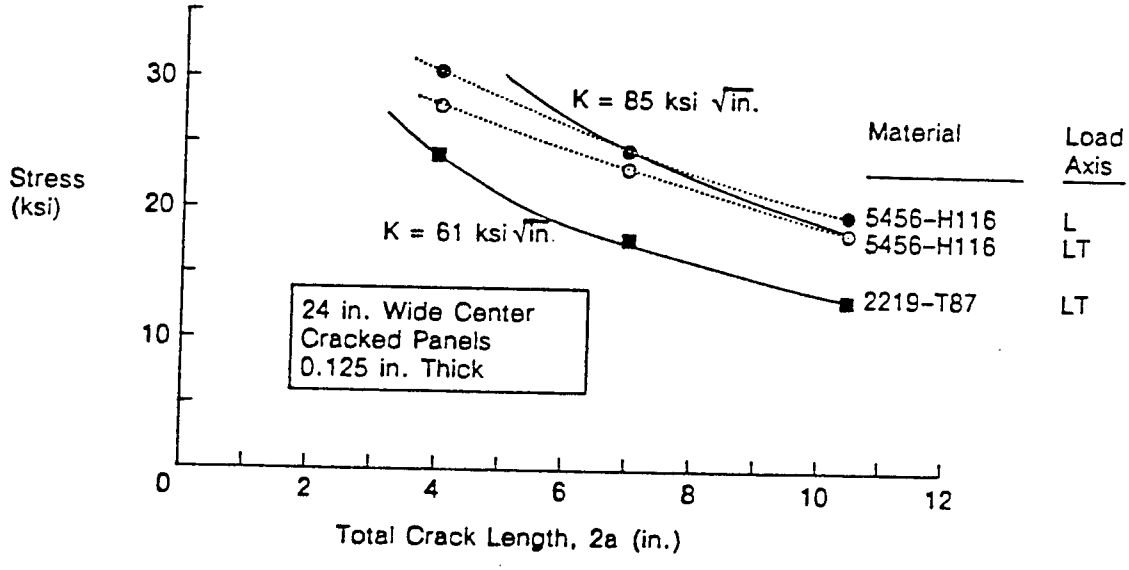


Fig. 7-4. Failure stress versus flaw size in 61 cm wide sheet of 2219 and 5456. [Elfer 88]

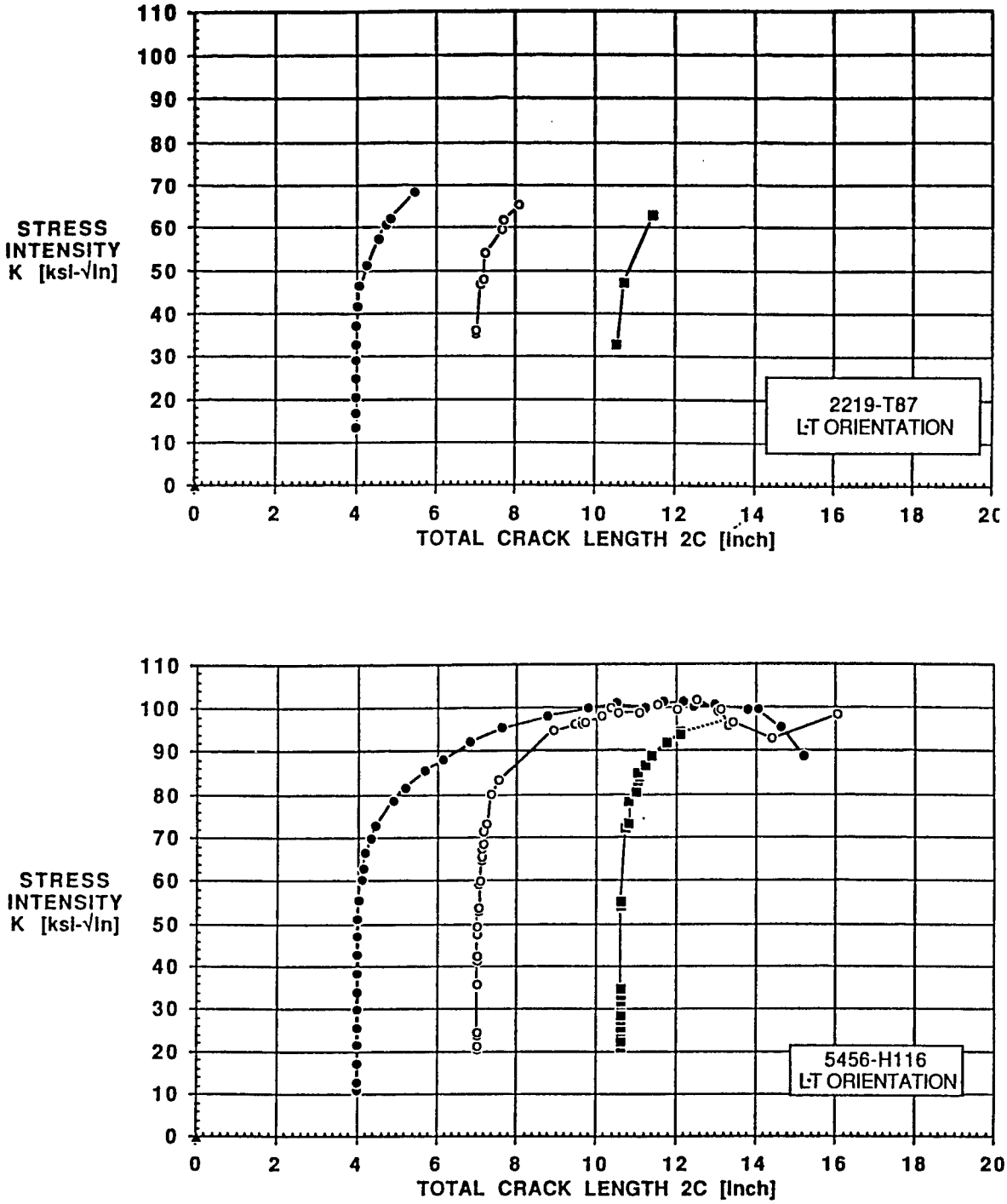


Fig. 7-5. R-curve versus physical flaw size a 61 cm wide sheet of 2219-T87 and 5456-H116. [Elfer 88] A flaw length was not necessarily measured at max stress.

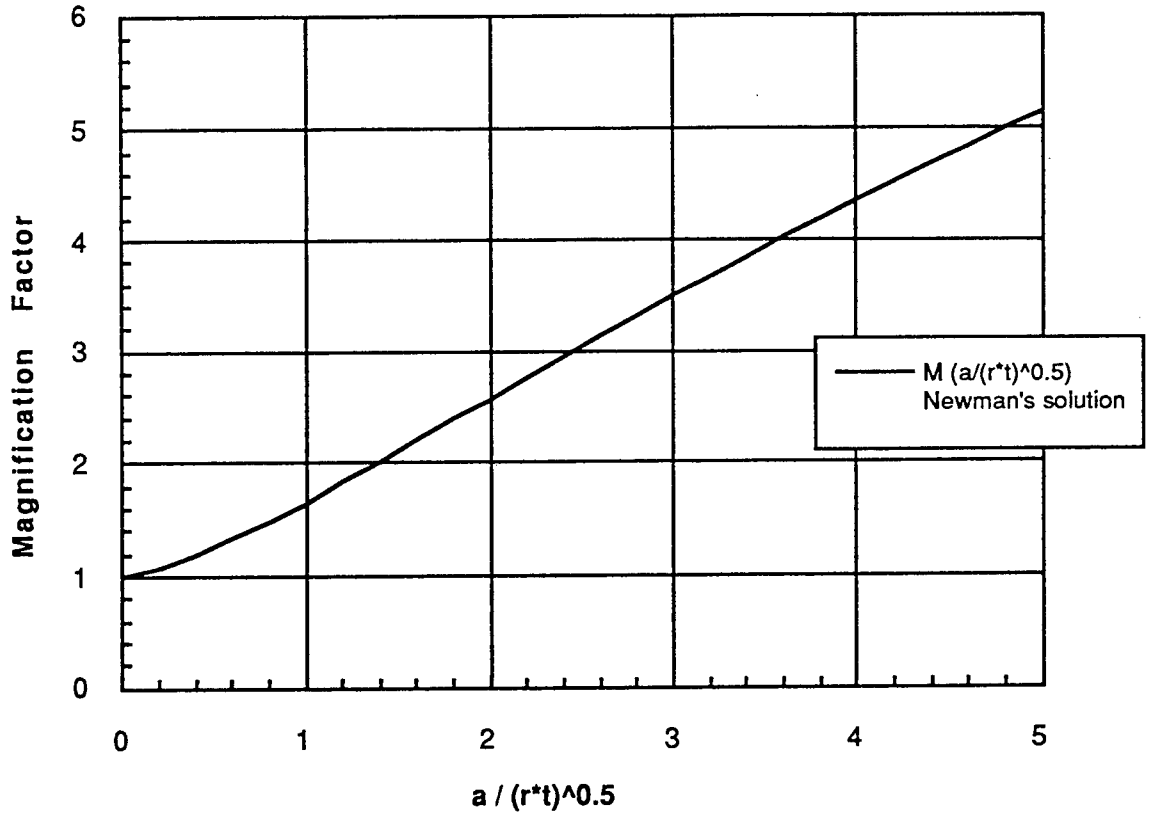


Fig. 7-6 Stress intensity magnification factor for a cylinder relative to a flat plate.

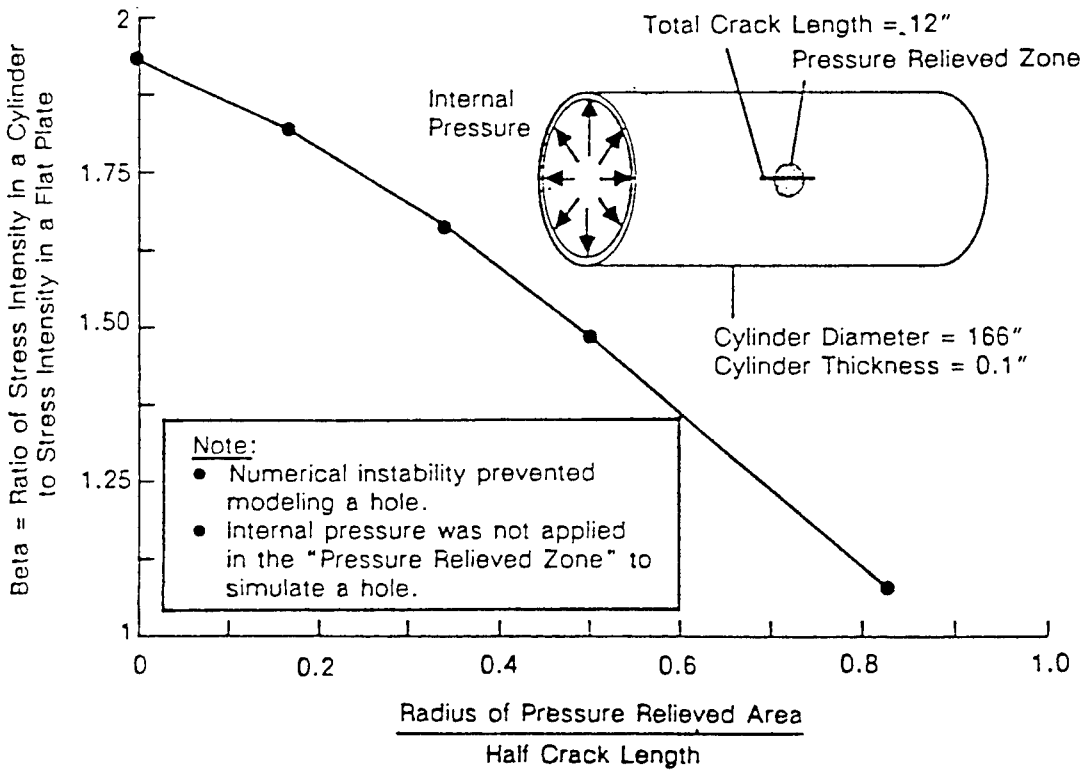


Fig. 7-7 Effect of a Hole (modeled as depressurized zone) on the Stress Intensity in a Cylinder. [Rajendran in Elfer88]

## Influence Function

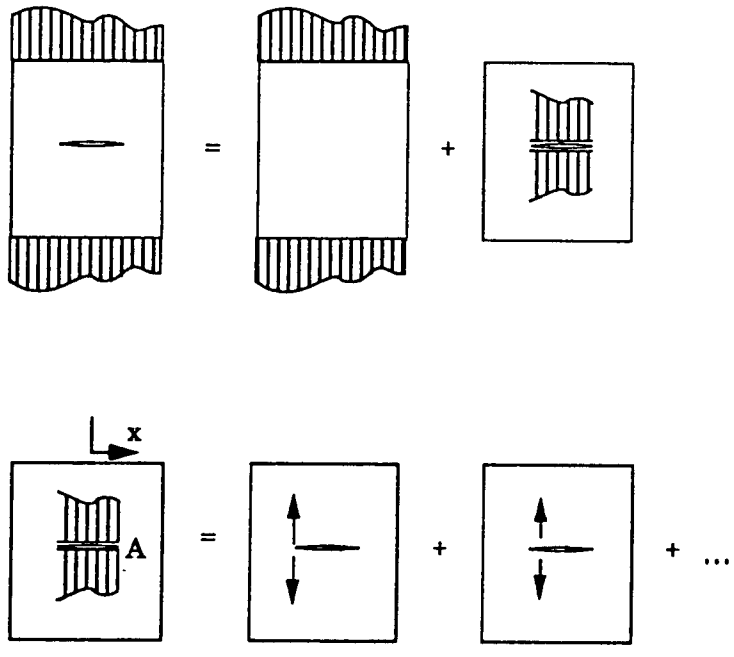


for a flat plate (solved using Green's function):

$$K_{IA} = \frac{P}{\sqrt{\pi a}} \frac{\sqrt{(a+x)}}{\sqrt{(a-x)}}$$

Fig. 7-8 Influence function for a flat plate.

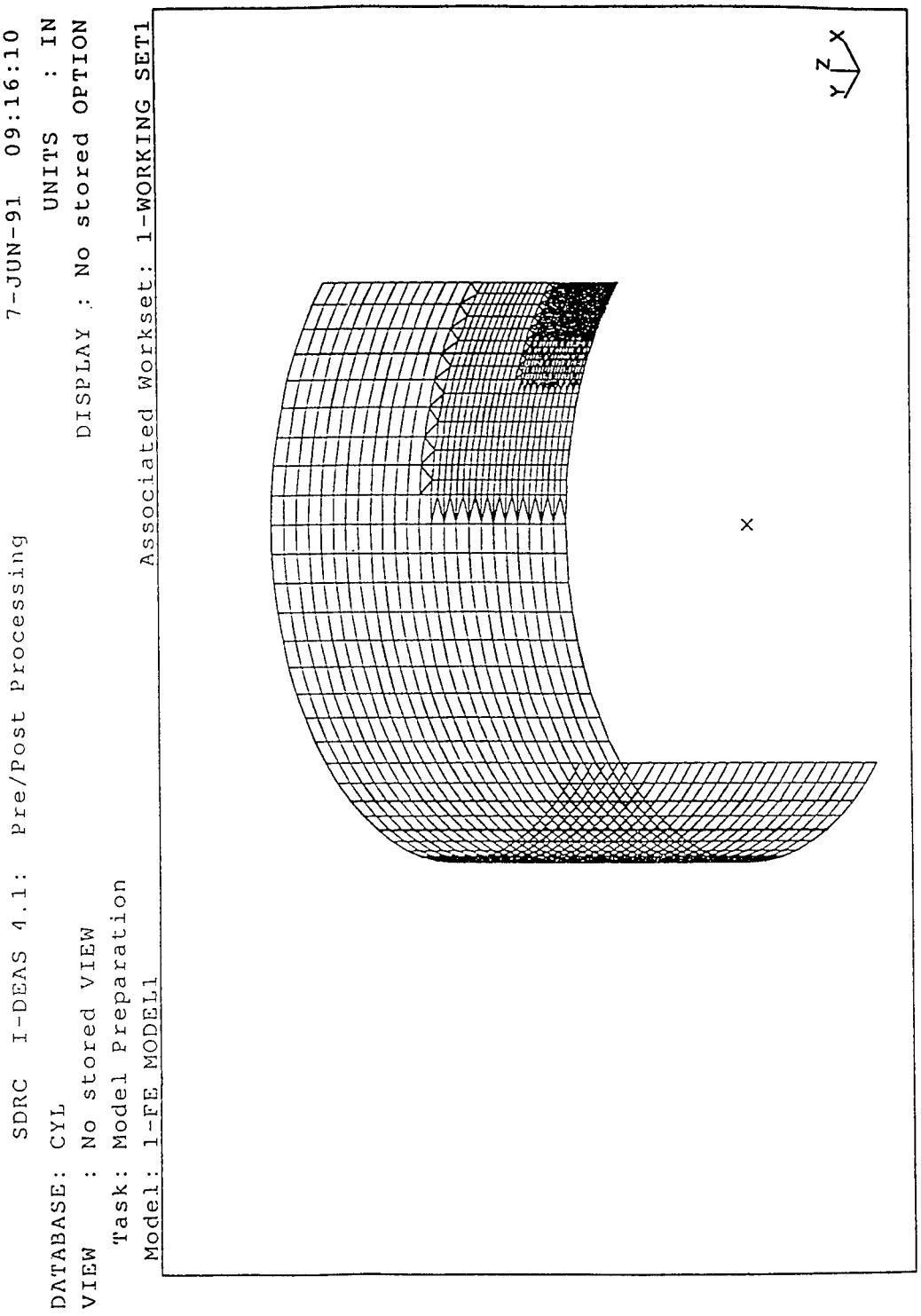


Fig. 7-9 NASTRAN 1/4 cylinder symmetric model.

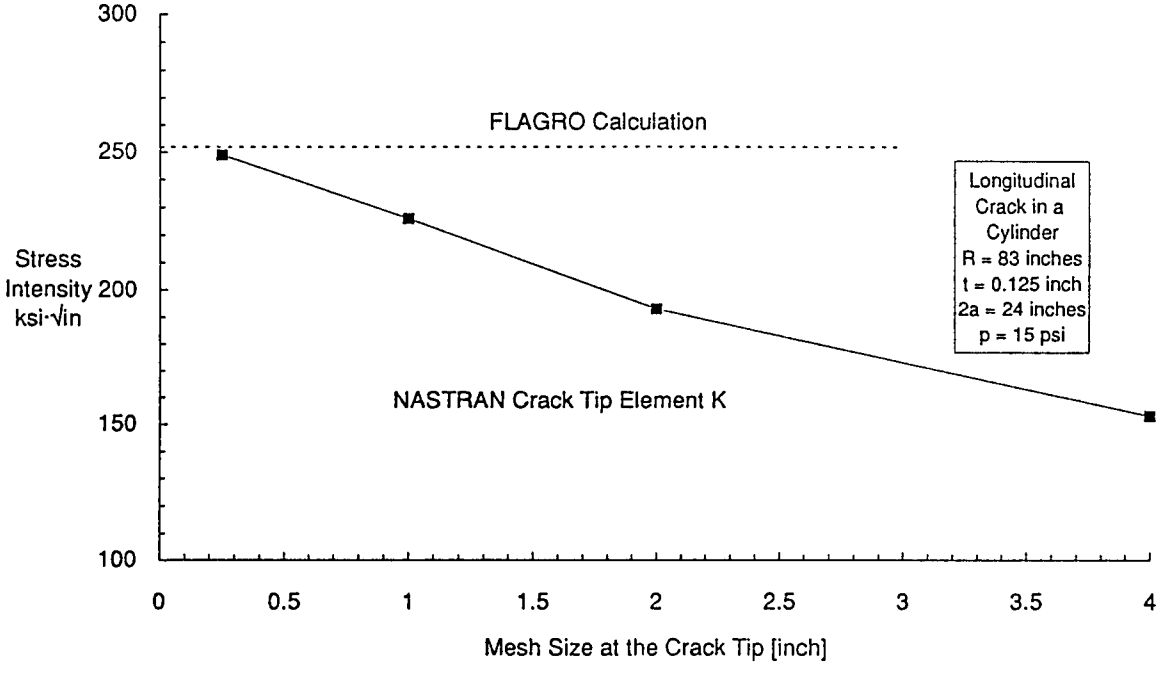


Fig. 7-10 Effect of mesh size on the calculated stress intensity for a cylinder (using NASTRAN crack tip element).

# Influence Function

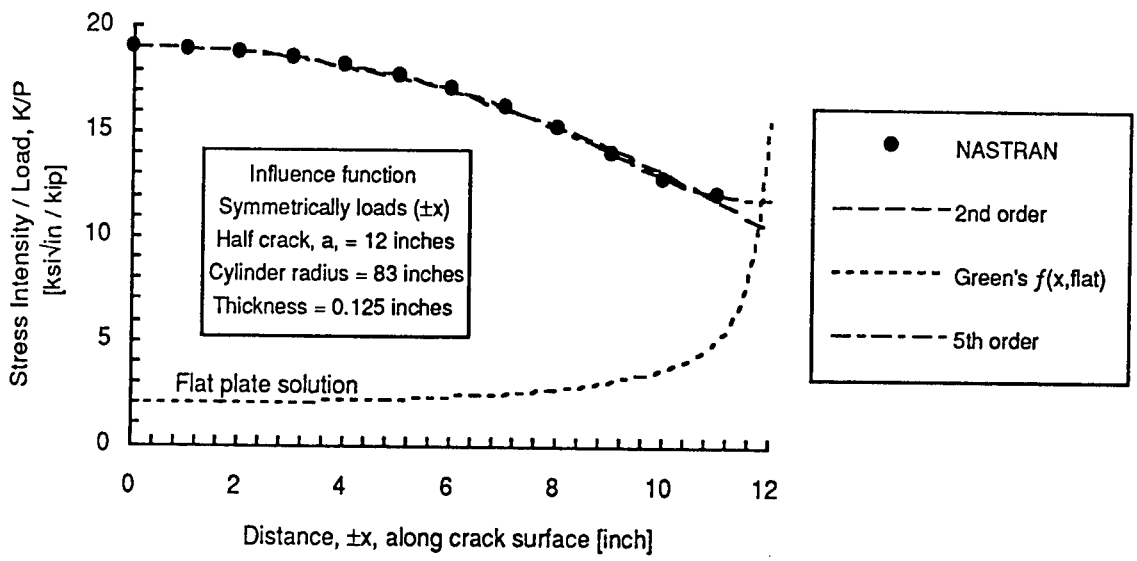


Fig. 7-11 Influence function for a crack in a cylinder.

CONTRACT NAS8-38856

# Structural Damage Prediction and Analysis for Hypervelocity Impact

# APPENDIX A

# EQUATIONS

## APPENDIX A - TABLE OF CONTENTS

TABLE OF CONTENTS ..... III

GLOSSARY ..... VI

UNIT CONVERSIONS ..... VII

Probability

Binomial Distribution ..... 1

Penetration - Cratering/Single Wall Penetration

Fish and Summers ..... 2

JSC (Modified Cour-Palais) ..... 3

Penetration - Multisheet Fragment Penetration

Burch ..... 4

Nysmith ..... 6

Penetration - Equations for Specific Shields

Whipple Bumper (Modified Cour-Palais) ..... 7

Nextel/Kevlar Intermediate Shield ..... 9

Multishock Shield (Christiansen) ..... 11

Mesh Double-Bumper (Christiansen) ..... 13

Penetration - Dispersion Angle

Wilkinson ..... 15

Penetration - Momentum Failure

Wilkinson ..... 17

Grove and Rajendran ..... 19

Housen and Schmidt ..... 20

Fracture Mechanics - Longitudinal Through Crack in a Cylinder

Tada solution ..... 22

Folias solution ..... 23

Plastic Zone correction by Hahn et al. to Folias solution ..... 24

Zahoor solution ..... 25

Zahoor limt load solution ..... 26

Newman solution ..... 27

Depressurized Area at Center of Crack

(or Hole at center of crack) - Elfer, Grove and Rajendran ..... 29

Membrane Load - Zahoor solution ..... 31

Wedge loads - Influence function ..... 33

Fracture Mechanics - Through Crack in a Sphere
Tada solution ..... 35
Erdogan and Kibler solution ..... 36
Fracture Mechanics Flat Plate
Radial cracks - Tada solution ..... 37
Wedge loads - Influence function ..... 38
Through cracks from a hole in a plate - Tada ..... 39
Through cracks from a hole in a plate - FLAGRO ..... 40
Fracture mechanics - Influence function
General equation for influence function ..... 41

## GLOSSARY

**Variable**

**Subscript**

c ---------- Speed of sound [km/s]
d ---------- Diameter [cm]
  frag .....fragment diameter from bumper impact
  p .....projectile diameter (spherical unless noted)
E---------- Young's Modulus [MPa]
G ---------- Shear Modulus [MPa]
h ---------- Spacecraft altitude from earth's surface [km]
H ---------- Energy per unit mass for melt/vaporization []
m---------- Mass [g]
PNCD---------- Probabilty of no Critical Damage
PNP ---------- Probability of no Penetration
POP ---------- Probability of (one or more) Penetrations (1-PNP)
r ---------- Radial distance
S---------- Spacing (front of bumper to rear of rear wall unless noted [cm]
  1,2,...n .....first, second, nth bumper to rear wall spacing. Bumpers counted from the initial projectile impact.
t ---------- Thickness [cm]
  b .....bumper
  rw .....rear wall
t ---------- time [s, or as listed]
v ---------- Velocity [km/s]
  E. .....initial projectile
  frag .....largest fragment from bumper impact
  orb .....orbital velocity of a spacecraft

$\beta$ ———————Obliquity angle
$\varepsilon$———————Strain
$\rho$ ---------- Density [g/cm$^3$]
$\sigma$ ---------- Stress [dynes/cm$^2$ or MPa]
  sp, ult, y .....spall, ultimate or yield strength
$\theta$---------- Average semivertex cone angle of debris cloud [rad]

**Subscripts**
b .....bumper
frag .....fragment from bumper impact
p .....projectile
rw .....rear wall
t.....target (for a single wall experiment)
1,2,...n .....first, second, nth bumper to rear wall.

# UNIT CONVERSIONS

| To Convert from | Multiply by | To Get |
|---|---|---|
| **Length** | | |
| Angstrom | 1.0 E+10 | meters [m] |
| centimeters [cm] | 0.3937 | inches [in] |
| centimeters [cm] | 3.281 E-2 | feet [ft] |
| feet [ft] | 1.894 E-4 | miles [mi] |
| feet [ft] | 1.645 E-4 | nautical miles |
| feet [ft] | 30.48 | centimeters [cm] |
| inches [in] | 2.54 | centimeters [cm] |
| kilometers [km] | 0.6214 | miles [mi] |
| kilometers [km] | 0.5396 | nautical miles |
| meters [m] | 1.0 E-10 | Angstrom |
| miles [mi] | 0.86842 | nautical miles |
| miles [mi] | 1.6093 | kilometers [km] |
| miles [mi] | 5,280. | feet [ft] |
| nautical miles | 1.8532 | kilometers [km] |
| nautical miles | 6,080. | feet [ft] |
| nautical miles | 1.1515 | miles [mi] |
| **Mass** | | |
| grain | 1.42857 E-4 | Pound mass [lbm] |
| grain | 6.47989 E-2 | gram (g) |
| gram (g) | 3.52741 E-2 | ounce (oz) |
| gram (g) | 2.20462 E-3 | Pound mass [lbm] |
| gram (g) | 15.4324 | grain |
| kilogram [kg] | 6.85218 E-2 | slug |
| ounce (oz) | 28.3494 | gram (g) |
| ounce (oz) | 28.3494 | gram (g) |
| Pound mass [lbm] | 32.174 | slug |
| Pound mass [lbm] | 7,000. | grain |
| Pound mass [lbm] | 453.5924 | gram (g) |
| slug | 3.1081 E-2 | Pound mass [lbm] |
| slug | 14.5939 | kg |
| **Velocity** | | |
| cm/s | 0. | km/s |
| ft/s | 6.8182 E-1 | mi/hr |
| ft/s | 3.048 E-3 | km/s |
| in/s | 2.54 E-4 | km/s |
| km/s | 1.0 E+5 | cm/s |
| km/s | 3,937. | in/s |
| km/s | 328.08 | ft/s |
| km/s | 6.2137 E-2 | mi/hr |
| mi/hr | 16.0934 | km/s |
| mi/hr | 1.4663 | ft/s |
| **Density** | | |
| gm/cm^3 | 3.613 E-2 | lbm/in^3 |
| lbm/in^3 | 27.6798 | gm/cm^3 |

| To Convert from | Multiply by | To Get |
|---|---|---|
| **Force** | | |
| dyne | 1.0 E-5 | Newton (N) |
| kg·m/s^2 | 1. | Newton (N) |
| kilogram-force | 9.8067 | Newton (N) |
| kip (1000 lbs) | 4,448. | Newton (N) |
| Newton (N) | 1.0 E+0 | kg·m/s^2 |
| Newton (N) | 2.24809 E-1 | Pound-force [lbf] |
| Newton (N) | 2.2482 E-4 | kip (1000 lbs) |
| Newton (N) | 1.01972 E-1 | kilogram-force [kgf] |
| Newton (N) | 100,000. | dyne |
| Pound-force [lbf] avoirdupois | 4.4482 | Newton (N) |
| **Areal Density** | | |
| gm/cm^2 | 0.2276 | oz/in^2 |
| gm/cm^2 | 32.7708 | oz/ft^2 |
| gm/cm^2 | 98.3123 | oz/yd^2 |
| gm/cm^2 | 1.422 E-2 | lbm/in^2 |
| gm/cm^2 | 2.0482 | lbm/ft^2 |
| gm/cm^2 | 6.1445 | lbm/yd^2 |
| gm/cm^2 | 10. | kg/m^2 |
| kg/m^2 | 0.1 | gm/cm^2 |
| lbm/ft^2 | 0.4882 | gm/cm^2 |
| lbm/in^2 | 70.3066 | gm/cm^2 |
| lbm/yd^2 | 0.1627 | gm/cm^2 |
| oz/ft^2 | 0.0305 | gm/cm^2 |
| oz/in^2 | 4.3942 | gm/cm^2 |
| oz/yd^2 | 0.0102 | gm/cm^2 |
| **Pressure - Stress** | | |
| atm (normal 760 Torr) | 101,325. | Pascal |
| atm (technical (1kgf/cm^2)) | 98,066.5 | Pascal |
| bar | 1.000 E+5 | Pascal (Pa) |
| dyne/cm^2 | 1.000 E-1 | Pascal (Pa) |
| kg-force/cm^2 | 98,070. | Pascal (Pa) |
| ksi (1000 psi) | 6.895 | MPa |
| MPascal [MPa] | 1.450 E-1 | ksi |
| Pascal (Pa) | 1.020 E-5 | kg-force/cm^2 |
| Pascal (Pa) | 9.869 E-6 | atm (normal 760 Torr) |
| Pascal (Pa) | 1.020 E-5 | atm (technical (1kgf/cm^2)) |
| Pascal (Pa) | 1.450 E-4 | psi |
| Pascal (Pa) | 1.0 E-5 | bar |
| Pascal (Pa) | 10. | dyne/cm^2 |
| lbf/sq inch [psi] | 6,895. | Pascal (Pa) |
| **Momentum** | | |
| g·km/s | 5.59974 E+2 | lbm·in/s |
| lbm·in/s | 1.7858 E-3 | g·km/s |

| To Convert from | Multiply by | To Get |
|---|---|---|
| **Stress Intensity** | | |
| ksi√in | 1.099 | MPa√m |
| MPa√m | 0.9099 | ksi√in |
| MPa√m | 31.6228 | MPa√mm |
| MPa√mm | 0.0316 | MPa√m |
| **Energy** | | |
| British Thermal Unit BTU (Int. Table) | 1,055.1 | Joule |
| Calorie (Int. Table) | 4.1868 | Joule |
| dyne-cm | 1.0 E-7 | Joule |
| Electronvolt (eV) | 1.6022 E-19 | Joule |
| erg | 1.0 E-7 | Joule |
| ft·lbf | 1.3558 | Joule |
| Joule | 1. | Newton-meter |
| Joule | 1. | Watt-second |
| Joule | 9.4782 E-4 | BTU (Int. Table) |
| Joule | 0.7376 | ft·lbf |
| Joule | 6.24146 E+18 | Electronvolt (eV) |
| Joule | 0.2388 | Calorie (Int. Table) |
| Joule | 1.0 E+7 | dyne-cm |
| Joule | 1.0 E+7 | erg |
| Joule | 0.10197 | Kgf-m |
| Kgf-m | 9.8067 | Joule |
| Newton-meter | 1. | Joule |
| Watt-second | 1. | Joule |
| **Energy per unit area** | | |
| ft·lbf/in^2 | 0.2102 | Joule/cm^2 |
| in·lbf/in^2 | 1.75127 E-2 | Joule/cm^2 |
| in·lbf/in^2 | 24.9089 | Pascal (Pa-cm) |
| Joule/cm^2 | 4.7585 | ft·lbf/in^2 |
| Joule/cm^2 | 57.1015 | in·lbf/in^2 |
| **Power** | | |
| BTU/s | 107.58 | Kgf·m/s |
| Ft-lbf/s | 1.81818 E-3 | Horsepower |
| ft-lbf/s | 1.3558 | Watt |
| ft-lbf/s | 0.1383 | Kgf·m/s |
| Horsepower | 550. | Ft-lbf/s |
| Joule/s | 1. | Watt |
| Kgf·m/s | 9.295 E-3 | BTU/s |
| Kgf·m/s | 7.233 | ft-lbf/s |
| Watt | 1.0 | Joule/s |
| Watt | 0.73756 | ft-lbf/s |

## Probability - Binomial Distribution
## Probability of n impacts or penetrations

**Reference** NASA SP-8042

**Relationship** $P = (F \cdot A \cdot t)^n \cdot (\exp(- F \cdot A \cdot t))/n!$

where

P = Probability of *n* impacts or penetrations

F = flux [consistent units]

A = area [consistent units]

t = time [consistent units]

and

n = number of impacts or penetrations

**Limitations** Binomial theory

**Comments** Flux and area must have similar definitions (e.g. flux and area for randomly tumbling plate vs. for a projected area. The flux and *n* may be determined in terms or impacts, penetrations or other phenomena.

## Penetration - Cratering/Single Wall Penetration
## Fish and Summers

**Reference** Frost (NASA SP-8042)

**Relationship**

$$P = K_i\, m_p^{0.352}\, \rho_p^{0.167}\, (V_p \cdot \cos(\beta))^{0.667} \quad \text{(CRATERING)}$$

where

$P$ = depth of penetration in cm

$K_i$ = material constant for semi-infinite material
= 0.42 for Al alloys
= 0.25 for 304 and 316 stainless steel

and

$V_p \cdot \cos(\beta)$ = projectile velocity normal to the surface [km/s].

$$t = K_i\, m_p^{0.352}\, \rho_p^{0.167}\, (V_p \cdot \cos(\beta))^{0.875} \quad \text{(PENETRATION)}$$

where

$t$ = thickness of plate penetrated [cm]

$K_i$ = material constant for penetration (pressure)
= 0.54 for visual penetration in Al alloys
= 0.57 in Al alloys
= 0.32 for 304 and 316 stainless steel
= 0.38 for 17-4 PH annealed CRES

**Limitations** $\beta < 45°$. Spherical cratering. Other variables unknown. Empirical fit to data.

**Comments** Tests indicate oblique impacts should use only the normal component of the impact velocity to calculate energy and crater volume. As the obliquity angle became large, greater than 45°, the crater becomes elongated, and at greater than 65° from the normal, the projectile primarily ricochets from the surface.

Hayashida and Robinson found that this equation and the JSC Cour-Palais equations gave adequate predictions of independent aluminum impact test data. Fish-Summers was the most conservative.

## Penetration - Cratering/Single Wall Penetration
## JSC (Modified Cour-Palais)

**Reference** Christiansen 1981

**Relationship**

$$p = 5.24\, d_p^{19/18} \cdot BH^{-.25} \cdot \left(\frac{\rho p}{\rho t}\right)^{0.5} \left(\frac{V_p \cdot \cos(\beta)}{C}\right)^{0.667}$$

where

$p$ = depth of penetration [cm]

$C$ = speed of sound in target [km/s]

$= \sqrt{E_t/\rho_t}$

$BH$ = Brinell Hardness for target.

$V_p \cdot \cos(\beta)$ = projectile velocity normal to the surface [km/s]

$t_{pen} = 1.8 \cdot p$ (PENETRATION)

$t_{spall} = 2.2 \cdot p$ (SPALL)

where

$t$ = thickness of plate penetrated or spalled [cm]

**Limitations** $\beta < 45°$. Spherical cratering. Other variables unknown. Empirical fit to data.

**Comments** Tests indicate oblique impacts should use only the normal component of the impact velocity to calculate energy and crater volume. As the obliquity angle became large, greater than 45°, the crater becomes elongated, and at greater than 65° from the normal, the projectile primarily ricochets from the surface.

Hayashida and Robinson found that this equation and the Fish-Summers equations gave adequate predictions of independent aluminum impact test data. Fish-Summers was the most conservative.

## Penetration - Multisheet Fragment Penetration
## Penetration and Dispersion Angle - Burch

**Reference** Burch[67]

**Relationship** $N_o$ = Number of sheets penetrated following the first sheet.

$$= \left(\frac{V}{C}\right)^{-4/3} \cdot \left(\frac{t_2}{D}\right)^{-7/12} \cdot \left(\frac{S_1}{D}\right)^{-5/12} f\left(\frac{t_1}{D}\right)$$

where

$$f\left(\frac{t_1}{D}\right) = 2.42 \cdot \left(\frac{t_1}{D}\right)^{-1/3} + 4.26 \cdot \left(\frac{t_1}{D}\right)^{+1/3} - 4.18$$

C = speed of sound in first sheet (16,650 f/s in aluminum)

S1 is the distance between the first and second sheets. Subsequent sheets are the same thickness as the second sheet. To equate the number of sheets of thickness "b" to sheets of thickness "a" use the following formula.

$$n_b \cdot (t_b)^{7/12} = n_a \cdot (t_a)^{7/12}$$

For oblique impacts the number of sheets after the first sheet, $N_f$, penetrated along the flight path was:

$$N_f = N_o + 0.63 \cdot f(\beta, t_1/D) \cdot \left(\frac{V}{C}\right)^{-4/3} \cdot \left(\frac{t_2}{D}\right)^{-7/12} \cdot \left(\frac{S_1}{D}\right)^{-5/12}$$

where

$$f(\beta, t_1/D) = \{0.5 - 1.87 \cdot \left(\frac{t_1}{D}\right)\} + \{5 \cdot \left(\frac{t_1}{D}\right) - 1.6\} \cdot \chi + \{1.7 - 12 \cdot \left(\frac{t_1}{D}\right)\} \cdot \chi$$

$$\text{for } \left(\frac{t_1}{D}\right) \leq 0.32;$$

$$= -(0.6 + 0.8 \cdot \chi^{-3}) \quad \text{for } \left(\frac{t_1}{D}\right) = 0.64$$

$$\chi = (\tan\beta - 0.5)$$

For oblique impacts the number of sheets after the first sheet, $N_n$, penetrated normal to the bumper was:

$$N_n = [0.32\cdot\left(\frac{t_1}{D}\right)^{5/6} + 0.48\cdot\left(\frac{t_1}{D}\right)^{1/3}\cdot\sin^3(\beta)]\cdot\left(\frac{V}{C}\right)^{-4/3}\cdot\left(\frac{D}{t_2}\right)$$

The major damage diameter, $D_{90}$, for aluminum on aluminum impacts was expressed as:

$$\left(\frac{D_{90}}{D}\right) = \left(\frac{t_1}{D\cdot\cos(\beta)}\right)^{1/4}\cdot\left(\frac{S_l}{D\cdot\cos(\beta)}\right)^{1/2}\cdot\lambda$$

where

$$\lambda = 5.55\cdot V\cdot\cos(\beta)/C - 2.52 \qquad \text{for } 0.6 \le V\cdot\cos(\beta)/C \le 1.05$$

$$= 1.56\cdot V\cdot\cos(\beta)/C + 1.66 \qquad \text{for } 1.05 \le V\cdot\cos(\beta)/C$$

and this was independent of second sheet material.

The equation for major spray diameter was

$$\left(\frac{D_{MS}}{D}\right) = \left(\frac{t_1}{D\cdot\cos(\beta)}\right)^{1/4}\cdot\left(\frac{S_l}{D\cdot\cos(\beta)}\right)^{1/2}\cdot\lambda_{MS}$$

where

$$\lambda_{MS} = 3.12\cdot V/C + 3.32 \qquad \text{for } 0.6 \le V\cdot\cos(\beta)/C \le 1.05$$

**Limitations**

The models were appropriate between 0.6 and 1.3 times the speed of sound.

## Penetration - Whipple Bumper
## Nysmith

**Reference** Nysmith[69]

**Relationship** The Ballistic Limit Velocity (km/s) is given by

$$V = 2.88 \cdot 10^{-3} \cdot \left(\frac{t_b}{d}\right)^{1.9} \cdot \left(\frac{t_{rw}}{d}\right)^{3.6} \cdot \left(\frac{S}{d}\right)^{5}$$

and also

$$V = 7.8 \cdot 10^{-5} \cdot \left(\frac{t_b + t_{rw}}{d}\right)^{5.5} \cdot \left(\frac{S}{d}\right)^{5}$$

(All terms are defined in the glossary.)

**Limitations** Developed by pyrex-glass spheres (2.23 g/cm$^3$) to simulate meteoroids. Tests up to 8.8 km/s. Targets were

$0.81 \text{ mm} \le t_b \le 1.24 \text{ mm}$

$1.63 \text{ mm} \le t_{rw} \le 3.18 \text{ mm}$

$17.5 \text{ mm} \le S \le 42.9 \text{ mm}$

**Comments** By combining the two equations Nysmith found the optimum ratio of bumper to rear wall thickness was 0.35.

## Penetration - Whipple Bumper
## Modified Cour-Palais Equations

**Reference** Christiansen [93]

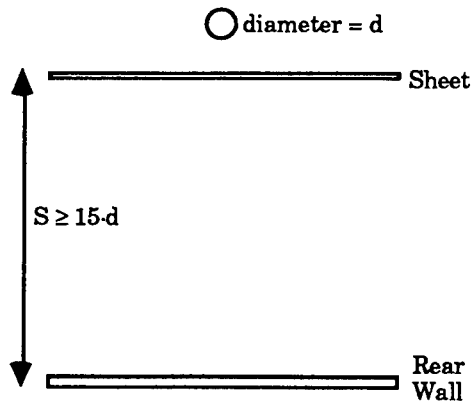


**Relationship** The critical diameter, $d_p$, to penetrate a given shield is

$$d_p = 3.918\, t_{rw}^{2/3} \cdot \rho_b^{-1/9} \cdot \rho_p^{-1/3} \cdot (V_p \cdot \cos(\beta))^{-2/3} \cdot S^{1/3} \cdot (\sigma_y/70)^{1/3}$$

for $V_n > 7$ km/s

$$= \left(\frac{t_{rw} \cdot \sqrt{\sigma_y/40} + t_b}{1.248 \cdot \rho_p^{0.5} \cos(\beta)}\right)^{\frac{18}{19}} \cdot (1.75 - V_n/4) +$$

$$(1.071 \cdot t_{rw}^{2/3} \cdot \rho_b^{-1/9} \cdot \rho_p^{-1/3} \cdot S^{1/3} \cdot (\sigma_y/70)^{1/3}) \cdot (V_n - 3)/4$$

for 3 km/s $< V_n <$ 7 km/s

$$= \left(\frac{t_{rw} \cdot \sqrt{\sigma_y/40} + t_b}{0.6 \cdot \rho_p^{0.5} \cdot V_n^{2/3} \cdot \cos^{5/3}(\beta)}\right)^{\frac{18}{19}} \quad \text{for } V_n < 3 \text{ km/s}$$

Above 65° obliquity the critical diameter is set to the 65° critical diameter.

$V_n = V_p \cdot \cos(\beta)$

= projectile velocity normal to the surface [km/s]

$S$ = Total spacing [cm]

and

$\sigma_y$ = rear wall yield strength (NB: standard units) [ksi]

The minimum design requirements for the above equations to be applicable are

$$t_b = c_b \cdot m_p/\rho_b = c_b \cdot d_p \cdot \rho_p/\rho_b$$

where

$$c_b = 0.25 \quad \text{when } S/d < 30$$
$$= 0.20 \quad \text{when } S/d \geq 30$$

$$t_w = c_w \cdot d^{0.5} \cdot (\rho_p \cdot \rho_b)^{1/6} \cdot M^{1/3} \cdot V_n/S^{0.5} \cdot (70/\sigma_y)^{0.5}$$

where

$$c_w = 0.16 \text{ cm}^2 \cdot \text{sec}/g^{2/3} \cdot \text{km}$$

**Limitations**

$S/d_p > 15$; above provisions on minimum bumper thickness.

**Comments**

The equation assumes constant initial projectile energy to penetrate. The low velocity equations provide a very compact alternate to the BUMPERII equations developed from the THOR equations. The 3 to 7 km/s regime is an interpolation between the low velocity equation and Christiansen's high velocity equation.

## Penetration - Nextel/Kevlar Intermediate Shield
## Enhanced Shield Equations

**Reference** Christiansen et al [92b]

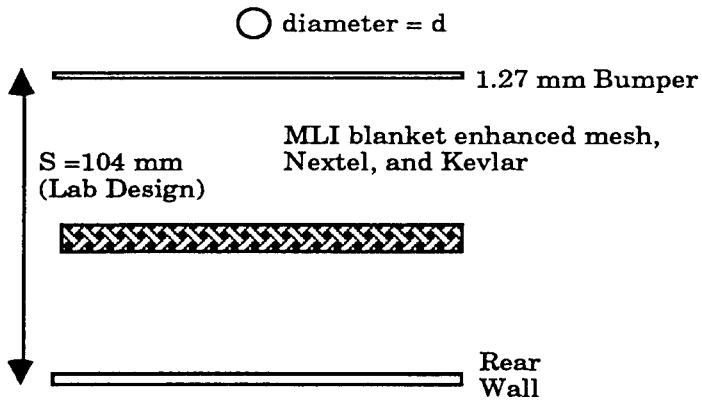


**Relationship** The critical diameter, $d_p$, to penetrate a given shield is

$$d_p = 0.62\,(t_{rw}\cdot\rho_{rw})^{1/3}\cdot\rho_p^{-1/3}\cdot V_p^{-1/3}\cdot\cos^{-1/2}(\beta)\cdot S^{2/3}\cdot(\sigma_y/40)^{1/6}$$

for $V\cdot\cos^{1/3}(\beta) > 6.5$ km/s

$$= 1.031\cdot\rho_p^{-1/2}\cdot[t_{rw}\cdot(\sigma_y/40)^{1/2}+0.37\cdot m_b]\cdot\cos^{-4/3}(\beta)$$

$$\cdot\{[6.5\cdot\cos^{-1/3}(\beta)-V]/[6.5\cdot\cos^{-1/3}(\beta)-2.7\cdot\cos^{-1/2}(\beta)]\}$$

$$+\ 0.332\cdot(t_{rw}\cdot\rho_{rw})^{1/3}\cdot\rho_p^{-1/3}\cdot\cos^{-7/18}(\beta)\cdot S^{2/3}\cdot(\sigma_y/40)^{1/6}$$

$$\cdot\{[V-2.7\cdot\cos^{-1/2}(\beta)]/[6.5\cdot\cos^{-1/3}(\beta)--2.7\cdot\cos^{-1/2}(\beta)]\}$$

for $2.7/\cos^{1/2}(\beta)$ km/s $< V < 6.5/\cos^{1/3}(\beta)$ km/s

$$= 2\left(\frac{t_{rw}\cdot\sqrt{\sigma_y/40}+0.37\cdot m_b}{\rho_p^{0.5}\cdot V_n^{2/3}\cdot\cos^{5/3}(\beta)}\right)$$

for $V\cdot\cos^{1/2}(\beta) \le 2.7$ km/s

$V = V_p$

= projectile velocity normal to the surface [km/s]

$m_b$ = Areal density of all bumpers and intermediate shields [g/cm$^2$]

and

$\sigma_y$ = rear wall yield strength (NB: standard units) [ksi]

The design is shown in the sketch.

**Limitations**

For 1.3 mm bumper and intermediate shield of MLI plus $0.03 g/cm^2$ mesh; $0.3 g/cm^2$ Nextel and $0.136 g/cm^2$ Kevlar. Blanket midway between bumper and rear wall.

**Comments**

High velocity curve is constant momentum extrapolation. This is different that Wilkinson, which assumes that there is an enhanced dispersion angle for smaller projectiles at higher velocities.

## Penetration - Multishock

## Modified Cour-Palais Multi-Shock

**Reference** Christiansen 1992

**Relationship** The critical diameter, $d_p$, to penetrate a given shield is

$$d_p = 0.354\, t_{rw}^{1/3} \cdot \rho_{rw}^{1/3} \cdot \rho_p^{-1/3} \cdot (V_p \cdot \cos(\beta))^{-1/3} \cdot S^{2/3} \cdot (40/\sigma_y/40)^{1/6}$$

for $V_n > 6$ km/s

$$= \left( \frac{t_{rw} \cdot \sqrt{\sigma_y/40} + 0.37 \cdot m_b}{0.624 \cdot \rho_p^{0.5} \cos(\beta)} \right)^{\frac{18}{19}} \cdot (2 - V_n/3) +$$

$$(0.1948 \cdot t_{rw}^{1/3} \cdot \rho_{rw}^{1/3} \cdot \rho_p^{-1/3} \cdot S^{2/3} \cdot (\sigma_y/40)^{1/6}) \cdot (V_n/3 - 1)$$

for 3 km/s $< V_n <$ 6 km/s

$$= \left( \frac{t_{rw} \cdot \sqrt{\sigma_y/40} + 0.37 \cdot m_b}{0.3 \cdot \rho_p^{0.5} \cdot V_n^{2/3} \cdot \cos(\beta)} \right)^{\frac{18}{19}} \quad \text{for } V_n < 3 \text{ km/s}$$

The design is defined by:

$$m_b = 0.19\, m_p = 0.19 \cdot d_p \cdot \rho_p$$

$$m_{rw} = 43.1 \cdot M_p \cdot V_n / S^2 \cdot \sqrt{40/\sigma_y}$$

where

$m_b$ = required total areal density of four bumper layers of alumina-boro-silica ceramic cloth (Nextel by 3M) [g/cm$^2$]

$m_p$ = areal density projectile [g/cm$^2$]

$m_{rw}$ = required areal density aluminum rear wall [g/cm$^2$]

$M_p$ = projectile mass [g]

$V_n$ = $V_p \cdot \cos(\beta)$

= projectile velocity normal to the surface [km/s]

$S$ = Total spacing with each layer located successively at one quarter of the total spacing [cm]

and

$\sigma_y$ = rear wall yield strength (NB: standard units) [ksi]

**Limitations** $S/d_p > 15$; with the stated provisions on minimum bumper thickness.

**Comments** Tested with aluminum projectiles to 0.32 cm. Primary weight savings is in rear wall required to stop a given threat particle. The required bumper thickness is not reflected in the rear wall equations. The rear wall equation accounts for strength but not for ductility, which may be more important.

## Penetration - Mesh Double-Bumper
## Christiansen Equations

**Reference** Christiansen 1992

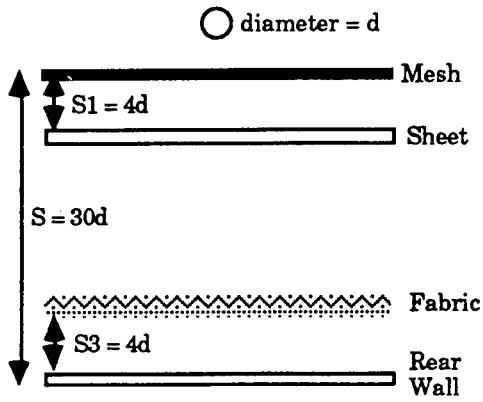


**Relationship** The critical diameter, $d_p$, to penetrate a given shield is

$$d_p = 0.38\, t_{rw}^{1/3} \cdot \rho_{rw}^{1/3} \cdot \rho_p^{-1/3} \cdot (V_p \cdot \cos(\beta))^{-1/3} \cdot S^{2/3} \cdot (\sigma_y/40)^{1/6}$$

for $V_n > 6$ km/s

$$= \left( \frac{t_{rw} \cdot \sqrt{\sigma_y/40} + 0.37 \cdot m_{b+I}}{0.83 \cdot \rho_p^{0.5} \cos(\beta)} \right)^{\frac{18}{19}} \cdot (2 - V_n/3) +$$

$$(0.209 \cdot t_{rw}^{1/3} \cdot \rho_{rw}^{1/3} \cdot \rho_p^{-1/3} \cdot S^{2/3} \cdot (\sigma_y/40)^{1/6}) \cdot (V_n/3 - 1)$$

for 3 km/s $< V_n <$ 6 km/s

$$= \left( \frac{t_{rw} \cdot \sqrt{\sigma_y/40} + 0.37 \cdot m_b}{0.4 \cdot \rho_p^{0.5} \cdot V_n^{2/3} \cdot \cos(\beta)} \right)^{\frac{18}{19}} \quad \text{for } V_n < 3 \text{ km/s}$$

Optimum design parameters:

$m_1 = c_1 \cdot d_p \cdot \rho_p$ (where $0.035 < c_1 < 0.057$)

= required total areal density of fine aluminum mesh first part of bumper [g/cm$^2$]

$m_2 = 0.93 \cdot d_p \cdot \rho_p$

= required total areal density of aluminum plate second part of bumper at spacing $S_1 = 4 \cdot d_p$ from first bumper [g/cm$^2$]

$m_3 = c_3 \cdot d_p \cdot \rho_p$

= required total areal density of intermediate catcher cloth (Nextel, Spectra or Kevlar) at spacing $S_3 = 4 \cdot d_p$ in front of rear wall [g/cm$^2$]

$c_3$ = 0.095 for Nextel

$c_3$ = 0.064 for Kevlar or Spectra

$m_{rw} = 34.8 \cdot M_p \cdot V_n / S^2 \cdot \sqrt{40/\sigma_y}$

where

$m_{rw}$ = required areal density aluminum rear wall [g/cm$^2$]

$m_{b+I}$ = total areal density of mesh, sheet and fabric [g/cm$^2$]

$M_p$ = projectile mass [g]

$V_n = V_p \cdot \cos(\beta)$

= projectile velocity normal to the surface [km/s]

$S = 30 \cdot d_p$

= Optimum total spacing [cm]

and

$\sigma_y$ = rear wall yield strength (NB: standard units) [ksi]

**Limitations** $S/d_p > 15$; the stated provisions on minimum bumper thickness

**Comments** Tested with aluminum projectiles to 0.32 cm. Primary weight savings is in rear wall required to stop a given threat particle. The rear wall equation accounts for strength but not for ductility, which may be more important.

## Penetration - Dispersion Angle

## Dispersion Angle - Wilkinson

**Reference** Wilkinson

**Relationship** $\theta$ = Average cone angle of debris cloud (Note: "Average" is defined below with a limiting condition and modifications defined in the comments.)

$$\theta = \arctan\left(0.6 \cdot \frac{\rho_b \cdot t_b}{\rho_p \cdot d_p}\right) \quad \text{for } \left(\frac{\rho_b \cdot t_b}{\rho_p \cdot d_p}\right) < 1$$

$$\theta = \arctan(0.6) = .54 \text{ rad} = 31° \quad \text{for } \left(\frac{\rho_b \cdot t_b}{\rho_p \cdot d_p}\right) \geq 1$$

where

$\rho_b$, $t_b$, $\rho_p$, and $d_p$ are the density and thickness of the bumper and projectile respectively.

$$\tan\theta = \frac{1}{S} \cdot \frac{\int_0^\infty r^2 \cdot D(r)dr}{\int_0^\infty r \cdot D(r)dr}$$

where

$D(r)$ = the momentum intensity distribution

and

$S$ = Spacing of bumper to location of $D(r)$.

The standard deviation of the momentum intensity distribution is given as:

$$\Delta = (2/\pi)^{1/2} \cdot S \cdot \tan(\theta)$$

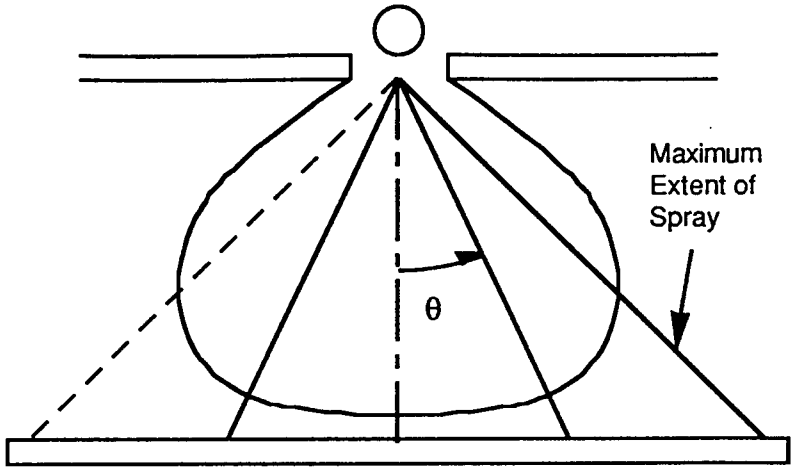


**Limitations** Based on hydrocode calculations in vaporization regime, as well as cadmium-on-cadmium tests at 6 to 7 km/s.

**Comments** Wilkinson's equation is based on vaporization, which is not appropriate to all space debris impacts. Average cone angle contains most of the mass but not all. If the momentum distribution is a step function, 1 inside $r_0$ and 0 outside of $r_o$, then $\tan\theta = 2/3 \cdot (r_o / S)$.

Elfer used 0.475 instead of 0.6 in the equation to correlate momentum failures at 6 to 7 km/s with aluminum projectiles on aluminum bumpers with Kevlar intermediate shields. This modification is probably appropriate up to 12 to 14 km/s when more aluminum-on-aluminum impacts will transition from predominantly liquid to vapor, thus increasing the dispertion angle to the original Wilkinson equation.

## Penetration Mechanics - Momentum Failure
## Wilkinson Equation with Modifications

**Reference** Wilkinson, modifications by Elfer [77] and Bjorkman [91]

**Relationship** For penetration to occur:

$$m_p V = 1.44 \cdot c_2 (\xi/c_2)_a \cdot m_2 \cdot S^2 \quad \text{for} \left(\frac{\rho_b \cdot t_b}{\rho_p \cdot d_p}\right) \geq 1$$

or

$$m_p V \rho_p d_p = 1.44 \cdot c_2 \left(\frac{\xi}{c_2}\right)_a \cdot m_2 \cdot S^2 \cdot m_1 \quad \text{for} \left(\frac{\rho_b \cdot t_b}{\rho_p \cdot d_p}\right) \geq 1$$

where

$c_2$ = speed of sound in the rear wall

$m_2$ = $\rho_{rw} \cdot t_{rw}$

$m_1$ = $\rho_b \cdot t_b$

and

$\left(\frac{\xi}{c_2}\right)_a$ = $f(\varepsilon_{max}, E/\sigma_y)$ given in the figure:

**Limitations** Assumes Wilkinson dispersion angle. Assumes rear wall loading can be modeled as a Gausian momentum intensity distribution. Assumes $\Delta/t_{rw} > 20$, and that the strain to failure is independent of $\Delta/t_{rw}$, where $\Delta$ is the standard deviation of the momentum intensity distribution given previously.

**Comments** Wilkinson assumed vaporization, and did not include loading rate effects in the rear wall, such as spall.

Elfer [88] and Bjorkman [91] suggested revising the critical projectile diameter to 80 percent of the original Wilkinson equation prediction, consistent with the observed critical diameters using intermediate shields. Elfer suggested this was due to a lower dispersion angle, caused by melting rather than vaporization of the projectile. Schmidt's cadmium-on-cadmium tests [94] did not show a change in the shape of the cloud with the transition from melting to vaporization, although there may be a different mass distribution within the cloud to account for the dramatic increase in penetration resistance. Bjorkman suggested the modification based on elastic

rebound. 100% rebound was not observed with intermediate shields or with Schmidt's tests which had vaporization.

For 2219-T87 using the normal strain rate room temperature typical yield strength, $E/\sigma_y$ = (72.4GPa/395MPa) = 184. The typical strain to failure is only 10 percent. This gives $(\xi/c_2)_a$ approximately 0.8 km/s. A uniaxial flow stress of 485 MPa and 30% strain to failure were measured at UDRI using a tensile Hopkinson bar at a strain rate of $10^3$ [Rajendran]. Using this flow stress $E/\sigma_y$ = 149, and a using a strain to failure of 25% percent, gives $(\xi/c_2)_a$ closer to the value of 0.27 km/s used by BUMPER and BUMPERII. Under biaxial load conditions, the effective flow stress will increase further, but the strain to failure will decrease.

It can be seen that a 10% improvement in the strain to failure should give a 25% improvement in the momentum that can be absorbed. However, for a 20% improvement in strength momentum absorption capability will increase by only about 10%. This is qualitatively consistent with the improvement seen in using 5456-H116 compared to 2219-T87 [Elfer]. When tested by UDRI at a high strain rate, 5456 showed similar strength to the 2219-T87 results mentioned in the preceding paragraph.

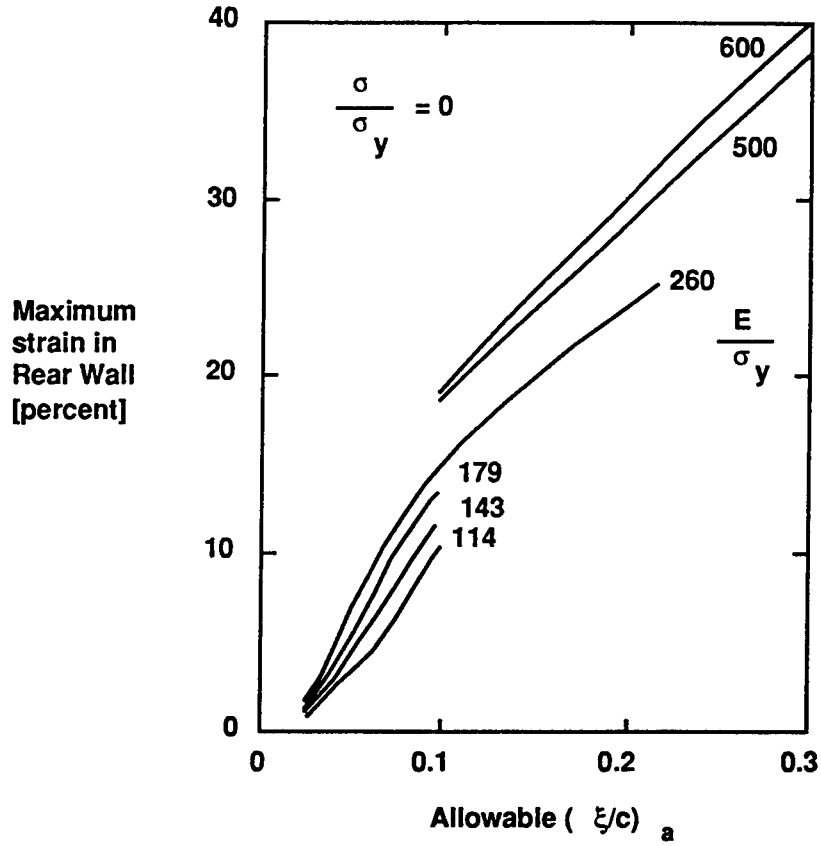


Figure - Wilkinson failure criteria, $(\xi/c_2)_a$ , in km/s.

## Penetration Mechanics - Momentum Failure
## Grove and Rajendran

**Reference** Grove [Appendix D]

**Relationship** For penetration to occur:

$$\gamma \geq -7.71338 \cdot 10^{-3} + 2.64191 \cdot 10^{-2} \cdot \varepsilon + 3.61467 \cdot 10^{-3} \cdot \varepsilon^2 - 1.24587 \cdot 10^{-4} \cdot \varepsilon^3 + 1.74572 \cdot 10^{-6} \cdot \varepsilon^4$$

where

$\varepsilon$ = effective rear wall strain at failure in percent

$\gamma$ = dimensionless parameter

$= \xi^2 \cdot \rho_{rw} \cdot e^{(t_{rw}/\Delta)} / \sigma_y$

$\xi = m_p \cdot V / \{4 \cdot \rho_{rw} \cdot t_{rw} \cdot S^2 \cdot \tan^2(\theta)\}$ (as in Wilkinson)

$\Delta = \sqrt{2/\pi} \cdot S \cdot \tan(\theta)$ (as in Wilkinson)

and

$\theta$ = Wilkinson dispersion angle (although Wilkinson constant of 0.6 may be adjusted as necessary.)

Alternative formula for $\varepsilon$ as a function of $\gamma$.

$$\varepsilon = 1.01152 + 18.295 \cdot \gamma - 2.35542 \cdot \gamma^2 + 0.113756 \cdot \gamma^3$$

**Limitations** Assumes rear wall loading can be modeled as a Gausian momentum intensity distribution. Assumes Wilkinson dispersion angle or a modification.

**Comments** Curve fit to maximum strain as a function of the dimensionless parameter, $\gamma$. To use as a ballistic limit equation solve for the mass of the projectile as a function of the other variables. For 2219-T87 aluminum, a critical strain of 0.2 (20%) was found to be appropriate from Hopkinson bar tensile tests.

## Penetration Mechanics - Momentum Failure
## Housen and Schmidt

**Reference**

Housen and Schmidt [95]

**Relationship**

For penetration to occur (aluminum-on-aluminum):

$$\frac{d}{t_b} \geq A + B\cdot\exp[-0.17(V\cdot\cos\beta - 7.5)^2] + C\cdot\exp[0.3\cdot V\cdot\cos\beta]$$

where

$$A(\pi_1) = \begin{cases} 0.87\cdot\pi_1^{0.157} & \pi_1 \leq 1.6\cdot10^4 \\ 0.218\cdot\pi_1^{0.3} & \pi_1 > 1.6\cdot10^4 \end{cases}$$

$$B(\pi_1) = \begin{cases} 0.003\cdot\pi_1^{0.624} & \pi_1 \leq 7000 \\ 0.75 & \pi_1 > 7000 \end{cases}$$

$$C(\pi_1) = \begin{cases} 0.001 & \pi_1 \leq 2000 \\ 2.17\cdot10^{-7}\cdot\pi_1^{1.11} & 7000 \leq \pi_1 \leq 1.6\cdot10^4 \\ 3.8\cdot10^{-3}\cdot\pi_1^{0.1} & \pi_1 > 1.6\cdot10^4 \end{cases}$$

and

$$\pi_1 = t_{rw}\cdot S^2/t_b$$

**Limitations**

7 km/s < V < 18km/s and $500 < \pi_1 < 10^5$

**Comments**

Empirical fit to cadmium-on-cadmium tests using a 3.1 velocity scaling factor. The diameter to penetrate increases between approximately 12 and 18 km/s. This is due to the transition from liquid to vapor in the debris cloud, and is comparable to a shift between modified Wilkinson and normal Wilkinson. Note that while the simulation has the correct debris cloud shape and momentum, the rate of momentum transfer to the rear wall is also 3.1 times slower than for an aluminum-on-aluminum impact. This effectively distributes the momentum over a larger area using Cd-on-Cd instead of Al-on-Al. This could overestimate the diameter to penetrate.

(Continued next page)

For penetrations below 3 km/s, Housen and Schmidt recommend Christiansen's Whipple shield equation and then they give a linear interpolation between this 3 and 7 km/s using a similar procedure as Christiansen. The equation is:

$d_p$ = Critical diameter to penetrate a given shield [cm]

$$= 0.5 \cdot \left( \frac{t_{rw} \cdot 1.14 + t_b}{\cos(\beta)} \right)^{\frac{18}{19}} \cdot (7 - V_n)/4$$

$$+ t_b \cdot (A + 0.958 \cdot B + 8.17C) \cdot (V_n - 3)/4$$

for 3 km/s < $V_n$ < 7 km/s

where all A, B, and C were previously defined.

## Fracture Mechanics - Cylinder

## Longitudinal Through Crack in a Cylinder - Tada solution

**Reference** Tada 83, Tada 85

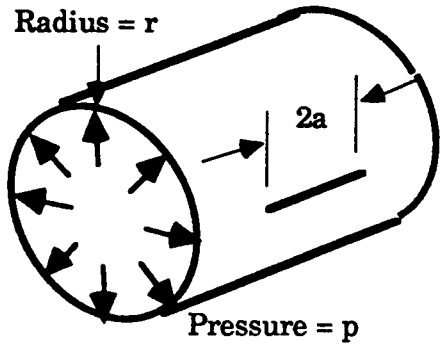


**Relationship**

K = Stress intensity.

A = Crack opening area.

$$K = \sigma \cdot \sqrt{\pi \cdot a} \cdot F(\lambda)$$

where

$$\sigma = p \cdot r/t$$

= pressure·(pressure vessel radius)/thickness

$$\lambda = a/\sqrt{r \cdot t}$$

and

$$F(\lambda) = \sqrt{1 + 1.25 \cdot \lambda^2} \quad \text{for } 0<\lambda\leq 1$$

$$= 0.6 + 0.9 \cdot \lambda \quad \text{for } 1\leq\lambda\leq 5$$

$$A = \sigma/E \cdot (2 \cdot \pi \cdot r \cdot t) \cdot G(\lambda)$$

where

$$G(\lambda) = \lambda^2 + .625 \cdot \lambda^4 \quad \text{for } 0<\lambda<1$$

$$= .14 + .36 \cdot \lambda^2 + .72 \cdot \lambda^3 + .405 \cdot \lambda^4 \quad \text{for } 1<\lambda<5$$

**Limitations** $\lambda<5$

## Fracture Mechanics - Cylinder

## Longitudinal Through Crack in a Cylinder - Folias solution

**Reference** Folias, Broeck

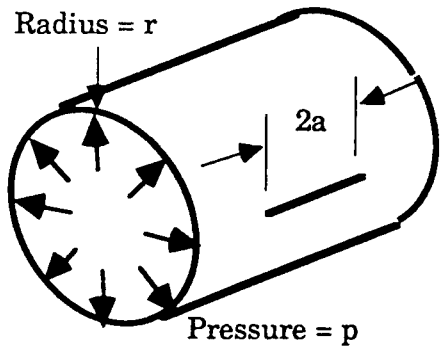


**Relationship** K = Stress intensity.

$$K = \sigma \cdot \sqrt{\pi \cdot a} \cdot M_f(\lambda)$$

where

$$\sigma = p \cdot r/t$$

$$\lambda = a/\sqrt{r \cdot t}$$

and

$$M_f(\lambda) = \sqrt{1 + 1.61 \cdot \lambda^2}$$

**Limitations** Linear elastic fracture mechanics; unknown in other terms.

**Comments**

## Fracture Mechanics - Cylinder
## Longitudinal Through Crack in a Cylinder - Plastic Zone correction by Hahn et al. to Folias solution

**Reference** Hahn et al. as referenced in Broeck

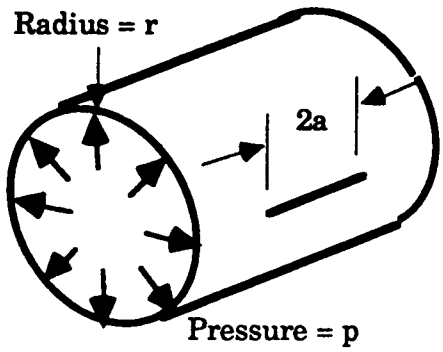


**Relationship**

$K$ = Stress intensity.

$$K = \sigma \cdot \sqrt{\pi \cdot a \cdot \phi} \cdot M_f(\lambda)$$

where

$$\sigma = p \cdot r / t$$

$$\lambda = a / \sqrt{r \cdot t}$$

$$M_f(\lambda) = \sqrt{1 + 1.61 \cdot \lambda^2}$$ , the Folias magnification factor.

$$\phi = 2 \cdot \left( \frac{2 \cdot \sigma_f}{\pi \cdot M_f \cdot \sigma} \right)^2 \cdot \ln \sec \left( \frac{\pi \cdot M_f \cdot \sigma}{2 \cdot \sigma_f} \right)$$

and

$\sigma_f$ = the effective yield or flow stress

$\approx (\sigma_{yield} + \sigma_{ult}) / 2$ .

**Limitations** Unknown.

**Comments** Verified for a variety of tough materials [Hahn et al.] including aluminum pressure vessels. [Anderson] The plastic zone correction only gives a 6% increase in K for $\sigma_f/\sigma = 6$ and $M_f = 3$.

## Fracture Mechanics - Cylinder

## Longitudinal Through Crack in a Cylinder - Zahoor solution

**Reference** Zahoor 89

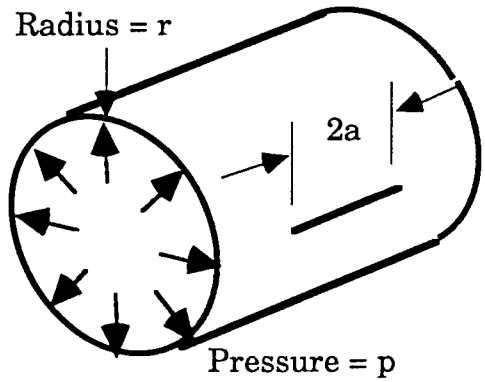


**Relationship** K = Stress intensity.

$$K = \sigma \cdot \sqrt{\pi \cdot a} \cdot M(\lambda)$$

where

$$\sigma = p \cdot r/t$$

$$\lambda = a/\sqrt{r \cdot t}$$

and

$$M(\lambda) = 1 + .72449 \cdot 10^{-2} \cdot \lambda + 0.64856 \cdot \lambda^2 - 0.2327 \cdot \lambda^3 + 3.8154 \cdot 10^{-2} \cdot \lambda^4 - 2.3487 \cdot 10^{-3} \cdot \lambda^5$$

**Limitations** $\lambda \leq 5$.

**Comments** Accuracy within 1% of [Erdogan and Kibler 69].

## Fracture Mechanics - Cylinder
## Longitudinal Through Crack in a Cylinder - Zahoor limt load solution

**Reference** Zahoor 89

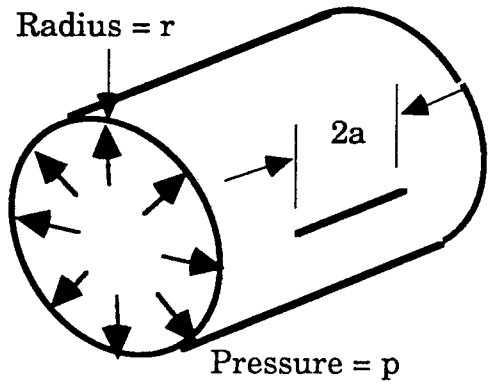


**Relationship** $p_l$ = limit pressure.

$$p_l = \sigma_f \cdot (t/R) \cdot M(\lambda)$$

where

$\sigma_f$ = reference stress (average of yield and ultimate)

$$\lambda = a/\sqrt{r \cdot t}$$

and

$$M(\lambda) = [1 + 1.2987\lambda^2 - 0.026905 \cdot \lambda^4 + 5.3549 \cdot 10^{-4} \cdot \lambda^6]^{0.5}$$

**Limitations** $0 \le \lambda \le 5$.

**Comments** Empirical solution.

## Fracture Mechanics - Cylinder

## Longitudinal Through Crack in a Cylinder-Newman solution

**Reference** Newman 76; Forman

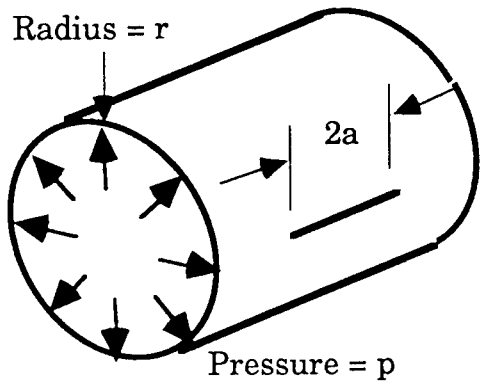


**Relationship** K = Stress intensity.

$$K = \sigma \cdot \sqrt{\pi \cdot a} \cdot M(\lambda)$$

where

$$\sigma = p \cdot r/t$$

$$\lambda = a/\sqrt{r \cdot t}$$

and

$$M(\lambda) = \sqrt{1 + .52 \cdot \lambda + 1.29 \cdot \lambda^2 - 0.074 \cdot \lambda^3}$$

**Limitations** $\lambda \leq 10$.

**Comments** TC07 in FLAGRO 2.0.

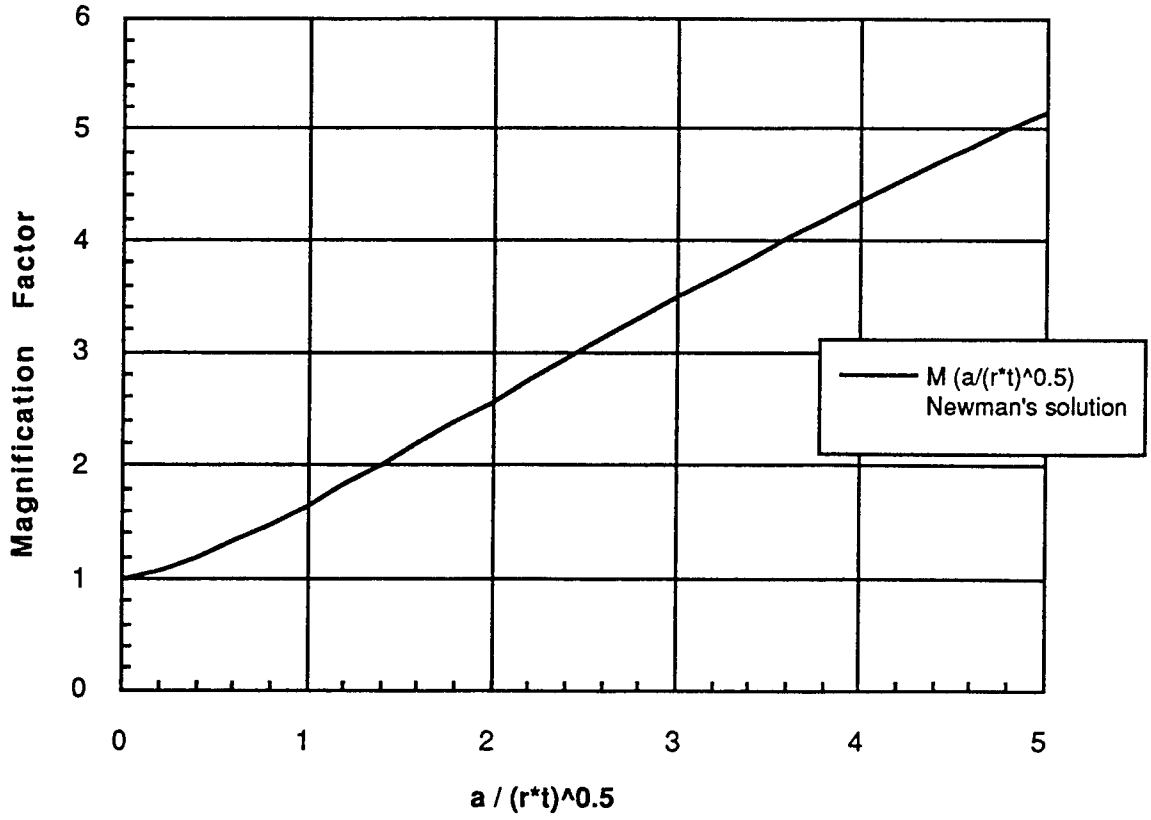
6
5
4
3
2
1
0
Magnification Factor
0
1
2
3
4
5
a / (r*t)^0.5
M (a/(r*t)^0.5)
Newman's solution

## Fracture Mechanics - Cylinder

## Longitudinal Through Crack in a Cylinder - Depressurized Area at Center of Crack (or Hole at center of crack)

**Reference** Elfer, Groove and Rajendran.

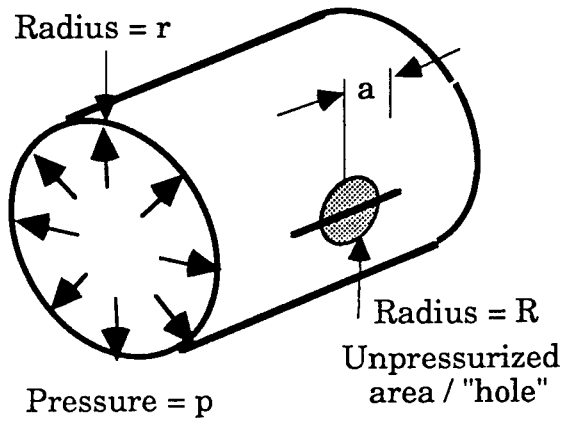


**Relationship** K = Stress intensity.

$$K = \sigma \cdot \sqrt{\pi \cdot a} \cdot M_n(\lambda) \cdot (M_h/M_f)$$

where

$$\sigma = p \cdot r/t$$

$$\lambda = a/\sqrt{r \cdot t}$$

and

$$M_n(\lambda) = \sqrt{1 + .52 \cdot \lambda + 1.29 \cdot \lambda^2 - 0.74 \cdot \lambda^3}$$

= Newman Magnification factor

$$M_f = \sqrt{1 + 1.61 \cdot a^2/(r \cdot t)}$$

= Folias Magnification factor

$M_h = \sqrt{1 + 1.61 \cdot a \cdot (a-R)/(r \cdot t)}$

= Folias modified for a hole (depressurized area)

2a = crack tip to crack tip distance

and

R = Radius of hole (depressurized area)

**Limitations** Unknown. Newman magnification factor limited to $\leq 10$. Estimate $a/r \geq 1.2$ due to modeling of hole as a depressurized zone.

**Comments** A hole was modeled as an unpressurized area and this will not be accurate as the size of the unpressurized area approaches the flaw length. If used to model a petalled hole, the pressure on the inward turned petals should also be considered. This may be used to model hydraulic ram effects by superposition.

## Fracture Mechanics - Cylinder
## Uniform Membrane Load Through Crack in a Cylinder
## - Zahoor solution

**Reference** Zahoor 89

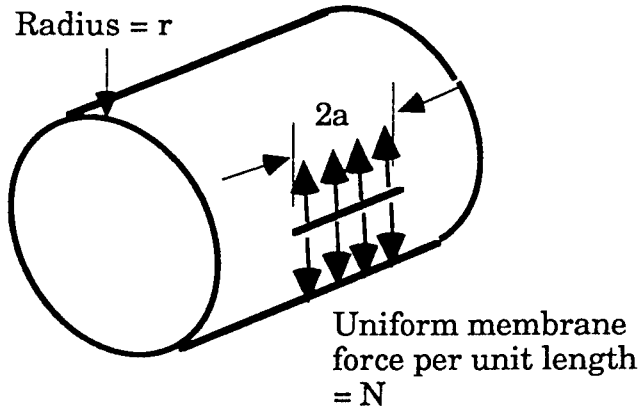


**Relationship**

$K$ = Stress intensity.

$$K = \sigma \cdot \sqrt{\pi \cdot a} \cdot ( M_m(\lambda) + (2 \cdot z/t) \cdot M_b(\lambda) )$$

where

$\sigma$ = $N/t$

$N$ = uniform membrane force per unit length

$\lambda$ = $a/\sqrt{r \cdot t}$

$z$ = $+t/2$ at outer surface

= $-t/2$ at innersurface

$M_m(\lambda)$ = Membrane component magnification factor

$$= 1 + .72449 \cdot 10^{-2} \cdot \lambda + 0.64856 \cdot \lambda^2 - 0.2327 \cdot \lambda^3 + 3.8154 \cdot 10^{-2} \cdot \lambda^4 - 2.3487 \cdot 10^{-3} \cdot \lambda^5$$

and

$M_b(\lambda) =$ bending component magnification factor

$$= .36811 \cdot \lambda + 0.067692 \cdot \lambda^2 - 0.14558 \cdot \lambda^3 + .036931 \cdot \lambda^4 - 3.0961 \cdot 10^{-3} \cdot \lambda^5$$

**Limitations** $\lambda \leq 5$.

**Comments** Accuracy within 1% of [Erdogan and Kibler 69].

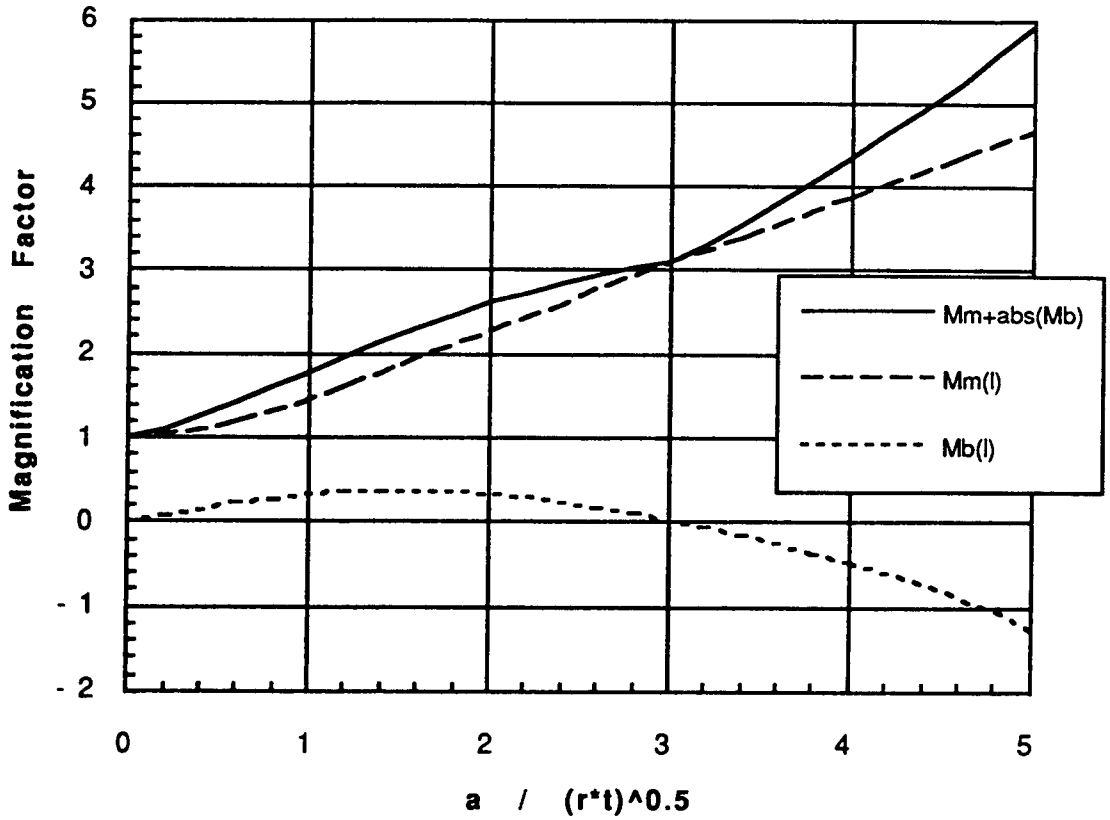

**Fracture Mechanics - Through crack in a Cylinder**
**Wedge loads on a Longitudinal Through Crack-**
**- Influence function by Elfer**

**Reference** Elfer92

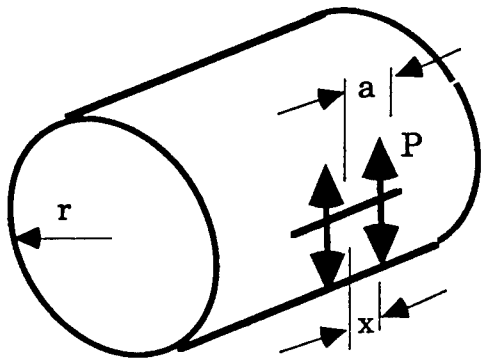


P typ 4 places

**Relationship** $K_I$ = Stress intensity at either crack tip due to wedge loads P at ±x.

$$K_I/P = \left(\frac{\sqrt{\pi \cdot a}}{(a \cdot t)}(M_{cyl}(\lambda)-1) \cdot h_{cyl}(x) + H_{plate}(x)\right)$$

where

$$M_{cyl}(\lambda) = \sqrt{1 + .52 \cdot \lambda + 1.29 \cdot \lambda^2 - 0.74 \cdot \lambda^3}$$

$$\lambda = a/\sqrt{r \cdot t}$$

$$h_{cyl}(x) = (1.269 - 0.070 \cdot y - 0.235 \cdot y^2 - 0.623 \cdot y^3)$$

$$y = x/a$$

$$H_{plate} = 2 \cdot \sqrt{a} / \sqrt{\pi \cdot (a^2 - x^2)} / t$$

$P$ = load

and

$x$ = load location, $0 \le x \le a$, with symmetric load at -x.

**Limitations** Unknown. Estimated ±5%. Integrates to Newman's solution for longitudinal

**Comments** The equations are based on a curve fit to NASTRAN symmetric wedge load solutions for 14.6 and 29.8 cm half crack lengths in a cylinder with thickness of 2.54*0.125 cm and a radius of 2.13 m. The equation uses Broeck's [82] solution for a flat plate and it integrates to the FLAGRO solution [Newman76].

## Fracture Mechanics - Sphere

## Through Crack in a Sphere - Tada solution

**Reference** Tada 85

**Relationship**

K = Stress intensity.
A = Crack opening area.

$$K = \sigma \cdot \sqrt{\pi \cdot a} \cdot F(\lambda)$$

where

$$\sigma = p \cdot r/(2 \cdot t)$$

$$\lambda = a/\sqrt{(r \cdot t)}$$

and

$$F(\lambda) = (1+1.41 \cdot \lambda^2+0.04 \cdot \lambda^3)^{0.5} \quad \text{for } 0<\lambda\leq 3.$$

$$A = \sigma/E \cdot (2 \cdot \pi \cdot r \cdot t) \cdot G(\lambda)$$

where

$$G(\lambda) = \lambda^2 + .705 \cdot \lambda^4 + 0.016 \cdot \lambda^5 \quad \text{for } 0<\lambda\leq 3.$$

**Limitations** $\lambda\leq 3$. Accuracy given as 1% on K and 2% on A.

**Comments** *a* is along a great meridian.

## Fracture Mechanics - Sphere

## Through Crack in a Sphere - Erdogan and Kibler solution

**Reference** Erdogan and Kibler; Forman

**Relationship** K = Stress intensity.

$$K = \sigma \cdot \sqrt{\pi \cdot a} \cdot F(\lambda)$$

where

$$\sigma = p \cdot r/(2 \cdot t)$$

$$\lambda = a/\sqrt{(r \cdot t)}$$

and

$$F(\lambda) = (1+3 \cdot \lambda^{1.9})^{0.4} \quad \text{for } 0<\lambda\leq 3.$$

**Limitations** $\lambda \leq 3$.

**Comments** TC06 dsolution in FLAGRO 2.0

## Fracture Mechanics - Infinite plate.
## Infinite plate with radiating cracks - Tada solution

**Reference** Tada 85 (21.12)

**Relationship** K = Stress intensity.

$$K = \sigma \cdot \sqrt{\pi \cdot a} \cdot F_A(n)$$

where

$$F_A(n) = (1/\sqrt{n}) \cdot (3 - 3.25 \cdot n^{-1} - .64 \cdot n^{-2} + 1.6 \cdot n^{-3}) \quad \text{for } n \geq 1$$

$$F_A(n) \rightarrow 3/\sqrt{n} \quad \text{as } n \rightarrow \infty$$

**Limitations** Accuracy quoted as "expected to be within 1%." Infinite plate solution.

**Comments** Cracks are radial at $2\pi/n$ angle. Solution is for first crack which is normal to tensile direction. Estimated by Tada from solutions for n = 1, 2, 4, and infinity.

## Fracture Mechanics - Flat Plate
## Wedge loads - Influence function

**Reference** Broeck 82

**Relationship**

$K_{IA}$ = Stress intensity at A (+a) location.

$K_{IB}$ = Stress intensity at B (-a) location.

$$K_{IA} = P/t/\sqrt{\pi \cdot a} \cdot \sqrt{(a+x)/(a-x)}$$

and

$$K_{IB} = P/t/\sqrt{\pi \cdot a} \cdot \sqrt{(a-x)/(a+x)}$$

where

P = load

and

x = load location, $-a \le x \le a$.

Special cases

$$K_{IA,B} = P/t/\sqrt{\pi \cdot a} \quad \text{for } x = 0.$$

$$K_{IA,B} = 2 \cdot P\sqrt{a}/t/\sqrt{\pi \cdot (a^2 - x^2)}$$

for symmetric loads, P at both $\pm x$.

**Limitations** Infinite plate solution.

**Comments**

## Fracture mechanics - Infinite Plate

## Through cracks (symmetric) from a hole in a plate - Tada

**Reference** Tada, Newman 71

**Relationship**

$K = \sigma \cdot \sqrt{\pi \cdot a} \cdot F_\lambda$

$F_\lambda = (1-\lambda) \cdot F_0 + \lambda \cdot F_1$

$\lambda$ = Ratio of (stress normal to crack/stress in crack direction)

$F_0 = 0.5 \cdot (3-s) \cdot (1+1.243 \cdot (1-s)^3)$

$F_1 = 1+(1+s) \cdot (0.5+0.743 \cdot (1-s)^2)$

$s = a / (R+a)$

and

$R$ = Radius of hole.

**Limitations** Unknown.

**Comments** Tada solution includes additional mode 3 loading, which is not included here. As $s \rightarrow 0$, $F1 \rightarrow 2.243$ and $F2 \rightarrow 3.365$.

## Fracture mechanics - Flat Plate
## Through crack from a hole in a plate - FLAGRO

**Reference** Forman

**Relationship**

$$K = \sigma \cdot \sqrt{\pi \cdot a} \cdot F_0$$

$$F_0 = G_0 \cdot G_W$$

$$G_0 = 0.7071 + 0.7548 \cdot z + 0.3415 \cdot z^2 + 0.642 \cdot z^3 + 0.9196 \cdot z^4$$

$$z = (1 + 2 \cdot a/D)^{-1}$$

$D$ = hole diameter

$a$ = crack length from hole edge

$$G_W = [\sec( \cdot (\sin((D/t-D/W))/(D/t-D/W)]^{0.5}$$

and

$$\lambda = (\pi/2) \cdot (1 + a/D)/(2 \cdot t/D - a/D)$$

**Limitations** Unknown.

**Comments** The FLAGRO solution includes pin loading of the hole, which is ignored here.

## Fracture mechanics - Influence function
## General equation for influence function

**Reference** NASCRAC 89, Besuner 81

**Relationship**

$$K = t \cdot \int_{o \text{ or } -a}^{a} \sigma(x) \cdot h(x)\, dx$$

or

$$K = 1/(t(a)) \cdot \int_{o \text{ or } -a}^{a} t(x) \cdot \sigma(x) \cdot h(x)\, dx$$

where

$t(x)$ = thickness variation,

$\sigma(x)$ = stress variation along the crack face,

and

$h(x)$ = K/P solution for a point load P at location x along the crack face.

= $1/t/\sqrt{\pi \cdot a} \cdot \sqrt{(a-x)/(a+x)}$ for a flat plate.

**Limitations** Linear superposition of K solutions.

**Comments**

## APPENDIX B - BIBLIOGRAPHY

## TABLE OF CONTENTS

Table of Contents.....i

Hypervelocity Impact ..... 1

Fracture ..... 7

## HYPERVELOCITY IMPACT BIBLIOGRAPHY


Baker, W. E. et al.: Workbook for Predicting Pressure Wave and Fragment Effects of Exploding Propellant Tanks and Gas Storage Vessels, NASA CR-134906 (Nov. 1975).

Bjork, R. L.: The Physics of Hypervelocity Lethality, *Int. J. of Impact Engr.*, **5**, 129-154 (1987).

Bjorkman, M.: Proceedings of the APS 1991 Topical Conference on Shock Compression on Condensed Matter, Williamsburg, VA, June 17-20, (1991).

Bodner, S. R.: Modelling Ballistic Perforation, *Int. Conf. on Structural Impact and Crashworthiness*, Imperial College, London, (1984).

Brewer, E. D.; Hendrich, W. R.; Thomas, D. G. and Smith, J. E.: Effects of Oblique Impact on Hypervelocity Shield Performance, ORNL/TM-11390 (1990).

Bruce, E. P.: Review and Analysis of High Velocity Impact Data, *Proceedings of the Fifth Symposium on Hypervelocity Impact*, Vol 1-Part 2, 439-474 (1961)

Burch, G. T.: Multiplate-Damage Study, AFATL-TR-67-116, (1967)

Chhabildas, L. C.: *A New Hypervelocity Launcher (HVL) for Space Science Applicaitons*, AIAA 92-1639, AIAA Space Programs and Technologies Conference, Huntsville, AL (1992).

Christiansen, E. L.: *Evaluation of Space Station Meteoroid Debris Shielding Materials*, NASA Contract NAS9-15800, Eagle Engineering Report 87-163 (1987).

Christiansen, E. L.: *Shield Sizing and Response Equations*, NASA SN3-91-42, (1991).

Christiansen, E. L.: Private Communication.(1991a)

Christiansen, E. L., Hyde, J. L. and Snell, G.: *Spacecraft Survivablility in the Meteoroid and Debris Environment*, AIAA 92-1409, AIAA Space Programs and Technologies Conference, Huntsville, AL (1992).

Christiansen, E. L.: *Performance Equations for Advanced Orbital Debris Shields*, AIAA 92-1462, AIAA Space Programs and Technologies Conference, Huntsville, AL (1992a).

Christiansen, E.L.; Crews, J.; Nolen, A.; Robinson, J. and Willaimsen, J.: The Space Station Freedom Shielding Tiger Team: Results of the Protection Enhancement Plan Shielding Study, attachment: Ballistic Limit Equations for SSF Shielding Enhancement Plan, NASA/JSC Memo SN3-92-175, (1992b).

Christiansen, E. L.: Design and Performance Equations for Advanced Meteoroid and Debris Shields, *Int. J. Impact Engng*, 14, 145-156 (1993)

Christman, D. R.; Gehring, J. W.; Maiden, C. J. and Wenzel, A. B.: *Study of the Phenomena of Hypervelocity Impact*, General Motor Defense Laboratories Report TR 63-216 (1963).

Coronado, A.R., Wright, M.A., and Stern, P.H.: Space Station Integrated Wall Design and Penetration Damage Control Contract NAS8-36426 Report D180-30550, July, 1987.

Cour-Palais, B. G. and Crews, J. L.: A Multi-Shock Concept for Spacecraft Shielding, *Hypervelocity Impact, Proceedings of the 1989 Symposium, Int. J. of Impact Engineering*, Vol.10, 135-146 (1989).

Cour-Palais, B. G. and Piekutowski, A. J.: The Multi-Shock Hypervelocity Impact Shield, *Proceedings of the American Physical Society 1991 Topical Conference on Shock Compression on Condensed Matter*, Williamsburg, VA.

Dickinson, D.L.; Yatteau, J.D. and Recht R.F.: Fragment breakup, *Int. J. of Impact Engr.*, 5, 249-260 (1987).

Eftis, J. and Nemes, J.A.: Modeling of Impact Induced Spall Fracture And Post Spall Behavior of a Circular Plate, *Int. J. Fracture*, **53**, 301-324 (1992).

Elfer, N. C.: *Space Debris and Meteoroid Protection*, Martin Marietta IR&D Report 826-2307, (1988).

Elfer, N. C.; Baillif, F. and Robinson, J.: *External Tank Space Debris Considerations*, AIAA 92-1411, AIAA Space Programs and Technologies Conference, Huntsville, AL (1992).

Elfer, N. C.; Meibaum, R. and Olsen, G.: *Space Debris Surfaces SD_SURF (Computer Program): Probability of No Penetration versus Impact Velocity and Obliquity*, AIAA 92-1407, AIAA Space Programs and Technologies Conference, Huntsville, AL (1992a).

Elfer, N. C.: *Structural Damage Pediction and Analysis for Hypervelocity Impact*, (This Handbook) Contract NAS8-38856 Report (1995).

Elfer, N. C.: *User's Manual for SD_SURF*, Contract NAS8-38856 Report 1995a.

Fish, R. H. and Summers, J. L.: The Effect of Material Properties on Yhreshold Penetration, *Proceedings of the Seventh Hypervelocity Impact Symposium*, VI, (1965).

Frost, V. C.: *Meteoroid Damage Assessment*, Aerospace Corporation, NASA SP-8042, (1970).

Gehring, J. W.: Theory of Impact on Thin Targets and Shields and Correlation with Experiment, *High Velocity Impact Phenomena*, R. Kinslow ed., Academic Press, New York, 105-156 (1970).

Gehring, J. W.: Engineering Considerations in Hypervelocity Impact, *High Velocity Impact Phenomena*, R. Kinslow ed., Academic Press, New York, 463-514 (1970).

Gilman, J. J. and Tuler, F. R.: Dynamic Fracture by Spallation in Metals, *Int. J. of Fracture Mech.*, **6**, 169-182 (1970).

Grady, D.E. and Kipp, M. E.: Fragmentation of Solids Under Dynamic Loading, *Structural Failure*, T. Weirzbicki ed., John Wiley & Sons, New York, 1-40 (1989).

Graves, R. and Smiley, J.: User's Guide for Design Analysis Code BUMPER-II, Report XD683-99402-1 on Contract NAS8-50000 (1991).

Grove, D. J. and Rajendran, A. M.: Modeling the Response of a Thin Sheet due to a Hypervelocity Debris Cloud Impact, Appendix D, Contract NAS8-38856 Report (1992).

Gurson, A. L.: The Effect of Geometric Scale on Impact Induced Fragmentation and its Application to the Design of Dual Plate Armor, *Hypervelocity Impact, Proceedings of the 1989 Symposium, Int. J. of Impact Engineering*, Vol.10, 135-146 (1989).

Hayashida, K. B. and Robinson, J. H.: *Single Wall Penetration Equations*, NASA TM 103565, (1991).

Hayashida, K. B. personal communication, NASA-MSFC (1995).

Henderson, B.J. and Zimmerschied, A.B.: Very High Velocity Penetration Model, NSWC TR 83-189, (1983).

Herrmann, W. and Wilbeck, J. S.: Review of Hypervelocity Penetration Theory, *Int. J. of Impact Engr.*, **5**, 307-322 (1987).

Holsapple, K. A.: Hypervelocity Impacts: Testing In Surrogate Materials, *Int. J. of Impact Engr.*, **14**, 335-345 (1993).

Holsapple, K. A. and Schmidt, R. M.: On the Scaling of Crater Dimensions to Impact Process, *J. Geophysical Research*, N87 vol B3 (1982).

Housen, K. R. and Schmidt, R. M.: Whipple Shields Characterized by a Nondimensional Geometry Parameter, *J. Spacecraft and Rockets.*, 32-1, 162-168 (1995).

Jolly, W. H. and Williamsen, J.E.: Statistical Ballistic Limit Curve Regression for Space Station Freedom Meteoroid/Orbital Debris Shielding, *Int. J. Impact Engng.*, **14**, 395-406 (1993).

Klinkrad, H. and Jehn, R.: The Space Debris Environment, *ESA Journal*, 16, 1-11 (1992).

Kulesz, J. J. and Vargas, L. M.: Prediction of fragment velcoities and trajectories, *Shock and Vibration Journal*, **1** (1979).

Lawrence, R. J.: *A Simple Approach for the Design and Optimization of Standoff Hypervelocity Particle Shields*, AIAA 92-1465, AIAA Space Programs and Technologies Conference, Huntsville, AL (1992).

McGill, P. and Mount, A.: Effectiveness of Metal Matrix and Ceramic Matrix Composites as Orbital Debris Shield Materials, AIAA 92-1461, AIAA Space Programs and Technologies Conference, Huntsville, AL (1992).

Mechtly, E. A.: The International System of Units Physical Constants and Conversion Factors, NASA SP-7012, 2nd Revision (1973).

Morrison, R. H.: A Preliminary Investigation of Projectile Shape Effects in Hypervelocity Impact of a Double-Sheet Structure, NASA TN D-6944 (1972).

Mullin, S. A.; Anderson, C. E. Jr.; and Wilbeck, J. S.: *Dissimilar Material Scaling Relationships for Hypervelocity Impact*, DNA-TR-89-112, Feb. 1989.

NASA SP-8042 see (Frost, V. C.: *Meteoroid Damage Assessment*, Aerospace Corporation, NASA SP-8042, (1970).)

Nicholas, T. and Rajendran, A. M.: Material Characterization at High Strain Rates, *High Velocity Impact Dynamics*, J. A. Zukas ed., John Wiley & Sons, New York, 127-297 (1990).

Nysmith, R. C.: An Experimental Impact Investigation of Aluminum Double Sheet Structures, AIAA Paper 69-374 (1969).

Piekutowski, A.J.: Debris Clouds Generated by Hypervelocity Impact of Cylindrical Projectiles with Thin Aluminum Plates, *Int. J. of Impact Engr.*, Vol. 5, pp.509-518, 1987.

Piekutowski, A. J.: A simple dynamic model for the formation of debris clouds, *Hypervelocity Impact, Proceedings of the 1989 Symposium, Int. J. of Impact Engineering,* Vol.10, 453-472 (1989).

Piekutowski, A. J.: Formation and Description of Debris Clouds Produced by Hypervelocity Impact, UDR-TR-95-46 (1995).

Rajendran, A. M. and Elfer, N. C.: Debris Protection of Space Structures, *Structural Failure*, T. Weirzbicki ed., John Wiley & Sons, New York, 41-78 (1989).

Recht, R. F.: High Velocity Impact Dynamics: Analytical Modeling and Plate Penetration Dynamics, *High Velocity Impact Dynamics*, J. A. Zukas ed., John Wiley & Sons, New York, 443-514 (1990).

Richardson, A.J.: Theoretical Penetration Mechanics of Multisheet Structures Based on Discrete Particle Modeling, *J. of Spacecraft and Rockets,* vol.7, pp.486-489, 1970.

Richardson, A.J., and Sanders, J.P.: Development of Dual Bumper Wall Construction for Advanced Spacecraft, *J. of Spacecraft and Rockets,* vol.9, pp448-451, 1972.

Schmidt, R. M.; Housen, K. R.; Piekutowski, A. J. and Poorman, K. L.: Cadmium Simulations of Orbital Debris Shield Performance to Scaled Velocities of 18 km/s, *J. of Spacecraft and Rockets,* 31-5, pp866-877 (1994).

Summers, J. L.: Investigation of High Speed Impact: Regions of Impact and impact at Oblique Angles, NASA TN D-94 (1959).

Swift, H. F. and Hopkins, A. K.: Effects of Bumper Material Properties on the Operation of Spaced Meteoroid Shields, AFML-TR-68-257 (1968) and *J. Spacecraft and Rockets*, vol. 7, no. 1, pp 73-77 (1970).

Swift, H. F.: Hypervelocity Impact Mechanics, *Impact Dynamics*, John Wiley and Sons, (1982)

Swift, H. F.; Bamford, R, and Chen, R.:Designing Dual Plate Meteoroid Shields - A New Analysis, NASA CR-169143, (1982).

Swift, H. F.: On Predicting Projectile Breakup During Thin Plate Impact, *Hypervelocity Impact, Proceedings of the 1989 Symposium, Int. J. of Impact Engineering,* Vol.10, 579-586 (1989).

Taylor, D. E. and Price, C. F.: Velocities of Fragments From Bursting Gas Reservoirs, *J. Engr. for Industry, Trans. ASME*, 981-985 (1971).

Trucano, T. G.; Grady, D. E. and McGlaun, J. M.: Fragmentation Statistics from Eulerian Hydrocode Calculations, *Hypervelocity Impact, Proceedings of the 1989 Symposium, Int. J. of Impact Engineering,* Vol.10, 587-599 (1989).

Tullos, R. J.; Mullen, S. A. and Graef, R.C.: An Evaluation of the Response of Advanced Structural Materials to Hypervelocity Impacts, SwR Final Report 06-1974-130 Air Force Contract F41608-87-A237 (1990)

Weldon, W. F.: Development of Hypervelocity Electromagnetic Launchers, *Int. J. of Impact Engr.*, **5**, 671-680 (1987).

Williamsen, J. E.: Orbital Debris Risk Analysis and Survivability Enhancement for Freedom Station Manned Modules, AIAA-92-1410, AIAA Space Programs and Technologies Conference, Huntsville, AL (1992).

Williamsen, J. E.: Vulnerability of Manned Spacecraft to Crew Loss from Orbital Debris Penetration, NASA TM-108452, (1994)

Yatteau, J.D.: *High Velocity Penetration Model*, NSWC TR 82-123 1982.

Zukas, J. A.: Survey of Computer Codes for Impact Simulation, *High Velocity Impact Dynamics*, J. A. Zukas ed., John Wiley & Sons, New York, 593-714 (1990).

## FRACTURE MECHANICS BIBLIOGRAPHY


Aminpour, M. A. and Holsapple, K. A.: Finite Element Solutions for Propagating Interface Cracks with Singular Elements, Engr. Fracture Mechanics, 39 no. 3, 451-468 (1991).

Anderson, R. B. and Sullivan, T. L.: *Fracture Mechanics of Through-Cracked Cylindrical Pressure Vessels*, NASA TN D-3252 (1966).

Atluri, S. N.; Nishioka, T.; Nakagaki, M.: Numerical Modeling of dynamic and nonlinear crack propagation in finite bodies by moving singular elements, Nonlinear and Dynamic Fracture Mechanics, N. Perrone and S. N. Atluri, ed., ASME, 35, 37-66 (1979).

Atkins, A. G.: Tearing of Thin Metal Sheet, Structural Failure, T. Weirzbicki ed., John Wiley & Sons, New York, 107-159 (1989).

Baker, B. R.: Dynamic Stresses Created by a Moving Crack, J. Applied Mech., 29, 449-545 (1962).

Besuner, P. M.: BIGIF - Fracture Mechanics Code for Structures, Electric Power Research Institute Report NP-1830-CCM, Palo Alto, CA (1981)

Broeck, D.: Elementary Engineering Fracture Mechanics, Martinus Nijhoff, Boston (1982).

Couque, H.; O'Donoghue, P.; Mullin, S.; and Kanninen, M.: Investigation of Crack Initiation and Unstable Propagation due to Meteoroid or Orbital Debris Impact into Space Station Freedom Pressure Vessels, Southwest Research Institute Project No. 06-5537 (1993).

Eichenberger, T. W.: *Fracture Resistance Data Summary*, Report DA-20947, (1962).

Eidinoff, H., Meyers,W. and Balderes: Fracture Mechanics Analysis of the Space Station Freedom Common Module, Grumman ASD Report SAR-93-01, Bethpage, N.Y., Presented at the 7th Meeting of the Space Station Freedom Meteoroid/Oribital Debris Advanced Fracture Mechanics Group, at Southwest Research Institute, San Antonio, (March 1993)

Elfer, N. C.: Space Debris and Meteoroid Protection, Martin Marietta IR&D Report 826-2307, 1988.

Elfer, N. C.: R-Curve Analysis of Surface Flaws, Final Report for TD 812, TBD [1991]

Erdogan, F. and Kibler, J. J.: Cylindrical and Spherical Shells with Cracks, *Int. J. of Frac. Mechanics*, **5** no. 3, 229-237 (1969).

Erdogan, F. and Ratwani, M.: Fracture of Cylindrical and Spherical Shells Containing a Crack, *Nuclear Engineering and Design*, Paper G6/4, p. 265-286, (1972).

Ernst, H.: Recent Developments in Elastic Plastic Crack Growth Characterization, *22nd National Fracture Mechanics Symposium,* ASTM STP 1131, 136-157 (1992).

Ernst, H.: Material Resistance and Instability Beyond J-Controlled Crack Growth, *Elastic-Plastic Fracture: Second Symposium, Vol.1 Inelastic Crack Analysis,* ASTM STP 803, C.F. Shih and J. P. Gudas, Eds., 191-213 (1983).

Folias, E. S.: A Finite Line Crack In A Pressurized Cylindrical Shell, *Int. J. of Fracture Mech.*, 1, 104-113 (1965).

Forman, R. G., Fatigue Crack Growth Computer Program "NASA/FLAGRO," NASA-Johnson Space Center Materials Branch Report 85-ES5-1 (1986).

Fruend, L. B.: Dynamic Crack Propagation, *The Mechanics of Fracture*, F. Erdogan ed., ASME Publ. No. AMD-19, 1976.

Gunther, C. K.; Holsapple, K. A. and Kobayashi, A. S.: Finite Element Analysis of Cracking Bodies, *AIAA J.* 19, 789-795 (1981).

Hahn, G. T.; Sarrate, M. and Rosenfield, A. R.: Criteria for Crack Extension In Cylindrical Pressure Vessels, *Int. J. Fracture Mechanics*, 5, 187-210 (1969).

Kanninen, M. F. and Popelar, C. H.: Dynamic Fracture Mechanics, *Advanced Fracture Mechanics*, Oxford Univ. Press, New York, 193-280, (1985).

Kanninen, M. F. Preliminary Dynamic Toughness Measurements on 2219-T87, Southwest Research Institute, San Antonio, TX, Presentation at the Eighth Meeting of the Space Station Freedom Meteoroid/Oribital Debris Advanced Fracture Mechanics Group, at GE Corporate Research and Development, Schenectady N.Y.(June, 1993). see Couque et al.

Kaufman, J. G., and Hunsicker: Fracture Toughness Testing at Alcoa Research Laboratories, ASTM STP.

Newman, J. C. Jr: *An Improved Method of Collocation for the Stress Analysis of Cracked Plates with Various Shaped Boundaries*, NASA TN D-6376, ( 1971).

Newman, J. C. Jr: *Fracture Analysis of Surface and Through Cracks in Cylindrical Pressure Vessels*, NASA TN D-8325, ( 1976).

Nied, H.F. and Bachrach, W. E. Several Topics in Fracture Mechanics, GE Corporate Research and Development (GE CR&D) Presentation at the Eighth Meeting of the Space Station Freedom Meteoroid/Oribital Debris Advanced Fracture Mechanics Group, at GE Corporate Research and Development, GE CR&D Schenectady N.Y.(June, 1993).

Pfluger, A. R.: *Fracture Toughness of 2219-T87 Aluminum*, NASA CR-60285 (1964). (note that toughness reported for maximum flaw length at maximum load, while max load actually occurs at shorter lengths.)

Poe, C.C.: Fatigue Crack Propagation in Stiffened Panels, *Damage Tolerance in Aircraft Structures*, ASTM STP 486, 79-97 (1971).

Schmidt, R.: Linear-Shaped Charge Experiments: Crack Geometry Effects on Unzipping. Boeing Defense and Space Group, Seattle Wa., Presentation at the Eighth Meeting of the Space Station Freedom Meteoroid/Oribital Debris Advanced Fracture Mechanics Group, at GE Corporate Research and Development, Schenectady N.Y.(June, 1993).

Tada, H.: The Effects Of Shell Corrections On Stress Intensity Factors And The Crack Opening Areas Of A Circumferential And A Longitudinal Through Crack In A Pipe, *The Application of Fracture Proof Design Methods Using Tearing Instability Theory to Nuclear Piping Postulating Circumferential Through Wall Cracks*, P. C. Paris and H. Tada ed., U.S. Nuclear Regulatory Commision, NUREG/CR-3464, Section III (1983).

Tada, H.; Paris, P. C. and Irwin, G.: The Stress Intensity Analysis of Cracks Handbook, Paris Productions Inc. (and Del Research Corporation) 226 Woodburne Dr. St. Louis, Mo 63105 (1985).

Zahor, A.: Axial Throughwall Crack, chapter 6 in *Ductile Fracture Handbook*, EPRI NP-6301-D (1989),

# APPENDIX C - TEST DATABASES

## TABLE OF CONTENTS

Table of Contents ..... i

Martin Marrietta IR&D Tests at UDRI [N. Elfer - Lockheed Martin]..... 1

NASA-MSFC 'Meteroid' Database (7/91) [D. Williams - Boeing]..... 7

JSC Whipple Database (7/91) [E. Christiansen - JSC]..... 36

JSC Mesh Double Bumper Database (7/91) [E. Christiansen - JSC]..... 46

JSC Multi-Shock Bumper Database (7/91)[E. Christiansen - JSC] ..... 49

| | | PROJECTILE CHARACTERISTICS | | | | | | BUMPER | | | REAR WALL | | | |
|---|---|---|---|---|---|---|---|---|---|---|---|---|---|---|
| UDRI | PROJECTILE | CYL. | MASS | DIA. | VELOC. | OBL. | BUMPER | THICK. | HOLE | SPACE | REAR WALL | THICK. | HOLEOUT | PEN |
| ID.NO. | MATERIAL | /SPHERE | g | in | km/s | deg | MATERIAL | in | DIA. in | in | MATERIAL | in | DIA. in | Y,N,T |
| | CELOTEX WITNESS MATERIALS | | | | | | | | | | | | | |
| | 2.54-4.0 | KM/SEC | | | | | Aluminum | | | | 1st Witness Plate | | | |
| 4-0327 | 2024-T4 | C | 1.0018 | 0.304 | 2.64 | 0 | 6061-T6 | 0.080 | 0.53 | 4 | 2024-T3 | 0.02 | 2 | |
| 4-0330 | 2017-T4 | S | 1.272 | 0.375 | 2.79 | 0 | 6061-T6 | 0.080 | 0.56 | 4 | 2024-T3 | 0.02 | 0.9 | |
| 4-0405 | 2024-T4 | C | 1 | 0.304 | 3.09 | 0 | 6061-T6 | 0.125 | 0.63 | 4 | 2024-T3 | 0.02 | 1.5 | |
| 4-0416 | 2024-T4 | C | 1 | 0.304 | 3.06 | 0 | 6061-T6 | 0.080 | 0.55 | 4 | 2024-T3 | 0.02 | 1.7 | |
| 4-0421 | 2024-T4 | C | 1 | 0.304 | 3.11 | 0 | 6061-T6 | 0.080 | 0.55 | 4 | 2024-T3 | 0.02 | 2 | |
| 4-0422 | 2024-T4 | C | 1 | 0.304 | 2.97 | 0 | 6061-T6 | 0.080 | 0.585 | 4 | 2024-T3 | 0.02 | 0.5x1.0 | |
| 4-0423 | 2024-T4 | C | 1.28 | 0.329 | 2.98 | 0 | 6061-T6 | 0.080 | 0.585 | 4 | 2024-T3 | 0.02 | 2 | |
| | | | | | | | Composites | | | | | | | |
| 4-0368 | 2024-T4 | C | 1 | 0.304 | 3.03 | 0 | IM6/3501 | 0.200 | 0.65 | 4 | 2024-T3 | 0.02 | 1.0x1.2 | |
| 4-0369 | 2024-T4 | C | 1 | 0.304 | 3.09 | 0 | S2/3501 | 0.100 | 0.5 | 4 | 2024-T3 | 0.02 | 1.5 | |
| 4-0370 | 2024-T4 | C | 1 | 0.304 | 3.03 | 0 | IM6/8551 | 0.200 | 0.65 | 4 | 2024-T3 | 0.02 | 1.0x1.5 | |
| 4-0371 | 2024-T4 | C | 1 | 0.304 | 3.08 | 0 | IM6-S2/3501 | 0.175 | 0.61 | 4 | 2024-T3 | 0.02 | 1.0x1.5 | |
| 4-0396 | 2024-T4 | C | 1 | 0.304 | 3.16 | 0 | KEVLAR 49/3501 | 0.160 | 0.54 | 4 | 2024-T3 | 0.02 | 0.7x1.5 | |
| 4-0397 | 2024-T4 | C | 1 | 0.304 | 3.13 | 0 | IM6/3501 | 0.150 | 0.6x0.9 | 4 | 2024-T3 | 0.02 | 1.5 | |
| 4-0419 | 2024-T4 | C | 1 | 0.304 | 3.04 | 0 | Al-Si C | 0.071 | 0.55 | 4 | 2024-T3 | 0.02 | 1.0x1.7 | |
| 4-0428 | 2024-T4 | C | 1.0011 | 0.304 | 3.01 | 0 | 3 PLIES VM3063 KEVLAR | TBD | TBD | 4 | 2024-T3 | 0.02 | 0.7 | |
| 4-0431 | 2024-T4 | C | 0.9985 | 0.304 | 3.02 | 0 | 2 PLIES VM3063 KEVLAR | 0.120 | 0.6 | 4 | 2024-T3 | 0.02 | 0.5x0.9 | |
| 4-0467 | 2024-T4 | C | 0.9996 | 0.304 | 3.12 | 0 | MMA II.2-06-001 | 0.175 | 0.75 | 6 | 2024-T3 | 0.02 | 0.5 | |
| 4-0486 | 2024-T4 | C | 0.9998 | 0.304 | 3.06 | 0 | 2(Al203)/Al | 0.075 | 0.865 | 6 | 2024-T3 | 0.02 | 1.5 | |
| 4-0589 | 2024-T4 | C | 1.0043 | 0.304 | 3.04 | 0 | 7740 GLASS/SiC | 0.100 | 0.8 | 4 | 2024-T3 | 0.02 | 1.8 | |
| | 4-6 KM/SEC | | | | | | Aluminum | | | | | | | |
| 4-0331 | 2017-T4 | S | 1.27 | 0.375 | 5.1 | 0 | 6061-T6 | 0.080 | 0.72 | 4 | 2024-T3 | 0.02 | 3 | |
| 4-0333 | 2024-T4 | C | 1 | 0.304 | 4.82 | 0 | 6061-T6 | 0.080 | 0.8 | 4 | 2024-T3 | 0.02 | 1.5x2.5 | |
| 4-0334 | 2024-T4 | C | 1 | 0.304 | 4.98 | 0 | 6061-T6 | 0.080 | 0.63 | 4 | 2024-T3 | 0.02 | 2.5 | |
| 4-0424 | 2024-T4 | C | 1.28 | 0.329 | 4.91 | 0 | 6061-T6 | 0.080 | 0.7 | 4 | 2024-T3 | 0.02 | 5 | |
| | 6+ KM/SEC | | | | | | Aluminum | | | | | | | |
| 4-0335 | 2024-T4 | C | 1 | 0.304 | 6.09 | 0 | 6061-T6 | 0.080 | 0.76 | 4 | 2024-T3 | 0.02 | 5.0x6.0 | |
| 4-0336 | 2024-T4 | C | 2.01 | 0.383 | 6.17 | 0 | 6061-T6 | 0.080 | 0.85 | 4 | 2024-T3 | 0.02 | 9 | |
| 4-0338 | 2024-T4 | C | 1 | 0.304 | 6.3 | 0 | 6061-T6 | 0.080 | 0.7 | 2 | 2024-T3 | 0.02 | 2 | |
| 4-0339 | 2017-T4 | S | 0.373 | 0.25 | 6.35 | 0 | 6061-T6 | 0.080 | 0.8 | 4 | 2024-T3 | 0.02 | 2.0-2.5 | |
| 4-0404 | 2024-T4 | C | 1 | 0.304 | 6.42 | 0 | 6061-T6 | 0.125 | 0.81 | 4 | 2024-T3 | 0.02 | 3 | |
| 4-0433 | 2024-T4 | C | 0.998 | 0.304 | 6.23 | 0 | 6061-T6 | 0.080 | 0.685 | 4 | 2024-T3 | 0.02 | 2.5 | |
| 4-0434 | 2024-T4 | C | 1.0039 | 0.304 | 6.34 | 0 | 6061-T6 | 0.080 | 0.65 | 4 | 2024-T3 | 0.02 | 4 | |
| | | | | | | | Composites | | | | | | | |
| 4-0360 | 2024-T4 | C | 0.9968 | 0.304 | 6.45 | 0 | IM6/3501 | 0.200 | 0.95 | 4 | 2024-T3 | 0.02 | 4.5 | |
| 4-0361 | 2024-T4 | C | 1 | 0.304 | 6.3 | 0 | S2/3501 | 0.100 | 0.65 | 4 | 2024-T3 | 0.02 | 3 | |
| 4-0362 | 2024-T4 | C | 1 | 0.304 | 6.42 | 0 | IM6/8551 | 0.200 | 0.95 | 4 | 2024-T3 | 0.02 | 2 | |
| 4-0363 | 2024-T4 | C | 1 | 0.304 | 6.54 | 0 | IM6-S2/3501 | 0.150 | 0.8 | 4 | 2024-T3 | 0.02 | 2.5 | |
| 4-0398 | 2024-T4 | C | 1 | 0.304 | 6.38 | 0 | KEVLAR 49/3501 | 0.160 | 0.7 | 4 | 2024-T3 | 0.02 | 2.5 | |
| 4-0415 | 2024-T4 | C | 1 | 0.304 | 6.33 | 0 | IM6/3501 | 0.150 | 7.75 | 4 | 2024-T3 | 0.02 | 2.5x3.0 | |
| 4-0420 | 2024-T4 | C | 1 | 0.304 | 6.43 | 0 | Al-Si C | 0.071 | 0.67 | 4 | 2024-T3 | 0.02 | 4 | |
| 4-0427 | 2024-T4 | C | 0.9984 | 0.304 | 6.36 | 0 | 2 PLIES KEVLAR 3063-1 | TBD | TBD | 4 | 2024-T3 | 0.02 | 4 | |
| 4-0430 | 2024-T4 | C | 1.0024 | 0.304 | 6.3 | 0 | 3 PLIES VM3063 KEVLAR | TBD | TBD | 4 | 2024-T3 | 0.02 | 8 | |
| 4-0468 | 2024-T4 | C | 0.9816 | 0.304 | 6.51 | 0 | MMA II.2-06-002 | 0.175 | 0.425 | 6 | 2024-T3 | 0.02 | 0 | |
| 4-0469 | 2024-T4 | C | 0.9805 | 0.304 | 6.54 | 0 | MMA II.2-06-003 | 0.175 | 0.95 | 6 | 2024-T3 | 0.02 | 4 | |
| 4-0485 | 2024-T4 | C | 1.0049 | 0.304 | 6.4 | 0 | Al02/Al 3 PLIES | 0.075 | 1 | 6 | 2024-T3 | 0.02 | 3 | |
| 4-0487 | 2024-T4 | C | 1.0028 | 0.304 | 6.46 | 0 | 8 PLIES TRIAX KEVLAR | 0.035 | TBD | 6 | 2024-T3 | 0.02 | 9.5 | |
| 4-0503 | 2024-T4 | C | 1.0035 | 0.304 | 6.4 | 0 | Al02/Al 3 PLIES | 0.075 | 1.0x1.26 | 4 | 2024-T3 | | 3 | |
| 4-0504 | 2024-T4 | C | 1.0028 | 0.304 | 6.36 | 0 | MMA II.2-10-001 | TBD | 0.9 | 4 | 2024-T3 | 0.02 | 9 | |
| 4-0588 | 2024-T4 | C | 1.0043 | 0.304 | 6.49 | 0 | MML 7740 GLASS/SiC | 0.080 | 1.7 X 2.5 | 4 | 2024-T3 | 0.02 | 3.5 | |

| UDRI ID.NO. | WITNESS MATERIALS | SPACING in | THICK. in | DEPTH of PEN. in | HOLEOUT DIA. in | COMMENTS |
|---|---|---|---|---|---|---|
| | | | | | | |
| | | | | | | |
| 4-0327 | CELOTEX | 0 | UNLIMITED | 2.05 | 2 | 6 CELOTEX PENETRATED |
| 4-0330 | CELOTEX | 0 | UNLIMITED | 4 | 1.6 | 8 SMALL HOLES OUTSIDE OF HOLEOUT |
| 4-0405 | CELOTEX | 0 | UNLIMITED | 2.67 | 1.5 | THICKER BUMPER,5 CELOTEX PENETRATED,1 CRUSH/DENTED |
| 4-0416 | CELOTEX | 0 | UNLIMITED | 1.63 | 1.0x1.7 | 4 FRAGMENTS THROUGH 2ND CELOTEX |
| 4-0421 | CELOTEX | 0 | UNLIMITED | 1.9 | 2 | 4 CELOTEX PENETRATED,1 CRUSH/DENTED, 7" DIA. CRATER AREA ON WITNESS PLATE |
| 4-0422 | CELOTEX | 0 | UNLIMITED | 3.61 | 0.7x1.5 | 7 CELOTEX PENETRATED,1 CRUSH/DENTED, 7" DIA. CRATER AREA ON WITNESS PLATE |
| 4-0423 | CELOTEX | 0 | UNLIMITED | 2.2 | 1.5x2.0 | 4 CELOTEX PENETRATED,1 CRUSH/DENTED, 7" DIA CRATER AREA ON WITNESS PLATE |
| | | | | | | |
| 4-0368 | CELOTEX | 0 | UNLIMITED | 2.1 | 1.5 | EQUIVALENT 0.110" Al,GRAPHITE BUMPER |
| 4-0369 | CELOTEX | 0 | UNLIMITED | 1.68 | 1.5x2.0 | EQUIVALENT 0.080" Al,FIBERGLASS BUMPER |
| 4-0370 | CELOTEX | 0 | UNLIMITED | 2.52 | 0.5x1.5 | EQUIVALENT 0.110" Al,FIBERGLASS BUMPER |
| 4-0371 | CELOTEX | 0 | UNLIMITED | 3.04 | 1.0x1.5 | ALTERNATING S-2 GLASS & IM6,EQUIVALENT 0.095" Al |
| 4-0396 | CELOTEX | 0 | UNLIMITED | 2.2 | 1.0x1.5 | EQUIVALENT 0.080" Al,3 CELOTEX PENETRATED,1 CRUSHED ,2 DENTED |
| 4-0397 | CELOTEX | 0 | UNLIMITED | 2.3 | 1.5 | EQUIVALENT 0.080" Al ,4 CELOTEX PENETRATED,1 CRUSHED,1DENTED |
| 4-0419 | CELOTEX | 0 | UNLIMITED | 2.2 | 2 | 4 CELOTEX PENETRATED,1 CRUSH/DENTED , 7" DIA CRATER AREA ON WITENSS PLATE |
| 4-0428 | CELOTEX | 0 | UNLIMITED | 3.78 | 1 | 8 CELOTEX PENETRATED 1 CRUSH/DENTED, (SMALL DIA), 5" DIA CRATER AREA ON WITNESS PLATE |
| 4-0431 | CELOTEX | 0 | UNLIMITED | 4.25 | 1.2 | 8 CELOTEX PENETRATED, 4" DIA CRATER AREA ON WITNESS PLATE |
| 4-0467 | CELOTEX | 0 | UNLIMITED | 3.76 | 1.5 | 8 CELOTEX SHEETS PENETRATED |
| 4-0486 | CELOTEX | 0 | UNLIMITED | 2.67 | 1.5x2.0 | AlO2 BUMPER 1PLY Al CREST4-0487,5 CELOTEX PENETRATED 2 CRUSH/DENTED |
| 4-0589 | CELOTEX | 0 | UNLIMITED | 2.37 | 1.8 | 5 CELOTEX PENETRATED, 1 DENTED |
| | | | | | | |
| 4-0331 | CELOTEX | 0 | UNLIMITED | 2.67 | 3 | |
| 4-0333 | CELOTEX | 0 | UNLIMITED | 1.8 | 2.5 | PARTIAL SABOT FAILURE |
| 4-0334 | CELOTEX | 0 | UNLIMITED | 1.88 | 2.5 | 4 CELOTEX PENETRATED,8.5" CRATER AREA ON WITNESS PLATE |
| 4-0424 | CELOTEX | 0 | UNLIMITED | 3.31 | 3 | 5 CELOTEX PENETRATED,1 CRUSH/DENTED,12 BROKEN,8" DIA CRATER AREA ON WITNESS PLATE |
| | | | | | | |
| 4-0335 | CELOTEX | 0 | UNLIMITED | 2.68 | 3.5 | PETALLING OF WITNESS PLATE |
| 4-0336 | CELOTEX | 0 | UNLIMITED | 2.37 | 9 | WITNESS PLATE TOO DAMAGED TO MEASURE; 1ST SEVEN CELOTEX FRACTURED,SABOT DAMAGE |
| 4-0338 | CELOTEX | 0 | UNLIMITED | 3.14 | 2.5x3.0 | SABOT DAMAGE, 7 CELOTEX PENETRATED |
| 4-0339 | CELOTEX | 0 | UNLIMITED | 0.49 | 0 | |
| 4-0404 | CELOTEX | 0 | UNLIMITED | 2.1 | 2.5 | 2 CELOTEX PENETRATED,1 CRUSH/DENTED,2 DENTED,SLIGHT SABOT DAMAGE |
| 4-0433 | CELOTEX | 0 | UNLIMITED | 2.37 | 3 | 3 CELOTEX PENETRATED, 9" DIA CRATER AREA ON WITNESS PLATE |
| 4-0434 | CELOTEX | 0 | UNLIMITED | 2.84 | 3 | 9" DIA CRATER AREA ON WITNESS PLATE |
| | | | | | | |
| 4-0360 | CELOTEX | 0 | UNLIMITED | 2.975 | 2.0x3.0 | EQUIVALENT 0.095" Al,GRAPHITE EPOXY BUMPER |
| 4-0361 | CELOTEX | 0 | UNLIMITED | 2.94 | 3.0x3.5 | EQUIVALENT 0.080" Al, FIBERGLASS BUMPER |
| 4-0362 | CELOTEX | 0 | UNLIMITED | 2.15 | 2 | EQUIVALENT 0.110" Al, GRAPHITE BUMPER |
| 4-0363 | CELOTEX | 0 | UNLIMITED | 2.17 | 2 | EQUIVALENT 0.110" Al,GRAPHITE BUMPER |
| 4-0398 | CELOTEX | 0 | UNLIMITED | 1.81 | 3.5 | EQUIVALENT 0.080" Al,4 CELOTEX PENETRATED, 4 PANELS CRACKED ENTIRELY, 1 DENTED |
| 4-0415 | CELOTEX | 0 | UNLIMITED | 2.67 | 2 | EQUIVALENT 0.080" Al, 4 CELOTEX PENTRATED,1 CRUSH /DENTED,2 DENTED |
| 4-0420 | CELOTEX | 0 | UNLIMITED | 2.84 | 2.5 | EQUIV. 0.080", 4 CELOTEX PENETRATED,1 CRUSH/ DENTED,2 DENTED,9" DIA CRATER AREA ON WIT. PLT. |
| 4-0427 | CELOTEX | 0 | UNLIMITED | 3.09 | 2.5 | 2 PLIES KEVLAR VM 3063-1 BUMPER,5 CELOTEX PEN.,1 C/D,2 DENTED, 7" DIA CRATER AREA ON WIT. PLT |
| 4-0430 | CELOTEX | 0 | UNLIMITED | 2.37 | 3.5 | 3 PLIES KEVLAR VM 3063-1 BUMPER,8" DIA CRATER AREA ON WITNESS PLATE |
| 4-0468 | CELOTEX | 0 | UNLIMITED | 0.005 | 0 | SABOT TURNED ?, ONE HALF AHEAD OF PROJECTILE,SMALL DENTS IN WITNESS PLATE |
| 4-0469 | CELOTEX | 0 | UNLIMITED | 2.35 | 3.74 | EQUIVALENT 0.080" Al BUMPER, 5 CELOTEX PENETRATED |
| 4-0485 | CELOTEX | 0 | UNLIMITED | 1.43 | 3.5 | 2 PLIES Al203/1 PLY Al/CREST,AlO2 TOWARD PROJECTILE,2 CELOTEX PENETRATED,2 CRACKED |
| 4-0487 | CELOTEX | 0 | UNLIMITED | 1.9 | 3.5 | 4 CELOTEX PENETRATED,2 CRUSH/DENT,WITNESS PLATE DESTROYED |
| 4-0503 | CELOTEX | 0 | UNLIMITED | 1.9 | 3.5 | 2 PLIES Al203/1 PLY Al/CREST,4 CELOTEX PENETRATED,2 CRACKED |
| 4-0504 | CELOTEX | 0 | UNLIMITED | 2.82 | 4 | 5 CELOTEX PENETRATED |
| 4-0588 | CELOTEX | 0 | UNLIMITED | 2.37 | 3 | 3 CELOTEX PENETRATED |

| | | PROJECTILE CHARACTERISTICS | | | | | | BUMPER | | | REAR WALL | | | |
|---|---|---|---|---|---|---|---|---|---|---|---|---|---|---|
| UDRI | PROJECTILE | CYL. | MASS | DIA. | VELOC. | OBL. | BUMPER | THICK. | HOLE | SPACE | REAR WALL | THICK. | HOLEOUT | PEN |
| ID.NO. | MATERIAL | /SPHERE | g | in | km/s | deg | MATERIAL | in | DIA. in | in | MATERIAL | in | DIA. in | Y,N,T |
| | MULTIWALL DESIGNS | | | | | | | | | | | | | |
| | | ALL ALUMINUM | | | | | | | | | | | | |
| PRELIM. | 2024-T4 | C | 0.75 | 0.23 | 5.2 | 0 | 6061-T6 | 0.040 | TBD | 2 | 2219-T87 | 0.07 | 2 | Y |
| PRELIM. | 2024-T4 | C | 0.75 | 0.23 | 5.2 | 0 | 6061-T6 | 0.020 | TBD | 4 | 2219-T87 | 0.125 | 0 | N |
| 4-0316 | 2024-T4 | C | 0.75 | 0.23 | 5.2 | 0 | 6061-T6 | 0.080 | 1.0x1.25 | 4 | 2219-T87 | 0.125 | 0.3x0.675 | Y |
| 4-0317 | 2024-T4 | C | 0.75 | 0.23 | 5.2 | 0 | 6061-T6 | 0.125 | 0.825 | 4 | 2219-T87 | 0.125 | 0.3x2.3 | Y |
| 4-0402 | 2024-T4 | C | 0.9991 | 0.304 | 6.31 | 0 | 6061-T6 | 0.080 | 0.735 | 4 | 2219-T851 | 0.125 | 1.5x2.5 | Y |
| 4-0408 | 2024-T4 | C | 1 | 0.304 | 6.38 | 0 | 6061-T6 | 0.080 | 0.7 | 4 | 2219-T851 | 0.2 | 0.5x1.5 | Y |
| 4-0417 | 2024-T4 | C | 1 | 0.304 | 6.27 | 0 | 6061-T6 | 0.080 | 0.675 | 4 | 2219-T851 | 0.25 | 0 | N |
| 4-0435 | 2024-T4 | C | 1 | 0.304 | 6.26 | 0 | 6061-T6 | 0.080 | 0.65 | 12 | 2219-T851 | 0.15 | 0.04 | Y |
| 4-0436 | 2024-T4 | C | 1.0018 | 0.304 | 6.24 | 0 | 6061-T6 | 0.080 | 0.63x0.75 | 4 | 2219-T851 | 0.225 | 0.7x2.2 | Y |
| 4-0438 | 2024-T4 | C | 1.0007 | 0.304 | 6.34 | 0 | 6061-T6 | 0.080 | 0.66x0.74 | 9/3 | (0.02") 2024-T3/2219-T851 | 0.15 | 0 | N |
| 4-0446 | 2024-T4 | C | 0.9988 | 0.304 | 6.28 | 0 | 6061-T6 | 0.080 | TBD | 12 | 2219-T851 | 0.175 | TBD | Y |
| | | Fabric Catchers + Aluminum Rear Walls | | | | | | | | | | | | |
| 4-0454 | 2024-T4 | C | 1.0004 | 0.304 | 6.44 | 0 | 6061-T6 | 0.080 | 0.69 | 2.5/1/1 | 2 PLIES (2X) TRIAXIAL KEVLAR/2219-T81 | 0.125 | 0 | N |
| 4-0455 | 2024-T4 | C | 1.0031 | 0.304 | 3.06 | 0 | 6061-T6 | 0.080 | 0.575 | 2.5/1/1 | 2 PLIES (2X) TRIAXIAL KEVLAR/2219-T81 | 0.125 | 0.3 | Y |
| 4-0456 | 2024-T4 | C | 1.2731 | 0.327 | 6.3 | 0 | 6061-T6 | 0.080 | 0.65x0.8 | 2.5/1/1 | 2 PLIES (2X) TRIAXIAL KEVLAR/2219-T81 | 0.125 | 0.2x1.0 | Y |
| 4-0457 | 2024-T4 | C | 0.4975 | 0.383 | 3 | 0 | 6061-T6 | 0.080 | 0.485 | 2.5/1/1 | 2 PLIES (2X) TRIAXIAL KEVLAR/2219-T81 | 0.125 | 0 | N |
| 4-0459 | 2024-T4 | C | 1.0024 | 0.304 | 6.24 | 0 | 6061-T6 | 0.080 | 0.725 | 3.5/1 | MMA II.2-08-005/2219-T81 | 0.125 | 0.5x7.0 | Y |
| 4-0462 | 2024-T4 | C | 1.0045 | 0.304 | 3.17 | 0 | 6061-T6 | 0.080 | 0.575 | 2.5/1/1 | 0.02" 2024/2 PLIES TRIAX KEVLAR/2219-T81 | 0.125 | 0.25 | Y |
| 4-0463 | 2024-T4 | C | 1.0011 | 0.304 | 6.43 | 0 | 6061-T6 | 0.080 | 0.685 | 2.5/1/1 | 0.02" 2024/2 PLIES TRIAX KEVLAR/2219-T81 | 0.125 | 0 | N |
| 4-0465 | 2024-T4 | C | 1.0021 | 0.304 | 6.37 | 0 | 6061-T6 | 0.080 | 0.675 | 2.5/.5/.5/1 | (3X)KEVLAR 49/EPOXY / 2219-T81 | 0.125 | 0 | N |
| 4-0466 | 2017-T4 | S | 1.2728 | 0.375 | 6.23 | 0 | 6061-T6 | 0.080 | TBD | 2.5/1/1 | 2 PLIES (2X) TRIAXIAL KEVLAR/2219-T81 | 0.125 | 0.7 | Y |
| 4-0474 | 2024-T4 | C | 0.9868 | 0.304 | 6.44 | 0 | 6061-T6 | 0.080 | 0.675 | 2.5/2 | 3 PLIES TRIAXIAL KEVLAR/2219-T81 | 0.125 | 0 | N |
| 4-0477 | 2024-T4 | C | 0.9869 | 0.304 | 6.39 | 0 | 6061-T6 | 0.080 | 0.71 | 2.5/2 | 2 PLIES TRIAXIAL KEVLAR/2219-T81 | 0.125 | 0 | N |
| 4-0478 | 2024-T4 | C | 1.2475 | 0.327 | 6.4 | 0 | 6061-T6 | 0.080 | 0.685 | 2.5/1/1 | 2 PLIES (2X) TRIAXIAL KEVLAR/2219-T81 | 0.125 | 0.5 | Y |
| 4-0479 | 2024-T4 | C | 1.0021 | 0.304 | 6.55 | 0 | 6061-T6 | 0.080 | 0.65 | 1/3.5 | 2 PLIES TRIAXIAL KEVLAR/2219-T81 | 0.125 | 0.4 | Y |
| 4-0480 | 2024-T4 | C | 1.0018 | 0.304 | 6.39 | 0 | 6061-T6 | 0.080 | 0.675 | 3.5/1 | 2 PLIES TRIAXIAL KEVLAR/2219-T81 | 0.125 | 0 | N |
| 4-0482 | 2024-T4 | C | 1.0028 | 0.304 | 6.36 | 0 | 6061-T6 | 0.080 | 0.62x0.75 | 2.5/2 | 6 PLIES SPECTRA 900 / 2219-T81 | 0.125 | 0.5x2.5 | Y |
| 4-0484 | 2024-T4 | C | 1.0019 | 0.304 | 6.42 | 0 | 6061-T6 | 0.063 | 0.69 | 2.5/2 | 2 PLIES TRIAXIAL KEVLAR/2219-T81 | 0.125 | 1.5 | Y |
| 4-0491 | 2024-T4 | C | 0.4973 | 0.241 | 2.96 | 0 | 6061-T6 | 0.080 | 0.465 | 3.5/1 | 2 PLIES TRIAX KEVLAR/ 2219-T87 | 0.125 | 0.29 | Y |
| 4-0492 | 2024-T4 | C | 2.015 | 0.383 | 6.36 | 0 | 6061-T6 | 0.080 | 0.765 | 4/1/1 | 2 PLIES (2X) TRIAXIAL KEVLAR/2219-T87 | 0.125 | 1.5 | Y |
| 4-0501 | 2024-T4 | C | 1.5095 | 0.348 | 6.42 | 0 | 6061-T6 | 0.080 | 0.735 | 4/1/1 | 2 PLIES (2X) TRIAXIAL KEVLAR/2219-T87 | 0.125 | 0.1 | T |
| 4-0502 | 2024-T4 | C | 1.0028 | 0.304 | 6.49 | 0 | 6061-T6 | 0.080 | 0.68 | 2.5/2 | 4 PLIES 8 OZ KEVLAR/2219-T87 | 0.125 | 0 | N |
| 4-0505 | 2024-T4 | C | 1.0053 | 0.304 | 6.42 | 0 | 6061-T6 | 0.080 | 0.678 | 3.5/1 | 2 PLIES 8 OZ KEVLAR/2219-T87 | 0.125 | 0.1 | Y |
| 4-0506 | 2024-T4 | C | 2.0232 | 0.383 | 6.36 | 0 | 2219-T87 | 0.125 | 0.95 | 9/3 | 8 PLIES 8 OZ KEVLAR/2219-T87 | 0.125 | 0 | N |
| 4-0507 | 2017-T4 | S | 1.2735 | 0.375 | 6.42 | 0 | 6061-T6 | 0.080 | 0.725 | 3.5/1 | 8 PLIES 8 OZ KEVLAR/ 5456-H116 | 0.125 | 0 | N |
| 4-0508 | 2024-T4 | C | 1.0038 | 0.304 | 6.42 | 0 | 6061-T6 | 0.080 | 0.69 | 3.5/1 | 4 PLIES 8 OZ KEVLAR/2219-T87 | 0.125 | 0 | T |
| 4-0509 | 2024-T4 | C | 1.0025 | 0.304 | 6.79 | 0 | 6061-T6 | 0.080 | 0.68 | 3.5/1 | 4 PLIES 8 OZ KEVLAR/2219-T87 | 0.125 | 0 | N |
| 4-0510 | 2024-T4 | C | 1.0038 | 0.304 | 6.96 | 0 | 6061-T6 | 0.080 | TBD | 3.5/1 | 4 PLIES 8 OZ KEVLAR/2219-T87 | 0.125 | TBD | Y |
| 4-0511 | 2017-T4 | S | 1.2747 | 0.375 | 6.42 | 0 | 6061-T6 | 0.080 | 0.73 | 2/1/1 | 2 PLIES (2X) 17 OZ KEVLAR /5456-H116 | 0.125 | 0 | N |
| 4-0512 | 2017-T4 | S | 1.2718 | 0.375 | 6.31 | 0 | 6061-T6 | 0.080 | TBD | 3.5/1 | 4 PLIES 8 OZ KEVLAR/5456-H116 | 0.125 | TBD | N |
| 4-0513 | 2024-T4 | C | 1.5053 | 0.348 | 6.34 | 0 | 6061-T6 | 0.080 | 0.74 | 3.5/1 | 8 PLIES 8 OZ KEVLAR/5456-H116 | 0.125 | 4.0 X 3.0 | Y |
| 4-0515 | 2017-T4 | S | 0.3733 | 0.25 | 3.01 | 0 | 6061-T6 | 0.080 | 0.43 | 3.5/1 | 4 PLIES 8 OZ KEVLAR 5456-H116 | 0.125 | 0.31 | Y |
| 4-0516 | 2017-T4 | S | 0.3729 | 0.25 | 3.93 | 0 | 6061-T6 | 0.080 | 0.48 | 3.5/1 | 4 PLIES 8 OZ KEVLAR 5456-H116 | 0.125 | 0 | N |
| 4-0517 | 2024-T4 | C | 2.025 | 0.383 | 6.3 | 0 | 2219-T87 | 0.125 | 0.92 | 6/2 | 8 PLIES 8 OZ KEVLAR/2219-T87 | 0.125 | 0.01 | Y |
| 4-0527 | 2024-T4 | C | 1.0021 | 0.304 | 6.31 | 0 | 6061-T6 | 0.080 | 0.71 | 4.5/0 | 4 PLIES 8 OZ KEVLAR/2219 -T87 | 0.125 | 2.0" SPLIT | Y |
| 4-0528 | 2024-T4 | C | 1.002 | 0.304 | 6.16 | 0 | 6061-T6 | 0.080 | 0.675 | 3.5/1 | 4 PLIES 8 OZ KEVLAR/2219-T87 | 0.125 | 0 | N |
| 4-0529 | 2024-T4 | C | 1.0004 | 0.304 | 6.17 | 0 | 6061-T6 | 0.063 | 0.625 | 3.5/1 | 4 PLIES 8 OZ KEVLAR/2219-T87 | 0.125 | 0.9 X 1.2 | Y |
| 4-0530 | 2024-T4 | C | 1.0004 | 0.304 | 6.1 | 0 | 2024-T3 | (3)0.020 | 0.40,1.47 | 3.5/1 | 4 PLIES 8 OZ KEVLAR/2219-T87 | 0.125 | 0.4 x0.56 | Y |
| 4-0531 | 2024-T4 | C | 1.0033 | 0.304 | 6.34 | 0 | COPPER | 0.026 | 0.525 | 3.5/1 | 4 PLIES 8 OZ KEVLAR/2219-T87 | 0.125 | 0 | N |
| 4-0533 | 2024-T4 | C | 1.0079 | 0.304 | 6.95 | 0 | 6061-T6 | 0.080 | 0.7 | 3.5/1 | 4 PLIES 8 OZ KEVLAR/ 5456-H116 | 0.1 | 0 | N |
| 4-0534 | 2024 -T4 | C | 1.0061 | 0.304 | 7 | 0 | 6061-T6 | 0.080 | 0.71 | 3.5/1 | 4 PLIES 8 OZ KEVLAR/5456-H116 | 0.08 | 1.5 | Y |
| 4-0535 | 2024-T4 | C | 1.0066 | 0.304 | 6.98 | 0 | 6061-T6 | 0.080 | 0.695 | 3.5/1 | 4 PLIES 8 OZ KEVLAR/5456-H116 | 0.1 | 1.28 | Y |
| 4-0541 | 2024-T4 | C | 2.0189 | 0.383 | 6.37 | 45 | 6061-T6 | 0.080 | 0.82x1.3 | 3.5/1 | 4 PLIES 8 OZ KEVLAR/5456-H116 | 0.125 | 3.5x5.0 | Y |
| 4-0542 | 2024-T4 | C | 1.5087 | 0.348 | 6.48 | 45 | 6061-T6 | 0.080 | 0.76x0.96 | 3.5/1 | 4 PLIES 8 OZ KEVLAR/ 5456-H116 | 0.125 | 0.65x1.0 | Y |
| 4-0543 | 2024-T4 | C | 1.2493 | 0.327 | 6.36 | 45 | 6061-T6 | 0.080 | 0.76x0.93 | 3.5/1 | 4 PLIES 8 OZ KEVLAR/ 5456-H116 | 0.125 | 1.2 | Y |

| UDRI ID.NO. | WITNESS MATERIALS | WITNESS MATERIALS SPACING in | WITNESS MATERIALS THICK. in | WITNESS MATERIALS DEPTH of PEN. in | HOLEOUT DIA. in | COMMENTS |
|---|---|---|---|---|---|---|
| | | | | | | |
| | | | | | | |
| PRELIM. | | | | | | PETALLED HOLE |
| PRELIM. | NONE | | | | | 1 " HOLE IN HEAT PIPE |
| 4-0316 | 2024-T3 | 4 | 0.002 | 0.02+ | 0.25 | 1 PINHOLE ONLY WALL,6 PENETRATIONS > 0.25" IN 1ST WITNESS PLATE, SABOT DAMAGE |
| 4-0317 | 2024-T3 | 4 | 0.02 | 0.02+ | 0.25 | BAD SHOT SABOT DAMAGE |
| 4-0402 | 2024-T3 | 0.5 | 0.02 | 0.02+ | 2.0x5.0 | 7" DIAMETER CRATER AREA ON WITNESS PLATE |
| 4-0408 | 2024-T3 | 4 | 0.02 | 0.1 | 3 | 5 WITNESS PLATES PENETRATED |
| 4-0417 | 2024-T3 | 0.5 | 0.02 | 0.04 | 0.5x2.5 | 2 WITNESS PLATES PENETRATED BY SPALL, 2" DIA. SPALL AREA |
| 4-0435 | 2024-T3 | 0.5 | 0.02 | 0.03 | 0 | SMALL DENT AND10"DIA CRATER AREA ON WITNESS PLATE |
| 4-0436 | 2024-T3 | 0.5 | 0.02 | 1.2 | 3 | 5 WITNESS PLATES PENETRATED,5" DIA CRATER ON 1ST WITNESS PLATE |
| 4-0438 | NONE | - | - | - | - | 0.02" 2024-T3 9" FROM BUMPER,12" SPACING, 6" DIA. CRATER ON WALL, 0.125" MAX CRATER DEPTH |
| 4-0446 | TBD | TBD | TBD | TBD | TBD | WITNESS PLATE DENTED |
| | | | | | | |
| 4-0454 | 2024-T3 | 0.5 | 0.02 | 0 | 0 | 0.3" DEEP, 3.8" DIA DENT IN WALL |
| 4-0455 | 2024-T3 | 0.5 | 0.02 | 0.04 | TBD | 1 FRAGMENT THROUGH WALL AND 2 WITNESS PLATES |
| 4-0456 | 2024-T3 | 0.5 | 0.02 | 0.8 | 0.75 | WALL SPLIT IN HALF, 4 WITNESS PLATES PENETRATED, 1 DENTED |
| 4-0457 | 2024-T3 | 0.5 | 0.02 | 0 | 0 | SMALL BULGE IN WALL NO FAILURE, DEEPEST CRATER 0.100" |
| 4-0459 | 2024-T3 | 0.5 | 0.02 | 0.06 | PLATE SPLIT | WALL SPLIT IN HALF- HIGH STRAIN FAILURE,3 WITNESS PLATES PENETRATED, 2 DENTED |
| 4-0462 | 2024-T3 | 0.5 | 0.02 | 0.02 | 0.5 | 0.02" 2024 &2 KEVLAR INTERMEDIATE LAYERS,2 SPLITS ~0.7" LONG IN WALL |
| 4-0463 | 2024-T3 | 0.5 | 0.02 | 0 | 0 | 0.02" 2024 &2 KEVLAR INTERMEDIATE LAYERS, WALL BULGE- 2.5"x 3.5", DENT IN FIRST WITNESS PLATE |
| 4-0465 | 2024-T3 | 0.5 | 0.02 | 0 | 0 | 3 SHEETS INTERMEDIATE KEVLAR/EPOXY,1.5" DIA BULGE IN WALL |
| 4-0466 | 2024-T3 | 0.5 | 0.02 | 0.6 | 1.7 | WALL SPLIT IN HALF |
| 4-0474 | 2024-T3 | 0.5 | 0.02 | 0 | 0 | 3 PLIES TRIAXIAL KEVLAR (2.5"); 0.2" DENT IN WALL; TARGET CLAMPED IN FOLLOWING TESTS |
| 4-0477 | 2024-T3 | 0.5 | 0.02 | 0 | 0 | 2 PLIES TRIAXIAL KEVLAR (2.5"); 0.25" DENT IN WALL |
| 4-0478 | 2024-T3 | 0.5 | 0.02 | 0.04 | SPLIT | 2 PLIES (2X) TRIAXIAL KEVLAR (2.5"/3.5"); PLATE SPLIT |
| 4-0479 | 2024-T3 | 0.5 | 0.02 | 0.08 | 1.5 | 2 PLIES TRIAXIAL KEVLAR (1"); "JET" HOLE THROUGH WALL AND WITNESS PLATES |
| 4-0480 | 2024-T3 | 0.5 | 0.02 | 0 | 0 | 2 PLIES TRIAXIAL KEVLAR (3.5"); 0.5 " DENT,WITNESS PLATE ALSO DENTED |
| 4-0482 | 2024-T3 | 0.5 | 0.02 | 0.06 | 1.1 | 3 WITNESS PLATES SPLIT , 1 DENTED |
| 4-0484 | 2024-T3 | 0.5 | 0.02 | 0.04 | 1.5 | 2 PLIES TRIAXIAL KEVLAR (2.5"),WALL SPLIT,2 WITNESS PLATES PENETRATED, 2 DENTED |
| 4-0491 | TBD | TBD | TBD | TBD | TBD | 2 WITNESS PLATES TORN,7 FRAGMENTS THROUGH WALL |
| 4-0492 | 2024-T3 | 0.5 | 0.02 | 0.12 | 2 | (4) 4.0" AVG LENGHT PETALS IN WALL, 6 WITNESS PLATES PETAL DAMAGED |
| 4-0501 | 2024-T3 | 0.5 | 0.02 | 0 | 0 | 10" DIA , 0.5" DEEP DENT IN WALL, 1ST WITNESS PLATE DENTED |
| 4-0502 | 2024-T3 | 0.5 | 0.02 | 0.02 | 0 | SOME Al SPRAY, 0.40" DEEP, 9.0" DIA. DENT IN WALL |
| 4-0505 | 2024-T3 | 0.5 | 0.02 | 0.02 | 0.5 | 0.5" BULGE IN WALL |
| 4-0506 | 2024-T3 | 0.5 | 0.02 | 0 | 0 | 3" DIA. CRATER PATTERN ON WALL, DEEPEST CRATER 0.02" |
| 4-0507 | 2024-T3 | 0.5 | 0.02 | 0 | 0 | FIBER PATTERN & 10" DIA,~1.325 DEEP DENT IN WALL ,3 WITNESS PLATES DENTED |
| 4-0508 | 2024-T3 | 0.5 | 0.02 | 0 | 0 | 10.0" DIA. , 0.60" DEEP DENT IN WALL |
| 4-0509 | 2024-T3 | 0.5 | 0.02 | 0 | 0 | 9.5" DIA ,0.7" DEEP DENT IN WALL, 1.5" DIA CRATER AREA AND DENT ON WITNESS PLATE |
| 4-0510 | 2024-T3 | 0.5 | 0.02 | 0.04 | 0.5x5 | 4 TEARS IN WALL , 2 WITNESS PLATES PENETRATED |
| 4-0511 | 2024-T3 | 0.5 | 0.02 | 0 | 0 | 10" DIA, 0.98" DEEP DENT IN WALL, 2 WITNESS PLATES DENTED |
| 4-0512 | 2024-T3 | 0.5 | 0.02 | 0 | 0 | 1.125" DEEP DENT IN WALL , 3 WITNESS PLATES DENTED |
| 4-0513 | 2024-T3 | 0.5 | 0.02 | 0.04 | 2 | (4) 3.0" AVG LENGHT PETALS IN WALL, 4 WITNESS PLATES DENTED |
| 4-0515 | 2024-T3 | 0.5 | 0.02 | 0.04 | 0.415 | 2.5" DIA CRATER AREA ON WALL |
| 4-0516 | 2024-T3 | 0.5 | 0.02 | 0 | 0 | SEVERAL DIMPLES,0.125" DEEP DENT IN WALL |
| 4-0517 | 2024-T3 | 0.5 | 0.02 | 0 | 0 | 0.375" DEEP DENT SEVERAL PINHOLES & DIMPLES IN WALL, WITNESS PLATE DAMAGED |
| 4-0527 | 2024-T3 | 0.5 | 0.02 | 0.08 | 1.0 SPLIT | CRESCENT SHAPED SPLIT IN WALL,4 WITNESS PLATES SPLIT, 2 DENTED |
| 4-0528 | 2024-T3 | 0.5 | 0.02 | 0 | 0 | DENT IN WALL, 0.05" DEEP DENT IN WITNESS PLATE |
| 4-0529 | 2024-T3 | 0.5 | 0.02 | 0.06 | 1.3 | (4) 2" AVG LENGHT PETALS IN WALL, 3 WITNESS PLATES PENETRATED, 1 DENTED |
| 4-0530 | 2024-T3 | 0.5 | 0.02 | 0.12 | 1.7 | MULTIPLE BUMPER TEST, 6 WITNESS PLATES PENETRATED |
| 4-0531 | 2024-T3 | 0.5 | 0.02 | 0 | 0 | ~ 0.5" DEEP DENT IN WALL , 0.03" DEEP DENT IN WITNESS PLATE |
| 4-0533 | 2024-T3 | 0.5 | 0.02 | 0 | 0 | 1.2" DEEP, 9.0" DIA DENT IN WALL;3 WITNESS PLATES DENTED |
| 4-0534 | 2024-T3 | 0.5 | 0.02 | 0.04 | 1 | (5)PETALS 2.0"AVG LENGTH IN WALL; 2 WITNESS PLATES BROKEN,2 DENTED |
| 4-0535 | 2024 T3 | 0.5 | 0.02 | 0 | 0 | "TRAPDOOR" FAILURE, NO WITNESS PLATES PENETRATED |
| 4-0541 | 2024-T3 | 0.5 | 0.02 | 0.04 | 2.5x3.0 | 45° OBLIQUE SHOT, (4) 2.0"AVG LENGHT PETALS IN WALL,2 WITNESS PLATES PENETRATED |
| 4-0542 | 2024-T3 | 0.5 | 0.02 | 0.04 | 1.7 | (2) 1" AVG LENGHT PETALS IN WALL , 2 WITNESS PLATES PENETRATED |
| 4-0543 | 2024-T3 | 0.5 | 0.02 | 0.04 | 0.2x1.7 | 2 WITNESS PLATES PENETRATED |

| | | PROJECTILE CHARACTERISTICS | | | | | | BUMPER | | | REAR WALL | | |
|---|---|---|---|---|---|---|---|---|---|---|---|---|---|
| UDRI | PROJECTILE | CYL. | MASS | DIA. | VELOC. | OBL. | BUMPER | THICK. | HOLE | SPACE | REAR WALL | THICK. | HOLEOUT | PEN |
| ID.NO. | MATERIAL | /SPHERE | g | in | km/s | deg | MATERIAL | in | DIA. in | in | MATERIAL | in | DIA. in | Y,N,T |
| 4-0544 | 2024-T4 | C | 0.9988 | 0.304 | 6.43 | 45 | 6061-T6 | 0.080 | 0.71x0.87 | 3.5/1 | 4 PLIES 8 OZ KEVLAR/5456-H116 | 0.125 | 0.65 | Y |
| 4-0545 | 2024-T4 | C | 1.0054 | 0.304 | 6.34 | 45 | CORR.Al 0.08 Eff. | 0.75(.08) | 5.0x0.68 | 3.5/1 | 4 PLIES 8 OZ KEVLAR/5456-H116 | 0.125 | 0 | N |
| 4-0571 | 2017-T4 | S | 1.2719 | 0.375 | 6.37 | 0 | 6061-T6 | 0.080 | 0.72 | 3.5/1 | 4 PLIES 8 OZ KEVLAR/ 6061-T6 | 0.125 | 0 | N |
| 4-0572 | 2024-T4 | C | 1.004 | 0.304 | 6.37 | 0 | CORR.Al 0.08 Eff. | 0.75(.08) | 0.47x0.61 | 3.5/1 | 4 PLIES 8 OZ KEVLAR/ 5456-H116 | 0.125 | 0.7 | Y |
| 4-0573 | 2017-T4 | S | 1.2728 | 0.375 | 6.54 | 65 | 6061-T6 | 0.080 | 0.74x1.25 | 3.5/1 | 4 PLIES 8 OZ KEVLAR/5456-H116 | 0.125 | 0.22 | Y |
| 4-0590 | 2024-T4 | C | 1.5085 | 0.348 | 6.51 | 0 | 6061-T6 | 0.080 | 0.755 | 3.5/1 | 8 PLIES 8 OZ KEVLAR/6061-T6 | 0.125 | 0.3x4.0 | N |
| 4-0591 | 2017-T4 | S | 1.2715 | 0.375 | 6.58 | 0 | 6061-T6 | 0.080 | 0.8 | 3.25/1.25 | 4 PLIES 8 OZ KEVLAR/5456-H116 | 1.25 | 0 | N |
| 4-0592 | 2024-T4 | C | 1.5055 | 0.348 | 6.57 | 0 | 6061-T6 | 0.080 | 0.74 | 3.25/1.25 | 6 PLIES 8 OZ KEVLAR/5456-H116 | 1.25 | 2.5x3.5 | Y |
| 4 -0593 | 2024-T4 | C | 2.0283 | 0.383 | 6.51 | 0 | 6061-T6 | 0.080 | 0.775 | 3.25/1.25 | 6 PLIES 8 OZ KEVLAR/5456-H116 | 1.25 | 3 x3.5 | Y |
| 4-0594 | Al | S | 0.1582 | 0.1875 | 2.79 | 0 | 6061-T6 | 0.080 | 0.325 | 3.5/1 | 4 PLIES 8 OZ KEVLAR/5456-H116 | 0.125 | 0 | N |
| 4-0595 | Al | S | 3.0072 | 0.5 | 6.42 | 0 | 2219-T87 | 0.125 | 1.1 | 6/2 | 12 PLIES 8 OZ KEVLAR/ 2219-T87 | 0.125 | 0 | N |
| 4-0597 | 2017-T4 | S | 2.9879 | 0.5 | 6.36 | 0 | 6061-T6 | 0.080 | TBD | 3.5/1 | 4 PLIES 8 OZ KEVLAR/2219-T87 | 0.125 | TBD | Y |
| 4-0599 | 2017-T4 | S | 1.2712 | 0.375 | 6.49 | 0 | 6061-T6 | 0.080 | 0.72 | 3.5/1 | 4 PLIES 8 OZ KEVLAR/2219-T62 | 0.125 | 0 | T |
| 4-0600 | 2024-T4 | C | 1.5049 | 0.348 | 6.48 | 0 | 6061-T6 | 0.080 | 0.75 | 3.5/1 | 8 PLIES 8 OZ KEVLAR/6061-T6 | 0.125 | 2.4 | Y |
| 4-0602 | 2017-T4 | S | 2.988 | 0.5 | 6.36 | 0 | 6061-T6 | 0.08 | TBD | 3.5/1 | 4 PLIES 8 OZ KEVLAR/5456-H116 | 0.125 | 8 | Y |
| 4-0603 | 2017-T4 | S | 1.2724 | 0.375 | 6.6 | 0 | 6061-T6 | 0.08 | 0.732 | 3.5/1 | 4 PLIES 8 OZ KEVLAR/5456-H116 | 0.125 | 2.5x0.4 | Y |
| 4-0604 | 2024-T4 | C | 1.0039 | 0.304 | 5.64 | 0 | 6061-T6 | 0.080 | TBD | 3.5/1 | 6 PLIES 8 OZ KEVLAR/5456-H116 | 0.125 | 1x2 | Y |
| 4-0605 | 2017-T4 | S | 0.3732 | 0.25 | 2.97 | 0 | 6061-T6 | 0.080 | 0.425 | 3.5/1 | 6 PLIES 8 OZ KEVLAR/5456-H116 | 0.125 | 0.275 | Y |
| 4-0608 | 2017-T4 | S | 1.2714 | 0.375 | 6.57 | 0 | 6061-T6 | 0.08 | 0.734 | 3.25/1.25 | 4 PLIES 8 OZ KEVLAR/2219-T851 | 0.125 | 8 | Y |
| 4-0609 | 2017-T4 | S | 2.9888 | 0.5 | 6.42 | 0 | 6061-T6 | 0.08 | 0.855 | 3.25/1.25 | 4 PLIES 8 OZ KEVLAR/2219-T851 | 0.125 | 8 | Y |
| 4-0610 | 2017-T4 | S | 1.2727 | 0.375 | 6.55 | 0 | 6061-T6 | 0.08 | 0.745 | 3.5/1 | 4 PLIES 8 OZ KEVLAR/2219-T87 | 0.125 | 0 | N |
| 4-0611 | 2017-T4 | S | 2.9885 | 0.5 | 6.28 | 0 | 6061-T6 | 0.08 | 0.84 | 3.25/1.25 | 4 PLIES 8 OZ KEVLAR/5456-H116 | 0.2 | TBD | Y |
| 4-0612 | 2017-T4 | S | 2.9881 | 0.5 | 6.28 | 0 | 6061-T6 | 0.08 | 0.85 | 3.25/1.25 | 4 PLIES 8 OZ KEVLAR/2219-T851 | 0.125 | TBD | Y |
| 4-0613 | 2017-T4 | S | 3.0014 | 0.5 | 6.36 | 0 | 6061-T6 | 0.08 | TBD | 3.5/1 | 4 PLIES 8 OZ KEVLAR/2219-T851 | TBD | TBD | |
| 4-0614 | 2017-T4 | S | 2.9999 | 0.5 | 6.28 | 0 | 6061-T6 | 0.08 | TBD | 3.5/1 | 4 PLIES 8 OZ KEVLAR/5456-H116 | TBD | TBD | |
| 4-0646 | 2017-T4 | S | 0.7336 | 0.312 | 6.74 | 0 | 6061-T6 | 0.063 | | 3/1.5 | 3 PLIES 8OZ KEVLAR/ 5456-H116 | 0.1 | | Y |
| 4-0647 | 2017-T4 | S | 0.1589 | 0.187 | 3.08 | 0 | 6061-T6 | 0.063 | | 3/1.5 | 3 PLIES 8OZ KEVLAR/ 5456-H116 | 0.1 | | Y |
| 4-0648 | 2017-T4 | S | 0.045 | 0.125 | 2.84 | 0 | 6061-T6 | 0.063 | | 3/1.5 | 3 PLIES 8OZ KEVLAR/ 5456-H116 | 0.1 | | N |
| 4-0650 | 2017-T4 | S | 0.3762 | 0.25 | | 45 | 6061-T6 | 0.063 | | 3/1.5 | 3 PLIES 8OZ KEVLAR/ 5456-H116 | 0.1 | | |
| 4-0651 | 2017-T4 | S | 0.3726 | 0.25 | 6.69 | 45 | 6061-T6 | 0.063 | | 3/1.5 | 3 PLIES 8OZ KEVLAR/ 5456-H116 | 0.1 | | N |
| 4-0652 | 2017-T4 | S | 0.3733 | 0.25 | 6.28 | 45 | 6061-T6 | 0.063 | | 3/1.5 | 3 PLIES 8OZ KEVLAR/ 5456-H116 | 0.1 | | Y |
| 4-0653 | 2017-T4 | S | 0.1588 | 0.187 | 5.1 | 45 | 6061-T6 | 0.063 | | 3/1.5 | 3 PLIES 8OZ KEVLAR/ 5456-H116 | 0.1 | | Y |
| 4-0654 | 2017-T4 | S | 0.1583 | 0.187 | 5.97 | 45 | 6061-T6 | 0.063 | | 3/1.5 | 3 PLIES 8OZ KEVLAR/ 5456-H116 | 0.1 | | N |
| 4-0655 | 2017-T4 | S | 0.3727 | 0.25 | 6.82 | 65 | 6061-T6 | 0.04 | | 3/1.5 | 3 PLIES 8OZ KEVLAR/ 5456-H116 | 0.1 | | N |
| 4-0656 | 2017-T4 | S | 0.3724 | 0.25 | 6.85 | 65 | 6061-T6 | 0.063 | | 3/1.5 | 3 PLIES 8OZ KEVLAR/ 5456-H116 | 0.1 | | N |
| 4-0657 | 2017-T4 | S | 0.7313 | 0.312 | 6.61 | 65 | 6061-T6 | 0.063 | | 3/1.5 | 3 PLIES 8OZ KEVLAR/ 5456-H116 | 0.1 | | Y |
| 4-0660 | 2017-T4 | S | 1.2716 | 0.375 | 6.67 | 0 | 6061-T6 | 0.63 | | 3/1.5 | 3 PLIES (2X) 8OZ KEVLAR/5456-H116 | 0.1 | | N |
| 4-0661 | 2017-T4 | S | 3.0014 | 0.5 | 6.24 | 0 | 6061-T6 | 0.63 | | 3/1.5 | 3 PLIES (3X) 8OZ KEVLAR/5456-H116 | 0.1 | | N |
| 4-0662 | 2017-T4 | S | 0.3725 | 0.25 | 6.33 | 45 | 6061-T6 | 0.63 | | 3/1.5 | 3 PLIES 8OZ KEVLAR/5456-H116 | 0.125 | | N |
| 4-0671 | 1100 | S | 0.0059 | 0.0625 | 6.75 | 0 | 3 PLIES 8OZ KEVLAR | | | 4 | 5456-H116 | 0.1 | 0 | N |
| 4-0673 | 2017-T4 | S | 0.3731 | 0.25 | 6.8 | 45 | 7075-T6 | 0.063 | | 3/1.5 | 3 PLIES 8OZ KEVLAR/5456-H116 | 0.1 | | Y |
| 4-0674 | 2017-T4 | S | 0.3731 | 0.25 | 6.8 | 45 | 7075-T6 | 0.04 | | 3/1.5 | 3 PLIES 8OZ KEVLAR/5456-H116 | 0.1 | | Y |
| 4-0675 | 2017-T4 | S | 3.0032 | 0.5 | 5.72 | 0 | 3 LAYERS 6061-T6 | 0.063 | | 3x(3/1.5) | 3 PLIES (3X) 8OZ KEVLAR/5456-H116 | 0.1 | | N |
| 4-0724 | 2017-T4 | S | 1.275 | 0.375 | 6.38 | 0 | 6061-T6 | 0.08 | | 3/1.5 | 2519-T81 (NOT 2219) | 0.125 | | Y |
| 4-0736 | 2017-T4 | S | 3.0028 | 0.5 | 4.37 | 0 | 3 LAYERS 6061-T6 | 0.063 | | 3x(3/1.5) | 3 PLIES (3X) 8OZ KEVLAR/5456-H116 | 0.1 | | N |
| 4-0737 | 2017-T4 | S | 1.2727 | 0.375 | 2.83 | 0 | 3 LAYERS 6061-T6 | 0.063 | | 3x(3/1.5) | 3 PLIES (3X) 8OZ KEVLAR/5456-H116 | 0.1 | | N |

| | | WITNESS MATERIALS | | | | |
|---|---|---|---|---|---|---|
| UDRI | WITNESS | SPACING | THICK. | DEPTH of | HOLEOUT | COMMENTS |
| ID.NO. | MATERIALS | in | in | PEN. in | DIA. in | |
| 4-0544 | 2024-T3 | TBD | 0.02 | 0.02 | 0.01 | 1 WITNESS PLATE PENETRATED |
| 4-0545 | 2024-T3 | TBD | 0.02 | 0 | 0 | CORRUGATED BUMPER (32/20/20MILS 0.75" THICK) SPLIT, DEPEST CRATER IN WALL 0.080" |
| 4-0571 | 2024-T3 | 0.5 | 0.02 | 0 | 0 | 1.0" DEEP,9.0" WIDE DENT IN WALL |
| 4-0572 | 2024-T3 | 0.5 | 0.02 | 0.04 | 0.2 | (4) 1" AVG LENGHT PETALS IN WALL, 2 WIT. PLT. PENETRATED, CORR.BUMPER(32/20/20MILS 0.75 THICK) |
| 4-0573 | 2024-T3 | 0.5 | 0.02 | TBD | TBD | 65° OBLIQUE SHOT, 3 SMALL HOLES IN WALL |
| 4-0590 | 2024-T3 | 0.5 | 0.02 | 0 | 0 | 10" X 10" AND 1.6 " DEEP DENT IN WALL,2 WITNESS PLATES DENTED |
| 4-0591 | 2024-T3 | 0.5 | 0.02 | 0 | 0 | ~ 0.625" DOUBLE BULGE, 0.60" DEEP DENT IN WALL |
| 4-0592 | 2024-T3 | 0.5 | 0.02 | 0 | 0 | 3"X 3.5" KITE-SHAPED HOLE, WALL TORN ON RIGHT SIDE OF RIB, WAFFLE WALL |
| 4 -0593 | 2024-T3 | 0.5 | 0.02 | 0 | 0 | TORN ON BOTH SIDES RIB,WAFFLE WALL |
| 4-0594 | 2024-T3 | 0.5 | 0.02 | 0 | 0 | WALL DENTED/CRATERED 1" X 2" CRATER AREA, DEEPEST CRATER 0.110" AND 0.215" DIA. |
| 4-0595 | 2024-T3 | 0.5 | 0.02 | 0 | 0 | 1.8" DEEP DENT IN 12" X12" WALL PANEL |
| 4-0597 | | | | | | WALL LOADED 1500#/IN |
| 4-0599 | 2024-T3 | 0.5 | 0.02 | 0 | 0 | 1.1" DEEP DENT IN WALL,NOTE: 0.60" LONG CRACK ON BACKSIDE BUT NO PENETRATRATION |
| 4-0600 | 2024-T3 | 0.5 | 0.02 | 0.04 | 1.0x2.0 | (3) 4" AVG LENGHT PETALS IN WALL, 2 WITNESS PLATES PENETRATED |
| 4-0602 | 2024-T3 | | | | | WALL LOADED 1500#/IN |
| 4-0603 | 2024-T3 | 0 | 0.02 | 0 | 0 | WALL LOADED 1500#/IN,WITNESS STANDOFF 4.625", WITNESS PLATE DENTED |
| 4-0604 | 2024-T3 | 0.5 | 0.02 | TBD | TBD | (4)1.5" AVG LENGHT PETALS IN WALL |
| 4-0605 | 2024-T3 | 0.5 | 0.02 | 0.02 | 0.275x0.43 | 1 CELOTEX PENETRATED AND 1 DENTED |
| 4-0608 | 2024-T3 | 4.125 | 0.02 | 7.02 | 4.0x2.0 | (7) PETALS IN WALL AVG LENGHT 7" (1.25",45°,WAFFLE WALL LOADED 1500#/IN) |
| 4-0609 | 2024-T3 | 4.125 | 0.02 | 7.02 | 4.0x2.0 | (7) 7" AVG LENGHT PETALS IN WALL (LOADED 1500#/IN) |
| 4-0610 | 2024-T3 | 4.125 | 0.02 | 0 | 0 | 8" DIA,0.5" DEEP DENT IN WALL (LOADED 1500#/IN) |
| 4-0611 | 2024-T3 | 4.625 | 0.02 | > 0.490 | 0.5x0.3 | 1" ORTHGONAL WALL (LOADED 2050#/IN) |
| 4-0612 | 2024-T3 | 4.625 | 0.02 | 0.49 | 1.5 | WALL CRACKED IN HALF (LOADED 2400#/IN),0.8"x0.6" HOLE IN CELOTEX |
| 4-0613 | 2024-T3 | 4.625 | 0.02 | TBD | TBD | WALL LOADED 1500#/IN |
| 4-0614 | 2024-T3 | 4.625 | 0.02 | TBD | TBD | CENTER RIB REMOVED FROM WALL (LOADED 2400#/IN) |
| 4-0646 | | | | | | |
| 4-0647 | | | | | | |
| 4-0648 | | | | | | |
| 4-0650 | | | | | | SABOT FAILED |
| 4-0651 | | | | | | |
| 4-0652 | | | | | | |
| 4-0653 | | | | | | |
| 4-0654 | | | | | | |
| 4-0655 | | | | | | RICOCHET PANEL RIVETED TO BUMPER |
| 4-0656 | | | | | | |
| 4-0657 | | | | | | |
| 4-0660 | | | | | | |
| 4-0661 | | | | | | |
| 4-0662 | | | | | | |
| 4-0671 | | | | | | |
| 4-0673 | | | | | | |
| 4-0674 | | | | | | |
| 4-0675 | | | | | | |
| 4-0724 | | | | | | PLATE SPLIT LIKE 2219. |
| 4-0736 | | | | | | |
| 4-0737 | | | | | | |
| | | | | | | |

| | standoff inch | rearwall gage inch | bumper gage inch | rearwall alloy | bumper alloy | mli present | mli location | prj. len to dia | prj. material | obliquity | projectile size | velocity avg km/s | rear penetr'n | rearhole inch | rearwall spall | bumper hole inch | vel hall km/s | vel xray km/s | witness penet. | rico con | test number | data source | test | date | comments |
|---|---|---|---|---|---|---|---|---|---|---|---|---|---|---|---|---|---|---|---|---|---|---|---|---|---|
| 1 | 0 | 0.13 | | 2219-T87 | B CLOTH | TPS | | | 1100-O | 0 | 0.13 | 7.7 | | 0.4 | | | 7.6 | 7.8 | | | 730 | | GRIT-9 | 08/16/88 | |
| 2 | 4 | 0.05 | 0.05 | 2219-T87 | 6061-T6 | B | 3.75 | | 1100-O | 75 | 0.31 | 7.1 | N | 0 | N | 1.53 | 7.1 | 7 | 0 | CRATERED | 1181 | | 4108-D | 11/27/90 | WALL CRATERED ONLY. |
| 3 | 4 | 0.06 | 0.03 | 2219-T87 | 6061-T6 | NO | | | 1100-O | 0 | 0.31 | 6 | Y | 0.8 | Y | 0.49 | 5.9 | 6.1 | 4 | | 406 | IWALL | SS-228A | 12/11/86 | |
| | 4 | 0.06 | 0.03 | 2219-T87 | 6061-T6 | NO | | | 1100-O | 0 | 0.31 | 6.8 | Y | 0.8 | Y | 0.5 | | 6.8 | 4 | | 407 | IWALL | SS-228B | 12/11/86 | |
| 4 | 4 | 0.06 | 0.03 | 2219-T87 | 6061-T6 | YES | | | 1100-O | 45 | 0.25 | 5.6 | Y | 0.5 | N | 0.6 | 5.5 | 5.6 | 3 | CAVITIES | 399 | IWALL | SS-227A | 12/04/86 | |
| | 4 | 0.06 | 0.03 | 2219-T87 | 6061-T6 | YES | | | 1100-O | 45 | 0.25 | 7.2 | Y | 1 | N | 0.6 | 7.1 | 7.3 | 2 | CAVITIES | 410 | IWALL | SS-227B | 12/12/86 | |
| 5 | 4 | 0.1 | 0.03 | 2219-T87 | 6061-T6 | YES | | | 1100-O | 45 | 0.25 | 4.5 | Y | 0.5 | N | 0.51 | 4.4 | 4.5 | 4 | CAVITIES | 394 | IWALL | SS-226A | 11/24/86 | |
| | 4 | 0.1 | 0.03 | 2219-T87 | 6061-T6 | YES | | | 1100-O | 45 | 0.25 | 5.5 | Y | 0.8 | N | 0.56 | | 5.5 | 4 | CAVITIES | 397 | IWALL | SS-226B | 12/01/86 | |
| | 4 | 0.1 | 0.03 | 2219-T87 | 6061-T6 | YES | | | 1100-O | 45 | 0.25 | 6.7 | Y | 0.4 | N | 0.7 | 6.7 | 6.8 | 2 | CAVITIES | 398 | IWALL | SS-226C | 12/03/86 | |
| 6 | 4 | 0.1 | 0.04 | 2219-T87 | 6061-T6 | YES | W | | 1100-O | 0 | 0.25 | 4.4 | Y | 0.3 | N | 0.48 | | 4.4 | 0 | | 178 | ADP SM1 | SS-P-034C-1 | 03/14/86 | |
| | 4 | 0.1 | 0.04 | 2219-T87 | 6061-T6 | YES | W | | 1100-O | 0 | 0.25 | 5.5 | N | 0 | N | 0.51 | | 5.5 | 0 | | 177 | ADP SM1 | SS-P-034C | 03/13/86 | |
| 7 | 4 | 0.13 | 0.03 | 2219-T87 | 6061-T6 | NO | | | 1100-O | 45 | 0.3 | 3.5 | Y | 0.5 | N | 0.63 | | 3.5 | 3 | | 175 | MARTIN | SS-114B | 03/12/86 | |
| 8 | 4 | 0.13 | 0.03 | 2219-T87 | 6061-T6 | YES | B | | 1100-O | 0 | 0.19 | 7.2 | Y | 0.2 | Y | 0.34 | 7.3 | 7.2 | | | 897 | | MLI-B3 | 12/12/89 | SPALL AROUND HOLES |
| | 4 | 0.13 | 0.03 | 2219-T87 | 6061-T6 | YES | B | | 1100-O | 0 | 0.19 | 7.8 | S | 0 | Y | 0.38 | 7.8 | 7.8 | | | 898 | | MLI-B4 | 12/13/89 | COUNT SPALL AS FAILURE |
| 9 | 4 | 0.13 | 0.03 | 2219-T87 | 6061-T6 | YES | W | | 1100-O | 0 | 0.19 | 4 | Y | 0.4 | Y | 0.28 | | 4 | 2 | | 798 | | 3001-A | 09/08/89 | SMALL CRATERS UP TO 0.12" DIA X 0.05" DEEP IN AREA APPROX. 3.5" DIA. NO DIMPLES ON REAR, SPALLING AROUND HOLE APPROX. 0.06" WIDE AND 0.05" DEEP. OTHER CRATERS 0.2" DIA AND 0.2" DEEP FEW VERY SLIGHT DIMPLES ON REAR. |
| | 4 | 0.13 | 0.03 | 2219-T87 | 6061-T6 | YES | W | | 1100-O | 0 | 0.19 | 5.8 | Y | 0.2 | N | 0.35 | 5.8 | 5.8 | 1 | | 799 | | 3001-B | 09/14/89 | 2 HOLES: APPROX. 0.2" DIA AND ONE PIN HOLE. NO SINK AREA, VERY FEW CRATERS, 2 CRATERS AT EDGE OF HOLE APPROX. .2" DIA AND .05" DEEP. OTHER CRATERS 0.2" DIA AND .02" DEEP, FEW VERY SLIGHT DIMPLES ON REAR. |
| | 4 | 0.13 | 0.03 | 2219-T87 | 6061-T6 | YES | W | | 1100-O | 0 | 0.19 | 6.3 | Y | 0.2 | N | 0.35 | 6.2 | 6.3 | 0 | | 800 | | 3001-C | 09/14/89 | 3 HOLES, APPROX. 0.2" DIA X 0.1" DIA, 0.06" DIA AND 0.03" DIA, FEW SMALL CRATERS, SLIGHT BULGE ON REAR. |
| | 4 | 0.13 | 0.03 | 2219-T87 | 6061-T6 | YES | W | | 1100-O | 0 | 0.19 | 6.8 | Y | 0.2 | N | 0.35 | 6.8 | 6.9 | 0 | | 802 | | 3001-E | 09/18/89 | HOLE .2X.1", MOST OF DAMAGE APPROX. 1" DIA, ONE CRATER APPROX. .2" f 10m HOLE APPROX. .15" DIA AND .07 DEEP. FEW SMALL CRATERS LESS THAN 0.060" DIA. |
| | 4 | 0.13 | 0.03 | 2219-T87 | 6061-T6 | YES | W | | 1100-O | 0 | 0.19 | 7.2 | N | 0 | N | 0.52 | 7.2 | 7.3 | | | 801 | | 3001-D | 09/15/89 | 3 VERY SLIGHT CRATERS |
| 10 | 4 | 0.13 | 0.03 | 2219-T87 | 6061-T6 | YES | W | | 1100-O | 0 | 0.25 | 7 | Y | 0.9 | N | 0.46 | 7 | 7.1 | | | 803 | | 3002-A | 09/18/89 | HOLE APPROX. .2" DIA X .1" DIA WITH CRACKS IN METAL APPROX. .7" AND .9" SINK APPROX. 2.5" DIA WITH MOST OF DAMAGE APPROX. 7" DIA. BULGE ON REAR APPROX .3" |
| | 4 | 0.13 | 0.03 | 2219-T87 | 6061-T6 | YES | W | | 1100-O | 0 | 0.25 | 7.4 | Y | 2 | N | 0.42 | 7.3 | 7.5 | 2 | | 804 | | 3002-B | 09/19/89 | HOLE 2X1". MOST OF DAMAGE AT ONE END OF PETALED HOLE APPROX. " DIA, 2 HOLES APPROX. .1" DIA x .2" DIA APPROX. .2" FROM HOLE. SEVERAL CRATERS IN PETAL AND EDGE OF HOLE. |

| | standoff inch | rearwall gage inch | bumper gage inch | rearwall alloy | bumper alloy | mil present | mil location | prj. len to dia | prj. material | obliquity | projectile size | velocity avg km/s | rear penetr'n | rearhole inch | rearwall spall | bumper hole inch | vel hail km/s | vel xray km/s | witness penet. | rico con | test number | data source | test | date | comments |
|---|---|---|---|---|---|---|---|---|---|---|---|---|---|---|---|---|---|---|---|---|---|---|---|---|---|
| | 4 | 0.13 | 0.03 | 2219-T87 | 6061-T6 | YES | W | | 1100-O | 0 | 0.25 | 7.7 | N | 0 | N | 0.46 | 7.5 | 7.8 | | | 806 | | 3002-C | 09/20/89 | SINK .3" DIA X .3" DIA DEEP WITH SMALL CRATERS,..FEW SMALL CRATERS.... |
| 11 | 4 | 0.13 | 0.03 | 2219-T87 | 6061-T6 | YES | W | | 1100-O | 45 | 0.19 | 6.1 | Y | 0.3 | N | 0.44 | 6.1 | 6.1 | 0 | | 963 | | 3203 | 03/19/90 | |
| | 4 | 0.13 | 0.03 | 2219-T87 | 6061-T6 | YES | W | | 1100-O | 45 | 0.19 | 6.6 | Y | 0.1 | N | 0.48 | 6.6 | 6.7 | 0 | | 810 | | 3004-B | 09/22/89 | HOLE 0.1" DIA, ONE CRATER APPROX. 0.25" DIA WITH..CRACK ON REAR. FEW VERY SMALL CRATERS. |
| | 4 | 0.13 | 0.03 | 2219-T87 | 6061-T6 | YES | W | | 1100-O | 45 | 0.19 | 7 | Y | 0 | N | 0.43 | 6.8 | 7.2 | | | 807 | | 3004-A | 09/21/89 | PINHOLE, DAMAGE AREA APPROX. 1.5" DIA X 1" DIA SEVERAL CRATERS IN THIS AREA UP TO .2" DIA AND .05" DEEP ALL IN PROJECTILE PATH. VERY SLIGHT CRATERING UNDER BUMPER HOLE. 4 SMALL DIMPLES ON REAR. |
| | 4 | 0.13 | 0.03 | 2219-T87 | 6061-T6 | YES | W | | 1100-O | 45 | 0.19 | 7.7 | C | 0 | N | 0.54 | 7.7 | 7.7 | 0 | | 964 | | 3204 | 03/19/90 | REAR SURFACE CRACK ON WALL, COUNT AS FAILURE |
| 12 | 4 | 0.13 | 0.03 | 2219-T87 | 6061-T6 | YES | W | | 1100-O | 45 | 0.25 | 6.5 | Y | 0.5 | N | 0.57 | 6.5 | 6.5 | 2 | | 970 | | 3207 | 03/23/90 | |
| | 4 | 0.13 | 0.03 | 2219-T87 | 6061-T6 | YES | W | | 1100-O | 45 | 0.25 | 7.5 | Y | 0.2 | N | 0.63 | 7.4 | 7.6 | 0 | | 808 | | 3005-A | 09/21/89 | 2 HOLES IN PROJECTILE PATH APPROX. .20" DIA X .12" DIA AND APPROX. .1" DIA, MOST OF DAMAGE IN AREA APPORX. 1.2" DIA. FEW CRATERS UP TO .2" DIA AND .05" DEEP. FEW DIMPLES ON REAR. |
| | 4 | 0.13 | 0.03 | 2219-T87 | 6061-T6 | YES | W | | 1100-O | 45 | 0.25 | 7.7 | N | 0 | N | 0.64 | 7.6 | 7.8 | 0 | | 811 | | 3005-B | 09/26/89 | DAMAGE AREA IN PROJECTILE PATH 1.7" DIA X 1" DIA WITH FEW CRATERS UP TO .12" DIA AND .040" DIA DEEP. FEW VERY SMALL CRATERS UNDER BUMPER PROJECTILE HOLE. SLIGHT BULGE ON REAR. |
| 13 | 4 | 0.13 | 0.03 | 2219-T87 | 6061-T6 | YES | W | | 1100-O | 45 | 0.31 | 7.1 | Y | 0.8 | N | 0.75 | 7 | 7.2 | 3 | | 812 | | 3006-A | 09/26/89 | SEVERE CRACKS DAMAGE APPROX. 2/3 CIRCUMFERENCE OF HOLE |
| 14 | 4 | 0.13 | 0.03 | 2219-T87 | 6061-T6 | YES | W | | 1100-O | 65 | 0.19 | 3.4 | N | 0 | N | 0.58 | 3.4 | 3.4 | | | 820 | | 3007-C | 10/02/89 | VERY LITTLE DAMAGE, FEW SMALL CRATERS UNDER BUMPER HOLE, NO DIMPLES ON REAR. |
| | 4 | 0.13 | 0.03 | 2219-T87 | 6061-T6 | YES | W | | 1100-O | 65 | 0.19 | 4.8 | N | 0 | N | 0.54 | 4.8 | 4.9 | 0 | | 819 | | 3007-B | 10/02/89 | CRATER IN PROJECTILE PATH APPROX. .2" DIA WITH DIMPLE ON REAR. FEW CRATERS BEGINNING UNDER BUMPER HOLE AND EXTENDING FOR AREA APPROX .3" DIA WIDE AND .3" DIA TOWARD PROJECTILE PATH. ONE CRATER .15" DIA AND .040" DIA DEEP WITH DIMPLE ON REAR. OTHER CRATER |
| | 4 | 0.13 | 0.03 | 2219-T87 | 6061-T6 | YES | W | | 1100-O | 65 | 0.19 | 6.6 | N | 0 | N | 0.85 | 6.5 | 6.6 | 0 | | 818 | | 3007-A | 09/29/89 | NO DAMAGE IN PROJECTILE PATH. FEW CRATERS BEGINNING UNDER BUMPER HOLE UP TO APPROX. .1" DIA. 3 VERY SMALL DIMPLES ON REAR. |
| 15 | 4 | 0.13 | 0.03 | 2219-T87 | 6061-T6 | YES | W | | 1100-O | 65 | 0.25 | 3.8 | N | 0 | N | 0.78 | 3.8 | 3.8 | 0 | | 971 | | 3208 | 03/23/90 | |
| | 4 | 0.13 | 0.03 | 2219-T87 | 6061-T6 | YES | W | | 1100-O | 65 | 0.25 | 4.3 | Y | 0.1 | N | 0.74 | 4.3 | 4.3 | 0 | | 822 | | 3008-B | 10/03/89 | FEW SMALL CRATERS IN SAME AREA. FEW SMALL CRATERS UNDER BUMPER HOLE NO DIMPLES ON REAR. |
| | 4 | 0.13 | 0.03 | 2219-T87 | 6061-T6 | YES | W | | 1100-O | 65 | 0.25 | 4.7 | N | 0 | N | 0.77 | 4.6 | 4.7 | 0 | | 821 | | 3008-A | 10/03/89 | CRATER IN PROJECTILE PATH APPROX. .287" DIA X .17" DIA AND .08" DIA DEEP WITH DIMPLE ON REAR. FEW SMALL CRATER IN SAME AREA UNDER BUMPER HOLE SLIGHT DAMAGE TO AREA APPROX. .4" DIA FEW CRATERS UP TO .1" DIA WITH 3 SMALL DIMPLES ON REAR. |
| | 4 | 0.13 | 0.03 | 2219-T87 | 6061-T6 | YES | W | | 1100-O | 65 | 0.25 | 5.6 | N | 0 | N | 0.95 | | 5.6 | 0 | | 974 | | 3210 | 03/27/90 | |
| 16 | 4 | 0.13 | 0.03 | 2219-T87 | 6061-T6 | YES | W | | 1100-O | 65 | 0.31 | 3.6 | Y | 0.3 | N | 0.95 | 3.6 | 3.6 | 1 | | 982 | | 3212-1 | 04/05/90 | |

| | standoff inch | rearwall gage inch | bumper gage inch | rearwall alloy | bumper alloy | mil present | mil location | prj. lan to dia | prj. material | obliquity | projectile size | velocity avg km/s | rear penetr'n | rearhole inch | rearwall spall | bumper hole inch | vel hall km/s | vel xray km/s | witness penet. | rico con | test number | data source | test | date | comments |
|---|---|---|---|---|---|---|---|---|---|---|---|---|---|---|---|---|---|---|---|---|---|---|---|---|---|
| | 4 | 0.13 | 0.03 | 2219-T87 | 6061-T6 | YES | W | | 1100-O | 65 | 0.31 | 4.6 | C | 0 | N | 1 | 4.5 | 4.6 | 0 | | 824 | | 3009-B | 10/04/89 | NO HOLE, NO LIGHT CAN BE SEEN THROUGH CRATER IN PROJECTILE PATH THAT IS APPROX. .26" DIA X .18" DIA AND .15" DIA DEEP. DIMPLE ON REAR WITH VERY SMALL CRACK (COUNT CRACK AS FAILURE. SEVERAL SMALL CRATERS. UNDER BUMPER HOLE DAMAGE AREA IS APPROX. .4" DIA W |
| | 4 | 0.13 | 0.03 | 2219-T87 | 6061-T6 | YES | W | | 1100-O | 65 | 0.31 | 5.2 | Y | 0 | N | 0.93 | 5.1 | 5.2 | | | 823 | | 3009-A | 10/04/89 | PIN HOLE IN PROJECTILE PATH, SMALL CRACK IN METAL AT BOTTOM OF CRATER THAT IS APPROX. .24" DIA X .2" DIA, 2 CRATERS IN AREA APPROX. .2" DIA WITH DIMPLES ON REAR, FEW OTHER SMALL CRATERS UNDER BUMPER HOLE CRATER COVER AN AREA APPROX. 3.5" DIA FEW CRATERS |
| | 4 | 0.13 | 0.03 | 2219-T87 | 6061-T6 | YES | W | | 1100-O | 65 | 0.31 | 6.1 | C | 0 | N | 1.05 | | 6.1 | 0 | | 979 | | 3217 | 04/02/90 | REAR SURFACE CRACK, COUNTED AS FAILURE |
| 17 | 4 | 0.13 | 0.04 | 2219-T87 | 6061-T6 | NO | | 1 | LEXAN | 0 | 0.38 | 6.4 | Y | 3 | N | 0.71 | 6.4 | | 4 | | 387 | IWALL | SS-225D-1 | 11/06/86 | |
| 18 | 4 | 0.13 | 0.04 | 2219-T87 | 6061-T6 | NO | | | 1100-O | 0 | 0.19 | 3.3 | Y | 0.1 | Y | 0.31 | 3.2 | 3.4 | | | 481 | MSFC | SS-T2-2 | 02/26/87 | |
| 19 | 4 | 0.13 | 0.04 | 2219-T87 | 6061-T6 | NO | | | 1100-O | 0 | 0.25 | 4.9 | Y | 0.2 | N | 0.44 | | 4.9 | 1 | | 182 | ADP SM1 | SS-P-033B | 03/20/86 | |
| | 4 | 0.13 | 0.04 | 2219-T87 | 6061-T6 | NO | | | 1100-O | 0 | 0.25 | 5.3 | Y | 0.3 | Y | 0.44 | | 5.3 | 1 | | 183 | ADP SM1 | SS-P-033B-1 | 03/24/86 | |
| | 4 | 0.13 | 0.04 | 2219-T87 | 6061-T6 | NO | | | 1100-O | 0 | 0.25 | 5.5 | C | 0 | N | 0.44 | | 5.5 | 0 | | 184 | ADP SM1 | SS-P-033C | 03/24/86 | REAR SURFACE CRACK COUNTED AS FAILURE |
| | 4 | 0.13 | 0.04 | 2219-T87 | 6061-T6 | NO | | | 1100-O | 0 | 0.25 | 7.2 | Y | 0.1 | Y | 0.52 | | 7.2 | 2 | | 181 | ADP SM1 | SS-P-033 | 03/17/86 | |
| 20 | 4 | 0.13 | 0.04 | 2219-T87 | 6061-T6 | NO | | | 1100-O | 0 | 0.31 | 4.3 | Y | 1 | N | 0.56 | 4.3 | 4.3 | | | 391 | MSFC | SS-PT6A | 11/19/86 | |
| | 4 | 0.13 | 0.04 | 2219-T87 | 6061-T6 | NO | | | 1100-O | 0 | 0.31 | 4.6 | Y | 1 | Y | 0.48 | 4.6 | 4.7 | | | 475 | MSFC | SS-T2-6 | 02/23/87 | |
| 21 | 4 | 0.13 | 0.04 | 2219-T87 | 6061-T6 | NO | | | 1100-O | 0 | 0.38 | 5.4 | Y | 1.8 | N | 0.53 | 5.4 | 5.5 | | | 495 | MSFC | SS-T2-16 | 03/11/87 | |
| 22 | 4 | 0.13 | 0.04 | 2219-T87 | 6061-T6 | NO | | | 1100-O | 45 | 0.13 | 3.3 | N | 0 | N | 0.29 | 3.3 | 3.3 | 0 | CAVITIES | 359 | IWALL | SS-222C | 10/15/86 | |
| | 4 | 0.13 | 0.04 | 2219-T87 | 6061-T6 | NO | | | 1100-O | 45 | 0.13 | 5 | N | 0 | N | 0.34 | | 5 | 0 | CAVITIES | 358 | IWALL | SS-222B | 10/14/86 | |
| | 4 | 0.13 | 0.04 | 2219-T87 | 6061-T6 | NO | | | 1100-O | 45 | 0.13 | 5.6 | N | 0 | N | 0.36 | | 5.6 | 0 | CAVITIES | 357 | IWALL | SS-222A | 10/14/86 | |
| 23 | 4 | 0.13 | 0.04 | 2219-T87 | 6061-T6 | NO | | | 1100-O | 45 | 0.19 | 3.2 | Y | 0.3 | N | 0.42 | 4.2 | 4.3 | 1 | | 215 | IWALL | SS-202B | 06/05/86 | |
| | 4 | 0.13 | 0.04 | 2219-T87 | 6061-T6 | NO | | | 1100-O | 45 | 0.19 | 3.5 | Y | 0.1 | N | 0.42 | 3.5 | 3.5 | 0 | | 214 | IWALL | SS-202A | 06/05/86 | |
| | 4 | 0.13 | 0.04 | 2219-T87 | 6061-T6 | NO | | | 1100-O | 45 | 0.19 | 5.3 | Y | 0.4 | N | 0.47 | 5.2 | 5.3 | 2 | SPRAY | 259 | IWALL | SS-202C | 07/14/86 | |
| | 4 | 0.13 | 0.04 | 2219-T87 | 6061-T6 | NO | | | 1100-O | 45 | 0.19 | 6 | Y | 0.2 | Y | 0.48 | 5.9 | 6 | 0 | | 504 | MARTIN | SS-154B | 04/02/87 | |
| | 4 | 0.13 | 0.04 | 2219-T87 | 6061-T6 | NO | | | 1100-O | 45 | 0.19 | 6.4 | Y | 0.3 | N | 0.46 | 6.4 | 6.5 | 1 | SPRAY | 261 | IWALL | SS-202D | 07/14/86 | |
| | 4 | 0.13 | 0.04 | 2219-T87 | 6061-T6 | NO | | | 1100-O | 45 | 0.19 | 6.8 | N | 0 | N | 0.55 | 6.8 | 6.9 | 0 | | 503 | MARTIN | SS-154A | 04/02/87 | |
| | 4 | 0.13 | 0.04 | 2219-T87 | 6061-T6 | NO | | | 1100-O | 45 | 0.19 | 7.2 | Y | 0.1 | N | 0.51 | 7.2 | 7.2 | 0 | SPRAYED | 262 | IWALL | SS-202E | 07/15/86 | |
| | 4 | 0.13 | 0.04 | 2219-T87 | 6061-T6 | NO | | | 1100-O | 45 | 0.19 | 7.5 | Y | 0.2 | N | 0.54 | | 7.5 | 0 | | 263 | IWALL | SS-202F | 07/15/86 | |
| 24 | 4 | 0.13 | 0.04 | 2219-T87 | 6061-T6 | NO | | | 1100-O | 65 | 0.25 | 3.2 | N | 0 | N | 0.72 | | 3.2 | 0 | HOLES | 265 | IWALL | SS-204D | 07/16/86 | |
| | 4 | 0.13 | 0.04 | 2219-T87 | 6061-T6 | NO | | | 1100-O | 65 | 0.25 | 4.3 | N | 0 | N | 0.83 | 4.2 | 4.3 | 0 | 2HOLES | 247 | IWALL | SS-204C | 07/01/86 | |
| | 4 | 0.13 | 0.04 | 2219-T87 | 6061-T6 | NO | | | 1100-O | 65 | 0.25 | 4.8 | Y | 0.1 | N | 0.78 | 4.7 | 4.8 | 0 | HOLES | 245 | IWALL | SS-204A | 06/30/86 | |

| | standoff inch | rearwall gage inch | bumper gage inch | rearwall alloy | bumper alloy | mli present | mli location | pri. len to dia | pri. material | obliquity | projectile size | velocity avg km/s | rear penetr'n | rearhole inch | rearwall spall | bumper hole inch | vel hall km/s | vel xray km/s | witness penet. | rico con | test number | data source | test | date | comments |
|---|---|---|---|---|---|---|---|---|---|---|---|---|---|---|---|---|---|---|---|---|---|---|---|---|---|
| | 4 | 0.13 | 0.04 | 2219-T87 | 6061-T6 | NO | | | 1100-O | 65 | 0.25 | 5.9 | C | 0 | N | 0.88 | 5.9 | 5.9 | 0 | HOLES | 246 | IWALL | SS-204B | 07/01/86 | CRACK ON BACK SIDE OF A DIMPLE. |
| 25 | 4 | 0.13 | 0.04 | 2219-T87 | 6061-T6 | NO | | | LEXAN | 0 | 0.35 | 4.3 | N | 0 | N | 0.51 | | 4.3 | 0 | | 384 | IWALL | SS-225C | 11/05/86 | |
| | 4 | 0.13 | 0.04 | 2219-T87 | 6061-T6 | NO | | | LEXAN | 0 | 0.35 | 4.9 | N | 0 | N | 0.51 | | 4.9 | 0 | | 383 | IWALL | SS-225B | 11/04/86 | |
| | 4 | 0.13 | 0.04 | 2219-T87 | 6061-T6 | NO | | | LEXAN | 0 | 0.35 | 5.8 | S | 0 | Y | 0.53 | | 5.8 | 0 | | 379 | IWALL | SS-225A | 10/31/86 | |
| 26 | 4 | 0.13 | 0.04 | 2219-T87 | CADMIUM | NO | | | CADMIUM | 0 | 0.22 | 3.7 | Y | | N | 0.5 | | 3.7 | 0 | | 298 | MARTIN | CD-134B | 08/20/86 | |
| | 4 | 0.13 | 0.04 | 2219-T87 | CADMIUM | NO | | | CADMIUM | 0 | 0.22 | 4.6 | Y | | Y | 0.55 | | 4.6 | 0 | | 297 | MARTIN | CD-134A | 08/19/86 | |
| | 4 | 0.13 | 0.04 | 2219-T87 | CADMIUM | NO | | | CADMIUM | 0 | 0.22 | 4.8 | N | | N | 0.55 | | 4.8 | 0 | | 299 | MARTIN | CD-134C | 08/21/86 | |
| 27 | 4 | 0.13 | 0.04 | 2219-T87 | CADMIUM | NO | | | CADMIUM | 0 | 0.24 | 2.8 | Y | 0.5 | N | 0.47 | | 2.8 | 1 | | 300 | MARTIN | CD-134D | 08/21/86 | |
| | 4 | 0.13 | 0.04 | 2219-T87 | CADMIUM | NO | | | CADMIUM | 0 | 0.24 | 3.5 | Y | 1 | N | 0.51 | | 3.5 | 0 | | 293 | MARTIN | CD-133A | 08/15/86 | |
| | 4 | 0.13 | 0.04 | 2219-T87 | CADMIUM | NO | | | CADMIUM | 0 | 0.24 | 4.6 | Y | 1.1 | N | 0.54 | | 4.6 | 3 | | 294 | MARTIN | CD-133B | 08/15/86 | |
| | 4 | 0.13 | 0.04 | 2219-T87 | CADMIUM | NO | | | CADMIUM | 0 | 0.24 | 5 | Y | 0.2 | N | 0.7 | | 5 | 0 | N | 295 | MARTIN | CD-133C | 08/18/86 | |
| | 4 | 0.13 | 0.04 | 2219-T87 | CADMIUM | NO | | | CADMIUM | 0 | 0.24 | | | | | 0.5 | | 5.4 | | | 296 | | CD-133D | 08/18/86 | |
| 28 | 4 | 0.13 | 0.04 | 2219-T87 | CADMIUM | NO | | | CADMIUM | 0 | 0.26 | 6 | Y | 0.1 | Y | 0.51 | | 6 | 0 | | 291 | MARTIN | CD-132C | 08/14/86 | |
| | 4 | 0.13 | 0.04 | 2219-T87 | CADMIUM | NO | | | CADMIUM | 0 | 0.26 | 6.5 | Y | 0.6 | N | 0.46 | | 6.5 | 1 | | 290 | MARTIN | CD-132B | 08/13/86 | |
| 29 | 4 | 0.13 | 0.04 | 2219-T87 | 6061-T6 | YES | W | 1 | 1100-O | 0 | 0.2 | 3.9 | Y | 0.2 | N | 0.39 | 3.8 | 3.9 | | | 493 | MSFC | SS-T2-14 | 03/10/87 | |
| 30 | 4 | 0.13 | 0.04 | 2219-T87 | 6061-T6 | YES | W | 1 | 6061-T6 | 45 | 0.26 | 5.7 | Y | 0.4 | N | 0.67 | | 5.7 | 4 | CAVITIES | 372 | IWALL | SS-223C | 10/27/86 | |
| | 4 | 0.13 | 0.04 | 2219-T87 | 6061-T6 | YES | W | 1 | 6061-T6 | 45 | 0.26 | 6.6 | Y | 0.3 | N | 0.7 | | 6.6 | 1 | NO CAVS. | 370 | IWALL | SS-223A | 10/24/86 | |
| | 4 | 0.13 | 0.04 | 2219-T87 | 6061-T6 | YES | W | 1 | 6061-T6 | 45 | 0.26 | 6.8 | Y | 0.4 | N | 0.8 | | 6.8 | 1 | SPRAY | 371 | IWALL | SS-223B | 10/24/86 | |
| 31 | 4 | 0.13 | 0.04 | 2219-T87 | 6061-T6 | YES | W | 1 | 6061-T6 | 65 | 0.26 | 3.7 | N | 0 | N | 0.89 | | 3.7 | 0 | 5HOLES | 376 | IWALL | SS-224C | 10/29/86 | |
| | 4 | 0.13 | 0.04 | 2219-T87 | 6061-T6 | YES | W | 1 | 6061-T6 | 65 | 0.26 | 4.8 | N | 0 | N | 1 | | 4.8 | 0 | 3HOLES | 375 | IWALL | SS-224B | 10/28/86 | |
| | 4 | 0.13 | 0.04 | 2219-T87 | 6061-T6 | YES | W | 1 | 6061-T6 | 65 | 0.26 | 6.5 | N | 0 | N | 1.02 | | 6.5 | 0 | HOLES | 374 | IWALL | SS-224A | 10/28/86 | |
| 32 | 4 | 0.13 | 0.04 | 2219-T87 | 6061-T6 | YES | W | | 1100-O | 0 | 0.19 | 2.5 | Y | 0.3 | N | 0.27 | 2.6 | 2.5 | | | 483 | MSFC | SS-T2-1 | 03/02/87 | |
| | 4 | 0.13 | 0.04 | 2219-T87 | 6061-T6 | YES | W | | 1100-O | 0 | 0.19 | 6 | Y | 0.6 | Y | 0.36 | 5.9 | 6 | 1 | | 813 | | 3010-A | 09/27/89 | 2 HOLES, 0.6X0.25", 0.05" DIA. DAMAGE MOSTLY IN 1.2" DIA AREA FEW CRATERS IN THIS AREA APPROX. .1" DIA AND .03" DIA DEEP. VERY SLIGHT EDGE ON REAR WITH SPALL AROUND HOLE APPROX. .1" DIA WIDE AND THIN LAYER OF METAL |
| | 4 | 0.13 | 0.04 | 2219-T87 | 6061-T6 | YES | W | | 1100-O | 0 | 0.19 | 6.6 | Y | 0.2 | N | 0.39 | 6.6 | 6.6 | 0 | | 965 | | 3201 | 03/20/90 | |

| | standoff inch | rearwall gage inch | bumper gage inch | rearwall alloy | bumper alloy | mli present | mli location | prj. len to dia | prj. material | obliquity | projectile size | velocity avg km/s | rear penetr'n | rearhole inch | rearwall spall | bumper hole inch | vel hall km/s | vel xray km/s | witness penet. | rico con | test number | data source | test | date | comments |
|---|---|---|---|---|---|---|---|---|---|---|---|---|---|---|---|---|---|---|---|---|---|---|---|---|---|
| | 4 | 0.13 | 0.04 | 2219-T87 | 6061-T6 | YES | W | | 1100-O | 0 | 0.19 | 7.1 | Y | 0.2 | N | 0.32 | | 7.1 | 0 | | 814 | | 3010-B | 09/27/89 | 2 HOLES, 0.2X0.12", 0.05" DIA. DAMAGE IN AREA APPROX. 1" DIA ONE CRATERS APPROX. .2" DIA AND .06" DIA DEEP WITH DIMPLE ON REAR SEVERAL OTHER SMALL CRATERS. LARGER HOLE HAS APPROX. .06" DIA WIDE SOME ARE AND EDGE AT HOLE. SLIGHT EDGE IN METAL ON REAR. |
| | 4 | 0.13 | 0.04 | 2219-T87 | 6061-T6 | YES | W | | 1100-O | 0 | 0.19 | 7.2 | N | 0 | N | 0.42 | 7.2 | 7.2 | 0 | | 966 | | 3202 | 03/20/90 | |
| | 4 | 0.13 | 0.04 | 2219-T87 | 6061-T6 | YES | W | | 1100-O | 0 | 0.19 | 7.5 | Y | 0.1 | N | 0.04 | 7.3 | 7.6 | 0 | | 815 | | 3010-C | 09/28/89 | HOLE 0.06" DIAM IN A CRATER APPROX. .15" DIA WITH ANOTHER CRATER JOINING APPROX. .12" DIA FEW VERY SMALL CRATERS WITHIN .3" DIA OF THE LARGER CRATERS. |
| 33 | 4 | 0.13 | 0.04 | 2219-T87 | 6061-T6 | YES | W | | 1100-O | 0 | 0.25 | 6.8 | N | 0 | N | 0.5 | 6.8 | 6.8 | 0 | | 967 | | 3205 | 03/21/90 | |
| | 4 | 0.13 | 0.04 | 2219-T87 | 6061-T6 | YES | W | | 1100-O | 0 | 0.25 | 6.8 | Y | 0.2 | Y | 0.46 | | 6.8 | 0 | | 969 | | 3206 | 03/22/90 | 4 HOLES, SMALL SPALL AROUND HOLES |
| | 4 | 0.13 | 0.04 | 2219-T87 | 6061-T6 | YES | W | | 1100-O | 0 | 0.25 | 6.8 | Y | 0.3 | N | 0.46 | 6.8 | 6.9 | 0 | | 817 | | 3010-B1 | 09/29/89 | HOLE 0.25" DIA, SLIGHTLY JAGGED, SINK IN AN AREA APPROX. .2" DIA, WITH MOST OF THE CRATERS IN AN AREA APPROX. .6" DIA X 1.5" DIA, MANY SMALL CRATERS IN THIS AREA UP TO .1" DIA AND .040" DIA DEEP. FEW CRATERS OUT TO 2" DIA AREA BULGE ON REAR WITH A SLIGH |
| | 4 | 0.13 | 0.04 | 2219-T87 | 6061-T6 | YES | W | | 1100-O | 0 | 0.25 | 7.3 | N | 0 | N | 0.51 | 7.2 | 7.4 | 0 | | 816 | | 3010-A1 | 09/28/89 | SINK AREA APPROX. .2" DIA WITH FEW CRATERS LESS THAN .1" DIA, SLIGHT BULGE OR REAR WITH ONE DIMPLE. |
| 34 | 4 | 0.13 | 0.04 | 2219-T87 | 6061-T6 | YES | W | | 1100-O | 0 | 0.31 | 4 | Y | 1 | N | 0.46 | 3.9 | 4 | | | 476 | MSFC | SS-T2-5 | 02/23/87 | PETALED |
| | 4 | 0.13 | 0.04 | 2219-T87 | 6061-T6 | YES | W | | 1100-O | 0 | 0.31 | 6.8 | Y | 2 | N | 0.52 | 6.8 | 6.9 | 1 | | 825 | | 3011-B | 10/05/89 | HOLE APPROX. 2" DIA WITH 5 PETALS PUSHED OUTWARDS APPROX. 2". METAL SPLIT ALONG PETALS APPROX. 3.5" DIA, 2.5" DIA, 4" DIA, 1.5" DIA AND 3" DIA. |
| | 4 | 0.13 | 0.04 | 2219-T87 | 6061-T6 | YES | W | | 1100-O | 0 | 0.31 | 7.1 | Y | 2.5 | N | 0.54 | 7 | 7.1 | 3 | | 826 | | 3011-A | 10/05/89 | HOLE 2.5X2". 6 PETALS PUSHED OUTWARD APPROX. 2." SPLIT IN METAL ALONG PETALS APPROX. 3", 2.5", 2.5", 2.5", 2.2" AND 2.1" |
| 35 | 4 | 0.13 | 0.04 | 2219-T87 | 6061-T6 | YES | W | | 1100-O | 0 | 0.38 | 5 | Y | 6 | N | 0.52 | 5 | 5.1 | | | 494 | MSFC | SS-T2-15 | 03/10/87 | PETALING |
| 36 | 4 | 0.13 | 0.04 | 2219-T87 | 6061-T6 | YES | W | | 1100-O | 30 | 0.19 | 2.7 | Y | 0.3 | N | 0.33 | 2.7 | 2.7 | 1 | | 827 | | 3012-B | 10/06/89 | HOLE 0.324X0.266" OBLONG IN PROJECTILE PATH. FEW SHALLOW CRATERS UNDER BUMPER HOLE |
| | 4 | 0.13 | 0.04 | 2219-T87 | 6061-T6 | YES | W | | 1100-O | 30 | 0.19 | 4 | N | 0 | N | 0.36 | 4 | 4 | 0 | | 829 | | 3012-C | 10/10/89 | NO HOLE, 2 CRATERS APPROX. .2" DIA X .08" DEEP, AMD .18" DIA X .08" DEEP WITH LARGE DIMPLES ON REAR SEVERAL SMALLER CRATERS. ALL DAMAGE IN AREA OF PROJECTILE PATH |
| | 4 | 0.13 | 0.04 | 2219-T87 | 6061-T6 | YES | W | | 1100-O | 30 | 0.19 | 4.3 | N | 0 | N | 0.39 | 4.3 | 4.3 | 0 | | 828 | | 3012-D | 10/06/89 | CRATERS APPROX. .15" DIA X .11 DEEP, .018" DIA X d.09" DEEP, .19" DIA X .11 DEEP. ALL WITH LARGE DIMPLES ON REAR. SEVERAL SMALLER CRATERS. DAMAGE ALL IN PROJECTILE PATH. |
| 37 | 4 | 0.13 | 0.04 | 2219-T87 | 6061-T6 | YES | W | | 1100-O | 30 | 0.25 | 7 | Y | 1.4 | N | 0.48 | 7 | 7.1 | 0 | | 830 | | 3013-A | 10/10/89 | HOLE IN PROJECTILE PATH APPROX. 1.4" X .8" WITH 2 PETALS PUSHED OUT ON BACK APPROX 0.8" WIDE X 1.0" LONG AND 0.6" WIDE X 1.2" LONG. FEW SMALL CRATERS IN PETALS AND AROUND EDGE OF HOLE. |

| | standoff inch | rearwall gage inch | bumper gage inch | rearwall alloy | bumper alloy | mil present | mil location | prj. len to dia | prj. material | obliquity | projectile size | velocity avg km/s | rear penetr'n | rearhole inch | rearwall spall | bumper hole inch | vel hall km/s | vel xray km/s | witness penet. | rico con | test number | data source | test | date | comments |
|---|---|---|---|---|---|---|---|---|---|---|---|---|---|---|---|---|---|---|---|---|---|---|---|---|---|
| 38 | 4 | 0.13 | 0.04 | 2219-T87 | 6061-T6 | YES | W | | 1100-O | 45 | 0.19 | 2.9 | N | 0 | N | 0.4 | 2.9 | 3 | 0 | CAVITIES | 535 | MSFC | SS-333 | 05/11/87 | |
| | 4 | 0.13 | 0.04 | 2219-T87 | 6061-T6 | YES | W | | 1100-O | 45 | 0.19 | 3.7 | N | 0 | N | 0.4 | 3.6 | 3.7 | 0 | CAVITIES | 533 | MSFC | SS-334 | 05/07/87 | |
| | 4 | 0.13 | 0.04 | 2219-T87 | 6061-T6 | YES | W | | 1100-O | 45 | 0.19 | 4.1 | c | 0 | N | 0.46 | 4 | 4.1 | 0 | CAVITIES | 347 | IWALL | SS-221D | 10/06/86 | COUNT REAR SURFACE CRACK AS FAILURE |
| | 4 | 0.13 | 0.04 | 2219-T87 | 6061-T6 | YES | W | | 1100-O | 45 | 0.19 | 4.6 | N | 0 | N | 0.45 | 4.6 | 4.6 | 0 | CAVITIES | 346 | IWALL | SS-221C | 10/03/86 | |
| | 4 | 0.13 | 0.04 | 2219-T87 | 6061-T6 | YES | W | | 1100-O | 45 | 0.19 | 5.9 | N | 0 | N | 0.54 | 5.9 | 6 | 0 | CAVITIES | 345 | IWALL | SS-221B | 10/03/86 | |
| | 4 | 0.13 | 0.04 | 2219-T87 | 6061-T6 | YES | W | | 1100-O | 45 | 0.19 | 6.4 | N | 0 | N | 0.48 | 6.4 | 6.5 | 0 | NODAMAG | 344 | IWALL | SS-221A | 10/02/86 | |
| 39 | 4 | 0.13 | 0.04 | 2219-T87 | 6061-T6 | YES | W | | 1100-O | 45 | 0.25 | 4.1 | Y | 0.5 | N | 0.52 | 4 | 4.2 | 1 | CAVITIES | 531 | MSFC | SS-335 | 05/05/87 | |
| | 4 | 0.13 | 0.04 | 2219-T87 | 6061-T6 | YES | W | | 1100-O | 45 | 0.25 | 4.3 | Y | 0.4 | N | 0.55 | | 4.3 | 1 | SPRAYED | 266 | IWALL | SS-201A | 07/17/86 | |
| | 4 | 0.13 | 0.04 | 2219-T87 | 6061-T6 | YES | W | | 1100-O | 45 | 0.25 | 4.5 | Y | 0.6 | N | 0.53 | 4.5 | 4.6 | 2 | CAVITIES | 532 | MSFC | SS-336 | 05/06/87 | |
| | 4 | 0.13 | 0.04 | 2219-T87 | 6061-T6 | YES | W | | 1100-O | 45 | 0.25 | 5.5 | Y | 0.5 | N | 0.53 | | 5.5 | 4 | CAVITIES | 267 | IWALL | SS-201B | 07/17/86 | |
| | 4 | 0.13 | 0.04 | 2219-T87 | 6061-T6 | YES | W | | 1100-O | 45 | 0.25 | 5.8 | C | 0 | N | 0.57 | 5.7 | 5.8 | 0 | CAVITIES | 536 | MSFC | SS-336A | 05/13/87 | "SMALL CRACK IN DIMPLE ON BACK"--COUNT AS PENETRATION |
| | 4 | 0.13 | 0.04 | 2219-T87 | 6061-T6 | YES | W | | 1100-O | 45 | 0.25 | 7.2 | Y | 0.1 | N | 0.53 | | 7.2 | 0 | CAVITIES | 268 | IWALL | SS-201C | 07/18/86 | |
| | 4 | 0.13 | 0.04 | 2219-T87 | 6061-T6 | YES | W | | 1100-O | 45 | 0.25 | 7.6 | Y | 0.6 | N | 0.65 | 7.5 | 7.7 | 2 | CAVITIES | 269 | IWALL | SS-201D | 07/21/86 | |
| 40 | 4 | 0.13 | 0.04 | 2219-T87 | 6061-T6 | YES | W | | 1100-O | 45 | 0.31 | 3 | Y | 1 | N | 0.65 | 2.9 | 3 | 4 | CAVITIES | 524 | MSFC | SS-319 | 04/24/87 | |
| | 4 | 0.13 | 0.04 | 2219-T87 | 6061-T6 | YES | W | | 1100-O | 45 | 0.31 | 4.1 | Y | 0.8 | N | 0.65 | 4.1 | 4.2 | 4 | CAVITIES | 527 | MSFC | SS-324 | 04/29/87 | |
| | 4 | 0.13 | 0.04 | 2219-T87 | 6061-T6 | YES | W | | 1100-O | 45 | 0.31 | 6.5 | Y | 3 | N | 0.76 | 6.5 | 6.6 | 4 | | 497 | MSFC | SS-003A | 03/25/87 | |
| | 4 | 0.13 | 0.04 | 2219-T87 | 6061-T6 | YES | W | | 1100-O | 45 | 0.31 | 6.9 | Y | 1.1 | N | 0.77 | 6.8 | 7 | 4 | CAVITIES | 540 | MSFC | SS-337 | 05/18/87 | |
| | 4 | 0.13 | 0.04 | 2219-T87 | 6061-T6 | YES | W | | 1100-O | 45 | 0.31 | 7 | Y | 1 | N | 0.84 | 7 | 7.1 | 2 | CAVITIES | 538 | MSFC | SS-338 | 05/14/87 | |
| 41 | 4 | 0.13 | 0.04 | 2219-T87 | 6061-T6 | YES | W | | 1100-O | 45 | 0.38 | 6.5 | Y | 2 | N | 0.83 | 6.5 | | 3 | 1HOLE | 544 | MSFC | SS-339 | 05/21/87 | |
| 42 | 4 | 0.13 | 0.04 | 2219-T87 | 6061-T6 | YES | W | | 1100-O | 65 | 0.25 | 4.6 | N | 0 | N | 0.88 | 4.6 | 4.5 | 0 | | 983 | | 3209-1 | 04/06/90 | |
| | 4 | 0.13 | 0.04 | 2219-T87 | 6061-T6 | YES | W | | 1100-O | 65 | 0.25 | 4.8 | N | 0 | N | 0.81 | | 4.8 | | | 833 | | 3017-C | 10/12/89 | NO HOLE, DAMAGE BOTH IN PROJ PATH AND UNDER BUMPER HOLE, CRATERS APPROX. SAME SIZE AND DEPTH, MORE CRATERS UNDER BUMPER HOLE, CRATERS UP TO .12" DIA X .04" DEEP WITH FEW VERY SLIGHT DIMPLES ON REAR. |
| | 4 | 0.13 | 0.04 | 2219-T87 | 6061-T6 | YES | W | | 1100-O | 65 | 0.25 | 5.7 | N | 0 | N | 0.8 | 5.7 | 5.7 | 0 | | 973 | | 3211 | 03/26/90 | |
| | 4 | 0.13 | 0.04 | 2219-T87 | 6061-T6 | YES | W | | 1100-O | 65 | 0.25 | 5.8 | N | 0 | N | 0.79 | 5.8 | 5.8 | 0 | | 972 | | 3209 | 03/26/90 | |
| | 4 | 0.13 | 0.04 | 2219-T87 | 6061-T6 | YES | W | | 1100-O | 65 | 0.25 | 6.3 | Y | 0.1 | N | 0.8 | 6.3 | 6.4 | | | 832 | | 3017-B | 10/11/89 | 2 HOLES, ONE IN PROJ PATH AND ONE UNDER BUMPER HOLE, DAMAGE AREA IN PROJ PATH APPROX .4" X .3" WITH HOLE APPROX .13" X .1. DAMAGE AREA UNDER BUMPER HOLE APPROX. 4.0" WIDE X 2.5" LONG (WITH PROJ TRAVEL), HOLE APPROX .09" DIA, CRATERS .1" DIA AND SMALLER |
| | 4 | 0.13 | 0.04 | 2219-T87 | 6061-T6 | YES | W | | 1100-O | 65 | 0.25 | 7 | N | 0 | N | 0.88 | 7 | 7.1 | | | 831 | | 3017-A | 10/11/89 | NO HOLE, NO DAMAGE INPROJECTILE PATH DAMAGE AREA UNDER PROJECTILE HOLE APPROX 3.5" DIA, ONE CRATER APPROX. .17" DIA AND .06" DEEP WITH DIMPLE ON BACK, OTHER CRATERS .1" DIA AND LESS WITH FEW SMALL DIMPLES ON REAR |
| 43 | 4 | 0.13 | 0.04 | 2219-T87 | 6061-T6 | YES | W | | 1100-O | 65 | 0.3 | 2.7 | N | 0 | N | 0.86 | 2.7 | 2.7 | 0 | HOLES | 255 | IWALL | SS-203C | 07/09/86 | |
| | 4 | 0.13 | 0.04 | 2219-T87 | 6061-T6 | YES | W | | 1100-O | 65 | 0.3 | 3.7 | N | 0 | N | 0.87 | 3.6 | 3.7 | 0 | HOLES | 254 | IWALL | SS-203B | 07/08/86 | |
| | 4 | 0.13 | 0.04 | 2219-T87 | 6061-T6 | YES | W | | 1100-O | 65 | 0.3 | 4.8 | N | 0 | N | 0.94 | | 4.8 | 0 | HOLES | 253 | IWALL | SS-203A | 07/08/86 | |
| | 4 | 0.13 | 0.04 | 2219-T87 | 6061-T6 | YES | W | | 1100-O | 65 | 0.3 | 5.6 | N | 0 | N | 0.93 | | 5.6 | 0 | HOLES | 256 | IWALL | SS-203D | 07/09/86 | |
| | 4 | 0.13 | 0.04 | 2219-T87 | 6061-T6 | YES | W | | 1100-O | 65 | 0.3 | 6.7 | N | 0 | N | 1.18 | 6.7 | 6.8 | 0 | HOLES | 270 | IWALL | SS-203E | 07/21/86 | |

| | standoff inch | rearwall gage inch | bumper gage inch | rearwall alloy | bumper alloy | mil present | mil location | prj. lan to dia | prj. material | obliquity | projectile size | velocity avg km/s | rear penetr'n | rearhole inch | rearwall spall | bumper hole inch | vel hall km/s | vel xray km/s | witness penet. | rico con | test number | data source | test | date | comments |
|---|---|---|---|---|---|---|---|---|---|---|---|---|---|---|---|---|---|---|---|---|---|---|---|---|---|
| 44 | 4 | 0.13 | 0.04 | 2219-T87 | 6061-T6 | YES | W | | 1100-O | 65 | 0.31 | 3.4 | Y | 0.3 | Y | 0.88 | 3.4 | 3.4 | 0 | | 975 | | 3212 | 03/28/90 | |
| | 4 | 0.13 | 0.04 | 2219-T87 | 6061-T6 | YES | W | | 1100-O | 65 | 0.31 | 4.4 | N | 0 | N | 1.27 | 4.5 | 4.4 | 0 | | 976 | | 3213 | 03/28/90 | |
| | 4 | 0.13 | 0.04 | 2219-T87 | 6061-T6 | YES | W | | 1100-O | 65 | 0.31 | 5.2 | N | 0 | N | 0.97 | 5.2 | 5.2 | 0 | | 977 | | 3214 | 03/29/90 | |
| | 4 | 0.13 | 0.04 | 2219-T87 | 6061-T6 | YES | W | | 1100-O | 65 | 0.31 | 5.7 | N | 0 | N | 1.04 | | 5.7 | 0 | | 978 | | 3215 | 04/02/90 | |
| | 4 | 0.13 | 0.04 | 2219-T87 | 6061-T6 | YES | W | | 1100-O | 65 | 0.31 | 6.3 | S | 0 | Y | 1.02 | 6.3 | 6.3 | 0 | | 980 | | 3216 | 04/04/90 | COUNT SPALL AS FAILURE |
| | 4 | 0.13 | 0.04 | 2219-T87 | 6061-T6 | YES | W | | 1100-O | 65 | 0.31 | 6.5 | N | 0 | N | 1.03 | 6.5 | 6.5 | 0 | | 981 | | 3218 | 04/05/90 | |
| 45 | 4 | 0.13 | 0.04 | 2219-T87 | 6061-T6 | YES | W | | 1100-O | 65 | 0.35 | 3.1 | C | 0 | N | 0.98 | 3.1 | 3 | 0 | HOLES | 277 | IWALL | SS-203F | 08/01/86 | SURFACE CRACK ON REAR OF WALL. |
| | 4 | 0.13 | 0.04 | 2219-T87 | 6061-T6 | YES | W | | 1100-O | 65 | 0.35 | 4.6 | Y | 0.2 | N | 1.1 | 4.6 | 4.7 | 0 | HOLES | 278 | IWALL | SS-203G | 08/01/86 | |
| 46 | 4 | 0.13 | 0.05 | 2219-T87 | 2024-T3 | B | 3.75 | | 1100-O | 45 | 0.31 | 4.1 | Y | 1 | N | 0.71 | 4.1 | 4.1 | 2 | CRATERED | 1189 | | 4102-B | 12/04/90 | 3 WALL HOLES, LARGEST 0.95X0.5, OTHERS 0.35,0.25 DIA. |
| 47 | 4 | 0.13 | 0.05 | 2219-T87 | 6061-T6 | B | 3.75 | | 1100-0 | 75 | 0.31 | 4 | N | 0 | N | 1.25 | 4 | 4 | 0 | CRATERED | 1179 | | 4108-B | 11/26/90 | WALL CRATERED ONLY. |
| 48 | 4 | 0.13 | 0.05 | 2219-T87 | 6061-T6 | B | 3.75 | | 1100-O | 45 | 0.25 | 6 | N | 0 | N | 0.67 | 5.9 | 6 | 0 | | 1173 | | 9001-C | 11/15/90 | WALL CRATERED ONLY. |
| | 4 | 0.13 | 0.05 | 2219-T87 | 6061-T6 | B | 3.75 | | 1100-O | 45 | 0.25 | 6 | Y | 0.3 | N | 0.66 | 6 | 6 | 0 | | 1171 | | 9001-A | 11/14/90 | WALL CRATERED PLUS HOLE. |
| | 4 | 0.13 | 0.05 | 2219-T87 | 6061-T6 | B | 3.75 | | 1100-O | 45 | 0.25 | 6.1 | Y | 0.2 | N | 0.65 | 6.1 | 6.1 | 0 ? | | 1174 | | 9001-D | 11/16/90 | WALL CRATERED PLUS HOLE. |
| | 4 | 0.13 | 0.05 | 2219-T87 | 6061-T6 | B | 3.75 | | 1100-O | 45 | 0.25 | 6.4 | N | 0 | N | 0.7 | 6.4 | 6.4 | 0 | | 1177 | | 9002-C | 11/20/90 | WALL CRATERED ONLY. |
| | 4 | 0.13 | 0.05 | 2219-T87 | 6061-T6 | B | 3.75 | | 1100-O | 45 | 0.25 | 6.4 | N | 0 | N | 0.65 | 6.4 | 6.4 | 0 | | 1178 | | 9002-D | 11/21/90 | WALL CRATERED ONLY. |
| | 4 | 0.13 | 0.05 | 2219-T87 | 6061-T6 | B | 3.75 | | 1100-O | 45 | 0.25 | 6.4 | Y | 0.2 | N | 0.65 | 6.4 | 6.4 | 2 | | 1175 | | 9002-A | 11/19/90 | HOLE SIZES NEED TO BE VERIFIED. |
| | 4 | 0.13 | 0.05 | 2219-T87 | 6061-T6 | B | 3.75 | | 1100-O | 45 | 0.25 | 6.4 | N | 0 | N | 0.7 | 6.4 | 6.5 | 0 | | 1176 | | 9002-B | 11/20/90 | WALL CRATERED ONLY. |
| 49 | 4 | 0.13 | 0.05 | 2219-T87 | 6061-T6 | B | 3.75 | | 1100-O | 45 | 0.31 | 3 | Y | 0.6 | N | 0.67 | 3 | | 2 | CRATERED | 1190 | | 4102-A | 12/04/90 | WALL ALSO CRATERED. |
| 50 | 4 | 0.13 | 0.05 | 2219-T87 | 6061-T6 | B | 3.75 | | 1100-O | 60 | 0.31 | 2.9 | Y | 0.4 | N | 0.83 | 2.9 | 2.9 | 2 | CRATERED | 1185 | | 4105-A | 11/29/90 | WALL JAGGED HOLE, PLUS CRATERS. |
| | 4 | 0.13 | 0.05 | 2219-T87 | 6061-T6 | B | 3.75 | | 1100-O | 60 | 0.31 | 3 | N | 0 | N | 0.85 | 3 | 3 | 0 | CRATERED | 1187 | | 4105-A1 | 12/03/90 | WALL CRATERED & REAR BUMPS. |
| | 4 | 0.13 | 0.05 | 2219-T87 | 6061-T6 | B | 3.75 | | 1100-O | 60 | 0.31 | 4 | N | 0 | N | 0.9 | 4 | 4.1 | 0 | CRATERED | 1184 | | 4105-B | 11/29/90 | WALL CRATERED & REAR BUMPS. |
| | 4 | 0.13 | 0.05 | 2219-T87 | 6061-T6 | B | 3.75 | | 1100-O | 60 | 0.31 | 6.2 | N | 0 | N | 0.98 | 6.2 | 6.1 | 0 | CRATERED | 1182 | | 4105-C | 11/27/90 | WALL CRATERED, SOME REAR BUMPS. |
| | 4 | 0.13 | 0.05 | 2219-T87 | 6061-T6 | B | 3.75 | | 1100-O | 60 | 0.31 | 7.3 | N | 0 | N | 1.1 | 7.2 | 7.3 | 0 | CRATERED | 1183 | | 4105-D | 11/28/90 | CRATERED ONLY. |
| 51 | 4 | 0.13 | 0.05 | 2219-T87 | 6061-T6 | B | 3.75 | | 1100-O | 75 | 0.31 | 3 | N | 0 | N | 1.29 | 3 | 3 | 0 | CRATERED | 1188 | | 4108-A1 | 12/03/90 | WALL CRATERED & 1 REAR BUMP. |
| | 4 | 0.13 | 0.05 | 2219-T87 | 6061-T6 | B | 3.75 | | 1100-O | 75 | 0.31 | 3.1 | N | 0 | N | 1.08 | 3.1 | 3.1 | 0 | CRATERED | 1186 | | 4108-A | 11/30/90 | CRATERED ONLY. |
| | 4 | 0.13 | 0.05 | 2219-T87 | 6061-T6 | B | 3.75 | | 1100-O | 75 | 0.31 | 6 | N | 0 | N | 1.5 | 6 | 5.9 | 0 | CRATERED | 1180 | | 4108-C | 11/26/90 | WALL CRATERED ONLY. |
| 52 | 4 | 0.13 | 0.05 | 2219-T87 | 6061-T6 | NO | 3.75 | | 1100-O | 45 | 0.25 | 6 | Y | 0.6 | N | 0.65 | 5.9 | 6 | 2 | | 1172 | | 9001-B | 11/15/90 | 2 HOLES IN WALL, PLUS CRATERS |
| 53 | 4 | 0.13 | 0.05 | 2219-T87 | 6061-T6 | YES | 3.75 | | 1100-O | 45 | 0.19 | 3 | N | 0 | N | 0.41 | 3 | 3 | 0 | SPRAY | 1105 | | 4100-A | 09/05/90 | |
| | 4 | 0.13 | 0.05 | 2219-T87 | 6061-T6 | YES | 3.75 | | 1100-O | 45 | 0.19 | 3.8 | N | 0 | N | 0.45 | 3.8 | 3.8 | 0 | SPRAYED | 1106 | | 4100-B | 09/06/90 | |
| | 4 | 0.13 | 0.05 | 2219-T87 | 6061-T6 | YES | 3.75 | | 1100-O | 45 | 0.19 | 5.6 | N | 0 | N | 0.48 | 5.7 | 5.6 | 0 | SPRAYED | 1108 | | 4100-C | 09/07/90 | |
| | 4 | 0.13 | 0.05 | 2219-T87 | 6061-T6 | YES | 3.75 | | 1100-O | 45 | 0.19 | 7.2 | N | 0 | N | 0.52 | 7.2 | 7.1 | 0 | SPRAYED | 1109 | | 4100-D | 09/07/90 | |
| 54 | 4 | 0.13 | 0.05 | 2219-T87 | 6061-T6 | YES | 3.75 | | 1100-O | 45 | 0.25 | 3.2 | Y | 0.4 | | 0.59 | 3.1 | 3.2 | 1 | SPRAYED | 1110 | | 4101-A | 09/10/90 | |
| | 4 | 0.13 | 0.05 | 2219-T87 | 6061-T6 | YES | 3.75 | | 1100-O | 45 | 0.25 | 4.1 | Y | 0.4 | N | 0.66 | 4.1 | 4.2 | 1 | CRATERED | 1111 | | 4101-B | 09/10/90 | |
| | 4 | 0.13 | 0.05 | 2219-T87 | 6061-T6 | YES | 3.75 | | 1100-O | 45 | 0.25 | 6.1 | Y | 0.4 | N | 0.65 | 6.1 | 6.1 | 2 | CRATERED | 1112 | | 4101-C | 09/11/90 | |
| | 4 | 0.13 | 0.05 | 2219-T87 | 6061-T6 | YES | 3.75 | | 1100-O | 45 | 0.25 | 7.5 | Y | 0.1 | N | 0.68 | 7.5 | 7.4 | 0 | SPRAYED | 1113 | | 4101-D | 09/12/90 | |
| 55 | 4 | 0.13 | 0.05 | 2219-T87 | 6061-T6 | YES | 3.75 | | 1100-O | 60 | 0.19 | 2.9 | N | 0 | N | 0.56 | 2.9 | 2.9 | 0 | SPRAYED | 1114 | | 4103-A | 09/12/90 | |
| | 4 | 0.13 | 0.05 | 2219-T87 | 6061-T6 | YES | 3.75 | | 1100-O | 60 | 0.19 | 3 | N | 0 | N | 0.52 | 3.1 | 3 | 0 | CRATERED | 1125 | | 4106-A | 09/24/90 | |

| | standoff inch | rearwall gage inch | bumper gage inch | rearwall alloy | bumper alloy | mli present | mli location | prj. len to dia | prj. material | obliquity | projectile size | velocity avg km/s | rear penetr'n | rearhole inch | rearwall spall | bumper hole inch | vel hall km/s | vel xray km/s | witness panel. | rico con | test number | data source | test | date | comments |
|---|---|---|---|---|---|---|---|---|---|---|---|---|---|---|---|---|---|---|---|---|---|---|---|---|---|
| | 4 | 0.13 | 0.05 | 2219-T87 | 6061-T6 | YES | 3.75 | | 1100-O | 60 | 0.19 | 4 | N | 0 | N | 0.54 | 4 | 4 | 0 | CRATERED | 1115 | | 4103-B | 09/13/90 | |
| | 4 | 0.13 | 0.05 | 2219-T87 | 6061-T6 | YES | 3.75 | | 1100-O | 60 | 0.19 | 4.1 | N | 0 | N | 0.59 | 4.1 | 4.1 | 0 | CRATERED | 1126 | | 4106-B | 09/25/90 | |
| | 4 | 0.13 | 0.05 | 2219-T87 | 6061-T6 | YES | 3.75 | | 1100-O | 60 | 0.19 | 5.9 | N | 0 | N | 0.69 | 5.9 | 5.9 | 0 | SPRAYED | 1116 | | 4103-C | 09/13/90 | |
| | 4 | 0.13 | 0.05 | 2219-T87 | 6061-T6 | YES | 3.75 | | 1100-O | 60 | 0.19 | 7.4 | N | 0 | N | 0.87 | 7.4 | | 0 | SPRAYED | 1121 | | 4103-D | 09/20/90 | |
| 56 | 4 | 0.13 | 0.05 | 2219-T87 | 6061-T6 | YES | 3.75 | | 1100-O | 60 | 0.25 | 3.2 | N | 0 | N | 0.71 | 3.2 | 3.2 | 0 | CRATERED | 1118 | | 4104-A | 09/17/90 | |
| | 4 | 0.13 | 0.05 | 2219-T87 | 6061-T6 | YES | 3.75 | | 1100-O | 60 | 0.25 | 4.2 | N | 0 | N | 0.76 | 4.2 | 4.2 | 0 | CRATERED | 1122 | | 4104-B | 09/20/90 | |
| | 4 | 0.13 | 0.05 | 2219-T87 | 6061-T6 | YES | 3.75 | | 1100-O | 60 | 0.25 | 6.1 | N | 0 | N | 0.88 | 6.1 | 6.1 | 0 | CRATERED | 1123 | | 4104-C | 09/21/90 | |
| | 4 | 0.13 | 0.05 | 2219-T87 | 6061-T6 | YES | 3.75 | | 1100-O | 60 | 0.25 | 7.6 | N | 0 | N | 0.76 | 7.5 | 7.6 | 0 | SPRAYED | 1124 | | 4104-D | 09/24/90 | |
| 57 | 4 | 0.13 | 0.05 | 2219-T87 | 6061-T6 | YES | 3.75 | | 1100-O | 75 | 0.19 | 3.1 | N | 0 | N | 0.73 | 3.1 | 3.1 | 0 | CRATERED | 1133 | | 4106-A1 | 10/09/90 | |
| | 4 | 0.13 | 0.05 | 2219-T87 | 6061-T6 | YES | 3.75 | | 1100-O | 75 | 0.19 | 4 | N | 0 | N | 0.59 | 4 | 4.1 | 0 | CRATERED | 1134 | | 4106-B1 | 10/09/90 | |
| | 4 | 0.13 | 0.05 | 2219-T87 | 6061-T6 | YES | 3.75 | | 1100-O | 75 | 0.19 | 6 | N | 0 | N | 0.75 | 6 | 6 | 0 | CRATERED | 1137 | | 4106-C | 10/11/90 | |
| | 4 | 0.13 | 0.05 | 2219-T87 | 6061-T6 | YES | 3.75 | | 1100-O | 75 | 0.19 | 7.6 | N | 0 | N | 0.93 | 7.6 | 7.6 | 0 | CRATERED | 1136 | | 4106-D | 10/10/90 | |
| 58 | 4 | 0.13 | 0.05 | 2219-T87 | 6061-T6 | YES | 3.75 | | 1100-O | 75 | 0.25 | 3.1 | N | 0 | N | 1.09 | 3.1 | 3.1 | 0 | CRATERED | 1128 | | 4107-A | 09/26/90 | |
| | 4 | 0.13 | 0.05 | 2219-T87 | 6061-T6 | YES | 3.75 | | 1100-O | 75 | 0.25 | 4.1 | N | 0 | N | 1.04 | 4.1 | 4.2 | 0 | CRATERED | 1130 | | 4107-B | 10/03/90 | |
| | 4 | 0.13 | 0.05 | 2219-T87 | 6061-T6 | YES | 3.75 | | 1100-O | 75 | 0.25 | 6.2 | N | 0 | N | 1.37 | 6.2 | 6.3 | 0 | CRATERED | 1131 | | 4107-C | 10/04/90 | |
| | 4 | 0.13 | 0.05 | 2219-T87 | 6061-T6 | YES | 3.75 | | 1100-O | 75 | 0.25 | 7.7 | N | 0 | N | 0.92 | 7.6 | 7.7 | 0 | CRATERED | 1132 | | 4107-D | 10/05/90 | |
| 59 | 4 | 0.13 | 0.06 | 2219-T87 | 6061-T6 | 2.0 | 2.0 | | 1100-O | 0 | 0.25 | 3.1 | Y | 0.5 | N | 0.43 | | 3.1 | 2 | | 1165 | | 3405-A | 11/06/90 | 30 LAYER MLI. WALL CRATERED PLUS HOLE. |
| | 4 | 0.13 | 0.06 | 2219-T87 | 6061-T6 | 2.0 | 2.0 | | 1100-O | 0 | 0.25 | 3.1 | Y | 0.3 | Y | 0.45 | 3.1 | 3.1 | 1 | | 1161 | | 3406-A | 11/01/90 | 2 BUMHOLES .45" DIA. 20 LAYER MLI. |
| | 4 | 0.13 | 0.06 | 2219-T87 | 6061-T6 | 2.0 | 2.0 | | 1100-O | 0 | 0.25 | 3.9 | Y | 0 | N | 0.48 | 3.8 | 3.9 | 1 | | 1166 | | 3405-B | 11/07/90 | 30 LAYER MLI. WALL CRATERED PLUS HOLE. |
| | 4 | 0.13 | 0.06 | 2219-T87 | 6061-T6 | 2.0 | 2.0 | | 1100-O | 0 | 0.25 | 4.1 | N | 0 | N | 0.5 | 4.1 | 4.1 | 0 | | 1162 | | 3406-B | 11/01/90 | WALL CRATERED ONLY. 20 LAYER MLI. |
| | 4 | 0.13 | 0.06 | 2219-T87 | 6061-T6 | 2.0 | 2.0 | | 1100-O | 0 | 0.25 | 5.1 | N | 0 | N | 0.53 | 5.1 | 5.2 | 0 | | 1167 | | 3405-C | 11/07/90 | 30 LAYER MLI. WALL CRATERED ONLY. |
| | 4 | 0.13 | 0.06 | 2219-T87 | 6061-T6 | 2.0 | 2.0 | | 1100-O | 0 | 0.25 | 5.2 | N | 0 | N | 0.48 | 5.2 | 5.2 | 0 | | 1163 | | 3406-C | 11/05/90 | WALL CRATERED ONLY. 20 LAYER MLI. |
| | 4 | 0.13 | 0.06 | 2219-T87 | 6061-T6 | 2.0 | 2.0 | | 1100-O | 0 | 0.25 | 5.6 | N | 0 | N | 0.5 | 5.6 | 5.6 | 0 | | 1164 | | 3406-D | 11/06/90 | WALL CRATERED ONLY. 20 LAYER MLI. |
| | 4 | 0.13 | 0.06 | 2219-T87 | 6061-T6 | 2.0 | 2.0 | | 1100-O | 0 | 0.25 | 6.1 | Y | 0.3 | N | 0.5 | 6.1 | 6.2 | 0 | | 1169 | | 3406-D1 | 11/09/90 | 20 LAYER MLI. WALL CRATERED PLUS 2 HOLES. |
| | 4 | 0.13 | 0.06 | 2219-T87 | 6061-T6 | 2.0 | 2.0 | | 1100-O | 0 | 0.25 | 6.2 | N | 0 | N | 0.52 | 6.2 | 6.2 | 0 | | 1168 | | 3405-D | 11/09/90 | 30 LAYER MLI. WALL CRATERED ONLY. |
| 60 | 4 | 0.13 | 0.06 | 2219-T87 | 6061-T6 | 2.0 | 2.0 | | 1100-O | 0 | 0.38 | 5.5 | Y | 6 | N | 0.7 | 5.5 | 5.5 | 2 | | 1156 | | 3404-D | 10/29/90 | WALL 7 PETALS TO 3" FROM IMPACT POINT. 20 LAYER MLI. |
| | 4 | 0.13 | 0.06 | 2219-T87 | 6061-T6 | 2.0 | 2.0 | | 1100-O | 0 | 0.38 | 6.2 | Y | 6 | N | 0.64 | 6.2 | | 3 | | 1154 | | 3404-C | 10/26/90 | WALL PETALED 6 WAYS TO 3" FROM IMPACT POINT. 20 LAYER MLI (NEW). |
| 61 | 4 | 0.13 | 0.06 | 2219-T87 | 6061-T6 | B | 3.75 | | 1100-O | 0 | 0.25 | 2.9 | Y | 0.5 | N | 0.44 | | 2.9 | 3 | | 1160 | | 3407-A | 10/31/90 | WALL HOLE JAGGED, APPROX. ROUND. 20 LAYER MLI. |
| | 4 | 0.13 | 0.06 | 2219-T87 | 6061-T6 | B | 3.75 | | 1100-O | 0 | 0.25 | 4 | Y | 1 | N | 0.47 | | 4 | 3 | | 1159 | | 3407-B | 10/31/90 | WALL JAGGED HOLE 1.04X0.65 INCHES. 20 LAYER MLI. |
| | 4 | 0.13 | 0.06 | 2219-T87 | 6061-T6 | B | 3.75 | | 1100-O | 0 | 0.25 | 4.8 | Y | 0.2 | N | 0.52 | 4.8 | 4.8 | 0 | | 1158 | | 3407-C | 10/30/90 | 20 LAYER MLI |
| | 4 | 0.13 | 0.06 | 2219-T87 | 6061-T6 | B | 3.75 | | 1100-O | 0 | 0.25 | 5.8 | N | 0 | N | 0.53 | 5.8 | 5.8 | 0 | | 1157 | | 3407-D | 10/30/90 | WALL CRATERED ONLY. 20 LAYER MLI. |
| 62 | 4 | 0.13 | 0.06 | 2219-T87 | 6061-T6 | B | 3.75 | | 1100-O | 45 | 0.25 | 6.1 | N | 0 | N | 0.74 | 6 | 6.1 | 0 | | 1170 | | 9001-1 | 11/13/90 | WALL CRATERED ONLY. |
| 63 | 4 | 0.13 | 0.06 | 2219-T87 | 6061-T6 | OPR | OPR | | 1100-O | 0 | 0.25 | 3.6 | Y | 0.6 | N | 0.43 | | 3.6 | 0 | | 426 | MARTIN | SS-148C | 01/06/87 | |
| | 4 | 0.13 | 0.06 | 2219-T87 | 6061-T6 | OPR | OPR | | 1100-O | 0 | 0.25 | 4.6 | S | 0 | Y | 0.46 | | 4.6 | | | 425 | MARTIN | SS-148B | 01/05/87 | |
| | 4 | 0.13 | 0.06 | 2219-T87 | 6061-T6 | OPR | OPR | | 1100-O | 0 | 0.25 | 5.7 | N | 0 | N | 0.5 | | 5.7 | N | | 424 | MARTIN | SS-148A | 12/22/86 | |

| | standoff inch | rearwall gage inch | bumper gage inch | rearwall alloy | bumper alloy | mli present | mli location | prj. len to dia | prj. material | obliquity | projectile size | velocity avg km/s | rear penetr'n | rearhole inch | rearwall spall | bumper hole inch | vel hall km/s | vel xray km/s | witness penet. | rico con | test number | data source | test | date | comments |
|---|---|---|---|---|---|---|---|---|---|---|---|---|---|---|---|---|---|---|---|---|---|---|---|---|---|
| 64 | 4 | 0.13 | 0.06 | 2219-T87 | 6061-T6 | NO | | 1 | 1100-O | 0 | 0.26 | 5.1 | Y | 2 | N | 0.58 | | 5.1 | 2 | | 131 | ADP SM1 | SS-P-022 | 01/14/86 | |
| | 4 | 0.13 | 0.06 | 2219-T87 | 6061-T6 | NO | | 1 | 1100-O | 0 | 0.26 | 6.9 | Y | 0.3 | N | 0.67 | | 6.9 | 2 | | 133 | ADP SM1 | SS-P-022B | 01/15/86 | AFT PLATE ZIGZAG SPLIT C. 2" LONG, PLUS 1" SPLIT AT TOP OF ZIGZAG SPLIT. |
| 65 | 4 | 0.13 | 0.06 | 2219-T87 | 6061-T6 | NO | | | 1100-O | 0 | 0.13 | 3 | N | 0 | N | 0.34 | | 3 | 0 | | 121 | ADP SM1 | SS-P-028 | 12/18/85 | |
| 66 | 4 | 0.13 | 0.06 | 2219-T87 | 6061-T6 | NO | | | 1100-O | 0 | 0.19 | 3.9 | Y | 0.2 | N | 0.38 | | 3.9 | 0 | | 116 | ADP SM1 | SS-P-027A | 12/13/85 | |
| | 4 | 0.13 | 0.06 | 2219-T87 | 6061-T6 | NO | | | 1100-O | 0 | 0.19 | 4.2 | Y | 0.1 | N | 0.41 | | 4.2 | 0 | | 117 | ADP SM1 | SS-P-027B | 12/16/85 | |
| | 4 | 0.13 | 0.06 | 2219-T87 | 6061-T6 | NO | | | 1100-O | 0 | 0.19 | 4.5 | N | 0 | N | 0.41 | | 4.5 | 0 | | 115 | ADP SM1 | SS-P-027 | 12/12/85 | |
| 67 | 4 | 0.13 | 0.06 | 2219-T87 | 6061-T6 | NO | | | 1100-O | 0 | 0.25 | 2.8 | Y | 0.5 | N | 0.41 | | 2.8 | 0 | | 43 | ADP SM1 | SS-P-001 | 08/19/85 | |
| | 4 | 0.13 | 0.06 | 2219-T87 | 6061-T6 | NO | | | 1100-O | 0 | 0.25 | 3 | Y | 0.4 | N | 0.42 | | 3 | 1 | | 44 | ADP SM1 | SS-P-002 | 08/20/85 | |
| | 4 | 0.13 | 0.06 | 2219-T87 | 6061-T6 | NO | | | 1100-O | 0 | 0.25 | 3.6 | Y | 0.5 | N | 0.42 | 3.6 | 3.7 | | | 395 | MSFC | SS-PT4A | 11/25/86 | |
| | 4 | 0.13 | 0.06 | 2219-T87 | 6061-T6 | NO | | | 1100-O | 0 | 0.25 | 4.3 | Y | 0.2 | Y | 0.46 | 4.2 | 4.3 | | | 396 | MSFC | SS-PT4B | 11/26/86 | |
| | 4 | 0.13 | 0.06 | 2219-T87 | 6061-T6 | NO | | | 1100-O | 0 | 0.25 | 4.9 | Y | 0.4 | Y | 0.49 | | 4.9 | | | 45 | ADP SM1 | SS-P-003 | 08/23/85 | |
| | 4 | 0.13 | 0.06 | 2219-T87 | 6061-T6 | NO | | | 1100-O | 0 | 0.25 | 5 | Y | 0.4 | | 0.51 | | 5 | 1 | | 46 | ADP SM1 | SS-P-004 | 08/26/85 | |
| | 4 | 0.13 | 0.06 | 2219-T87 | 6061-T6 | NO | | | 1100-O | 0 | 0.25 | 5.9 | Y | 0 | Y | 0.51 | 5.9 | 5.9 | 1 | | 681 | MSFC | EHSS-2B | 03/04/88 | PINHOLES, PLUS SPALL OF REAR WALL |
| | 4 | 0.13 | 0.06 | 2219-T87 | 6061-T6 | NO | | | 1100-O | 0 | 0.25 | 6.1 | Y | 0.8 | Y | 0.51 | 6.2 | 6 | 3 | | 931 | | 2004-C | 02/16/90 | SPALL AROUND HOLES IN REAR WALL |
| | 4 | 0.13 | 0.06 | 2219-T87 | 6061-T6 | NO | | | 1100-O | 0 | 0.25 | 6.4 | S | 0 | Y | 0.57 | 6.3 | 6.4 | 0 | | 680 | MSFC | EHSS-2A | 03/02/88 | COUNT SPALL AS FAILURE |
| | 4 | 0.13 | 0.06 | 2219-T87 | 6061-T6 | NO | | | 1100-O | 0 | 0.25 | 6.9 | Y | 0 | N | 0.56 | | 6.9 | 0 | | 47 | ADP SM1 | SS-P-005 | 08/28/85 | |
| | 4 | 0.13 | 0.06 | 2219-T87 | 6061-T6 | NO | | | 1100-O | 0 | 0.25 | 6.9 | Y | 0 | Y | 0.55 | 6.9 | 6.9 | 1 | | 939 | | 2004-B | 02/21/90 | |
| | 4 | 0.13 | 0.06 | 2219-T87 | 6061-T6 | NO | | | 1100-O | 0 | 0.25 | 7 | Y | 0 | Y | 0.59 | | 7 | 0 | | 49 | ADP SM1 | SS-P-006A | 08/30/85 | COUNT SPALL AS PENETRATION |
| | 4 | 0.13 | 0.06 | 2219-T87 | 6061-T6 | NO | | | 1100-O | 0 | 0.25 | 7.1 | Y | 1 | Y | 0.57 | | 7.1 | 0 | | 176 | ADP SM1 | SS-P-034B | 03/13/86 | REAR PLATE SPLIT 1" L X 0.1" W |
| | 4 | 0.13 | 0.06 | 2219-T87 | 6061-T6 | NO | | | 1100-O | 0 | 0.25 | 7.2 | Y | 2 | Y | 0.57 | | 7.2 | 1 | | 941 | | 2004-A | 02/26/90 | |
| 68 | 4 | 0.13 | 0.06 | 2219-T87 | 6061-T6 | NO | | | 1100-O | 0 | 0.3 | 6.5 | Y | 2 | N | 0.62 | | 6.5 | 3 | | 127 | ADP SM1 | SS-P-021A | 01/09/86 | |
| | 4 | 0.13 | 0.06 | 2219-T87 | 6061-T6 | NO | | | 1100-O | 0 | 0.3 | 6.6 | Y | 1.5 | Y | 0.62 | | 6.6 | 2 | | 126 | ADP SM1 | SS-P-021 | 01/09/86 | |
| 69 | 4 | 0.13 | 0.06 | 2219-T87 | 6061-T6 | NO | | | 1100-O | 0 | 0.31 | 3.4 | Y | 1 | Y | 0.5 | 3.4 | 3.4 | | | 477 | MSFC | SS-T2-8 | 02/24/87 | |
| | 4 | 0.13 | 0.06 | 2219-T87 | 6061-T6 | NO | | | 1100-O | 0 | 0.31 | 4.4 | Y | 1.4 | N | 0.54 | 4.3 | 4.4 | | | 392 | MSFC | SS-PT8A | 11/20/86 | |
| | 4 | 0.13 | 0.06 | 2219-T87 | 6061-T6 | NO | | | 1100-O | 0 | 0.31 | 4.4 | Y | 1.4 | N | 0.56 | 4.3 | 4.4 | | | 393 | MSFC | SS-PT8B | 11/21/86 | |
| | 4 | 0.13 | 0.06 | 2219-T87 | 6061-T6 | NO | | | 1100-O | 0 | 0.31 | 4.6 | Y | 1.8 | N | 0.61 | 4.6 | 4.7 | | | 484 | MSFC | SS-T2-6A | 03/03/87 | |
| | 4 | 0.13 | 0.06 | 2219-T87 | 6061-T6 | NO | | | 1100-O | 0 | 0.31 | 6.6 | Y | 1.3 | Y | 0.57 | 6.6 | 6.7 | 2 | | 703 | MSFC | EHSS-6C | 06/09/88 | SPALL AROUND EDGE OF HOLE |

| | standoff inch | rearwall gage inch | bumper gage inch | rearwall alloy | bumper alloy | mli present | mli location | prj. len to dia | prj. material | obliquity | projectile size | velocity avg km/s | rear penetr'n | rearhole inch | rearwall spall | bumper hole inch | vel hall km/s | vel xray km/s | witness penet. | rico con | test number | data source | test | date | comments |
|---|---|---|---|---|---|---|---|---|---|---|---|---|---|---|---|---|---|---|---|---|---|---|---|---|---|
| | 4 | 0.13 | 0.06 | 2219-T87 | 6061-T6 | NO | | | 1100-O | 0 | 0.31 | 6.6 | Y | 2 | N | 0.61 | 6.6 | | 2 | | 636 | MSFC | EH3-A | 09/21/87 | BUMPER - .611" DIA. HOLE, 1" LOW, SOME DEBRIS, FEW DEBRIS HOLES. WALL - HOLE 2" X 1.5", METAL SPLIT 1" LONG & PEELED BACK SLIGHTLY. HEAVY CONCENTRATION OF CAVATIES OVER 5" DIA. DAMAGE AREA 9" DIA. AREA. WITNESS #1 - HOLE, 3.5" DIA. WITH PETALS PEELED B |
| | 4 | 0.13 | 0.06 | 2219-T87 | 6061-T6 | NO | | | 1100-O | 0 | 0.31 | 6.8 | Y | 8 | N | 0.66 | 6.7 | 6.8 | 2 | | 676 | MSFC | EH4-B | 12/11/87 | WALL: 5 PETALS, CRACKS 4-6" EACH |
| 70 | 4 | 0.13 | 0.06 | 2219-T87 | 6061-T6 | NO | | | 1100-O | 0 | 0.38 | 5.1 | Y | 2 | Y | 0.7 | 5 | 5.1 | | | 487 | MSFC | SS-T2-18 | 03/04/87 | |
| 71 | 4 | 0.13 | 0.06 | 2219-T87 | 6061-T6 | NO | | | 1100-O | 30 | 0.19 | 5.1 | Y | 0.2 | N | 0.46 | 5 | 5.2 | 0 | NO CAV. | 546 | MARTIN | SS-162B | 05/27/87 | |
| | 4 | 0.13 | 0.06 | 2219-T87 | 6061-T6 | NO | | | 1100-O | 30 | 0.19 | 6.5 | S | 0 | Y | 0.55 | 6.5 | | 0 | CAVITIES | 545 | MARTIN | SS-162A | 05/26/87 | COUNT SPALL AS FAILURE |
| 72 | 4 | 0.13 | 0.06 | 2219-T87 | 6061-T6 | NO | | | 1100-O | 30 | 0.25 | 5.9 | Y | 0.8 | N | 0.6 | 5.8 | 5.9 | 2 | | 303 | MARTIN | SS-135A | 08/26/86 | |
| | 4 | 0.13 | 0.06 | 2219-T87 | 6061-T6 | NO | | | 1100-O | 30 | 0.25 | 6.7 | Y | 1 | Y | 0.56 | 6.6 | 6.8 | 1 | | 305 | MARTIN | SS-135C | 08/27/86 | |
| | 4 | 0.13 | 0.06 | 2219-T87 | 6061-T6 | NO | | | 1100-O | 30 | 0.25 | 6.8 | Y | 1.3 | Y | 0.54 | 6.8 | 6.9 | 2 | CAVITIES | 691 | MSFC | EHSS-3C | 04/15/88 | REAR WALL HOLED PLUS SPALLED |
| | 4 | 0.13 | 0.06 | 2219-T87 | 6061-T6 | NO | | | 1100-O | 30 | 0.25 | 6.9 | Y | 1 | N | 0.56 | 6.8 | 6.9 | 2 | | 306 | MARTIN | SS-135D | 08/28/86 | |
| | 4 | 0.13 | 0.06 | 2219-T87 | 6061-T6 | NO | | | 1100-O | 30 | 0.25 | 7.2 | Y | 0.1 | Y | 0.65 | 7.1 | 7.2 | 0 | | 304 | MARTIN | SS-135B | 08/27/86 | |
| | 4 | 0.13 | 0.06 | 2219-T87 | 6061-T6 | NO | | | 1100-O | 30 | 0.25 | 7.2 | Y | 0.2 | N | 0.63 | 7.1 | 7.3 | 0 | | 307 | MARTIN | SS-135E | 08/29/86 | |
| 73 | 4 | 0.13 | 0.06 | 2219-T87 | 6061-T6 | NO | | | 1100-O | 30 | 0.31 | 7.1 | Y | 1.5 | N | 0.67 | 7.1 | 7.2 | 4 | OK | 336 | MSFC | SS-EH1A | 09/26/86 | |
| 74 | 4 | 0.13 | 0.06 | 2219-T87 | 6061-T6 | NO | | | 1100-O | 45 | 0.19 | 3.2 | N | 0 | N | 0.42 | 3.2 | 3.2 | 0 | CAVITIES | 230 | IWALL | SS-206E | 06/17/86 | |
| | 4 | 0.13 | 0.06 | 2219-T87 | 6061-T6 | NO | | | 1100-O | 45 | 0.19 | 3.7 | C | 0 | N | 0.46 | | 3.7 | 0 | | 220 | IWALL | SS-206D | 06/10/86 | COUNT REAR SURFACE CRACK AS FAILURE |
| | 4 | 0.13 | 0.06 | 2219-T87 | 6061-T6 | NO | | | 1100-O | 45 | 0.19 | 4.8 | Y | 0.2 | Y | 0.46 | 4.8 | 4.8 | 1 | | 217 | IWALL | SS-206A | 06/06/86 | |
| | 4 | 0.13 | 0.06 | 2219-T87 | 6061-T6 | NO | | | 1100-O | 45 | 0.19 | 5.1 | N | 0 | N | 0.52 | | 5.1 | 0 | | 218 | IWALL | SS-206B | 06/09/86 | |
| | 4 | 0.13 | 0.06 | 2219-T87 | 6061-T6 | NO | | | 1100-O | 45 | 0.19 | 5.4 | Y | 0.1 | N | 0.52 | | 5.4 | 0 | | 219 | IWALL | SS-206C | 06/09/86 | |
| | 4 | 0.13 | 0.06 | 2219-T87 | 6061-T6 | NO | | | 1100-O | 45 | 0.19 | 6.2 | N | 0 | N | 0.53 | 6.1 | 6.2 | 0 | CAVITIES | 231 | IWALL | SS-206F | 06/18/86 | |
| | 4 | 0.13 | 0.06 | 2219-T87 | 6061-T6 | NO | | | 1100-O | 45 | 0.19 | 7 | Y | 0.2 | N | 0.52 | 7 | 7 | 0 | CAVITIES | 510 | MARTIN | SS-155A | 04/09/87 | |
| | 4 | 0.13 | 0.06 | 2219-T87 | 6061-T6 | NO | | | 1100-O | 45 | 0.19 | 7.4 | Y | 0.1 | N | 0.61 | 7.3 | 7.4 | 0 | CAVITIES | 720 | MSFC | EHRP-8 | 07/28/88 | |
| 75 | 4 | 0.13 | 0.06 | 2219-T87 | 6061-T6 | NO | | | 1100-O | 45 | 0.25 | 5.2 | Y | 0.6 | N | 0.63 | 5.2 | 5.2 | 3 | CAVITIES | 453 | IWALL | SS-230C | 02/03/87 | |
| | 4 | 0.13 | 0.06 | 2219-T87 | 6061-T6 | NO | | | 1100-O | 45 | 0.25 | 5.6 | Y | 0.4 | N | 0.64 | 5.5 | 5.6 | 2 | CAVITIES | 456 | IWALL | SS-230D | 02/04/87 | |
| | 4 | 0.13 | 0.06 | 2219-T87 | 6061-T6 | NO | | | 1100-O | 45 | 0.25 | 6.6 | Y | 0.3 | N | 0.7 | 6.5 | 6.6 | 1 | CAVITIES | 457 | IWALL | SS-230E | 02/05/87 | |
| | 4 | 0.13 | 0.06 | 2219-T87 | 6061-T6 | NO | | | 1100-O | 45 | 0.25 | 7 | Y | 0.7 | N | 0.71 | 6.9 | 7.1 | 2 | CAVITIES | 445 | MARTIN | SS-150A | 01/27/87 | |
| 76 | 4 | 0.13 | 0.06 | 2219-T87 | 6061-T6 | NO | | | 1100-O | 45 | 0.31 | 6.5 | Y | 1.2 | Y | 0.8 | 6.4 | 6.6 | 4 | HOLE | 466 | MSFC | SS-002A | 02/12/87 | |
| | 4 | 0.13 | 0.06 | 2219-T87 | 6061-T6 | NO | | | 1100-O | 45 | 0.31 | 7 | Y | 0.5 | N | 0.83 | 7 | 7.1 | 4 | CAVITIES | 337 | MSFC | SS-EH1B | 09/26/86 | |
| 77 | 4 | 0.13 | 0.06 | 2219-T87 | 6061-T6 | NO | | | 1100-O | 55 | 0.25 | 6.3 | Y | 0.3 | Y | 0.72 | | 6.3 | 1 | | 308 | MARTIN | SS-136A | 08/29/86 | |

| | standoff inch | rearwall gage inch | bumper gage inch | rearwall alloy | bumper alloy | mil present | mil location | prj. len to dia | prj. material | obliquity | projectile size | velocity avg km/s | rear penetr'n | rearhole inch | rearwall spall | bumper hole inch | vel hall km/s | vel xray km/s | witness penet. | rico con | test number | data source | test | date | comments |
|---|---|---|---|---|---|---|---|---|---|---|---|---|---|---|---|---|---|---|---|---|---|---|---|---|---|
| | 4 | 0.13 | 0.06 | 2219-T87 | 6061-T6 | NO | | | 1100-O | 55 | 0.25 | 6.7 | Y | 0.3 | N | 0.69 | | 6.7 | 1 | | 310 | MARTIN | SS-136C | 09/02/86 | |
| | 4 | 0.13 | 0.06 | 2219-T87 | 6061-T6 | NO | | | 1100-O | 55 | 0.25 | 7.2 | C | 0 | Y | 0.83 | 7.2 | 7.3 | 0 | | 309 | MARTIN | SS-136B | 09/02/86 | |
| 78 | 4 | 0.13 | 0.06 | 2219-T87 | 6061-T6 | NO | | | 1100-O | 60 | 0.19 | 7.4 | N | 0 | N | 0.68 | | 7.4 | 0 | 2HOLES | 517 | MARTIN | SS-157A | 04/16/87 | |
| | 4 | 0.13 | 0.06 | 2219-T87 | 6061-T6 | NO | | | 1100-O | 60 | 0.19 | 8 | Y | 0.1 | N | 0.66 | 8 | 8.1 | 0 | CAVITIES | 717 | MSFC | EHRP-7 | 07/25/88 | |
| 79 | 4 | 0.13 | 0.06 | 2219-T87 | 6061-T6 | NO | | | 1100-O | 60 | 0.31 | 7.2 | Y | 0.3 | N | 1 | 7.1 | 7.2 | 0 | HOLES | 338 | MSFC | SS-EH1C | 09/29/86 | |
| 80 | 4 | 0.13 | 0.06 | 2219-T87 | 6061-T6 | NO | | | 1100-O | 65 | 0.19 | 2.4 | N | 0 | N | 0.42 | 2.4 | 2.5 | 0 | HOLE | 509 | IWALL | SS-231B | 04/09/87 | |
| | 4 | 0.13 | 0.06 | 2219-T87 | 6061-T6 | NO | | | 1100-O | 65 | 0.19 | 3.3 | N | 0 | N | 0.47 | 3.3 | 3.4 | 0 | HOLE | 508 | IWALL | SS-231A | 04/08/87 | |
| | 4 | 0.13 | 0.06 | 2219-T87 | 6061-T6 | NO | | | 1100-O | 65 | 0.19 | 4.2 | N | 0 | N | 0.63 | | 4.2 | | HOLE | 516 | MARTIN | SS-156C | 04/16/87 | |
| | 4 | 0.13 | 0.06 | 2219-T87 | 6061-T6 | NO | | | 1100-O | 65 | 0.19 | 6 | C | 0 | N | 0.63 | | 6 | | HOLES | 515 | MARTIN | SS-156B | 04/15/87 | SURFACE CRACK ON BACK OF WALL |
| | 4 | 0.13 | 0.06 | 2219-T87 | 6061-T6 | NO | | | 1100-O | 65 | 0.19 | 7.1 | N | 0 | N | 0.75 | | 7.1 | | HOLES | 514 | MARTIN | SS-156A | 04/15/87 | |
| | 4 | 0.13 | 0.06 | 2219-T87 | 6061-T6 | NO | | | 1100-O | 65 | 0.19 | 7.3 | N | 0 | N | 0.62 | 7.3 | 7.4 | 0 | CAVITIES | 721 | MSFC | EHRP-9 | 07/29/88 | |
| 81 | 4 | 0.13 | 0.06 | 2219-T87 | 6061-T6 | NO | | | 1100-O | 65 | 0.25 | 3.3 | N | 0 | N | 0.8 | 3.2 | 3.4 | 0 | 2HOLES | 228 | IWALL | SS-208C | 06/16/86 | |
| | 4 | 0.13 | 0.06 | 2219-T87 | 6061-T6 | NO | | | 1100-O | 65 | 0.25 | 4.3 | Y | 0.2 | N | 0.73 | 4.2 | 4.4 | 0 | | 227 | IWALL | SS-208B | 06/13/86 | |
| | 4 | 0.13 | 0.06 | 2219-T87 | 6061-T6 | NO | | | 1100-O | 65 | 0.25 | 5 | N | 0 | N | 0.82 | 4.9 | 5 | 0 | | 226 | IWALL | SS-208A | 06/13/86 | |
| | 4 | 0.13 | 0.06 | 2219-T87 | 6061-T6 | NO | | | 1100-O | 65 | 0.25 | 5.6 | C | 0 | N | 0.79 | | 5.6 | 0 | HOLES | 229 | IWALL | SS-208D | 06/17/86 | COUNT REAR SURFACE CRACK AS FAILURE |
| | 4 | 0.13 | 0.06 | 2219-T87 | 6061-T6 | NO | | | 1100-O | 65 | 0.25 | 6.5 | Y | 0.2 | N | 0.83 | 6.5 | 6.5 | 1 | HOLES | 264 | IWALL | SS-208E | 07/16/86 | |
| 82 | 4 | 0.13 | 0.06 | 2219-T87 | 6061-T6 | NO | | | 1100-O | 65 | 0.31 | 6.6 | Y | 0.2 | Y | 1.21 | 6.6 | 6.6 | | HOLES | 511 | IWALL | SS-231C | 04/10/87 | |
| | 4 | 0.13 | 0.06 | 2219-T87 | 6061-T6 | NO | | | 1100-O | 65 | 0.31 | 7.3 | Y | 0.2 | Y | 1 | 7.1 | 7.3 | 0 | HOLES | 512 | IWALL | SS-231D | 04/13/87 | |
| 83 | 4 | 0.13 | 0.06 | 2219-T87 | 6061-T6 | NO | | | 1100-O | 75 | 0.25 | 7.3 | Y | 0.2 | N | 1.11 | 7.2 | 7.4 | | CAVITIES | 598 | MSFC | EH1-B | 07/27/87 | |
| 84 | 4 | 0.13 | 0.06 | 2219-T87 | 6061-T6 | NO | | | 1100-O | 75 | 0.31 | 6.9 | Y | 0.2 | N | 1.28 | 6.8 | 7 | 1 | HOLE | 593 | | EH1-A | 07/22/87 | |
| | 4 | 0.13 | 0.06 | 2219-T87 | 6061-T6 | NO | | | 1100-O | 75 | 0.31 | 6.9 | Y | 0.1 | N | 1.32 | 6.9 | 7 | 1 | HOLES | 594 | | EH1-AA | 07/23/87 | |
| | 4 | 0.13 | 0.06 | 2219-T87 | 6061-T6 | NO | | | 1100-O | 75 | 0.31 | 6.9 | Y | 0.2 | N | 1.49 | 6.9 | 7 | | CAVITIES | 597 | | EH1-AB | 07/24/87 | |
| | 4 | 0.13 | 0.06 | 2219-T87 | 6061-T6 | NO | | | 1100-O | 75 | 0.31 | 7.2 | Y | 0.2 | N | 1.41 | 7.1 | 7.2 | 1 | HOLES | 340 | MSFC | SS-EH1D | 09/30/86 | |
| 85 | 4 | 0.13 | 0.06 | 2219-T87 | 6061-T6 | NO | | | 6061-T6 | 0 | 0.3 | 7 | Y | 0.7 | Y | 0.61 | | 7 | 2 | | 81 | ADP SM1 | SS-P-017 | 10/17/85 | |
| 86 | 4 | 0.13 | 0.06 | 2219-T87 | 6061-T6 | NO | | | 6061-T6 | 45 | 0.25 | 3.2 | Y | 0.4 | N | 0.58 | | 3.2 | 3 | | 171 | MARTIN | SS-113A | 03/10/86 | |
| 87 | 4 | 0.13 | 0.06 | 2219-T87 | 6061-T6 | NO | | | 6061-T6 | 60 | 0.25 | 3.2 | N | 0 | N | 0.73 | | 3.2 | | | 170 | MARTIN | SS-113 | 03/10/86 | |
| 88 | 4 | 0.13 | 0.06 | 2219-T87 | 6061-T6 | NO | | | 6061-T6 | 60 | 0.3 | 3.3 | N | 0 | N | 0.87 | | 3.3 | 0 | | 172 | MARTIN | SS-114 | 03/11/86 | |
| 89 | 4 | 0.13 | 0.06 | 2219-T87 | 6061-T6 | NO | | | GLASS | 0 | 0.38 | 5.4 | N | 0 | N | 1.5 | 5.4 | | | | 557 | | SS-165B | 06/04/87 | PROJECTILE SHATTERED |

| | standoff inch | rearwall gage inch | bumper gage inch | rearwall alloy | bumper alloy | mli present | mli location | prj. len to dia | prj. material | obliquity | projectile size | velocity avg km/s | rear penetr'n | rearhole inch | rearwall spall | bumper hole inch | vel hall km/s | vel xray km/s | witness penet. | rico con | test number | data source | test | date | comments |
|---|---|---|---|---|---|---|---|---|---|---|---|---|---|---|---|---|---|---|---|---|---|---|---|---|---|
| | 4 | 0.13 | 0.06 | 2219-T87 | 6061-T6 | NO | | | GLASS | 0 | 0.38 | 6.4 | N | 0 | N | 1.1 | 6.4 | | | | 555 | | SS-165A | 06/03/87 | |
| 90 | 4 | 0.13 | 0.06 | 2219-T87 | 6061-T6 | NO | | | STEEL | 0 | 0.13 | 7 | Y | 1 | Y | 0.37 | | 7 | 2 | | 388 | MARTIN | SS-146A | 11/07/86 | |
| | 4 | 0.13 | 0.06 | 2219-T87 | 6061-T6 | NO | | | STEEL | 0 | 0.13 | 7.4 | Y | 0.1 | Y | 0.36 | | 7.4 | 1 | | 389 | MARTIN | SS-146B | 11/07/86 | |
| 91 | 4 | 0.13 | 0.06 | 5456 | 6061-T6 | NO | | | 1100-O | 0 | 0.25 | 6 | Y | 1 | Y | 0.52 | 6 | 6.1 | 1 | | 678 | MSFC | EHSS-1B | 02/22/88 | |
| | 4 | 0.13 | 0.06 | 5456 | 6061-T6 | NO | | | 1100-O | 0 | 0.25 | 6.4 | Y | 0.2 | Y | 0.55 | 6.3 | 6.5 | 1 | | 679 | MSFC | EHSS-1C | 02/24/88 | |
| | 4 | 0.13 | 0.06 | 5456 | 6061-T6 | NO | | | 1100-O | 0 | 0.25 | 6.9 | N | | Y | 0.57 | 6.9 | 6.9 | 1 | | 677 | MSFC | EHSS-1A | 02/18/88 | |
| 92 | 4 | 0.13 | 0.06 | 5456 | 6061-T6 | NO | | | 1100-O | 0 | 0.31 | 6.6 | Y | 0.7 | Y | 0.65 | 6.5 | 6.6 | 2 | | 695 | MSFC | EHSS-6A | 05/02/88 | |
| | 4 | 0.13 | 0.06 | 5456 | 6061-T6 | NO | | | 1100-O | 0 | 0.31 | 6.6 | Y | 1.8 | | 0.58 | 6.6 | 6.7 | 2 | | 696 | MSFC | EHSS-6B | 05/09/88 | |
| 93 | 4 | 0.13 | 0.06 | 5456 | 6061-T6 | NO | | | 1100-O | 25 | 0.25 | 5 | Y | 0.6 | | 0.56 | 4.9 | 5 | 2 | | 690 | MSFC | EHSS-5B | 04/12/88 | |
| 94 | 4 | 0.13 | 0.06 | 5456 | 6061-T6 | NO | | | 1100-O | 30 | 0.25 | 6.8 | Y | 0.2 | Y | 0.64 | 6.7 | 6.9 | 1 | | 683 | MSFC | EHSS-3A | 03/17/88 | |
| | 4 | 0.13 | 0.06 | 5456 | 6061-T6 | NO | | | 1100-O | 30 | 0.25 | 7.1 | Y | 1.3 | Y | 0.66 | 7 | 7.1 | 2 | | 686 | MSFC | EHSS-3B | 03/30/88 | |
| 95 | 4 | 0.13 | 0.06 | 5456 | 6061-T6 | NO | | | 1100-O | 45 | 0.25 | 4.1 | Y | 0.4 | N | 0.53 | 4.1 | 4.1 | 2 | | 689 | MSFC | EHSS-5A | 04/07/88 | |
| | 4 | 0.13 | 0.06 | 5456 | 6061-T6 | NO | | | 1100-O | 45 | 0.25 | 5.6 | Y | 0.6 | Y | 0.67 | 5.5 | 5.6 | 1 | | 712 | MSFC | EHSS-4C | 07/14/88 | |
| | 4 | 0.13 | 0.06 | 5456 | 6061-T6 | NO | | | 1100-O | 45 | 0.25 | 6.8 | Y | 0.3 | | 0.76 | 6.8 | 6.8 | 1 | | 687 | MSFC | EHSS-4A | 04/01/88 | |
| | 4 | 0.13 | 0.06 | 5456 | 6061-T6 | NO | | | 1100-O | 45 | 0.25 | 7 | Y | 0.5 | Y | 0.71 | 6.9 | 7 | 2 | | 688 | MSFC | EHSS-4B | 04/04/88 | |
| | 4 | 0.13 | 0.06 | 5456 | 6061-T6 | NO | | | 1100-O | 45 | 0.25 | 7.6 | Y | 0.2 | Y | 0.8 | 7.6 | 7.7 | 1 | | 715 | MSFC | EHRP-6 | 07/19/88 | |
| 96 | 4 | 0.13 | 0.06 | 5456 | 6061-T6 | NO | | | 1100-O | 45 | 0.31 | 6.6 | Y | 1.3 | | 0.84 | 6.6 | 6.6 | 2 | | 697 | MSFC | EHSS-7A | 05/11/88 | |
| | 4 | 0.13 | 0.06 | 5456 | 6061-T6 | NO | | | 1100-O | 45 | 0.31 | 6.8 | Y | 1 | Y | 0.81 | 6.8 | 6.9 | 2 | | 707 | MSFC | EHRP-3 | 06/30/88 | |
| | 4 | 0.13 | 0.06 | 5456 | 6061-T6 | NO | | | 1100-O | 45 | 0.31 | 7 | Y | 1.4 | Y | 0.86 | 7 | 7.1 | 2 | | 699 | MSFC | EHSS-7B | 05/17/88 | |
| 97 | 4 | 0.13 | 0.06 | 5456 | 6061-T6 | NO | | | 1100-O | 60 | 0.25 | 7.7 | Y | 0.3 | | 0.84 | 7.7 | 7.8 | 1 | | 713 | MSFC | EHRP-4 | 07/15/88 | |
| 98 | 4 | 0.13 | 0.06 | 5456 | 6061-T6 | NO | | | 1100-O | 60 | 0.31 | 6.9 | Y | 0.4 | | 1.2 | 6.9 | 7 | 1 | | 705 | MSFC | EHRP-1 | 06/28/88 | |
| 99 | 4 | 0.13 | 0.06 | 5456 | 6061-T6 | NO | | | 1100-O | 65 | 0.25 | 4.3 | Y | 0.2 | | 0.79 | 4.2 | 4.3 | 0 | | 694 | MSFC | EHSS-5D | 04/28/88 | |
| | 4 | 0.13 | 0.06 | 5456 | 6061-T6 | NO | | | 1100-O | 65 | 0.25 | 5.3 | Y | 0.1 | Y | 0.85 | 5.2 | 5.3 | 0 | | 693 | MSFC | EHSS-5C | 04/20/88 | |
| | 4 | 0.13 | 0.06 | 5456 | 6061-T6 | NO | | | 1100-O | 65 | 0.25 | 7.6 | Y | 0.3 | | 0.87 | 7.5 | 7.6 | 1 | | 714 | MSFC | EHRP-5 | 07/18/88 | |
| 100 | 4 | 0.13 | 0.06 | 5456 | 6061-T6 | NO | | | 1100-O | 65 | 0.31 | 6.9 | Y | 0.3 | | 1.3 | 6.8 | 6.9 | 1 | | 706 | MSFC | EHRP-2 | 06/29/88 | |
| 101 | 4 | 0.13 | 0.06 | 5456 | 6061-T6 | NO | | | 1100-O | 75 | 0.31 | 7.1 | Y | 0.2 | | 1.43 | 7 | 7.2 | 0 | | 701 | MSFC | EHSS-8A | 05/26/88 | |
| 102 | 4 | 0.13 | 0.06 | 2219-T87 | 6061-T6 | YES | 0.9 | | 1100-O | 0 | 0.38 | 6.6 | Y | 8 | N | 0.65 | 6.7 | 6.6 | 3 | | 1002 | | 3227-B | 04/24/90 | HOLE IN REARWALL 8" L X 2" WIDE, PETALLED OUT. |
| 103 | 4 | 0.13 | 0.06 | 2219-T87 | 6061-T6 | YES | 2.0 | | 1100-O | 0 | 0.31 | 5 | Y | | N | 0.57 | 5 | 5.1 | 1 | | 1141 | | 3402-D | 10/16/90 | WALL: 4 PETALS, PLUS CRATERS 20 LAYER MLI |
| | 4 | 0.13 | 0.06 | 2219-T87 | 6061-T6 | YES | 2.0 | | 1100-O | 0 | 0.31 | 5.3 | Y | 0.3 | N | 0.58 | 5.3 | 5.3 | 1 | | 1138 | | 3401-D | 10/11/90 | WALL CRACKED ABOUT 1" EACH L/R, .8" EACH U/D. 30 LAYER MLI |
| | 4 | 0.13 | 0.06 | 2219-T87 | 6061-T6 | YES | 2.0 | | 1100-O | 0 | 0.31 | 6.2 | Y | | N | 0.61 | 6.1 | 6.2 | 0 | | 1139 | | 3401-C | 10/15/90 | 30 LAYER MLI |
| | 4 | 0.13 | 0.06 | 2219-T87 | 6061-T6 | YES | 2.0 | | 1100-O | 0 | 0.31 | 6.2 | Y | 0.3 | N | 0.61 | 6.2 | 6.2 | 0 | | 1142 | | 3402-C | 10/17/90 | WALL HOLED + 4 PETALS TO 1.75" LONG 20 LAYER MLI |

| | standoff inch | rearwall gage inch | bumper gage inch | rearwall alloy | bumper alloy | mli present | mli location | prj. len to dia | prj. material | obliquity | projectile size | velocity avg km/s | rear penetr'n | rearhole inch | rearwall spall | bumper hole inch | vel hall km/s | vel xray km/s | witness penet. | rico con | test number | data source | test | date | comments |
|---|---|---|---|---|---|---|---|---|---|---|---|---|---|---|---|---|---|---|---|---|---|---|---|---|---|
| | 4 | 0.13 | 0.06 | 2219-T87 | 6061-T6 | YES | 2.0 | | 1100-O | 0 | 0.31 | 7.1 | Y | 0.4 | N | 0.67 | 7.1 | 7.1 | 2 | | 1144 | | 3401-B | 10/18/90 | WALL HOLED PLUS 6 CRACKS TO 1.75" FROM IMPACT 30 LAYER MLI |
| | 4 | 0.13 | 0.06 | 2219-T87 | 6061-T6 | YES | 2.0 | | 1100-O | 0 | 0.31 | 7.1 | Y | 0.4 | N | 0.66 | 7.1 | 7.2 | 2 | | 1145 | | 3402-B | 10/19/90 | WALL 5 CRACKS UP TO 1.25" LONG, PETALED 20 LAYER MLI |
| | 4 | 0.13 | 0.06 | 2219-T87 | 6061-T6 | YES | 2.0 | | 1100-O | 0 | 0.31 | 7.2 | Y | 0.4 | N | 0.68 | 7.2 | 7.2 | 2 | | 1143 | | 3402-A | 10/17/90 | WALL HOLED PLUS 4 CRACKS TO 1.5" LONG FROM IMPACT 20 LAYER MLI |
| | 4 | 0.13 | 0.06 | 2219-T87 | 6061-T6 | YES | 2.0 | | 1100-O | 0 | 0.31 | 7.2 | Y | | N | 0.68 | 7.2 | 7.2 | 3 | | 1140 | | 3401-A | 10/15/90 | WALL: 5 PETALS W/CRACKS UP TO 2" 30 LAYER MLI |
| 104 | 4 | 0.13 | 0.06 | 2219-T87 | 6061-T6 | YES | 2.0 | | 1100-O | 0 | 0.38 | 6.9 | Y | 1.8 | N | 0.66 | 6.9 | | 3 | | 1153 | | 3404-B | 10/26/90 | 7 WALL PETALS TO 3.5" RADIUS. 20 LAYER NEW MLI |
| | 4 | 0.13 | 0.06 | 2219-T87 | 6061-T6 | YES | 2.0 | | 1100-O | 0 | 0.38 | 6.9 | Y | 2 | N | 0.66 | 6.9 | | 3 | | 1152 | | 3404-A | 10/25/90 | 5 WALL PETALS TO 3" RADIUS. 20 LAYER NEW MLI |
| 105 | 4 | 0.13 | 0.06 | 2219-T87 | 6061-T6 | YES | 3.75 | | 1100-O | 0 | 0.19 | 3.8 | C | 0 | N | 0.43 | 3.8 | 3.8 | 0 | | 1024 | | 3305-C | 05/21/90 | REAR SURFACE CRACK COUNTED AS FAILURE |
| | 4 | 0.13 | 0.06 | 2219-T87 | 6061-T6 | YES | 3.75 | | 1100-O | 0 | 0.19 | 4.2 | N | 0 | N | 0.4 | 4.2 | 4.2 | 0 | | 1023 | | 3305-B | 05/18/90 | |
| | 4 | 0.13 | 0.06 | 2219-T87 | 6061-T6 | YES | 3.75 | | 1100-O | 0 | 0.19 | 4.6 | N | 0 | N | 0.38 | 4.6 | | 0 | | 1025 | | 3305-A | 05/21/90 | |
| 106 | 4 | 0.13 | 0.06 | 2219-T87 | 6061-T6 | YES | 3.75 | | 1100-O | 0 | 0.25 | 5.2 | N | 0 | N | 0.52 | 5.2 | 5.2 | 0 | | 1026 | | 3306-A | 05/22/90 | |
| | 4 | 0.13 | 0.06 | 2219-T87 | 6061-T6 | YES | 3.75 | | 1100-O | 0 | 0.25 | 7 | N | 0 | N | 0.54 | 7 | | 0 | | 1031 | | 3306-B | 05/24/90 | |
| | 4 | 0.13 | 0.06 | 2219-T87 | 6061-T6 | YES | 3.75 | | 1100-O | 0 | 0.25 | 7 | Y | 0.1 | N | 0.51 | 7 | | 0 | | 1028 | | 3306-D | 05/23/90 | |
| | 4 | 0.13 | 0.06 | 2219-T87 | 6061-T6 | YES | 3.75 | | 1100-O | 0 | 0.25 | 7.1 | Y | 0.2 | Y | 0.52 | 7.1 | | 0 | | 1027 | | 3306-C | 05/22/90 | |
| 107 | 4 | 0.13 | 0.06 | 2219-T87 | 6061-T6 | YES | 3.75 | | 1100-O | 0 | 0.31 | 5.1 | Y | 0.8 | N | 0.67 | 5 | 5.1 | 2 | | 1146 | | 3403-D | 10/19/90 | WALL PETALED. 20 LAYER MLI |
| | 4 | 0.13 | 0.06 | 2219-T87 | 6061-T6 | YES | 3.75 | | 1100-O | 0 | 0.31 | 6.2 | Y | 0.6 | N | 0.64 | 6.2 | 6.2 | 2 | | 1147 | | 3403-C | 10/22/90 | WALL: 5 PETALS W/CRACKS TO 1.2". 20 LAYER MLI |
| | 4 | 0.13 | 0.06 | 2219-T87 | 6061-T6 | YES | 3.75 | | 1100-O | 0 | 0.31 | 7.1 | Y | 1 | N | 0.66 | 7.1 | 7.2 | 2 | | 1148 | | 3403-B | 10/22/90 | LITTLE WALL PETALING. 20 LAYER MLI |
| | 4 | 0.13 | 0.06 | 2219-T87 | 6061-T6 | YES | 3.75 | | 1100-O | 0 | 0.31 | 7.2 | Y | 0.8 | N | 0.64 | 7.2 | 7.2 | 2 | | 1149 | | 3403-A | 10/23/90 | WALL PETALED TO 0.75" CRACKS. 20 LAYER NEW MLI |
| | 4 | 0.13 | 0.06 | 2219-T87 | 6061-T6 | YES | 3.75 | | 1100-O | 0 | 0.31 | 7.2 | Y | 0.6 | N | 0.66 | 7.2 | 7.2 | 2 | | 1150 | | MLI-BURN2 | 10/24/90 | WALL PETALED TO 1.75" RADIUS. 20 LAYER OLD MLI |
| 108 | 4 | 0.13 | 0.06 | 2219-T87 | 6061-T6 | YES | 3.75 | | 1100-O | 45 | 0.19 | 4.8 | N | 0 | N | 0.48 | 4.8 | 4.8 | 0 | | 1032 | | 3307-A | 05/30/90 | |
| | 4 | 0.13 | 0.06 | 2219-T87 | 6061-T6 | YES | 3.75 | | 1100-O | 45 | 0.19 | 6.3 | N | 0 | N | 0.59 | 6.3 | 6.3 | 0 | | 1033 | | 3307-B | 05/31/90 | |
| 109 | 4 | 0.13 | 0.06 | 2219-T87 | 6061-T6 | YES | 3.75 | | 1100-O | 45 | 0.25 | 5.2 | Y | 0 | N | 0.65 | 5.2 | 5.1 | 0 | | 1034 | | 3308-A | 05/31/90 | |
| | 4 | 0.13 | 0.06 | 2219-T87 | 6061-T6 | YES | 3.75 | | 1100-O | 45 | 0.25 | 6.2 | Y | 0.3 | N | 0.56 | 6.2 | 6.2 | 1 | | 1035 | | 3308-B | 06/01/90 | 3 HOLES: .26X.203, .27X.205, PINHOLE |
| 110 | 4 | 0.13 | 0.06 | 2219-T87 | 6061-T6 | YES | 3.75 | | 1100-O | 75 | 0.31 | 7.1 | N | 0 | N | 1.37 | 7.1 | 7.1 | 0 | F HOLED | 1047 | | 4002-D | 06/18/90 | SIDE RICOCHET PLATES VERY FINE CRATERS |
| 111 | 4 | 0.13 | 0.06 | 2219-T87 | 6061-T6 | YES | B | | 1100-O | 0 | 0.31 | 7.1 | Y | 0.7 | N | 0.07 | 7.1 | 7.1 | | | 894 | | MLI-B1 | 12/11/89 | MLI ON BUMPER |
| 112 | 4 | 0.13 | 0.06 | 2219-T87 | 6061-T6 | YES | B | | 1100-O | 0 | 0.38 | 6.9 | Y | 2 | N | 0.75 | 6.9 | 6.8 | | | 896 | | MLI-B2 | 12/12/89 | |
| | 4 | 0.13 | 0.06 | 2219-T87 | 6061-T6 | YES | B | | 1100-O | 0 | 0.38 | 6.9 | Y | 2 | Y | 0.67 | 6.9 | 6.9 | 3 | | 1000 | | 3227-D | 04/23/90 | |
| 113 | 4 | 0.13 | 0.06 | 2219-T87 | 6061-T6 | YES | B--AL | | 1100-O | 0 | 0.31 | 6.9 | Y | 0.8 | Y | 0.67 | 6.9 | 6.9 | | | 905 | | BLKT-AL-1 | 12/19/89 | AL FOIL OF SAME AREAL WEIGHT AS MLI |
| 114 | 4 | 0.13 | 0.06 | 2219-T87 | 6061-T6 | YES | W | 1 | 1100-O | 0 | 0.2 | 3.1 | Y | 0.2 | N | 0.43 | 3 | 3.1 | | | 492 | MSFC | SS-T2-13 | 03/09/87 | |
| 115 | 4 | 0.13 | 0.06 | 2219-T87 | 6061-T6 | YES | W | 1 | 1100-O | 0 | 0.26 | 6.2 | Y | 1.3 | N | 0.6 | | 6.2 | 6 | | 132 | ADP SM1 | SS-P-022A | 01/15/86 | |
| 116 | 4 | 0.13 | 0.06 | 2219-T87 | 6061-T6 | YES | W | | 1100-O | 0 | 0.19 | 2.2 | Y | 0.3 | N | 0.29 | | 2.2 | | | 447 | MSFC | MD-TEST-A | 01/29/87 | |
| | 4 | 0.13 | 0.06 | 2219-T87 | 6061-T6 | YES | W | | 1100-O | 0 | 0.19 | 2.5 | C | 0 | N | 0.31 | | 2.5 | 0 | | 448 | MSFC | MD-TEST-B | 01/29/87 | |

| | standoff inch | rearwall gage inch | bumper gage inch | rearwall alloy | bumper alloy | mli present | mli location | prj. len to dia | prj. material | obliquity | projectile size | velocity avg km/s | rear penetr'n | rearhole inch | rearwall spall | bumper hole inch | vel hall km/s | vel xray km/s | witness penet. | rico con | test number | data source | test | date | comments |
|---|---|---|---|---|---|---|---|---|---|---|---|---|---|---|---|---|---|---|---|---|---|---|---|---|---|
| | 4 | 0.13 | 0.06 | 2219-T87 | 6061-T6 | YES | W | | 1100-O | 0 | 0.19 | 2.5 | C | 0 | N | 0.32 | 2.5 | 2.6 | | | 451 | | MD-TEST-A1 | 02/02/87 | |
| | 4 | 0.13 | 0.06 | 2219-T87 | 6061-T6 | YES | W | | 1100-O | 0 | 0.19 | 2.5 | N | 0 | N | 0.3 | | 2.5 | 0 | | 125 | ADP SM1 | SS-P-027F | 01/06/86 | |
| | 4 | 0.13 | 0.06 | 2219-T87 | 6061-T6 | YES | W | | 1100-O | 0 | 0.19 | 2.8 | N | 0 | N | 0.32 | | 2.8 | 0 | | 120 | ADP SM1 | SS-P-027E | 12/18/85 | |
| | 4 | 0.13 | 0.06 | 2219-T87 | 6061-T6 | YES | W | | 1100-O | 0 | 0.19 | 3.1 | N | 0 | N | 0.34 | | 3.1 | 0 | | 119 | ADP SM1 | SS-P-027D | 12/17/85 | |
| | 4 | 0.13 | 0.06 | 2219-T87 | 6061-T6 | YES | W | | 1100-O | 0 | 0.19 | 3.7 | N | 0 | N | 0.38 | | 3.7 | 0 | | 118 | ADP SM1 | SS-P-027C | 12/16/85 | |
| 117 | 4 | 0.13 | 0.06 | 2219-T87 | 6061-T6 | YES | W | | 1100-O | 0 | 0.25 | 2.9 | Y | 0.4 | | 0.41 | | 2.9 | 0 | | 50 | ADP SM1 | SS-P-007 | 09/04/85 | |
| | 4 | 0.13 | 0.06 | 2219-T87 | 6061-T6 | YES | W | | 1100-O | 0 | 0.25 | 3 | Y | 0.4 | Y | 0.41 | | 3 | 1 | | 51 | ADP SM1 | SS-P-008 | 09/05/85 | |
| | 4 | 0.13 | 0.06 | 2219-T87 | 6061-T6 | YES | W | | 1100-O | 0 | 0.25 | 3 | Y | 0.2 | N | 0.42 | 3 | 3 | | | 480 | MSFC | SS-T2-3 | 02/25/87 | |
| | 4 | 0.13 | 0.06 | 2219-T87 | 6061-T6 | YES | W | | 1100-O | 0 | 0.25 | 4 | N | 0 | N | 0.45 | | 4 | 0 | | 124 | ADP SM1 | SS-P-012D | 01/03/86 | |
| | 4 | 0.13 | 0.06 | 2219-T87 | 6061-T6 | YES | W | | 1100-O | 0 | 0.25 | 4.3 | Y | 0.2 | Y | 0.45 | 4.3 | 4.4 | | | 479 | MSFC | SS-T2-4 | 02/25/87 | |
| | 4 | 0.13 | 0.06 | 2219-T87 | 6061-T6 | YES | W | | 1100-O | 0 | 0.25 | 4.3 | N | 0 | N | 0.46 | | 4.3 | 0 | | 123 | ADP SM1 | SS-P-012C | 01/02/86 | |
| | 4 | 0.13 | 0.06 | 2219-T87 | 6061-T6 | YES | W | | 1100-O | 0 | 0.25 | 5 | N | 0 | | 0.5 | | 5 | 0 | | 53 | ADP SM1 | SS-P-010 | 09/09/85 | |
| | 4 | 0.13 | 0.06 | 2219-T87 | 6061-T6 | YES | W | | 1100-O | 0 | 0.25 | 5.2 | N | 0 | N | 0.5 | | 5.2 | 0 | | 179 | ADP SM1 | SS-P-034C-2 | 03/14/86 | |
| | 4 | 0.13 | 0.06 | 2219-T87 | 6061-T6 | YES | W | | 1100-O | 0 | 0.25 | 5.3 | N | 0 | | 0.52 | | 5.3 | 0 | | 52 | ADP SM1 | SS-P-009 | 09/06/85 | |
| | 4 | 0.13 | 0.06 | 2219-T87 | 6061-T6 | YES | W | | 1100-O | 0 | 0.25 | 6.6 | N | 0 | | 0.58 | | 6.6 | 0 | | 54 | ADP SM1 | SS-P-011 | 09/11/85 | |
| | 4 | 0.13 | 0.06 | 2219-T87 | 6061-T6 | YES | W | | 1100-O | 0 | 0.25 | 6.8 | N | 0 | | 0.55 | | 6.8 | 0 | | 57 | ADP SM1 | SS-P-012B | 09/12/85 | |
| 118 | 4 | 0.13 | 0.06 | 2219-T87 | 6061-T6 | YES | W | | 1100-O | 0 | 0.3 | 5.9 | Y | 2 | N | 0.59 | | 5.9 | 1 | | 130 | ADP SM1 | SS-P-021D | 01/13/86 | AFT PLATE CRACKED THROUGH-THICKNESS 1" UP, 1" LEFT, 1" RIGHT. PART-THROUGH CRACKS UP TO 2" UP, 3" LEFT, 3" RIGHT. |
| | 4 | 0.13 | 0.06 | 2219-T87 | 6061-T6 | YES | W | | 1100-O | 0 | 0.3 | 6.6 | N | 0 | N | 0.61 | | 6.6 | 0 | | 129 | ADP SM1 | SS-P-021C | 01/10/86 | |
| | 4 | 0.13 | 0.06 | 2219-T87 | 6061-T6 | YES | W | | 1100-O | 0 | 0.3 | 6.9 | N | 0 | N | 0.63 | | 6.9 | 0 | | 128 | ADP SM1 | SS-P-021B | 01/10/86 | |
| 119 | 4 | 0.13 | 0.06 | 2219-T87 | 6061-T6 | YES | W | | 1100-O | 0 | 0.31 | 3.3 | Y | 0.6 | N | 0.49 | 3.2 | 3.3 | | | 478 | MSFC | SS-T2-7 | 02/24/87 | SOME CRACKS AROUND HOLE |
| | 4 | 0.13 | 0.06 | 2219-T87 | 6061-T6 | YES | W | | 1100-O | 0 | 0.31 | 3.3 | Y | 0.7 | N | 0.55 | 3.2 | 3.3 | | | 488 | MSFC | SS-T2-7A | 03/05/87 | PETALING AND CRACKS |
| | 4 | 0.13 | 0.06 | 2219-T87 | 6061-T6 | YES | W | | 1100-O | 0 | 0.31 | 5.6 | Y | 1 | N | 0.6 | 5.6 | 5.7 | 0 | | 485 | MSFC | MD-TEST-D | 03/03/87 | |
| | 4 | 0.13 | 0.06 | 2219-T87 | 6061-T6 | YES | W | | 1100-O | 0 | 0.31 | 6.1 | Y | 11 | N | 0.6 | 6.1 | 6.2 | 2 | | 675 | MSFC | EH4-A | 12/01/87 | |
| | 4 | 0.13 | 0.06 | 2219-T87 | 6061-T6 | YES | W | | 1100-O | 0 | 0.31 | 6.6 | Y | 10 | N | 0.62 | 6.6 | 6.7 | | | 618 | MSFC | EH2-C | 08/25/87 | BUMPER - .619" DIA. HOLE, 1" LOW, .6" RIGHT, SOME DEBRIS. BUMPER BENT OUT .6" AT CENTER. WALL - MATERIAL SPLIT 5" DOWN, 5" UP, & 3" TO THE RIGHT. SINK 3.5" DIA. & 1" DEEP. WALL PANEL BENT OUT FOR .4". MLI - HOLE 6" DIA. & FLUFFED OUT. |

| | standoff inch | rearwall gage inch | bumper gage inch | rearwall alloy | bumper alloy | mli present | mli location | prj. len to dia | prj. material | obliquity | projectile size | velocity avg km/s | rear penetr'n | rearhole inch | rearwall spall | bumper hole inch | vel hall km/s | vel xray km/s | witness penet. | rico con | test number | data source | test | date | comments |
|---|---|---|---|---|---|---|---|---|---|---|---|---|---|---|---|---|---|---|---|---|---|---|---|---|---|
| | 4 | 0.13 | 0.06 | 2219-T87 | 6061-T6 | YES | W | | 1100-O | 0 | 0.31 | 6.7 | Y | 10 | N | 0.64 | 6.6 | 6.7 | | | 619 | MSFC | EH2-D | 08/26/87 | BUMPER - .635" DIA. HOLE, 1" LOW, .2" RIGHT, 3 DEBRIS HOLES .15" DIA. BUMPER BENT OUTWARD .8" AT CENTER. WALL - HOLE, METAL SPLIT 5" UP, & 5" DOWN, 4" LEFT. PANEL BENT OUTWARD .8" AT EDGES. LARGE CAVITY 4" DIA. & 1" DEEP. |
| | 4 | 0.13 | 0.06 | 2219-T87 | 6061-T6 | YES | W | | 1100-O | 0 | 0.31 | 6.7 | N | 0 | N | 0.77 | 6.6 | 6.7 | | | 613 | MSFC | EH2-B | 08/14/87 | BUMPER - .766" DIA. HOLE, 1" LOW, SOME DEBRIS. BENT OUT 1.1" AT CENTER. WALL - NO HOLE, CAVITY 6" DIA. AND .55" DEEP. MLI - HOLE 6" DIA. AND FLUFFED OUT. |
| | 4 | 0.13 | 0.06 | 2219-T87 | 6061-T6 | YES | W | | 1100-O | 0 | 0.31 | 6.7 | Y | 9.3 | N | 0.63 | | 6.7 | 0 | | 844 | | 3020-A | 10/24/89 | HOLE, METAL SPLIT 4 WAYS, HORIZONTAL-4.75" LEFT AND 4.5" RIGHT, VERTICAL-2.75" UP AND 2.75" DOWN. DOES NOT SEEM TO BE A PROJECTILE PENETRATION. 4 PETALS PUSHED OUT APPROX. 1.3". |
| | 4 | 0.13 | 0.06 | 2219-T87 | 6061-T6 | YES | W | | 1100-O | 0 | 0.31 | 6.8 | Y | 4 | N | 0.58 | 6.7 | 6.9 | | | 620 | MSFC | EH2-E | 08/27/87 | BUMPER - .584" DIA. HOLE, 1" LOW, .2" LEFT, SOME DEBRIS, BENT OUTWARD .55" AT CENTER. WALL - HOLE 3" X 4" WITH THE SECTION PEELED BACK. |
| | 4 | 0.13 | 0.06 | 2219-T87 | 6061-T6 | YES | W | | 1100-O | 0 | 0.31 | 6.9 | Y | 7 | N | 0.7 | 6.9 | 6.9 | 1 | | 859 | | N2PURGE1 | 11/07/89 | METAL SPLIT 4 PETALS, CRACKS ALONG PETALS APPROX. 4", 3.5", 4.2" AND 2.8" LONG. DAMAGE IN CENTER AREA OF PETALS APPROX. 2" DIA OF SMALL CRATERS. |
| | 4 | 0.13 | 0.06 | 2219-T87 | 6061-T6 | YES | W | | 1100-O | 0 | 0.31 | 6.9 | Y | 0.8 | N | 0.64 | 6.9 | 7 | | | 756 | | EHSS-M4 | 03/22/89 | |
| | 4 | 0.13 | 0.06 | 2219-T87 | 6061-T6 | YES | W | | 1100-O | 0 | 0.31 | 7.1 | Y | 5 | N | 0.63 | 7 | 7.1 | | | 606 | MSFC | EH2-A | 08/05/87 | BUMPER - .634" DIA. HOLE, .9" LOW, .3" LEFT, FEW DEBRIS CAVITIES, ONE DEBRIS HOLE .2" DIA. BUMPER BENT OUTWARD 1". WALL - HOLE, METAL SPLIT 4 DIRECTIONS LENGTH 5", 3.5", 4", AND 4". (NO PRESSURE READINGS) |
| | 4 | 0.13 | 0.06 | 2219-T87 | 6061-T6 | YES | W | | 1100-O | 0 | 0.31 | 7.1 | Y | 11 | N | 0.65 | 7.1 | 7.2 | 0 | | 834 | | 3020-B | 10/13/89 | METAL SPLIT, NO PROJECTILE HOLE, LARGE SINK APPROX. 1" DEEP AND 6" DIA, WITH SPLIT IN BOTTOM, SPLIT IN METAL HORIZONTAL APPROX. 5.5" BOTH WAYS. SPLIT OPEN APPROX. .5" AT BOTTOM OF SINK. |
| | 4 | 0.13 | 0.06 | 2219-T87 | 6061-T6 | YES | W | | 1100-O | 0 | 0.31 | 7.2 | N | 0 | N | 0.65 | 7.2 | 7.3 | | | 845 | | 3021-A | 10/24/89 | NO HOLE, SINK APPROX. 5" DIA AND .5" DEEP, FEW SMALL CRATERS. PUSHED OUT ON REAR, NO DIMPLES. |
| 120 | 4 | 0.13 | 0.06 | 2219-T87 | 6061-T6 | YES | W | | 1100-O | 0 | 0.38 | 4.6 | Y | 5.5 | N | 0.61 | 4.6 | 4.6 | | | 491 | MSFC | SS-T2-17 | 03/09/87 | PETALING |
| | 4 | 0.13 | 0.06 | 2219-T87 | 6061-T6 | YES | W | | 1100-O | 0 | 0.38 | 6.8 | Y | 6 | N | 0.7 | 6.8 | 6.8 | 3 | | 997 | | 3227-A | 04/19/90 | REARWALL PETALLED |
| 121 | 4 | 0.13 | 0.06 | 2219-T87 | 6061-T6 | YES | W | | 1100-O | 30 | 0.19 | 2.2 | N | 0 | N | 0.43 | | 2.2 | | | 836 | | 3022-A | 10/16/89 | NO HOLE, CRATER IN PROJECTILE PATH APPROX. .25" DIA AND LESS THAN .050" DEEP, SLIGHT DIMPLE ON REAR. FEW SMALL CRATERS. |
| | 4 | 0.13 | 0.06 | 2219-T87 | 6061-T6 | YES | W | | 1100-O | 30 | 0.19 | 3.4 | N | 0 | N | 0.37 | | 3.4 | | | 835 | | 3022-B | 10/16/89 | NO HOLE, CRATER APPROX .3" X .25" IN PROJ PATH WITH LARGE DIMPLE ON REAR. FEW SMALL CRATERS UNDER BUMPER HOLE. |
| | 4 | 0.13 | 0.06 | 2219-T87 | 6061-T6 | YES | W | | 1100-O | 30 | 0.19 | 4.1 | Y | 0.3 | N | 0.41 | | 4.1 | | | 842 | | 3022-C | 10/23/89 | HOLE 0.338" DIA. ONE CRATER APPROX. .2" DIA AND .05" DEEP IN PROJECTILE PATH. SEVERAL SMALL CRATERS IN AREA APPROX. 3.5" DIA. |
| | 4 | 0.13 | 0.06 | 2219-T87 | 6061-T6 | YES | W | | 1100-O | 30 | 0.19 | 4.9 | Y | 0.2 | N | 0.44 | 4.9 | 4.9 | 1 | | 843 | | 3022-D | 10/23/89 | 2 HOLES IN PROJECTILE PATH, .21" X .13" AND .15" X .70" WITH FEW SMALL CRATERS FROM HOLE UP TO AREA UNDER BUMPER HOLE. |

| | standoff inch | rearwall gage inch | bumper gage inch | rearwall alloy | bumper alloy | mli present | mli location | pri. len to dia | pri. material | obliquity | projectile size | velocity avg km/s | rear penetr'n | rearhole inch | rearwall spall | bumper hole inch | vel hall km/s | vel xray km/s | witness penet. | rico con | test number | data source | test | date | comments |
|---|---|---|---|---|---|---|---|---|---|---|---|---|---|---|---|---|---|---|---|---|---|---|---|---|---|
| 122 | 4 | 0.13 | 0.06 | 2219-T87 | 6061-T6 | YES | W | | 1100-O | 30 | 0.25 | 6.2 | Y | 0 | N | 0.61 | 6.2 | 6.2 | | | 839 | | 3023-B | 10/19/89 | PIN HOLE BOTTOM OF CRATER .18" WIDE X .13" DEEP WITH CRACK IN DIMPLE ON REAR. SEVERAL CRATERS IN APPROX. 3" DIA AREA UP TO .15" DIA X .07" DEEP WITH FEW DIMPLES ON REAR. |
| | 4 | 0.13 | 0.06 | 2219-T87 | 6061-T6 | YES | W | | 1100-O | 30 | 0.25 | 7 | N | 0 | N | 0.62 | 6.9 | 7 | | | 840 | | 3023-A | 10/20/89 | NO HOLE, SINK AREA APPROX. 2.5" DIA X .15" DEEP WITH SMALL CRATER IN SINK AREA UP TO .15" DIA, VERY SMALL SIMPLES ON REAR. |
| 123 | 4 | 0.13 | 0.06 | 2219-T87 | 6061-T6 | YES | W | | 1100-O | 30 | 0.31 | 7 | Y | 7 | N | 0.73 | 7 | 7 | 0 | | 841 | | 3024-B | 10/20/89 | PROJECTILE HOLE WITH SPLIT HORIZONTALLY ACCROSS METAL |
| 124 | 4 | 0.13 | 0.06 | 2219-T87 | 6061-T6 | YES | W | | 1100-O | 45 | 0.19 | 3.2 | N | 0 | N | 0.47 | | 3.2 | 0 | CAVITIES | 386 | IWALL | SS-230B | 11/06/86 | |
| | 4 | 0.13 | 0.06 | 2219-T87 | 6061-T6 | YES | W | | 1100-O | 45 | 0.19 | 4.4 | N | 0 | N | 0.48 | | 4.4 | 0 | CAVITIES | 385 | IWALL | SS-230A | 11/05/86 | |
| 125 | 4 | 0.13 | 0.06 | 2219-T87 | 6061-T6 | YES | W | | 1100-O | 45 | 0.25 | 3.2 | Y | 0.4 | N | 0.58 | | 3.2 | 2 | CAVITIES | 242 | IWALL | SS-205E | 06/27/86 | |
| | 4 | 0.13 | 0.06 | 2219-T87 | 6061-T6 | YES | W | | 1100-O | 45 | 0.25 | 4.2 | Y | 0.2 | N | 0.61 | 4.1 | 4.2 | 0 | CAVITIES | 238 | IWALL | SS-205A | 06/24/86 | |
| | 4 | 0.13 | 0.06 | 2219-T87 | 6061-T6 | YES | W | | 1100-O | 45 | 0.25 | 4.6 | Y | 0.2 | N | 0.65 | 4.6 | 4.6 | 0 | 1HOLE | 239 | IWALL | SS-205B | 06/25/86 | |
| | 4 | 0.13 | 0.06 | 2219-T87 | 6061-T6 | YES | W | | 1100-O | 45 | 0.25 | 5.3 | Y | 0.3 | N | 0.6 | | 5.3 | 1 | CAVITIES | 240 | IWALL | SS-205C | 06/25/86 | |
| | 4 | 0.13 | 0.06 | 2219-T87 | 6061-T6 | YES | W | | 1100-O | 45 | 0.25 | 6.3 | C | 0 | N | 0.63 | 6.2 | 6.4 | 0 | SPRAY | 241 | IWALL | SS-205D | 06/26/86 | COUNT REAR SURFACE CRACK AS FAILURE |
| | 4 | 0.13 | 0.06 | 2219-T87 | 6061-T6 | YES | W | | 1100-O | 45 | 0.25 | 7 | Y | 0 | N | 0.7 | 6.9 | 7.1 | | | 847 | | 3027-A | 10/26/89 | PIN HOLE, IN PROJECTILE PATH, ONE CRATER APPROX. .16" DIA X .08" DEEP WITH DIMPLE ON REAR, SEVERAL OTHER SMALL CRATERS IN AREA. MANY VERY SMALL CRATERS UNDER BUMPER HOLE |
| 126 | 4 | 0.13 | 0.06 | 2219-T87 | 6061-T6 | YES | W | | 1100-O | 45 | 0.3 | 6.3 | Y | 1.1 | N | 0.81 | 6.2 | 6.4 | 2 | CAVITIES | 284 | IWALL | SS-212B | 08/06/86 | |
| 127 | 4 | 0.13 | 0.06 | 2219-T87 | 6061-T6 | YES | W | | 1100-O | 45 | 0.31 | 3.1 | Y | 0.2 | N | 0.74 | 3 | 3.1 | 0 | CAVITIES | 525 | MSFC | SS-320 | 04/28/87 | CRACK IN C. 0.25" CAVITY |
| | 4 | 0.13 | 0.06 | 2219-T87 | 6061-T6 | YES | W | | 1100-O | 45 | 0.31 | 3.7 | Y | 0.6 | N | 0.74 | 3.7 | 3.8 | 2 | CAVITIES | 599 | MSFC | SS-303A | 07/27/87 | |
| | 4 | 0.13 | 0.06 | 2219-T87 | 6061-T6 | YES | W | | 1100-O | 45 | 0.31 | 4.3 | Y | 0.3 | N | 0.77 | 4.1 | 4.4 | 1 | CAVITIES | 528 | MSFC | SS-325 | 05/01/87 | |
| | 4 | 0.13 | 0.06 | 2219-T87 | 6061-T6 | YES | W | | 1100-O | 45 | 0.31 | 6.5 | Y | 0.2 | N | 0.81 | 6.4 | 6.5 | 0 | CAVITIES | 467 | MSFC | SS-002B | 02/12/87 | |
| | 4 | 0.13 | 0.06 | 2219-T87 | 6061-T6 | YES | W | | 1100-O | 45 | 0.31 | 7.1 | Y | 1.1 | N | 0.84 | 7 | 7.1 | 1/+ | | 846 | | 3028-A | 10/25/89 | METAL HAS SMALL CRACK FROM ONE EDGE OF HOLE APPROX .7" LONG. SEVERAL CRATERS AROUND HOLE UP TO .2" DIA AND .07" DEEP, WITH FEW DIMPLES ON REAR. MANY VERY SMALL CRATERS UNDER BUMPER HOLE WITH NO DIMPLES ON REAR. #2 WITNESS HAS |
| 128 | 4 | 0.13 | 0.06 | 2219-T87 | 6061-T6 | YES | W | | 1100-O | 45 | 0.35 | 5.9 | Y | 1.1 | N | 0.86 | 5.9 | 5.9 | 4 | CAVITIES | 282 | IWALL | SS-211B | 08/05/86 | |
| | 4 | 0.13 | 0.06 | 2219-T87 | 6061-T6 | YES | W | | 1100-O | 45 | 0.35 | 7 | Y | 1.3 | N | 0.91 | 6.8 | 7.1 | 4 | CAVITIES | 283 | IWALL | SS-211D | 08/06/86 | |
| 129 | 4 | 0.13 | 0.06 | 2219-T87 | 6061-T6 | YES | W | | 1100-O | 65 | 0.19 | 3.9 | N | 0 | N | 0.44 | | 3.9 | | | 848 | | 3029-C | 10/26/89 | NO, HOLE NO DAMAGE IN PROJ PATH. FEW CRATERS UNDER BUMPER HOLE AND FOR APPROX. 3" IN DIRECTION OF PROJ TRAVEL. 3 CRATERS APPROX. .15" DIA AND .05" DEEP WITH SMALL DIMPLES ON REAR. |
| 130 | 4 | 0.13 | 0.06 | 2219-T87 | 6061-T6 | YES | W | | 1100-O | 65 | 0.25 | 3.5 | N | 0 | N | 0.91 | | 3.5 | | | 849 | | 3030-A | 10/30/89 | NO HOLE, NO DAMAGE IN PROJ PATH, FEW CRATERS UNDER BUMPER HOLE AND FOR APPROX. 3" IN DIRECTION OF PROJ TRAVEL. 2 CRATERS APPROX. .17" DIA X .06" DEEP WITH DIMPLES ON REAR, OTHER CRATERS SMALLER. |
| | 4 | 0.13 | 0.06 | 2219-T87 | 6061-T6 | YES | W | | 1100-O | 65 | 0.25 | 4.3 | N | 0 | N | 0.69 | 4.2 | 4.4 | 0 | HOLES | 274 | IWALL | SS-209A | 07/25/86 | |

| | standoff inch | rearwall gage inch | bumper gage inch | rearwall alloy | bumper alloy | mli present | mli location | prj. len to dia | prj. material | obliquity | projectile size | velocity avg km/s | rear penetr'n | rearhole inch | rearwall spall | bumper hole inch | vel hall km/s | vel xray km/s | witness penet. | rico con | test number | data source | test | date | comments |
|---|---|---|---|---|---|---|---|---|---|---|---|---|---|---|---|---|---|---|---|---|---|---|---|---|---|
| | 4 | 0.13 | 0.06 | 2219-T87 | 6061-T6 | YES | W | | 1100-O | 65 | 0.25 | 6.4 | N | 0 | N | 0.87 | 6.3 | 6.4 | 0 | HOLES | 275 | IWALL | SS-209B | 07/31/86 | |
| | 4 | 0.13 | 0.06 | 2219-T87 | 6061-T6 | YES | W | | 1100-O | 65 | 0.25 | 7.3 | N | 0 | N | 0.77 | 7.3 | 7.4 | 0 | HOLES | 276 | IWALL | SS-209D | 07/31/86 | |
| 131 | 4 | 0.13 | 0.06 | 2219-T87 | 6061-T6 | YES | W | | 1100-O | 65 | 0.3 | 5.7 | Y | 0.2 | N | 0.88 | 5.6 | 5.9 | 0 | HOLES | 249 | IWALL | SS-207A | 07/03/86 | |
| | 4 | 0.13 | 0.06 | 2219-T87 | 6061-T6 | YES | W | | 1100-O | 65 | 0.3 | 6.3 | Y | 0.1 | N | 0.92 | 6.3 | 6.5 | 0 | HOLES | 271 | IWALL | SS-207B | 07/23/86 | |
| | 4 | 0.13 | 0.06 | 2219-T87 | 6061-T6 | YES | W | | 1100-O | 65 | 0.3 | 7 | N | 0 | N | 1.02 | 7 | 7.1 | 0 | HOLES | 273 | IWALL | SS-207C | 07/24/86 | |
| 132 | 4 | 0.13 | 0.06 | 2219-T87 | 6061-T6 | YES | W | | 1100-O | 65 | 0.31 | 3.5 | N | 0 | N | 0.92 | | 3.5 | | | 851 | | 3031-B | 11/01/89 | NO HOLE, VERY LITTLE DAMAGE IN PROJ PATH. CRATERS UNDER BUMPER HOLE OVER AN AREA APPROX. 3.5" DIA. FEW OF THE LARGER CRATERS UP TO .2" DIA AND .9" DEEP WITH DIMPLES ON REAR |
| | 4 | 0.13 | 0.06 | 2219-T87 | 6061-T6 | YES | W | | 1100-O | 65 | 0.31 | 7 | N | 0 | N | 1.11 | 7 | 7.1 | | | 850 | | 3031-C | 10/31/89 | NO HOLE, ALMOST NO DAMAGE IN PROJ PATH. FEW VERY LIGHT CRATERS. MANY CRATERS UNDER BUMPER HOLE OVER AN AREA APPROX 5" WIDE X 3.5" LONG PROJ TRAVEL. SEVERAL CRATER APPROX. .15" DIA X .07" DEEP WITH SMALL DIMPLES ON REAR |
| 133 | 4 | 0.13 | 0.06 | 2219-T87 | 6061-T6 | YES | W | | 1100-O | 65 | 0.35 | 5.7 | Y | 0.1 | N | 1.13 | 5.7 | 5.7 | 0 | HOLES | 280 | IWALL | SS-210B | 08/04/86 | |
| | 4 | 0.13 | 0.06 | 2219-T87 | 6061-T6 | YES | W | | 1100-O | 65 | 0.35 | 6.9 | Y | 0.2 | N | 1.4 | 6.8 | 7.1 | 1 | HOLES | 281 | IWALL | SS-210D | 08/05/86 | |
| 134 | 4 | 0.13 | 0.06 | 2219-T87 | 6061-T6 | YES | W--AL | | 1100-O | 0 | 0.31 | 6.8 | Y | 0.6 | N | | 6.9 | 6.8 | | | 909 | | BLKT-AL-2 | 01/03/90 | AL FOIL INSTEAD OF MLI |
| 135 | 4 | 0.13 | 0.06 | 2219-T87 | 2219-T87 | YES | | | 1100-O | 0 | 0.31 | 6.9 | Y | 3 | N | 0.62 | 6.9 | 7 | 2 | | 543 | MSFC | PR-EH2 | 05/20/87 | |
| | 4 | 0.13 | 0.06 | 2219-T87 | 2219-T87 | YES | | | 1100-O | 0 | 0.31 | 7 | Y | 3 | N | 0.62 | 7 | 7.1 | 2 | | 542 | MSFC | PR-EH1 | 05/20/87 | |
| 136 | 4 | 0.13 | 0.06 | 5456H116 | 6061-T6 | YES | | | 1100-O | 0 | 0.31 | | | 1.5 | | 0.73 | 6.9 | 7.1 | | | 745 | | EHSS-M1 | 03/04/89 | |
| | 4 | 0.13 | 0.06 | 5456H116 | 6061-T6 | YES | | | 1100-O | 0 | 0.31 | | | | | 0.65 | 6.9 | 7.1 | | | 747 | | EHSS-M3 | 03/06/89 | |
| 137 | 4 | 0.13 | 0.06 | 5456H116 | 6061-T6 | YES | | | 1100-O | 45 | 0.31 | | | 0.4 | | 0.85 | 7 | 7.2 | | | 746 | | EHSS-M2 | 03/06/89 | |
| 138 | 4 | 0.13 | 0.08 | 2219-T87 | 6061-T6 | NO | | | 1100-O | 0 | 0.19 | 2 | N | 0 | N | 0.32 | | 2 | 0 | | 166 | MARTIN | SS-109D | 03/04/86 | |
| | 4 | 0.13 | 0.08 | 2219-T87 | 6061-T6 | NO | | | 1100-O | 0 | 0.19 | 2.6 | S | 0 | Y | 0.35 | | 2.6 | | | 165 | MARTIN | SS-109C | 03/04/86 | COUNT SPALL AS PENETRATION |
| | 4 | 0.13 | 0.08 | 2219-T87 | 6061-T6 | NO | | | 1100-O | 0 | 0.19 | 3.1 | Y | 0.3 | N | 0.35 | | 3.1 | 2 | | 134 | MARTIN | SS-101 | 01/16/86 | |
| | 4 | 0.13 | 0.08 | 2219-T87 | 6061-T6 | NO | | | 1100-O | 0 | 0.19 | 3.6 | N | 0 | N | 0.39 | | 3.6 | 0 | | 164 | MARTIN | SS-109B | 03/03/86 | |
| | 4 | 0.13 | 0.08 | 2219-T87 | 6061-T6 | NO | | | 1100-O | 0 | 0.19 | 3.7 | Y | 0.2 | N | 0.37 | | 3.7 | 1 | | 135 | MARTIN | SS-101A | 01/17/86 | |
| | 4 | 0.13 | 0.08 | 2219-T87 | 6061-T6 | NO | | | 1100-O | 0 | 0.19 | 4.1 | N | 0 | N | 0.43 | | 4.1 | 0 | | 163 | MARTIN | SS-109A | 03/03/86 | |
| | 4 | 0.13 | 0.08 | 2219-T87 | 6061-T6 | NO | | | 1100-O | 0 | 0.19 | 4.3 | C | 0 | N | 0.44 | | 4.3 | 0 | | 136 | MARTIN | SS-101B | 01/21/86 | COUNT REAR SURFACE CRACK AS FAILURE |
| | 4 | 0.13 | 0.08 | 2219-T87 | 6061-T6 | NO | | | 1100-O | 0 | 0.19 | 7.4 | N | 0 | N | 0.53 | | 7.4 | 0 | | 153 | MARTIN | SS-109 | 02/14/86 | |
| 139 | 4 | 0.13 | 0.08 | 2219-T87 | 6061-T6 | NO | | | 1100-O | 0 | 0.3 | 7.2 | Y | 0 | Y | 0.72 | | 7.2 | 0 | | 137 | MARTIN | SS-102 | 01/21/86 | |

| | standoff inch | rearwall gage inch | bumper gage inch | rearwall alloy | bumper alloy | mli present | mli location | prj. len to dia | prj. material | obliquity | projectile size | velocity avg km/s | rear penetr'n | rearhole inch | rearwall spall | bumper hole inch | vel hall km/s | vel xray km/s | witness penet. | rico con | test number | data source | test | date | comments |
|---|---|---|---|---|---|---|---|---|---|---|---|---|---|---|---|---|---|---|---|---|---|---|---|---|---|
| 140 | 4 | 0.13 | 0.08 | 2219-T87 | 6061-T6 | NO | | | 1100-O | 0 | 0.35 | 6.8 | Y | 0.8 | Y | 0.74 | | 6.8 | 4 | | 155 | MARTIN | SS-107 | 02/19/86 | |
| 141 | 4 | 0.13 | 0.08 | 2219-T87 | 6061-T6 | NO | | | 1100-O | 45 | 0.25 | 6.9 | Y | 0.3 | N | 0.72 | 6.8 | 6.9 | 0 | HOLE | 461 | MARTIN | SS-151A | 02/09/87 | |
| 142 | 4 | 0.13 | 0.08 | 2219-T87 | 6061-T6 | NO | | | 1100-O | 45 | 0.31 | 6.6 | Y | 0.4 | N | 0.83 | 6.6 | 6.6 | 2 | CAVITIES | 463 | MSFC | SS-001A | 02/10/87 | |
| 143 | 4 | 0.13 | 0.08 | 2219-T87 | 6061-T6 | NO | | | 1100-O | 45 | 0.35 | 3.5 | Y | 0.6 | N | 0.81 | | 3.5 | 0 | | 149 | MARTIN | SS-105 | 02/06/86 | REAR WALL HIT OVER THICK PART OF SAMPLE HOLDER |
| | 4 | 0.13 | 0.08 | 2219-T87 | 6061-T6 | NO | | | 1100-O | 45 | 0.35 | 6.8 | Y | 1.3 | N | 0.93 | | 6.8 | 6 | | 157 | MARTIN | SS-106 | 02/21/86 | |
| 144 | 4 | 0.13 | 0.08 | 2219-T87 | 6061-T6 | NO | | | 1100-O | 60 | 0.35 | 4.1 | Y | 0.4 | N | 1.05 | | 4.1 | 1 | | 150 | MARTIN | SS-105A | 02/07/86 | |
| | 4 | 0.13 | 0.08 | 2219-T87 | 6061-T6 | NO | | | 1100-O | 60 | 0.35 | 6.8 | Y | 0.3 | N | 1.14 | | 6.8 | 1 | | 158 | MARTIN | SS-106-1 | 02/24/86 | |
| 145 | 4 | 0.13 | 0.08 | 2219-T87 | 6061-T6 | NO | | | 1100-O | 60 | 0.38 | 6.7 | Y | 0.5 | N | 1.28 | | 6.7 | 3 | | 160 | MARTIN | SS-106A | 02/26/86 | |
| 146 | 4 | 0.13 | 0.08 | 2219-T87 | 6061-T6 | NO | | | 1100-O | 75 | 0.35 | 3.9 | N | 0 | N | 1.4 | | 3.9 | 0 | | 151 | MARTIN | SS-105B | 02/11/86 | |
| | 4 | 0.13 | 0.08 | 2219-T87 | 6061-T6 | NO | | | 1100-O | 75 | 0.35 | 6.7 | Y | 0.1 | N | 1.53 | | 6.7 | 0 | | 159 | MARTIN | SS-106-2 | 02/25/86 | |
| 147 | 4 | 0.13 | 0.08 | 2219-T87 | 6061-T6 | NO | | | 1100-O | 75 | 0.38 | 6.7 | Y | 0.2 | N | 1.77 | | 6.7 | 2 | | 161 | MARTIN | SS-106B | 02/27/86 | |
| 148 | 4 | 0.13 | 0.08 | 2219-T87 | 6061-T6 | NO | | | 6061-T6 | 0 | 0.3 | 7.1 | Y | 0.8 | Y | 0.71 | | 7.1 | 1 | | 152 | MARTIN | SS-110 | 02/12/86 | |
| 149 | 4 | 0.13 | 0.08 | 5456H116 | 6061-T6 | W | | | LEXAN | 0 | 0.5 | | | 6 | | 0.98 | 6.4 | 6.4 | | | 920 | | FLASH-2 | 01/16/90 | 20 LAYERS AL FOIL INSTEAD OF MLI |
| 150 | 4 | 0.13 | 0.08 | 2219-T87 | 6061-T6 | YES | 3.75 | | 1100-O | 0 | 0.25 | 5 | Y | 0.2 | Y | 0.51 | 5 | | 0 | | 1029 | | 3301-E | 05/23/90 | |
| 151 | 4 | 0.13 | 0.08 | 2219-T87 | 6061-T6 | YES | 3.75 | | 1100-O | 0 | 0.31 | 6.2 | Y | 2 | N | 0.66 | 6.2 | | 2 | | 1030 | | 3302-E | 05/24/90 | |
| 152 | 4 | 0.13 | 0.08 | 2219-T87 | 6061-T6 | YES | 3.75 | | 1100-O | 45 | 0.19 | 3.3 | N | 0 | N | 0.46 | 3.3 | 3.3 | 0 | CRATERED | 1058 | | 4109-A | 07/03/90 | |
| | 4 | 0.13 | 0.08 | 2219-T87 | 6061-T6 | YES | 3.75 | | 1100-O | 45 | 0.19 | 4.1 | N | 0 | N | 0.47 | | 4.1 | 0 | CRATERED | 1059 | | 4109-B | 07/05/90 | |
| | 4 | 0.13 | 0.08 | 2219-T87 | 6061-T6 | YES | 3.75 | | 1100-O | 45 | 0.19 | 5.7 | Y | 0.1 | Y | 0.52 | 5.7 | 5.7 | 0 | | 1021 | | 3303-D | 05/17/90 | |
| | 4 | 0.13 | 0.08 | 2219-T87 | 6061-T6 | YES | 3.75 | | 1100-O | 45 | 0.19 | 6.1 | N | 0 | N | 0.54 | 6.1 | | 0 | | 1016 | | 3303-C | 05/11/90 | |
| | 4 | 0.13 | 0.08 | 2219-T87 | 6061-T6 | YES | 3.75 | | 1100-O | 45 | 0.19 | 6.4 | Y | 0.1 | N | 0.56 | 6.4 | 6.4 | | | 1014 | | 3303-A | 05/09/90 | |
| | 4 | 0.13 | 0.08 | 2219-T87 | 6061-T6 | YES | 3.75 | | 1100-O | 45 | 0.19 | 6.5 | N | 0 | N | 0.56 | 6.5 | 6.5 | 0 | CRATERED | 1060 | | 4109-C | 07/05/90 | RICOCHET CRATERS < 0.05"D |
| | 4 | 0.13 | 0.08 | 2219-T87 | 6061-T6 | YES | 3.75 | | 1100-O | 45 | 0.19 | 6.8 | N | 0 | N | 0.57 | 6.8 | 6.8 | 0 | | 1015 | | 3303-B | 05/10/90 | |
| | 4 | 0.13 | 0.08 | 2219-T87 | 6061-T6 | YES | 3.75 | | 1100-O | 45 | 0.19 | 7.4 | N | 0 | N | 0.59 | 7.5 | 7.4 | 0 | SPRAYED | 1062 | | 4109-D | 07/09/90 | |
| 153 | 4 | 0.13 | 0.08 | 2219-T87 | 6061-T6 | YES | 3.75 | | 1100-O | 45 | 0.25 | 3.3 | N | 0 | N | 0.58 | 3.3 | 3.3 | 0 | CRATERED | 1064 | | 4110-A | 07/10/90 | |
| | 4 | 0.13 | 0.08 | 2219-T87 | 6061-T6 | YES | 3.75 | | 1100-O | 45 | 0.25 | 4 | N | 0 | N | 0.62 | 4 | 4 | 0 | CRATERED | 1065 | | 4110-B | 07/11/90 | |

| | standoff inch | rearwall gage inch | bumper gage inch | rearwall alloy | bumper alloy | mil present | mil location | prj. len to dia | prj. material | obliquity | projectile size | velocity avg km/s | rear penetr'n | rearhole inch | rearwall spall | bumper hole inch | vel hall km/s | vel xray km/s | witness penet. | rico con | test number | data source | test | date | comments |
|---|---|---|---|---|---|---|---|---|---|---|---|---|---|---|---|---|---|---|---|---|---|---|---|---|---|
| | 4 | 0.13 | 0.08 | 2219-T87 | 6061-T6 | YES | 3.75 | | 1100-O | 45 | 0.25 | 5.8 | Y | 0.1 | N | 0.75 | 5.8 | 5.8 | 0 | CRATERED | 1068 | | 4110-C | 07/12/90 | SM. CRATERS ON RICO. PLATE UP TO 0.07"DIA X 0.03"DEEP |
| | 4 | 0.13 | 0.08 | 2219-T87 | 6061-T6 | YES | 3.75 | | 1100-O | 45 | 0.25 | 6.1 | Y | 0.2 | N | 0.71 | 6.2 | 6 | 0 | | 1017 | | 3304-A | 05/11/90 | |
| | 4 | 0.13 | 0.08 | 2219-T87 | 6061-T6 | YES | 3.75 | | 1100-O | 45 | 0.25 | 6.2 | Y | 0.4 | N | 0.72 | 6.3 | 6.1 | 1 | | 1018 | | 3304-B | 05/14/90 | BUMPER HOLE .722" X .568", 0.6" LOW, 0.4" LEFT, NO DEBRIS. |
| | 4 | 0.13 | 0.08 | 2219-T87 | 6061-T6 | YES | 3.75 | | 1100-O | 45 | 0.25 | 6.9 | Y | 0.4 | N | 0.66 | 6.8 | 6.9 | 1 | | 1019 | | 3304-C | 05/14/90 | BUMPER: HOLE 0.661" X 0.590" OBLONG, 1" LOW, 1.1" RIGHT. |
| | 4 | 0.13 | 0.08 | 2219-T87 | 6061-T6 | YES | 3.75 | | 1100-O | 45 | 0.25 | 6.9 | Y | 0.1 | Y | 0.69 | 6.9 | 6.8 | 0 | | 1020 | | 3304-D | 05/17/90 | BUMPER HOLE .693"X.611" OBLONG, 0.3" LOW, 0.2" RIGHT. NO DEBRIS. |
| | 4 | 0.13 | 0.08 | 2219-T87 | 6061-T6 | YES | 3.75 | | 1100-O | 45 | 0.25 | 6.9 | N | 0 | N | 0.71 | 7 | 6.9 | 0 | CRATERED | 1069 | | 4110-D | 07/13/90 | RICO PLATE SMALL CRATERS UP TO 0.1" DIA X 0.03"DEEP |
| 154 | 4 | 0.13 | 0.08 | 2219-T87 | 6061-T6 | YES | 3.75 | | 1100-O | 45 | 0.31 | 2.9 | Y | 0.3 | N | 0.7 | | 2.9 | 0 | CRATERED | 1070 | | 4111-A | 07/16/90 | RICO PLATE CRATERS UP TO 0.1" DIA X 0.03" DEEP |
| | 4 | 0.13 | 0.08 | 2219-T87 | 6061-T6 | YES | 3.75 | | 1100-O | 45 | 0.31 | 3.2 | Y | 0.5 | N | 0.68 | 3.2 | 3.2 | 3 | CRATERED | 1051 | | 4003-C | 06/21/90 | |
| | 4 | 0.13 | 0.08 | 2219-T87 | 6061-T6 | YES | 3.75 | | 1100-O | 45 | 0.31 | 3.2 | Y | 0.5 | N | 0.71 | 3.2 | 3.2 | 3 | CRATERED | 1042 | | 4001-A | 06/13/90 | |
| | 4 | 0.13 | 0.08 | 2219-T87 | 6061-T6 | YES | 3.75 | | 1100-O | 45 | 0.31 | 3.4 | Y | 0.7 | N | 0.7 | 3.4 | 3.4 | 3 | F CRATER | 1048 | | 4003-A | 06/19/90 | FRONT RICOCHET PLATE CRATERED. |
| | 4 | 0.13 | 0.08 | 2219-T87 | 6061-T6 | YES | 3.75 | | 1100-O | 45 | 0.31 | 3.9 | Y | 0.6 | N | 0.73 | 3.9 | 3.9 | 2 | CRATERED | 1071 | | 4111-B | 07/18/90 | RICO PLATE CRATERS UP TO 0.1" DIA X 0.03" DEEP |
| | 4 | 0.13 | 0.08 | 2219-T87 | 6061-T6 | YES | 3.75 | | 1100-O | 45 | 0.31 | 4.3 | Y | 0.9 | N | 0.76 | 4.3 | 4.2 | 2 | CRATERS | 1040 | | 4001-B | 06/12/90 | LEFT RICOCHET PANEL CRATERED OVERALL ABOVE BUMPER. |
| | 4 | 0.13 | 0.08 | 2219-T87 | 6061-T6 | YES | 3.75 | | 1100-O | 45 | 0.31 | 6 | Y | 0.6 | Y | 0.83 | | 6 | 3 | CRATERED | 1072 | | 4111-C | 07/19/90 | RICO PLATE CRATERS UP TO 0.11" DIA X 0.05" DEEP. WALL SPALL AROUND HOLE 0.07" WIDE |
| | 4 | 0.13 | 0.08 | 2219-T87 | 6061-T6 | YES | 3.75 | | 1100-O | 45 | 0.31 | 6.1 | Y | 0.8 | N | 0.85 | 6.1 | 6.1 | 2 | CRATERED | 1041 | | 4001-C | 06/12/90 | L&R RICOCHET PANELS CRATERED OVERALL |
| | 4 | 0.13 | 0.08 | 2219-T87 | 6061-T6 | YES | 3.75 | | 1100-O | 45 | 0.31 | 6.2 | Y | 0.6 | N | 0.79 | 6.2 | 6.3 | 1 | CRATERED | 1050 | | 4003-D | 06/20/90 | 2 HOLES IN WALL: 0.6X0.3, 0.21D |
| | 4 | 0.13 | 0.08 | 2219-T87 | 6061-T6 | YES | 3.75 | | 1100-O | 45 | 0.31 | 6.3 | Y | 0.6 | N | 0.79 | 6.3 | 6.3 | 2 | CRATERED | 1049 | | 4003-B | 06/19/90 | 4 HOLES, .57X.35, .5X.3, .25D, .05D |
| | 4 | 0.13 | 0.08 | 2219-T87 | 6061-T6 | YES | 3.75 | | 1100-O | 45 | 0.31 | 6.7 | Y | 0.3 | N | 0.83 | 6.7 | 6.7 | 1 | CRATERED | 1043 | | 4001-D | 06/13/90 | |
| | 4 | 0.13 | 0.08 | 2219-T87 | 6061-T6 | YES | 3.75 | | 1100-O | 45 | 0.31 | 6.8 | Y | 0.2 | N | 0.77 | 6.8 | | 0 | CRATERED | 1073 | | 4111-D | 07/19/90 | RICO PLATE CRATERS UP TO 0.1" DIA X 0.03" DEEP |
| 155 | 4 | 0.13 | 0.08 | 2219-T87 | 6061-T6 | YES | 3.75 | | 1100-O | 60 | 0.19 | 3.3 | N | 0 | N | 0.55 | 3.3 | 3.4 | 0 | CRATERED | 1074 | | 4112-A | 07/20/90 | RICO PLATE CRATERS UP TO 0.11" DIA X 0.04" DEEP |
| | 4 | 0.13 | 0.08 | 2219-T87 | 6061-T6 | YES | 3.75 | | 1100-O | 60 | 0.19 | 4 | N | 0 | N | 0.52 | 4.1 | 4 | 0 | CRATERED | 1075 | | 4112-B | 07/20/90 | ONE RICO CRATER 0.1" DIA X 0.1" DEEP, OTHERS 0.03" DEEP MX |
| | 4 | 0.13 | 0.08 | 2219-T87 | 6061-T6 | YES | 3.75 | | 1100-O | 60 | 0.19 | 5.9 | N | 0 | N | 0.6 | 5.9 | 5.9 | 0 | CRATERED | 1076 | | 4112-C | 07/23/90 | RICO PLATE CRATERS UP TO 0.15" DIA X 0.05" DEEP |
| | 4 | 0.13 | 0.08 | 2219-T87 | 6061-T6 | YES | 3.75 | | 1100-O | 60 | 0.19 | 7.5 | N | 0 | N | 0.69 | 7.5 | 7.5 | 0 | CRATERED | 1077 | | 4112-D | 07/23/90 | RICO PLATE CRATERS UP TO 0.12" DIA X 0.04" DEEP |
| 156 | 4 | 0.13 | 0.08 | 2219-T87 | 6061-T6 | YES | 3.75 | | 1100-O | 60 | 0.25 | 3 | N | 0 | N | 0.65 | | 3 | 0 | CRATERED | 1078 | | 4113-A | 07/24/90 | RICO PLATE CRATERS UP TP 0.13" DIA X 0.08" DEEP |
| | 4 | 0.13 | 0.08 | 2219-T87 | 6061-T6 | YES | 3.75 | | 1100-O | 60 | 0.25 | 3.8 | N | 0 | N | 0.7 | 3.8 | 3.8 | 0 | CRATERED | 1079 | | 4113-B | 07/25/90 | |
| | 4 | 0.13 | 0.08 | 2219-T87 | 6061-T6 | YES | 3.75 | | 1100-O | 60 | 0.25 | 6.3 | Y | 0.1 | N | 0.78 | 6.3 | 6.3 | 0 | CRATERED | 1080 | | 4113-C | 07/25/90 | |
| | 4 | 0.13 | 0.08 | 2219-T87 | 6061-T6 | YES | 3.75 | | 1100-O | 60 | 0.25 | 7.1 | N | 0 | N | 0.78 | 7.1 | 7.1 | 0 | CRATERED | 1082 | | 4113-D | 07/26/90 | |
| 157 | 4 | 0.13 | 0.08 | 2219-T87 | 6061-T6 | YES | 3.75 | | 1100-O | 60 | 0.31 | 3.1 | N | 0 | N | 0.83 | 3.1 | 3.2 | 0 | CRATERED | 1083 | | 4114-A | 07/27/90 | |
| | 4 | 0.13 | 0.08 | 2219-T87 | 6061-T6 | YES | 3.75 | | 1100-O | 60 | 0.31 | 4 | N | 0 | N | 1 | 4 | | 0 | CRATERED | 1084 | | 4114-B | 07/27/90 | |
| | 4 | 0.13 | 0.08 | 2219-T87 | 6061-T6 | YES | 3.75 | | 1100-O | 60 | 0.31 | 5.9 | Y | 0 | N | 0.97 | 5.9 | 5.9 | 0 | CRATERED | 1085 | | 4114-C | 08/02/90 | |
| | 4 | 0.13 | 0.08 | 2219-T87 | 6061-T6 | YES | 3.75 | | 1100-O | 60 | 0.31 | 7.4 | Y | 0.1 | Y | 0.71 | 7.4 | 7.4 | 0 | CRATERED | 1086 | | 4114-D | 08/02/90 | |
| 158 | 4 | 0.13 | 0.08 | 2219-T87 | 6061-T6 | YES | 3.75 | | 1100-O | 75 | 0.19 | 3.1 | N | 0 | N | 0.63 | 3.1 | 3.2 | 0 | CRATERED | 1089 | | 4115-A | 08/06/90 | |
| | 4 | 0.13 | 0.08 | 2219-T87 | 6061-T6 | YES | 3.75 | | 1100-O | 75 | 0.19 | 4.1 | N | 0 | N | 0.35 | 4.1 | 4.1 | 0 | CRATERED | 1088 | | 4115-B | 08/03/90 | |
| | 4 | 0.13 | 0.08 | 2219-T87 | 6061-T6 | YES | 3.75 | | 1100-O | 75 | 0.19 | 6.1 | N | 0 | N | 0.47 | 6.1 | 6.1 | 0 | CRATERED | 1090 | | 4115-C | 08/07/90 | |
| | 4 | 0.13 | 0.08 | 2219-T87 | 6061-T6 | YES | 3.75 | | 1100-O | 75 | 0.19 | 7.3 | N | 0 | N | 0.51 | 7.3 | 7.3 | 0 | CRATERED | 1091 | | 4115-D | 08/07/90 | |
| 159 | 4 | 0.13 | 0.08 | 2219-T87 | 6061-T6 | YES | 3.75 | | 1100-O | 75 | 0.25 | 2.9 | N | 0 | N | 0.63 | 2.9 | 2.9 | 0 | CRATERED | 1092 | | 4116-A | 08/08/90 | |
| | 4 | 0.13 | 0.08 | 2219-T87 | 6061-T6 | YES | 3.75 | | 1100-O | 75 | 0.25 | 4.5 | N | 0 | N | 0.84 | 4.5 | 4.5 | 0 | CRATERED | 1093 | | 4116-B | 08/09/90 | |

| | standoff inch | rearwall gage inch | bumper gage inch | rearwall alloy | bumper alloy | mli present | mli location | prj. lan to dia | prj. material | obliquity | projectile size | velocity avg km/s | rear penetr'n | rearhole inch | rearwall spall | bumper hole inch | vel hall km/s | vel xray km/s | witness penet. | rico con | test number | data source | test | date | comments |
|---|---|---|---|---|---|---|---|---|---|---|---|---|---|---|---|---|---|---|---|---|---|---|---|---|---|
| | 4 | 0.13 | 0.08 | 2219-T87 | 6061-T6 | YES | 3.75 | | 1100-O | 75 | 0.25 | 6.2 | N | 0 | N | 0.96 | 6.2 | 6.2 | 0 | CRATERED | 1094 | | 4116-C | 08/14/90 | |
| | 4 | 0.13 | 0.08 | 2219-T87 | 6061-T6 | YES | 3.75 | | 1100-O | 75 | 0.25 | 7.4 | N | 0 | N | 0.72 | 7.4 | 7.3 | 0 | CRATERED | 1095 | | 4116-D | 08/15/90 | |
| 160 | 4 | 0.13 | 0.08 | 2219-T87 | 6061-T6 | YES | 3.75 | | 1100-O | 75 | 0.31 | 3.1 | N | 0 | N | 0.91 | 3.1 | 3.1 | 0 | CRATERED | 1096 | | 4117-A | 08/15/90 | |
| | 4 | 0.13 | 0.08 | 2219-T87 | 6061-T6 | YES | 3.75 | | 1100-O | 75 | 0.31 | 3.2 | N | 0 | N | 1.48 | 3.2 | 3.2 | 0 | CRATERED | 1052 | | 4004-A | 06/22/90 | |
| | 4 | 0.13 | 0.08 | 2219-T87 | 6061-T6 | YES | 3.75 | | 1100-O | 75 | 0.31 | 3.2 | N | 0 | N | 1.01 | 3.2 | 3.2 | 0 | F HOLED | 1046 | | 4002-A | 06/15/90 | SIDE RICOCHET PLATES SPRAYED W/PARTICLES |
| | 4 | 0.13 | 0.08 | 2219-T87 | 6061-T6 | YES | 3.75 | | 1100-O | 75 | 0.31 | 4 | N | 0 | N | 1.06 | 4 | 4 | 0 | CRATERED | 1044 | | 4002-B | 06/14/90 | |
| | 4 | 0.13 | 0.08 | 2219-T87 | 6061-T6 | YES | 3.75 | | 1100-O | 75 | 0.31 | 4.1 | Y | 0.4 | N | 1.1 | 4.1 | 4.1 | 0 | CRATERED | 1097 | | 4117-B | 08/24/90 | |
| | 4 | 0.13 | 0.08 | 2219-T87 | 6061-T6 | YES | 3.75 | | 1100-O | 75 | 0.31 | 6 | N | 0 | N | 1.24 | 6 | 6 | 0 | CRATERED | 1098 | | 4117-C | 08/24/90 | |
| | 4 | 0.13 | 0.08 | 2219-T87 | 6061-T6 | YES | 3.75 | | 1100-O | 75 | 0.31 | 6.1 | Y | 0.1 | N | 1.33 | 6.1 | 6.1 | 0 | CRATERED | 1053 | | 4004-B | 06/25/90 | |
| | 4 | 0.13 | 0.08 | 2219-T87 | 6061-T6 | YES | 3.75 | | 1100-O | 75 | 0.31 | 6.2 | C | 0 | N | 1.25 | 6.2 | 6.2 | 0 | HOLE | 1054 | | 4004-C | 06/26/90 | COUNT REAR SURFACE CRACK AS FAILURE |
| | 4 | 0.13 | 0.08 | 2219-T87 | 6061-T6 | YES | 3.75 | | 1100-O | 75 | 0.31 | 6.3 | Y | 0.2 | N | 1.35 | 6.3 | 6.3 | 0 | F HOLED | 1045 | | 4002-C | 06/14/90 | SIDE RICOCHET PLATES SPRAYED W/PARTICLES, FRONT HOLED |
| | 4 | 0.13 | 0.08 | 2219-T87 | 6061-T6 | YES | 3.75 | | 1100-O | 75 | 0.31 | 6.4 | N | 0 | N | 1.21 | 6.4 | 6.3 | 0 | HOLE .1D | 1056 | | 4002-E | 07/02/90 | |
| | 4 | 0.13 | 0.08 | 2219-T87 | 6061-T6 | YES | 3.75 | | 1100-O | 75 | 0.31 | 7.1 | N | 0 | N | 1.44 | 7.2 | 7 | 0 | CRATERED | 1103 | | 4117-D | 09/04/90 | |
| 161 | 4 | 0.13 | 0.08 | 2219-T87 | 6061-T6 | YES | B | | 1100-O | 0 | 0.25 | 3.9 | Y | 0.1 | N | 0.5 | 3.9 | 3.8 | 0 | | 1005 | | 3301-A | 05/02/90 | |
| | 4 | 0.13 | 0.08 | 2219-T87 | 6061-T6 | YES | B | | 1100-O | 0 | 0.25 | 4.3 | Y | 0.4 | N | 0.49 | | 4.3 | 3 | | 1006 | | 3301-B | 05/02/90 | |
| | 4 | 0.13 | 0.08 | 2219-T87 | 6061-T6 | YES | B | | 1100-O | 0 | 0.25 | 5.5 | N | 0 | N | 0.59 | 5.5 | 5.5 | 0 | | 1008 | | 3301-D | 05/04/90 | |
| | 4 | 0.13 | 0.08 | 2219-T87 | 6061-T6 | YES | B | | 1100-O | 0 | 0.25 | 6.3 | N | 0 | N | 0.55 | 6.3 | 6.3 | 0 | | 1007 | | 3301-C | 05/03/90 | |
| 162 | 4 | 0.13 | 0.08 | 2219-T87 | 6061-T6 | YES | B | | 1100-O | 0 | 0.31 | 6.2 | Y | 0.3 | N | 0.7 | 6.2 | 6.2 | 1 | | 1010 | | 3302-A | 05/07/90 | |
| | 4 | 0.13 | 0.08 | 2219-T87 | 6061-T6 | YES | B | | 1100-O | 0 | 0.31 | 6.4 | Y | 1 | N | 0.66 | 6.4 | 6.4 | 1 | | 1011 | | 3302-B | 05/07/90 | |
| | 4 | 0.13 | 0.08 | 2219-T87 | 6061-T6 | YES | B | | 1100-O | 0 | 0.31 | 6.7 | Y | 0.6 | N | 0.73 | 6.7 | 6.6 | 0 | | 1012 | | 3302-C | 05/08/90 | |
| 163 | 4 | 0.13 | 0.08 | 2219-T87 | 6061-T6 | YES | W | | 1100-O | 0 | 0.25 | 3.4 | N | 0 | N | 0.47 | | 3.4 | | | 853 | | 3033-B | 11/02/89 | NO HOLE, DAMAGE AREA APPROX. 3.5" DIA WITH SINK AREA APPROX 1.5" DIA AND .15" DEEP, CRATERS IN SINK AREA UP TO .15" DIA X .06" DEEP, WITH SEVERAL DIMPLES ON REAR. |
| | 4 | 0.13 | 0.08 | 2219-T87 | 6061-T6 | YES | W | | 1100-O | 0 | 0.25 | 3.8 | N | 0 | N | 0.47 | 3.9 | 3.8 | | | 852 | | 3033-A | 11/01/89 | NO HOLE, MOST OF CRATERS OVER AND AREA APPROX. 2" DIA. FEW SMALL CRATERS OVER A 4" DIA AREA. FEW OF THE CRATERS IN THE CENTER ARE UP TO .2" DIA AND .1" DEEP. ONE CRATER HAS A DIMPLE ON REAR WITH A CRACK IN METAL. SEVERAL SMAL DIMPLES ON REAR. |
| | 4 | 0.13 | 0.08 | 2219-T87 | 6061-T6 | YES | W | | 1100-O | 0 | 0.25 | 5.6 | C | 0 | N | 0.56 | 5.6 | 5.6 | | | 869 | | 3033-C | 11/13/89 | NO HOLE, ONE CRATER .226" DIA X .06" DEEP, DIMPLE ON REAR WITH CRACK IN METAL. VERY SMALL CRATERS OVER AN AREA OF 4" DIA. COUNT CRACK AS FAILURE |
| 164 | 4 | 0.13 | 0.08 | 2219-T87 | 6061-T6 | YES | W | | 1100-O | 0 | 0.3 | 3.8 | Y | 0.2 | N | 0.57 | | 3.8 | 0 | | 141 | MARTIN | SS-102D | 01/24/86 | |
| | 4 | 0.13 | 0.08 | 2219-T87 | 6061-T6 | YES | W | | 1100-O | 0 | 0.3 | 4.7 | C | 0 | N | 0.61 | | 4.7 | 0 | | 140 | MARTIN | SS-102C | 01/23/86 | COUNT REAR SURFACE CRACK AS FAILURE |
| | 4 | 0.13 | 0.08 | 2219-T87 | 6061-T6 | YES | W | | 1100-O | 0 | 0.3 | 5.4 | N | 0 | N | 0.67 | | 5.4 | 0 | | 138 | MARTIN | SS-102A | 01/22/86 | |
| | 4 | 0.13 | 0.08 | 2219-T87 | 6061-T6 | YES | W | | 1100-O | 0 | 0.3 | 6 | N | 0 | N | 0.65 | | 6 | 0 | | 139 | MARTIN | SS-102B | 01/23/86 | |

| | standoff inch | rearwall gage inch | bumper gage inch | rearwall alloy | bumper alloy | mil present | mil location | prj. lan to dia | prj. material | obliquity | projectile size | velocity avg km/s | rear penetr'n | rearhole inch | rearwall spall | bumper hole inch | vel hail km/s | vel xray km/s | witness panel. | rico con | test number | data source | test | date | comments |
|---|---|---|---|---|---|---|---|---|---|---|---|---|---|---|---|---|---|---|---|---|---|---|---|---|---|
| 165 | 4 | 0.13 | 0.08 | 2219-T87 | 6061-T6 | YES | W | | 1100-O | 0 | 0.31 | 3.7 | Y | 0.3 | N | 0.57 | | 3.7 | 0 | | 855 | | 3034-B | 11/03/89 | HOLE APPROX. .25" DIA WITH CRACK IN METAL APPROX. 1.3" LEFT, 1.5" RIGHT, .5" UP, AND .5" DOWN. CRATERS OVER SINK AREA APPROX. 4" DIA. SINK APPROX. .45" DEEP. CRATERS UP TO .15" DIA X .07" DEEP. |
| | 4 | 0.13 | 0.08 | 2219-T87 | 6061-T6 | YES | W | | 1100-O | 0 | 0.31 | 4.5 | Y | 0.5 | N | 0.62 | 4.5 | 4.4 | 0 | | 854 | | 3034-A | 11/02/89 | HOLE APPROX .5" X .15" WITH METAL CRACK APPROX. 1.5" LEFT, 1.4" RIGHT, AND .6" UP. SINK APPROX. 4" DIA WITH APPROX 2: DIA COVERED WITH CRATERS UP TO .13" DIA AND .5" DEEP. |
| | 4 | 0.13 | 0.08 | 2219-T87 | 6061-T6 | YES | W | | 1100-O | 0 | 0.31 | 5.6 | Y | 5.5 | N | 0.66 | 5.6 | 5.6 | 0 | | 856 | | 3034-C | 11/03/89 | PANEL SPLIT, CRACK 3" LONG LEFT, 2.5" LONG RIGHT, AND 2.3" LONG DOWN, SINK AREA APPROX. 5" DIA X .8" DEEP. MANY SMALL CRATER IN CENTER OF SINK COVERING APPROX. 3" DIA. METAL SEPARATED APPROX. .3" AT CENTER. |
| 166 | 4 | 0.13 | 0.08 | 2219-T87 | 6061-T6 | YES | W | | 1100-O | 45 | 0.19 | 5.3 | Y | 0.2 | N | 0.53 | 5.3 | 5.3 | 0 | | 863 | | 3035-A | 11/08/89 | HOLE .215" DIA IN PROJ PATH, VERY LITTLE OTHER DAMAGE IN PROJ PATH. FEW CRATERS UNDER BUMPER HOLE, 4 SMALL DIMPLES ON REAR. |
| | 4 | 0.13 | 0.08 | 2219-T87 | 6061-T6 | YES | W | | 1100-O | 45 | 0.19 | 5.9 | C | 0 | N | 0.57 | | 5.9 | | | 864 | | 3035-B | 11/08/89 | NO HOLE, ONE CRATER UNDER BUMPER HOLE .15" DIA X .14" DEEP WITH A CRACK IN THE DIMPLE ON REAR (COUNT CRACK AS FAILURE). FEW SMALL CRATERS UNDER BUMPER HOLE. FEW SMALL CRATER IN PROJ PATH WITH VERY SLIGHT DIMPLES ON REAR. |
| 167 | 4 | 0.13 | 0.08 | 2219-T87 | 6061-T6 | YES | W | | 1100-O | 45 | 0.25 | 5.6 | Y | 0.3 | N | 0.66 | 5.5 | 5.6 | 1 | | 857 | | 3036-A | 11/06/89 | 2 HOLES IN PROJ PATH, ONE PIN HOLE IN CRATER APPROX. .170" DIA. ONE HOLE APPROX .346" X .265", FEW CRATER OVER AREA APPROX. 2" DIA AND UP TO .12" DIA AND .06" DEEP. FEW CRATERS UNDER BUMPER HOLE OVER AREA APPROX. 2" HORZ X 4" VERT., ONE DIMPLE ON BACK A |
| | 4 | 0.13 | 0.08 | 2219-T87 | 6061-T6 | YES | W | | 1100-O | 45 | 0.25 | 6.4 | N | 0 | N | 0.75 | 6.4 | 6.4 | | | 858 | | 3036-B | 11/06/89 | NO HOLE, FEW CRATERS IN PROJECTIL PATH AND UNDER BUMPER HOLE. SLIGHTLY DEEPER CRATERS IN PROJ PATH. CRATERS IN PROJ PATH UP TO .15" DIA AND .05" DEEP. |
| 168 | 4 | 0.13 | 0.08 | 2219-T87 | 6061-T6 | YES | W | | 1100-O | 45 | 0.31 | 3 | Y | 0.4 | N | 0.7 | 3 | 3.1 | 2 | CAVITIES | 526 | MSFC | SS-321 | 04/28/87 | |
| | 4 | 0.13 | 0.08 | 2219-T87 | 6061-T6 | YES | W | | 1100-O | 45 | 0.31 | 4.3 | Y | 0.4 | N | 0.76 | 4.2 | 4.3 | 3 | CAVITIES | 529 | MSFC | SS-326 | 05/01/87 | |
| | 4 | 0.13 | 0.08 | 2219-T87 | 6061-T6 | YES | W | | 1100-O | 45 | 0.31 | 6.5 | Y | 0.4 | N | 0.83 | 6.5 | 6.6 | 0 | CAVITIES | 464 | MSFC | SS-001B | 02/10/87 | |
| | 4 | 0.13 | 0.08 | 2219-T87 | 6061-T6 | YES | W | | 1100-O | 45 | 0.31 | 7.1 | Y | 0.1 | N | 0.86 | 7.1 | 7.1 | 0 | | 861 | | 3037-A | 11/07/89 | HOLE APPROX. .08" DIA IN PROJ PATH, DAMAGE AREA APPROX. 2" DIA WITH A FEW CRATERS UP TO .15" DIA X .06" DEEP. FEW VERY SMALL CRATERS UNDER BUMPER HOLE. |
| 169 | 4 | 0.13 | 0.08 | 2219-T87 | 6061-T6 | YES | W | | 1100-O | 65 | 0.19 | 5.1 | N | 0 | N | 0.69 | 5 | 5.1 | | | 870 | | 3038-A | 11/13/89 | NO HOLE, FEW CRATERS UNDER BUMPER HOLE, ONE CRATER .15" DIA X .05" DEEP. DAMAGE IN PROJ PATH. |
| | 4 | 0.13 | 0.08 | 2219-T87 | 6061-T6 | YES | W | | 1100-O | 65 | 0.19 | 6.4 | N | 0 | N | 0.7 | 6.4 | 6.4 | | | 871 | | 3038-B | 11/14/89 | NO HOLE, SLIGHT DAMAGE UNDER BUMPER HOLE, NO DAMAGE IN PROJ PATH, FEW CRATERS UNDER BUMPER HOLE UP TO .156" DIA AND .03" DEEP. FEW VERY SMALL SIMPLES ON REAR. |

| | standoff inch | rearwall gage inch | bumper gage inch | rearwall alloy | bumper alloy | mli present | mli location | prj. len to dia | prj. material | obliquity | projectile size | velocity avg km/s | rear penetr'n | rearhole inch | rearwall spall | bumper hole inch | vel hall km/s | vel xray km/s | witness penet. | rico con | test number | data source | test | date | comments |
|---|---|---|---|---|---|---|---|---|---|---|---|---|---|---|---|---|---|---|---|---|---|---|---|---|---|
| 170 | 4 | 0.13 | 0.08 | 2219-T87 | 6061-T6 | YES | W | | 1100-O | 65 | 0.25 | 4.6 | N | 0 | N | 0.73 | 4.5 | 4.6 | | | 867 | | 3039-B | 11/10/89 | NO HOLE, FEW CRATERS, ONE CRATER .170" DIA AND .09" DEEP. 5 OTHER CRATERS UP TO .2" DIA AND .04" DEEP. ALL DAMAGE UNDER BUMPER HOLE. FEW DIMPLES ON REAR. |
| | 4 | 0.13 | 0.08 | 2219-T87 | 6061-T6 | YES | W | | 1100-O | 65 | 0.25 | 5.7 | Y | 0.1 | N | 0.82 | 5.7 | 5.6 | 0 | | 866 | | 3039-A | 11/10/89 | HOLE .090" UNDER BUMPER HOLE SEVERAL CRATER UP TO .075" DIA X .050" DEEP, FEW SMALL DIMPLES ON REAR. |
| | 4 | 0.13 | 0.08 | 2219-T87 | 6061-T6 | YES | W | | 1100-O | 65 | 0.25 | 6.3 | Y | 0.2 | N | 0.87 | 6.3 | 6.3 | 1 | | 868 | | 3039-C | 11/13/89 | 2 HOLES .192" AND .175" DIA, ALL DAMAGE UNDER BUMPER HOLE, FEW CRATERS UP TO .125" DIA AND .07" DEEP. DAMAGE AREA APPROX. 4" DIA. |
| 171 | 4 | 0.13 | 0.08 | 2219-T87 | 6061-T6 | YES | W | | 1100-O | 65 | 0.31 | 6.3 | N | 0 | N | 0.93 | 6.3 | 6.3 | | | 498 | MSFC | SS-004A | 03/26/87 | |
| | 4 | 0.13 | 0.08 | 2219-T87 | 6061-T6 | YES | W | | 1100-O | 65 | 0.31 | 6.9 | Y | 0.2 | N | 1.87 | 6.9 | 6.9 | 0 | | 865 | | 3040-A | 11/09/89 | 2 HOLES UNDER BUMPER HOLE .140" X .180" AND .115" DIA. DAMAGE AREA APPROX. 4.5" DIA. CRATER UP TO .16" DIA X .1" DEEP, 2 CRATERS WITH SLIGHT CRACK IN DIMPLES ON REAR |
| 172 | 4 | 0.13 | 0.08 | 2219-T87 | 6061-T6 | YES | W | | LEXAN | 0 | 0.5 | 6.3 | Y | 8 | N | 1.02 | 6.3 | | | | 919 | | FLASH-1 | 01/15/90 | 20 LAYERS AL FOIL INSTEAD OF MLI |
| 173 | 4 | 0.13 | 0.13 | 2219-T87 | 2219-T87 | NO | | | 1100-O | 0 | 0.25 | 4.4 | Y | 0.2 | Y | 0.56 | 4.4 | 4.4 | 1 | | 333 | MSFC | SS-139B | 09/24/86 | |
| | 4 | 0.13 | 0.13 | 2219-T87 | 2219-T87 | NO | | | 1100-O | 0 | 0.25 | 5 | N | | Y | 0.61 | 5 | 5.1 | 0 | | 332 | MSFC | SS-139A | 09/24/86 | |
| 174 | 4 | 0.16 | 0.06 | 2219-T87 | 6061-T6 | YES | W | | 1100-O | 45 | 0.25 | 2.9 | N | 0 | N | 0.54 | 3 | 2.9 | 0 | CAVITIES | 595 | MSFC | SS-301 | 07/23/87 | |
| 175 | 4 | 0.16 | 0.06 | 2219-T87 | 6061-T6 | YES | | | 1100-O | 45 | 0.31 | 4.4 | N | | N | 0.71 | 4.3 | 4.5 | 0 | CAVITIES | 605 | MSFC | SS-303B | 07/31/87 | |
| | 4 | 0.16 | 0.06 | 2219-T87 | 6061-T6 | YES | | | 1100-O | 45 | 0.31 | 4.7 | N | | N | 0.73 | 4.6 | 4.7 | 0 | CAVITIES | 592 | MSFC | SS-303 | 07/22/87 | |
| 176 | 4 | 0.16 | 0.06 | 2219-T87 | 6061-T6 | YES | | | 1100-O | 45 | 0.38 | 6.4 | Y | 2.1 | N | 0.89 | 6.3 | 6.5 | 2 | 3HOLES | 596 | MSFC | SS-306 | 07/24/87 | |
| 177 | 4 | 0.19 | 0.03 | 2219-T87 | 6061-T6 | NO | | | 1100-O | 0 | 0.25 | 6.6 | Y | 0.1 | Y | 0.44 | 6.5 | 6.7 | 1 | | 500 | IWALL | SS-228D | 03/30/87 | |
| | 4 | 0.19 | 0.03 | 2219-T87 | 6061-T6 | NO | | | 1100-O | 0 | 0.25 | 7 | Y | 0.1 | Y | 0.45 | 6.9 | 7 | 2 | | 499 | IWALL | SS-228C | 03/27/87 | |
| 178 | 4 | 0.19 | 0.04 | 2219-T87 | 6061-T6 | NO | | | 1100-O | 0 | 0.25 | 4.5 | Y | 0.1 | Y | 0.41 | 4.5 | 4.6 | 0 | | 316 | IWALL | SS-214D | 09/05/86 | |
| | 4 | 0.19 | 0.04 | 2219-T87 | 6061-T6 | NO | | | 1100-O | 0 | 0.25 | 4.8 | Y | 0.1 | Y | 0.41 | 4.7 | 4.8 | 0 | | 313 | IWALL | SS-214C | 09/04/86 | |
| | 4 | 0.19 | 0.04 | 2219-T87 | 6061-T6 | NO | | | 1100-O | 0 | 0.25 | 5.6 | N | | Y | 0.42 | 5.6 | 5.7 | 0 | | 311 | IWALL | SS-214A | 09/03/86 | |
| 179 | 4 | 0.19 | 0.04 | 2219-T87 | 6061-T6 | NO | | | 1100-O | 15 | 0.25 | 4.9 | Y | 0.3 | | 0.4 | 4.9 | 5 | 1 | | 312 | IWALL | SS-214B | 09/03/86 | |
| 180 | 4 | 0.19 | 0.04 | 2219-T87 | 6061-T6 | NO | | | 1100-O | 45 | 0.25 | 6.1 | Y | 0.3 | N | 0.63 | | 6.1 | 1 | CAVITIES | 441 | IWALL | SS-217C | 01/21/87 | |
| | 4 | 0.19 | 0.04 | 2219-T87 | 6061-T6 | NO | | | 1100-O | 45 | 0.25 | 6.5 | Y | 0.2 | Y | 0.58 | | 6.5 | 1 | CAVITIES | 442 | IWALL | SS-217D | 01/22/87 | |
| | 4 | 0.19 | 0.04 | 2219-T87 | 6061-T6 | NO | | | 1100-O | 45 | 0.25 | 7.1 | Y | 0.5 | Y | 0.58 | | 7.1 | 2 | CAVITIES | 443 | IWALL | SS-217E | 01/23/87 | |
| 181 | 4 | 0.19 | 0.04 | 2219-T87 | 6061-T6 | NO | | | 1100-O | 45 | 0.31 | 6.6 | Y | 1 | N | 0.75 | 6.5 | 6.7 | 4 | CAVITIES | 329 | IWALL | SS-217A | 09/22/86 | |
| | 4 | 0.19 | 0.04 | 2219-T87 | 6061-T6 | NO | | | 1100-O | 45 | 0.31 | 7.1 | Y | 1.1 | N | 0.72 | | 7.1 | 4 | CAVITIES | 331 | IWALL | SS-217B | 09/23/86 | |
| 182 | 4 | 0.19 | 0.04 | 2219-T87 | 6061-T6 | YES | | | 1100-O | 0 | 0.35 | 4.6 | Y | 0.5 | N | 0.49 | 4.6 | 4.7 | 3 | | 314 | IWALL | SS-215A | 09/04/86 | |
| | 4 | 0.19 | 0.04 | 2219-T87 | 6061-T6 | YES | | | 1100-O | 0 | 0.35 | 5.5 | Y | 0.4 | N | 0.52 | | 5.5 | 1 | | 315 | IWALL | SS-215B | 09/05/86 | |
| | 4 | 0.19 | 0.04 | 2219-T87 | 6061-T6 | YES | | | 1100-O | 0 | 0.35 | 6.1 | Y | 0.3 | N | 0.53 | 6.1 | 6.2 | 1 | | 325 | IWALL | SS-215D | 09/16/86 | |
| | 4 | 0.19 | 0.04 | 2219-T87 | 6061-T6 | YES | | | 1100-O | 0 | 0.35 | 6.2 | N | | N | 0.54 | 6.1 | 6.3 | 0 | | 324 | IWALL | SS-215C | 09/16/86 | |

| | standoff inch | rearwall gage inch | bumper gage inch | rearwall alloy | bumper alloy | mil present | mil location | prj. lan to dia | prj. material | obliquity | projectile size | velocity avg km/s | rear penetr'n | rearhole inch | rearwall spall | bumper hole inch | vel hall km/s | vel xray km/s | witness penet. | rico con | test number | data source | test | date | comments |
|---|---|---|---|---|---|---|---|---|---|---|---|---|---|---|---|---|---|---|---|---|---|---|---|---|---|
| 183 | 4 | 0.19 | 0.04 | 2219-T87 | 6061-T6 | YES | | | 1100-O | 45 | 0.35 | 5.8 | Y | 0.7 | N | 0.58 | 5.7 | 5.8 | 4 | | 326 | IWALL | SS-218A | 09/19/86 | |
| | 4 | 0.19 | 0.04 | 2219-T87 | 6061-T6 | YES | | | 1100-O | 45 | 0.35 | 6.3 | Y | 0.7 | N | 0.8 | 6.2 | 6.4 | 4 | HOLES | 327 | IWALL | SS-218B | 09/19/86 | |
| | 4 | 0.19 | 0.04 | 2219-T87 | 6061-T6 | YES | | | 1100-O | 45 | 0.35 | 6.8 | Y | 1.2 | N | 0.84 | 6.8 | 6.9 | 4 | CAVITIES | 328 | IWALL | SS-218C | 09/22/86 | |
| 184 | 4 | 0.19 | 0.08 | 2219-T87 | 6061-T6 | NO | | | 1100-O | 0 | 0.25 | 4.4 | Y | 0.2 | Y | 0.49 | | 4.4 | 1 | | 439 | IWALL | SS-213C | 01/16/87 | |
| | 4 | 0.19 | 0.08 | 2219-T87 | 6061-T6 | NO | | | 1100-O | 0 | 0.25 | 5.1 | N | | Y | 0.54 | | 5.1 | 0 | | 440 | IWALL | SS-213D | 01/20/87 | |
| 185 | 4 | 0.19 | 0.08 | 2219-T87 | 6061-T6 | NO | | | 1100-O | 0 | 0.31 | 4.9 | Y | 0.3 | Y | 0.62 | 5 | 4.9 | 3 | | 334 | IWALL | SS-213A | 09/25/86 | |
| | 4 | 0.19 | 0.08 | 2219-T87 | 6061-T6 | NO | | | 1100-O | 0 | 0.31 | 5.8 | Y | 0.4 | Y | 0.65 | 5.7 | 5.9 | 0 | | 335 | IWALL | SS-213B | 09/25/86 | |
| 186 | 4 | 0.19 | 0.08 | 2219-T87 | 6061-T6 | NO | | | 1100-O | 45 | 0.31 | 6.9 | Y | 0.3 | Y | 0.84 | 6.9 | 7 | 1 | CAVITIES | 465 | IWALL | SS-216C | 02/11/87 | |
| 187 | 4 | 0.19 | 0.08 | 2219-T87 | 6061-T6 | NO | | | 1100-O | 45 | 0.35 | 6 | Y | 1.3 | N | 0.89 | 5.9 | 6.1 | 4 | | 317 | IWALL | SS-216A | 09/08/86 | |
| | 4 | 0.19 | 0.08 | 2219-T87 | 6061-T6 | NO | | | 1100-O | 45 | 0.35 | 6.5 | Y | 1.6 | N | 0.9 | 6.5 | 6.6 | 4 | CAVITIES | 318 | IWALL | SS-216B | 09/08/86 | |
| 188 | 4 | 0.19 | 0.08 | 2219-T87 | 6061-T6 | YES | | | 1100-O | 0 | 0.31 | 3.1 | Y | 0.5 | Y | 0.51 | | 3.1 | 2 | | 421 | IWALL | SS-229B | 12/19/86 | |
| | 4 | 0.19 | 0.08 | 2219-T87 | 6061-T6 | YES | | | 1100-O | 0 | 0.31 | 3.6 | Y | 0.3 | Y | 0.55 | | 3.6 | 0 | | 422 | IWALL | SS-229C | 12/19/86 | |
| | 4 | 0.19 | 0.08 | 2219-T87 | 6061-T6 | YES | | | 1100-O | 0 | 0.31 | 5.3 | N | | N | 0.63 | | 5.3 | 0 | | 420 | IWALL | SS-229A | 12/18/86 | |
| 189 | 4 | 0.19 | 0.08 | GR/E | 6061-T6 | YES | W | | 1100-O | 0 | 0.31 | 3.8 | Y | 1.2 | | 0.56 | 3.7 | 3.8 | 0 | | 1039 | | CRW-4 | 06/08/90 | 1.2 DIA HOLE, 1-4 FRONT PLIES, 4 REAR PLIES DAMAGED |
| | 4 | 0.19 | 0.08 | GR/E | 6061-T6 | YES | W | | 1100-O | 0 | 0.31 | 4.7 | Y | 1.5 | N | 0.61 | 4.7 | 4.7 | 0 | | 1038 | | CRW-3 | 06/07/90 | HOLE .7X1.5 |
| | 4 | 0.19 | 0.08 | GR/E | 6061-T6 | YES | W | | 1100-O | 0 | 0.31 | 5.4 | Y | 2 | | 0.67 | 5.4 | 5.4 | 0 | | 1037 | | CRW-2 | 06/04/90 | HOLE .5X2, 1-3 TOP PLIES DAMAGED, 4-5 REAR PLIES DAMAGED |
| | 4 | 0.19 | 0.08 | GR/E | 6061-T6 | YES | W | | 1100-O | 0 | 0.31 | 5.7 | N | 0 | | 0.66 | 5.7 | 5.7 | | | 1036 | | CRW-1 | 06/01/90 | FRONT: 3 PLIES DAMAGED |
| 190 | 4 | 0.2 | 0.08 | 2219-T87 | 6061-T6 | NO | | | 1100-O | 0 | 0.35 | 6.7 | Y | 0.4 | Y | 0.73 | | 6.7 | 4 | | 156 | MARTIN | SS-107A | 02/20/86 | |
| 191 | 4 | 0.23 | 0.08 | 2219-T87 | 6061-T6 | NO | | | 1100-O | 0 | 0.35 | 6.8 | Y | 0.4 | Y | 0.73 | | 6.8 | 2 | | 162 | MARTIN | SS-107B | 02/28/86 | |
| 192 | 4 | 0.25 | 0.13 | 2219-T87 | 2219-T87 | NO | | | 1100-O | 0 | 0.25 | 4 | Y | 0.1 | Y | 0.53 | | 4 | 1 | | 369 | MARTIN | SS-144C | 10/23/86 | |
| | 4 | 0.25 | 0.13 | 2219-T87 | 2219-T87 | NO | | | 1100-O | 0 | 0.25 | 4.5 | Y | 0.4 | Y | 0.57 | | 4.5 | 1 | | 368 | MARTIN | SS-144B | 10/23/86 | |
| | 4 | 0.25 | 0.13 | 2219-T87 | 2219-T87 | NO | | | 1100-O | 0 | 0.25 | 4.9 | N | | Y | 0.61 | | 4.9 | 0 | | 367 | MARTIN | SS-144A | 10/22/86 | |
| 193 | 5 | 0.13 | 0.08 | 316SS | 6061-T6 | NO | | | 1100-O | 0 | 0.25 | 6.7 | N | 0 | N | 0.57 | 6.6 | 6.7 | | N | 1119 | | DEBRIS-Z1 | 09/18/90 | MOMENTUM SENSOR TEST #1 |
| 194 | 5 | 0.13 | 0.08 | 316SS | 6061-T6 | NO | | | 1100-O | 0 | 0.38 | 6.8 | N | 0 | N | 0.48 | 6.8 | 6.7 | | N | 1120 | | DEBRIS-Z2 | 09/19/90 | MOMENTUM SENSOR TEST #2 |
| 195 | 6 | 0.13 | 0.06 | 2219-T87 | 6061-T6 | NO | | 1 | 6061-T6 | 0 | 0.26 | 7.1 | Y | 3.8 | N | 0.65 | | 7.1 | 3 | | 82 | ADP SM1 | SS-P-018RV | 10/18/85 | |
| 196 | 6 | 0.13 | 0.06 | 2219-T87 | 6061-T6 | NO | | | 1100-O | 0 | 0.13 | 2.9 | N | 0 | N | 0.23 | | 2.9 | 0 | | 67 | ADP SM1 | SS-P-015 | 09/27/85 | |
| | 6 | 0.13 | 0.06 | 2219-T87 | 6061-T6 | NO | | | 1100-O | 0 | 0.13 | 3 | N | 0 | N | 0.23 | | 3 | 0 | | 70 | ADP SM1 | SS-P-015C | 10/02/85 | |

| | standoff inch | rearwall gage inch | bumper gage inch | rearwall alloy | bumper alloy | mli present | mli location | prj. len to dia | prj. material | obliquity | projectile size | velocity avg km/s | rear penetr'n | rearhole inch | rearwall spall | bumper hole inch | vel hall km/s | vel xray km/s | witness penet. | rico con | test number | data source | test | date | comments |
|---|---|---|---|---|---|---|---|---|---|---|---|---|---|---|---|---|---|---|---|---|---|---|---|---|---|
| 197 | 6 | 0.13 | 0.06 | 2219-T87 | 6061-T6 | NO | | | 1100-O | 0 | 0.19 | 3.3 | Y | 0.1 | N | 0.36 | | 3.3 | 0 | | 71 | ADP SM1 | SS-P-014D | 10/03/85 | |
| | 6 | 0.13 | 0.06 | 2219-T87 | 6061-T6 | NO | | | 1100-O | 0 | 0.19 | 3.7 | N | 0 | N | 0.38 | | 3.7 | 0 | | 65 | ADP SM1 | SS-P-014B | 09/25/85 | |
| | 6 | 0.13 | 0.06 | 2219-T87 | 6061-T6 | NO | | | 1100-O | 0 | 0.19 | 3.7 | Y | 0.2 | N | 0.3 | | 3.7 | 1 | | 63 | ADP SM1 | SS-P-014 | 09/23/85 | |
| | 6 | 0.13 | 0.06 | 2219-T87 | 6061-T6 | NO | | | 1100-O | 0 | 0.19 | 3.8 | Y | 0.2 | N | 0.36 | 3.8 | 3.7 | 0 | | 960 | | 2001-A | 03/15/90 | |
| | 6 | 0.13 | 0.06 | 2219-T87 | 6061-T6 | NO | | | 1100-O | 0 | 0.19 | 3.9 | Y | 0.2 | Y | 0.36 | 3.9 | 3.9 | 0 | | 962 | | 2001- | 03/16/90 | |
| | 6 | 0.13 | 0.06 | 2219-T87 | 6061-T6 | NO | | | 1100-O | 0 | 0.19 | 4.1 | S | 0 | Y | 0.36 | 4.1 | 4.1 | | | 961 | | 2001-C | 03/15/90 | COUNT SPALL AS FAILURE |
| | 6 | 0.13 | 0.06 | 2219-T87 | 6061-T6 | NO | | | 1100-O | 0 | 0.19 | 4.2 | Y | 0.2 | N | 0.39 | | 4.2 | 1 | | 64 | ADP SM1 | SS-P-014A | 09/24/85 | |
| 198 | 6 | 0.13 | 0.06 | 2219-T87 | 6061-T6 | NO | | | 1100-O | 0 | 0.25 | 4.8 | Y | 0.2 | Y | 0.35 | | 4.8 | 1 | | 58 | ADP SM1 | SS-P-013 | 09/17/85 | |
| | 6 | 0.13 | 0.06 | 2219-T87 | 6061-T6 | NO | | | 1100-O | 0 | 0.25 | 4.9 | Y | 0.5 | | 0.55 | | 4.9 | | | 59 | | SS-P-13A | 09/17/85 | |
| | 6 | 0.13 | 0.06 | 2219-T87 | 6061-T6 | NO | | | 1100-O | 0 | 0.25 | 5.8 | Y | 0.6 | Y | 0.53 | | 5.8 | 2 | | 61 | ADP SM1 | SS-P-013C | 09/19/85 | |
| | 6 | 0.13 | 0.06 | 2219-T87 | 6061-T6 | NO | | | 1100-O | 0 | 0.25 | 6.1 | Y | 0.2 | Y | 0.5 | 6.1 | 6.1 | 1 | | 929 | | 2002-A | 02/15/90 | |
| | 6 | 0.13 | 0.06 | 2219-T87 | 6061-T6 | NO | | | 1100-O | 0 | 0.25 | 6.2 | S | 0 | Y | 0.63 | | 6.2 | 0 | | 60 | ADP SM1 | SS-P-013B | 09/18/85 | COUNT SPALL AS PENETRATION |
| | 6 | 0.13 | 0.06 | 2219-T87 | 6061-T6 | NO | | | 1100-O | 0 | 0.25 | 6.5 | Y | 0.1 | Y | 0.57 | 6.5 | 6.5 | 0 | | 930 | | 2002-B | 02/15/90 | |
| | 6 | 0.13 | 0.06 | 2219-T87 | 6061-T6 | NO | | | 1100-O | 0 | 0.25 | 6.7 | Y | 0.2 | Y | 0.53 | 6.8 | 6.7 | 1 | | 940 | | 2002-C | 02/22/90 | SPALL AROUND HOLES IN WALL |
| | 6 | 0.13 | 0.06 | 2219-T87 | 6061-T6 | NO | | | 1100-O | 0 | 0.25 | 7.1 | Y | 0.2 | Y | 0.55 | | 7.1 | 0 | | 949 | | 2003-A | 03/05/90 | WALL: 5 HOLES, SPALL AROUND HOLES |
| 199 | 6 | 0.13 | 0.06 | 2219-T87 | 6061-T6 | NO | | | 1100-O | 0 | 0.3 | 6.6 | Y | 0.1 | Y | 0.6 | | 6.6 | 1 | | 89 | ADP SM1 | SS-P-020C | 11/01/85 | |
| | 6 | 0.13 | 0.06 | 2219-T87 | 6061-T6 | NO | | | 1100-O | 0 | 0.3 | 7 | S | 0 | Y | 0.65 | | 7 | 0 | | 88 | ADP SM1 | SS-P-020B | 10/30/85 | COUNT SPALL AS PENETRATION |
| 200 | 6 | 0.13 | 0.06 | 2219-T87 | 6061-T6 | NO | | | 1100-O | 0 | 0.31 | 4.7 | Y | 1.5 | Y | 0.63 | 4.7 | 4.8 | | | 489 | MSFC | SS-T2-20 | 03/06/87 | |
| 201 | 6 | 0.13 | 0.06 | 2219-T87 | 6061-T6 | NO | | | 1100-O | 0 | 0.35 | 6.7 | Y | 2 | Y | 0.66 | | 6.7 | 1 | | 168 | ADP SM1 | SS-P-035 | 03/06/86 | |
| 202 | 6 | 0.13 | 0.06 | 2219-T87 | 6061-T6 | NO | | | 1100-O | 5 | 0.25 | 6 | N | 0 | N | 0.58 | 6 | 6 | | | 959 | | 2003-A1 | 03/14/90 | |
| | 6 | 0.13 | 0.06 | 2219-T87 | 6061-T6 | NO | | | 1100-O | 5 | 0.25 | 6.6 | Y | 0.4 | Y | 0.51 | 6.6 | 6.6 | 1 | | 956 | | 2003-B1 | 03/12/90 | SPALL AROUND HOLES IN WALL |
| | 6 | 0.13 | 0.06 | 2219-T87 | 6061-T6 | NO | | | 1100-O | 5 | 0.25 | 7.1 | Y | 0.4 | Y | 5.56 | 7.1 | 7.1 | 0 | | 944 | | 2003-B | 02/28/90 | SPALL AROUND HOLES IN WALL |
| | 6 | 0.13 | 0.06 | 2219-T87 | 6061-T6 | NO | | | 1100-O | 5 | 0.25 | 7.3 | Y | 1.4 | Y | 0.59 | 7.3 | 7.3 | 1 | | 945 | | 2003-C | 02/28/90 | |
| 203 | 6 | 0.13 | 0.06 | 2219-T87 | 6061-T6 | NO | | | 6061-T6 | 0 | 0.19 | 2.3 | Y | 0.3 | N | 0.3 | | 2.3 | 2 | | 122 | ADP SM1 | SS-P-025B | 12/22/85 | |
| | 6 | 0.13 | 0.06 | 2219-T87 | 6061-T6 | NO | | | 6061-T6 | 0 | 0.19 | 2.6 | N | 0 | N | 0.33 | | 2.6 | 0 | | 104 | ADP SM1 | SS-P-025C | 11/25/85 | |
| | 6 | 0.13 | 0.06 | 2219-T87 | 6061-T6 | NO | | | 6061-T6 | 0 | 0.19 | 3.3 | N | 0 | N | 0.35 | | 3.3 | 0 | | 103 | ADP SM1 | SS-P-025A | 11/22/85 | |
| | 6 | 0.13 | 0.06 | 2219-T87 | 6061-T6 | NO | | | 6061-T6 | 0 | 0.19 | 3.7 | N | 0 | N | 0.37 | | 3.7 | 0 | | 102 | ADP SM1 | SS-P-025 | 11/21/85 | |

| | standoff inch | rearwall gage inch | bumper gage inch | rearwall alloy | bumper alloy | mil present | mil location | pri. len to dia | pri. material | obliquity | projectile size | velocity avg km/s | rear penetr'n | rearhole inch | rearwall spall | bumper hole inch | vel hall km/s | vel xray km/s | witness penet. | rico con | test number | data source | test | date | comments |
|---|---|---|---|---|---|---|---|---|---|---|---|---|---|---|---|---|---|---|---|---|---|---|---|---|---|
| 204 | 6 | 0.13 | 0.06 | 2219-T87 | 6061-T6 | NO | | | 6061-T6 | 0 | 0.25 | 5.8 | Y | 0.1 | N | 0.53 | | 5.8 | 0 | | 97 | ADP SM1 | SS-P-024C | 11/13/85 | |
| | 6 | 0.13 | 0.06 | 2219-T87 | 6061-T6 | NO | | | 6061-T6 | 0 | 0.25 | 5.9 | Y | 0.1 | Y | 0.52 | | 5.9 | 0 | | 100 | ADP SM1 | SS-P-024F | 11/20/85 | |
| | 6 | 0.13 | 0.06 | 2219-T87 | 6061-T6 | NO | | | 6061-T6 | 0 | 0.25 | 6 | Y | 0 | Y | 0.53 | | 6 | | | 98 | | SS-P-24D | 11/14/85 | COUNT SPALL AS PENETRATION |
| 205 | 6 | 0.13 | 0.06 | 2219-T87 | 6061-T6 | NO | | | 6061-T6 | 0 | 0.3 | 5.1 | Y | 1 | Y | 0.54 | | 5.1 | 2 | | 72 | ADP SM1 | SS-P-016 | 10/04/85 | |
| | 6 | 0.13 | 0.06 | 2219-T87 | 6061-T6 | NO | | | 6061-T6 | 0 | 0.3 | 6 | Y | 1 | N | 0.57 | | 6 | 2 | | 73 | | SS-P-016A | 10/04/85 | |
| | 6 | 0.13 | 0.06 | 2219-T87 | 6061-T6 | NO | | | 6061-T6 | 0 | 0.3 | 6.3 | Y | 1 | Y | 0.58 | | 6.3 | 1 | | 74 | ADP SM1 | SS-P-016B | 10/07/85 | |
| | 6 | 0.13 | 0.06 | 2219-T87 | 6061-T6 | NO | | | 6061-T6 | 0 | 0.3 | 6.6 | Y | 0.8 | Y | 0.6 | | 6.6 | 1 | | 75 | ADP SM1 | SS-P-016C | 10/08/85 | |
| | 6 | 0.13 | 0.06 | 2219-T87 | 6061-T6 | NO | | | 6061-T6 | 0 | 0.3 | 6.8 | Y | 1 | Y | 0.62 | | 6.8 | 0 | | 77 | ADP SM1 | SS-P-016E | 10/10/85 | |
| | 6 | 0.13 | 0.06 | 2219-T87 | 6061-T6 | NO | | | 6061-T6 | 0 | 0.3 | 7.2 | Y | 0 | Y | 0.65 | | 7.2 | 0 | | 79 | ADP SM1 | SS-P-016G | 10/15/85 | COUNT SPALL AS PENETRATION |
| 206 | 6 | 0.13 | 0.06 | 2219-T87 | AL-LI | NO | | | 1100-O | 0 | 0.31 | 3.5 | Y | 0.8 | N | 0.47 | | 3.5 | 3 | | 360 | | SS-219A | 10/15/86 | |
| 207 | 6 | 0.13 | 0.06 | 2219-T87 | 6061-T6 | YES | W | | 1100-O | 0 | 0.13 | 2.1 | N | 0 | N | 0.21 | | 2.1 | 0 | | 69 | ADP SM1 | SS-P-015B | 10/01/85 | |
| 208 | 6 | 0.13 | 0.06 | 2219-T87 | 6061-T6 | YES | W | | 1100-O | 0 | 0.19 | 2.8 | Y | 0.3 | N | 0.33 | | 2.8 | 0 | | 107 | ADP SM1 | SS-P-014E | 12/02/85 | |
| | 6 | 0.13 | 0.06 | 2219-T87 | 6061-T6 | YES | W | | 1100-O | 0 | 0.19 | 3 | N | 0 | N | 0.34 | | 3 | 0 | | 106 | ADP SM1 | SS-P-014F | 12/02/85 | |
| | 6 | 0.13 | 0.06 | 2219-T87 | 6061-T6 | YES | W | | 1100-O | 0 | 0.19 | 3.7 | N | 0 | N | 0.38 | | 3.7 | 0 | | 66 | ADP SM1 | SS-P-014C | 09/26/85 | |
| 209 | 6 | 0.13 | 0.06 | 2219-T87 | 6061-T6 | YES | W | | 1100-O | 0 | 0.25 | 3.9 | C | 0 | N | 0.48 | | 3.9 | 0 | | 108 | ADP SM1 | SS-P-013E | 12/03/85 | COUNT REAR SURFACE CRACK AS FAILURE |
| | 6 | 0.13 | 0.06 | 2219-T87 | 6061-T6 | YES | W | | 1100-O | 0 | 0.25 | 6 | N | 0 | N | 0.55 | | 6 | 0 | | 62 | ADP SM1 | SS-P-013D | 09/20/85 | |
| 210 | 6 | 0.13 | 0.06 | 2219-T87 | 6061-T6 | YES | W | | 1100-O | 0 | 0.3 | 4.3 | Y | 1 | N | 0.48 | | 4.3 | 2 | | 93 | ADP SM1 | SS-P-020G | 11/06/85 | 0- |
| | 6 | 0.13 | 0.06 | 2219-T87 | 6061-T6 | YES | W | | 1100-O | 0 | 0.3 | 4.7 | Y | 0.5 | N | 0.54 | | 4.7 | 0 | | 114 | ADP SM1 | SS-P-020H | 12/12/85 | |
| | 6 | 0.13 | 0.06 | 2219-T87 | 6061-T6 | YES | W | | 1100-O | 0 | 0.3 | 5 | N | 0 | N | 0.55 | | 5 | 0 | | 92 | ADP SM1 | SS-P-020F | 11/05/85 | |
| 211 | 6 | 0.13 | 0.06 | 2219-T87 | 6061-T6 | YES | W | | 1100-O | 0 | 0.31 | 2.9 | Y | 0.8 | N | 0.57 | 2.9 | 2.9 | | | 496 | MSFC | SS-T2-19B | 03/11/87 | PETALED |
| | 6 | 0.13 | 0.06 | 2219-T87 | 6061-T6 | YES | W | | 1100-O | 0 | 0.31 | 3 | Y | 0.3 | N | 0.53 | 3 | 3 | | | 490 | MSFC | SS-T2-19A | 03/06/87 | |
| | 6 | 0.13 | 0.06 | 2219-T87 | 6061-T6 | YES | W | | 1100-O | 0 | 0.31 | 4.1 | N | 0 | N | 0.58 | 4.1 | 4.1 | | | 486 | MSFC | SS-T2-19 | 03/04/87 | |
| 212 | 6 | 0.13 | 0.06 | 2219-T87 | 6061-T6 | YES | W | | 1100-O | 0 | 0.35 | 6.3 | N | 0 | N | 0.64 | | 6.3 | 0 | | 169 | ADP SM1 | SS-P-035B | 03/07/86 | |

| | standoff inch | rearwall gage inch | bumper gage inch | rearwall alloy | bumper alloy | mli present | mli location | prj. len to dia | prj. material | obliquity | projectile size | velocity avg km/s | rear penetr'n | rearhole inch | rearwall spall | bumper hole inch | vel hall km/s | vel xray km/s | witness penet. | rico con | test number | data source | test | date | comments |
|---|---|---|---|---|---|---|---|---|---|---|---|---|---|---|---|---|---|---|---|---|---|---|---|---|---|
| 213 | 6 | 0.13 | 0.06 | 2219-T87 | 6061-T6 | YES | W | | 6061-T6 | 0 | 0.19 | 1.6 | S | 0 | Y | 0.27 | | 1.6 | 0 | | 105 | ADP SM1 | SS-P-025D | 11/26/85 | COUNT SPALL AS PENETRATION |
| 214 | 6 | 0.13 | 0.06 | 2219-T87 | 6061-T6 | YES | W | | 6061-T6 | 0 | 0.25 | 4.3 | S | 0 | Y | 0.46 | | 4.3 | 0 | | 101 | ADP SM1 | SS-P-024G | 11/21/85 | COUNT SPALL AS PENETRATION |
| 215 | 6 | 0.13 | 0.06 | 2219-T87 | 6061-T6 | YES | W | | 6061-T6 | 0 | 0.3 | 3.4 | Y | 0.3 | N | 0.49 | | 3.4 | 2 | | 110 | ADP SM1 | SS-P-016M | 12/04/85 | |
| | 6 | 0.13 | 0.06 | 2219-T87 | 6061-T6 | YES | W | | 6061-T6 | 0 | 0.3 | 3.8 | Y | 0.3 | N | 0.51 | | 3.8 | 3 | | 111 | ADP SM1 | SS-P-016N | 12/10/85 | |
| | 6 | 0.13 | 0.06 | 2219-T87 | 6061-T6 | YES | W | | 6061-T6 | 0 | 0.3 | 4.2 | Y | 0.3 | N | 0.51 | | 4.2 | 1 | | 112 | ADP SM1 | SS-P-016P | 12/11/85 | |
| | 6 | 0.13 | 0.06 | 2219-T87 | 6061-T6 | YES | W | | 6061-T6 | 0 | 0.3 | 4.8 | N | 0 | N | 0.54 | | 4.8 | 0 | | 109 | ADP SM1 | SS-P-016L | 12/03/85 | |
| | 6 | 0.13 | 0.06 | 2219-T87 | 6061-T6 | YES | W | | 6061-T6 | 0 | 0.3 | 6.7 | N | 0 | N | 0.59 | | 6.7 | 0 | | 85 | ADP SM1 | SS-P-016K | 10/25/85 | |
| | 6 | 0.13 | 0.06 | 2219-T87 | 6061-T6 | YES | W | | 6061-T6 | 0 | 0.3 | 6.7 | N | 0 | N | 0.6 | | 6.7 | 0 | | 84 | ADP SM1 | SS-P-016J | 10/22/85 | |
| | 6 | 0.13 | 0.06 | 2219-T87 | 6061-T6 | YES | W | | 6061-T6 | 0 | 0.3 | 7.1 | N | 0 | N | 0.61 | | 7.1 | 0 | | 80 | ADP SM1 | SS-P-016H | 10/16/85 | |
| 216 | 6 | 0.13 | 0.08 | 2219-T87 | 6061-T6 | NO | | | 1100-O | 0 | 0.3 | 6.6 | Y | 0.2 | Y | 0.63 | 6.4 | 6.7 | 2 | | 206 | MARTIN | SS-121-2 | 05/22/86 | |
| | 6 | 0.13 | 0.08 | 2219-T87 | 6061-T6 | NO | | | 1100-O | 0 | 0.3 | 6.8 | Y | 0.1 | Y | 0.66 | 6.7 | 6.9 | | | 205 | MARTIN | SS-121-1 | 05/21/86 | |
| 217 | 6 | 0.13 | 0.08 | 2219-T87 | 6061-T6 | YES | W | | 1100-O | 0 | 0.35 | 5.7 | Y | 12 | N | 0.63 | | 5.7 | 2 | | 173 | ADP SM1 | SS-P-035C | 03/11/86 | SPLIT IN TWO. |
| 218 | 6 | 0.19 | 0.19 | 2219-T87 | 2219-T87 | NO | | | 6061-T6 | 0 | 0.5 | 6 | Y | 4 | N | 1.3 | 5.9 | 6.1 | 2 | | 648 | MSFC | SS-185A | 10/14/87 | BUMBER - 1.303" DIA. HOLE WITH RING KNOCKED OUT .1" WIDE AND .080" DEEP FRONT AND BACK. NO DEBRIS HOLES, SOME DEBRIS, .5" LEFT, .7" LOW. WALL - HOLE SECTION 3" X 4" KNOCKED OUT. 1/3 OF SECTION BROKE OFF, THE REMAINING PORTION OF SECTION HANGING BY 1" S |
| 219 | 8 | 0.25 | 0.13 | 2219-T87 | 2219-T87 | NO | | | 1100-O | 0 | 0.25 | 3.4 | N | | | 0.5 | 3.4 | 3.4 | | | 353 | MARTIN | SS-142A | 10/09/86 | |
| 220 | 8 | 0.25 | 0.13 | 2219-T87 | 2219-T87 | NO | | | 1100-O | 0 | 0.31 | 2.9 | N | | Y | 0.55 | 2.8 | 2.9 | | | 356 | MARTIN | SS-143B | 10/10/86 | |
| | 8 | 0.25 | 0.13 | 2219-T87 | 2219-T87 | NO | | | 1100-O | 0 | 0.31 | 3.8 | N | | N | 0.63 | 3.8 | 3.9 | | | 355 | MSFC | SS-143A | 10/10/86 | |
| 221 | 12 | 0.13 | 0.03 | 2219-T87 | 6061-T6 | YES | W | | 1100-O | 0 | 0.19 | 4.3 | Y | 0.3 | N | 0.29 | | 4.3 | 1 | | 876 | | 3119-A | 11/16/89 | 2 HOLES, FEW VERY SMALL CRATERS |
| | 12 | 0.13 | 0.03 | 2219-T87 | 6061-T6 | YES | W | | 1100-O | 0 | 0.19 | 4.8 | N | 0 | N | 0.3 | 4.8 | 4.8 | | | 877 | | 3119-B | 11/17/89 | NO HOLE, FEW SMALL CRATERS |
| | 12 | 0.13 | 0.03 | 2219-T87 | 6061-T6 | YES | W | | 1100-O | 0 | 0.19 | 5.5 | Y | 0.1 | N | 0.31 | 5.6 | 5.5 | | | 988 | | 3222-A | 04/11/90 | |
| 222 | 12 | 0.13 | 0.03 | 2219-T87 | 6061-T6 | YES | W | | 1100-O | 0 | 0.25 | 4.9 | Y | 0.2 | Y | 0.4 | 5 | 4.9 | 0 | | 874 | | 3120-A | 11/15/89 | 3 HOLES, FEW CRATERS, PIN HOLE & SPALLING OFF REAR, |
| | 12 | 0.13 | 0.03 | 2219-T87 | 6061-T6 | YES | W | | 1100-O | 0 | 0.25 | 5.4 | Y | 0.1 | N | 0.44 | 5.4 | 5.5 | | | 875 | | 3120-B | 11/16/89 | HOLE IN BOTTOM, MOST DAMAGE IN .5" DIA AREA |

| | standoff inch | rearwall gage inch | bumper gage inch | rearwall alloy | bumper alloy | mil present | mil location | prj. len to dia | prj. material | obliquity | projectile size | velocity avg km/s | rear penetr'n | rearhole inch | rearwall spall | bumper hole inch | vel hall km/s | vel xray km/s | witness penet. | rico con | test number | data source | test | date | comments |
|---|---|---|---|---|---|---|---|---|---|---|---|---|---|---|---|---|---|---|---|---|---|---|---|---|---|
| | 12 | 0.13 | 0.03 | 2219-T87 | 6061-T6 | YES | W | | 1100-O | 0 | 0.25 | 6.2 | Y | 0.3 | Y | 0.38 | 6.2 | 6.1 | 0 | | 986 | | 3221-A | 04/10/90 | SPALL AROUND SOME HOLES AND ON DIMPLES |
| | 12 | 0.13 | 0.03 | 2219-T87 | 6061-T6 | YES | W | | 1100-O | 0 | 0.25 | 6.4 | Y | 0.2 | Y | 0.4 | 6.4 | 6.4 | 0 | | 987 | | 3221-B | 04/10/90 | SPALL AROUND HOLES |
| 223 | 12 | 0.13 | 0.03 | 2219-T87 | 6061-T6 | YES | W | | 1100-O | 0 | 0.31 | 4.6 | Y | 0.5 | N | 0.46 | 4.6 | 4.6 | 2 | | 873 | | 3121-B | 11/15/89 | 5 HOLES, SEVERAL CRATERS WITH DIMPLES ON REAR, DAMAGE |
| | 12 | 0.13 | 0.03 | 2219-T87 | 6061-T6 | YES | W | | 1100-O | 0 | 0.31 | 5.6 | Y | 0 | N | 0.46 | 5.6 | 5.6 | | | 872 | | 3121-A | 11/14/89 | 2 PIN HOLES, SINK AREA, CRATERS OVER AREA, SEVERAL DIMPLES |
| | 12 | 0.13 | 0.03 | 2219-T87 | 6061-T6 | YES | W | | 1100-O | 0 | 0.31 | 6 | Y | 0.1 | Y | 0.47 | 6 | | | | 984 | | 3220-A | 04/06/90 | |
| | 12 | 0.13 | 0.03 | 2219-T87 | 6061-T6 | YES | W | | 1100-O | 0 | 0.31 | 6.5 | Y | 0.2 | N | 0.47 | 6.5 | 6.5 | 0 | | 985 | | 3220-B | 04/09/90 | |
| 224 | 12 | 0.13 | 0.03 | 2219-T87 | 6061-T6 | YES | W | | 1100-O | 0 | 0.38 | 5.9 | Y | 0.7 | N | 0.5 | 5.9 | 5.8 | 2 | | 993 | | 3225-A | 04/17/90 | HOLE, METAL SPLIT, PETALS PUSHED OUT ON REAR |
| | 12 | 0.13 | 0.03 | 2219-T87 | 6061-T6 | YES | W | | 1100-O | 0 | 0.38 | 5.9 | Y | 0.5 | N | 0.5 | 5.9 | 5.9 | 1 | | 992 | | 3225-B | 04/16/90 | HOLE, METAL SPLIT, METAL MISSSING FROM CENTER, 4 PETALS PUSHED |
| | 12 | 0.13 | 0.03 | 2219-T87 | 6061-T6 | YES | W | | 1100-O | 0 | 0.38 | 6.2 | Y | 1.5 | N | 0.53 | 6.2 | 6.2 | 1 | | 1009 | | 3225-C | 05/04/90 | |
| 225 | 12 | 0.13 | 0.03 | 2219-T87 | 6061-T6 | YES | W | | 1100-O | 45 | 0.19 | 4.9 | Y | 0.3 | N | 0.45 | 4.9 | 5 | 0 | | 900 | | 3122-C | 12/14/89 | HOLE, 6 SM CRATERS NEAR HOLE, SM CRATER UNDER BUMPER HOLE |
| | 12 | 0.13 | 0.03 | 2219-T87 | 6061-T6 | YES | W | | 1100-O | 45 | 0.19 | 5.5 | N | 0 | N | 0.47 | 5.4 | 5.5 | | | 901 | | 3122-D | 12/15/89 | |
| | 12 | 0.13 | 0.03 | 2219-T87 | 6061-T6 | YES | W | | 1100-O | 45 | 0.19 | 6.3 | N | 0 | N | 0.45 | 6.3 | 6.3 | 0 | | 895 | | 3122-B | 12/11/89 | NO HOLE, 10 CRATERS, 3 DIMPLES ON REAR, FEW SMALL CRATERS UNDER BUMPER HOLE |
| | 12 | 0.13 | 0.03 | 2219-T87 | 6061-T6 | YES | W | | 1100-O | 45 | 0.19 | 7.4 | N | 0 | N | 0.57 | 7.4 | 7.4 | | | 890 | | 3122-A | 12/06/89 | NO HOLE, 1 SMALL CRATER IN PROJECTILE PATH |
| 226 | 12 | 0.13 | 0.03 | 2219-T87 | 6061-T6 | YES | W | | 1100-O | 45 | 0.25 | 7.2 | Y | 0.3 | Y | 0.62 | 7.2 | 7.2 | 2 | | 888 | | 3123-A | 12/05/89 | HOLE, 1 PIN HOLE IN CRATER W/SPALL OFF DIMPLE ON REAR, 5 CRATERS |
| | 12 | 0.13 | 0.03 | 2219-T87 | 6061-T6 | YES | W | | 1100-O | 45 | 0.25 | 7.6 | Y | 0.2 | Y | 0.6 | 7.6 | 7.6 | 0 | | 889 | | 3123-B | 12/05/89 | 2 HOLES, FEW CRATERS W/DIMPLES ON REAR, NO DAM UNDER BUMPER HOLE |
| 227 | 12 | 0.13 | 0.03 | 2219-T87 | 6061-T6 | YES | W | | 1100-O | 45 | 0.31 | 5 | Y | 0.7 | N | 0.68 | 5 | 4.9 | 2 | | 884 | | 3124-A | 11/27/89 | HOLE, 2 CRATERS W/DIMPLES ON REAR, FEW SMALL CRATERS. |
| | 12 | 0.13 | 0.03 | 2219-T87 | 6061-T6 | YES | W | | 1100-O | 45 | 0.31 | 6.2 | Y | 0.7 | N | 0.77 | 6.2 | 6.2 | 2 | | 885 | | 3124-B | 11/28/89 | 5 HOLES, FEW CRATERS W/DIMPLE ON REAR, FEW UNDER BUMPER HOLE |
| | 12 | 0.13 | 0.03 | 2219-T87 | 6061-T6 | YES | W | | 1100-O | 45 | 0.31 | 6.7 | Y | 0.6 | N | 0.72 | 6.7 | 6.6 | 2 | | 886 | | 3124-C | 11/29/89 | 5 HOLES IN PROJECTILE PATH, FEW SMALL CRATERS |
| 228 | 12 | 0.13 | 0.04 | 2219-T87 | 6061-T6 | TPS | TPS | | 1100-O | 0 | 0.31 | 6.8 | N | 0 | N | 0.55 | 6.8 | 6.9 | | | 732 | | GRIT-11 | 08/18/88 | |
| 229 | 12 | 0.13 | 0.04 | 2219-T87 | 6061-T6 | TPS | TPS | | 1100-O | 0 | 0.38 | 6.7 | Y | 0.2 | N | 0.56 | 6.6 | 6.7 | 0 | | 729 | | GRIT-8 | 08/15/88 | |
| 230 | 12 | 0.13 | 0.06 | 2219-T87 | 6061-T6 | TPS | TPS | | 1100-O | 0 | 0.38 | 5.9 | Y | 0.1 | N | 0.64 | 5.8 | 5.9 | 0 | | 731 | | GRIT-10 | 08/17/88 | |
| 231 | 12 | 0.13 | 0.06 | 2219-T87 | 6061-T6 | YES | W | | 1100-O | 0 | 0.19 | 3.6 | Y | 0.2 | N | 0.36 | | 3.6 | 0 | | 882 | | 3128-A | 11/22/89 | HOLE .2" DIA, FEW SMALL CRATER SCATTERED OVER PANEL |
| | 12 | 0.13 | 0.06 | 2219-T87 | 6061-T6 | YES | W | | 1100-O | 0 | 0.19 | 4.2 | N | 0 | N | 0.39 | 4.2 | 4.2 | | | 883 | | 3128-B | 11/22/89 | NO HOLE, SCATTERING SM CRATERS, FEW VERY SM CRATERS TO EDGE PANEL |
| 232 | 12 | 0.13 | 0.06 | 2219-T87 | 6061-T6 | YES | W | | 1100-O | 0 | 0.25 | 4.3 | Y | 0.4 | N | 0.45 | 4.3 | 4.3 | 0 | | 880 | | 3129-A | 11/20/89 | 5 HOLES, FEW CRATERS, FEW VERY SM CRATERS OUT TO EDGE OF PANEL |
| | 12 | 0.13 | 0.06 | 2219-T87 | 6061-T6 | YES | W | | 1100-O | 0 | 0.25 | 4.8 | Y | 0.2 | Y | 0.47 | 4.8 | 4.8 | 1 | | 881 | | 3129-B | 11/21/89 | 2 HOLES W/SPALLING OFF REAR |
| | 12 | 0.13 | 0.06 | 2219-T87 | 6061-T6 | YES | W | | 1100-O | 0 | 0.25 | 5.2 | Y | 0.1 | Y | 0.49 | 5.2 | 5.2 | 0 | | 990 | | 3224-A | 04/13/90 | |
| | 12 | 0.13 | 0.06 | 2219-T87 | 6061-T6 | YES | W | | 1100-O | 0 | 0.25 | 5.3 | N | 0 | N | 0.53 | 5.3 | 5.3 | 0 | | 989 | | 3224-B | 04/12/90 | |

| | standoff inch | rearwall gage inch | bumper gage inch | rearwall alloy | bumper alloy | mli present | mli location | prj. len. to dia | prj. material | obliquity | projectile size | velocity avg km/s | rear penetr'n | rearhole inch | rearwall spall | bumper hole inch | vel hall km/s | vel xray km/s | witness penet. | rico con | test number | data source | test | date | comments |
|---|---|---|---|---|---|---|---|---|---|---|---|---|---|---|---|---|---|---|---|---|---|---|---|---|---|
| 233 | 12 | 0.13 | 0.06 | 2219-T87 | 6061-T6 | YES | W | | 1100-O | 0 | 0.31 | 4.6 | Y | 0.3 | N | 0.56 | 4.6 | 4.6 | 0 | | 879 | | 3130-B | 11/20/89 | 4 HOLES |
| | 12 | 0.13 | 0.06 | 2219-T87 | 6061-T6 | YES | W | | 1100-O | 0 | 0.31 | 5.3 | C | 0 | N | 0.58 | 5.3 | 5.3 | | | 878 | | 3130-A | 11/17/89 | NO HOLE,SOME DAMAGE,FEW CRATERS W/DIMPLES,2 DIMPLES W/SM CRACKS. COUNT REAR SURFACE CRACKS AS FAILURES. |
| | 12 | 0.13 | 0.06 | 2219-T87 | 6061-T6 | YES | W | | 1100-O | 0 | 0.31 | 5.9 | N | 0 | N | 0.62 | 5.9 | 5.9 | 0 | | 991 | | 3223-A | 04/16/90 | |
| 234 | 12 | 0.13 | 0.06 | 2219-T87 | 6061-T6 | YES | W | | 1100-O | 0 | 0.38 | 5.6 | Y | 0.9 | Y | 0.64 | 5.6 | 5.5 | 1 | | 994 | | 3226-B | 04/17/90 | 3 HOLES, SPALL AROUND HOLES, FEW SMALL CRATERS OUTSIDE MLI BLNKS |
| | 12 | 0.13 | 0.06 | 2219-T87 | 6061-T6 | YES | W | | 1100-O | 0 | 0.38 | 5.6 | Y | 0.1 | N | 0.63 | 5.6 | 5.6 | 0 | | 995 | | 3226-A | 04/18/90 | 3 HOLES, 2 HOLES TOGETHER IN CENTER W/METAL PUSHED UP ON REAR |
| | 12 | 0.13 | 0.06 | 2219-T87 | 6061-T6 | YES | W | | 1100-O | 0 | 0.38 | 6 | S | 0 | Y | 0.64 | 6 | 5.9 | 0 | | 996 | | 3226-C | 04/18/90 | COUNT SPALL AS FAILURE |
| | 12 | 0.13 | 0.06 | 2219-T87 | 6061-T6 | YES | W | | 1100-O | 0 | 0.38 | 6.6 | N | 0 | N | 0.66 | 6.6 | 6.6 | 0 | | 998 | | 3227-C | 04/20/90 | |
| 235 | 12 | 0.13 | 0.06 | 2219-T87 | 6061-T6 | YES | W | | 1100-O | 45 | 0.19 | 3.6 | N | 0 | N | 0.46 | | 3.6 | | | 918 | | 3131-C | 01/11/90 | |
| | 12 | 0.13 | 0.06 | 2219-T87 | 6061-T6 | YES | W | | 1100-O | 45 | 0.19 | 3.9 | N | 0 | N | 0.49 | 3.9 | 3.9 | | | 903 | | 3131-B | 12/18/89 | |
| | 12 | 0.13 | 0.06 | 2219-T87 | 6061-T6 | YES | W | | 1100-O | 45 | 0.19 | 4.1 | N | 0 | N | 0.5 | 4.1 | 4.1 | | | 902 | | 3131-A | 12/15/89 | |
| 236 | 12 | 0.13 | 0.06 | 2219-T87 | 6061-T6 | YES | W | | 1100-O | 45 | 0.25 | 5.4 | Y | 0.3 | N | 0.67 | 5.4 | 5.3 | 1 | | 915 | | 3132-A | 01/09/90 | |
| | 12 | 0.13 | 0.06 | 2219-T87 | 6061-T6 | YES | W | | 1100-O | 45 | 0.25 | 6.4 | Y | 0.2 | N | 0.69 | 6.4 | 6.4 | 0 | | 917 | | 3132-C | 01/10/90 | |
| | 12 | 0.13 | 0.06 | 2219-T87 | 6061-T6 | YES | W | | 1100-O | 45 | 0.25 | 7 | N | 0 | N | 0.69 | 7 | 7 | | | 916 | | 3132-B | 01/09/90 | |
| 237 | 12 | 0.13 | 0.06 | 2219-T87 | 6061-T6 | YES | W | | 1100-O | 45 | 0.31 | 6.3 | Y | 0.3 | Y | 0.82 | 6.4 | 6.3 | 1 | | 910 | | 3133-B | 01/04/90 | |
| | 12 | 0.13 | 0.06 | 2219-T87 | 6061-T6 | YES | W | | 1100-O | 45 | 0.31 | 6.8 | Y | 0.6 | N | 0.82 | 6.8 | 6.8 | 2 | | 914 | | 3133-D | 01/08/90 | |
| | 12 | 0.13 | 0.06 | 2219-T87 | 6061-T6 | YES | W | | 1100-O | 45 | 0.31 | 6.9 | Y | 0.3 | N | 0.82 | 6.9 | 6.9 | 1 | | 911 | | 3133-C | 01/05/90 | |
| 238 | 12 | 0.13 | 0.06 | 2219-T87 | 6061-T87 | YES | W | | 1100-O | 45 | 0.31 | 5.1 | Y | 0.4 | N | 0.76 | | 5.1 | 1 | | 904 | | 3133-A | 12/19/89 | |
| 239 | 12 | 0.13 | 0.08 | 2219-T87 | 6061-T6 | NO | | | 1100-O | 0 | 0.35 | 6.9 | Y | 0.2 | N | 0.69 | | 6.9 | 0 | | 154 | MARTIN | SS-108 | 02/18/86 | |
| 240 | 12 | 0.13 | 0.13 | 2219-T87 | 2219-T87 | NO | | | 1100-O | 0 | 0.5 | 6.1 | Y | 0.1 | N | 1.08 | 6.1 | | | | 661 | MSFC | SS-189B | 11/02/87 | |
| | 12 | 0.13 | 0.13 | 2219-T87 | 2219-T87 | NO | | | 1100-O | 0 | 0.5 | 6.1 | Y | 0.2 | N | 1.07 | 6.1 | 6.2 | 1 | | 660 | MSFC | SS-189A | 10/30/87 | |
| 241 | 12 | 0.13 | 0.13 | 2219-T87 | 2219-T87 | TPS | | | 1100-O | 0 | 0.38 | | | | | 0.95 | 6.7 | 6.7 | | | 722 | | GRIT-1 | 08/03/88 | |
| | 12 | 0.13 | 0.13 | 2219-T87 | 2219-T87 | TPS | | | 1100-O | 0 | 0.38 | | | | | 0.95 | 6.8 | 6.9 | | | 723 | | GRIT-2 | 08/04/88 | |
| 242 | 12 | 0.13 | 0.13 | 2219-T87 | 2219-T87 | TPS | | | 1100-O | 0 | | | | 0.2 | | 1.15 | 6.4 | 6.5 | | | 727 | | GRIT-6 | 08/11/88 | |
| 243 | 12 | 0.13 | | 2219-T87 | B-CLOTH | TPS | | | 1100-O | 0 | 0.13 | | | | | 0.17 | 7.4 | 7.5 | | | 728 | | GRIT-7 | 08/12/88 | |
| 244 | 12 | 0.19 | 0.19 | 2219-T87 | 2219-T87 | NO | | | 6061-T6 | 0 | 0.5 | 5.3 | Y | 0.1 | Y | 1.22 | 5.2 | 5.4 | | | 647 | MARTIN | SS-184B | 10/08/87 | BUMBER - 1.216" DIA. HOLE WITH RING .1" WIDE AND .08" DEEP AROUND HOLE FRONT AND BACK. SOME DEBRIS, 1.5" LOW, .5" LEFT. WALL - 2 HOLES, .1" DIA. IN A CAVIVITY .25" DIA. AND LOCATED AT 11:00 O'CLOCK AND 3" FROM CENTER. SECOND HOLE .050" DIA. IN A CAVITY |

| | standoff inch | rearwall gage inch | bumper gage inch | rearwall alloy | bumper alloy | mli present | mli location | prj. len to dia | prj. material | obliquity | projectile size | velocity avg km/s | rear penetr'n | rearhole inch | rearwall spall | bumper hole inch | vel hall km/s | vel xray km/s | witness penet. | rico con | test number | data source | test | date | comments |
|---|---|---|---|---|---|---|---|---|---|---|---|---|---|---|---|---|---|---|---|---|---|---|---|---|---|
| | 12 | 0.19 | 0.19 | 2219-T87 | 2219-T87 | NO | | | 6061-T6 | 0 | 0.5 | 5.7 | N | 0 | Y | 1.25 | | 5.7 | | | 646 | MARTIN | SS-184A | 10/07/87 | BUMBER - 1.253" DIA. HOLE, WITH A RING .1" WIDE AND .80" DEEP KNOCKED OFF AROUND THE HOLE, .7" LOW, .2" LEFT, SOME DEBRIS BUT NO DEBRIS HOLES. WALL - NO HOLE, SPALLING OFF 3 DIMPLES ON BACK FEW OTHER DIMPLES WITH CRACKED METAL. DIMPLES ON BACK OVER 80% |
| 245 | 12 | 0.13 | 0.06 | 2219-T87 | 6061-T6 | TPS | TPS | | 1100-O | 0 | 0.38 | 6.8 | N | 0 | N | 0.68 | 6.7 | 6.9 | | | 726 | | GRIT-5 | 08/10/88 | |
| 246 | 36 | 0.13 | 0.13 | PLEXIGLA | 2219-T87 | NO | | | 1100-O | 0 | 0.31 | 5.5 | Y | 0.1 | N | 0.73 | | 5.5 | 0 | | 364 | MSFC | PT-1 | 10/20/86 | |

# WHIPPLE_EXCEL DATA

Translated from Lotus by L.Thompson (714) 896-4495

## Whipple Database

| | Shot No. | Site | Proj. Mat'l | Proj. Dia. (cm) | Proj. Dens. (g/cc) | Proj. Mass (g) | Vel. (km/sec) | Impact Angle (deg) | Normal Vel. (km/sec) | Bumper Mat'l | Bumper Thk (cm) | tb/d | Bumper Dens. (g/cc) | Spacing (cm) | S/d | Wall Th'k (cm) | tw/d | Wall Mat'l | Yield Stress (ksi) | (tb+tw)/d | Category |
|---|---|---|---|---|---|---|---|---|---|---|---|---|---|---|---|---|---|---|---|---|---|
| 1 | 4613 | JSC-orig | Glass | 0.079 | 2.25 | 0.00059 | 7.13 | 0 | 7.13 | Al2024T3 | 0.025 | 0.32 | 2.796 | 5.08 | 64 | 0.025 | 0.32 | Al2024-T3 | 47 | 0.640 | E2 |
| 2 | 4637 | JSC-orig | Glass | 0.079 | 2.25 | 0.00059 | 7.22 | 0 | 7.22 | Aluminum | 0.015 | 0.19 | 2.78 | 5.08 | 64 | 0.025 | 0.32 | Al2024-T3 | 47 | 0.512 | E4 |
| 3 | 4638 | JSC-orig | Glass | 0.079 | 2.25 | 0.00059 | 7.53 | 0 | 7.53 | Aluminum | 0.015 | 0.19 | 2.78 | 7.62 | 96 | 0.025 | 0.32 | Al2024-T3 | 47 | 0.512 | E4 |
| 4 | 4658 | JSC-orig | Al1100 | 0.079 | 2.71 | 0.00071 | 7.25 | 0 | 7.25 | Aluminum | 0.015 | 0.19 | 2.78 | 5.08 | 64 | 0.025 | 0.32 | Al2024-T3 | 47 | 0.512 | E4 |
| 5 | 4679 | JSC-orig | Al1100 | 0.079 | 2.71 | 0.00071 | 7.16 | 0 | 7.16 | Aluminum | 0.051 | 0.64 | 2.78 | 7.62 | 96 | 0.025 | 0.32 | Al2024-T3 | 47 | 0.960 | D2 |
| 6 | 4681 | JSC-orig | Al1100 | 0.079 | 2.71 | 0.00071 | 7.34 | 0 | 7.34 | Aluminum | 0.051 | 0.64 | 2.78 | 2.54 | 32 | 0.041 | 0.51 | Al2024-T3 | 47 | 1.152 | D2 |
| 7 | 4691 | JSC-orig | Glass | 0.159 | 2.54 | 0.0053 | 7.25 | 0 | 7.25 | Aluminum | 0.051 | 0.32 | 2.78 | 7.62 | 48 | 0.041 | 0.26 | Al2024-T3 | 47 | 0.576 | E4 |
| 8 | 4695 | JSC-orig | Glass | 0.159 | 2.54 | 0.0053 | 7.56 | 0 | 7.56 | Aluminum | 0.051 | 0.32 | 2.78 | 5.08 | 32 | 0.064 | 0.40 | Al2024-T3 | 47 | 0.720 | E2 |
| 9 | 4706 | JSC-orig | Glass | 0.159 | 2.54 | 0.0053 | 7.26 | 0 | 7.26 | Aluminum | 0.025 | 0.16 | 2.78 | 7.62 | 48 | 0.041 | 0.26 | Al2024-T3 | 47 | 0.416 | E4 |
| 10 | 4709 | JSC-orig | Glass | 0.159 | 2.54 | 0.0053 | 7.26 | 0 | 7.26 | Aluminum | 0.025 | 0.16 | 2.78 | 5.08 | 32 | 0.064 | 0.40 | Al2024-T3 | 47 | 0.560 | E2 |
| 11 | 4736 | JSC-orig | Al1100 | 0.159 | 2.71 | 0.0057 | 7.31 | 0 | 7.31 | Aluminum | 0.051 | 0.32 | 2.78 | 7.62 | 48 | 0.041 | 0.26 | Al2024-T3 | 47 | 0.576 | E4 |
| 12 | 4738 | JSC-orig | Al1100 | 0.159 | 2.71 | 0.0057 | 7.20 | 0 | 7.20 | Aluminum | 0.051 | 0.32 | 2.78 | 5.08 | 32 | 0.064 | 0.40 | Al2024-T3 | 47 | 0.720 | E1 |
| 13 | A201 | JSC-orig | Glass | 0.079 | 2.25 | 0.00059 | 6.70 | 0 | 6.70 | Al1100-H14 | 0.030 | 0.38 | 2.713 | 7.62 | 96 | 0.030 | 0.38 | Al1100-H14 | 17 | 0.768 | E4 |
| 14 | A250 | JSC-orig | Glass | 0.079 | 2.25 | 0.00059 | 6.52 | 0 | 6.52 | Al7075-T6 | 0.030 | 0.38 | 2.796 | 2.54 | 32 | 0.030 | 0.38 | Al7075-T6 | 68 | 0.768 | E2 |
| 15 | A337 | JSC-orig | Glass | 0.079 | 2.25 | 0.00059 | 5.44 | 0 | 5.44 | Aluminum | 0.025 | 0.32 | 2.78 | 2.54 | 32 | 0.025 | 0.32 | Al2024-T4 | 47 | 0.640 | E1 |
| 16 | A358 | JSC-orig | Glass | 0.040 | 2.25 | 7.36E-05 | 5.56 | 0 | 5.56 | Al2024-T4 | 0.015 | 0.38 | 2.796 | 2.54 | 64 | 0.015 | 0.38 | Al2024-T4 | 47 | 0.768 | E1 |
| 17 | AV26 | AVCO | Glass | 0.127 | 2.25 | 0.0024 | 5.72 | 0 | 5.72 | Al7178T6 | 0.041 | 0.32 | 2.823 | 2.54 | 20 | 0.041 | 0.32 | Al7178-T6 | 78 | 0.640 | D1 |
| 18 | 1376 | JSC-HIRL | Al1100 | 0.079 | 2.713 | 0.00071 | 7.20 | 0 | 7.20 | Al6061T6 | 0.064 | 0.80 | 2.713 | 3.33 | 42 | 0.635 | 8.00 | Al1100 | 10 | 8.800 | E1 |
| 19 | 1378 | JSC-HIRL | Al1100 | 0.040 | 2.713 | 0.00009 | 8.00 | 0 | 8.00 | Al6061T6 | 0.064 | 1.60 | 2.713 | 3.33 | 84 | 0.635 | 16.00 | Al1100 | 10 | 17.600 | E1 |
| 20 | 1403 | JSC-HIRL | Al1100 | 0.079 | 2.713 | 0.00071 | 3.55 | 0 | 3.55 | Al6061-0 | 0.015 | 0.19 | 2.713 | 2.54 | 32 | 0.064 | 0.80 | Al2024-T3 | 47 | 0.992 | D4 |
| 21 | 1421 | JSC-HIRL | Al2017T4 | 0.079 | 2.796 | 0.00073 | 6.40 | 45 | 4.53 | Al6061-0 | 0.015 | 0.19 | 2.713 | 2.54 | 32 | 0.064 | 0.80 | Al6061-T6 | 36 | 0.992 | C2 |
| 22 | 1423 | JSC-HIRL | Al2017T4 | 0.079 | 2.796 | 0.00073 | 7.04 | 45 | 4.98 | Al6061-0 | 0.015 | 0.19 | 2.713 | 2.54 | 32 | 0.064 | 0.80 | Al2024-T3 | 47 | 0.992 | C4 |
| 23 | 1425 | JSC-HIRL | Al1100 | 0.079 | 2.713 | 0.00071 | 6.13 | 45 | 4.33 | Al6061-0 | 0.015 | 0.19 | 2.713 | 2.54 | 32 | 0.064 | 0.80 | Al2024-T3 | 47 | 0.992 | C4 |
| 24 | 1431 | JSC-HIRL | Al2024T3 | 0.081 | 2.796 | 0.00078 | 6.57 | 45 | 4.65 | Al6061-0 | 0.015 | 0.19 | 2.713 | 2.54 | 31 | 0.064 | 0.78 | Al2024-T3 | 47 | 0.971 | C4 |
| 25 | 1435 | JSC-HIRL | Al2017T4 | 0.080 | 2.796 | 0.00076 | 6.52 | 0 | 6.52 | Al6061-0 | 0.015 | 0.19 | 2.713 | 2.54 | 32 | 0.064 | 0.79 | Al2024-T3 | 47 | 0.980 | E2 |
| 26 | 1436 | JSC-HIRL | Al1100 | 0.079 | 2.713 | 0.00069 | 6.60 | 0 | 6.60 | Al6061-0 | 0.015 | 0.19 | 2.713 | 2.54 | 32 | 0.030 | 0.39 | Al2024-T3 | 47 | 0.582 | C4 |
| 27 | 1444 | JSC-HIRL | Al2017T4 | 0.079 | 2.796 | 0.00072 | 3.72 | 0 | 3.72 | Al6061-0 | 0.015 | 0.19 | 2.713 | 2.54 | 32 | 0.064 | 0.80 | Al2024-T3 | 47 | 0.998 | A3/D4 |
| 28 | 1449 | JSC-HIRL | Al2024T4 | 0.081 | 2.796 | 0.00079 | 3.01 | 0 | 3.01 | Al6061-0 | 0.015 | 0.19 | 2.713 | 2.54 | 31 | 0.064 | 0.78 | Al2024-T3 | 47 | 0.967 | A3 |
| 29 | 1450 | JSC-HIRL | Al1100 | 0.079 | 2.713 | 0.00071 | 3.89 | 0 | 3.89 | Al6061-0 | 0.015 | 0.19 | 2.713 | 2.54 | 32 | 0.064 | 0.80 | Al2024-T3 | 47 | 0.992 | D4 |
| 30 | 1452 | JSC-HIRL | Al1100 | 0.079 | 2.713 | 0.00071 | 3.21 | 0 | 3.21 | Al6061-0 | 0.015 | 0.19 | 2.713 | 2.54 | 32 | 0.064 | 0.80 | Al2024-T3 | 47 | 0.992 | D4 |
| 31 | 1453 | JSC-HIRL | Al2017T4 | 0.080 | 2.796 | 0.00074 | 3.14 | 0 | 3.14 | Al6061-0 | 0.015 | 0.19 | 2.713 | 2.54 | 32 | 0.064 | 0.80 | Al2024-T3 | 47 | 0.988 | D4 |
| 32 | 1462 | JSC-HIRL | Al2024T4 | 0.081 | 2.796 | 0.00077 | 6.85 | 45 | 4.84 | Al6061-0 | 0.015 | 0.19 | 2.713 | 2.54 | 31 | 0.064 | 0.79 | Al2024-T3 | 47 | 0.975 | C4 |
| 33 | 1463 | JSC-HIRL | Al2017T4 | 0.079 | 2.796 | 0.00072 | 6.20 | 45 | 4.38 | Al6061-0 | 0.015 | 0.19 | 2.713 | 2.54 | 32 | 0.064 | 0.80 | Al2024-T3 | 47 | 0.998 | C4 |
| 34 | 1468 | JSC-HIRL | Al2017T4 | 0.081 | 2.796 | 0.00078 | 6.70 | 0 | 6.70 | Al6061-0 | 0.015 | 0.19 | 2.713 | 2.54 | 31 | 0.030 | 0.38 | Al2024-T3 | 47 | 0.565 | E2 |
| 35 | 1470 | JSC-HIRL | Al1100 | 0.080 | 2.713 | 0.00072 | 6.50 | 0 | 6.50 | Al6061-0 | 0.015 | 0.19 | 2.713 | 2.54 | 32 | 0.064 | 0.80 | Al2024-T3 | 47 | 0.988 | E2/C2 |
| 36 | 1472 | JSC-HIRL | Al1100 | 0.079 | 2.713 | 0.00071 | 6.30 | 0 | 6.30 | Al6061-0 | 0.015 | 0.19 | 2.713 | 2.54 | 32 | 0.064 | 0.80 | Al2024-T3 | 47 | 0.992 | E2/C2 |
| 37 | 1473 | JSC-HIRL | Al1100 | 0.079 | 2.713 | 0.00071 | 6.40 | 0 | 6.40 | Al6061-0 | 0.015 | 0.19 | 2.713 | 2.54 | 32 | 0.030 | 0.38 | Al2024-T3 | 47 | 0.576 | E4/C4 |
| 38 | 1475 | JSC-HIRL | Al2017T4 | 0.040 | 2.796 | 9.15E-05 | 7.99 | 0 | 7.99 | Al3003-0 | 0.010 | 0.26 | 2.74 | 1.27 | 32 | 0.025 | 0.64 | Al3003-H14 | 21 | 0.896 | F3 |
| 39 | 1476 | JSC-HIRL | Al2017T4 | 0.040 | 2.796 | 9.15E-05 | 8.06 | 0 | 8.06 | Al3003-0 | 0.010 | 0.26 | 2.74 | 1.27 | 32 | 0.027 | 0.68 | Al3003-H14 | 21 | 0.936 | F3 |
| 40 | 1481 | JSC-HIRL | Al2017T4 | 0.040 | 2.796 | 9.15E-05 | 7.10 | 0 | 7.10 | Al3003-0 | 0.010 | 0.26 | 2.74 | 1.27 | 32 | 0.010 | 0.26 | Al3003-H12 | 18 | 0.512 | F4 |
| 41 | 1486 | JSC-HIRL | Al2017T4 | 0.040 | 2.713 | 8.88E-05 | 7.90 | 0 | 7.90 | Al3003-0 | 0.010 | 0.26 | 2.74 | 1.27 | 32 | 0.015 | 0.38 | Al3003-H12 | 18 | 0.640 | F3/E2 |
| 42 | 1487 | JSC-HIRL | Al1100 | 0.040 | 2.713 | 8.88E-05 | 7.30 | 0 | 7.30 | Al3003-0 | 0.010 | 0.26 | 2.74 | 1.27 | 32 | 0.015 | 0.38 | Al3003-H12 | 18 | 0.640 | F3/E2 |
| 43 | 1488 | JSC-HIRL | Al1100 | 0.040 | 2.713 | 8.88E-05 | 7.30 | 0 | 7.30 | Al3003-0 | 0.010 | 0.26 | 2.74 | 1.27 | 32 | 0.015 | 0.38 | Al3003-H12 | 18 | 0.640 | F3/E2 |
| 44 | 1499 | JSC-HIRL | Al1100 | 0.082 | 2.713 | 0.00078 | 3.70 | 0 | 3.70 | Al6061-0 | 0.015 | 0.19 | 2.713 | 2.54 | 31 | 0.064 | 0.78 | Al2024-T3 | 47 | 0.962 | A3/D4 |
| 45 | 1644 | JSC-HIRL | CuBe | 0.018 | 8.24 | 0.000024 | 7.97 | 0 | 7.97 | Al6061-T6 | 0.064 | 3.57 | 2.796 | 2.54 | 143 | 0.025 | 1.43 | Al3003-H12 | 18 | 5.000 | E2 |
| 46 | A150 | JSC-HIRL | Al1100 | 0.318 | 2.713 | 0.0455 | 6.45 | 0 | 6.45 | Al6061T6 | 0.081 | 0.26 | 2.713 | 5.08 | 16 | 0.159 | 0.50 | Al2024-T3 | 47 | 0.756 | D4 |
| 47 | A151 | JSC-HIRL | Al1100 | 0.318 | 2.713 | 0.0455 | 6.60 | 0 | 6.60 | Al6061T6 | 0.081 | 0.26 | 2.713 | 5.08 | 16 | 0.127 | 0.40 | Al2024-T3 | 47 | 0.656 | D4 |
| 48 | A235 | JSC-HIRL | Al2017T4 | 0.318 | 2.796 | 0.0469 | 6.98 | 0 | 6.98 | Al1100 | 0.056 | 0.18 | 2.713 | 10.16 | 32 | 0.159 | 0.50 | Al2024-T3 | 47 | 0.676 | E3 |
| 49 | A240 | JSC-HIRL | Al2017T4 | 0.318 | 2.796 | 0.0469 | 6.58 | 0 | 6.58 | Al6061T6 | 0.081 | 0.26 | 2.713 | 10.16 | 32 | 0.127 | 0.40 | Al2024-T3 | 47 | 0.656 | E2 |
| 50 | A315 | JSC-HIRL | Al1100 | 0.317 | 2.713 | 0.0453 | 6.08 | 45 | 4.30 | Al6061T6 | 0.081 | 0.26 | 2.713 | 5.08 | 16 | 0.127 | 0.40 | Al2024-T3 | 47 | 0.657 | C5 |

# WHIPPLE_EXCEL DATA

Translated from

K=tw*(Y/70)^.5*S^.5*(pp*pb)^-1/6*Vn^-1*M^-1/3
K"=tw*(Y/70)^.5*S^.5*(pp*pb)^-1/6*Vn^-1*M^-1/3*d^-.5

K=tw*(Y/70)^.5*S^.5*(pp*pb)^
K"=tw*(Y/70)^.5*S^.5*(pp*pb)^

| | Shot No. | Damage Description | JSC Whipple Eqns. dcrit (cm) | dcrit-d (cm) | Fail? 1=Y, 0=N) | Perf. Pred. | Safe Acc? | Pred. Accurate? | Comments | dc/d | K | K" | ELC JSC Whipple Eq Category (cm) |
|---|---|---|---|---|---|---|---|---|---|---|---|---|---|
| 1 | 4613 | No perfs or spall:v.fine filament craters | 0.094 | 0.0143 | 0 | 0 | 1 | 1 | | 1.180 | 0.0578 | 0.2050 | 0.096806 |
| 2 | 4637 | No tear or hole;v.small perfs in 2.7cm ring | 0.093 | 0.0136 | 1 | 0 | 0 | 0 | | 1.171 | 0.0571 | 0.2027 | 0.098579 |
| 3 | 4638 | No tear or hole;v.small perfs in 4.4cm ring | 0.103 | 0.0241 | 1 | 0 | 0 | 0 | | 1.303 | 0.0671 | 0.2380 | 0.119325 |
| 4 | 4658 | No tear or hole;v.small perfs in 2.7cm ring | 0.087 | 0.0077 | 1 | 0 | 0 | 0 | | 1.097 | 0.0518 | 0.1839 | 0.093167 |
| 5 | 4679 | No tear or perfs; small central dimples | 0.101 | 0.0212 | 0 | 0 | 1 | 1 | | 1.267 | 0.0643 | 0.2281 | 0.104367 |
| 6 | 4681 | No tear or perfs; small central dimples | 0.094 | 0.0144 | 0 | 0 | 1 | 1 | | 1.182 | 0.0579 | 0.2055 | 0.100454 |
| 7 | 4691 | No tear or hole; 3 small perfs | 0.139 | -0.0194 | 1 | 1 | 1 | 1 | | 0.878 | 0.0524 | 0.1316 | 0.148133 |
| 8 | 4695 | No tear or perfs; small central craters | 0.159 | 0.0007 | 0 | 0 | 1 | 1 | | 1.004 | 0.0642 | 0.1610 | 0.18161 |
| 9 | 4706 | No tear or hole; perf ring 3.4 cm; 4 perfs | 0.139 | -0.0195 | 1 | 1 | 1 | 1 | | 0.877 | 0.0524 | 0.1314 | 0.14928 |
| 10 | 4709 | No tear or perfs; 2cm dimple ring | 0.164 | 0.0050 | 0 | 0 | 1 | 1 | | 1.032 | 0.0668 | 0.1677 | 0.175167 |
| 11 | 4736 | No tear or hole; perf ring 5.6 cm; 4 perfs | 0.136 | -0.0231 | 1 | 1 | 1 | 1 | | 0.854 | 0.0503 | 0.1264 | 0.14628 |
| 12 | 4738 | No tear,hole or perfs; small central craters | 0.161 | 0.0024 | 0 | 0 | 1 | 1 | | 1.015 | 0.0652 | 0.1637 | 0.169118 |
| 13 | A201 | No hole or spall; 1 perf | 0.084 | 0.0041 | 1 | 0 | 0 | 0 | | 1.052 | 0.0546 | 0.1938 | 0.083503 |
| 14 | A250 | No hole or spall; near perf | 0.090 | 0.0106 | 0 | 0 | 1 | 1 | | 1.133 | 0.0645 | 0.2288 | 0.089947 |
| 15 | A337 | No hole, spall or perfs | 0.059 | -0.0201 | 0 | 1 | 1 | 0 | | 0.746 | 0.0536 | 0.1902 | 0.059247 |
| 16 | A358 | No hole, spall or perfs | 0.042 | 0.0022 | 0 | 0 | 1 | 1 | | 1.054 | 0.0629 | 0.3155 | 0.041838 |
| 17 | AV26 | No hole or spall; front surface eroded | 0.102 | -0.0247 | 0 | 1 | 1 | 0 | | 0.805 | 0.0655 | 0.1837 | 0.102258 |
| 18 | 1376 | Many craters, no spall | 0.389 | 0.3097 | 0 | 0 | 1 | 1 | | 4.901 | 0.4891 | 1.7359 | 0.406226 |
| 19 | 1378 | Many craters, no spall | 0.363 | 0.3230 | 0 | 0 | 1 | 1 | | 9.138 | 0.8803 | 4.4190 | 0.445023 |
| 20 | 1403 | Small perf., spall bubbles/dimples | 0.060 | -0.0197 | 1 | 1 | 1 | 1 | | 0.752 | 0.1877 | 0.6662 | 0.05971 |
| 21 | 1421 | No perf., craters and dimples | 0.082 | 0.0028 | 0 | 0 | 1 | 1 | | 1.035 | 0.1269 | 0.4506 | 0.082155 |
| 22 | 1423 | Small perf., spall bubbles/dimples | 0.097 | 0.0181 | 1 | 0 | 0 | 0 | | 1.228 | 0.1319 | 0.4680 | 0.097474 |
| 23 | 1425 | Small perf., spall bubbles/dimples | 0.088 | 0.0090 | 1 | 0 | 0 | 0 | | 1.114 | 0.1538 | 0.5458 | 0.088386 |
| 24 | 1431 | 3 perfs, craters/dimples | 0.092 | 0.0112 | 1 | 0 | 0 | 0 | | 1.138 | 0.1383 | 0.4859 | 0.092227 |
| 25 | 1435 | No tear or hole; dimples | 0.120 | 0.0392 | 0 | 0 | 1 | 1 | | 1.488 | 0.0994 | 0.3507 | 0.11959 |
| 26 | 1436 | ~14 perfs. (small) | 0.075 | -0.0036 | 1 | 1 | 1 | 1 | | 0.954 | 0.0489 | 0.1745 | 0.074974 |
| 27 | 1444 | 1 large perf. (1.8x1.4 mm), some dmpls | 0.062 | -0.0165 | 1 | 1 | 1 | 1 | | 0.791 | 0.1774 | 0.6315 | 0.06241 |
| 28 | 1449 | 1 large perf. (1.8 mm) | 0.048 | -0.0335 | 1 | 1 | 1 | 1 | | 0.588 | 0.2126 | 0.7451 | 0.047911 |
| 29 | 1450 | 1 pinhole perf. (0.5mm), craters/dimples | 0.067 | -0.0127 | 1 | 1 | 1 | 1 | | 0.841 | 0.1713 | 0.6082 | 0.066706 |
| 30 | 1452 | Large hole (1.7mm); little projectile breakup | 0.053 | -0.0267 | 1 | 1 | 1 | 1 | | 0.664 | 0.2076 | 0.7368 | 0.052714 |
| 31 | 1453 | Large hole (1.7mm); little projectile breakup | 0.051 | -0.0291 | 1 | 1 | 1 | 1 | Vel. Estimated | 0.635 | 0.2083 | 0.7380 | 0.050566 |
| 32 | 1462 | 1 perf. (1.2x.6mm); dmpls (4) | 0.095 | 0.0146 | 1 | 0 | 0 | 0 | | 1.181 | 0.1333 | 0.4690 | 0.095353 |
| 33 | 1463 | 1 perf. (1.3mm); dmpls (6) | 0.088 | 0.0092 | 1 | 0 | 0 | 0 | | 1.116 | 0.1506 | 0.5359 | 0.088097 |
| 34 | 1468 | No tear or hole; dimples | 0.075 | -0.0055 | 0 | 1 | 1 | 0 | | 0.932 | 0.0461 | 0.1620 | 0.07549 |
| 35 | 1470 | No perf, dimples (2) | 0.120 | 0.0407 | 0 | 0 | 1 | 1 | | 1.510 | 0.1021 | 0.3614 | 0.120411 |
| 36 | 1472 | No perf, dimples (7) | 0.116 | 0.0369 | 0 | 0 | 1 | 1 | | 1.465 | 0.1058 | 0.3754 | 0.116295 |
| 37 | 1473 | Small perfs (13), diffuse impact pattern | 0.072 | -0.0070 | 1 | 1 | 1 | 1 | | 0.912 | 0.0500 | 0.1774 | 0.072398 |
| 38 | 1475 | No perfs; v. slight impulsive bulge | 0.039 | -0.0007 | 0 | 1 | 1 | 0 | | 0.982 | 0.0310 | 0.1557 | 0.048868 |
| 39 | 1476 | No perfs; v. slight impulsive bulge | 0.040 | 0.0007 | 0 | 0 | 1 | 1 | | 1.017 | 0.0327 | 0.1640 | 0.051377 |
| 40 | 1481 | Several perfs; impulsive bulge with dimples | 0.022 | -0.0179 | 1 | 1 | 1 | 1 | | 0.548 | 0.0129 | 0.0649 | 0.022243 |
| 41 | 1486 | No perfs; impulsive bulge with dimples | 0.027 | -0.0129 | 0 | 1 | 1 | 0 | | 0.675 | 0.0177 | 0.0888 | 0.032756 |
| 42 | 1487 | No perfs; impulsive bulge with dimples | 0.028 | -0.0114 | 0 | 1 | 1 | 0 | | 0.712 | 0.0191 | 0.0961 | 0.030293 |
| 43 | 1488 | No perfs; impulsive bulge with dimples | 0.028 | -0.0114 | 0 | 1 | 1 | 0 | | 0.712 | 0.0191 | 0.0961 | 0.030293 |
| 44 | 1499 | 1 large perf. (1.5x1.3 mm), some dmpls | 0.063 | -0.0191 | 1 | 1 | 1 | 1 | | 0.767 | 0.1746 | 0.6101 | 0.062796 |
| 45 | 1644 | No perf, craters & dimples | 0.033 | 0.0147 | 0 | 0 | 1 | 1 | | 1.829 | 0.0528 | 0.3956 | 0.037404 |
| 46 | A150 | No hole, detached spall, through crack | 0.281 | -0.0370 | 1 | 1 | 1 | 1 | | 0.884 | 0.0913 | 0.1621 | 0.28054 |
| 47 | A151 | Hole, detached spall, cracks | 0.247 | -0.0703 | 1 | 1 | 1 | 1 | | 0.779 | 0.0714 | 0.1267 | 0.247242 |
| 48 | A235 | No hole or tear; 1 spall split | 0.377 | 0.0596 | 0 | 0 | 1 | 1 | | 1.188 | 0.1175 | 0.2086 | 0.377068 |
| 49 | A240 | No hole or tear; attached spall | 0.304 | -0.0133 | 0 | 1 | 1 | 0 | | 0.958 | 0.0998 | 0.1770 | 0.304218 |
| 50 | A315 | 7 Perfs. (max 8.1x3.8mm) | 0.197 | -0.1199 | 1 | 1 | 1 | 1 | 16mil 3003-0 wit: 48 perfs | 0.622 | 0.1097 | 0.1948 | 0.197262 |

Translated from Lotus by L.Thompson (714) 896-4495

## Whipple Database

| | Shot No. | Site | Proj. Mat'l | Proj. Dia. (cm) | Proj. Dens. (g/cc) | Proj. Mass (g) | Vel. (km/sec) | Impact Angle (deg) | Normal Vel. (km/sec) | Bumper Mat'l | Bumper Thk (cm) | tb/d | Bumper Dens. (g/cc) | Spacing (cm) | S/d | Wall Th'k (cm) | tw/d | Wall Mat'l | Yield Stress (ksi) | (tb+tw)/d | Category |
|---|---|---|---|---|---|---|---|---|---|---|---|---|---|---|---|---|---|---|---|---|---|
| 51 | A316 | JSC-HIRL | Al1100 | 0.317 | 2.713 | 0.0452 | 5.99 | 45 | 4.24 | Al6061T6 | 0.081 | 0.26 | 2.713 | 5.08 | 16 | 0.159 | 0.50 | Al2024-T3 | 47 | 0.758 | C5 |
| 52 | A481 | JSC-HIRL | Al2017T4 | 0.318 | 2.796 | 0.0469 | 6.38 | 0 | 6.38 | Al1100 | 0.056 | 0.18 | 2.713 | 12.7 | 40 | 0.127 | 0.40 | Al6061-T6 | 36 | 0.576 | E4 |
| 53 | A558 | JSC-HIRL | Al2017T4 | 0.318 | 2.796 | 0.0469 | 2.64 | 0 | 2.64 | Al1100 | 0.056 | 0.18 | 2.713 | 12.7 | 40 | 0.483 | 1.52 | Al6061-T6 | 36 | 1.696 | D2/C2 |
| 54 | A570 | JSC-HIRL | Al2017T4 | 0.318 | 2.796 | 0.0469 | 2.48 | 0 | 2.48 | Al1100 | 0.056 | 0.18 | 2.713 | 12.7 | 40 | 0.635 | 2.00 | Al1100-0 | 10 | 2.176 | D2/C2 |
| 55 | A689 | JSC-HIRL | Al2017T4 | 0.318 | 2.796 | 0.0469 | 6.5 | 45 | 4.60 | Al1100 | 0.056 | 0.18 | 2.713 | 10.16 | 32 | 0.160 | 0.50 | Al2024-T3 | 47 | 0.680 | C5 |
| 56 | A690 | JSC-HIRL | Al2017T4 | 0.318 | 2.796 | 0.0469 | 5.65 | 45 | 4.00 | Al1100 | 0.056 | 0.18 | 2.713 | 10.16 | 32 | 0.160 | 0.50 | Al2024-T3 | 47 | 0.680 | C5 |
| 57 | A939 | JSC-HIRL | Al2O3 | 0.317 | 3.9 | 0.0650 | 5.67 | 0 | 5.67 | Al1100 | 0.056 | 0.18 | 2.713 | 12.7 | 40.1 | 0.160 | 0.50 | Al2024-T3 | 47 | 0.681 | D3 |
| 58 | A1005 | JSC-HIRL | Al2017T4 | 0.318 | 2.796 | 0.0472 | 5.86 | 0 | 5.86 | Al3003H12 | 0.064 | 0.20 | 2.74 | 10.16 | 31.9 | 0.081 | 0.26 | Al2024-T3 | 47 | 0 455 | D5/E4 |
| 59 | A1076 | JSC-HIRL | Al2017T4 | 0.200 | 2.796 | 0.0117 | 6.37 | 0 | 6.37 | Al1100 | 0.064 | 0.32 | 2.713 | 6.0 | 30 | 0.041 | 0.20 | Al6061-T6 | 36 | 0.521 | E4 |
| 60 | A1077 | JSC-HIRL | Al2017T4 | 0.200 | 2.796 | 0.0117 | 6.77 | 0 | 6.77 | Al1100 | 0.041 | 0.20 | 2.713 | 6.0 | 30 | 0.064 | 0.32 | Al6061-T6 | 36 | 0.521 | E2 |
| 61 | A1112 | JSC-HIRL | Al2017T4 | 0.318 | 2.796 | 0.0469 | 6.20 | 45 | 4.38 | Al1100 | 0.051 | 0.16 | 2.713 | 10.16 | 32 | 0.318 | 1.00 | Al2024-T3 | 47 | 1 160 | D5 |
| 62 | A1114 | JSC-HIRL | Al2017T4 | 0.318 | 2.796 | 0.0469 | 6.21 | 0 | 6.21 | Al1100 | 0.051 | 0.16 | 2.713 | 10.16 | 32 | 0.159 | 0.50 | Al2024-T3 | 47 | 0.660 | E4 |
| 63 | A1184 | JSC-HIRL | Al2017T4 | 0.238 | 2.796 | 0.0198 | 6.34 | 45 | 4.48 | Al1100 | 0.041 | 0.17 | 2.713 | 7.62 | 32 | 0.318 | 1.33 | Al2024-T3 | 47 | 1.504 | C2 |
| 64 | A1193 | JSC-HIRL | Al2017T4 | 0.318 | 2.796 | 0.0469 | 6.25 | 0 | 6.25 | Al1100 | 0.051 | 0.16 | 2.713 | 10.16 | 32 | 0.203 | 0.64 | Al6061-T6 | 36 | 0.800 | E4 |
| 65 | A1195 | JSC-HIRL | Al2017T4 | 0.318 | 2.796 | 0.0469 | 5.97 | 45 | 4.22 | Al1100 | 0.051 | 0.16 | 2.713 | 10.16 | 32 | 0.483 | 1.52 | Al6061-T6 | 36 | 1.680 | C2 |
| 66 | A1196 | JSC-HIRL | Al2017T4 | 0.200 | 2.796 | 0.0117 | 7.20 | 0 | 7.20 | Al1100 | 0.036 | 0.18 | 2.713 | 6.35 | 31.8 | 0.159 | 0.79 | Al2024-T3 | 47 | 0.972 | E2 |
| 67 | A1199 | JSC-HIRL | Al2017T4 | 0.200 | 2.796 | 0.0117 | 5.70 | 0 | 5.70 | Al1100 | 0.036 | 0.18 | 2.713 | 6.35 | 31 8 | 0.483 | 2.41 | Al6061-T6 | 36 | 2.591 | E1 |
| 68 | A1210 | JSC-HIRL | Al2017T4 | 0.318 | 2.796 | 0.0469 | 6.27 | 0 | 6.27 | Al1100 | 0.051 | 0.16 | 2.713 | 10.16 | 32 | 0.203 | 0.64 | Al2024-T3 | 47 | 0.800 | E3 |
| 69 | A1211 | JSC-HIRL | Al2017T4 | 0.200 | 2.796 | 0.0117 | 5.06 | 0 | 5.06 | Al1100 | 0.036 | 0.18 | 2.713 | 6.35 | 31 8 | 0.483 | 2.41 | Al6061-T6 | 36 | 2 591 | E1 |
| 70 | A1221 | JSC-HIRL | Al2017T4 | 0.200 | 2.796 | 0.0117 | 5.42 | 0 | 5.42 | Al1100 | 0.036 | 0.18 | 2.713 | 6.35 | 31 8 | 0.318 | 1.59 | Al2024-T3 | 47 | 1 765 | E1 |
| 71 | A1222 | JSC-HIRL | Al2017T4 | 0.200 | 2.796 | 0.0117 | 4.48 | 0 | 4.48 | Al1100 | 0.036 | 0.18 | 2.713 | 6.35 | 31.8 | 0.318 | 1.59 | Al2024-T3 | 47 | 1 765 | E2 |
| 72 | A1281 | JSC-HIRL | Nylon | 0.318 | 1.145 | 0.0192 | 6.70 | 0 | 6.70 | Al1100 | 0.025 | 0.08 | 2.713 | 10.16 | 32 | 0.081 | 0.26 | Al2024-T3 | 47 | 0.336 | E4 |
| 73 | A1331 | JSC-HIRL | Al2017T4 | 0.319 | 2.796 | 0.0473 | 6.58 | 0 | 6.58 | Al1100 | 0.056 | 0.18 | 2.713 | 10 16 | 31 9 | 0.160 | 0.50 | Al2024-T3 | 47 | 0 678 | E2 |
| 74 | A1332 | JSC-HIRL | Al1100 | 0.317 | 2.713 | 0.0453 | 6.47 | 0 | 6.47 | Al1100 | 0.056 | 0.18 | 2.713 | 10.16 | 32 0 | 0.127 | 0.40 | Al6061-T6 | 36 | 0.577 | D5/E4 |
| 75 | A1333 | JSC-HIRL | Al2024T4 | 0.315 | 2.796 | 0.0458 | 6.58 | 0 | 6.58 | Al1100 | 0.056 | 0.18 | 2.713 | 10.16 | 32.2 | 0.127 | 0.40 | Al6061-T6 | 36 | 0.580 | D4/E4 |
| 76 | A1334 | JSC-HIRL | Al2017T4 | 0.317 | 2.796 | 0.0468 | 6.25 | 0 | 6.25 | Al1100 | 0.056 | 0.18 | 2.713 | 10 16 | 32.0 | 0.127 | 0.40 | Al6061-T6 | 36 | 0.576 | D5/E4 |
| 77 | A1342 | JSC-HIRL | Al2017T4 | 0.318 | 2.796 | 0.0469 | 3.96 | 0 | 3.96 | Al6061T6 | 0.127 | 0.40 | 2.713 | 10.16 | 32.0 | 0.318 | 1.00 | Al2219-T87 | 52 | 1.400 | E2/D2 |
| 78 | A1343 | JSC-HIRL | Al2017T4 | 0.359 | 2.796 | 0.0678 | 3.72 | 0 | 3.72 | Al6061T6 | 0.127 | 0.35 | 2.713 | 10 16 | 28.3 | 0.318 | 0.88 | Al2219-T87 | 52 | 1.238 | E2/D2 |
| 79 | A1344 | JSC-HIRL | Al2017T4 | 0.358 | 2.796 | 0.0674 | 3.19 | 0 | 3.19 | Al6061T6 | 0.127 | 0.35 | 2.713 | 10.16 | 28.4 | 0.318 | 0.89 | Al2219-T87 | 52 | 1.241 | D4 |
| 80 | A1347 | JSC-HIRL | Al2017T4 | 0.358 | 2.796 | 0.0673 | 2.93 | 0 | 2.93 | Al6061T6 | 0.127 | 0.35 | 2.713 | 10.16 | 28.4 | 0.318 | 0.89 | Al2219-T87 | 52 | 1.241 | D4 |
| 81 | A1360 | JSC-HIRL | Al2017T4 | 0.357 | 2.796 | 0.0667 | 5.96 | 75 | 1 54 | Al6061T6 | 0.051 | 0.14 | 2.713 | 10.16 | 28.4 | 0.127 | 0.36 | Al2024-T3 | 47 | 0.498 | C2 |
| 82 | A1363 | JSC-HIRL | Al2017T4 | 0.357 | 2.796 | 0.0667 | 6.20 | 0 | 6.20 | Al7075T6 | 0.064 | 0.18 | 2.796 | 10.16 | 28.4 | 0.127 | 0.36 | Al7075-T73 | 56 | 0.533 | D4 |
| 83 | B31 | JSC-HIRL | Al2017T4 | 0.635 | 2.796 | 0.3748 | 7.08 | 0 | 7.08 | Al6061T6 | 0.127 | 0.20 | 2.713 | 20.32 | 32 | 0.229 | 0.36 | Al6061-T6 | 36 | 0.560 | E2 |
| 84 | B37 | JSC-HIRL | Al2017T4 | 0.635 | 2.796 | 0.3748 | 6.39 | 0 | 6.39 | Al2024T3 | 0.159 | 0.25 | 2.796 | 10.16 | 16 | 0.318 | 0.50 | Al6061-T6 | 36 | 0.750 | E4 |
| 85 | B71 | JSC-HIRL | Al2017T4 | 0.635 | 2.796 | 0.3748 | 6.77 | 0 | 6.77 | Al6061T6 | 0.127 | 0.20 | 2.796 | 10.16 | 16 | 0.254 | 0.40 | Al2024-T3 | 47 | 0.600 | D5/F5 |
| 86 | B72 | JSC-HIRL | Al2017T4 | 0.635 | 2.796 | 0.3748 | 7.22 | 0 | 7.22 | Al6061T6 | 0.127 | 0.20 | 2.796 | 10.16 | 16 | 0.318 | 0.50 | Al2219-T87 | 52 | 0.700 | D3 |
| 87 | B73 | JSC-HIRL | Al2017T4 | 0.635 | 2.796 | 0.3748 | 6.80 | 0 | 6.80 | Al6061T6 | 0.127 | 0.20 | 2.796 | 10.16 | 16 | 0.318 | 0.50 | Al6061-T6 | 36 | 0.700 | D5/F5 |
| 88 | B74 | JSC-HIRL | Al2017T4 | 0.634 | 2.796 | 0.3730 | 7.20 | 60 | 3.60 | Al6061T6 | 0.127 | 0.20 | 2.796 | 10.16 | 16.0 | 0.318 | 0.50 | Al2219-T87 | 52 | 0.701 | C5 |
| 89 | GM-1 | GMRL | Aluminum | 0.318 | 2.713 | 0.0455 | 6.8 | 0 | 6.80 | Al1100 | 0.064 | 0.20 | 2.713 | 5.08 | 16 0 | 0.318 | 1.00 | Al7075-T6 | 68 | 1.200 | D1 |
| 90 | D1584 | GMRL | Aluminum | 0.318 | 2.713 | 0.0455 | 7.4 | 30 | 6.41 | Al1100 | 0.064 | 0.20 | 2.713 | 5.08 | 16.0 | 0.159 | 0.50 | Al7075-T6 | 68 | 0.700 | C3 |
| 91 | D1585 | GMRL | Aluminum | 0.318 | 2.713 | 0.0455 | 7.4 | 45 | 5.23 | Al1100 | 0.064 | 0.20 | 2.713 | 5.08 | 16.0 | 0.159 | 0.50 | Al7075-T6 | 68 | 0.700 | C5 |
| 92 | D1586 | GMRL | Aluminum | 0.318 | 2.713 | 0.0455 | 7.4 | 60 | 3.70 | Al1100 | 0.064 | 0.20 | 2.713 | 5.08 | 16.0 | 0.159 | 0.50 | Al7075-T6 | 68 | 0.700 | C3 |
| 93 | GM-5 | GMRL | Aluminum | 0.318 | 2.713 | 0.0455 | 7.4 | 30 | 6.41 | Al1100 | 0.102 | 0.32 | 2.713 | 5.08 | 16.0 | 0.159 | 0.50 | Al7075-T6 | 68 | 0.820 | C2 |
| 94 | GM-6 | GMRL | Aluminum | 0.318 | 2.713 | 0.0455 | 7.4 | 45 | 5.23 | Al1100 | 0.102 | 0.32 | 2.713 | 5.08 | 16.0 | 0.159 | 0.50 | Al7075-T6 | 68 | 0.820 | C5 |
| 95 | GM-7 | GMRL | Aluminum | 0.318 | 2.713 | 0.0455 | 7.4 | 60 | 3.70 | Al1100 | 0.102 | 0.32 | 2.713 | 5.08 | 16.0 | 0.159 | 0.50 | Al7075-T6 | 68 | 0.820 | C4 |
| 96 | GM-8 | GMRL | Aluminum | 0.318 | 2.713 | 0.0455 | 7.4 | 30 | 6.41 | Al1100 | 0.159 | 0.50 | 2.713 | 5.08 | 16.0 | 0.159 | 0.50 | Al7075-T6 | 68 | 1.000 | C2 |
| 97 | GM-9 | GMRL | Aluminum | 0.318 | 2.713 | 0.0455 | 7.4 | 45 | 5.23 | Al1100 | 0.159 | 0.50 | 2.713 | 5.08 | 16.0 | 0.159 | 0.50 | Al7075-T6 | 68 | 1.000 | C4 |
| 98 | GM-10 | GMRL | Aluminum | 0.318 | 2.713 | 0.0455 | 7.57 | 45 | 5.35 | Al1100 | 0.064 | 0.20 | 2.713 | 5.08 | 16.0 | 0.318 | 1.00 | Al7075-T6 | 68 | 1.200 | C3 |
| 99 | GM-11 | GMRL | Aluminum | 0.318 | 2.713 | 0.0455 | 7.57 | 60 | 3.79 | Al1100 | 0.064 | 0.20 | 2.713 | 5.08 | 16.0 | 0.318 | 1.00 | Al7075-T6 | 68 | 1.200 | C2 |
| 100 | GM-12 | GMRL | Aluminum | 0.318 | 2.713 | 0.0455 | 7.57 | 45 | 5.35 | Al1100 | 0.102 | 0.32 | 2.713 | 5.08 | 16.0 | 0.318 | 1.00 | Al7075-T6 | 68 | 1.320 | C2 |

# WHIPPLE_EXCEL DATA

Translated from

K=tw*(Y/70)^.5*S^.5*(pp*pb)^-1/6*Vn^-1*M^-1/3
K"=tw*(Y/70)^.5*S^.5*(pp*pb)^-1/6*Vn^-1*M^-1/3*d^-.5

K=tw*(Y/70)^.5*S^.5*(pp*pb)^
K"=tw*(Y/70)^.5*S^.5*(pp*pb)^

| | Shot No. | Damage Description | JSC Whipple Eqns. dcrit (cm) | dcrit-d (cm) | Fail? 1=Y, 0=N) | Perf. Pred. | Safe Acc? | Pred. Accurate? | Comments | dc/d | K | K" | ELC JSC Whipple Eq Category (cm) |
|---|---|---|---|---|---|---|---|---|---|---|---|---|---|
| 51 | A316 | 4 Perfs. (max 10.7x2.3mm) | 0.226 | -0.0910 | 1 | 1 | 1 | 1 | 16mil 3003-0 wit: 11 perfs | 0.713 | 0.1394 | 0.2476 | 0.225761 |
| 52 | A481 | No hole; att'd spall 0.5cm dia; thru crack | 0.286 | -0.0310 | 1 | 1 | 1 | 1 | | 0.902 | 0.1007 | 0.1787 | 0.286466 |
| 53 | A558 | No Perf (?) | 0.287 | -0.0302 | 0 | 1 | 1 | 0 | | 0.905 | 0.9245 | 1.6407 | 0.218443 |
| 54 | A570 | No Perf (?) | 0.221 | -0.0966 | 0 | 1 | 1 | 0 | | 0.696 | 0.6825 | 1.2112 | 0.141647 |
| 55 | A689 | 6 Perfs: 7x5mm max | 0.255 | -0.0627 | 1 | 1 | 1 | 1 | | 0.803 | 0.1799 | 0.3193 | 0.254797 |
| 56 | A690 | 4 Perfs: 3 interconnected 12mmx5mm | 0.223 | -0.0941 | 1 | 1 | 1 | 1 | | 0.704 | 0.2070 | 0.3674 | 0.223402 |
| 57 | A939 | Detached spall (7x10mm) | 0.280 | -0.0370 | 1 | 1 | 1 | 1 | | 0.883 | 0.1384 | 0.2458 | 0.279839 |
| 58 | A1005 | Perfs (25): 3.2x4.4mm max., many dmpls | 0.197 | -0.1216 | 1 | 1 | 1 | 1 | | 0.618 | 0.0714 | 0.1265 | 0.19671 |
| 59 | A1076 | Numerous perforations and spall dimples | 0.108 | -0.0921 | 1 | 1 | 1 | 1 | | 0.539 | 0.0353 | 0.0789 | 0.107858 |
| 60 | A1077 | No perfs, numerous spall (attached) dimples | 0.152 | -0.0479 | 0 | 1 | 1 | 0 | | 0.761 | 0.0519 | 0.1161 | 0.152132 |
| 61 | A1112 | Perforated, hole 6mm, surface cratered | 0.395 | 0.0779 | 1 | 0 | 0 | 0 | | 1.245 | 0.3743 | 0.6643 | 0.395434 |
| 62 | A1114 | Thin spall 1cm dia; 2 perfs | 0.327 | 0.0099 | 1 | 0 | 0 | 0 | | 1.031 | 0.1321 | 0.2345 | 0.327352 |
| 63 | A1184 | No hole; large craters and attached spall | 0.378 | 0.1403 | 0 | 0 | 1 | 1 | | 1.589 | 0.4227 | 0.8662 | 0.378433 |
| 64 | A1193 | No hole or tear; thin spall 2 mm dia; 1 perf | 0.356 | 0.0386 | 1 | 0 | 0 | 0 | | 1.122 | 0.1471 | 0.2610 | 0.356084 |
| 65 | A1195 | No hole, large craters and spall (attached) | 0.475 | 0.1576 | 0 | 0 | 1 | 1 | | 1.496 | 0.5171 | 0.9177 | 0.475074 |
| 66 | A1196 | No tear,hole or perfs; small central craters | 0.317 | 0.1174 | 0 | 0 | 1 | 1 | | 1.587 | 0.1430 | 0.3198 | 0.334038 |
| 67 | A1199 | Too thick; central and ring craters | 0.502 | 0.3021 | 0 | 0 | 1 | 1 | | 2.511 | 0.4806 | 1.0748 | 0.502148 |
| 68 | A1210 | No tear, hole or perfs; thin spall 2.5 mm dia | 0.391 | 0.0735 | 1 | 0 | 0 | 0 | | 1.232 | 0.1675 | 0.2973 | 0.391023 |
| 69 | A1211 | Too thick; central and ring craters | 0.444 | 0.2436 | 0 | 0 | 1 | 1 | | 2.218 | 0.5414 | 1.2107 | 0.443584 |
| 70 | A1221 | Too thick; central and ring craters | 0.389 | 0.1893 | 0 | 0 | 1 | 1 | | 1.946 | 0.3800 | 0.8497 | 0.389284 |
| 71 | A1222 | Beginning central and ring spallation | 0.315 | 0.1154 | 0 | 0 | 1 | 1 | | 1.577 | 0.4597 | 1.0279 | 0.315386 |
| 72 | A1281 | Many small, dispersed perforations | 0.309 | -0.0086 | 1 | 1 | 1 | 1 | | 0.973 | 0.0980 | 0.1739 | 0.308874 |
| 73 | A1331 | No perf, s. bulge, craters, dimples | 0.353 | 0.0348 | 0 | 0 | 1 | 1 | | 1.109 | 0.1253 | 0.2220 | 0.353385 |
| 74 | A1332 | Perfs (7): 2.5 mm max., ring perfs | 0.274 | -0.0428 | 1 | 1 | 1 | 1 | .025" Al3003H14 wit: 1 dmpl | 0.865 | 0.0902 | 0.1602 | 0.274343 |
| 75 | A1333 | Perfs (4): 0.7 mm max., ring perfs | 0.277 | -0.0381 | 1 | 1 | 1 | 1 | 025" Al3003H14 wit: s.crater | 0.879 | 0.0879 | 0.1566 | 0.277104 |
| 76 | A1334 | Perfs (12): 3x2 mm max., ring perfs | 0.260 | -0.0570 | 1 | 1 | 1 | 1 | 025" Al3003H14 wit: 1 dmpl | 0.820 | 0.0919 | 0.1632 | 0.260433 |
| 77 | A1342 | No perfs, craters & dimples | 0.341 | 0.0237 | 0 | 0 | 1 | 1 | | 1.075 | 0.4358 | 0.7733 | 0.341307 |
| 78 | A1343 | No perfs, craters & dimples | 0.319 | -0.0399 | 0 | 1 | 1 | 0 | | 0.889 | 0.4102 | 0.6845 | 0.319212 |
| 79 | A1344 | 1 Perf (<1mm), 8mm det. spall, 4mm thru crack | 0.270 | -0.0879 | 1 | 1 | 1 | 1 | Wit .025" Al3003H14: lrg dmpl | 0.755 | 0.4794 | 0.8010 | 0.27042 |
| 80 | A1347 | 1 Perf (.6 mm), 6mm det. spall | 0.257 | -0.1015 | 1 | 1 | 1 | 1 | Wit .025"Al3003H14:perf/split (5mmx1m | 0.717 | 0.5222 | 0.8725 | 0.246484 |
| 81 | A1360 | No perf, ~30 dmpls | 0.561 | 0.2042 | 0 | 0 | 1 | 1 | | 1.572 | 0.3782 | 0.6329 | 0.384406 |
| 82 | A1363 | 8 perfs (max 1.5 mm), det.spall (13x7mm) | 0.299 | -0.0585 | 1 | 1 | 1 | 1 | Wit 025"Al3003H14:5-6 dmpls, no perf | 0.836 | 0.1022 | 0.1710 | 0.2987 |
| 83 | B31 | Central and ring dimples/spallation | 0.552 | -0.0832 | 0 | 1 | 1 | 0 | | 0.869 | 0.1033 | 0.1296 | 0.563672 |
| 84 | B37 | Small hole, detached spall (30 mm dia.) | 0.501 | -0.1344 | 1 | 1 | 1 | 1 | | 0.788 | 0.1118 | 0.1403 | 0.500553 |
| 85 | B71 | Petalled Hole (~11mm), Det.Spall (37mm) | 0.498 | -0.1367 | 1 | 1 | 1 | 1 | Wit (.04" Al2024): large dmpls | 0.785 | 0.0965 | 0.1211 | 0.498269 |
| 86 | B72 | No perf, detached spall (35 x 28 mm) | 0.606 | -0.0287 | 1 | 1 | 1 | 1 | Wit (.04" Al2024): dmpls | 0.955 | 0.1189 | 0.1493 | 0.639234 |
| 87 | B73 | Perf, split (20 mm long), det. spall(40x30mm) | 0.531 | -0.1036 | 1 | 1 | 1 | 1 | Wit (.04" Al2024): dmpls | 0.837 | 0.1051 | 0.1319 | 0.531444 |
| 88 | B74 | 3 Perfs (11x6mm max), craters, det. spall | 0.507 | -0.1265 | 1 | 1 | 1 | 1 | Wit (.04" Al2024): dmpls | 0.800 | 0.2389 | 0.3001 | 0.507439 |
| 89 | GM-1 | No perf or spall | 0.530 | 0.2124 | 0 | 0 | 1 | 1 | | 1.669 | 0.2084 | 0.3698 | 0.529897 |
| 90 | D1584 | No perf, detached spall | 0.317 | -0.0003 | 1 | 1 | 1 | 1 | | 0.999 | 0.1105 | 0.1962 | 0.317151 |
| 91 | D1585 | Perf (~5x2mm) | 0.281 | -0.0362 | 1 | 1 | 1 | 1 | | 0.886 | 0.1354 | 0.2403 | 0.281314 |
| 92 | D1586 | No perf, detached spall | 0.293 | -0.0245 | 1 | 1 | 1 | 1 | | 0.923 | 0.1915 | 0.3398 | 0.292954 |
| 93 | GM-5 | No perf or detached spall | 0.320 | 0.0029 | 0 | 0 | 1 | 1 | | 1.009 | 0.1105 | 0.1962 | 0.320449 |
| 94 | GM-6 | Perf | 0.293 | -0.0242 | 1 | 1 | 1 | 1 | | 0.924 | 0.1354 | 0.2403 | 0.293259 |
| 95 | GM-7 | Perf | 0.324 | 0.0064 | 1 | 0 | 0 | 0 | | 1.020 | 0.1915 | 0.3398 | 0.323925 |
| 96 | GM-8 | No perf or detached spall | 0.325 | 0.0079 | 0 | 0 | 1 | 1 | | 1.025 | 0.1105 | 0.1962 | 0.325358 |
| 97 | GM-9 | Perf | 0.311 | -0.0065 | 1 | 1 | 1 | 1 | | 0.980 | 0.1354 | 0.2403 | 0.311035 |
| 98 | GM-10 | No perf, detached spall | 0.464 | 0.1463 | 1 | 0 | 0 | 0 | | 1.461 | 0.2647 | 0.4698 | 0.463759 |
| 99 | GM-11 | No perf or detached spall | 0.496 | 0.1781 | 0 | 0 | 1 | 1 | | 1.561 | 0.3743 | 0.6644 | 0.495635 |
| 100 | GM-12 | No perf or detached spall | 0.475 | 0.1571 | 0 | 0 | 1 | 1 | | 1.495 | 0.2647 | 0.4698 | 0.47458 |

Translated from Lotus by L.Thompson (714) 896-4495

## Whipple Database

| | Shot No. | Site | Proj. Mat'l | Proj. Dia. (cm) | Proj. Dens. (g/cc) | Proj. Mass (g) | Vel. (km/sec) | Impact Angle (deg) | Normal Vel. (km/sec) | Bumper Mat'l | Bumper Thk (cm) | tb/d | Bumper Dens. (g/cc) | Spacing (cm) | S/d | Wall Th'k (cm) | tw/d | Wall Mat'l | Yield Stress (ksi) | (tb+tw)/d | Category |
|---|---|---|---|---|---|---|---|---|---|---|---|---|---|---|---|---|---|---|---|---|---|
| 101 | GM-13 | GMRL | Aluminum | 0.318 | 2.713 | 0.0455 | 7.57 | 60 | 3.79 | Al1100 | 0.102 | 0.32 | 2.713 | 5.08 | 16.0 | 0.318 | 1.00 | Al7075-T6 | 68 | 1.320 | C2 |
| 102 | GM-14 | GMRL | Aluminum | 0.318 | 2.713 | 0.0455 | 7.57 | 45 | 5.35 | Al1100 | 0.159 | 0.50 | 2.713 | 5.08 | 16.0 | 0.318 | 1.00 | Al7075-T6 | 68 | 1.500 | C2 |
| 103 | GM-15 | GMRL | Aluminum | 0.318 | 2.713 | 0.0455 | 7.57 | 60 | 3.79 | Al1100 | 0.159 | 0.50 | 2.713 | 5.08 | 16.0 | 0.318 | 1.00 | Al7075-T6 | 68 | 1.500 | C2 |
| 104 | GM-16 | GMRL | Aluminum | 0.318 | 2.713 | 0.0455 | 7.62 | 30 | 6.60 | Al1100 | 0.064 | 0.20 | 2.713 | 5.08 | 16.0 | 0.635 | 2.00 | Al7075-T6 | 68 | 2.200 | C2 |
| 105 | GM-17 | GMRL | Aluminum | 0.318 | 2.713 | 0.0455 | 7.62 | 45 | 5.39 | Al1100 | 0.064 | 0.20 | 2.713 | 5.08 | 16.0 | 0.635 | 2.00 | Al7075-T6 | 68 | 2.200 | C2 |
| 106 | A86/1 | ARC | Al2017T4 | 0.953 | 2.796 | 1.2651 | 6.65 | 0 | 6.65 | Al2024T3 | 0.159 | 0.17 | 2.796 | 30.48 | 32 | 0.635 | 0.67 | Al2024-T351 | 47 | 0.833 | D1 |
| 107 | A86/2 | ARC | Al2017T4 | 0.953 | 2.796 | 1.2651 | 6.64 | 0 | 6.64 | Al2024T3 | 0.318 | 0.33 | 2.796 | 30.48 | 32 | 0.229 | 0.24 | Al2024-T3 | 47 | 0.573 | F2 |
| 108 | A86/3 | ARC | Al2017T4 | 0.953 | 2.796 | 1.2651 | 6.65 | 0 | 6.65 | Al2024T3 | 0.159 | 0.17 | 2.796 | 30.48 | 32 | 0.229 | 0.24 | Al2024-T3 | 47 | 0.407 | F4 |
| 109 | A86/4 | ARC | Al2017T4 | 0.953 | 2.796 | 1.2651 | 6.40 | 0 | 6.40 | Al2024T3 | 0.483 | 0.51 | 2.796 | 30.48 | 32 | 0.229 | 0.24 | Al2024-T3 | 47 | 0.747 | E4 |
| 110 | 1732 | ARC | Al2017T4 | 0.953 | 2.796 | 1.2651 | 6.47 | 0 | 6.47 | Al2024T3 | 0.159 | 0.17 | 2.796 | 30.48 | 32 | 0.318 | 0.33 | Al2024-T3 | 47 | 0.500 | F4 |
| 111 | 1761 | ARC | Al2017T4 | 0.953 | 2.796 | 1.2651 | 6.50 | 45 | 4.60 | Al2024T3 | 0.159 | 0.17 | 2.796 | 30.48 | 32 | 0.318 | 0.33 | Al6061-T6 | 36 | 0.500 | C5 |
| 112 | 1868 | ARC | Al2017T4 | 0.953 | 2.796 | 1.2651 | 7.10 | 0 | 7.10 | Al2024T3 | 0.159 | 0.17 | 2.796 | 30.48 | 32 | 0.318 | 0.33 | Al6061-T6 | 36 | 0.500 | F3 |
| 113 | 1869 | ARC | Al2024T4 | 0.893 | 2.796 | 1.0436 | 6.70 | 0 | 6.70 | Al2024T3 | 0.159 | 0.18 | 2.796 | 15.24 | 17.1 | 0.127 | 0.14 | Al2024-T3 | 47 | 0.320 | D5 |
| 114 | 1870 | ARC | Al2024T4 | 0.954 | 2.796 | 1.2697 | 6.53 | 0 | 6.53 | Al2024T3 | 0.159 | 0.17 | 2.796 | 15.24 | 16.0 | 0.483 | 0.51 | Al6061-T6 | 36 | 0.673 | D5 |
| 115 | 1871 | ARC | SS316 | 0.955 | 7.86 | 3.5872 | 5.44 | 0 | 5.44 | Al2024T3 | 0.318 | 0.33 | 2.796 | 30.48 | 31.9 | 0.635 | 0.66 | Al6061-T6 | 36 | 0.997 | E5 |
| 116 | 1872 | ARC | SS316 | 0.955 | 7.86 | 3.5870 | 5.45 | 0 | 5.45 | Al2024T3 | 0.318 | 0.33 | 2.796 | 45.72 | 47.9 | 0.635 | 0.66 | Al6061-T6 | 36 | 0.997 | E5 |
| 117 | 1873 | ARC | Al2017T4 | 0.953 | 2.796 | 1.2681 | 6.89 | 0 | 6.89 | Al2024T3 | 0.081 | 0.09 | 2.796 | 30.48 | 32.0 | 0.635 | 0.67 | Al6061-T6 | 36 | 0.751 | E2 |
| 118 | 1874 | ARC | SS316 | 0.955 | 7.86 | 3.5870 | 5.45 | 0 | 5.45 | Al2024T3 | 0.318 | 0.33 | 2.796 | 30.48 | 31.9 | 0.635 | 0.66 | Al2024-T351 | 47 | 0.997 | E5 |
| 119 | 1875 | ARC | Al2017T4 | 0.953 | 2.796 | 1.2651 | 6.75 | 0 | 6.75 | Al2024T3 | 0.159 | 0.17 | 2.796 | 30.48 | 32 | 0.318 | 0.33 | Al6061-T6 | 36 | 0.500 | F3 |
| 120 | 1894 | ARC | Al2017T4 | 0.953 | 2.796 | 1.2651 | 6.74 | 45 | 4.77 | Al2024T3 | 0.159 | 0.17 | 2.796 | 30.48 | 32 | 0.795 | 0.83 | Al2024-T351 | 47 | 1.001 | C4 |
| 121 | 1895 | ARC | Al2017T4 | 0.953 | 2.796 | 1.2651 | 6.89 | 0 | 6.89 | Al2024T3 | 0.159 | 0.17 | 2.796 | 30.48 | 32 | 0.318 | 0.33 | Al6061-T6 | 36 | 0.500 | F3 |
| 122 | 1899 | ARC | Al2017T4 | 0.953 | 2.796 | 1.2651 | 6.83 | 0 | 6.83 | Al2024T3 | 0.159 | 0.17 | 2.796 | 15.24 | 16 | 0.635 | 0.67 | Al2024-T351 | 47 | 0.833 | D3 |
| 123 | 1907 | ARC | Al2017T4 | 1.270 | 2.796 | 2.9988 | 6.53 | 0 | 6.53 | Al2024T3 | 0.318 | 0.25 | 2.796 | 50.80 | 40 | 0.483 | 0.38 | Al2024-T351 | 47 | 0.630 | E4 |
| 124 | 1913 | ARC | Al2017T4 | 1.270 | 2.796 | 2.9988 | 6.71 | 0 | 6.71 | Al2024T3 | 0.318 | 0.25 | 2.796 | 50.80 | 40 | 0.483 | 0.38 | Al6061-T6 | 36 | 0.630 | D2 |
| 125 | 1917 | ARC | Al2017T4 | 0.953 | 2.796 | 1.2651 | 6.72 | 0 | 6.72 | Al2024T3 | 0.159 | 0.17 | 2.796 | 22.86 | 24 | 0.483 | 0.51 | Al2024-T351 | 47 | 0.673 | D2 |
| 126 | 1918 | ARC | Al2017T4 | 0.953 | 2.796 | 1.2651 | 6.83 | 0 | 6.83 | Al2024T3 | 0.159 | 0.17 | 2.796 | 38.10 | 40 | 0.318 | 0.33 | Al2024-T3 | 47 | 0.500 | E2 |
| 127 | 1921 | ARC | Al2017T4 | 1.270 | 2.796 | 2.9988 | 6.80 | 0 | 6.80 | Al2024T3 | 0.159 | 0.13 | 2.796 | 22.86 | 18 | 0.635 | 0.50 | Al2024-T351 | 47 | 0.625 | D3 |
| 128 | MD15 | MDAC | Aluminum | 0.884 | 2.78 | 1.0053 | 7.08 | 0 | 7.08 | Al2024T351 | 0.229 | 0.26 | 2.796 | 26.52 | 30 | 0.201 | 0.23 | Al2024-T351 | 47 | 0.486 | E3 |
| 129 | MD27 | MDAC | Aluminum | 1.908 | 2.78 | 10.1106 | 7.15 | 0 | 7.15 | Al2024T351 | 0.406 | 0.21 | 2.796 | 28.58 | 15.0 | 2.827 | 1.48 | Al2024-T351 | 47 | 1.695 | D2 |
| 130 | MD28 | MDAC | Aluminum | 1.908 | 2.78 | 10.1106 | 7.08 | 0 | 7.08 | Al2024T351 | 0.406 | 0.21 | 2.796 | 57.15 | 30.0 | 0.968 | 0.51 | Al2024-T351 | 47 | 0.720 | E2 |
| 131 | MD29 | MDAC | Aluminum | 1.908 | 2.78 | 10.1106 | 7.08 | 0 | 7.08 | Al2024T351 | 0.406 | 0.21 | 2.796 | 76.2 | 39.9 | 0.622 | 0.33 | Al2024-T351 | 47 | 0.539 | E3 |
| 132 | MD31 | MDAC | Aluminum | 1.908 | 2.78 | 10.1106 | 7.15 | 0 | 7.15 | Al2024T351 | 0.813 | 0.43 | 2.796 | 57.15 | 30.0 | 0.800 | 0.42 | Al2024-T351 | 47 | 0.845 | E2 |
| 133 | 1675 | Burch-BAC | Al2017 | 0.635 | 2.796 | 0.3748 | 4.97 | 0 | 4.97 | Al2024T3 | 0.102 | 0.16 | 2.796 | 7.62 | 12.0 | 0.051 | 0.08 | Al2024-T4 | 47 | 0.240 | C5 |
| 134 | 1676 | Burch-BAC | Al2017 | 0.635 | 2.796 | 0.3748 | 5.79 | 0 | 5.79 | Al2024T3 | 0.102 | 0.16 | 2.796 | 7.62 | 12.0 | 0.051 | 0.08 | Al2024-T4 | 47 | 0.240 | C5 |
| 135 | 1677 | Burch-BAC | Al2017 | 0.635 | 2.796 | 0.3748 | 5.33 | 30 | 4.62 | Al2024T3 | 0.102 | 0.16 | 2.796 | 7.62 | 12.0 | 0.051 | 0.08 | Al2024-T4 | 47 | 0.240 | C5 |
| 136 | 1678 | Burch-BAC | Al2017 | 0.635 | 2.796 | 0.3748 | 5.09 | 45 | 3.60 | Al2024T3 | 0.102 | 0.16 | 2.796 | 7.62 | 12.0 | 0.051 | 0.08 | Al2024-T4 | 47 | 0.240 | C5 |
| 137 | 1679 | Burch-BAC | Al2017 | 0.635 | 2.796 | 0.3748 | 5.24 | 30 | 4.54 | Al2024T3 | 0.203 | 0.32 | 2.796 | 7.62 | 12.0 | 0.051 | 0.08 | Al2024-T4 | 47 | 0.400 | C5 |
| 138 | 1680 | Burch-BAC | Al2017 | 0.635 | 2.796 | 0.3748 | 5.27 | 45 | 3.73 | Al2024T3 | 0.203 | 0.32 | 2.796 | 7.62 | 12.0 | 0.051 | 0.08 | Al2024-T4 | 47 | 0.400 | C5 |
| 139 | 1681 | Burch-BAC | Al2017 | 0.635 | 2.796 | 0.3748 | 5.09 | 30 | 4.41 | Al2024T3 | 0.406 | 0.64 | 2.796 | 7.62 | 12.0 | 0.051 | 0.08 | Al2024-T4 | 47 | 0.720 | C5 |
| 140 | 1682 | Burch-BAC | Al2017 | 0.635 | 2.796 | 0.3748 | 5.36 | 45 | 3.79 | Al2024T3 | 0.406 | 0.64 | 2.796 | 7.62 | 12.0 | 0.051 | 0.08 | Al2024-T4 | 47 | 0.720 | C5 |
| 141 | 1683 | Burch-BAC | Al2017 | 0.635 | 2.796 | 0.3748 | 5.09 | 60 | 2.55 | Al2024T3 | 0.102 | 0.16 | 2.796 | 7.62 | 12.0 | 0.051 | 0.08 | Al2024-T4 | 47 | 0.240 | C5 |
| 142 | 1684 | Burch-BAC | Al2017 | 0.635 | 2.796 | 0.3748 | 5.24 | 60 | 2.62 | Al2024T3 | 0.203 | 0.32 | 2.796 | 7.62 | 12.0 | 0.051 | 0.08 | Al2024-T4 | 47 | 0.400 | C5 |
| 143 | 1685 | Burch-BAC | Al2017 | 0.635 | 2.796 | 0.3748 | 5.09 | 60 | 2.55 | Al2024T3 | 0.406 | 0.64 | 2.796 | 7.62 | 12.0 | 0.051 | 0.08 | Al2024-T4 | 47 | 0.720 | C5 |
| 144 | 1686 | Burch-BAC | Al2017 | 0.635 | 2.796 | 0.3748 | 5.36 | 30 | 4.65 | Al2024T3 | 0.102 | 0.16 | 2.796 | 15.24 | 24.0 | 0.051 | 0.08 | Al2024-T4 | 47 | 0.240 | C5 |
| 145 | 1687 | Burch-BAC | Al2017 | 0.635 | 2.796 | 0.3748 | 5.12 | 45 | 3.62 | Al2024T3 | 0.102 | 0.16 | 2.796 | 15.24 | 24.0 | 0.051 | 0.08 | Al2024-T4 | 47 | 0.240 | C5 |
| 146 | 1688 | Burch-BAC | Al2017 | 0.635 | 2.796 | 0.3748 | 4.63 | 60 | 2.32 | Al2024T3 | 0.102 | 0.16 | 2.796 | 15.24 | 24.0 | 0.051 | 0.08 | Al2024-T4 | 47 | 0.240 | C5 |
| 147 | 1689 | Burch-BAC | Al2017 | 0.635 | 2.796 | 0.3748 | 5.09 | 45 | 3.60 | Al2024T3 | 0.102 | 0.16 | 2.796 | 22.86 | 36.0 | 0.051 | 0.08 | Al2024-T4 | 47 | 0.240 | C5 |
| 148 | 1690 | Burch-BAC | Al2017 | 0.635 | 2.796 | 0.3748 | 4.97 | 60 | 2.48 | Al2024T3 | 0.102 | 0.16 | 2.796 | 22.86 | 36.0 | 0.051 | 0.08 | Al2024-T4 | 47 | 0.240 | C5 |
| 149 | 1691 | Burch-BAC | Al2017 | 0.635 | 2.796 | 0.3748 | 4.57 | 70 | 1.56 | Al2024T3 | 0.102 | 0.16 | 2.796 | 7.62 | 12.0 | 0.051 | 0.08 | Al2024-T4 | 47 | 0.240 | C5 |
| 150 | 1692 | Burch-BAC | Al2017 | 0.635 | 2.796 | 0.3748 | 3.41 | 45 | 2.41 | Al2024T3 | 0.102 | 0.16 | 2.796 | 7.62 | 12.0 | 0.051 | 0.08 | Al2024-T4 | 47 | 0.240 | C5 |

# WHIPPLE_EXCEL DATA

Translated from

K=tw*(Y/70)^.5*S^.5*(pp*pb)^-1/6*Vn^-1*M^-1/3
K"=tw*(Y/70)^.5*S^.5*(pp*pb)^-1/6*Vn^-1*M^-1/3*d^-.5

K=tw*(Y/70)^.5*S^.5*(pp*pb)^
K"=tw*(Y/70)^.5*S^.5*(pp*pb)^

| | Shot No. | Damage Description | JSC Whipple Eqns. dcrit (cm) | dcrit-d (cm) | Fail? 1=Y, 0=N) | Perf. Pred. | Safe Acc? | Pred. Accurate? | Comments | dc/d | K | K" | JSC Whipple Eq Category (cm) |
|---|---|---|---|---|---|---|---|---|---|---|---|---|---|
| 101 | GM-13 | No perf or detached spall | 0.525 | 0.2075 | 0 | 0 | 1 | 1 | | 1.653 | 0.3743 | 0.6644 | 0.524963 |
| 102 | GM-14 | No perf or detached spall | 0.491 | 0.1732 | 0 | 0 | 1 | 1 | | 1.546 | 0.2647 | 0.4698 | 0.490734 |
| 103 | GM-15 | No perf or detached spall | 0.569 | 0.2512 | 0 | 0 | 1 | 1 | | 1.791 | 0.3743 | 0.6644 | 0.568745 |
| 104 | GM-16 | No perf or detached spall | 0.830 | 0.5124 | 0 | 0 | 1 | 1 | | 2.614 | 0.4294 | 0.7621 | 0.829883 |
| 105 | GM-17 | No perf or detached spall | 0.770 | 0.4522 | 0 | 0 | 1 | 1 | | 2.424 | 0.5259 | 0.9334 | 0.7697 |
| 106 | A86/1 | No hole or spall; front surface erosion | 1.288 | 0.3352 | 0 | 0 | 1 | 1 | | 1.352 | 0.2835 | 0.2905 | 1.287739 |
| 107 | A86/2 | No hole or tear; impulsive dent;1 incip spall | 0.657 | -0.2953 | 0 | 1 | 1 | 0 | | 0.690 | 0.1022 | 0.1047 | 0.657206 |
| 108 | A86/3 | Dented with 0.16 cm crack; incip spall ring | 0.651 | -0.3011 | 1 | 1 | 1 | 1 | | 0.684 | 0.1021 | 0.1046 | 0.651404 |
| 109 | A86/4 | No hole or tear; perf ring; no central spall | 0.645 | -0.3075 | 1 | 1 | 1 | 1 | | 0.677 | 0.1061 | 0.1087 | 0.644964 |
| 110 | 1732 | Dented with 3 cracks; 3 sm perfs; thin spall | 0.783 | -0.1692 | 1 | 1 | 1 | 1 | JSC A86/5 | 0.822 | 0.1457 | 0.1493 | 0.783329 |
| 111 | 1761 | Perfs (20): Max ~30mm x 12 mm | 0.514 | -0.4381 | 1 | 1 | 1 | 1 | Wit .063" Al: 3 perfs (1.5mm) | 0.540 | 0.1795 | 0.1839 | 0.514377 |
| 112 | 1868 | Dented; no tear or spall; A1732 w/6061-T6 | 0.782 | -0.1703 | 0 | 1 | 1 | 0 | | 0.821 | 0.1162 | 0.1191 | 0.803666 |
| 113 | 1869 | Perforated (L/D=3 proj., hit parallel) | 0.356 | -0.5374 | 1 | 1 | 1 | 1 | .125" Al 3rd perf. @ 6" | 0.398 | 0.0424 | 0.0449 | 0.355892 |
| 114 | 1870 | Perforated, 55 mm diameter spall | 0.768 | -0.1852 | 1 | 1 | 1 | 1 | Wit .125 Al6061: dented | 0.806 | 0.1356 | 0.1389 | 0.768434 |
| 115 | 1871 | Cooking cutter perf (? mm dia) | 0.652 | -0.3033 | 1 | 1 | 1 | 1 | Wit .125 Al6061: | 0.682 | 0.1804 | 0.1846 | 0.651949 |
| 116 | 1872 | Cooking cutter perf (? mm dia) | 0.732 | -0.2230 | 1 | 1 | 1 | 1 | Wit .125 Al6061: bul,cr,dmpl | 0.767 | 0.2205 | 0.2256 | 0.732212 |
| 117 | 1873 | No perf | 1.229 | 0.2757 | 0 | 0 | 1 | 1 | | 1.289 | 0.2393 | 0.2451 | 1.228938 |
| 118 | 1874 | Cooking cutter perf (103 mm dia) | 0.714 | -0.2415 | 1 | 1 | 1 | 1 | Wit .125 Al6061: bul,cr,dmpl | 0.747 | 0.2057 | 0.2105 | 0.713689 |
| 119 | 1875 | Dented; no tear or spall; #1868 w/ 2mm press. | 0.755 | -0.1971 | 0 | 1 | 1 | 0 | | 0.793 | 0.1222 | 0.1252 | 0.755435 |
| 120 | 1894 | 2 perfs (0.9 and 0.5 cm) | 1.097 | 0.1441 | 1 | 0 | 0 | 0 | | 1.151 | 0.4953 | 0.5075 | 1.096637 |
| 121 | 1895 | Dented; no tear or spall; #1868 repeat | 0.775 | -0.1778 | 0 | 1 | 1 | 0 | | 0.813 | 0.1197 | 0.1227 | 0.774727 |
| 122 | 1899 | No hole or tear; thin, 5cm detached spall | 1.060 | 0.1071 | 0 | 0 | 1 | 1 | | 1.112 | 0.1952 | 0.2000 | 1.059555 |
| 123 | 1907 | No tear; 1 perf 0.48cm; attached spall | 1.244 | -0.0262 | 1 | 1 | 1 | 1 | | 0.979 | 0.2125 | 0.1885 | 1.243794 |
| 124 | 1913 | No tear or spall; some impulsive denting | 1.177 | -0.0933 | 0 | 1 | 1 | 0 | | 0.927 | 0.1810 | 0.1606 | 1.176681 |
| 125 | 1917 | No hole or tear; attached spall with crack | 0.989 | 0.0361 | 0 | 0 | 1 | 1 | | 1.038 | 0.1847 | 0.1892 | 0.988596 |
| 126 | 1918 | No hole or perf; ring & central incip spalls | 0.901 | -0.0510 | 0 | 1 | 1 | 0 | | 0.946 | 0.1543 | 0.1581 | 0.901479 |
| 127 | 1921 | No hole or tear; thin 7.6cm detached spall | 1.204 | -0.0659 | 1 | 1 | 1 | 1 | | 0.948 | 0.1801 | 0.1598 | 1.204124 |
| 128 | MD15 | No hole or tear; discrete spallations | 0.603 | -0.2806 | 1 | 1 | 1 | 1 | | 0.683 | 0.0848 | 0.0902 | 0.615616 |
| 129 | MD27 | No hole or tear; attached spall, split | 3.585 | 1.6766 | 0 | 0 | 1 | 1 | | 1.879 | 0.5691 | 0.4120 | 3.712186 |
| 130 | MD28 | No hole or tear; attached spall dimples | 2.225 | 0.3166 | 0 | 0 | 1 | 1 | | 1.166 | 0.2782 | 0.2014 | 2.272769 |
| 131 | MD29 | No hole or tear; incip spalls, some detached | 1.824 | -0.0838 | 1 | 1 | 1 | 1 | | 0.956 | 0.2066 | 0.1496 | 1.864576 |
| 132 | MD31 | No hole or tear; attached spall dimples | 1.947 | 0.0388 | 0 | 0 | 1 | 1 | | 1.020 | 0.2278 | 0.1649 | 2.018569 |
| 133 | 1675 | Perforated (2") | 0.123 | -0.5124 | 1 | 1 | 1 | 1 | 4 20mil 2024T3 wit perf LOF | 0.193 | 0.0228 | 0.0286 | 0.12257 |
| 134 | 1676 | Perforated (2.2") | 0.138 | -0.4972 | 1 | 1 | 1 | 1 | 3.3 20mil 2024T3 wit perf LOF | 0.217 | 0.0195 | 0.0245 | 0.137846 |
| 135 | 1677 | Perforated (2.1"x2.6") | 0.124 | -0.5114 | 1 | 1 | 1 | 1 | 4.3 20mil 2024T3 wit perf LOF | 0.195 | 0.0245 | 0.0307 | 0.12357 |
| 136 | 1678 | Perforated (1.8"x2.6") | 0.126 | -0.5094 | 1 | 1 | 1 | 1 | 4.1 20mil 2024T3 wit perf LOF | 0.198 | 0.0314 | 0.0394 | 0.125587 |
| 137 | 1679 | Perforated (2.8") | 0.159 | -0.4759 | 1 | 1 | 1 | 1 | 3.3 20mil 2024T3 wit perf LOF | 0.251 | 0.0249 | 0.0313 | 0.159073 |
| 138 | 1680 | Perforated (2.0"x3.7") | 0.186 | -0.4489 | 1 | 1 | 1 | 1 | 3.3 20mil 2024T3 wit perf LOF | 0.293 | 0.0303 | 0.0381 | 0.186091 |
| 139 | 1681 | Perforated (3.0"x3.5") | 0.234 | -0.4008 | 1 | 1 | 1 | 1 | 3 20mil 2024T3 wit perf LOF | 0.369 | 0.0257 | 0.0322 | 0.234203 |
| 140 | 1682 | Perforated (2.8"x3.5") | 0.298 | -0.3367 | 1 | 1 | 1 | 1 | 3 20mil 2024T3 wit perf LOF | 0.470 | 0.0298 | 0.0374 | 0.298316 |
| 141 | 1683 | Perforated (1.7"x2.7") | 0.184 | -0.4509 | 1 | 1 | 1 | 1 | 6 20mil 2024T3 wit perf LOF | 0.290 | 0.0444 | 0.0558 | 0.166545 |
| 142 | 1684 | Perforated (1.7"x2.5") | 0.290 | -0.3449 | 1 | 1 | 1 | 1 | 3.2LOF & 4Norm 20mil wit perf | 0.457 | 0.0432 | 0.0542 | 0.276444 |
| 143 | 1685 | Perforated | 0.512 | -0.1228 | 1 | 1 | 1 | 1 | 1.5LOF & 5.8Norm 20mil perf | 0.807 | 0.0444 | 0.0558 | 0.49595 |
| 144 | 1686 | Perforated (2.5"x3.5") | 0.141 | -0.4939 | 1 | 1 | 1 | 1 | 3.3LOF 20mil 2024T3 wit perf | 0.222 | 0.0344 | 0.0432 | 0.141118 |
| 145 | 1687 | Perforated (1.2"x2") | 0.132 | -0.5027 | 1 | 1 | 1 | 1 | 4.7LOF 20mil 2024T3 wit perf | 0.208 | 0.0442 | 0.0554 | 0.132273 |
| 146 | 1688 | Perforated (0.8"x1.4") | 0.195 | -0.4397 | 1 | 1 | 1 | 1 | 4LOF 20mil 2024T3 wit perf | 0.308 | 0.0691 | 0.0867 | 0.159748 |
| 147 | 1689 | Perforated (0.5"x0.9") | 0.136 | -0.4988 | 1 | 1 | 1 | 1 | 5LOF 20mil 2024T3 wit perf | 0.214 | 0.0544 | 0.0683 | 0.136207 |
| 148 | 1690 | Perforated | 0.187 | -0.4481 | 1 | 1 | 1 | 1 | 4LOF 20mil 2024T3 wit perf | 0.294 | 0.0789 | 0.0990 | 0.157489 |
| 149 | 1691 | Perforated (1.1"x1.8") | 0.359 | -0.2762 | 1 | 1 | 1 | 1 | 3.8LOF 20mil 2024T3 wit perf | 0.565 | 0.0723 | 0.0908 | 0.265551 |
| 150 | 1692 | Perforated (0.7"x0.9") | 0.137 | -0.4980 | 1 | 1 | 1 | 1 | 7LOF 20mil 2024T3 wit perf | 0.216 | 0.0469 | 0.0588 | 0.113493 |

Translated from Lotus by L.Thompson (714) 896-4495

## Whipple Database

| | Shot No. | Site | Proj. Mat'l | Proj. Dia. (cm) | Proj. Dens. (g/cc) | Proj. Mass (g) | Vel. (km/sec) | Impact Angle (deg) | Normal Vel. (km/sec) | Bumper Mat'l | Bumper Thk (cm) | tb/d | Bumper Dens. (g/cc) | Spacing (cm) | S/d | Wall Th'k (cm) | tw/d | Wall Mat'l | Yield Stress (ksi) | (tb+tw)/d | Category |
|---|---|---|---|---|---|---|---|---|---|---|---|---|---|---|---|---|---|---|---|---|---|
| 151 | 1693 | Burch-BAC | Al2017 | 0.318 | 2.796 | 0.0469 | 4.48 | 45 | 3.17 | Al2024T3 | 0.102 | 0.32 | 2.796 | 7.62 | 24.0 | 0.025 | 0.08 | Al2024-T4 | 47 | 0.400 | C5 |
| 152 | 1694 | Burch-BAC | Al2017 | 0.318 | 2.796 | 0.0469 | 5.82 | 45 | 4.12 | Al2024T3 | 0.102 | 0.32 | 2.796 | 7.62 | 24.0 | 0.051 | 0.16 | Al2024-T4 | 47 | 0.480 | C5 |
| 153 | 1695 | Burch-BAC | Al2017 | 0.635 | 2.796 | 0.3748 | 5.36 | 45 | 3.79 | Al2024T3 | 0.102 | 0.16 | 2.796 | 7.62 | 12.0 | 0.102 | 0.16 | Al2024-T4 | 47 | 0.320 | C5 |
| 154 | 1696 | Burch-BAC | Al2017 | 0.635 | 2.796 | 0.3748 | 5.33 | 45 | 3.77 | Al2024T3 | 0.102 | 0.16 | 2.796 | 7.62 | 12.0 | 0.102 | 0.16 | Al2024-T4 | 47 | 0.320 | C5 |
| 155 | 1697 | Burch-BAC | Al2017 | 0.635 | 2.796 | 0.3748 | 5.64 | 45 | 3.99 | Al2024T3 | 0.051 | 0.08 | 2.796 | 7.62 | 12.0 | 0.051 | 0.08 | Al2024-T4 | 47 | 0.160 | C5 |
| 156 | 1699 | Burch-BAC | Al2017 | 0.635 | 2.796 | 0.3748 | 4.05 | 60 | 2.03 | Al2024T3 | 0.051 | 0.08 | 2.796 | 7.62 | 12.0 | 0.051 | 0.08 | Al2024-T4 | 47 | 0.160 | C5 |
| 157 | 1702 | Burch-BAC | Al2017 | 0.318 | 2.796 | 0.0469 | 3.96 | 60 | 1.98 | Al2024T3 | 0.102 | 0.32 | 2.796 | 7.62 | 24.0 | 0.051 | 0.16 | Al2024-T4 | 47 | 0.480 | C5 |
| 158 | 1703 | Burch-BAC | Al2017 | 0.318 | 2.796 | 0.0469 | 4.18 | 60 | 2.09 | Al2024T3 | 0.102 | 0.32 | 2.796 | 7.62 | 24.0 | 0.025 | 0.08 | Al2024-T4 | 47 | 0.400 | C5 |
| 159 | 1705 | Burch-BAC | Al2017 | 0.635 | 2.796 | 0.3748 | 4.54 | 45 | 3.21 | Al2024T3 | 0.051 | 0.08 | 2.796 | 7.62 | 12.0 | 0.051 | 0.08 | Al2024-T4 | 47 | 0.160 | C5 |
| 160 | 1706 | Burch-BAC | Al2017 | 0.635 | 2.796 | 0.3748 | 5.49 | 60 | 2.74 | Al2024T3 | 0.051 | 0.08 | 2.796 | 7.62 | 12.0 | 0.051 | 0.08 | Al2024-T4 | 47 | 0.160 | C5 |
| 161 | 1707 | Burch-BAC | Al2017 | 0.635 | 2.796 | 0.3748 | 5.30 | 30 | 4.59 | Al2024T3 | 0.102 | 0.16 | 2.796 | 7.62 | 12.0 | 0.051 | 0.08 | Al2024-T4 | 47 | 0.240 | C5 |
| 162 | 1708 | Burch-BAC | Al2017 | 0.635 | 2.796 | 0.3748 | 5.52 | 45 | 3.90 | Al2024T3 | 0.102 | 0.16 | 2.796 | 7.62 | 12.0 | 0.051 | 0.08 | Al2024-T4 | 47 | 0.240 | C5 |
| 163 | 1709 | Burch-BAC | Al2017 | 0.635 | 2.796 | 0.3748 | 5.21 | 60 | 2.61 | Al2024T3 | 0.102 | 0.16 | 2.796 | 7.62 | 12.0 | 0.051 | 0.08 | Al2024-T4 | 47 | 0.240 | C5 |
| 164 | 1710 | Burch-BAC | Al2017 | 0.635 | 2.796 | 0.3748 | 5.12 | 30 | 4.43 | Al2024T3 | 0.203 | 0.32 | 2.796 | 7.62 | 12.0 | 0.051 | 0.08 | Al2024-T4 | 47 | 0.400 | C5 |
| 165 | 1711 | Burch-BAC | Al2017 | 0.635 | 2.796 | 0.3748 | 5.21 | 45 | 3.69 | Al2024T3 | 0.203 | 0.32 | 2.796 | 7.62 | 12.0 | 0.051 | 0.08 | Al2024-T4 | 47 | 0.400 | C5 |
| 166 | 1712 | Burch-BAC | Al2017 | 0.635 | 2.796 | 0.3748 | 5.30 | 60 | 2.65 | Al2024T3 | 0.203 | 0.32 | 2.796 | 7.62 | 12.0 | 0.051 | 0.08 | Al2024-T4 | 47 | 0.400 | C5 |
| 167 | 1713 | Burch-BAC | Al2017 | 0.635 | 2.796 | 0.3748 | 5.24 | 30 | 4.54 | Al2024T3 | 0.406 | 0.64 | 2.796 | 7.62 | 12.0 | 0.051 | 0.08 | Al2024-T4 | 47 | 0.720 | C5 |
| 168 | 1714 | Burch-BAC | Al2017 | 0.635 | 2.796 | 0.3748 | 5.36 | 45 | 3.79 | Al2024T3 | 0.406 | 0.64 | 2.796 | 7.62 | 12.0 | 0.051 | 0.08 | Al2024-T4 | 47 | 0.720 | C5 |
| 169 | 1715 | Burch-BAC | Al2017 | 0.635 | 2.796 | 0.3748 | 4.69 | 60 | 2.35 | Al2024T3 | 0.406 | 0.64 | 2.796 | 7.62 | 12.0 | 0.051 | 0.08 | Al2024-T4 | 47 | 0.720 | C5 |
| 170 | 1716 | Burch-BAC | Al2017 | 0.635 | 2.796 | 0.3748 | 5.21 | 30 | 4.51 | Al2024T3 | 0.051 | 0.08 | 2.796 | 5.08 | 8.0 | 0.051 | 0.08 | Al2024-T4 | 47 | 0.160 | C5 |
| 171 | 1717 | Burch-BAC | Al2017 | 0.635 | 2.796 | 0.3748 | 5.00 | 45 | 3.53 | Al2024T3 | 0.051 | 0.08 | 2.796 | 5.08 | 8.0 | 0.051 | 0.08 | Al2024-T4 | 47 | 0.160 | C5 |
| 172 | 1719 | Burch-BAC | Al2017 | 0.635 | 2.796 | 0.3748 | 5.12 | 30 | 4.43 | Al2024T3 | 0.051 | 0.08 | 2.796 | 12.7 | 20.0 | 0.051 | 0.08 | Al2024-T4 | 47 | 0.160 | C5 |
| 173 | 1721 | Burch-BAC | Al2017 | 0.635 | 2.796 | 0.3748 | 5.46 | 60 | 2.73 | Al2024T3 | 0.051 | 0.08 | 2.796 | 12.7 | 20.0 | 0.051 | 0.08 | Al2024-T4 | 47 | 0.160 | C5 |
| 174 | 1722 | Burch-BAC | Al2017 | 0.635 | 2.796 | 0.3748 | 3.23 | 0 | 3.23 | Al2024T3 | 0.051 | 0.08 | 2.796 | 7.62 | 12.0 | 0.051 | 0.08 | Al2024-T4 | 47 | 0.160 | C5 |
| 175 | 1723 | Burch-BAC | Al2017 | 0.635 | 2.796 | 0.3748 | 3.57 | 0 | 3.57 | Al2024T3 | 0.102 | 0.16 | 2.796 | 7.62 | 12.0 | 0.051 | 0.08 | Al2024-T4 | 47 | 0.240 | C5 |
| 176 | 1724 | Burch-BAC | Al2017 | 0.635 | 2.796 | 0.3748 | 3.78 | 0 | 3.78 | Al2024T3 | 0.203 | 0.32 | 2.796 | 7.62 | 12.0 | 0.051 | 0.08 | Al2024-T4 | 47 | 0.400 | C5 |
| 177 | 1725 | Burch-BAC | Al2017 | 0.318 | 2.796 | 0.0469 | 5.30 | 30 | 4.59 | Al2024T3 | 0.051 | 0.16 | 2.796 | 2.54 | 8.0 | 0.051 | 0.16 | Al2024-T4 | 47 | 0.320 | C5 |
| 178 | 1726 | Burch-BAC | Al2017 | 0.635 | 2.796 | 0.3748 | 5.27 | 30 | 4.57 | Al2024T3 | 0.102 | 0.16 | 2.796 | 7.62 | 12.0 | 0.102 | 0.16 | Al2024-T4 | 47 | 0.320 | C5 |
| 179 | 1727 | Burch-BAC | Al2017 | 0.635 | 2.796 | 0.3748 | 5.15 | 45 | 3.64 | Al2024T3 | 0.102 | 0.16 | 2.796 | 7.62 | 12.0 | 0.102 | 0.16 | Al2024-T4 | 47 | 0.320 | C5 |
| 180 | 1728 | Burch-BAC | Al2017 | 0.635 | 2.796 | 0.3748 | 5.30 | 60 | 2.65 | Al2024T3 | 0.102 | 0.16 | 2.796 | 7.62 | 12.0 | 0.102 | 0.16 | Al2024-T4 | 47 | 0.320 | C5 |
| 181 | 1171 | ESA | Aluminum | 0.2 | 2.713 | 0.0114 | 3.3 | 30 | 2.86 | Al2024T3 | 0.150 | 0.75 | 2.796 | 20 | 100.0 | 0.150 | 0.75 | Al2219-T851 | 46 | 1.500 | D2 |
| 182 | 1172 | ESA | Aluminum | 0.2 | 2.713 | 0.0114 | 3.3 | 45 | 2.33 | Al2024T3 | 0.150 | 0.75 | 2.796 | 20 | 100.0 | 0.150 | 0.75 | Al2219-T851 | 46 | 1.500 | D2 |
| 183 | 1173 | ESA | Aluminum | 0.2 | 2.713 | 0.0114 | 3.3 | 60 | 1.65 | Al2024T3 | 0.150 | 0.75 | 2.796 | 20 | 100.0 | 0.150 | 0.75 | Al2219-T851 | 46 | 1.500 | D1 |
| 184 | 1647 | ESA | Aluminum | 0.4 | 2.713 | 0.0909 | 7 | 0 | 7.00 | Al2024T3 | 0.200 | 0.50 | 2.796 | 15 | 37.5 | 0.150 | 0.38 | Al2219-T851 | 46 | 0.875 | D3 |
| 185 | 1648 | ESA | Aluminum | 0.4 | 2.713 | 0.0909 | 7.1 | 0 | 7.10 | Al2024T3 | 0.200 | 0.50 | 2.796 | 20 | 50.0 | 0.150 | 0.38 | Al2219-T851 | 46 | 0.875 | D2 |
| 186 | 1650 | ESA | Aluminum | 0.4 | 2.713 | 0.0909 | 7.1 | 0 | 7.10 | Al2024T3 | 0.200 | 0.50 | 2.796 | 30 | 75.0 | 0.150 | 0.38 | Al2219-T851 | 46 | 0.875 | D2 |
| 187 | 1716 | ESA | Aluminum | 0.5 | 2.713 | 0.1776 | 3.2 | 0 | 3.20 | Al2024T3 | 0.150 | 0.30 | 2.796 | 20 | 40.0 | 0.150 | 0.30 | Al2219-T851 | 46 | 0.600 | D4 |
| 188 | 1717 | ESA | Aluminum | 0.5 | 2.713 | 0.1776 | 3.2 | 0 | 3.20 | Al2024T3 | 0.180 | 0.36 | 2.796 | 20 | 40.0 | 0.318 | 0.64 | Al2219-T851 | 46 | 0.995 | D4 |
| 189 | 1718 | ESA | Aluminum | 0.5 | 2.713 | 0.1776 | 3.1 | 0 | 3.10 | Al2024T3 | 0.200 | 0.40 | 2.796 | 20 | 40.0 | 0.600 | 1.20 | Al2219-T851 | 46 | 1.600 | D2 |
| 190 | 1720 | ESA | Aluminum | 0.5 | 2.713 | 0.1776 | 5.6 | 0 | 5.60 | Al2024T3 | 0.150 | 0.30 | 2.796 | 20 | 40.0 | 0.150 | 0.30 | Al2219-T851 | 46 | 0.600 | D4 |
| 191 | 1721 | ESA | Aluminum | 0.5 | 2.713 | 0.1776 | 5.8 | 0 | 5.80 | Al2024T3 | 0.180 | 0.36 | 2.796 | 20 | 40.0 | 0.318 | 0.64 | Al2219-T851 | 46 | 0.995 | D2 |
| 192 | 1720 | ESA | Aluminum | 0.5 | 2.713 | 0.1776 | 5.8 | 0 | 5.80 | Al2024T3 | 0.200 | 0.40 | 2.796 | 20 | 40.0 | 0.600 | 1.20 | Al2219-T851 | 46 | 1.600 | D1 |
| 193 | 1724 | ESA | Aluminum | 0.5 | 2.713 | 0.1776 | 6.5 | 0 | 6.50 | Al2024T3 | 0.150 | 0.30 | 2.796 | 20 | 40.0 | 0.150 | 0.30 | Al2219-T851 | 46 | 0.600 | D3 |
| 194 | 1725 | ESA | Aluminum | 0.5 | 2.713 | 0.1776 | 6.4 | 0 | 6.40 | Al2024T3 | 0.180 | 0.36 | 2.796 | 20 | 40.0 | 0.318 | 0.64 | Al2219-T851 | 46 | 0.995 | D2 |
| 195 | 1726 | ESA | Aluminum | 0.5 | 2.713 | 0.1776 | 6.4 | 0 | 6.40 | Al2024T3 | 0.200 | 0.40 | 2.796 | 20 | 40.0 | 0.600 | 1.20 | Al2219-T851 | 46 | 1.600 | D1 |
| 196 | 1729 | ESA | Aluminum | 1.0 | 2.713 | 1.4205 | 3.1 | 0 | 3.10 | Al2024T3 | 0.180 | 0.18 | 2.796 | 20 | 20.0 | 0.318 | 0.32 | Al2219-T851 | 46 | 0.498 | D5 |
| 197 | 1730 | ESA | Aluminum | 1.0 | 2.713 | 1.4205 | 3.1 | 0 | 3.10 | Al2024T3 | 0.200 | 0.20 | 2.796 | 20 | 20.0 | 0.600 | 0.60 | Al2219-T851 | 46 | 0.800 | D5 |
| 198 | 1739 | ESA | Aluminum | 0.5 | 2.713 | 0.1776 | 3.2 | 0 | 3.20 | Al2024T3 | 0.180 | 0.36 | 2.796 | 20 | 40.0 | 0.318 | 0.64 | Al2219-T851 | 46 | 0.995 | D4 |
| 199 | 1762 | ESA | Aluminum | 0.4 | 2.713 | 0.0909 | 3.1 | 0 | 3.10 | Al2024T3 | 0.200 | 0.50 | 2.796 | 20 | 50.0 | 0.150 | 0.38 | Al2219-T851 | 46 | 0.875 | C5 |
| 200 | 1763 | ESA | Aluminum | 0.4 | 2.713 | 0.0909 | 2.7 | 0 | 2.70 | Al2024T3 | 0.200 | 0.50 | 2.796 | 30 | 75.0 | 0.150 | 0.38 | Al2219-T851 | 46 | 0.875 | C5 |

# WHIPPLE_EXCEL DATA

Translated from

K=tw*(Y/70)^.5*S^.5*(pp*pb)^-1/6*Vn^-1*M^-1/3
K"=tw*(Y/70)^.5*S^.5*(pp*pb)^-1/6*Vn^-1*M^-1/3*d^-.5

K=tw*(Y/70)^.5*S^.5*(pp*pb)*
K"=tw*(Y/70)^.5*S^.5*(pp*pb)*

| | Shot No. | Damage Description | JSC Whipple Eqns. dcrit (cm) | dcrit-d (cm) | Fail? 1=Y, 0=N) | Perf. Pred. | Safe Acc? | Pred. Accurate? | Comments | dc/d | K | K" | ELC JSC Whipple Eq Category Cdtargory (cm) |
|---|---|---|---|---|---|---|---|---|---|---|---|---|---|
| 151 | 1693 | Perforated (0.6"x0.7") | 0.100 | -0.2180 | 1 | 1 | 1 | 1 | 4LOF 10mil 2024T3 wit perf | 0.314 | 0.0357 | 0.0634 | 0 099546 |
| 152 | 1694 | Perforated (0.7"x1.3") | 0.131 | -0.1866 | 1 | 1 | 1 | 1 | 3LOF 20mil 2024T3 wit perf | 0.412 | 0.0550 | 0.0975 | 0.130865 |
| 153 | 1695 | Perforated (1.4"x2.6") | 0.178 | -0.4571 | 1 | 1 | 1 | 1 | 3LOF 40mil 2024T3 wit perf | 0.280 | 0.0596 | 0.0748 | 0.177867 |
| 154 | 1696 | Perforated (1.2"x2.2") | 0.177 | -0.4576 | 1 | 1 | 1 | 1 | 3LOF 40mil 2024T3 wit perf | 0.279 | 0.0600 | 0.0753 | 0.177352 |
| 155 | 1697 | Perforated (1.5"x2.3") | 0.102 | -0.5334 | 1 | 1 | 1 | 1 | 6LOF 20mil 2024T3 wit perf | 0.160 | 0.0284 | 0.0356 | 0 101634 |
| 156 | 1699 | Perforated (1.8"x1.8") | 0.147 | -0.4884 | 1 | 1 | 1 | 1 | 5.1LOF 20mil 2024T3 wit perf | 0.231 | 0.0558 | 0.0700 | 0.103296 |
| 157 | 1702 | Perforated | 0.216 | -0.1019 | 1 | 1 | 1 | 1 | 2LOF 20mil 2024T3 wit perf | 0.679 | 0.1142 | 0.2027 | 0.167338 |
| 158 | 1703 | Perforated | 0.174 | -0.1438 | 1 | 1 | 1 | 1 | 3.5LOF 10mil 2024T3 wit perf | 0.547 | 0.0542 | 0.0962 | 0.146624 |
| 159 | 1705 | Perforated (1"x0.7") | 0.087 | -0.5485 | 1 | 1 | 1 | 1 | 5.5LOF 20mil 2024T3 wit perf | 0.136 | 0.0352 | 0.0442 | 0 08653 |
| 160 | 1706 | Perforated (1"x0.8") | 0.121 | -0.5139 | 1 | 1 | 1 | 1 | 3.5LOF 20mil 2024T3 wit perf | 0.191 | 0.0412 | 0.0517 | 0.111504 |
| 161 | 1707 | Perforated (2.2"x2.8") | 0.123 | -0.5118 | 1 | 1 | 1 | 1 | 3.5LOF 20mil 2024T3 wit perf | 0.194 | 0.0246 | 0.0309 | 0.123163 |
| 162 | 1708 | Perforated (1.5") | 0.129 | -0.5063 | 1 | 1 | 1 | 1 | 4.3LOF 20mil 2024T3 wit perf | 0.203 | 0.0290 | 0.0364 | 0 128666 |
| 163 | 1709 | Perforated (0.9"x1.1") | 0.181 | -0.4537 | 1 | 1 | 1 | 1 | 3.5LOF 20mil 2024T3 wit perf | 0.286 | 0.0434 | 0.0545 | 0.16646 |
| 164 | 1710 | Perforated (1.8"x2.4") | 0.159 | -0.4760 | 1 | 1 | 1 | 1 | 3.3LOF 20mil 2024T3 wit perf | 0.250 | 0.0255 | 0.0320 | 0 159022 |
| 165 | 1711 | Perforated (1.1"x2.2") | 0.186 | -0.4486 | 1 | 1 | 1 | 1 | 3.1LOF 20mil 2024T3 wit perf | 0.294 | 0.0307 | 0 0385 | 0 186431 |
| 166 | 1712 | Perforated (0.8"x0.5") | 0.288 | -0.3470 | 1 | 1 | 1 | 1 | 3.6LOF 20mil 2024T3 wit perf | 0.454 | 0.0427 | 0.0535 | 0 275635 |
| 167 | 1713 | Perforated (2.2"x2.1") | 0.230 | -0.4046 | 1 | 1 | 1 | 1 | 3LOF 20mil 2024T3 wit perf | 0.363 | 0.0249 | 0.0313 | 0 230439 |
| 168 | 1714 | Perforated (0.4"x1.8") | 0.298 | -0.3367 | 1 | 1 | 1 | 1 | 2.7LOF & 3.6Norm .02 wit perf | 0.470 | 0.0298 | 0.0374 | 0 298316 |
| 169 | 1715 | Perforated | 0.539 | -0.0959 | 1 | 1 | 1 | 1 | 3.9Norm .02 2024T3 wit perf | 0.849 | 0.0482 | 0.0605 | 0 510878 |
| 170 | 1716 | Perforated (1"x0.9") | 0.095 | -0.5397 | 1 | 1 | 1 | 1 | 5.1LOF 20mil 2024T3 wit perf | 0.150 | 0.0205 | 0.0257 | 0 095265 |
| 171 | 1717 | Perforated (0.8"x0.8") | 0.090 | -0.5449 | 1 | 1 | 1 | 1 | 6.1LOF 20mil 2024T3 wit perf | 0.142 | 0.0261 | 0.0328 | 0 090115 |
| 172 | 1719 | Perforated (1.6"x1.7") | 0.112 | -0.5232 | 1 | 1 | 1 | 1 | 4.3LOF 20mil 2024T3 wit perf | 0.176 | 0.0329 | 0.0413 | 0 111778 |
| 173 | 1721 | Perforated (0.8"x1") | 0.122 | -0.5135 | 1 | 1 | 1 | 1 | 3.8LOF 20mil 2024T3 wit perf | 0.191 | 0.0535 | 0.0672 | 0 109306 |
| 174 | 1722 | Perforated (0.4") | 0.065 | -0.5698 | 1 | 1 | 1 | 1 | 7.7LOF 20mil 2024T3 wit perf | 0.103 | 0.0350 | 0.0439 | 0 065175 |
| 175 | 1723 | Perforated (0.9") | 0.097 | -0.5385 | 1 | 1 | 1 | 1 | 5.6LOF 20mil 2024T3 wit perf | 0.152 | 0.0317 | 0.0398 | 0 096544 |
| 176 | 1724 | Perforated (1.8") | 0.142 | -0.4925 | 1 | 1 | 1 | 1 | 5.2LOF 20mil 2024T3 wit perf | 0.224 | 0.0299 | 0.0376 | 0 142461 |
| 177 | 1725 | Perforated (0.7"x0.6") | 0.085 | -0.2323 | 1 | 1 | 1 | 1 | 3.3LOF 20mil 2024T3 wit perf | 0.268 | 0.0284 | 0.0505 | 0.085187 |
| 178 | 1726 | Perforated (1.3"x1.8") | 0.179 | -0.4556 | 1 | 1 | 1 | 1 | 4.5LOF 40mil 2024T3 wit perf | 0.283 | 0.0495 | 0.0622 | 0.179437 |
| 179 | 1727 | Perforated (1"x1.4") | 0.174 | -0.4607 | 1 | 1 | 1 | 1 | 4.9LOF 40mil 2024T3 wit perf | 0.274 | 0.0621 | 0.0779 | 0 174265 |
| 180 | 1728 | Perforated (0.6"x1.1") | 0.239 | -0.3964 | 1 | 1 | 1 | 1 | 3.6LOF 40mil 2024T3 wit perf | 0.376 | 0.0853 | 0.1071 | 0.217756 |
| 181 | 1171 | Buckled | 0.197 | -0.0026 | 0 | 1 | 1 | 0 | | 0.987 | 0.6038 | 1.3501 | 0.182004 |
| 182 | 1172 | Buckled | 0.272 | 0.0718 | 0 | 0 | 1 | 1 | | 1.359 | 0.7395 | 1.6535 | 0.194552 |
| 183 | 1173 | No perf. or spall | 0.470 | 0.2698 | 0 | 0 | 1 | 1 | | 2.349 | 1.0458 | 2.3384 | 0.276779 |
| 184 | 1647 | Spall, buckled | 0.415 | 0.0145 | 1 | 0 | 0 | 0 | | 1.036 | 0.1067 | 0.1688 | 0.414638 |
| 185 | 1648 | Buckled | 0.452 | 0.0519 | 0 | 0 | 1 | 1 | | 1.130 | 0.1215 | 0.1921 | 0.462968 |
| 186 | 1650 | Buckled | 0.517 | 0.1173 | 0 | 0 | 1 | 1 | | 1.293 | 0.1488 | 0.2353 | 0.530662 |
| 187 | 1716 | Perf., spall, buckled; witness buckled | 0.181 | -0.3185 | 1 | 1 | 1 | 1 | | 0.363 | 0.2157 | 0.3050 | 0.181499 |
| 188 | 1717 | Perf., buckled; witness buckled | 0.296 | -0.2038 | 1 | 1 | 1 | 1 | | 0.592 | 0.4565 | 0.6457 | 0.296192 |
| 189 | 1718 | Buckled | 0.448 | -0.0520 | 0 | 1 | 1 | 0 | | 0.896 | 0.8906 | 1.2595 | 0.448002 |
| 190 | 1720 | Perf., spall, buckled; witness buckled | 0.355 | -0.1449 | 1 | 1 | 1 | 1 | | 0.710 | 0.1233 | 0.1743 | 0.3551 |
| 191 | 1721 | Buckled | 0.608 | 0.1083 | 0 | 0 | 1 | 1 | | 1.217 | 0.2519 | 0.3562 | 0.608296 |
| 192 | 1720 | No perf. or spall | 0.934 | 0.4340 | 0 | 0 | 1 | 1 | | 1.868 | 0.4760 | 0.6732 | 0.933983 |
| 193 | 1724 | Spall, buckled | 0.420 | -0.0798 | 1 | 1 | 1 | 1 | | 0.840 | 0.1062 | 0.1502 | 0.420201 |
| 194 | 1725 | Buckled | 0.680 | 0.1803 | 0 | 0 | 1 | 1 | | 1.361 | 0.2283 | 0.3228 | 0.68032 |
| 195 | 1726 | No perf. or spall | 1.042 | 0.5420 | 0 | 0 | 1 | 1 | | 2.084 | 0.4314 | 0.6101 | 1.041979 |
| 196 | 1729 | Perf., spall, buckled | 0.284 | -0.7158 | 1 | 1 | 1 | 1 | | 0.284 | 0.2356 | 0.2356 | 0.284188 |
| 197 | 1730 | Perf., spall, buckled | 0.448 | -0.5520 | 1 | 1 | 1 | 1 | | 0.448 | 0.4453 | 0.4453 | 0.448002 |
| 198 | 1739 | Backwall perforated, .5mm witness dented | 0.296 | -0.2038 | 1 | 1 | 1 | 1 | | 0.592 | 0.4565 | 0.6457 | 0.296192 |
| 199 | 1762 | 2 Perfs (max: 7 mm) | 0.199 | -0.2010 | 1 | 1 | 1 | 1 | | 0.497 | 0.2783 | 0.4401 | 0.198982 |
| 200 | 1763 | 1 Perf (dia.: 6 mm) | 0.206 | -0.1944 | 1 | 1 | 1 | 1 | | 0.514 | 0.3914 | 0.6188 | 0.16763 |

# WHIPPLE_EXCEL DATA

Translated from Lotus by L.Thompson (714) 896-4495

## Whipple Database

| | Shot No. | Site | Proj. Mat'l | Proj. Dia. (cm) | Proj. Dens. (g/cc) | Proj. Mass (g) | Vel. (km/sec) | Impact Angle (deg) | Normal Vel. (km/sec) | Bumper Mat'l | Bumper Thk (cm) | tb/d | Bumper Dens. (g/cc) | Spacing (cm) | S/d | Wall Th'k (cm) | tw/d | Wall Mat'l | Yield Stress (ksi) | (tb+tw)/d | Category |
|---|---|---|---|---|---|---|---|---|---|---|---|---|---|---|---|---|---|---|---|---|---|
| 201 | 1764 | ESA | Aluminum | 0.4 | 2.713 | 0.0909 | 3.2 | 0 | 3.20 | Al2024T3 | 0.200 | 0.50 | 2.796 | 30 | 75.0 | 0.150 | 0.38 | Al2219-T851 | 46 | 0.875 | C5 |
| 202 | 1765 | ESA | Aluminum | 0.4 | 2.713 | 0.0909 | 3.4 | 0 | 3.40 | Al2024T3 | 0.200 | 0.50 | 2.796 | 15 | 37.5 | 0.150 | 0.38 | Al2219-T851 | 46 | 0.875 | C4 |
| 203 | 1780 | ESA | Aluminum | 0.5 | 2.713 | 0.1776 | 5.7 | 30 | 4.94 | Al2024T3 | 0.180 | 0.36 | 2.796 | 20 | 40.0 | 0.318 | 0.64 | Al2219-T851 | 46 | 0.995 | D4 |
| 204 | 1784 | ESA | Aluminum | 0.5 | 2.713 | 0.1776 | 5.7 | 45 | 4.03 | Al2024T3 | 0.180 | 0.36 | 2.796 | 20 | 40.0 | 0.318 | 0.64 | Al2219-T851 | 46 | 0.995 | D2 |
| 205 | 1785 | ESA | Aluminum | 0.5 | 2.713 | 0.1776 | 5.6 | 60 | 2.80 | Al2024T3 | 0.180 | 0.36 | 2.796 | 20 | 40.0 | 0.318 | 0.64 | Al2219-T851 | 46 | 0.995 | D2 |
| 206 | 1788 | ESA | Aluminum | 0.5 | 2.713 | 0.1776 | 6.5 | 0 | 6.50 | Al2024T3 | 0.180 | 0.36 | 2.796 | 20 | 40.0 | 0.200 | 0.40 | Al2219-T851 | 46 | 0.760 | D2 |
| 207 | 1795 | ESA | Aluminum | 1.0 | 2.713 | 1.4205 | 3.1 | 0 | 3.10 | Al2024T3 | 0.200 | 0.20 | 2.796 | 20 | 20.0 | 1.000 | 1.00 | Al2219-T851 | 46 | 1.200 | D3 |
| 208 | 1815 | ESA | Aluminum | 0.5 | 2.713 | 0.1776 | 5.3 | 0 | 5.30 | Al2024T3 | 0.150 | 0.30 | 2.796 | 20 | 40.0 | 0.250 | 0.50 | Al2219-T851 | 46 | 0.800 | D4 |
| 209 | 1821 | ESA | Aluminum | 0.5 | 2.713 | 0.1776 | 6.2 | 0 | 6.20 | Al2024T3 | 0.150 | 0.30 | 2.796 | 20 | 40.0 | 0.250 | 0.50 | Al2219-T851 | 46 | 0.800 | D2 |
| 210 | 1822 | ESA | Aluminum | 0.5 | 2.713 | 0.1776 | 6.4 | 0 | 6.40 | Al2024T3 | 0.180 | 0.36 | 2.796 | 15 | 30.0 | 0.318 | 0.64 | Al2219-T851 | 46 | 0.995 | D2 |
| 211 | 1824 | ESA | Aluminum | 0.5 | 2.713 | 0.1776 | 3.2 | 0 | 3.20 | Al2024T3 | 0.150 | 0.30 | 2.796 | 20 | 40.0 | 0.318 | 0.64 | Al2219-T851 | 46 | 0.935 | D5 |
| 212 | 1825 | ESA | Aluminum | 0.5 | 2.713 | 0.1776 | 1.6 | 0 | 1.60 | Al2024T3 | 0.150 | 0.30 | 2.796 | 20 | 40.0 | 0.318 | 0.64 | Al2219-T851 | 46 | 0.935 | D5 |
| 213 | 1826 | ESA | Aluminum | 0.5 | 2.713 | 0.1776 | 5.7 | 0 | 5.70 | Al2024T3 | 0.150 | 0.30 | 2.796 | 20 | 40.0 | 0.100 | 0.20 | Al2219-T851 | 46 | 0.500 | D4 |
| 214 | 1827 | ESA | Aluminum | 0.5 | 2.713 | 0.1776 | 7.3 | 0 | 7.30 | Al2024T3 | 0.150 | 0.30 | 2.796 | 20 | 40.0 | 0.100 | 0.20 | Al2219-T851 | 46 | 0.500 | D4 |
| 215 | 6266 | ESA | Aluminum | 1.0 | 2.713 | 1.4205 | 5.2 | 0 | 5.20 | Al2024T3 | 0.200 | 0.20 | 2.796 | 20 | 20.0 | 0.600 | 0.60 | Al2219-T851 | 46 | 0.800 | D5 |
| 216 | 6267 | ESA | Aluminum | 1.0 | 2.713 | 1.4205 | 5.2 | 0 | 5.20 | Al2024T3 | 0.180 | 0.18 | 2.796 | 20 | 20.0 | 0.318 | 0.32 | Al2219-T851 | 46 | 0.498 | D5 |
| 217 | 6274 | ESA | Aluminum | 1.0 | 2.713 | 1.4205 | 5.6 | 0 | 5.60 | Al2024T3 | 0.200 | 0.20 | 2.796 | 20 | 20.0 | 0.600 | 0.60 | Al2219-T851 | 46 | 0.800 | D5 |

# WHIPPLE_EXCEL DATA

Translated from

K=tw*(Y/70)^.5*S^.5*(pp*pb)^-1/6*Vn^-1*M^-1/3
K"=tw*(Y/70)^.5*S^.5*(pp*pb)^-1/6*Vn^-1*M^-1/3*d^-.5

K=tw*(Y/70)^.5*S^.5*(pp*pb)^
K"=tw*(Y/70)^.5*S^.5*(pp*pb)^

| | Shot No. | Damage Description | JSC Whipple Eqns. dcrit (cm) | dcrit-d (cm) | Fail? 1=Y, 0=N) | Perf. Pred. | Safe Acc? | Pred. Accurate? | Comments | dc/d | K | K" | BLC JSC Whipple Eq Category (cm) |
|---|---|---|---|---|---|---|---|---|---|---|---|---|---|
| 201 | 1764 | 1 Perf (dia.: 7 mm) | 0.209 | -0.1911 | 1 | 1 | 1 | 1 | | 0.522 | 0.3302 | 0.5221 | 0.208883 |
| 202 | 1765 | Small perf holes and spall | 0.215 | -0.1854 | 1 | 1 | 1 | 1 | | 0.537 | 0.2198 | 0.3475 | 0.214608 |
| 203 | 1780 | Perforation, spall, buckled | 0.525 | 0.0251 | 1 | 0 | 0 | 0 | | 1.050 | 0.2960 | 0.4186 | 0.525123 |
| 204 | 1784 | Buckled | 0.474 | -0.0256 | 0 | 1 | 1 | 0 | | 0.949 | 0.3625 | 0.5126 | 0.474417 |
| 205 | 1785 | Buckled | 0.548 | 0.0482 | 0 | 0 | 1 | 1 | | 1.096 | 0.5218 | 0.7379 | 0.513492 |
| 206 | 1788 | Buckled | 0.510 | 0.0099 | 0 | 0 | 1 | 1 | | 1.020 | 0.1416 | 0.2002 | 0.509909 |
| 207 | 1795 | Spall | 0.659 | -0.3406 | 1 | 1 | 1 | 1 | | 0.659 | 0.7422 | 0.7422 | 0.659351 |
| 208 | 1815 | Perf. (1mm), spall, buckled | 0.463 | -0.0371 | 1 | 1 | 1 | 1 | | 0.926 | 0.2170 | 0.3070 | 0.462877 |
| 209 | 1821 | Buckled | 0.557 | 0.0575 | 0 | 0 | 1 | 1 | | 1.115 | 0.1855 | 0.2624 | 0.557456 |
| 210 | 1822 | Buckled | 0.622 | 0.1218 | 0 | 0 | 1 | 1 | | 1.244 | 0.1977 | 0.2796 | 0.621845 |
| 211 | 1824 | Perf. (6mm), buckled | 0.282 | -0.2179 | 1 | 1 | 1 | 1 | | 0.564 | 0.4565 | 0.6457 | 0.28205 |
| 212 | 1825 | Perf. (5.5mm), buckled | 0.383 | -0.1173 | 1 | 1 | 1 | 1 | | 0.765 | 0.9131 | 1.2913 | 0.084031 |
| 213 | 1826 | Perf., spall, buckled | 0.280 | -0.2195 | 1 | 1 | 1 | 1 | | 0.561 | 0.0807 | 0.1142 | 0.280457 |
| 214 | 1827 | Perf. (1mm), buckled | 0.339 | -0.1614 | 1 | 1 | 1 | 1 | | 0.677 | 0.0630 | 0.0891 | 0.363924 |
| 215 | 6266 | Perf., spall, buckled | 0.826 | -0.1740 | 1 | 1 | 1 | 1 | | 0.826 | 0.2655 | 0.2655 | 0.825988 |
| 216 | 6267 | Perf., spall, buckled | 0.536 | -0.4637 | 1 | 1 | 1 | 1 | | 0.536 | 0.1405 | 0.1405 | 0.536272 |
| 217 | 6274 | Perf., spall, buckled | 0.898 | -0.1020 | 1 | 1 | 1 | 1 | | 0.898 | 0.2465 | 0.2465 | 0.897985 |

NASA JSC
Hypervelocity Impact Research Laboratory (HIRL)

Translated from Lotus by L. Thompson (714) 896-4495

## Aluminum Mesh Double-Bumper Shots

. MESH, AL 2ND BUMPER, KEVLAR OR SPECTRA INTERMEDIATE, AL REAR WALL

| | | PROJECTILE CONDITIONS | | | | | | | TARGET CONDITIONS | | | | | | | | |
|---|---|---|---|---|---|---|---|---|---|---|---|---|---|---|---|---|---|
| Shot No. | Site | Mat'l | Dia. (cm) | Density (g/cc) | Mass (g) | Vel. (km/sec) | Impact Angle (deg) | Vn (km/sec) | 1st Bumper Mat'l | 1st Areal Density (g/cm^2) | 2nd Bumper Mat'l | 2nd Areal Density (g/cm^2) | Intermediate Layer Mat'l (# sheets) | Intermed. Areal Density (g/cm^2) | Total Bump+I A.D. (g/cm^2) | Overall Spacing (cm) | Back-Wall Mat'l |
| A954 | JSC-HIRL | Al2017T4 | 0.318 | 2.796 | 0.0469 | 6.39 | 0 | 6.39 | Almesh 30x30 .012" wire | 0.051 | Al6061-0 | 0.110 | Spectra 618(2) | 0.056 | 0.217 | 5.08 | Al2024T3 |
| A962 | JSC-HIRL | Al2017T4 | 0.320 | 2.796 | 0.0478 | 6.38 | 0 | 6.38 | Almesh 30x30 .012" wire | 0.051 | Al6061-0 | 0.083 | Spectra 618(3) | 0.084 | 0.218 | 5.08 | Al2024T3 |
| A963 | JSC-HIRL | Al2017T4 | 0.320 | 2.796 | 0.0478 | 6.35 | 0 | 6.35 | Almesh 30x30 .012" wire | 0.051 | Al6061-0 | 0.083 | Spectra 618(2) | 0.056 | 0.190 | 5.08 | Al2024T3 |
| A971 | JSC-HIRL | Al2017T4 | 0.317 | 2.796 | 0.0464 | 6.62 | 0 | 6.62 | Almesh 30x30 .012" wire | 0.051 | Al6061-0 | 0.083 | Spectra 618(2) | 0.056 | 0.190 | 10.16 | Al3003H12 |
| A978 | JSC-HIRL | Al2017T4 | 0.318 | 2.796 | 0.0473 | 6.58 | 0 | 6.58 | Almesh 30x30 .012" wire | 0.051 | Al6061-0 | 0.083 | Spectra 618(2) | 0.056 | 0.190 | 10.16 | Al6061-0 |
| A1060 | JSC-HIRL | Al2017T4 | 0.318 | 2.796 | 0.0469 | 6.32 | 0 | 6.32 | Almesh 30x30 .012" wire | 0.051 | Al6061-0 | 0.083 | Spectra 618(2) | 0.056 | 0.190 | 10.16 | Al2024T3 |
| A1061 | JSC-HIRL | Al2017T4 | 0.318 | 2.796 | 0.0469 | 6.11 | 45 | 4.32 | Almesh 30x30 .012" wire | 0.051 | Al6061-0 | 0.083 | Spectra 618(2) | 0.056 | 0.190 | 10.16 | Al2024T3 |
| A1068 | JSC-HIRL | Al2017T4 | 0.318 | 2.796 | 0.0469 | 5.87 | 60 | 2.94 | Almesh 30x30 .012" wire | 0.051 | Al6061-0 | 0.083 | Spectra 618(2) | 0.056 | 0.190 | 10.16 | Al3003H12 |
| A1069 | JSC-HIRL | Al2017T4 | 0.318 | 2.796 | 0.0469 | 6.08 | 45 | 4.30 | Almesh 30x30 .012" wire | 0.051 | Al6061-0 | 0.083 | Spectra 618(2) | 0.056 | 0.190 | 10.16 | Al3003H12 |
| A1111 | JSC-HIRL | Al2017T4 | 0.318 | 2.796 | 0.0469 | 6.02 | 60 | 3.01 | Almesh 30x30 .012" wire | 0.051 | Al6061-0 | 0.083 | Spectra 618(3) | 0.084 | 0.218 | 10.16 | Al2024T3 |
| A1275 | JSC-HIRL | Al2017T4 | 0.318 | 2.796 | 0.0469 | 5.9 | 0 | 5.90 | Almesh 30x30 .013" wire | 0.057 | Al6061-0 | 0.083 | Spectra 618(2) | 0.056 | 0.196 | 10.16 | Al2024T3 |
| A1276 | JSC-HIRL | Al2017T4 | 0.318 | 2.796 | 0.0469 | 6.2 | 0 | 6.20 | Almesh 50x50 .009" wire | 0.0304 | Al6061-0 | 0.083 | Kevlar 095(2) | 0.056 | 0.169 | 10.16 | Al2024T3 |
| A1285 | JSC-HIRL | Al2017T4 | 0.318 | 2.796 | 0.0469 | 6.42 | 0 | 6.42 | Almesh 50x50 .009" wire | 0.0304 | Al6061-0 | 0.083 | Kevlar 095(2) | 0.056 | 0.169 | 10.16 | Al2024T3 |
| A1289 | JSC-HIRL | Al2017T4 | 0.318 | 2.796 | 0.0469 | 6.24 | 0 | 6.24 | Almesh 50x50 .009" wire | 0.0304 | Al6061-0 | 0.083 | Spectra 618(2) | 0.056 | 0.169 | 10.16 | Al2024T3 |
| A1351 | JSC-HIRL | Al2017T4 | 0.239 | 2.796 | 0.01989 | 4.46 | 45 | 3.15 | Almesh 50x50 .009" wire | 0.0304 | Al6061-0 | 0.083 | Kevlar710(2) | 0.064 | 0.177 | 10.16 | Al2024T3 |
| A1364 | JSC-HIRL | Al2017T4 | 0.357 | 2.796 | 0.06672 | 6 | 75 | 1.55 | Almesh 50x50 .009" wire | 0.0304 | Al6061-0 | 0.083 | Kevlar710(2) | 0.064 | 0.177 | 5.08 | Al2024T3 |
| 1414 | JSC-HIRL | Al2017T4 | 0.079 | 2.796 | 0.00073 | 3.5 | 0 | 3.50 | Almesh 50x50 .009" wire | 0.051 | Al6061-0 | 0.083 | Spectra 618 (2) | 0.056 | 0.190 | 10.16 | Al2024T3 |
| 1418 | JSC-HIRL | Al2017T4 | 0.079 | 2.796 | 0.00073 | 4.1 | 0 | 4.10 | Almesh 50x50 .009" wire | 0.051 | Al6061-0 | 0.083 | Spectra 618 (2) | 0.056 | 0.190 | 10.16 | Al2024T3 |
| 1650 | JSC-HIRL | Al2017T4 | 0.160 | 2.796 | 0.00598 | 3 | 0 | 3.00 | Almesh 50x50 .009" wire | 0.0304 | Al6061-0 | 0.083 | Kevlar710(2) | 0.064 | 0.177 | 10.16 | Al2024T3 |
| 1651 | JSC-HIRL | Al2017T4 | 0.149 | 2.796 | 0.00485 | 2.63 | 0 | 2.63 | Almesh 50x50 .009" wire | 0.0304 | Al6061-0 | 0.083 | Kevlar710(2) | 0.064 | 0.177 | 10.16 | Al2024T3 |
| 1652 | JSC-HIRL | Al2017T4 | 0.160 | 2.796 | 0.00596 | 3.44 | 45 | 2.43 | Almesh 50x50 .009" wire | 0.0304 | Al6061-0 | 0.083 | Kevlar710(2) | 0.064 | 0.177 | 10.16 | Al2024T3 |
| 1653 | JSC-HIRL | Al2017T4 | 0.160 | 2.796 | 0.00596 | 3.31 | 60 | 1.66 | Almesh 50x50 .009" wire | 0.0304 | Al6061-0 | 0.083 | Kevlar710(2) | 0.064 | 0.177 | 10.16 | Al2024T3 |
| 1654 | JSC-HIRL | Al2017T4 | 0.160 | 2.796 | 0.00596 | 3.41 | 60 | 1.71 | Almesh 50x50 .009" wire | 0.0304 | Al6061-0 | 0.083 | Kevlar710(2) | 0.064 | 0.177 | 10.16 | Al2024T3 |
| 1655 | JSC-HIRL | Al2017T4 | 0.143 | 2.796 | 0.00425 | 2.96 | 0 | 2.96 | Almesh 50x50 .009" wire | 0.0304 | Al6061-0 | 0.083 | Kevlar710(2) | 0.064 | 0.177 | 10.16 | Al2024T3 |
| 1656 | JSC-HIRL | Al2017T4 | 0.125 | 2.796 | 0.00288 | 3.19 | 0 | 3.19 | Almesh 50x50 .009" wire | 0.0304 | Al6061-0 | 0.083 | Kevlar710(2) | 0.064 | 0.177 | 10.16 | Al2024T3 |
| 1660 | JSC-HIRL | Al2017T4 | 0.160 | 2.796 | 0.00595 | 4.81 | 45 | 3.40 | Almesh 50x50 .009" wire | 0.0304 | Al6061-0 | 0.083 | Kevlar710(2) | 0.064 | 0.177 | 10.16 | Al2024T3 |
| 1661 | JSC-HIRL | Al2017T4 | 0.160 | 2.796 | 0.00597 | 5.74 | 60 | 2.87 | Almesh 50x50 .009" wire | 0.0304 | Al6061-0 | 0.083 | Kevlar710(2) | 0.064 | 0.177 | 10.16 | Al2024T3 |
| B27 | JSC-HIRL | Al2017T4 | 0.635 | 2.796 | 0.374 | 6.69 | 0 | 6.69 | Almesh 24x24 .023" wire | 0.130 | Al3003H14 | 0.174 | Spectra 618(4) | 0.112 | 0.416 | 20.32 | Al2024T3 |
| B77 | JSC-HIRL | Al2017T4 | 0.635 | 2.796 | 0.374 | 7.53 | 0 | 7.53 | Almesh 24x24 .023" wire | 0.130 | Al6061T6 | 0.172 | Kevlar710(4) | 0.128 | 0.430 | 10.16 | Al2024T3 |
| B81 | JSC-HIRL | Al2017T4 | 0.634 | 2.796 | 0.3734 | 7.29 | 0 | 7.29 | Almesh 24x24 .023" wire | 0.130 | Al6061T6 | 0.172 | Kevlar710(4) | 0.128 | 0.430 | 10.16 | Al2024T3 |
| 4-1172 | UDRI | Al2017T4 | 0.953 | 2.796 | 1.2651 | 6.65 | 0 | 6.65 | Almesh 12x12 .032" wire | 0.135 | Al2024T3 | 0.284 | Kevlar903(7) | 0.161 | 0.580 | 30.48 | Al2024T3 |

# MDB_EXCEL DATA

Hypervel

**Alumini**

. MESH, AL 2ND BUMPE

| Shot No. | Site | Wall Thick (cm) | Wall Areal Density (g/cm^2) | Yield Stress (ksi) | Damage Class | Wall Damage (P=Perforation, S=Detached Spall) | Total Areal Density (g/cm^2) | SN3-91-42 dcrit (cm) | dcrit-d (cm) | ratio dcrit/d | Predict Fail? (1=Y,0=N) | Fail? | Safety Accurate? | All Acc? | Comments | 3<Vn<6 dcrit (cm) | Wire Thick (mm) | Min Ratio t1/d |
|---|---|---|---|---|---|---|---|---|---|---|---|---|---|---|---|---|---|---|
| A954 | JSC-HIRL | 0.079 | 0.222 | 47 | F3 | No P or S, some dimples | 0.439 | 0.267 | -0.050 | 0.841 | 1 | 0 | 1 | 0 | Si=.25",1.5",.25" | 0.291 | 0.305 | 0.096 |
| A962 | JSC-HIRL | 0.079 | 0.222 | 47 | F3 | No P or S, bulge | 0.440 | 0.267 | -0.052 | 0.836 | 1 | 0 | 1 | 0 | Si=.25",1.5",.25" | 0.290 | 0.305 | 0.095 |
| A963 | JSC-HIRL | 0.079 | 0.222 | 47 | F3 | No P or S, bulge | 0.412 | 0.268 | -0.052 | 0.838 | 1 | 0 | 1 | 0 | Si=.25",1.5",.25" | 0.290 | 0.305 | 0.095 |
| A971 | JSC-HIRL | 0.064 | 0.174 | 18 | F3 | No P or S, bulge | 0.364 | 0.329 | 0.013 | 1.040 | 0 | 0 | 1 | 1 | Si=.25",3.5",.25" | 0.391 | 0.305 | 0.096 |
| A978 | JSC-HIRL | 0.064 | 0.172 | 8 | F3 | No P or S, bulge | 0.362 | 0.287 | -0.031 | 0.902 | 1 | 0 | 1 | 0 | Si=.3",3.45",.25" | 0.338 | 0.305 | 0.096 |
| A1060 | JSC-HIRL | 0.079 | 0.222 | 47 | F3 | No P or S, s.bulge | 0.412 | 0.426 | 0.108 | 1.340 | 0 | 0 | 1 | 1 | Si=.375",3.25",.375" | 0.466 | 0.305 | 0.096 |
| A1061 | JSC-HIRL | 0.079 | 0.222 | 47 | C2 | No P or S, dmpls | 0.412 | 0.289 | -0.029 | 0.909 | 1 | 0 | 1 | 0 | Si=.375",3.25",.375" | 0.289 | 0.305 | 0.096 |
| A1068 | JSC-HIRL | 0.064 | 0.174 | 18 | C4 | 1 P, 1.3mm | 0.364 | 0.181 | -0.137 | 0.570 | 1 | 1 | 1 | 1 | Si=.375",3.25",.375" | 0.175 | 0.305 | 0.096 |
| A1069 | JSC-HIRL | 0.064 | 0.174 | 18 | C2 | No P or S, dmpls | 0.364 | 0.220 | -0.097 | 0.694 | 1 | 0 | 1 | 0 | Si=.375",3.25",.375" | 0.220 | 0.305 | 0.096 |
| A1111 | JSC-HIRL | 0.064 | 0.178 | 47 | C2 | No P or S, dmpls | 0.395 | 0.234 | -0.084 | 0.737 | 1 | 0 | 1 | 0 | Si=.375",3.25",.375" | 0.234 | 0.305 | 0.096 |
| A1275 | JSC-HIRL | 0.041 | 0.114 | 47 | F3 | No P or S, bulge | 0.309 | 0.338 | 0.020 | 1.064 | 0 | 0 | 1 | 1 | Si=.5",3",.5" | 0.338 | 0.330 | 0.104 |
| A1276 | JSC-HIRL | 0.041 | 0.114 | 47 | F3 | No P or S, bulge | 0.283 | 0.343 | 0.025 | 1.079 | 0 | 0 | 1 | 1 | Si=.5",3",.5" | 0.363 | 0.229 | 0.072 |
| A1285 | JSC-HIRL | 0.030 | 0.085 | 47 | F3 | No P or S, bulge | 0.254 | 0.308 | -0.010 | 0.969 | 1 | 0 | 1 | 0 | Si=.5",3",.5" | 0.348 | 0.229 | 0.072 |
| A1289 | JSC-HIRL | 0.030 | 0.085 | 47 | F3 | No P or S, bulge | 0.254 | 0.311 | -0.007 | 0.979 | 1 | 0 | 1 | 0 | Si=.5",3",.5" | 0.333 | 0.229 | 0.072 |
| A1351 | JSC-HIRL | 0.051 | 0.142 | 47 | C4 | 4 Ps, 1.5x1mm max | 0.319 | 0.149 | -0.089 | 0.626 | 1 | 1 | 1 | 1 | Si=.5",3",.5" | 0.149 | 0.229 | 0.096 |
| A1364 | JSC-HIRL | 0.051 | 0.142 | 47 | C1 | No P or S, sm.dmpls | 0.319 | 0.538 | 0.180 | 1.505 | 0 | 0 | 1 | 1 | Si=.5",3",.5" | 0.414 | 0.229 | 0.064 |
| 1414 | JSC-HIRL | 0.030 | 0.085 | 47 | C1/C0 | No P or S, No damage | 0.275 | 0.123 | 0.044 | 1.556 | 0 | 0 | 1 | 1 | Si=.5",3",.5" | 0.123 | 0.229 | 0.288 |
| 1418 | JSC-HIRL | 0.030 | 0.085 | 47 | C1/C0 | No P or S, No damage | 0.275 | 0.169 | 0.090 | 2.134 | 0 | 0 | 1 | 1 | Si=.5",3",.5" | 0.169 | 0.229 | 0.288 |
| 1650 | JSC-HIRL | 0.051 | 0.142 | 47 | C4 | 2 Ps, 1.5x0.8mm & 0.7mm | 0.319 | 0.099 | -0.061 | 0.617 | 1 | 1 | 1 | 1 | Si=.5",3",.5" | 0.099 | 0.229 | 0.143 |
| 1651 | JSC-HIRL | 0.051 | 0.142 | 47 | C4 | 1 P, 0.8mm | 0.319 | 0.107 | -0.042 | 0.719 | 1 | 1 | 1 | 1 | Si=.5",3",.5" | 0.065 | 0.229 | 0.153 |
| 1652 | JSC-HIRL | 0.051 | 0.142 | 47 | C2 | No P or S, dmpls | 0.319 | 0.156 | -0.003 | 0.979 | 1 | 0 | 1 | 0 | Si=.5",3",.5" | 0.093 | 0.229 | 0.143 |
| 1653 | JSC-HIRL | 0.051 | 0.142 | 47 | C1 | No P or S, no dmpls | 0.319 | 0.277 | 0.117 | 1.733 | 0 | 0 | 1 | 1 | Si=.5",3",.5" | 0.109 | 0.229 | 0.143 |
| 1654 | JSC-HIRL | 0.051 | 0.142 | 47 | C1 | No P or S, no dmpls | 0.319 | 0.272 | 0.112 | 1.701 | 0 | 0 | 1 | 1 | Si=.5",3",.5" | 0.112 | 0.229 | 0.143 |
| 1655 | JSC-HIRL | 0.051 | 0.142 | 47 | C4 | 4 Ps, 1mm max | 0.319 | 0.099 | -0.043 | 0.697 | 1 | 1 | 1 | 1 | Si=.5",3",.5" | 0.095 | 0.229 | 0.160 |
| 1656 | JSC-HIRL | 0.051 | 0.142 | 47 | C4 | Small P, 0.7mm | 0.319 | 0.116 | -0.009 | 0.927 | 1 | 1 | 1 | 1 | Si=.5",3",.5" | 0.116 | 0.229 | 0.182 |
| 1660 | JSC-HIRL | 0.051 | 0.142 | 47 | C2 | No P or S, dmpls | 0.319 | 0.169 | 0.009 | 1.057 | 0 | 0 | 1 | 1 | Si=.5",3",.5" | 0.169 | 0.229 | 0.143 |
| 1661 | JSC-HIRL | 0.051 | 0.142 | 47 | C1/C0 | No P or S, No damage | 0.319 | 0.195 | 0.036 | 1.224 | 0 | 0 | 1 | 1 | No perf of Kevlar, Si=.5",3' | 0.183 | 0.229 | 0.143 |
| B27 | JSC-HIRL | 0.079 | 0.222 | 47 | F3 | No P or S, bulge | 0.638 | 0.663 | 0.028 | 1.045 | 0 | 0 | 1 | 1 | Si=1",6",1" | 0.801 | 0.584 | 0.092 |
| B77 | JSC-HIRL | 0.180 | 0.504 | 47 | F3 | No P or S, bulge | 0.935 | 0.528 | -0.107 | 0.832 | 1 | 0 | 1 | 0 | Si=1",2",1" | 0.719 | 0.584 | 0.092 |
| B81 | JSC-HIRL | 0.180 | 0.504 | 47 | F3 | No P or S, bulge | 0.935 | 0.534 | -0.101 | 0.841 | 1 | 0 | 1 | 0 | Si=1",2",1" | 0.696 | 0.584 | 0.092 |
| 4-1172 | UDRI | 0.180 | 0.504 | 47 | F3 | No P or S, s.bulge | 1.084 | 1.144 | 0.192 | 1.201 | 0 | 0 | 1 | 1 | Si=1.5",8.5",2" | 1.372 | 0.813 | 0.085 |
| | | | | | | | | | | | no. | 6 | 31 | 19 | | | | |
| | | | | | | | | | | | count | 31 | 31 | 31 | | | | |
| | | | | | | | | | | | % | 19.4% | 100.0% | 61.3% | | | | |

C-47

Hypervel

**Alumini**

. MESH, AL 2ND BUMPE

| Shot No. | Site | Max Ratio t1/d | Wires per inch | Wires "Cut" | Ratio Shield to proj. | Ratio AD 1st to proj. | Ratio AD 2nd to proj. | Ratio Int. to proj. | Ratio AD 1&2 to proj. | Ratio AD B&I to proj. | Ratio Wall to proj. | Ratio W&I to proj. | 2nd Thick (cm) | Ratio (t1 min+t2)/ proj dia |
|---|---|---|---|---|---|---|---|---|---|---|---|---|---|---|
| A954 | JSC-HIRL | 0.192 | 30 | 3.8 | 0.495 | 0.057 | 0.124 | 0.063 | 0.182 | 0.245 | 0.250 | 0.313 | 0.041 | 0.224 |
| A962 | JSC-HIRL | 0.191 | 30 | 3.8 | 0.492 | 0.057 | 0.093 | 0.094 | 0.150 | 0.244 | 0.248 | 0.342 | 0.030 | 0.191 |
| A963 | JSC-HIRL | 0.191 | 30 | 3.8 | 0.461 | 0.057 | 0.093 | 0.063 | 0.150 | 0.212 | 0.248 | 0.311 | 0.030 | 0.191 |
| A971 | JSC-HIRL | 0.193 | 30 | 3.7 | 0.411 | 0.058 | 0.093 | 0.063 | 0.151 | 0.214 | 0.197 | 0.260 | 0.030 | 0.193 |
| A978 | JSC-HIRL | 0.191 | 30 | 3.8 | 0.406 | 0.057 | 0.093 | 0.063 | 0.150 | 0.213 | 0.193 | 0.256 | 0.030 | 0.191 |
| A1060 | JSC-HIRL | 0.192 | 30 | 3.8 | 0.464 | 0.057 | 0.093 | 0.063 | 0.151 | 0.214 | 0.250 | 0.313 | 0.030 | 0.192 |
| A1061 | JSC-HIRL | 0.192 | 30 | 3.8 | 0.464 | 0.057 | 0.093 | 0.063 | 0.151 | 0.214 | 0.250 | 0.313 | 0.030 | 0.192 |
| A1068 | JSC-HIRL | 0.192 | 30 | 3.8 | 0.410 | 0.057 | 0.093 | 0.063 | 0.151 | 0.214 | 0.196 | 0.259 | 0.030 | 0.192 |
| A1069 | JSC-HIRL | 0.192 | 30 | 3.8 | 0.410 | 0.057 | 0.093 | 0.063 | 0.151 | 0.214 | 0.196 | 0.259 | 0.030 | 0.192 |
| A1111 | JSC-HIRL | 0.192 | 30 | 3.8 | 0.445 | 0.057 | 0.093 | 0.095 | 0.151 | 0.245 | 0.200 | 0.295 | 0.030 | 0.192 |
| A1275 | JSC-HIRL | 0.208 | 30 | 3.8 | 0.348 | 0.064 | 0.093 | 0.063 | 0.157 | 0.220 | 0.128 | 0.191 | 0.030 | 0.200 |
| A1276 | JSC-HIRL | 0.144 | 50 | 6.3 | 0.318 | 0.034 | 0.093 | 0.063 | 0.127 | 0.190 | 0.128 | 0.191 | 0.030 | 0.168 |
| A1285 | JSC-HIRL | 0.144 | 50 | 6.3 | 0.286 | 0.034 | 0.093 | 0.063 | 0.127 | 0.190 | 0.096 | 0.159 | 0.030 | 0.168 |
| A1289 | JSC-HIRL | 0.144 | 50 | 6.3 | 0.286 | 0.034 | 0.093 | 0.063 | 0.127 | 0.190 | 0.096 | 0.159 | 0.030 | 0.168 |
| A1351 | JSC-HIRL | 0.192 | 50 | 4.7 | 0.478 | 0.046 | 0.124 | 0.096 | 0.170 | 0.265 | 0.213 | 0.309 | 0.030 | 0.224 |
| A1364 | JSC-HIRL | 0.128 | 50 | 7.0 | 0.320 | 0.030 | 0.083 | 0.064 | 0.113 | 0.177 | 0.142 | 0.206 | 0.030 | 0.149 |
| 1414 | JSC-HIRL | 0.576 | 50 | 1.6 | 1.239 | 0.230 | 0.373 | 0.252 | 0.602 | 0.855 | 0.384 | 0.636 | 0.030 | 0.672 |
| 1418 | JSC-HIRL | 0.576 | 50 | 1.6 | 1.239 | 0.230 | 0.373 | 0.252 | 0.602 | 0.855 | 0.384 | 0.636 | 0.030 | 0.672 |
| 1650 | JSC-HIRL | 0.286 | 50 | 3.1 | 0.714 | 0.068 | 0.185 | 0.143 | 0.253 | 0.396 | 0.318 | 0.461 | 0.030 | 0.334 |
| 1651 | JSC-HIRL | 0.307 | 50 | 2.9 | 0.766 | 0.073 | 0.198 | 0.154 | 0.271 | 0.425 | 0.341 | 0.494 | 0.030 | 0.358 |
| 1652 | JSC-HIRL | 0.286 | 50 | 3.1 | 0.715 | 0.068 | 0.185 | 0.143 | 0.253 | 0.397 | 0.318 | 0.461 | 0.030 | 0.334 |
| 1653 | JSC-HIRL | 0.286 | 50 | 3.1 | 0.715 | 0.068 | 0.185 | 0.143 | 0.253 | 0.397 | 0.318 | 0.461 | 0.030 | 0.334 |
| 1654 | JSC-HIRL | 0.286 | 50 | 3.1 | 0.715 | 0.068 | 0.185 | 0.143 | 0.253 | 0.397 | 0.318 | 0.461 | 0.030 | 0.334 |
| 1655 | JSC-HIRL | 0.320 | 50 | 2.8 | 0.800 | 0.076 | 0.207 | 0.160 | 0.284 | 0.444 | 0.356 | 0.517 | 0.030 | 0.374 |
| 1656 | JSC-HIRL | 0.365 | 50 | 2.5 | 0.911 | 0.087 | 0.236 | 0.183 | 0.323 | 0.505 | 0.405 | 0.588 | 0.030 | 0.426 |
| 1660 | JSC-HIRL | 0.286 | 50 | 3.1 | 0.715 | 0.068 | 0.185 | 0.143 | 0.253 | 0.397 | 0.318 | 0.462 | 0.030 | 0.334 |
| 1661 | JSC-HIRL | 0.286 | 50 | 3.1 | 0.714 | 0.068 | 0.185 | 0.143 | 0.253 | 0.396 | 0.318 | 0.461 | 0.030 | 0.334 |
| B27 | JSC-HIRL | 0.184 | 24 | 6.0 | 0.360 | 0.073 | 0.098 | 0.063 | 0.171 | 0.234 | 0.125 | 0.188 | 0.064 | 0.192 |
| B77 | JSC-HIRL | 0.184 | 24 | 6.0 | 0.527 | 0.073 | 0.097 | 0.072 | 0.170 | 0.243 | 0.284 | 0.356 | 0.064 | 0.192 |
| B81 | JSC-HIRL | 0.184 | 24 | 6.0 | 0.527 | 0.073 | 0.097 | 0.072 | 0.170 | 0.243 | 0.284 | 0.357 | 0.064 | 0.192 |
| 4-1172 | UDRI | 0.171 | 12 | 4.5 | 0.407 | 0.051 | 0.107 | 0.060 | 0.157 | 0.218 | 0.189 | 0.250 | 0.102 | 0.192 |

# MS_EXCEL DATA

Eric L. Christiansen
NASA/Johnson Space Center
Mail Code SN3
Translated from Lotus by L.Thompson (714)896-4495

## Multi-Shock Shield Database

Nextel Bumpers, Aluminum Rear Wall

| Projectile Parameters | | | | | | | | | Bumper | | | | Back Wall | | | |
|---|---|---|---|---|---|---|---|---|---|---|---|---|---|---|---|---|
| Shot No. | Site | Mat'l | Dia. (cm) | Dens. (g/cc) | Mass (g) | Vel. (km/sec) | Obliquity (deg) | Vn (km/sec) | Mat'l | Number Sheets | Areal D. (g/cm^2) | Overall Spacing (cm) | Mat'l | Thk (cm) | Areal D. (g/cm^2) | Yield Stress (ksi) |
| A433 | JSC | Al2017T4 | 0.3175 | 2.796 | 0.0469 | 6.6 | 0 | 6.6 | Nextel | 4 | 0.172 | 10.16 | Al6061T6 | 0.079 | 0.215 | 36 |
| A436 | JSC | Al2017T4 | 0.3175 | 2.796 | 0.0469 | 6.55 | 0 | 6.55 | Nextel | 4 | 0.172 | 10.16 | Al6061T6 | 0.079 | 0.215 | 36 |
| A624 | JSC | Al2017T4 | 0.3175 | 2.796 | 0.0469 | 6.6 | 0 | 6.6 | Nextel | 2 | 0.172 | 5.08 | Al2024T3 | 0.127 | 0.355 | 47 |
| A725 | JSC | Al2017T4 | 0.3175 | 2.796 | 0.0469 | 6.17 | 0 | 6.17 | Nextel | 2 | 0.284 | 5.08 | Al2024T3 | 0.127 | 0.355 | 47 |
| A726 | JSC | Al2017T4 | 0.3175 | 2.796 | 0.0469 | 5.93 | 0 | 5.93 | Nextel | 2 | 0.256 | 5.08 | Al2024T3 | 0.127 | 0.355 | 47 |
| A727 | JSC | Al2017T4 | 0.3175 | 2.796 | 0.0469 | 6.14 | 0 | 6.14 | Nextel | 2 | 0.22 | 5.08 | Al2024T3 | 0.127 | 0.355 | 47 |
| A729 | JSC | Al2017T4 | 0.3175 | 2.796 | 0.0469 | 6.14 | 0 | 6.14 | Nextel | 3 | 0.165 | 7.62 | Al6061T6 | 0.079 | 0.215 | 36 |
| A731 | JSC | Al2017T4 | 0.3175 | 2.796 | 0.0469 | 6.15 | 0 | 6.15 | Nextel | 3 | 0.129 | 7.62 | Al6061T6 | 0.079 | 0.215 | 36 |
| A732 | JSC | Al2017T4 | 0.3175 | 2.796 | 0.0469 | 6.15 | 0 | 6.15 | Nextel | 4 | 0.22 | 10.16 | Al3003H12 | 0.064 | 0.174 | 18 |
| A958 | JSC | Al2O3 | 0.3175 | 3.9 | 0.0654 | 6 | 0 | 6 | Nextel | 5 | 0.258 | 12.7 | Al2024T3 | 0.079 | 0.222 | 47 |
| A1066 | JSC | Al2017T4 | 0.3175 | 2.796 | 0.0469 | 6.34 | 60 | 3.17 | Nextel AF26 | 4 | 0.172 | 10.16 | Al2024T3 | 0.079 | 0.222 | 47 |
| A1067 | JSC | Al2017T4 | 0.3175 | 2.796 | 0.0469 | 5.91 | 45 | 4.18 | Nextel AF26 | 4 | 0.172 | 10.16 | Al2024T3 | 0.079 | 0.222 | 47 |
| A1229 | JSC | Al2017T4 | 0.3175 | 2.796 | 0.0469 | 6.49 | 0 | 6.49 | Nextel AF26 | 4 | 0.172 | 10.16 | Al2024T3 | 0.051 | 0.142 | 47 |
| A1230 | JSC | Al2017T4 | 0.3175 | 2.796 | 0.0469 | 6.32 | 0 | 6.32 | Nextel AF26 | 4 | 0.172 | 10.16 | Al6061T6 | 0.064 | 0.172 | 36 |
| A1231 | JSC | Al2017T4 | 0.3175 | 2.796 | 0.0469 | 6.39 | 0 | 6.39 | Nextel AF26 | 4 | 0.172 | 10.16 | Al2024T3 | 0.041 | 0.114 | 47 |
| A1235 | JSC | Al2017T4 | 0.3175 | 2.796 | 0.0469 | 6.24 | 0 | 6.24 | Nextel AF26 | 4 | 0.172 | 10.16 | Al2024T3 | 0.064 | 0.178 | 47 |
| A1237 | JSC | Al2017T4 | 0.3175 | 2.796 | 0.0469 | 6.2 | 0 | 6.2 | Nextel AF26 | 4 | 0.172 | 7.62 | Al2024T3 | 0.079 | 0.222 | 47 |
| A1239 | JSC | Al2017T4 | 0.3175 | 2.796 | 0.0469 | 4.87 | 0 | 4.87 | Nextel AF26 | 4 | 0.172 | 10.16 | Al2024T3 | 0.079 | 0.222 | 47 |
| A1252 | JSC | Al2017T4 | 0.3175 | 2.796 | 0.0469 | 6.23 | 0 | 6.23 | Nextel AF26 | 4 | 0.172 | 5.08 | Al6061T6 | 0.127 | 0.355 | 36 |
| A1253 | JSC | Al2017T4 | 0.3175 | 2.796 | 0.0469 | 6.51 | 0 | 6.51 | Nextel AF26 | 4 | 0.172 | 5.08 | Al2024T3 | 0.159 | 0.444 | 47 |
| A1256 | JSC | Al2017T4 | 0.3175 | 2.796 | 0.0469 | 6.47 | 0 | 6.47 | Nextel AF26 | 4 | 0.172 | 10.16 | Al2024T3 | 0.030 | 0.085 | 47 |
| A1257 | JSC | Al2017T4 | 0.3175 | 2.796 | 0.0469 | 6.32 | 0 | 6.32 | Nextel AF26 | 4 | 0.172 | 10.16 | Al2024T3 | 0.030 | 0.085 | 47 |
| A1264 | JSC | Al2017T4 | 0.3175 | 2.796 | 0.0469 | 5.47 | 0 | 5.47 | Nextel AF26 | 4 | 0.172 | 10.16 | Al2024T3 | 0.051 | 0.142 | 47 |
| A1265 | JSC | Al2017T4 | 0.238 | 2.796 | 0.0198 | 6.71 | 0 | 6.71 | Nextel AF26 | 4 | 0.172 | 10.16 | Al2024T3 | 0.064 | 0.178 | 47 |
| A1283 | JSC | Al2017T4 | 0.3175 | 2.796 | 0.0469 | 6.23 | 0 | 6.23 | Nextel AF26 | 4 | 0.172 | 10.16 | Al2024T3 | 0.030 | 0.085 | 47 |
| A1284 | JSC | Al2017T4 | 0.3175 | 2.796 | 0.0469 | 6.29 | 0 | 6.29 | Nextel AF26 | 4 | 0.172 | 10.16 | Al2024T3 | 0.030 | 0.085 | 47 |
| A1291 | JSC | Al2017T4 | 0.3175 | 2.796 | 0.0469 | 5.44 | 0 | 5.44 | Nextel AF26 | 4 | 0.172 | 10.16 | Al2024T3 | 0.051 | 0.142 | 47 |
| A1312 | JSC | Al2017T4 | 0.3 | 2.796 | 0.0395 | 5.58 | 0 | 5.58 | Nextel AF26 | 4 | 0.172 | 10.16 | Al2024T3 | 0.051 | 0.142 | 47 |
| A1313 | JSC | Al2017T4 | 0.28 | 2.796 | 0.0321 | 5.3 | 0 | 5.3 | Nextel AF26 | 4 | 0.172 | 10.16 | Al2024T3 | 0.051 | 0.142 | 47 |
| A1314 | JSC | Al2017T4 | 0.2805 | 2.796 | 0.0323 | 5.69 | 0 | 5.69 | Nextel AF26 | 4 | 0.172 | 10.16 | Al2024T3 | 0.051 | 0.142 | 47 |
| A1315 | JSC | Al2017T4 | 0.26 | 2.796 | 0.0257 | 5.59 | 0 | 5.59 | Nextel AF26 | 4 | 0.172 | 10.16 | Al2024T3 | 0.051 | 0.142 | 47 |
| A1316 | JSC | Al2017T4 | 0.2191 | 2.796 | 0.0154 | 4.9 | 0 | 4.9 | Nextel AF26 | 4 | 0.172 | 10.16 | Al2024T3 | 0.051 | 0.142 | 47 |
| A1317 | JSC | Al2017T4 | 0.3176 | 2.796 | 0.0469 | 6.23 | 45 | 4.41 | Nextel AF26 | 4 | 0.172 | 10.16 | Al2024T3 | 0.051 | 0.142 | 47 |

# MS_EXCEL DATA

Eric L. Christians
NASA/Johnson S
Mail Code SN3
Translated from

Vn>6km/sec: K=mw*S^2*(Y/40)^0.5/(M*Vn) [sec/km] {K=43.1 for Nextel bumpers w/ Al rear wall}
Vn<6 km/sec: K2=mw*S*(Y/40)^0.5*Vn/M [km/sec-cm]
K3=mw*[S^2*[(Vn/3-1)+((2-Vn/(3*S^2))]*(Y/40)^0.5/M [km/sec-cm]

| Shot No. | Damage Class | Damage Description | Ratio AD Bumper to Proj. | Total Areal D. (g/cm^2) | K >6km/s | K2 <6km/s | K3 <6km/s | Comments |
|---|---|---|---|---|---|---|---|---|
| A433 | F3 | Bulged, intact | 0.194 | 0.387 | 68.2 | | | |
| A436 | F3 | Bulged, intact | 0.194 | 0.387 | 68.7 | | | |
| A624 | F3 | Bulged, intact | 0.194 | 0.527 | 32.1 | | | |
| A725 | F3 | Bulged, intact | 0.320 | 0.639 | 34.4 | | | |
| A726 | F5 | Bulged, perforated | 0.288 | 0.611 | | 247.5 | 549 | |
| A727 | F3 | Bulged, intact | 0.248 | 0.575 | 34.5 | | | |
| A729 | F5 | Bulged, perforated | 0.186 | 0.380 | 41.2 | | | |
| A731 | F5 | Bulged, perforated | 0.145 | 0.344 | 41.2 | | | |
| A732 | F3 | Bulged, intact | 0.248 | 0.394 | 41.8 | | | |
| A958 | F3 | Bulged, intact | 0.208 | 0.480 | 98.9 | | | NEXTEL:1,1,1,1,2 |
| A1066 | C1/F1 | No perf, surface craters only | 0.194 | 0.394 | | 165.4 | 1035 | |
| A1067 | C2 | No perf, cratering & dimples | 0.194 | 0.394 | | 218.0 | 1196 | |
| A1229 | F3 | Bulged (1 v.small dimple) | 0.194 | 0.314 | 52.3 | | | |
| A1230 | F3 | Bulged, intact | 0.194 | 0.344 | 57.0 | | | |
| A1231 | F3 | Bulged, intact | 0.194 | 0.286 | 42.5 | | | |
| A1235 | F3 | Bulged, intact | 0.194 | 0.350 | 67.9 | | | |
| A1237 | F3 | Bulged, intact | 0.194 | 0.394 | 48.1 | | | |
| A1239 | C5 | perforated (1 hole 1.5x1mm) | 0.194 | 0.394 | | 254.0 | 1306 | |
| A1252 | F5/D4 | Bulged, Pet. Perf. (5 x 3 mm) | 0.194 | 0.527 | 29.8 | | | |
| A1253 | F3 | Bulged, intact | 0.194 | 0.616 | 40.7 | | | |
| A1256 | F5 | Bulged, perforated | 0.194 | 0.257 | 31.5 | | | Si=.75",.75",.75",1.75" |
| A1257 | F5 | Bulged, perforated | 0.194 | 0.257 | 32.2 | | | Si=.5",.75",.75",2" |
| A1264 | F4/C4 | Bulged, 7 perfs, max 1.8x1.5mm | 0.194 | 0.314 | | 182.6 | 897 | |
| A1265 | F1 | No bulge, intact | 0.258 | 0.350 | 149.8 | | | |
| A1283 | F4 | Bulged, split (8mm) | 0.194 | 0.257 | 32.7 | | | Si=1",.5",.5",2"; frame size (115 x 120mm) |
| A1284 | F5 | Bulged, split (no dmpls/holes) | 0.194 | 0.257 | 32.4 | | | Si=1",.5",.5",2"; small frame (90 x 95 mm) |
| A1291 | C4 | 5 perforations, Dmax=1.5 mm | 0.194 | 0.314 | | 181.6 | 894 | Witness: craters & Al powder |
| A1312 | F4/C4 | bulge, 1 hole (1 mm) & dimples | 0.205 | 0.314 | | 220.8 | 1076 | Witness: no craters, soot |
| A1313 | C4 | 1 tiny pinhole (~.2mm) & 7 dimples | 0.220 | 0.314 | | 258.0 | 1282 | Witness: no damage |
| A1314 | F3/C2 | Bulged, 2 dimples | 0.219 | 0.314 | | 275.6 | 1333 | |
| A1315 | F3/C2 | Bulged, 11 small dimples | 0.237 | 0.314 | | 339.8 | 1655 | |
| A1316 | F3/C2 | Bulged, 10 dimples (2 lrg) | 0.281 | 0.314 | | 498.0 | 2553 | |
| A1317 | F3/C2 | s. bulge, 12 dimples (2 large) | 0.194 | 0.314 | | 147.0 | 788 | |

# MS_EXCEL DATA

Eric L. Christiansen
NASA/Johnson Space Center
Mail Code SN3
Translated from Lotus by L.Thompson (714)896-4495

## Multi-Shock Shield Database

Nextel Bumpers, Aluminum Rear Wall

| | Projectile Parameters | | | | | | | | Bumper | | | | Back Wall | | | |
|---|---|---|---|---|---|---|---|---|---|---|---|---|---|---|---|---|
| Shot No. | Site | Mat'l | Dia. (cm) | Dens. (g/cc) | Mass (g) | Vel. (km/sec) | Obliquity (deg) | Vn (km/sec) | Mat'l | Number Sheets | Areal D. (g/cm^2) | Overall Spacing (cm) | Mat'l | Thk (cm) | Areal D. (g/cm^2) | Yield Stress (ksi) |
| A1318 | JSC | Al2017T4 | 0.2806 | 2.796 | 0.0324 | 5.5 | 45 | 3.89 | Nextel AF26 | 4 | 0.172 | 10.16 | Al2024T3 | 0.051 | 0.142 | 47 |
| A1319 | JSC | Al2017T4 | 0.2992 | 2.796 | 0.0392 | 5.36 | 45 | 3.79 | Nextel AF26 | 4 | 0.172 | 10.16 | Al2024T3 | 0.051 | 0.142 | 47 |
| A1320 | JSC | Al2017T4 | 0.2595 | 2.796 | 0.0256 | 4.52 | 45 | 3.20 | Nextel AF26 | 4 | 0.172 | 10.16 | Al2024T3 | 0.051 | 0.142 | 47 |
| A1322 | JSC | Al2017T4 | 0.238 | 2.796 | 0.0198 | 4.53 | 45 | 3.20 | Nextel AF26 | 4 | 0.172 | 10.16 | Al2024T3 | 0.051 | 0.142 | 47 |
| A1325 | JSC | Al2017T4 | 0.2200 | 2.796 | 0.0156 | 4.7 | 45 | 3.32 | Nextel AF26 | 4 | 0.172 | 10.16 | Al2024T3 | 0.051 | 0.142 | 47 |
| A1327 | JSC | Al2017T4 | 0.3176 | 2.796 | 0.0469 | 4.00 | 0 | 4.00 | Nextel AF26 | 4 | 0.344 | 20.32 | Al2024T3 | 0.102 | 0.284 | 47 |
| A1328 | JSC | Al2017T4 | 0.3174 | 2.796 | 0.0468 | 2.91 | 0 | 2.91 | Nextel AF26 | 4 | 0.344 | 20.32 | Al2024T3 | 0.102 | 0.284 | 47 |
| A1329 | JSC | Al2017T4 | 0.3174 | 2.796 | 0.0468 | 4.82 | 45 | 3.41 | Nextel AF26 | 4 | 0.344 | 20.32 | Al2024T3 | 0.102 | 0.284 | 47 |
| A1330 | JSC | Al2017T4 | 0.3175 | 2.796 | 0.0468 | 3.62 | 45 | 2.56 | Nextel AF26 | 4 | 0.344 | 20.32 | Al2024T3 | 0.102 | 0.284 | 47 |
| A1335 | JSC | Al2017T4 | 0.3174 | 2.796 | 0.0468 | 5.57 | 60 | 2.79 | Nextel AF26 | 4 | 0.172 | 10.16 | Al2024T3 | 0.051 | 0.142 | 47 |
| A1336 | JSC | Al2017T4 | 0.2994 | 2.796 | 0.0393 | 6.27 | 60 | 3.14 | Nextel AF26 | 4 | 0.172 | 10.16 | Al2024T3 | 0.051 | 0.142 | 47 |
| A1337 | JSC | Al2017T4 | 0.2806 | 2.796 | 0.0323 | 5.46 | 60 | 2.73 | Nextel AF26 | 4 | 0.172 | 10.16 | Al2024T3 | 0.051 | 0.142 | 47 |
| A1338 | JSC | Al2017T4 | 0.2601 | 2.796 | 0.0258 | 5.49 | 60 | 2.75 | Nextel AF26 | 4 | 0.172 | 10.16 | Al2024T3 | 0.051 | 0.142 | 47 |
| A1339 | JSC | Al2017T4 | 0.3172 | 2.796 | 0.0467 | 4.75 | 60 | 2.38 | Nextel AF26 | 4 | 0.172 | 10.16 | Al2024T3 | 0.051 | 0.142 | 47 |
| A1340 | JSC | Al2017T4 | 0.3583 | 2.796 | 0.0674 | 6.24 | 60 | 3.12 | Nextel AF26 | 4 | 0.172 | 10.16 | Al2024T3 | 0.051 | 0.142 | 47 |
| A1341 | JSC | Al2017T4 | 0.3585 | 2.796 | 0.0675 | 6.13 | 0 | 6.13 | Nextel AF26 | 4 | 0.172 | 10.16 | Al2024T3 | 0.051 | 0.142 | 47 |
| A1361 | JSC | Al2017T4 | 0.3572 | 2.796 | 0.0667 | 6.09 | 75 | 1.58 | Nextel AF26 | 4 | 0.172 | 10.16 | Al2024T3 | 0.030 | 0.085 | 47 |
| B39 | JSC | Al2017T4 | 0.6265 | 2.796 | 0.3600 | 6.92 | 0 | 6.92 | Nextel AF26 | 4 | 0.344 | 20.32 | Al2024T3 | 0.081 | 0.227 | 47 |
| B70 | JSC | Al2017T4 | 0.6265 | 2.796 | 0.3600 | 7.07 | 0 | 7.07 | Nextel AF26 | 4 | 0.344 | 20.32 | Al2024T3 | 0.102 | 0.284 | 47 |
| B75 | JSC | Al2017T4 | 0.6343 | 2.796 | 0.3736 | 7.48 | 0 | 7.48 | Nextel AF26 | 4 | 0.344 | 10.16 | Al2024T3 | 0.254 | 0.710 | 47 |
| B79 | JSC | Al2017T4 | 0.6350 | 2.796 | 0.3748 | 7.76 | 0 | 7.76 | Nextel AF26 | 4 | 0.43 | 10.16 | Al2024T3 | 0.180 | 0.504 | 47 |
| B80 | JSC | Al2017T4 | 0.6340 | 2.796 | 0.3731 | 7.41 | 0 | 7.41 | Nextel AF26 | 4 | 0.43 | 10.16 | Al2024T3 | 0.180 | 0.504 | 47 |
| B82 | JSC | Al2017T4 | 0.6340 | 2.796 | 0.3730 | 7.51 | 0 | 7.51 | AF26,BF54 | 3 | 0.302 | 10.16 | Al2024T3 | 0.180 | 0.504 | 47 |
| B83 | JSC | Al2017T4 | 0.6340 | 2.796 | 0.3730 | 7.48 | 0 | 7.48 | AF62,BF54 | 3 | 0.416 | 10.16 | Al2024T3 | 0.180 | 0.504 | 47 |
| B84 | JSC | Al2017T4 | 0.6350 | 2.796 | 0.3748 | 7.29 | 0 | 7.29 | AF62,26+BF54 | 3 | 0.459 | 10.16 | Al2024T3 | 0.180 | 0.504 | 47 |
| B85 | JSC | Al2017T4 | 0.6340 | 2.796 | 0.3730 | 7.39 | 0 | 7.39 | AF62,26+BF54 | 3 | 0.459 | 10.16 | Al2024T3 | 0.180 | 0.504 | 47 |
| B86 | JSC | Al2017T4 | 0.6344 | 2.796 | 0.3738 | 7.34 | 0 | 7.34 | 62,26+62,2-62 | 3 | 0.486 | 10.16 | Al2024T3 | 0.180 | 0.504 | 47 |
| B87 | JSC | Al2017T4 | 0.6342 | 2.796 | 0.3734 | 7.51 | 0 | 7.51 | AF26:2,3,3,3 | 4 | 0.473 | 10.16 | Al2024T3 | 0.180 | 0.504 | 47 |
| B88 | JSC | Al2017T4 | 0.6342 | 2.796 | 0.3734 | 7.06 | 0 | 7.06 | :2,2,2,4(2/Batti | 4 | 0.447 | 10.16 | Al2024T3 | 0.180 | 0.504 | 47 |
| B89 | JSC | Al2017T4 | 0.6350 | 2.796 | 0.3748 | 7.22 | 0 | 7.22 | AF26:2,2,2,2 | 4 | 0.344 | 10.16 | Al2024T3 | 0.254 | 0.710 | 47 |
| B95 | JSC | Al2017T4 | 0.6350 | 2.796 | 0.3748 | 7.36 | 0 | 7.36 | \F62(2),AF26(5 | 2 | 0.415 | 10.16 | Al2024T3 | 0.229 | 0.639 | 47 |
| 1512 | JSC | Al2017T4 | 0.1599 | 2.796 | 0.00598 | 3.26 | 0 | 3.26 | Nextel AF26 | 4 | 0.172 | 10.16 | Al2024T3 | 0.051 | 0.142 | 47 |
| 1513 | JSC | Al2017T4 | 0.1598 | 2.796 | 0.00597 | 4.33 | 0 | 4.33 | Nextel AF26 | 4 | 0.172 | 10.16 | Al2024T3 | 0.051 | 0.142 | 47 |
| 1523 | JSC | Al2017T4 | 0.1253 | 2.796 | 0.00288 | 3.94 | 0 | 3.94 | Nextel AF26 | 4 | 0.172 | 10.16 | Al2024T3 | 0.051 | 0.142 | 47 |

# MS_EXCEL DATA

Eric L. Christians
NASA/Johnson S
Mail Code SN3
Translated from

Vn>6km/sec: K=mw*S^2*(Y/40)^0.5/(M*Vn) [sec/km] {K=43.1 for Nextel bumpers w/ Al rear wall}
Vn<6 km/sec: K2=mw*S*(Y/40)^0.5*Vn/M [km/sec-cm]
K3=mw*[S^2*[(Vn/3-1)+((2-Vn/(3*S^2))]*(Y/40)^0.5/M [km/sec-cm]

| Shot No. | Damage Class | Damage Description | Ratio AD Bumper to Proj. | Total Areal D. (g/cm^2) | K >6km/s | K2 <6km/s | K3 <6km/s | Comments |
|---|---|---|---|---|---|---|---|---|
| A1318 | C2 | 14 dimples (2 large) | 0.219 | 0.314 | | 188.1 | 1065 | |
| A1319 | C4 | 2 Perfs (max=1 mm) 12 dimples | 0.206 | 0.314 | | 151.2 | 867 | Witness: no damage |
| A1320 | C4 | 7 Perfs (max=2x1.5 mm) 15 dmpl | 0.237 | 0.314 | | 195.5 | 1219 | Witness: craters |
| A1322 | C4 | 1 Perfs (2x1.5 mm) 13 dmpl | 0.258 | 0.314 | | 253.5 | 1578 | Witness: craters & dimples |
| A1325 | C2 | 15 dimples (3 large) | 0.280 | 0.314 | | 333.7 | 2039 | |
| A1327 | C2 | No perforation, craters & dmpl | 0.387 | 0.628 | | 533.9 | 6150 | |
| A1328 | C5 | 3 perfs, Max 3 mm | 0.388 | 0.628 | | 389.1 | 5222 | Witness: 1 hole (1 mm), cr. |
| A1329 | C1 | No perforation, s. cratering | 0.388 | 0.628 | | 455.4 | 5648 | |
| A1330 | C2 | No perforation, craters & dmpl | 0.388 | 0.628 | | 341.9 | 4917 | |
| A1335 | C1/F1 | No perfs, s.craters only | 0.194 | 0.314 | | 93.0 | 623 | |
| A1336 | C1/F1 | No perfs, no cratering | 0.205 | 0.314 | | 124.8 | 786 | 4th Nextel was perforated |
| A1337 | C2 | No perfs, craters & 2 dmpls | 0.219 | 0.314 | | 132.1 | 895 | |
| A1338 | C2 | No perfs, craters & 1 dmpl | 0.237 | 0.314 | | 166.8 | 1126 | |
| A1339 | C2 | No perfs, craters & 5 dmpls | 0.194 | 0.314 | | 79.5 | 583 | |
| A1340 | C2 | No perfs, craters & 5 dmpls | 0.172 | 0.314 | | 72.5 | 457 | |
| A1341 | F5 | Large petalled perf (25mm) | 0.172 | 0.314 | 38.4 | | | Wit: perf (3x2mm); some secondaries |
| A1361 | C0 | No perf, No damage | 0.172 | 0.257 | | 22.2 | 211 | No perf of 4th Nextel |
| B39 | F4 | Bulge, 2 small perf(1.5mm max) | 0.196 | 0.571 | 40.8 | | | Many secondarys (Redo) |
| B70 | F3 | Deep bulge (~8mm) | 0.196 | 0.628 | 50.0 | | | Center of wall bulge has dmpl |
| B75 | F5 | Pet Perf (12x15mm),s.cratering | 0.194 | 1.054 | 28.4 | | | Si=1.5",.75",.75",1":Wit:dmpl, molten splash |
| B79 | D5 | Perf (~12 mm) | 0.242 | 0.934 | 19.4 | | | 1/4Sabot (Redo), AF26:3,2,2,3;.04"Wit:8mm perfs |
| B80 | F5 | Pet Perf (~30mm), 70mm cracks | 0.243 | 0.934 | 20.4 | | | AF26:3,2,1,4; .04"Wit:splash (no perf) |
| B82 | F5 | Petalled Perf (~50mm) | 0.170 | 0.806 | 20.1 | | | AF26,AF26,2*BF54; Wit:2 perfs (3/4" max) |
| B83 | F5 | Petalled Perf (~40mm) | 0.235 | 0.920 | 20.2 | | | AF62,AF62,2*BF54; Wit:no perf, dimples |
| B84 | F5 | Petalled Perf (~25mm) | 0.259 | 0.963 | 20.6 | | | AF62,AF62,AF26+2*BF54; Wit:no perf; Si=1.5",1.5", |
| B85 | F5 | Petalled Perf (~25mm) | 0.259 | 0.963 | 20.5 | | | AF62,AF62,AF26+2*BF54; Wit:no perf; Si=1.3",1.3" |
| B86 | F5 | Petalled Perf (~20x30mm), particulates | 0.274 | 0.990 | 20.6 | | | Wit: s.bulge, no perf; AF62,AF26+AF62,AF26+2*AF |
| B87 | F5 | Petalled Perf (~35x45mm), impulsive | 0.267 | 0.977 | 20.1 | | | Wit: no perf, no dmpls; Si=1",1",1",1" |
| B88 | F5 | Petalled Perf (~50x20mm), particulates | 0.252 | 0.951 | 21.4 | | | Wit: no perf, 5 s.dmpls; (2)AF26, (2)AF26, (2)AF2 |
| B89 | F5 | Petalled Perf (~15x19mm), particulates/holes in petals | 0.194 | 1.054 | 29.4 | | | Wit: no perf, many dmpls; Si=1",1",1",1" |
| B95 | F4 | Bulge, 1 s. perf (1.6 mm) | 0.234 | 1.054 | 25.9 | | | Wit: no perf; Si=2",2" |
| 1512 | C4 | 3 Perfs (max=1.2 mm), dimples | 0.385 | 0.314 | | 852.8 | 5261 | Witness: craters & dimples |
| 1513 | C2 | No perforation, dimples | 0.385 | 0.314 | | 1134.6 | 6126 | |
| 1523 | C2 | No perf., dimples (1 Large) | 0.491 | 0.314 | | 2140.0 | 12053 | |

# MS_EXCEL DATA

Eric L. Christiansen
NASA/Johnson Space Center
Mail Code SN3
Translated from Lotus by L.Thompson (714)896-4495

## Multi-Shock Shield Database

Nextel Bumpers, Aluminum Rear Wall

| | Projectile Parameters | | | | | | | | Bumper | | | | Back Wall | | | |
|---|---|---|---|---|---|---|---|---|---|---|---|---|---|---|---|---|
| Shot No. | Site | Mat'l | Dia. (cm) | Dens. (g/cc) | Mass (g) | Vel. (km/sec) | Obliquity (deg) | Vn (km/sec) | Mat'l | Number Sheets | Areal D. (g/cm^2) | Overall Spacing (cm) | Mat'l | Thk (cm) | Areal D. (g/cm^2) | Yield Stress (ksi) |
| 1525 | JSC | Al2017T4 | 0.1488 | 2.796 | 0.00482 | 3.89 | 0 | 3.89 | Nextel AF26 | 4 | 0.172 | 10.16 | Al2024T3 | 0.051 | 0.142 | 47 |
| 1526 | JSC | Al2017T4 | 0.1598 | 2.796 | 0.00597 | 3.32 | 45 | 2.35 | Nextel AF26 | 4 | 0.172 | 10.16 | Al2024T3 | 0.051 | 0.142 | 47 |
| 1528 | JSC | Al2017T4 | 0.1599 | 2.796 | 0.00598 | 4.57 | 45 | 3.23 | Nextel AF26 | 4 | 0.172 | 10.16 | Al2024T3 | 0.051 | 0.142 | 47 |
| 1540 | JSC | Al2017T4 | 0.1595 | 2.796 | 0.00594 | 3.57 | 30 | 3.09 | Nextel AF26 | 4 | 0.172 | 10.16 | Al2024T3 | 0.051 | 0.142 | 47 |
| 1550 | JSC | Al2017T4 | 0.1600 | 2.796 | 0.00600 | 4.24 | 30 | 3.67 | Nextel AF26 | 4 | 0.172 | 10.16 | Al2024T3 | 0.051 | 0.142 | 47 |
| 1585 | JSC | Al2017T4 | 0.1596 | 2.796 | 0.00595 | 3.57 | 60 | 1.79 | Nextel AF26 | 4 | 0.172 | 10.16 | Al2024T3 | 0.051 | 0.142 | 47 |
| 1586 | JSC | Al2017T4 | 0.1598 | 2.796 | 0.00597 | 4.81 | 60 | 2.41 | Nextel AF26 | 4 | 0.172 | 10.16 | Al2024T3 | 0.051 | 0.142 | 47 |
| 1587 | JSC | Al2017T4 | 0.1596 | 2.796 | 0.00595 | 3.79 | 0 | 3.79 | Nextel AF26 | 4 | 0.344 | 10.16 | Al2024T3 | 0.102 | 0.284 | 47 |
| 1588 | JSC | Al2017T4 | 0.1252 | 2.796 | 0.00287 | 3.77 | 0 | 3.77 | Nextel AF26 | 4 | 0.172 | 10.16 | Al2024T3 | 0.051 | 0.142 | 47 |
| 1589 | JSC | Al2017T4 | 0.1597 | 2.796 | 0.00596 | 3.45 | 0 | 3.45 | Nextel AF26 | 4 | 0.172 | 10.16 | Al2024T3 | 0.051 | 0.142 | 47 |
| 1590 | JSC | Al2017T4 | 0.1256 | 2.796 | 0.00290 | 4.04 | 0 | 4.04 | Nextel AF26 | 4 | 0.172 | 10.16 | Al2024T3 | 0.051 | 0.142 | 47 |
| 1591 | JSC | Al2017T4 | 0.1154 | 2.796 | 0.00225 | 4.14 | 0 | 4.14 | Nextel AF26 | 4 | 0.172 | 10.16 | Al2024T3 | 0.051 | 0.142 | 47 |
| 1594 | JSC | Al2017T4 | 0.1156 | 2.796 | 0.00226 | 2.85 | 0 | 2.85 | Nextel AF26 | 4 | 0.172 | 10.16 | Al2024T3 | 0.051 | 0.142 | 47 |
| 1595 | JSC | Al2017T4 | 0.1154 | 2.796 | 0.00225 | 4.1 | 0 | 4.10 | Nextel AF26 | 4 | 0.172 | 10.16 | Al2024T3 | 0.051 | 0.142 | 47 |
| 1597 | JSC | Al2017T4 | 0.1157 | 2.796 | 0.00227 | 3.44 | 0 | 3.44 | Nextel AF26 | 4 | 0.172 | 10.16 | Al2024T3 | 0.051 | 0.142 | 47 |
| 1598 | JSC | Al2017T4 | 0.1001 | 2.796 | 0.00147 | 4.27 | 0 | 4.27 | Nextel AF26 | 4 | 0.172 | 10.16 | Al2024T3 | 0.051 | 0.142 | 47 |
| 1603 | JSC | Al2017T4 | 0.1001 | 2.796 | 0.00147 | 3.79 | 0 | 3.79 | Nextel AF26 | 4 | 0.172 | 10.16 | Al2024T3 | 0.051 | 0.142 | 47 |
| 1604 | JSC | Al2017T4 | 0.0997 | 2.796 | 0.00145 | 3.62 | 0 | 3.62 | Nextel AF26 | 4 | 0.172 | 10.16 | Al2024T3 | 0.051 | 0.142 | 47 |
| 1625 | JSC | Al2017T4 | 0.1006 | 2.796 | 0.00149 | 3.39 | 0 | 3.39 | Nextel AF26 | 4 | 0.172 | 10.16 | Al2024T3 | 0.051 | 0.142 | 47 |
| 1628 | JSC | Al2017T4 | 0.1004 | 2.796 | 0.00148 | 2.47 | 0 | 2.47 | Nextel AF26 | 4 | 0.172 | 10.16 | Al2024T3 | 0.051 | 0.142 | 47 |
| 1632 | JSC | Al2017T4 | 0.0794 | 2.796 | 0.00073 | 3.08 | 0 | 3.08 | Nextel AF26 | 4 | 0.172 | 10.16 | Al2024T3 | 0.051 | 0.142 | 47 |
| 1635 | JSC | Al2017T4 | 0.0804 | 2.796 | 0.00076 | 2.68 | 0 | 2.68 | Nextel AF26 | 4 | 0.172 | 10.16 | Al2024T3 | 0.051 | 0.142 | 47 |
| 1636 | JSC | Nylon | 0.2373 | 1.14 | 0.00798 | 3.2 | 0 | 3.20 | Nextel AF26 | 4 | 0.172 | 10.16 | Al2024T3 | 0.051 | 0.142 | 47 |
| 1637 | JSC | Nylon | 0.2387 | 1.14 | 0.00812 | 3.16 | 0 | 3.16 | Nextel AF26 | 4 | 0.172 | 10.16 | Al2024T3 | 0.051 | 0.142 | 47 |
| 1638 | JSC | Nylon | 0.2399 | 1.14 | 0.00824 | 3.15 | 0 | 3.15 | Nextel AF26 | 4 | 0.172 | 10.16 | Al2024T3 | 0.051 | 0.142 | 47 |
| 1639 | JSC | Nylon | 0.2361 | 1.14 | 0.00786 | 3.78 | 0 | 3.78 | Nextel AF26 | 4 | 0.172 | 10.16 | Al2024T3 | 0.051 | 0.142 | 47 |
| 1640 | JSC | Al2017T4 | 0.1596 | 2.796 | 0.00595 | 2.97 | 30 | 2.57 | Nextel AF26 | 4 | 0.172 | 10.16 | Al2024T3 | 0.051 | 0.142 | 47 |
| 1641 | JSC | Al2017T4 | 0.1485 | 2.796 | 0.00479 | 2.90 | 30 | 2.51 | Nextel AF26 | 4 | 0.172 | 10.16 | Al2024T3 | 0.051 | 0.142 | 47 |
| 1642 | JSC | Al2017T4 | 0.1489 | 2.796 | 0.00483 | 3.01 | 30 | 2.61 | Nextel AF26 | 4 | 0.172 | 10.16 | Al2024T3 | 0.051 | 0.142 | 47 |
| 1643 | JSC | Al2017T4 | 0.1486 | 2.796 | 0.00480 | 3.36 | 45 | 2.38 | Nextel AF26 | 4 | 0.172 | 10.16 | Al2024T3 | 0.051 | 0.142 | 47 |
| ? | ARC | Al2017T4 | 0.9525 | 2.796 | 1.26512 | 6.5 | 0 | 6.50 | Nextel AF26 | 4 | 0.516 | 30.48 | Al2024T3 | 0.229 | 0.639 | 47 |
| 1150 | UDRI | Al2017T4 | 0.9525 | 2.796 | 1.26512 | 6.77 | 0 | 6.77 | Nextel AF26 | 4 | 0.516 | 30.48 | Al6061T6 | 0.229 | 0.620 | 36 |
| 1151 | UDRI | Al2017T4 | 0.9525 | 2.796 | 1.26512 | 6.78 | 0 | 6.78 | Nextel AF62 | 5 | 0.500 | 38.1 | Al6061T6 | 0.229 | 0.620 | 36 |
| 1152 | UDRI | Al2017T4 | 0.9525 | 2.796 | 1.26512 | 6.78 | 0 | 6.78 | Nextel BF54 | 4 | 0.434 | 30.48 | Al6061T6 | 0.229 | 0.620 | 36 |

# MS_EXCEL DATA

Eric L. Christians
NASA/Johnson S
Mail Code SN3
Translated from

Vn>6km/sec: K=mw*S^2*(Y/40)^0.5/(M*Vn) [sec/km] {K=43.1 for Nextel bumpers w/ Al rear wall}
Vn<6 km/sec: K2=mw*S*(Y/40)^0.5*Vn/M [km/sec-cm]
K3=mw*{S^2*[(Vn/3-1)+((2-Vn/(3*S^2))]}*(Y/40)^0.5/M [km/sec-cm]

| Shot No. | Damage Class | Damage Description | Ratio AD Bumper to Proj. | Total Areal D. (g/cm^2) | K >6km/s | K2 <6km/s | K3 <6km/s | Comments |
|---|---|---|---|---|---|---|---|---|
| 1525 | C2 | No perf., dimples | 0.414 | 0.314 | | 1262.5 | 7152 | |
| 1526 | C4 | 1 Perf (1.5x1 mm) | 0.385 | 0.314 | | 615.1 | 4540 | Witness: dimple |
| 1528 | C2 | No perf., dimples (2 large) | 0.385 | 0.314 | | 845.3 | 5239 | |
| 1540 | C4 | 1 Perf (1.8x1.5mm), dimples | 0.386 | 0.314 | | 814.2 | 5162 | Witness: 1.5x.7 mm hole |
| 1550 | C2 | No perf., dimples (1 large) | 0.384 | 0.314 | | 957.3 | 5572 | |
| 1585 | C1 | No perf., v.slight cratering | 0.385 | 0.314 | | 469.3 | 4104 | Barely perforated 4th Nextel |
| 1586 | C1 | No perf., no craters, clean | 0.385 | 0.314 | | 630.2 | 4586 | Barely perforated 3rd Nextel |
| 1587 | C1 | No perf., cratering | 0.771 | 0.628 | | 1992.8 | 11427 | |
| 1588 | C4 | 2 Perfs (max=1.8 mm) | 0.492 | 0.314 | | 2054.8 | 11812 | Witness: craters & 3 dimples |
| 1589 | C5 | 1 Perf (3 mm), 3 dimples | 0.385 | 0.314 | | 905.5 | 5431 | Witness: 1 perf (2mm) & 10dmp |
| 1590 | C2 | No perf., 1 dimple | 0.490 | 0.314 | | 2179.2 | 12134 | |
| 1591 | C2 | No perf., 5 dimples (3 lrg) | 0.533 | 0.314 | | 2878.3 | 15852 | |
| 1594 | C5 | 1 Perf (3 mm) | 0.532 | 0.314 | | 1972.6 | 13055 | Witness: 7 dimples (1 lrg) |
| 1595 | C1 | No perf., v.slight cratering | 0.533 | 0.314 | | 2850.5 | 15767 | |
| 1597 | C4 | 1 perf (1.3x1 mm), dimples | 0.531 | 0.314 | | 2370.5 | 14239 | Witness: craters, 3 small dmp |
| 1598 | C1 | No perf., v.slight cratering | 0.614 | 0.314 | | 4543.9 | 24685 | Barely perforated 4th Nextel |
| 1603 | C1 | No perf., 3 dimples (1 lrg) | 0.614 | 0.314 | | 4033.1 | 23126 | |
| 1604 | C1 | No perf., 1 small dimple | 0.617 | 0.314 | | 3905.3 | 22885 | |
| 1625 | C2 | No perf., 2 small dimples | 0.612 | 0.314 | | 3559.0 | 21533 | |
| 1628 | C4 | 1 Perf (~1.2 mm circ) | 0.613 | 0.314 | | 2610.7 | 18710 | Wit: no perf, dmpls & melt |
| 1632 | C1 | No perf | 0.775 | 0.314 | | 6580.8 | 41801 | Secondary impact (half sabot) |
| 1635 | C2/D2 | No perf, 1 impact: dimple | 0.765 | 0.314 | | 5516.1 | 37754 | |
| 1636 | A2 | No perf, 1 large dmpl (D=3mm) | 0.636 | 0.314 | | 627.3 | 3907 | Slug DxL:.0798"x.0854"; est Vel |
| 1637 | C2 | No perf, surface marks, s.dmpl | 0.632 | 0.314 | | 608.8 | 3816 | Nylon Slug: D=.0798",L=.0869" |
| 1638 | C1 | No perf, surface marks | 0.629 | 0.314 | | 598.0 | 3755 | Nylon Slug: D=.0798",L=.0882" |
| 1639 | C1 | No perf, no damage | 0.639 | 0.314 | | 752.3 | 4319 | DxL:.0798"x.0882";4thNex no-perf |
| 1640 | C5/A3 | 1 perf (2.4 x 1.6 mm), dmpls | 0.385 | 0.314 | | 676.2 | 4736 | Wit: perf (1.6x1.2 mm), dmpls |
| 1641 | C4/A3 | 1 perf (2 mm), dmpls | 0.414 | 0.314 | | 820.2 | 5822 | Wit: no perf, dmpls |
| 1642 | C5/A3 | 1 perf (2.4x2 mm), dmpls | 0.413 | 0.314 | | 844.2 | 5868 | Wit: pinhole (~0.4 mm), dmpls |
| 1643 | C4/A3 | 1 perf (2x1.1 mm), 2dmpls | 0.414 | 0.314 | | 774.3 | 5675 | Wit: pinhole (~0.4 mm), dmpls |
| ? | F3 | No perf., bulge, molten splash | 0.194 | 1.155 | 78.3 | | | Chk Shot No., Vel.,M |
| 1150 | F3 | No perf., bulge, molten splash | 0.194 | 1.136 | 63.8 | | | Chk Proj Mass |
| 1151 | F3 | No perf., bulge, molten splash | 0.188 | 1.120 | 99.6 | | | Chk Proj Mass |
| 1152 | F3 | No perf., bulge, molten splash | 0.163 | 1.054 | 63.7 | | | Chk Proj Mass |

# MS_EXCEL DATA

Eric L. Christiansen
NASA/Johnson Space Center
Mail Code SN3
Translated from Lotus by L.Thompson (714)896-4495

## Multi-Shock Shield Database

Nextel Bumpers, Aluminum Rear Wall

| | Projectile Parameters | | | | | | | | Bumper | | | | Back Wall | | | |
|---|---|---|---|---|---|---|---|---|---|---|---|---|---|---|---|---|
| Shot No. | Site | Mat'l | Dia. (cm) | Dens. (g/cc) | Mass (g) | Vel. (km/sec) | Obliquity (deg) | Vn (km/sec) | Mat'l | Number Sheets | Areal D. (g/cm^2) | Overall Spacing (cm) | Mat'l | Thk (cm) | Areal D. (g/cm^2) | Yield Stress (ksi) |
| 1153 | UDRI | Al2017T4 | 0.9525 | 2.796 | 1.26512 | 6.75 | 0 | 6.75 | AF62 & BF54 | 4 | 0.417 | 30.48 | Al6061T6 | 0.203 | 0.551 | 36 |
| 1154 | UDRI | Al2017T4 | 0.9525 | 2.796 | 1.26512 | 6.94 | 0 | 6.94 | AF62 & BF54 | 4 | 0.417 | 30.48 | Al6061T6 | 0.203 | 0.551 | 36 |
| 1170 | UDRI | Al2017T4 | 0.9525 | 2.796 | 1.26512 | 6.72 | 0 | 6.72 | Nextel AF40 | 4 | 0.342 | 30.48 | Al6061T6 | 0.203 | 0.551 | 36 |
| 1173 | UDRI | Al2017T4 | 0.9525 | 2.796 | 1.26512 | 6.67 | 0 | 6.67 | Nextel AF62 | 4 | 0.400 | 22.86 | Al6061T6 | 0.203 | 0.551 | 36 |
| 1174 | UDRI | Al2017T4 | 0.9525 | 2.796 | 1.26512 | 6.57 | 0 | 6.57 | Nextel AF40 | 5 | 0.427 | 38.1 | Al6061T6 | 0.203 | 0.551 | 36 |
| 1250 | UDRI | Al2017T4 | 0.9549 | 2.796 | 1.27480 | 6.73 | 0 | 6.73 | Nextel BF54 | 4 | 0.434 | 30.48 | Al6061T6 | 0.203 | 0.551 | 36 |
| 1251 | UDRI | Al2017T4 | 0.9549 | 2.796 | 1.27490 | 6.80 | 0 | 6.80 | Nextel AF40 | 5 | 0.427 | 30.48 | Al6061T6 | 0.203 | 0.551 | 36 |
| 1253 | UDRI | Al2017T4 | 0.9550 | 2.796 | 1.27500 | 6.76 | 0 | 6.76 | (3) AF26 | 4 | 0.516 | 30.48 | Al6061T6 | 0.160 | 0.434 | 36 |
| 1293 | UDRI | Al2017T4 | 0.9550 | 2.796 | 1.27500 | 6.67 | 0 | 6.67 | AF62 | 4 | 0.400 | 30.48 | Al6061T6 | 0.229 | 0.620 | 36 |

# MS_EXCEL DATA

Eric L. Christians
NASA/Johnson S
Mail Code SN3
Translated from

Vn>6km/sec: K=mw*S^2*(Y/40)^0.5/(M*Vn) [sec/km] {K=43.1 for Nextel bumpers w/ Al rear wall}
Vn<6 km/sec: K2=mw*S*(Y/40)^0.5*Vn/M [km/sec-cm]
K3=mw*[S^2*[(Vn/3-1)+((2-Vn/(3*S^2))]*(Y/40)^0.5/M [km/sec-cm]

| Shot No. | Damage Class | Damage Description | Ratio AD Bumper to Proj. | Total Areal D. (g/cm^2) | K >6km/s | K2 <6km/s | K3 <6km/s | Comments |
|---|---|---|---|---|---|---|---|---|
| 1153 | F4 | Small perf. (trailing debris?) | 0.157 | 0.968 | 56.9 | | | 2 AF62, 2 BF54 (Chk Mass) |
| 1154 | F4 | Small perf. (trailing debris?) | 0.157 | 0.968 | 55.3 | | | 2 AF54, 2 BF62 (Chk Mass) |
| 1170 | F5 | Large petalled hole | 0.128 | 0.893 | 57.2 | | | Wit: molten splash (Chk M) |
| 1173 | F5 | Large petalled hole | 0.150 | 0.951 | 32.4 | | | Wit: molten splash (Chk M) |
| 1174 | F4 | Small perf. (trailing debris?) | 0.160 | 0.978 | 91.3 | | | (Chk M, S) |
| 1250 | F4 | Pin hole, 3/4" deep bulge | 0.162 | 0.985 | 56.6 | | | (Chk Wit.) |
| 1251 | F4 | 3 Cracks(L=3.5"-4"),deep bulge | 0.160 | 0.978 | 56.0 | | | Si=2",2",2",3",3" (Chk Wit) |
| 1253 | F4 | 3 Perfs (1.6-2.5 mm), d. bulge | 0.193 | 0.950 | 44.4 | | | Wit: s.hole |
| 1293 | F3 | No perf. Bulge, molten splash | 0.150 | 1.020 | 64.3 | | | |

# Appendix D

## MODELING THE RESPONSE OF A THIN SHEET DUE TO A HYPERVELOCITY DEBRIS CLOUD IMPACT

D. J. GROVE AND A. M. RAJENDRAN
UNIVERSITY OF DAYTON RESEARCH INSTITUTE
DAYTON, OHIO 45469-0120

A spacecraft can be protected from hypervelocity meteoroid impacts through the use of a thin sacrificial shield, or bumper. The presence of a bumper shield causes the meteoroid to vaporize and expand before it reaches the rear (inner) wall of the space structure. Spreading the meteoroid's momentum over a larger surface area helps prevent a catastrophic failure of the rear wall. Additional protection may be achieved by placing intermediate blankets, such as honeycomb, fiber composites, etc., between the bumper and rear wall. The loading conditions on the rear wall due to the impact of debris that passes through the intermediate layers are extremely complex and difficult to measure or calculate. However, a simplistic approach to the loading calculation using an impulse based model proposed earlier by Wilkinson [1] seems to yield encouraging solutions to this complex problem. Recently, Rajendran and Elfer [2] presented a comprehensive summary on "Debris-Impact Protection of Space Structures".

In modeling the deflection of the rear wall due to a debris cloud impact, Wilkinson chose an impulse-velocity-based approach, in which the cloud imparts a sudden velocity to the rear wall. Thus, only the rear wall is modeled, and no attempt is made to model the physical details of the debris cloud. Assuming a 1:1 momentum transfer, Wilkinson proposed the following expression for the initial velocity of the rear wall:

$$V_i(r) = \xi \exp\left(\frac{-r^2}{2\Delta^2}\right) \tag{1}$$

where

$$\xi = \frac{m_p V_p}{4 m_r S^2 \tan^2 \bar{\theta}} \tag{2}$$

and

$$\Delta = \left(\frac{2}{\pi}\right)^{\frac{1}{2}} S \tan \bar{\theta} \tag{3}$$

In the above expressions, $m_p$ and $V_p$ are the mass and velocity of the projectile, respectively. S is the inner spacing between the bumper and the rear wall, $m_r$ is the mass per unit area of the rear wall, and r is the radial distance from the center of the circular portion on the rear wall through which the momentum of the debris cloud is transferred. In this model, the parameters $m_p$, $V_p$, S, and $m_r$ are known based on the experimental configuration. The only parameter that has to be determined from the experiments is the debris cloud's spray angle $\bar{\theta}$. Wilkinson presented an empirical expression for tan $\bar{\theta}$ as

$$\tan \bar{\theta} = \begin{cases} \beta \left( \dfrac{m_b}{\rho_p d_p} \right)^{\frac{1}{2}} & \dfrac{m_b}{\rho_p d_p} < 1 \\ \beta & \dfrac{m_b}{\rho_p d_p} \geq 1 \end{cases} \tag{4}$$

where $m_b$ is the mass per unit area of the bumper sheet, $\rho_p$ is the density of the projectile, $d_p$ is the diameter of the projectile, and $\beta$ is an empirical parameter. Based on various hypervelocity experiments with lead and cadmium and hydrodynamic computer code calculations of vaporized aluminum, Wilkinson suggested a value of 0.6 for $\beta$.

After incorporating Wilkinson's model into the 2D STEALTH [3] finite difference code, numerous simulations were performed to evaluate the model for various impact velocities, bumper thicknesses, spacings between the bumper and rear wall, and rear wall yield strengths. Table 1 lists the configurations for the STEALTH simulations; the last column in the table lists the computed values of maximum effective strain ($\varepsilon_{eff}^{max}$) in the rear wall. The projectile, bumper, and rear wall were assumed to consist of aluminum, so $\rho_p = \rho_b = \rho_r = 2785$ kg/m$^3$ in all the simulations. Other constant simulation parameters were the rear wall thickness ($t_r = 3.175 \times 10^{-3}$ m) and Wilkinson's model parameter ($\beta = 0.392$).

TABLE 1

STEALTH SIMULATION CASES

| Case | $m_p$ (kg) | $d_p$ (m) | $V_p$ (m/s) | $m_pV_p$ (kg-m/s) | $t_b$ (m) | $Y_r$ (Pa) | S (m) | Computed $\varepsilon_{eff}^{max}$ (%) |
|---|---|---|---|---|---|---|---|---|
| 1 | $1.0\times10^{-3}$ | $7.7216\times10^{-3}$ | 6500 | 6.500 | $2.032\times10^{-3}$ | $4.0\times10^{8}$ | $109.093\times10^{-3}$ | 19.40 |
| 2 | $2.0232\times10^{-3}$ | $9.7282\times10^{-3}$ | 6360 | 12.870 | $3.175\times10^{-3}$ | $4.0\times10^{8}$ | $298.450\times10^{-3}$ | 0.42 |
| 3 | $1.0\times10^{-3}$ | $7.7216\times10^{-3}$ | 6986 | 6.986 | $2.032\times10^{-3}$ | $4.0\times10^{8}$ | $109.093\times10^{-3}$ | 21.75 |
| 4 | $1.0\times10^{-3}$ | $7.7216\times10^{-3}$ | 6170 | 6.170 | $2.032\times10^{-3}$ | $4.0\times10^{8}$ | $109.093\times10^{-3}$ | 17.90 |
| 5 | $1.0\times10^{-3}$ | $7.7216\times10^{-3}$ | 6170 | 6.170 | $1.600\times10^{-3}$ | $4.0\times10^{8}$ | $109.525\times10^{-3}$ | 26.20 |
| 6 | $1.0\times10^{-3}$ | $7.7216\times10^{-3}$ | 1625 | 1.625 | $2.032\times10^{-3}$ | $4.0\times10^{8}$ | $77.1404\times10^{-3}$ | 8.00 |
| 7 | $1.0\times10^{-3}$ | $7.7216\times10^{-3}$ | 3250 | 3.250 | $2.032\times10^{-3}$ | $4.0\times10^{8}$ | $109.093\times10^{-3}$ | 7.40 |
| 8 | $1.0\times10^{-3}$ | $7.7216\times10^{-3}$ | 6500 | 6.500 | $2.032\times10^{-3}$ | $4.0\times10^{8}$ | $154.281\times10^{-3}$ | 5.90 |
| 9 | $1.0\times10^{-3}$ | $7.7216\times10^{-3}$ | 2600 | 2.600 | $2.032\times10^{-3}$ | $4.0\times10^{8}$ | $77.1404\times10^{-3}$ | 15.50 |
| 10 | $1.0\times10^{-3}$ | $7.7216\times10^{-3}$ | 5200 | 5.200 | $2.032\times10^{-3}$ | $4.0\times10^{8}$ | $109.093\times10^{-3}$ | 13.70 |
| 11 | $1.0\times10^{-3}$ | $7.7216\times10^{-3}$ | 10400 | 10.400 | $2.032\times10^{-3}$ | $4.0\times10^{8}$ | $154.281\times10^{-3}$ | 12.45 |
| 12 | $1.0\times10^{-3}$ | $7.7216\times10^{-3}$ | 3250 | 3.250 | $2.032\times10^{-3}$ | $4.0\times10^{8}$ | $77.1404\times10^{-3}$ | 20.90 |
| 13 | $1.0\times10^{-3}$ | $7.7216\times10^{-3}$ | 13000 | 13.000 | $2.032\times10^{-3}$ | $4.0\times10^{8}$ | $154.281\times10^{-3}$ | 18.10 |

TABLE 1 (continued)

STEALTH SIMULATION CASES

| Case | $m_p$ (kg) | $d_p$ (m) | $V_p$ (m/s) | $m_pV_p$ (kg-m/s) | $t_b$ (m) | $Y_r$ (Pa) | S (m) | Computed $\varepsilon_{eff}^{max}$ (%) |
|---|---|---|---|---|---|---|---|---|
| 14 | $1.0x10^{-3}$ | $7.7216x10^{-3}$ | 4110 | 4.110 | $2.032x10^{-3}$ | $4.0x10^{8}$ | $77.1404x10^{-3}$ | 30.00 |
| 15 | $1.0x10^{-3}$ | $7.7216x10^{-3}$ | 8220 | 8.220 | $2.032x10^{-3}$ | $4.0x10^{8}$ | $109.093x10^{-3}$ | 28.30 |
| 16 | $1.0x10^{-3}$ | $7.7216x10^{-3}$ | 16440 | 16.440 | $2.032x10^{-3}$ | $4.0x10^{8}$ | $154.281x10^{-3}$ | 27.00 |
| 17 | $1.0x10^{-3}$ | $7.7216x10^{-3}$ | 4875 | 4.875 | $2.032x10^{-3}$ | $4.0x10^{8}$ | $77.1404x10^{-3}$ | 38.40 |
| 18 | $1.0x10^{-3}$ | $7.7216x10^{-3}$ | 9750 | 9.750 | $2.032x10^{-3}$ | $4.0x10^{8}$ | $109.093x10^{-3}$ | 36.00 |
| 19 | $1.0x10^{-3}$ | $7.7216x10^{-3}$ | 19500 | 19.500 | $2.032x10^{-3}$ | $4.0x10^{8}$ | $154.281x10^{-3}$ | 34.50 |
| 20 | $1.0x10^{-3}$ | $7.7216x10^{-3}$ | 5500 | 5.500 | $2.032x10^{-3}$ | $4.0x10^{8}$ | $77.1404x10^{-3}$ | 44.50 |
| 21 | $1.0x10^{-3}$ | $7.7216x10^{-3}$ | 11000 | 11.000 | $2.032x10^{-3}$ | $4.0x10^{8}$ | $109.093x10^{-3}$ | 41.75 |
| 22 | $1.0x10^{-3}$ | $7.7216x10^{-3}$ | 22000 | 22.000 | $2.032x10^{-3}$ | $4.0x10^{8}$ | $154.281x10^{-3}$ | 39.75 |
| 23 | $1.0x10^{-3}$ | $7.7216x10^{-3}$ | 6500 | 6.500 | $2.032x10^{-3}$ | $4.0x10^{8}$ | $77.1404x10^{-3}$ | 51.00 |
| 24 | $1.0x10^{-3}$ | $7.7216x10^{-3}$ | 13000 | 13.000 | $2.032x10^{-3}$ | $4.0x10^{8}$ | $109.093x10^{-3}$ | 46.70 |
| 25 | $1.0x10^{-3}$ | $7.7216x10^{-3}$ | 26000 | 26.000 | $2.032x10^{-3}$ | $4.0x10^{8}$ | $154.281x10^{-3}$ | 43.50 |
| 26 | $1.0x10^{-3}$ | $7.7216x10^{-3}$ | 8250 | 8.250 | $2.032x10^{-3}$ | $4.0x10^{8}$ | $77.1404x10^{-3}$ | 56.70 |

TABLE 1 (concluded)

STEALTH SIMULATION CASES

| Case | $m_p$ (kg) | $d_p$ (m) | $V_p$ (m/s) | $m_pV_p$ (kg-m/s) | $t_b$ (m) | $Y_r$ (Pa) | S (m) | Computed $\varepsilon_{eff}^{max}$ (%) |
|---|---|---|---|---|---|---|---|---|
| 27 | $1.0\times10^{-3}$ | $7.7216\times10^{-3}$ | 3250 | 3.250 | $2.032\times10^{-3}$ | $3.0\times10^{8}$ | $109.093\times10^{-3}$ | 8.55 |
| 28 | $1.0\times10^{-3}$ | $7.7216\times10^{-3}$ | 6500 | 6.500 | $2.032\times10^{-3}$ | $3.0\times10^{8}$ | $109.093\times10^{-3}$ | 24.30 |
| 29 | $1.0\times10^{-3}$ | $7.7216\times10^{-3}$ | 9750 | 9.750 | $2.032\times10^{-3}$ | $3.0\times10^{8}$ | $109.093\times10^{-3}$ | 41.70 |
| 30 | $1.0\times10^{-3}$ | $7.7216\times10^{-3}$ | 13000 | 13.000 | $2.032\times10^{-3}$ | $3.0\times10^{8}$ | $109.093\times10^{-3}$ | 49.50 |
| 31 | $1.0\times10^{-3}$ | $7.7216\times10^{-3}$ | 3250 | 3.250 | $2.032\times10^{-3}$ | $5.0\times10^{8}$ | $109.093\times10^{-3}$ | 6.53 |
| 32 | $1.0\times10^{-3}$ | $7.7216\times10^{-3}$ | 6500 | 6.500 | $2.032\times10^{-3}$ | $5.0\times10^{8}$ | $109.093\times10^{-3}$ | 16.50 |
| 33 | $1.0\times10^{-3}$ | $7.7216\times10^{-3}$ | 9750 | 9.750 | $2.032\times10^{-3}$ | $5.0\times10^{8}$ | $109.093\times10^{-3}$ | 31.50 |
| 34 | $1.0\times10^{-3}$ | $7.7216\times10^{-3}$ | 13000 | 13.000 | $2.032\times10^{-3}$ | $5.0\times10^{8}$ | $109.093\times10^{-3}$ | 44.10 |
| 35 | $1.0\times10^{-3}$ | $7.7216\times10^{-3}$ | 3250 | 3.250 | $2.032\times10^{-3}$ | $6.0\times10^{8}$ | $109.093\times10^{-3}$ | 5.45 |
| 36 | $1.0\times10^{-3}$ | $7.7216\times10^{-3}$ | 6500 | 6.500 | $2.032\times10^{-3}$ | $6.0\times10^{8}$ | $109.093\times10^{-3}$ | 14.30 |
| 37 | $1.0\times10^{-3}$ | $7.7216\times10^{-3}$ | 9750 | 9.750 | $2.032\times10^{-3}$ | $6.0\times10^{8}$ | $109.093\times10^{-3}$ | 27.10 |
| 38 | $1.0\times10^{-3}$ | $7.7216\times10^{-3}$ | 13000 | 13.000 | $2.032\times10^{-3}$ | $6.0\times10^{8}$ | $109.093\times10^{-3}$ | 40.80 |
| 39 | $1.0\times10^{-3}$ | $7.7216\times10^{-3}$ | 6807 | 6.807 | $2.032\times10^{-3}$ | $4.0\times10^{8}$ | $109.093\times10^{-3}$ | 20.90 |

The first five simulation cases corresponded to actual experiments, as indicated by Table 2. In each of these experiments, the rear wall consisted of 2219-T87 aluminum, and several intermediate layers of Kevlar cloth were placed between the bumper and rear wall. From split Hopkinson bar experiments, a critical strain to failure of 0.2 was determined for the 2219-T87 aluminum. Based on this failure strain, Wilkinson's model parameter $\beta$ was calibrated to match experiments 4-0502 (no failure) and 4-0510 (failure), which had identical configurations except for their impact velocities. Using Wilkinson's model, the response of the rear wall was simulated for each of the five experiments. Figure 1 shows the computed strain histories (at the center of the rear wall) from the five simulations. Comparing these results with the experimental observations (last column of Table 2) reveals that Wilkinson's model correctly predicted (at least qualitatively) the rear wall response in experiments 4-0506, 4-0528, and 4-0529.

More recently, we incorporated Wilkinson's model into the EPIC-2 [4] finite element code and used it to simulate an experiment for which the final deformation and the bulged shape of the rear wall were available. In this experiment, the impact velocity was 6.5 km/s, the aluminum ball projectile was 9.525 mm in diameter, the 6061-T6 aluminum bumper shield was 2.032 mm thick, the ductile 5456-H116 aluminum rear wall was 3.175 mm thick, and the inner spacing between the bumper and rear wall was about 109 mm. As in previous experiments, intermediate layers of Kevlar cloth were placed between the bumper and rear wall. We simulated this experimental configuration and compared the results with experimental measurements [5]. We chose a value of $\beta$ that produced the correct final thickness at the center of the thin sheet (rear wall). The simulated thickness reduction elsewhere in the sheet compared well with the experimental results, as illustrated by Figure 2.

We performed additional calculations to determine the effects of varying the boundary conditions on the thin sheet. We simulated a free boundary, a fixed boundary, and a boundary that was fixed in the vertical (z) direction and free in the

TABLE 2

EXPERIMENTS

| Simulation Case Number | Experiment Case Number | Experimentally Observed Rear Wall Response |
|---|---|---|
| 1 | 4-0502 | Bulged; no failure |
| 2 | 4-0506 | Insignificant bulge |
| 3 | 4-0510 | Tearing |
| 4 | 4-0528 | Bulged; no failure |
| 5 | 4-0529 | Tearing |

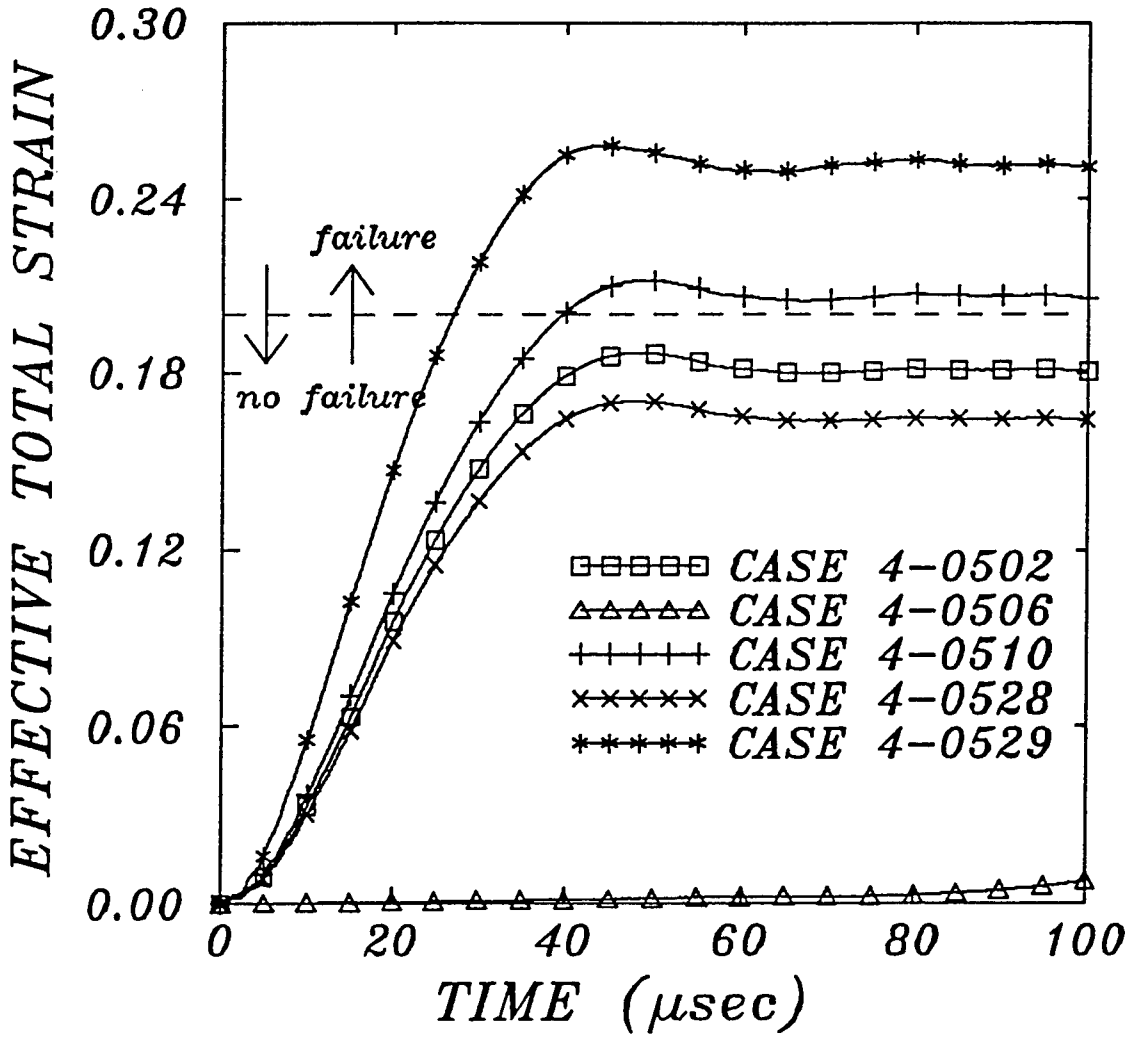


Figure 1. Calculated strain histories in rear wall

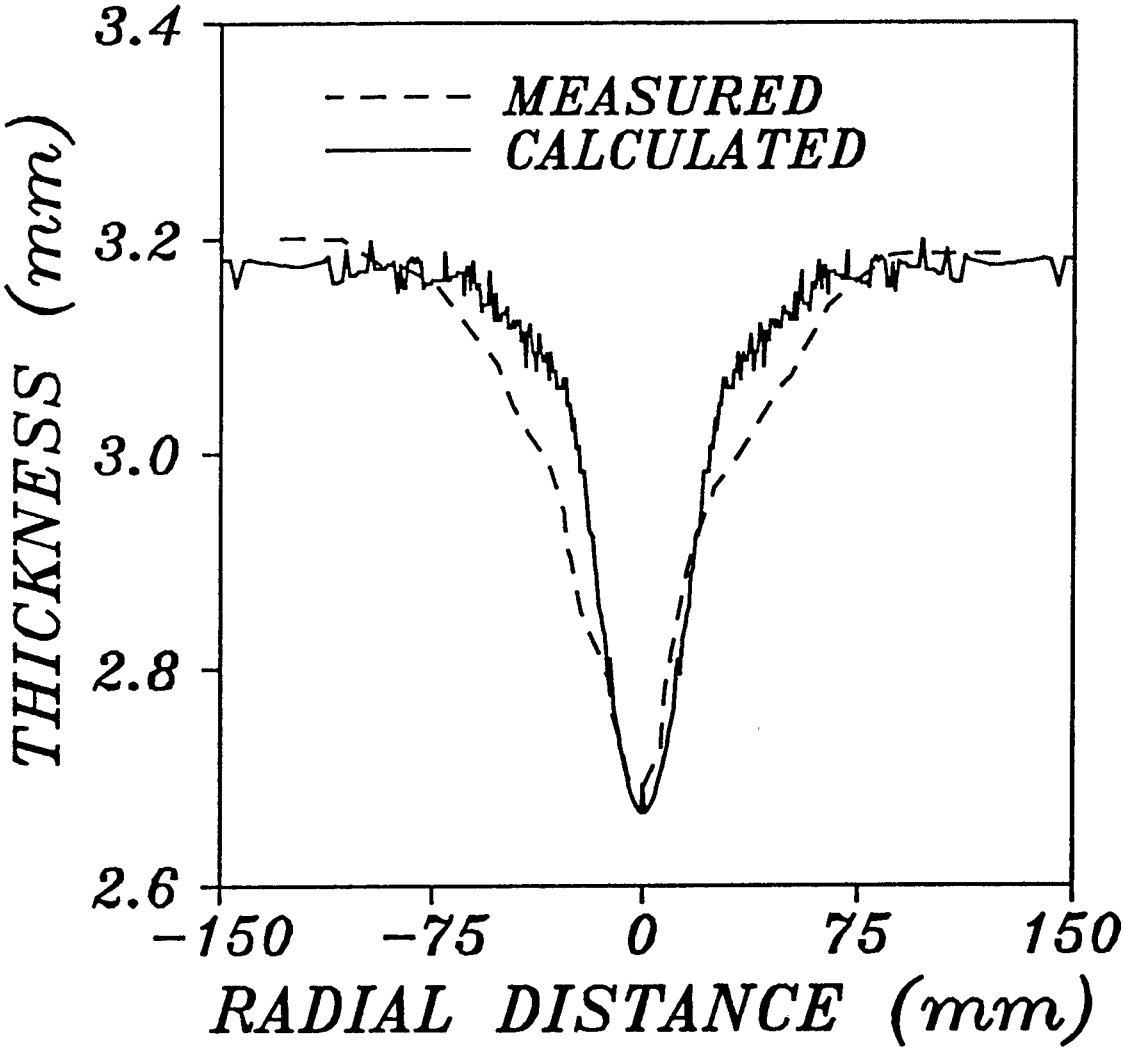


Figure 2. Comparison of final thickness profiles of rear wall

horizontal (r) direction. Since the simulations were all axisymmetric, the boundary conditions applied to the entire circumference of the circular thin sheet. In the actual experiment, the thin sheet was square and was held in place by a "picture frame" apparatus. The simulated shape of the rear wall deflection was sensitive to the boundary conditions imposed, and we were unable to achieve the amount of deflection measured by the experiment. However, the simulated thickness profile (see Figure 2) was independent of the boundary conditions.

Experimentally evaluating the effectiveness of various bumper shield configurations can be a time-consuming, expensive task. Since Wilkinson's model seems to generate a reasonable rear wall response, correlation of the above simulation results with some sort of design parameter may provide useful design criteria. Using $\xi$ and $\Delta$ from Equations (2) and (3), we can define a dimensionless design parameter $\gamma$ as follows:

$$\gamma = \frac{\xi^2 \rho_r e^{\left(\frac{t_r}{\Delta}\right)}}{Y_r} \tag{5}$$

where $\rho_r$, $t_r$, and $Y_r$ are the density, thickness, and yield strength, respectively, of the rear wall. Using the results from the 39 STEALTH simulations, we plotted the maximum effective strains experienced by the rear wall (as predicted by the simulations, using Wilkinson's model) versus the corresponding $\gamma$ values, as shown in Figure 3. There is definitely a correlation between $\gamma$ and the maximum effective strain experienced by the rear wall. The "best fit" line shown in Figure 3 is a cubic polynomial, defined as follows:

$$\%\varepsilon_{eff}^{max} = 1.01152 + 18.2953\gamma - 2.35542\gamma^2 + 0.113756\gamma^3 \tag{6}$$

Alternatively, we can define $\gamma$ as a function of $\varepsilon_{eff}^{max}$, so that a critical value of $\gamma$ can

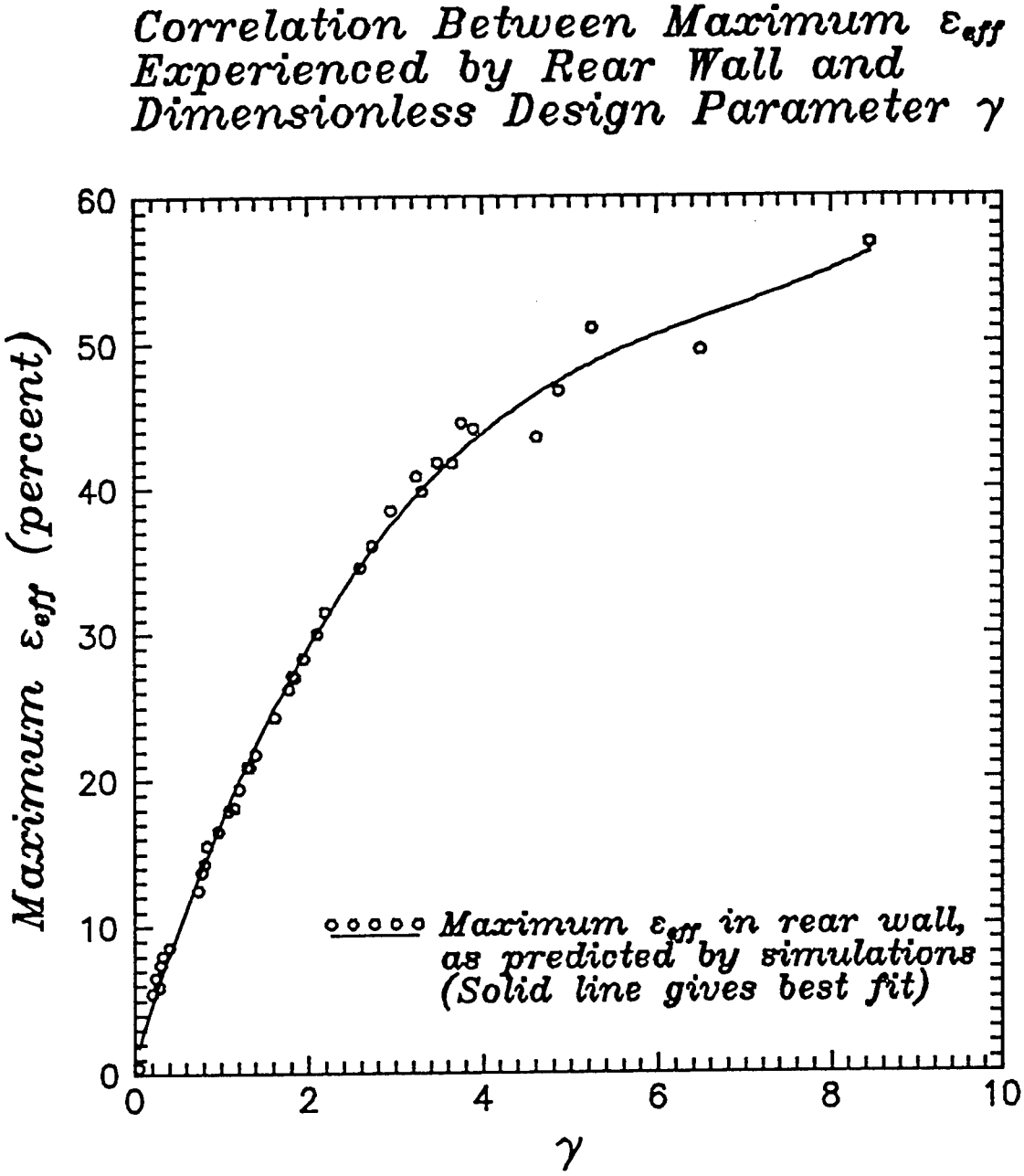


Figure 3. Correlation Between $\varepsilon_{eff}$ in Rear Wall, as Predicted by Simulations, and Dimensionless Design Parameter $\gamma$.

be calculated from the critical $\varepsilon_{eff}$ for rear wall failure. The resulting expression is a fourth degree polynomial:

$$\gamma = (-7.71338x10^{-3}) + (2.64191x10^{-2})(\%\varepsilon_{eff}^{max}) + (3.61467x10^{-3})(\%\varepsilon_{eff}^{max})^2 + (-1.24587x10^{-4})(\%\varepsilon_{eff}^{max})^3 + (1.74572x10^{-6})(\%\varepsilon_{eff}^{max})^4 \quad (7)$$

Knowing the critical $\varepsilon_{eff}$ for rear wall failure, the bumper/rear wall geometry can then be designed so that $\gamma$ is less than the critical value defined by Equation (7).

Using Equations (2)-(5) and (7), design curves were generated for various values of projectile momentum ($M_p$), rear wall thickness ($t_r$), rear wall strength ($Y_r$), and $\beta$. As in the simulations, the projectile, bumper, and rear wall materials were assumed to be aluminum. Each case considered four different levels of $\varepsilon_{eff}$ for rear wall failure (0.10, 0.20, 0.30, and 0.40). For each rear wall failure strain, the inner spacing (S) between the bumper and rear wall was plotted as a function of the ratio of bumper thickness ($t_b$) to projectile diameter ($d_p$). Given $\beta$, $t_r$, $Y_r$, and anticipated values of $M_p$ and $d_p$, these curves can be used to estimate the minimum S required for a given $t_b$ (or the minimum $t_b$ required for a given S). The various design curves are shown in Figures 4-84. Figure 4 provides the curves for the case when $\beta = 0.20$, $M_p = 6$ kg-m/s, $t_r = 1$ mm, and $Y_r = 0.20$ GPa. If the anticipated $d_p$ is 2 mm and the desired $t_b$ is 1 mm, then the S values corresponding to $t_b/d_p = 0.5$ reveal the critical inner spacings for the various rear wall failure strains. In this case ($t_b/d_p = 0.5$), for instance, the design curves predict that the rear wall will experience a maximum strain of 10% for an inner spacing of about 375 mm, and a maximum strain of 40% for an inner spacing of about 230 mm.

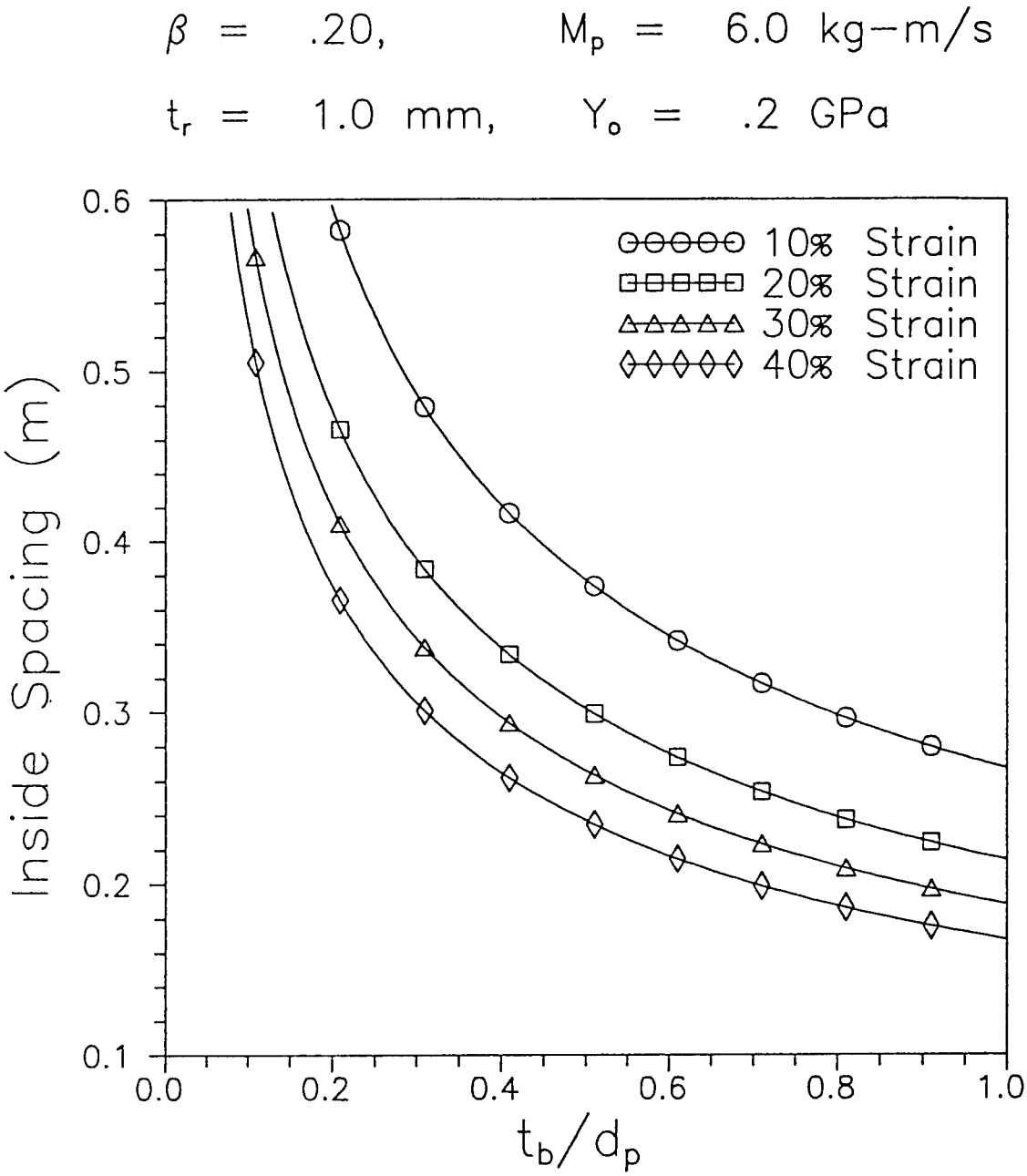


Figure 4. Design Curves for $\beta = 0.2$, $M_p = 6$ kg-m/s, $t_r = 1$ mm, and $Y_r = 0.2$ GPa

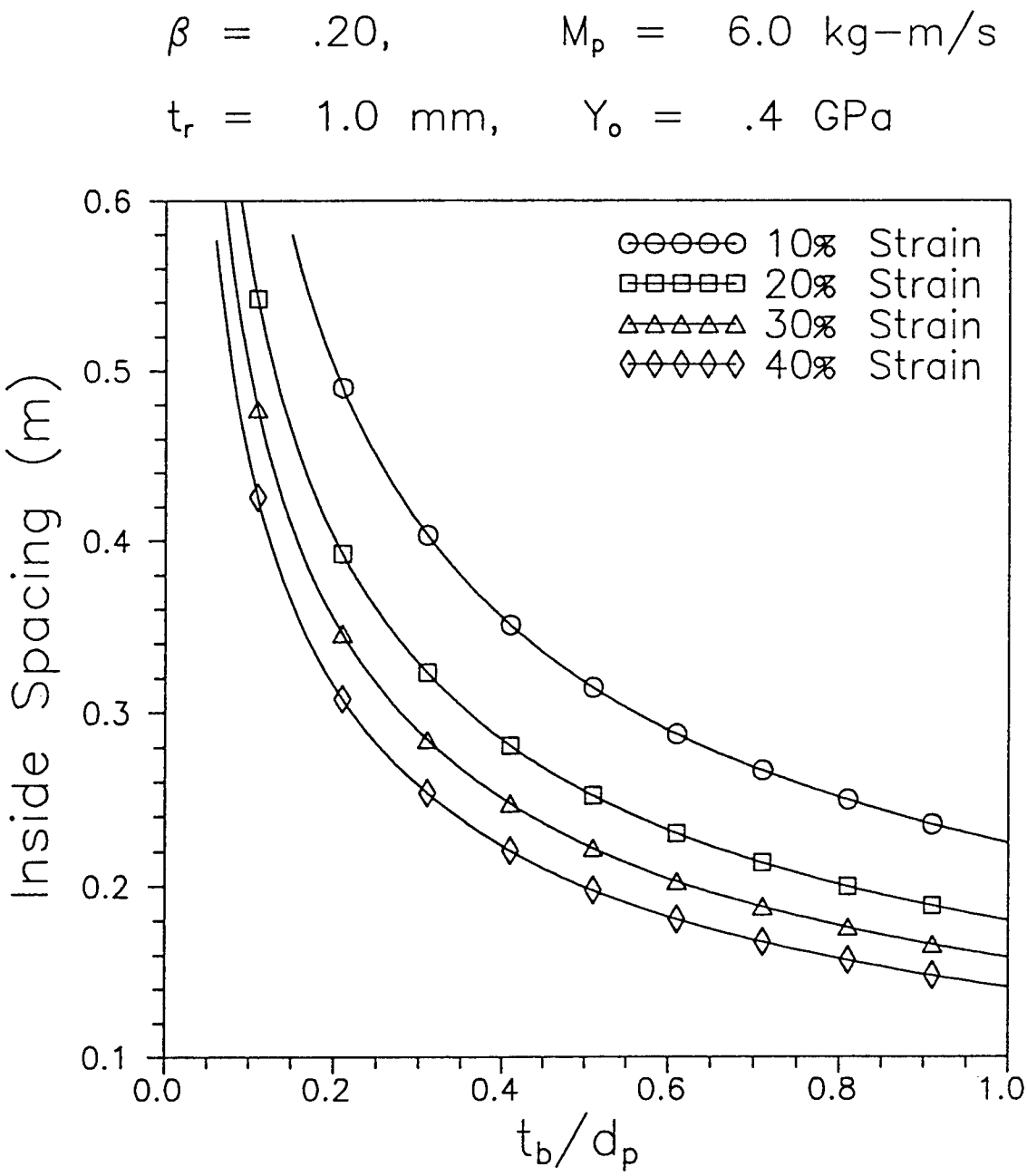


**Figure 5.** Design Curves for $\beta = 0.2$, $M_p = 6$ kg-m/s, $t_r = 1$ mm, and $Y_r = 0.4$ GPa

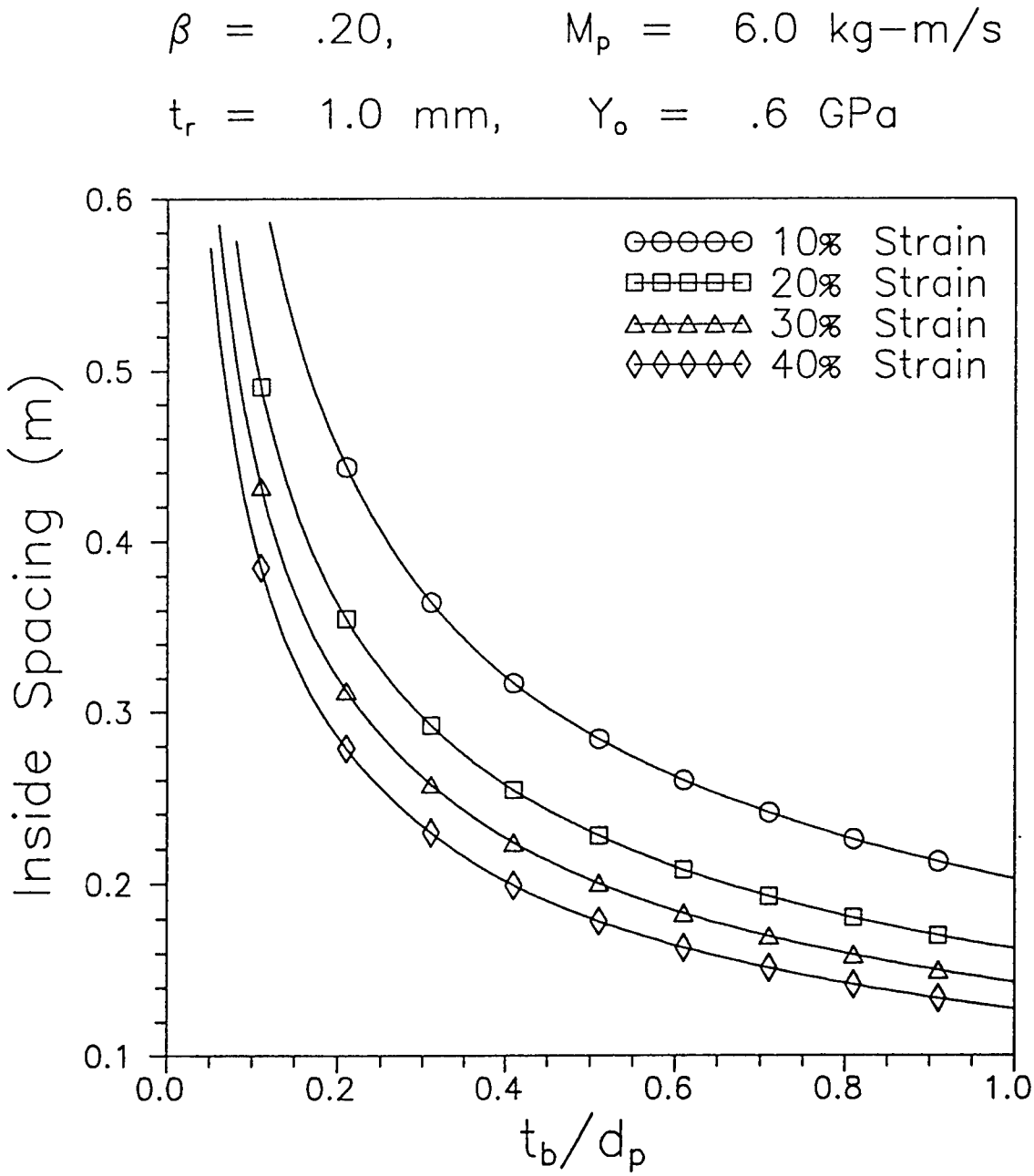


**Figure 6.** Design Curves for $\beta = 0.2$, $M_p = 6$ kg-m/s, $t_r = 1$ mm, and $Y_r = 0.6$ GPa

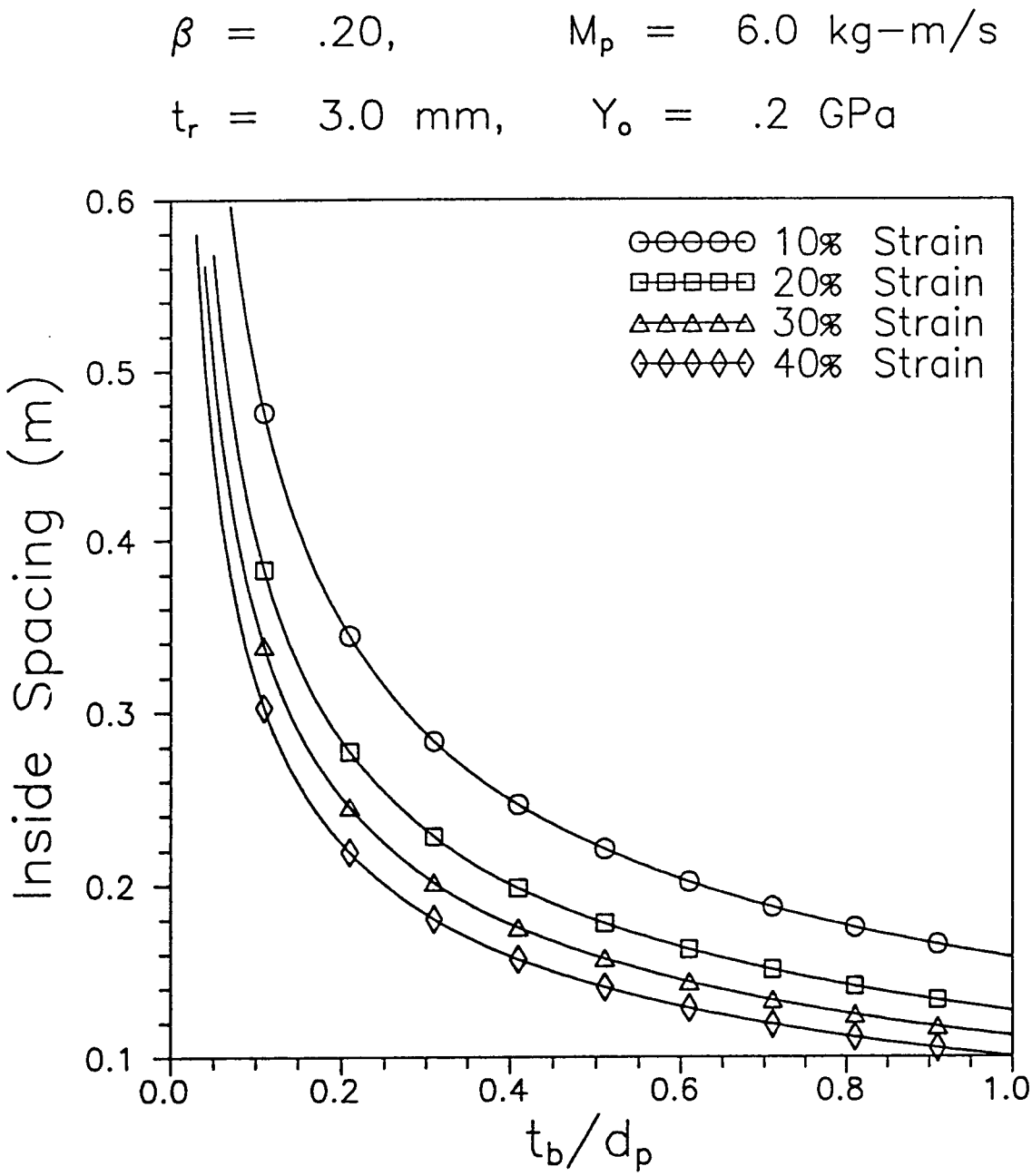


**Figure 7.** **Design Curves for $\beta = 0.2$, $M_p = 6$ kg-m/s, $t_r = 3$ mm, and $Y_r = 0.2$ GPa**

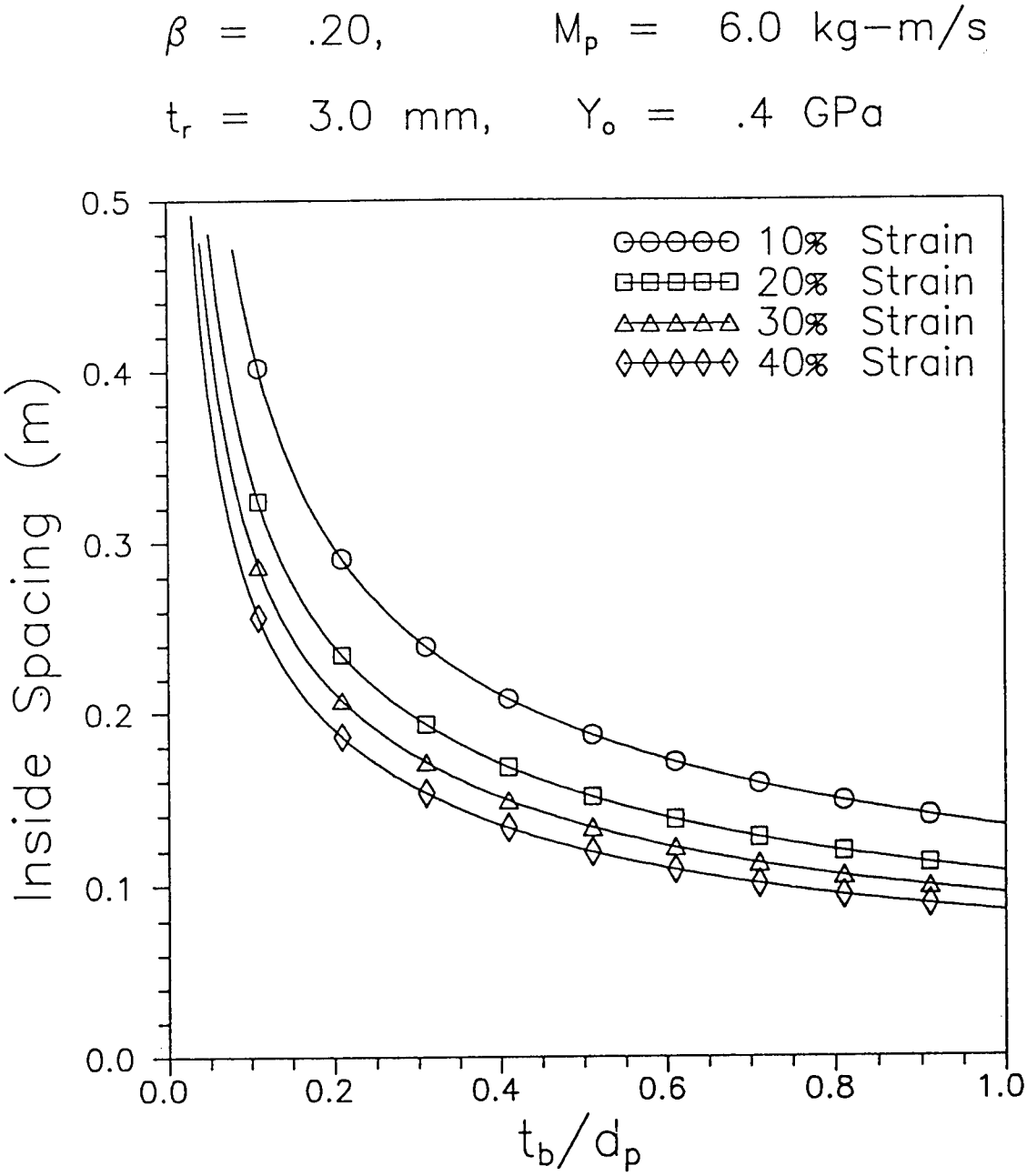


Figure 8. Design Curves for $\beta = 0.2$, $M_p = 6$ kg-m/s, $t_r = 3$ mm, and $Y_r = 0.4$ GPa

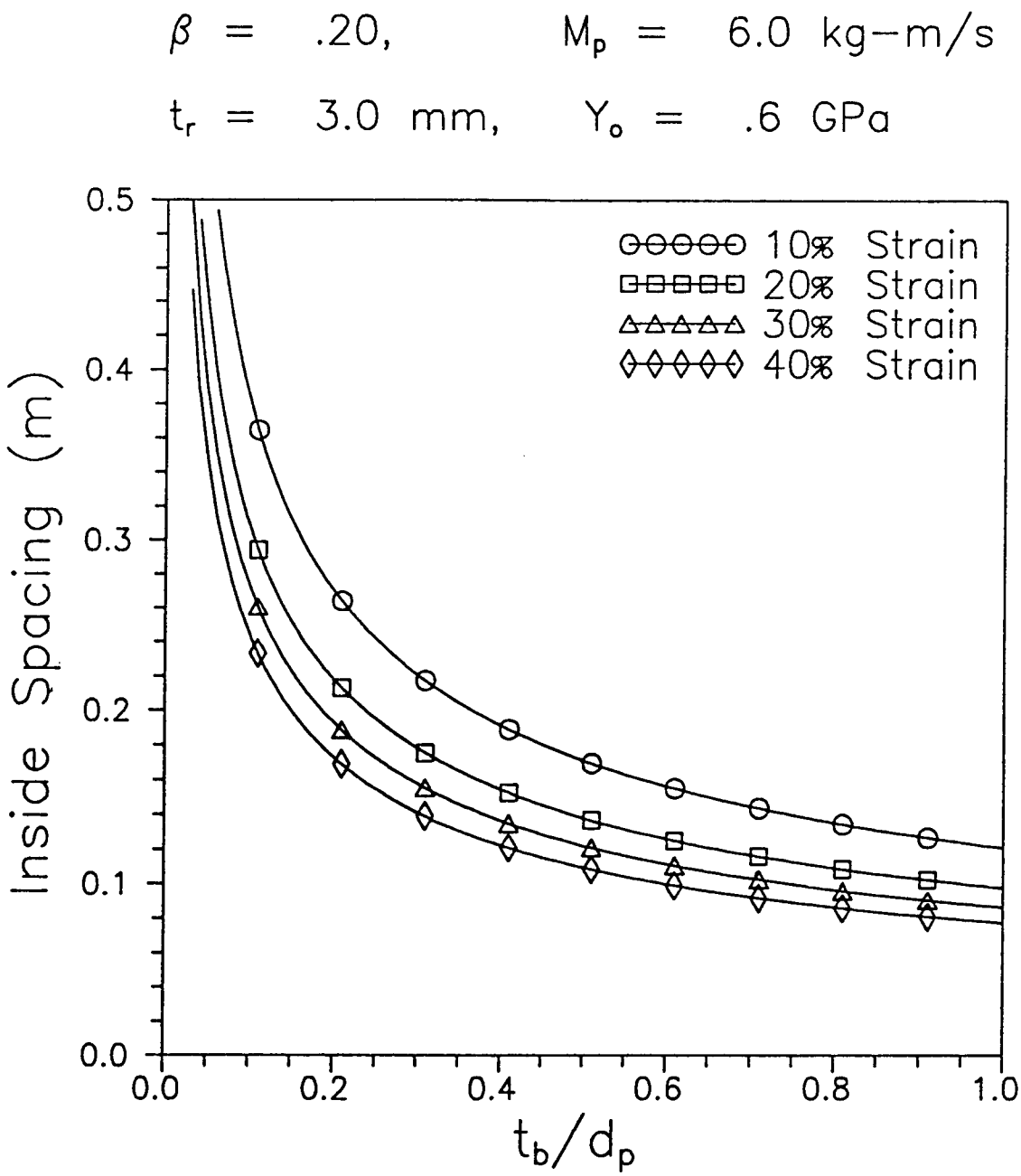


**Figure 9.** **Design Curves for $\beta = 0.2$, $M_p = 6$ kg-m/s, $t_r = 3$ mm, and $Y_r = 0.6$ GPa**

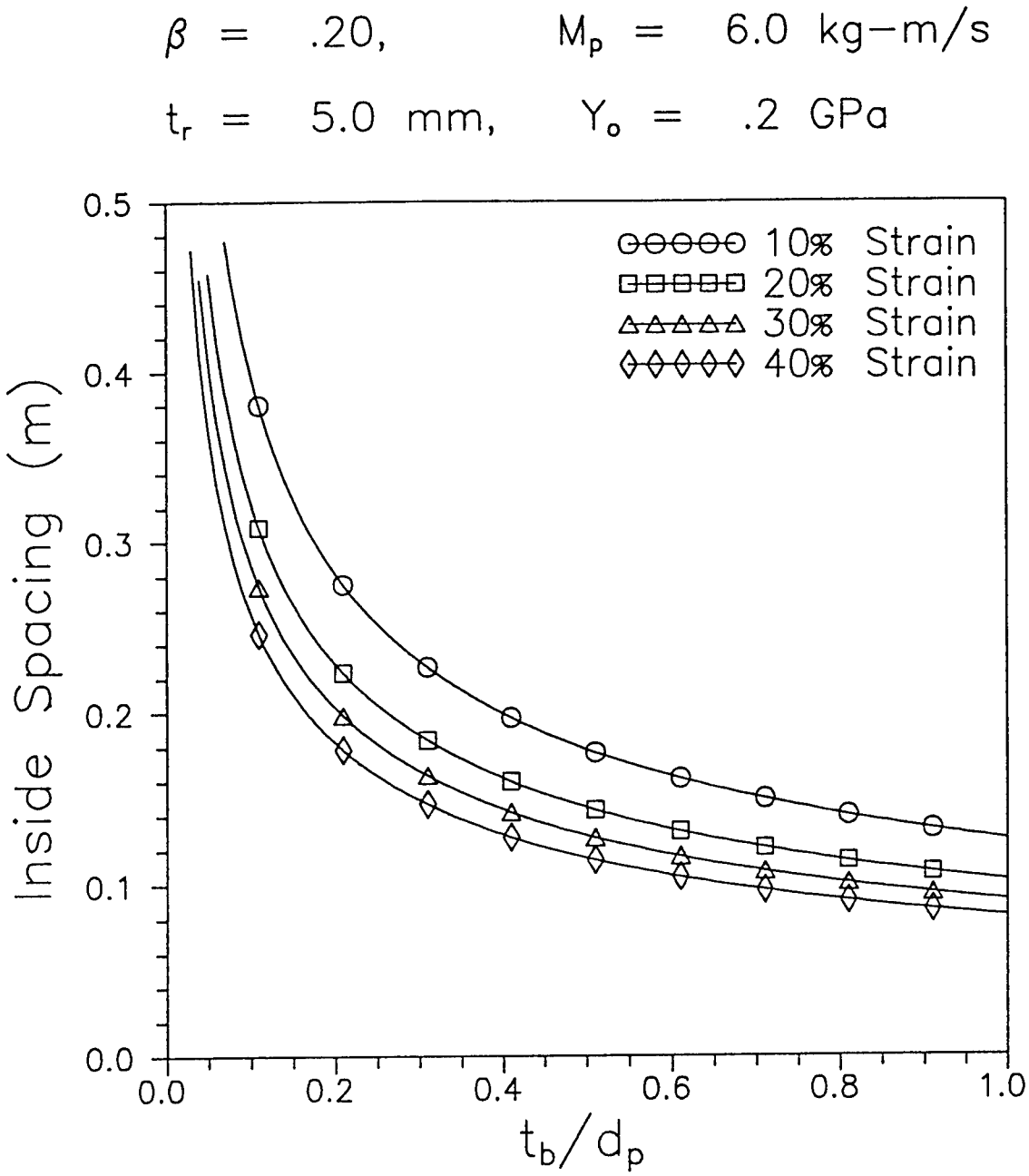


Figure 10. Design Curves for $\beta = 0.2$, $M_p = 6$ kg-m/s, $t_r = 5$ mm, and $Y_r = 0.2$ GPa

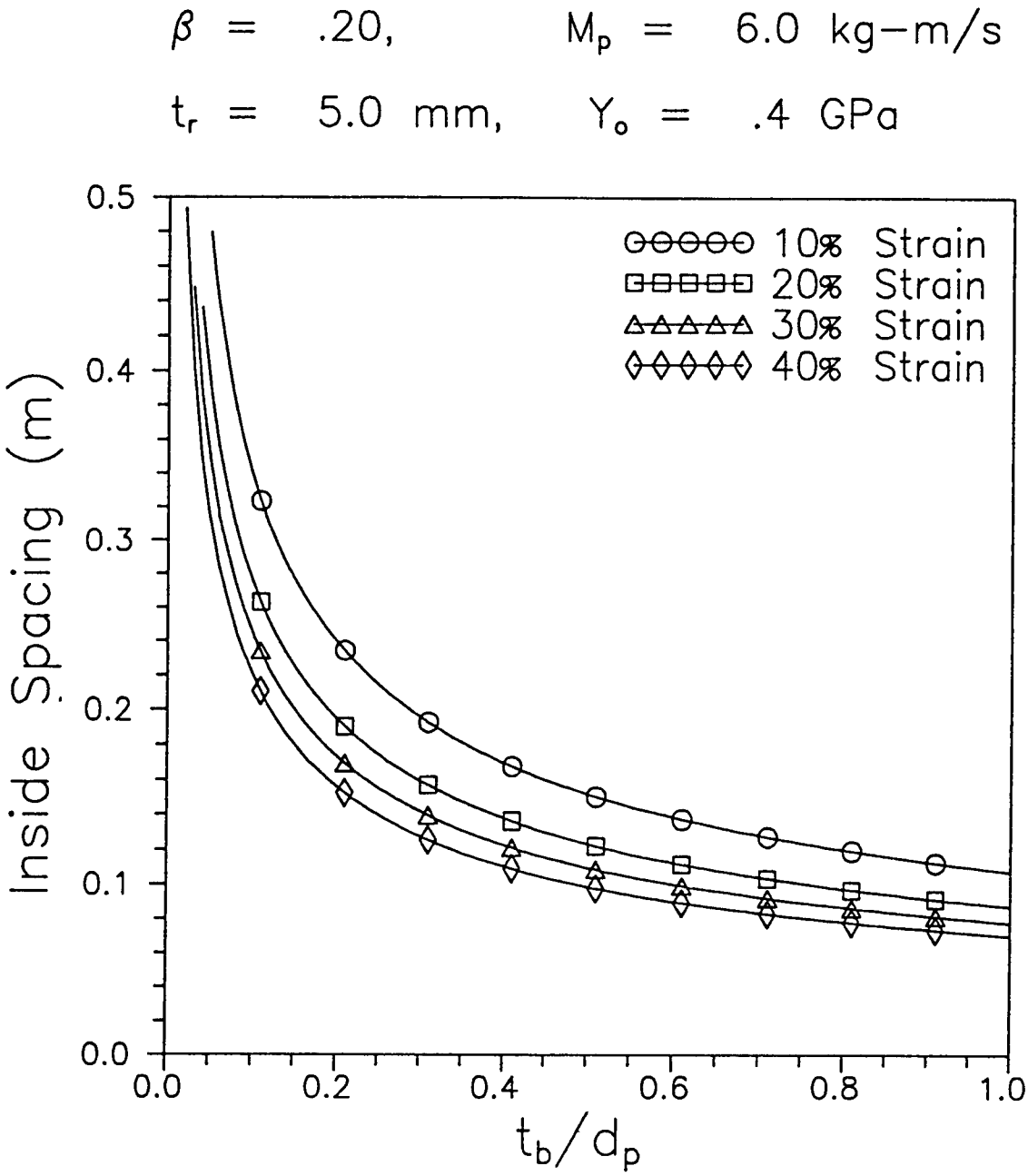


**Figure 11.** Design Curves for $\beta = 0.2$, $M_p = 6$ kg-m/s, $t_r = 5$ mm, and $Y_r = 0.4$ GPa

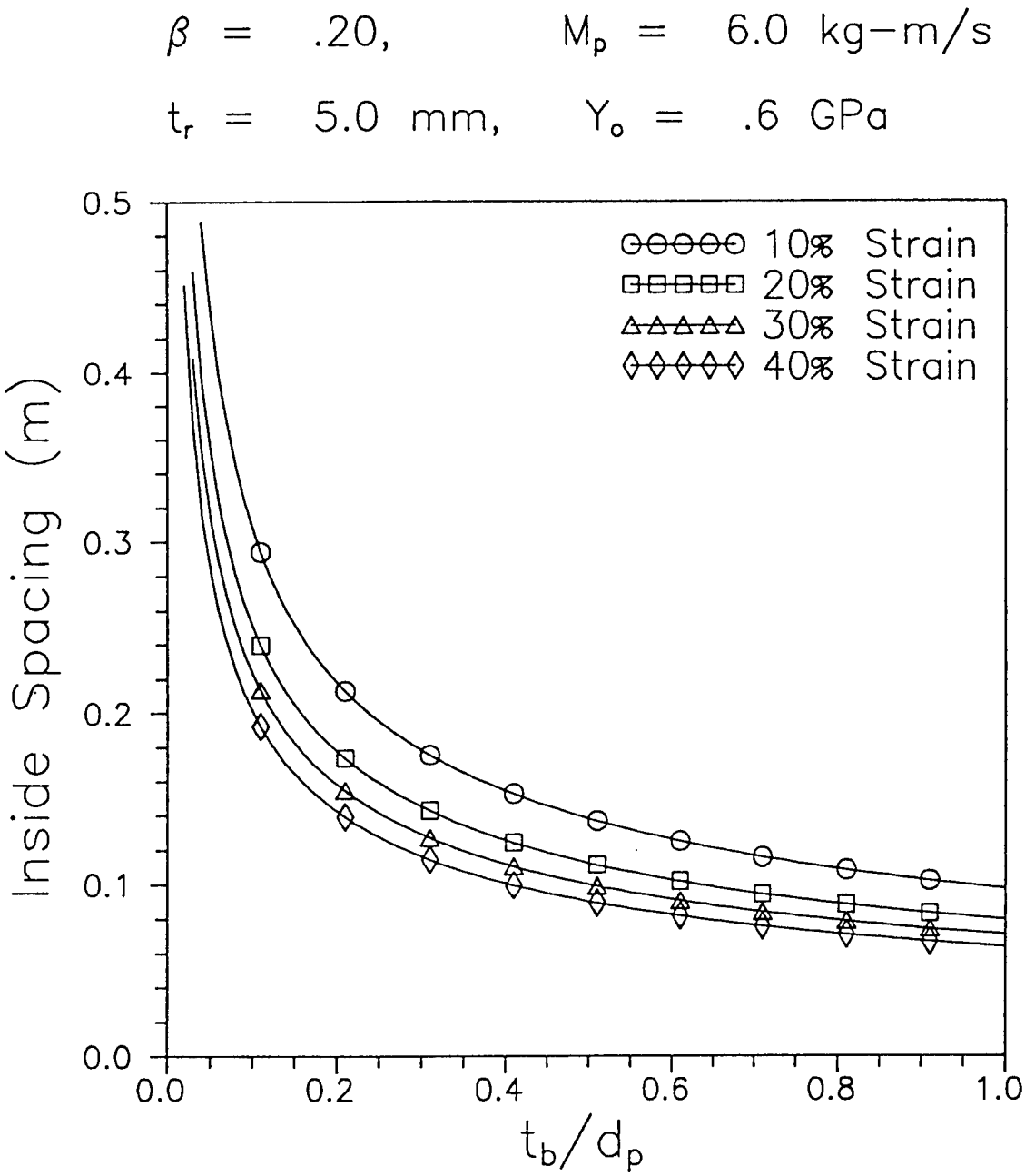


Figure 12. Design Curves for $\beta = 0.2$, $M_p = 6$ kg-m/s, $t_r = 5$ mm, and $Y_r = 0.6$ GPa

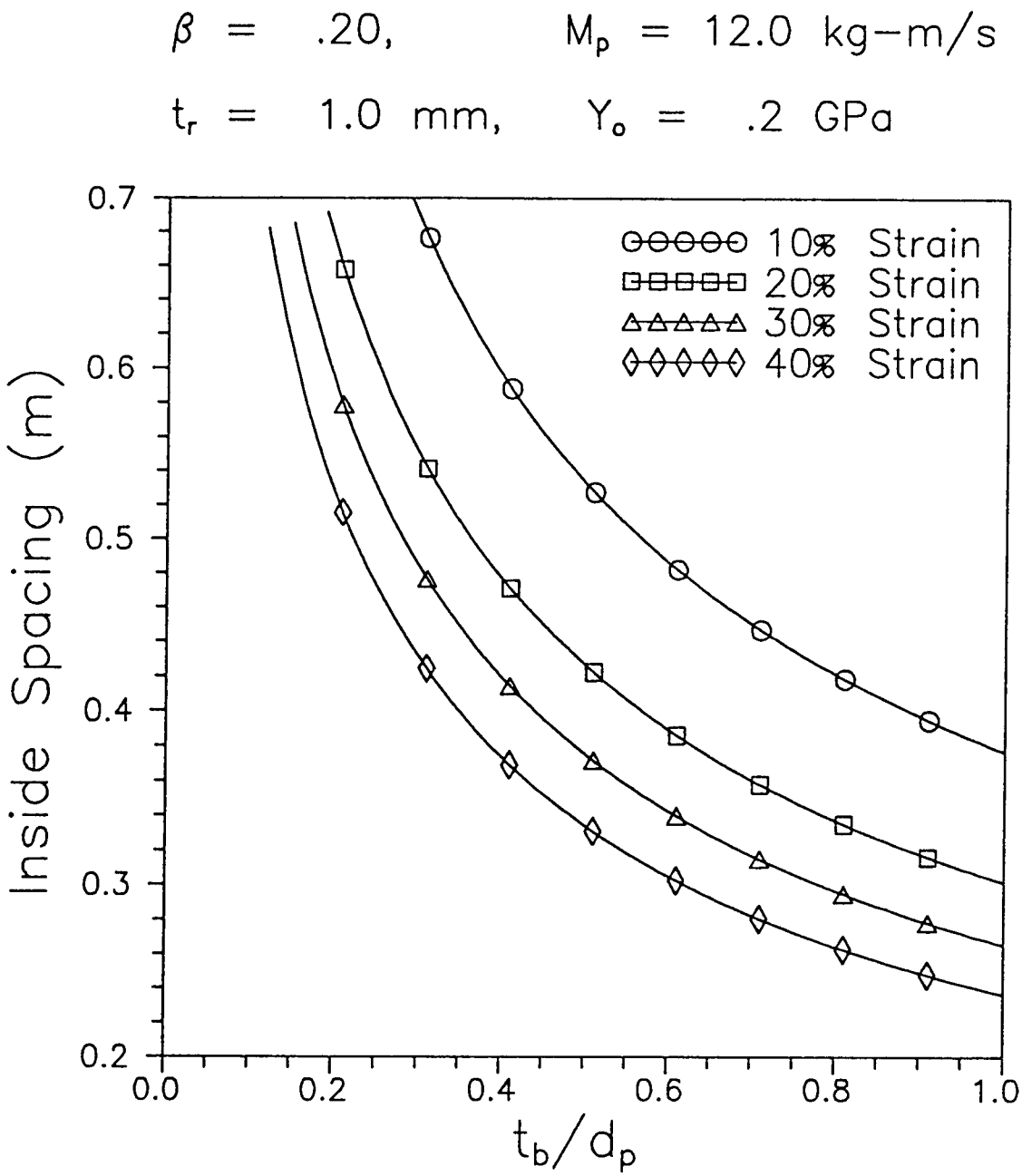


Figure 13. Design Curves for $\beta = 0.2$, $M_p = 12$ kg-m/s, $t_r = 1$ mm, and $Y_r = 0.2$ GPa

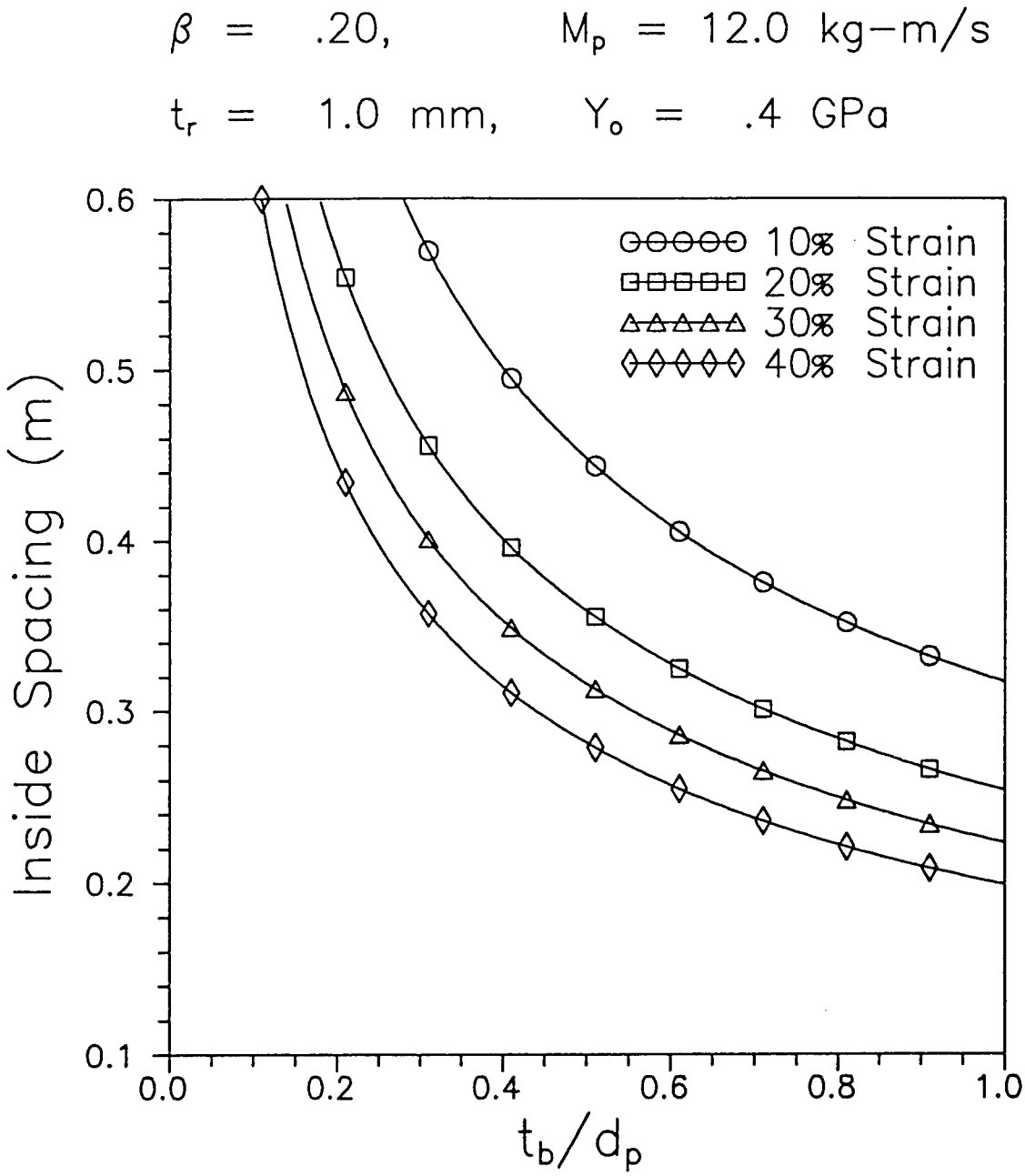


**Figure 14.** Design Curves for $\beta = 0.2$, $M_p = 12$ kg-m/s, $t_r = 1$ mm, and $Y_r = 0.4$ GPa

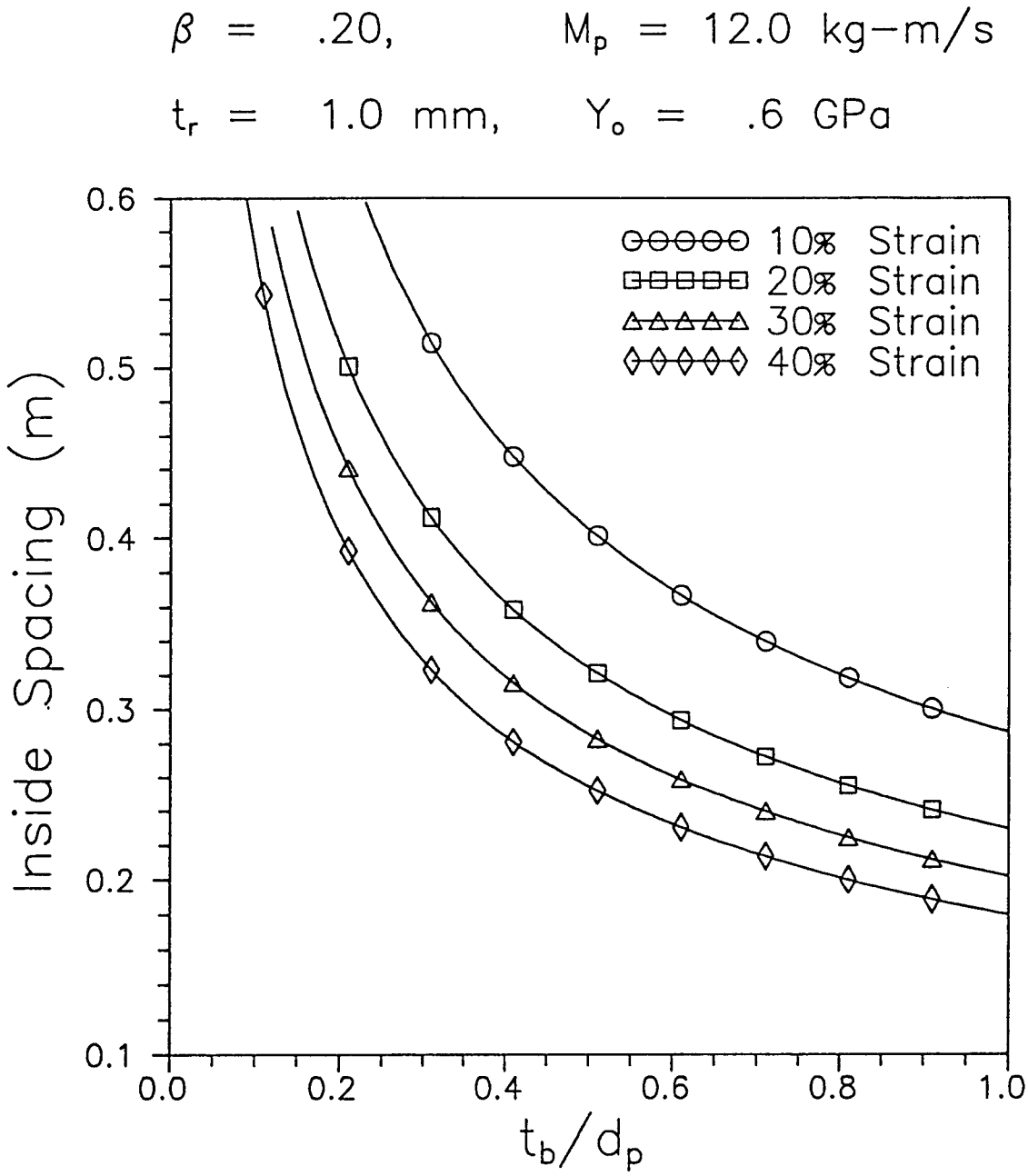


**Figure 15.** Design Curves for $\beta = 0.2$, $M_p = 12$ kg-m/s, $t_r = 1$ mm, and $Y_r = 0.6$ GPa

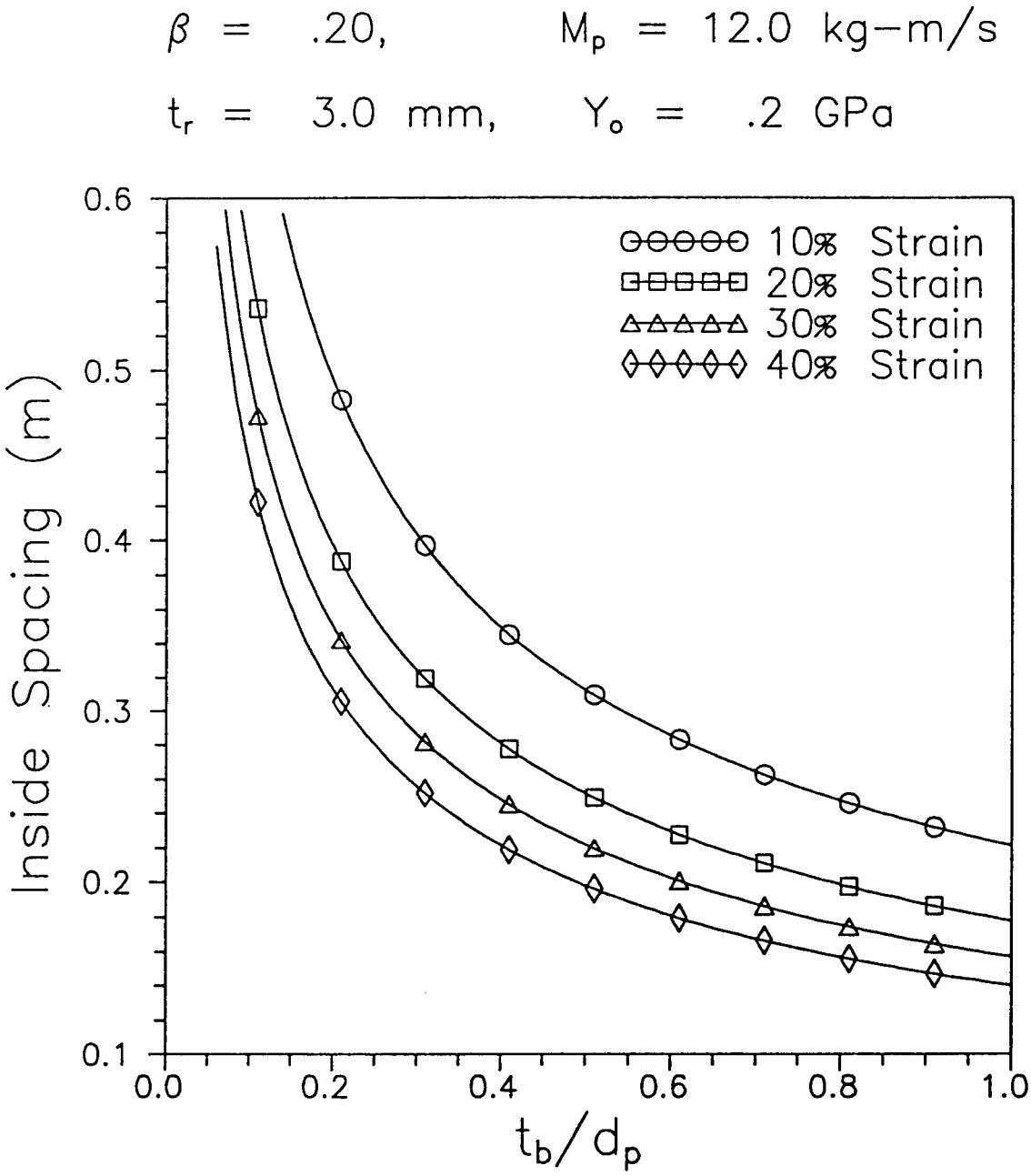


**Figure 16. Design Curves for $\beta$ = 0.2, $M_p$ = 12 kg-m/s, $t_r$ = 3 mm, and $Y_r$ = 0.2 GPa**

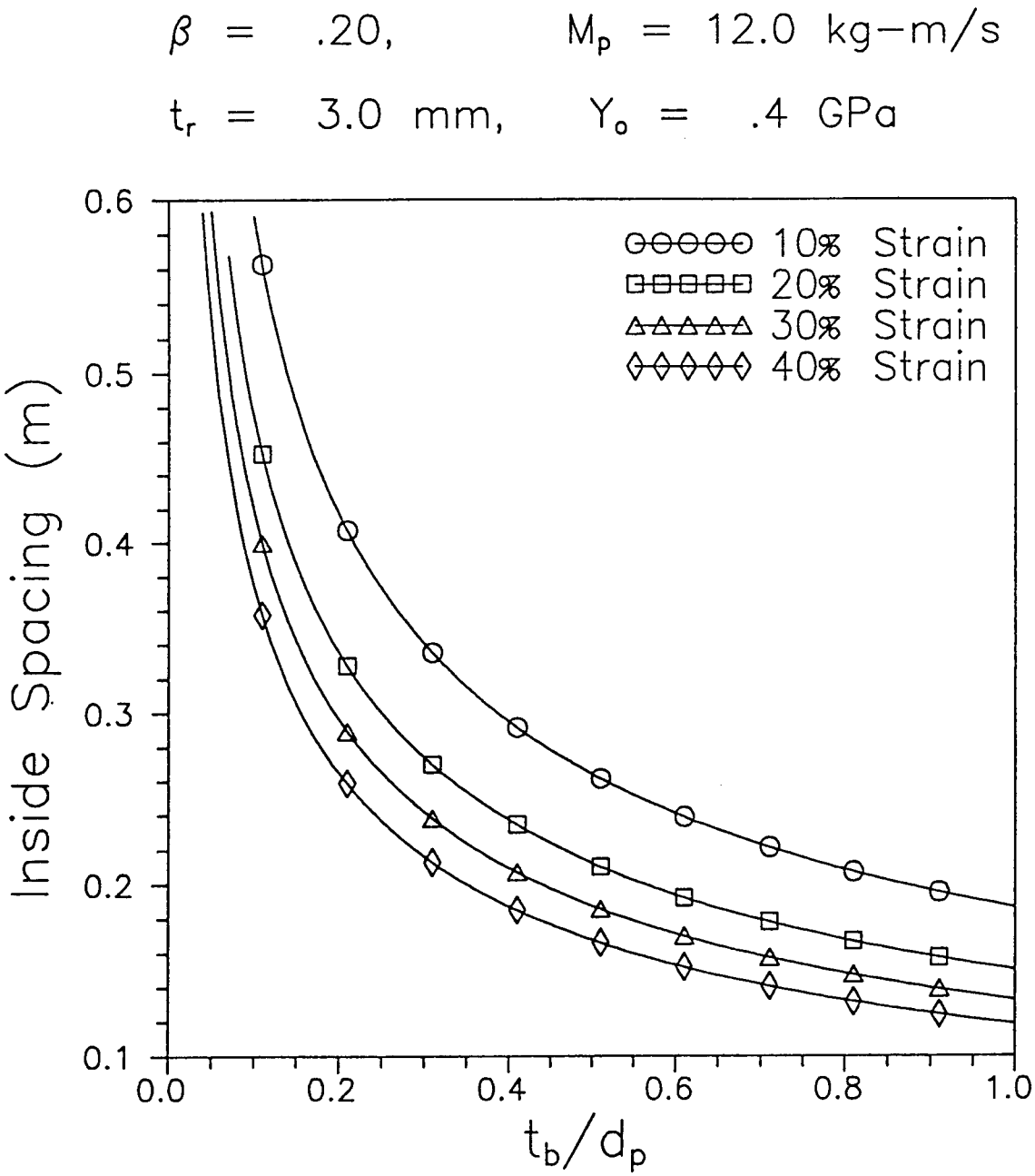


**Figure 17.** Design Curves for $\beta = 0.2$, $M_p = 12$ kg-m/s, $t_r = 3$ mm, and $Y_r = 0.4$ GPa

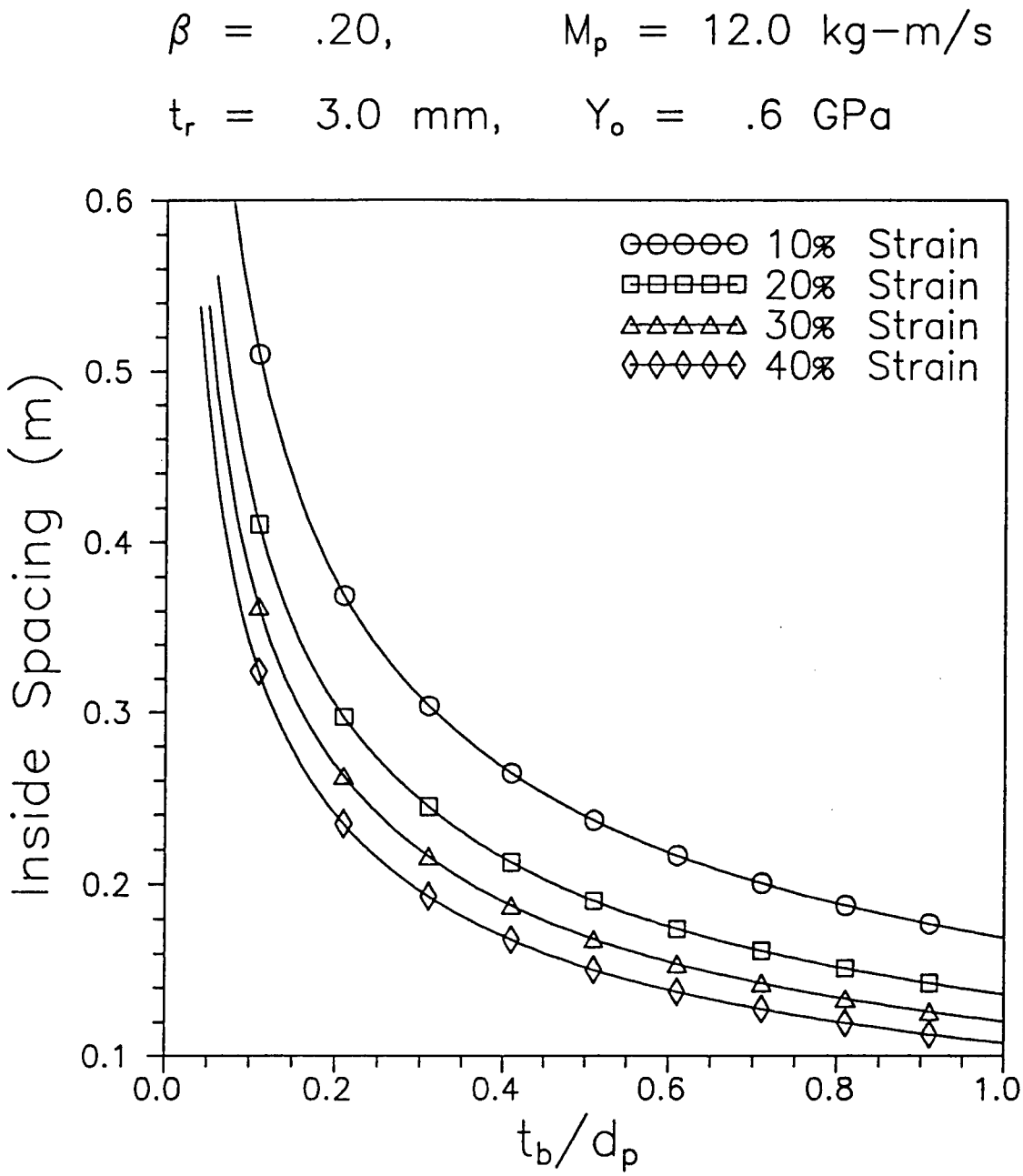


Figure 18. Design Curves for $\beta = 0.2$, $M_p = 12$ kg-m/s, $t_r = 3$ mm, and $Y_r = 0.6$ GPa

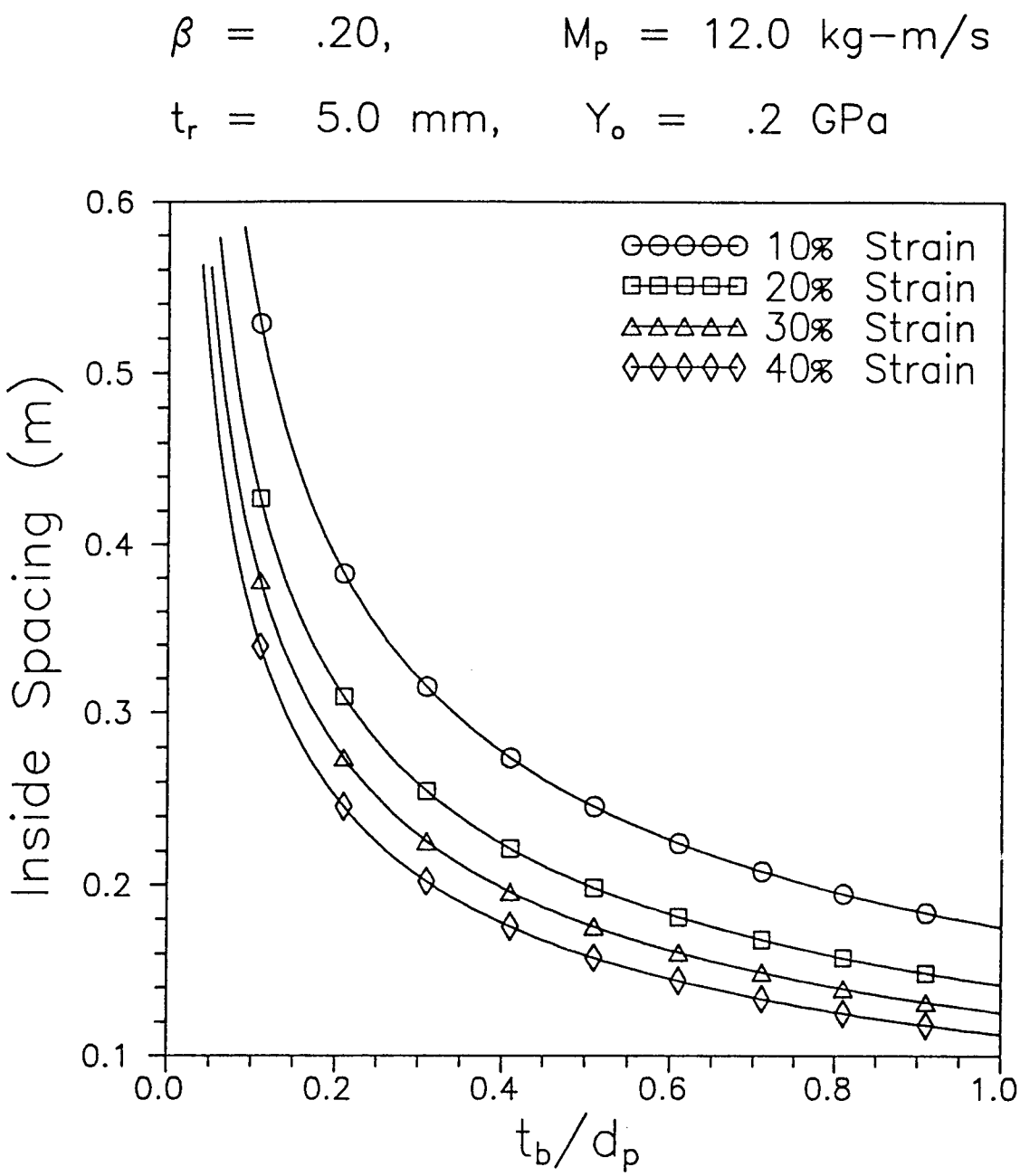


Figure 19. Design Curves for $\beta = 0.2$, $M_p = 12$ kg-m/s, $t_r = 5$ mm, and $Y_r = 0.2$ GPa

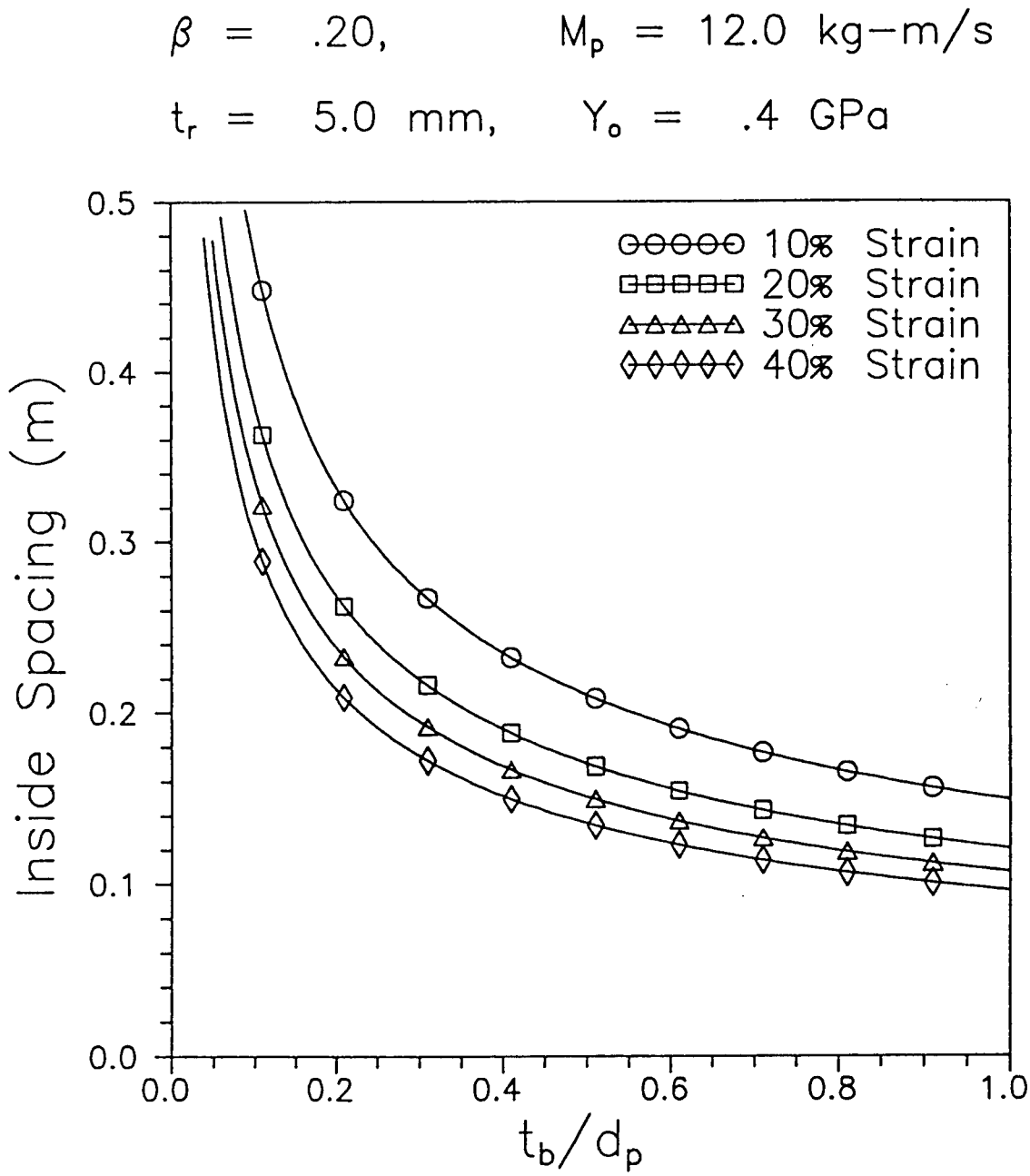


**Figure 20.** Design Curves for $\beta = 0.2$, $M_p = 12$ kg-m/s, $t_r = 5$ mm, and $Y_r = 0.4$ GPa

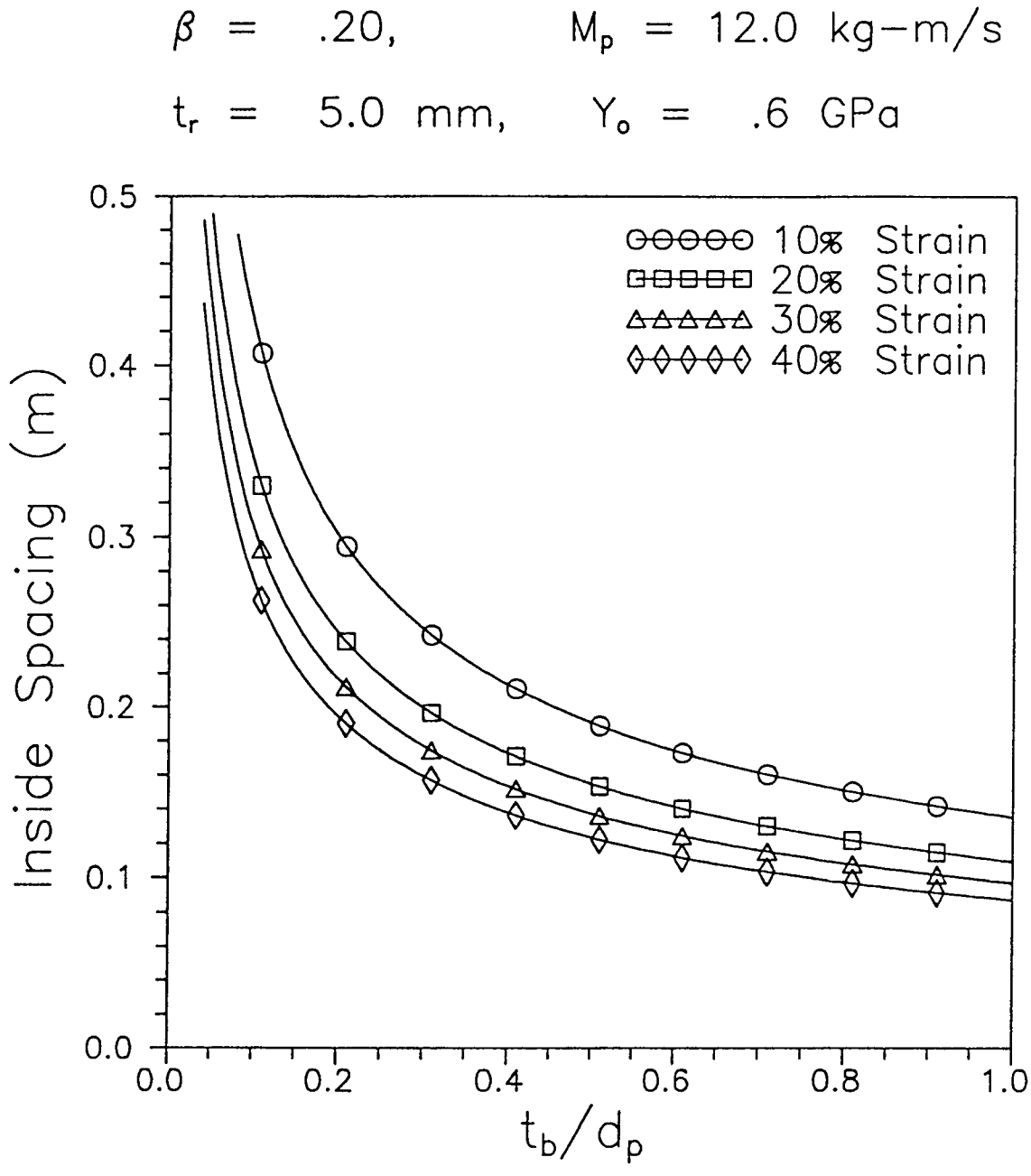


Figure 21. Design Curves for $\beta = 0.2$, $M_p = 12$ kg-m/s, $t_r = 5$ mm, and $Y_r = 0.6$ GPa

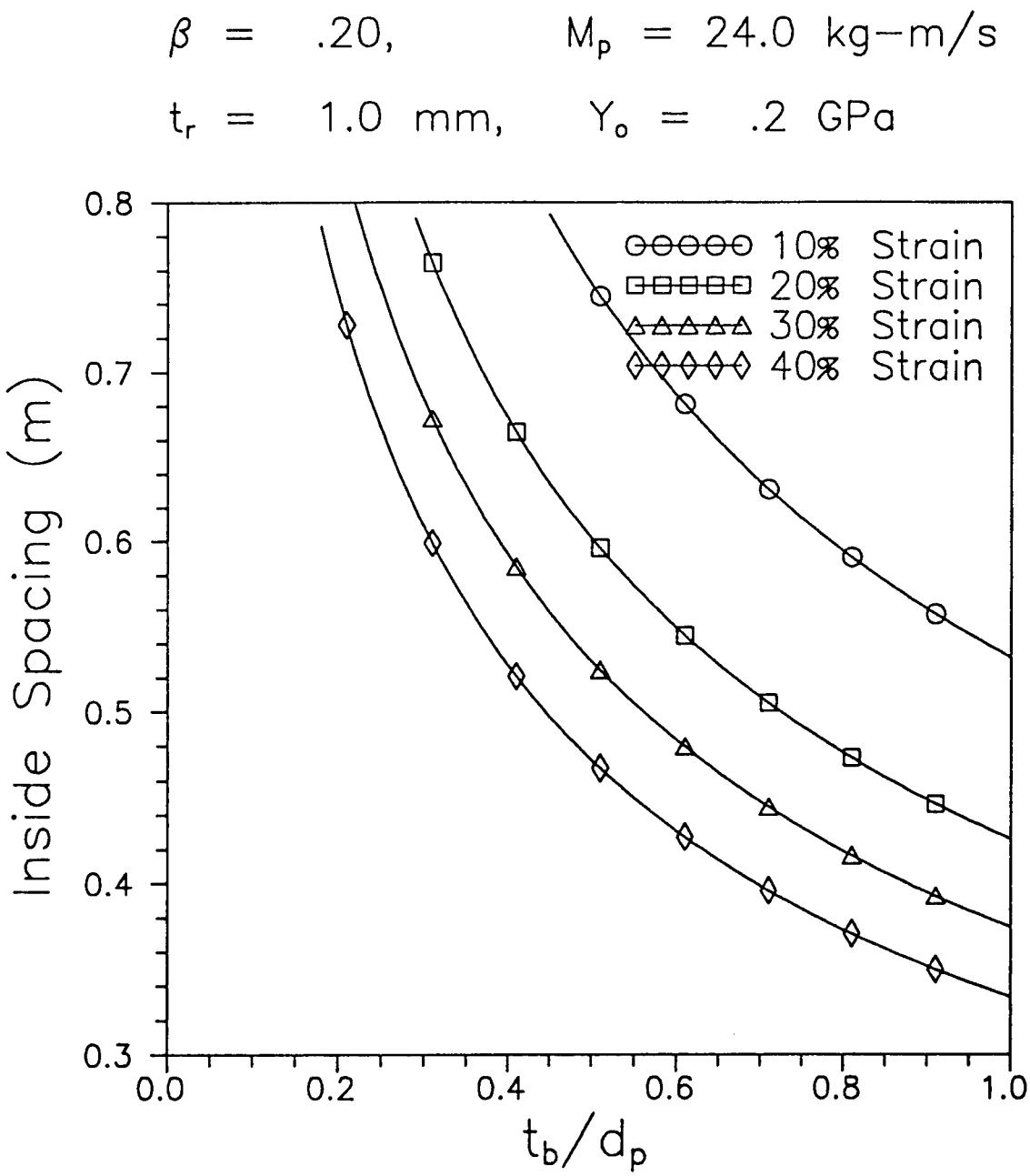


**Figure 22.** Design Curves for $\beta = 0.2$, $M_p = 24$ kg-m/s, $t_r = 1$ mm, and $Y_r = 0.2$ GPa

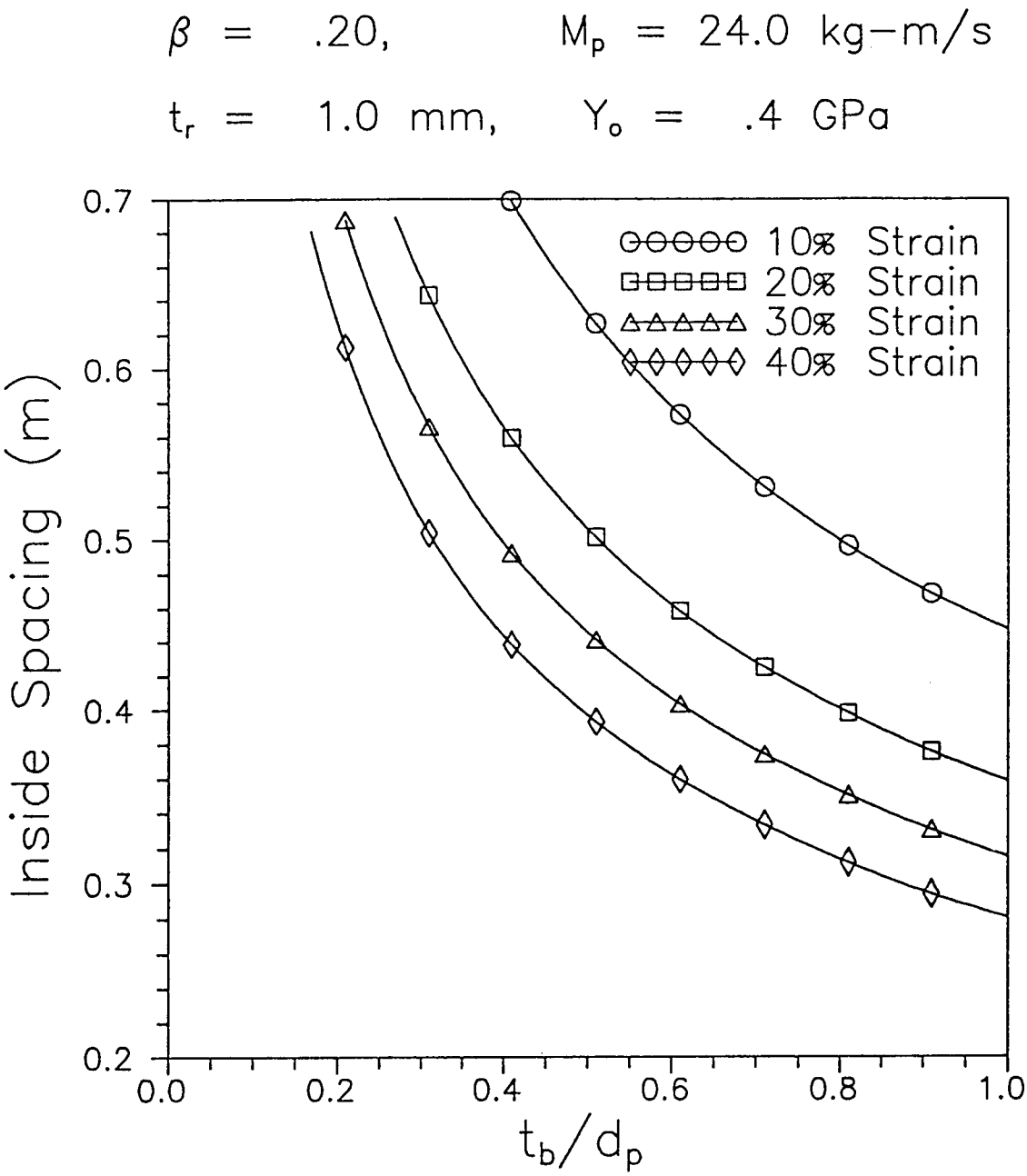


Figure 23. Design Curves for $\beta = 0.2$, $M_p = 24$ kg-m/s, $t_r = 1$ mm, and $Y_r = 0.4$ GPa

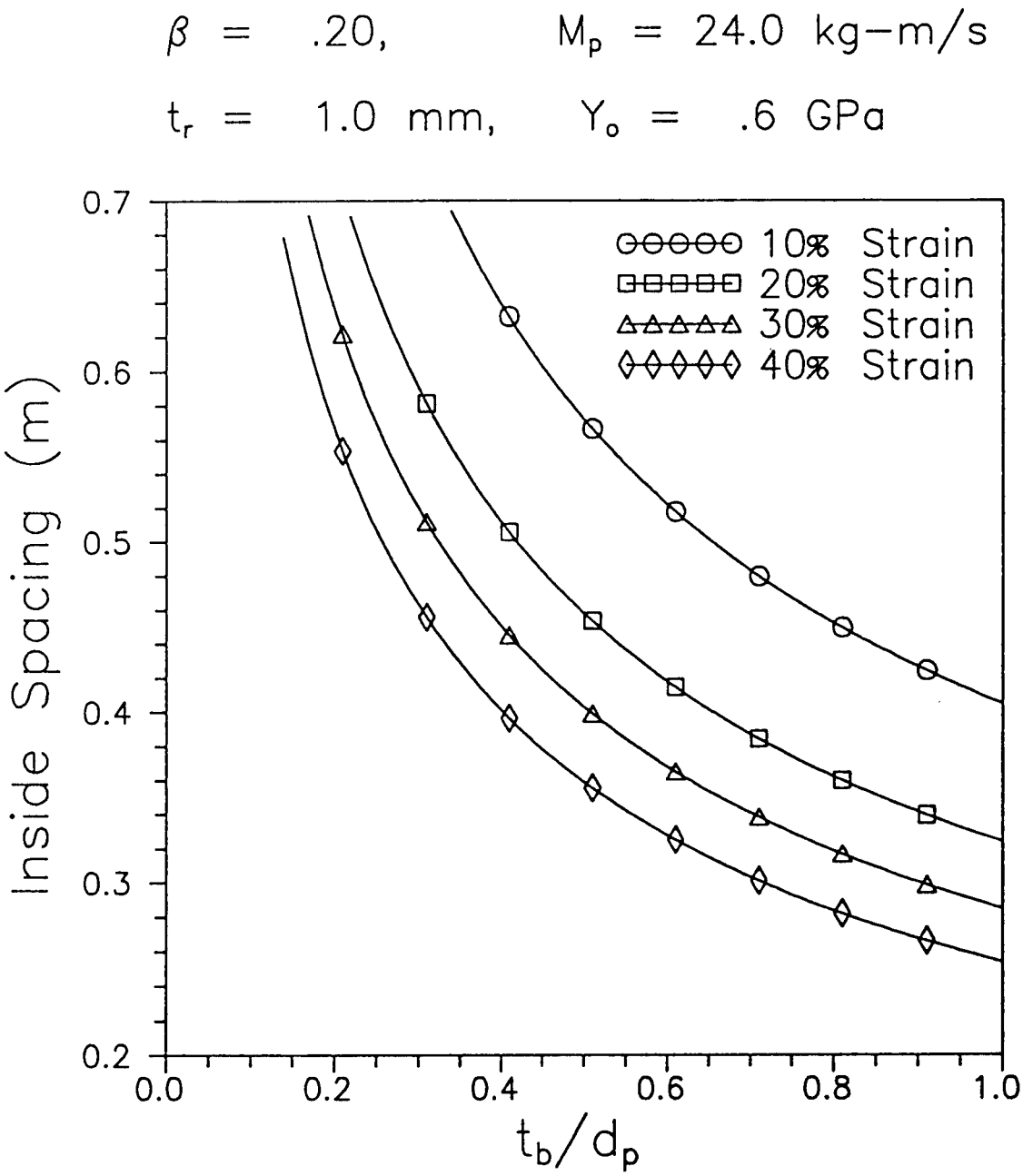


**Figure 24. Design Curves for $\beta = 0.2$, $M_p = 24$ kg-m/s, $t_r = 1$ mm, and $Y_r = 0.6$ GPa**

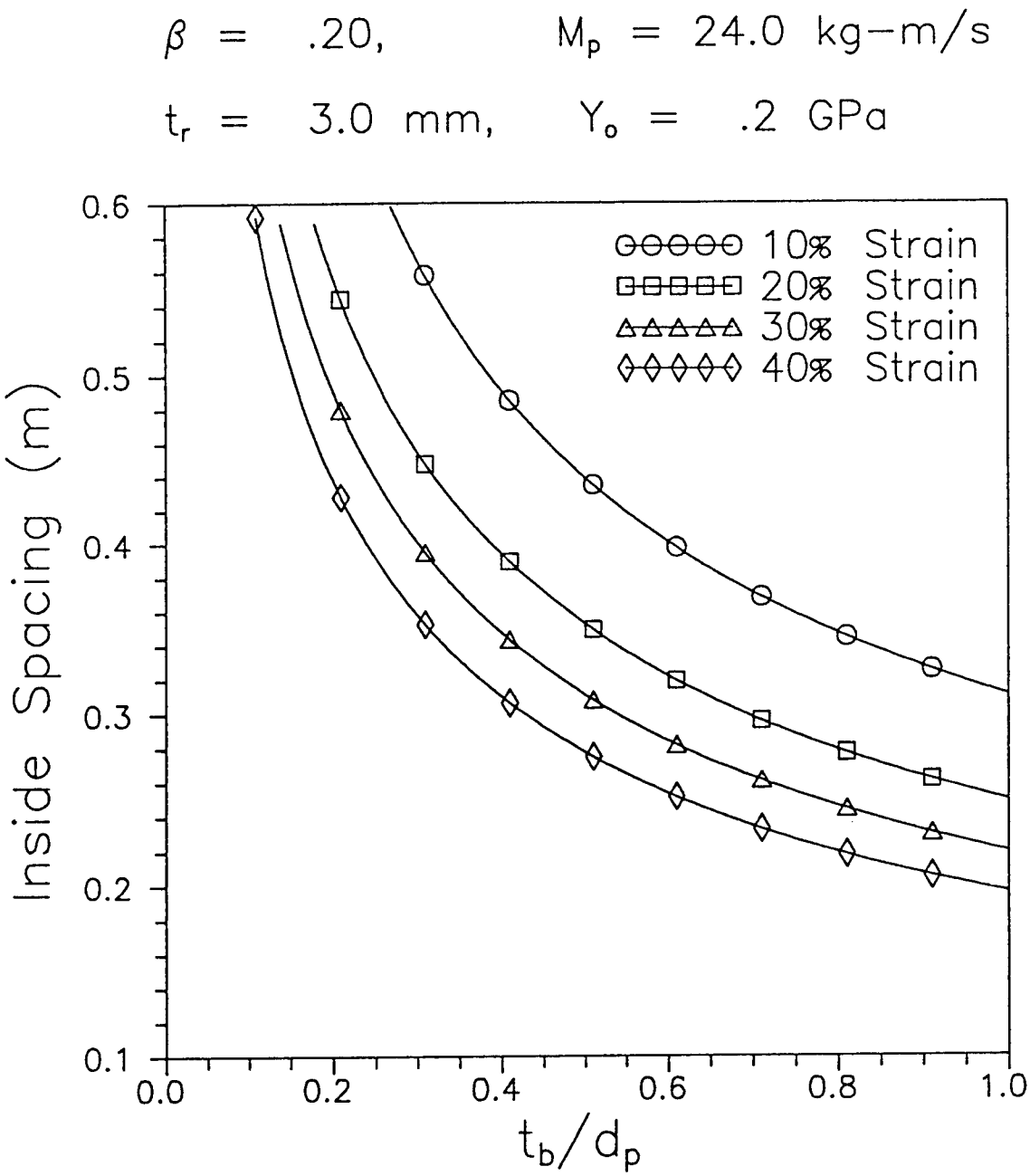


Figure 25. Design Curves for $\beta = 0.2$, $M_p = 24$ kg-m/s, $t_r = 3$ mm, and $Y_r = 0.2$ GPa

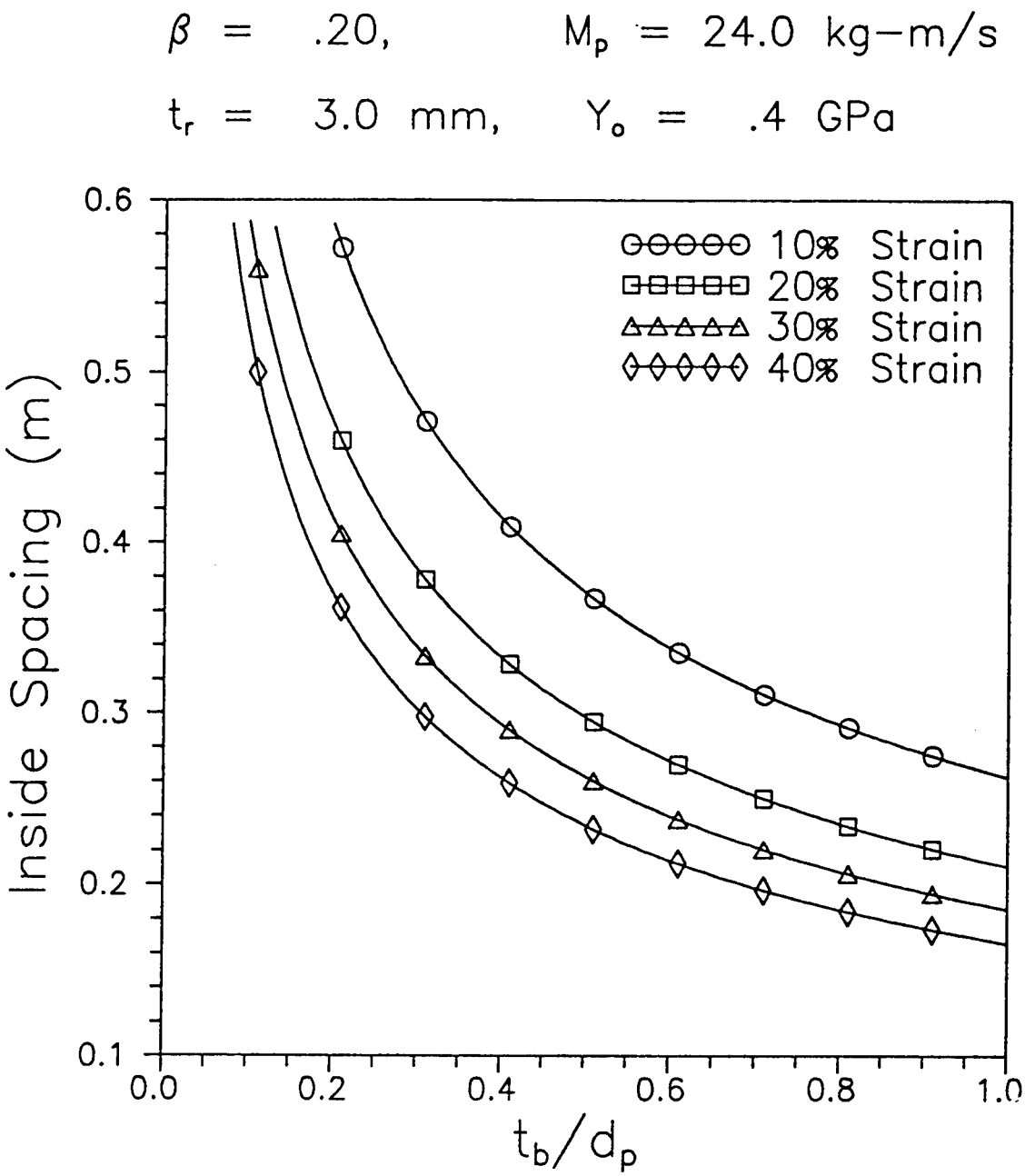


**Figure 26. Design Curves for $\beta = 0.2$, $M_p = 24$ kg-m/s, $t_r = 3$ mm, and $Y_r = 0.4$ GPa**

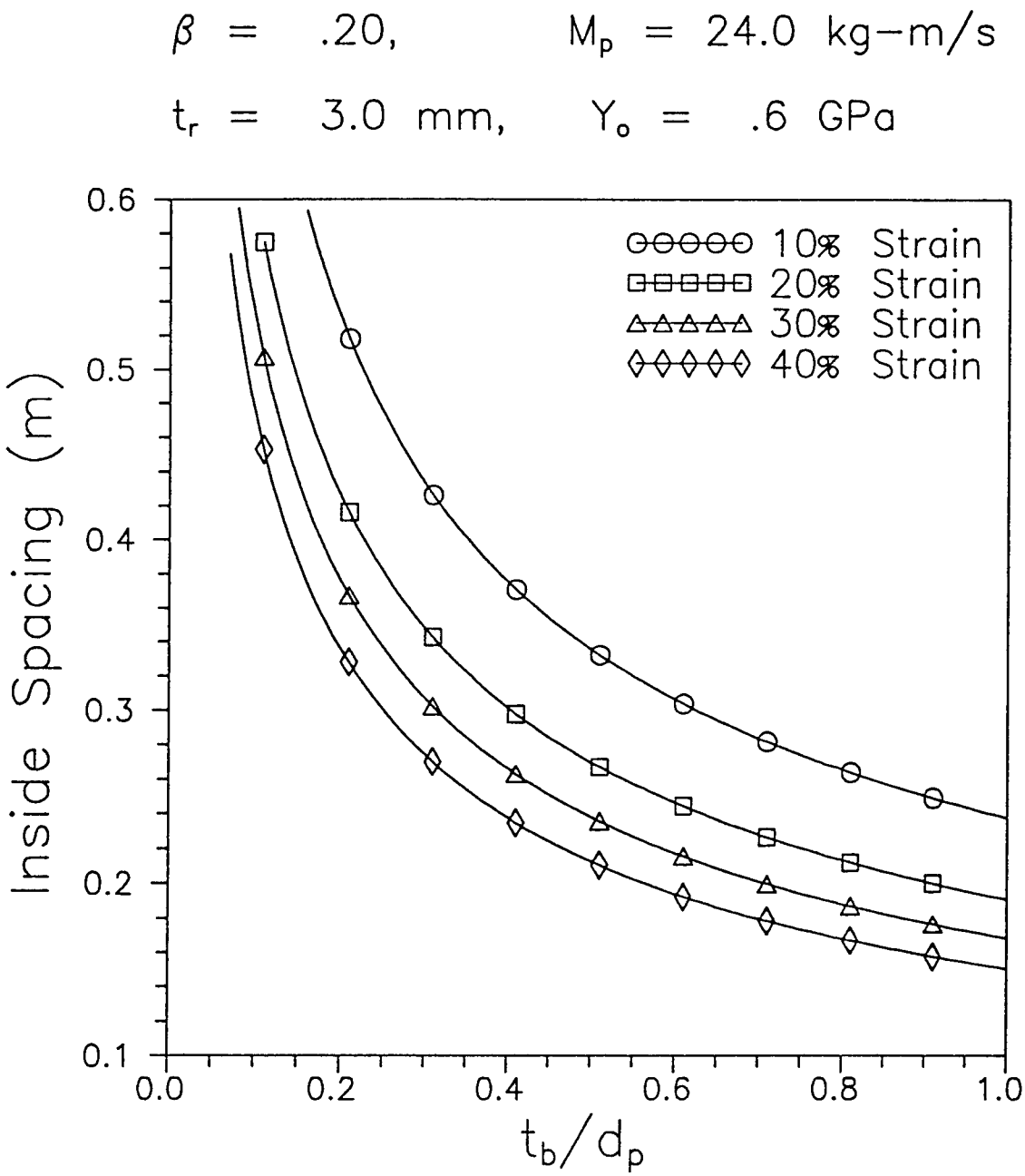


Figure 27. Design Curves for $\beta = 0.2$, $M_p = 24$ kg-m/s, $t_r = 3$ mm, and $Y_r = 0.6$ GPa

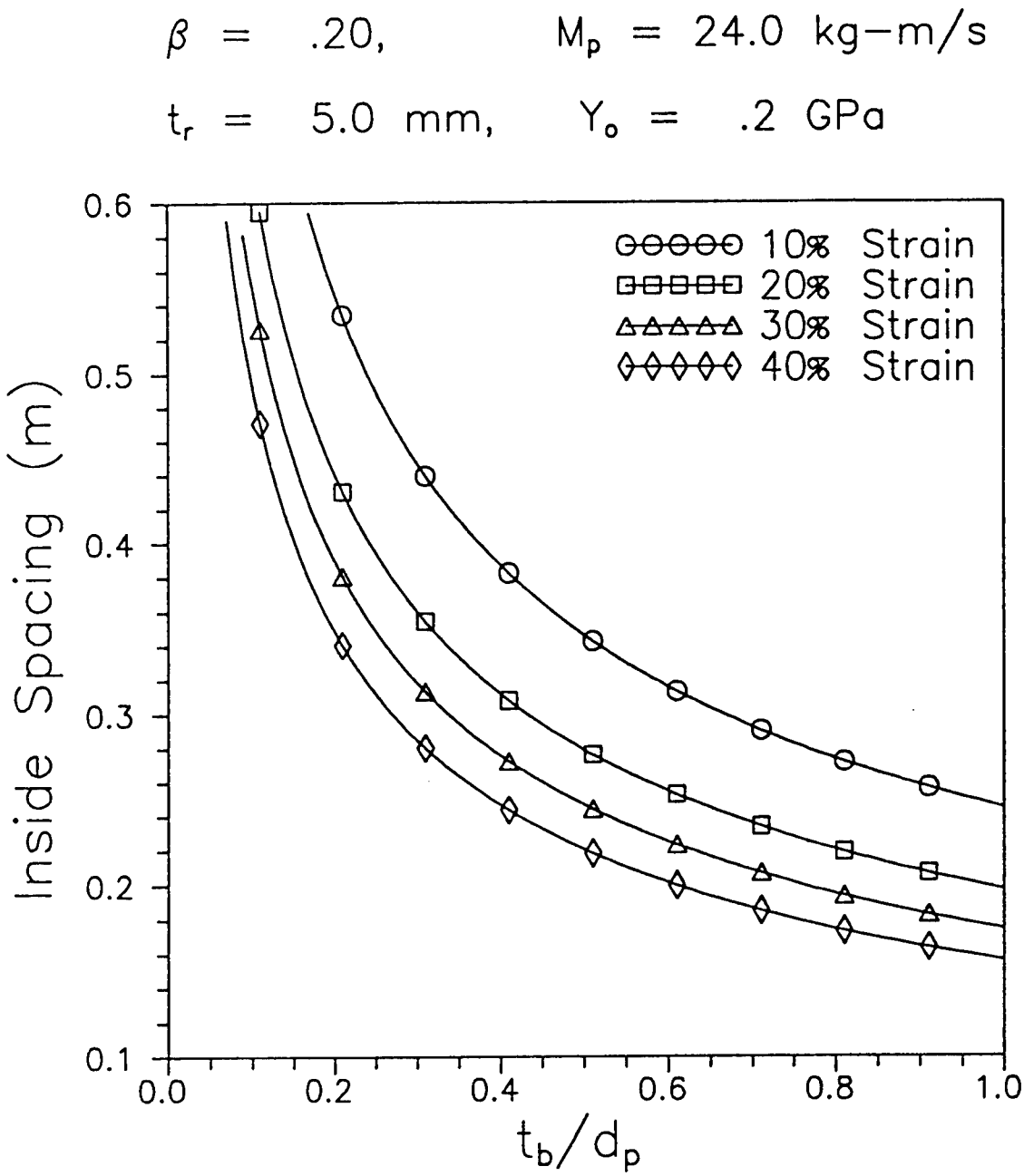


Figure 28. Design Curves for $\beta = 0.2$, $M_p = 24$ kg-m/s, $t_r = 5$ mm, and $Y_r = 0.2$ GPa

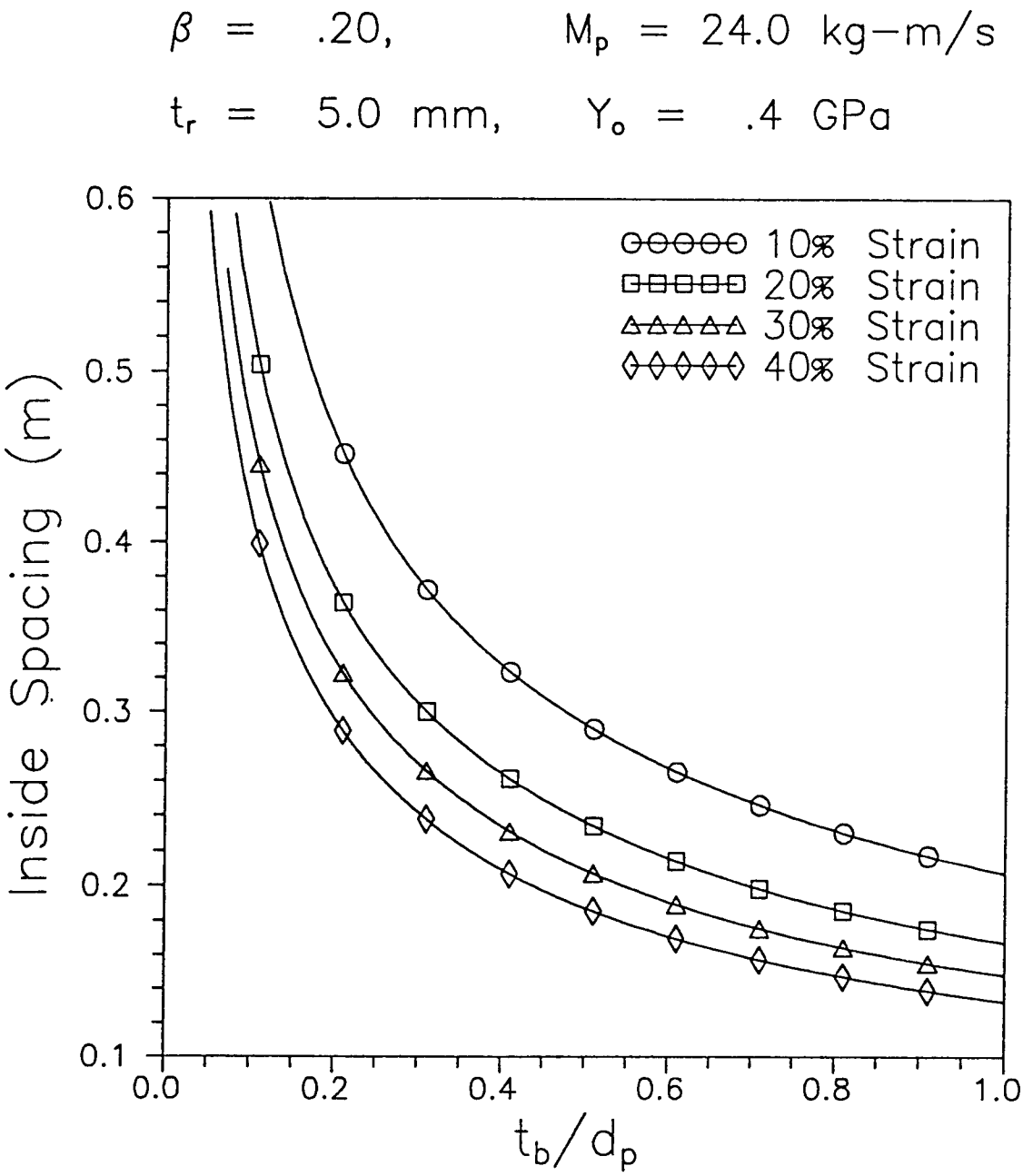


Figure 29. Design Curves for $\beta = 0.2$, $M_p = 24$ kg-m/s, $t_r = 5$ mm, and $Y_r = 0.4$ GPa

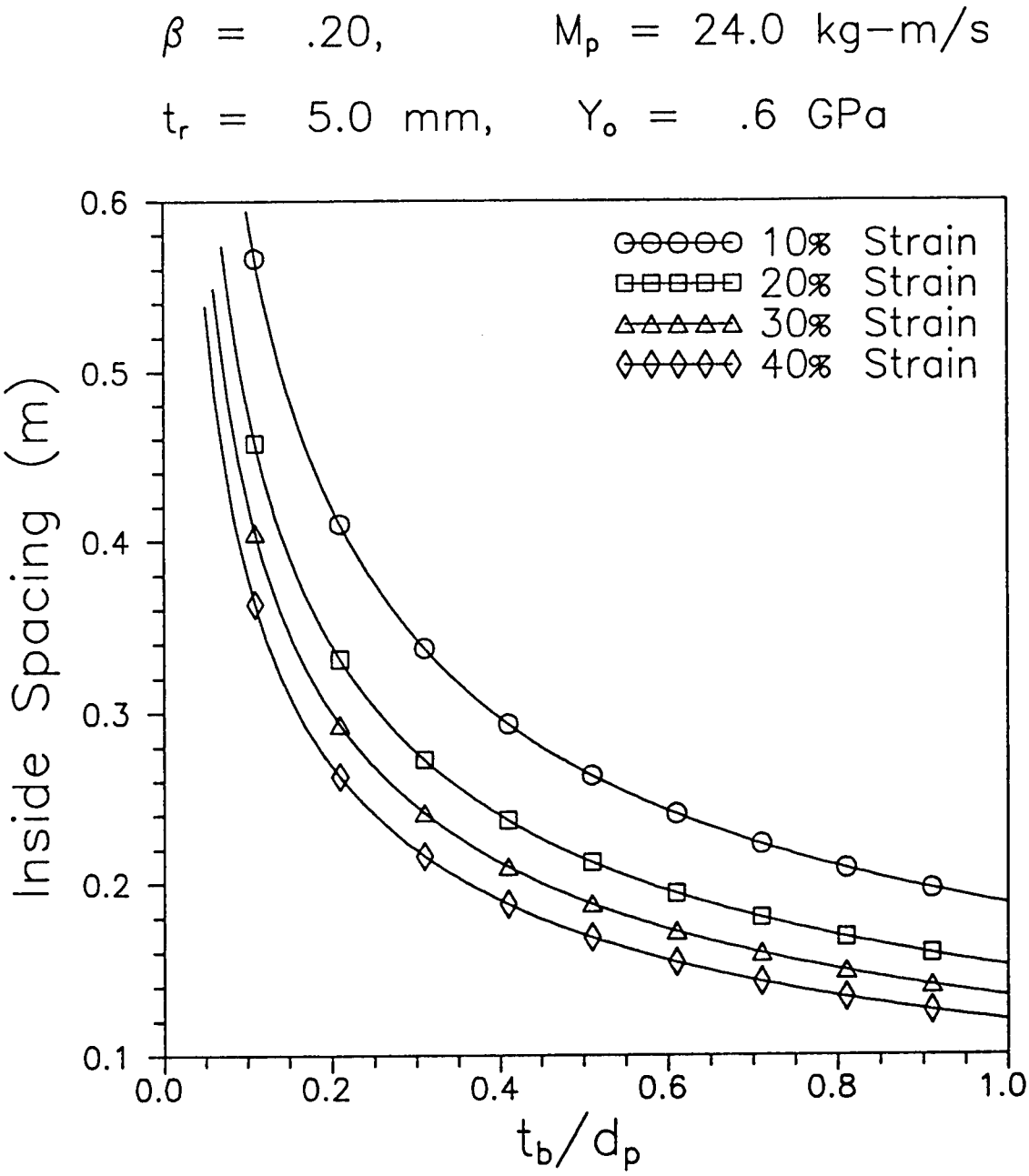


**Figure 30.** Design Curves for $\beta = 0.2$, $M_p = 24$ kg-m/s, $t_r = 5$ mm, and $Y_r = 0.6$ GPa

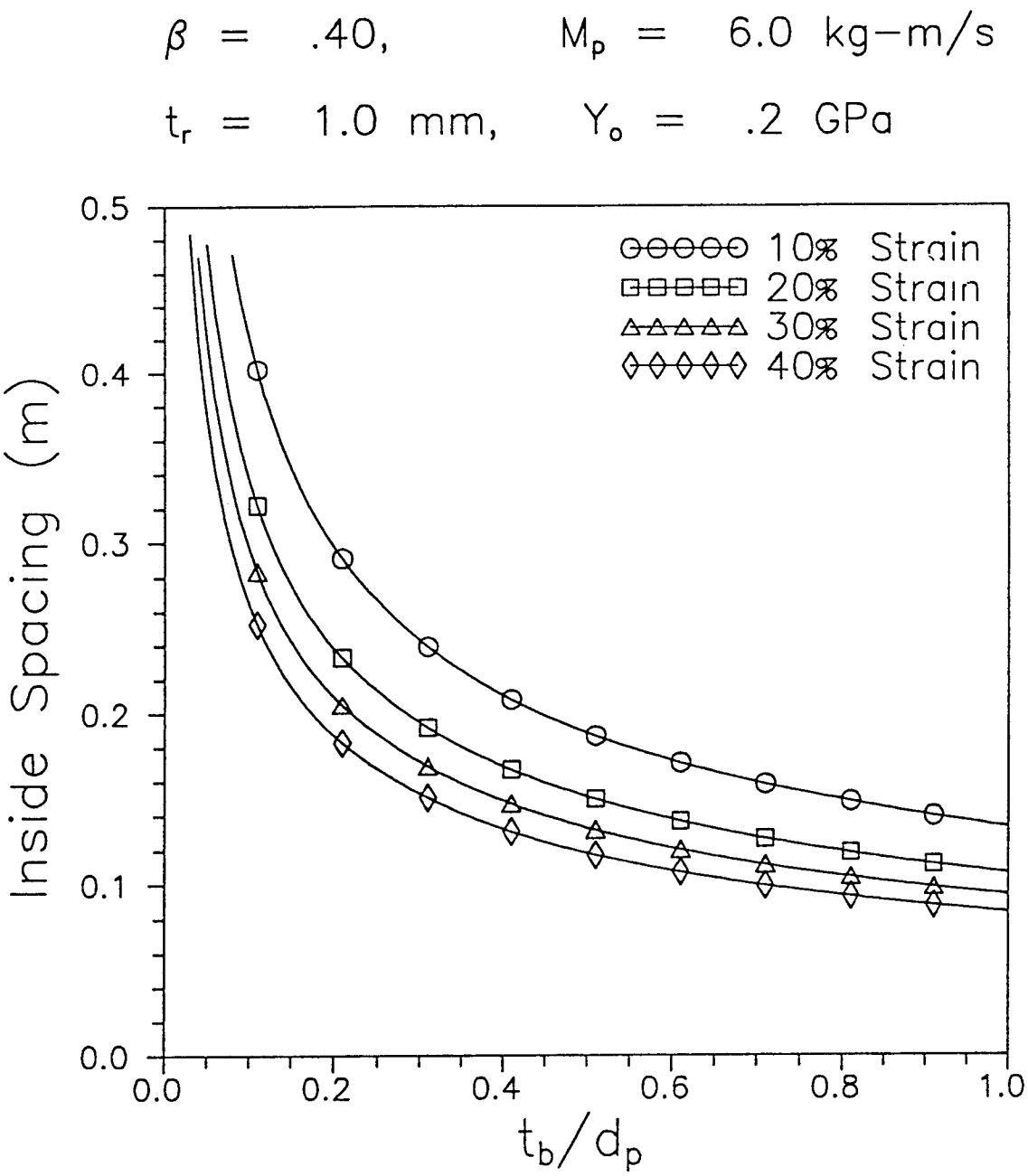


Figure 31. Design Curves for $\beta = 0.4$, $M_p = 6$ kg-m/s, $t_r = 1$ mm, and $Y_r = 0.2$ GPa

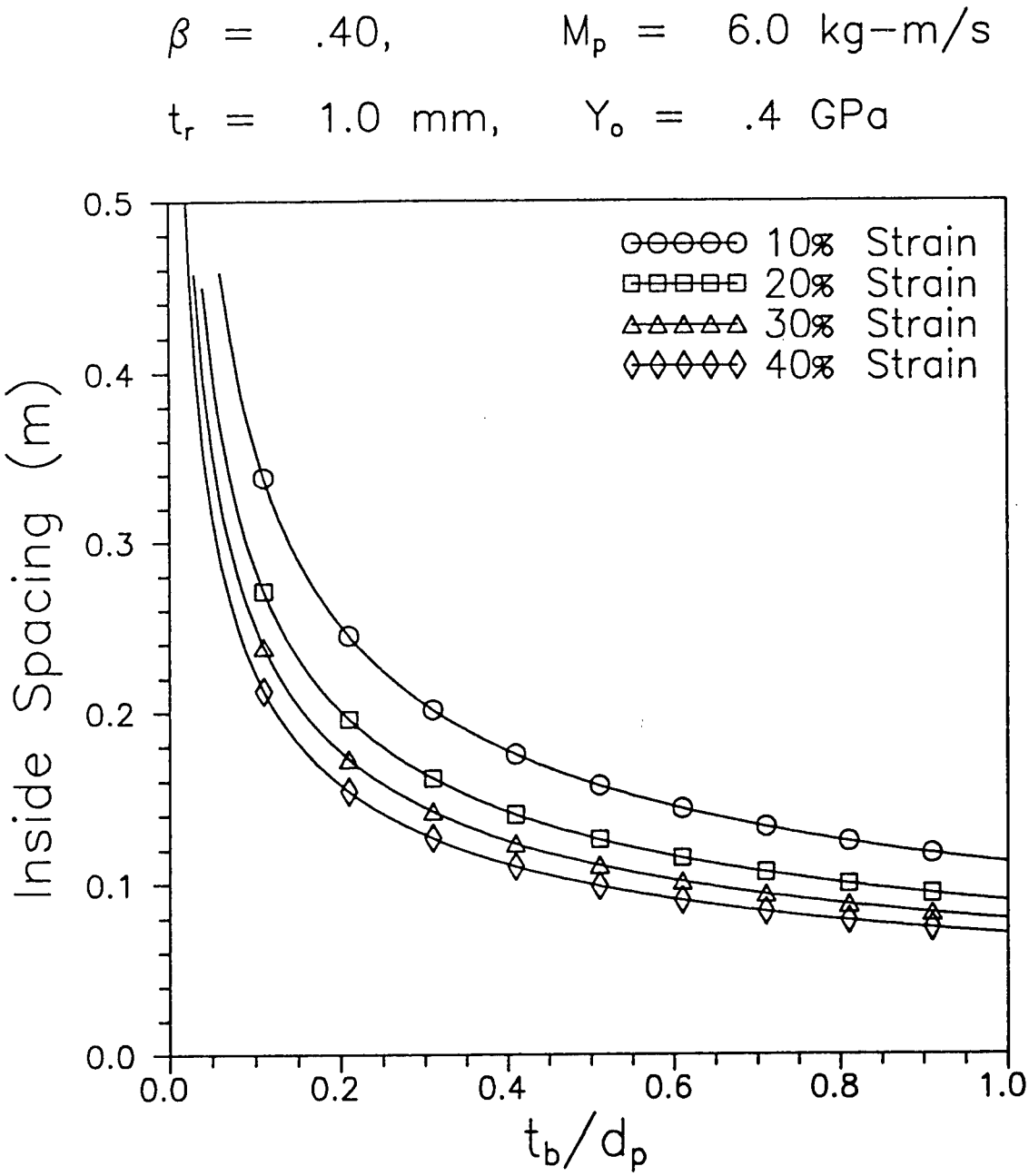


Figure 32. Design Curves for $\beta = 0.4$, $M_p = 6$ kg-m/s, $t_r = 1$ mm, and $Y_r = 0.4$ GPa

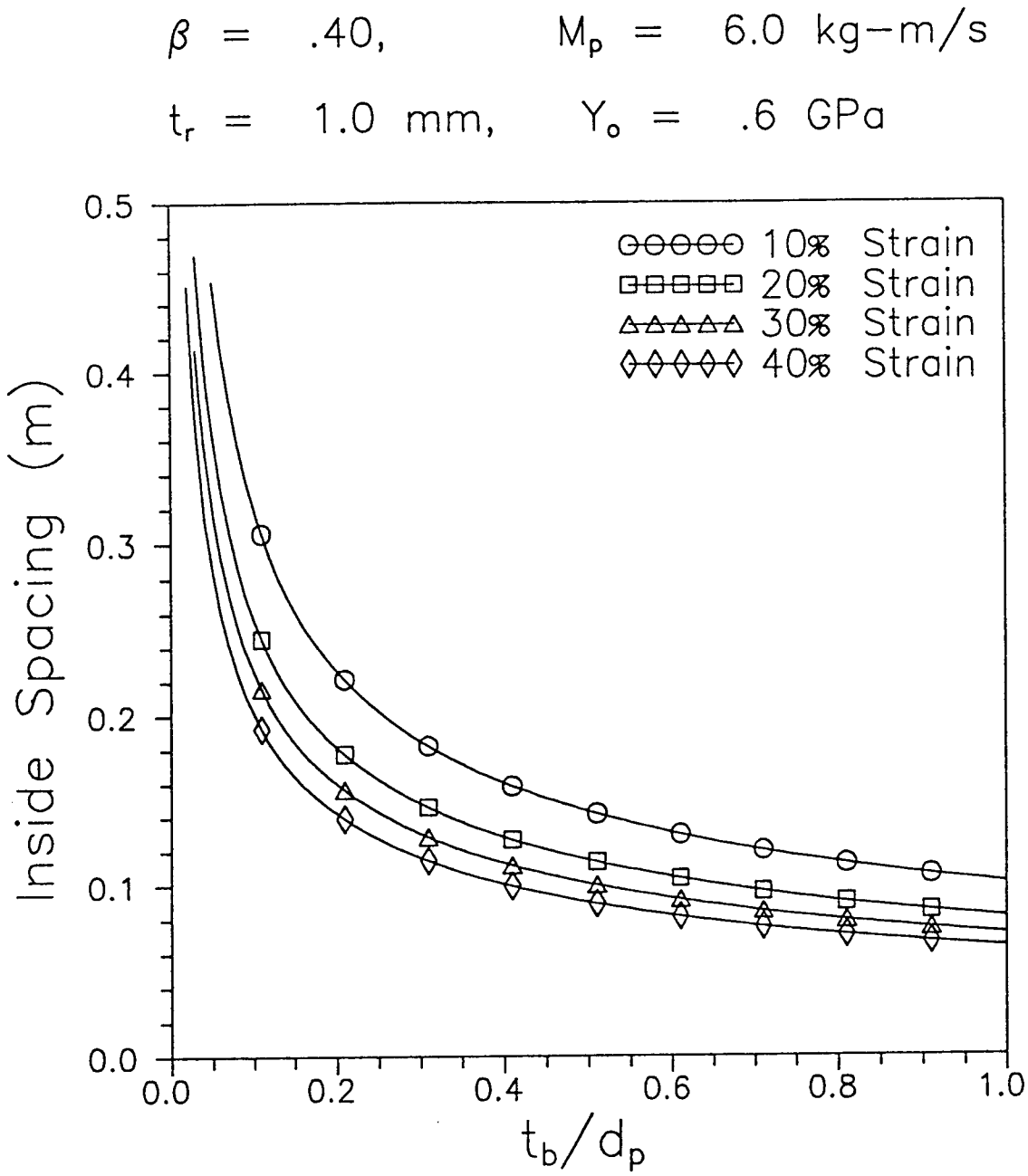


Figure 33. Design Curves for $\beta = 0.4$, $M_p = 6$ kg-m/s, $t_r = 1$ mm, and $Y_r = 0.6$ GPa

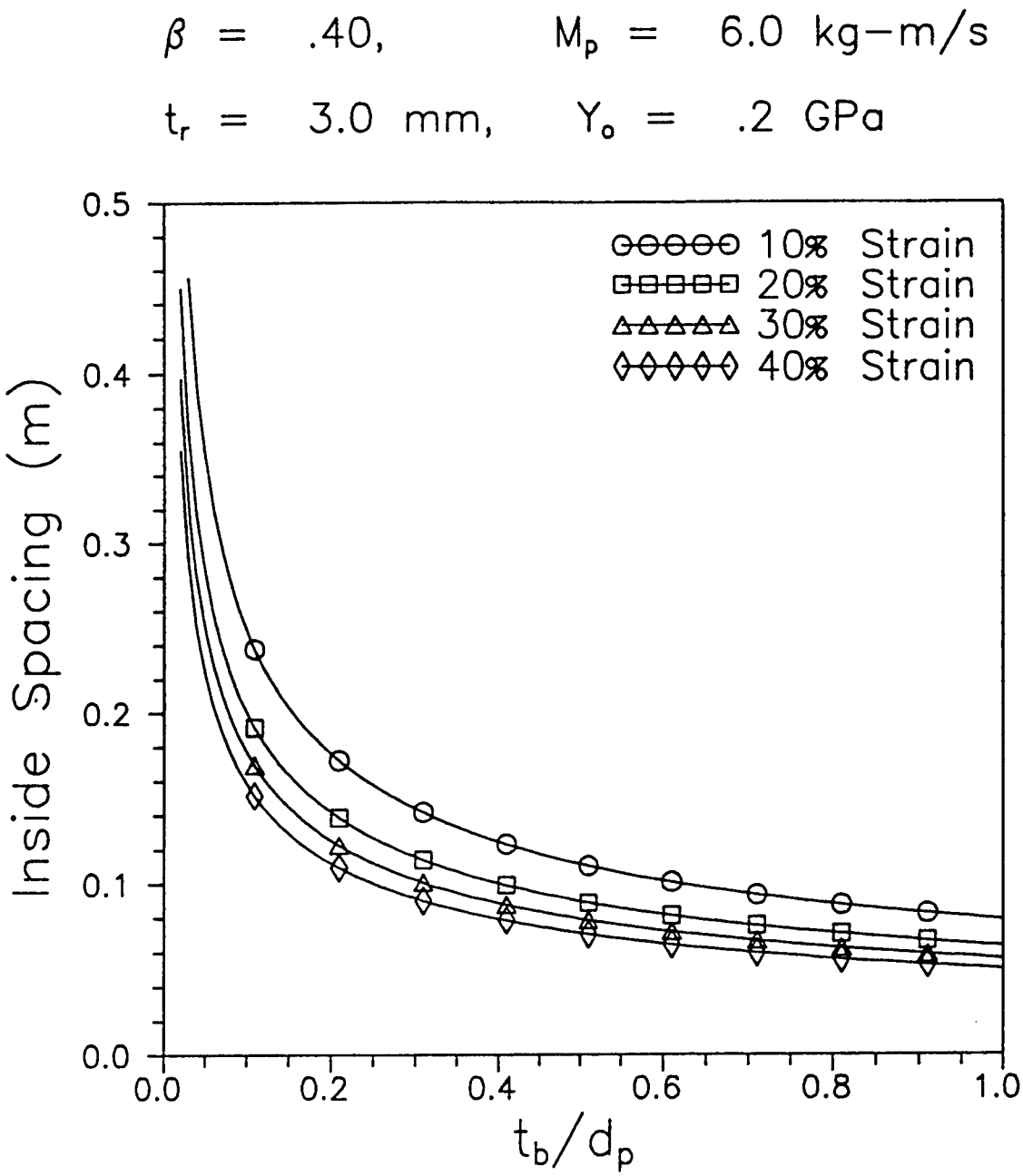


Figure 34. Design Curves for $\beta = 0.4$, $M_p = 6$ kg-m/s, $t_r = 3$ mm, and $Y_r = 0.2$ GPa

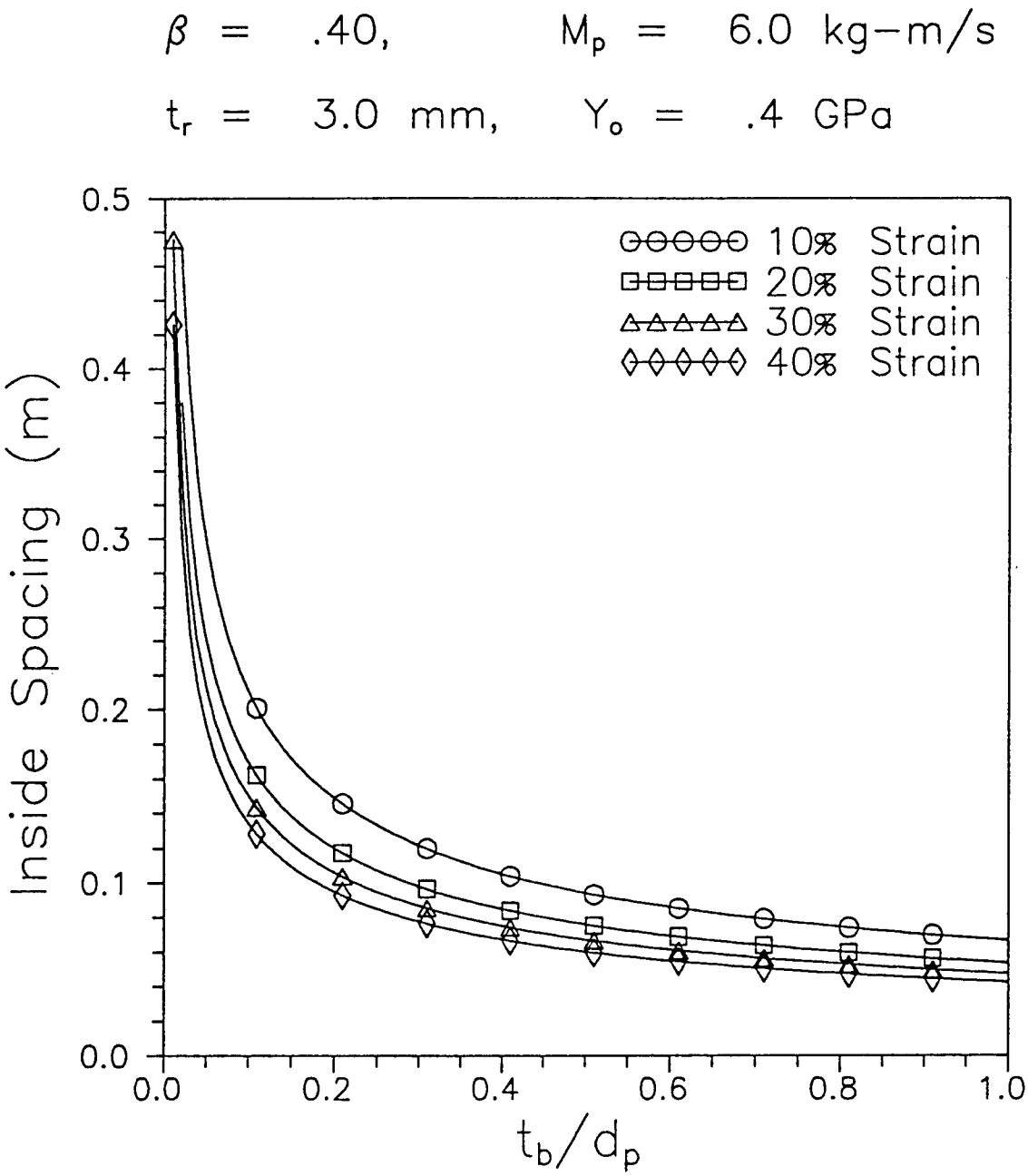


Figure 35. Design Curves for $\beta = 0.4$, $M_p = 6$ kg-m/s, $t_r = 3$ mm, and $Y_r = 0.4$ GPa

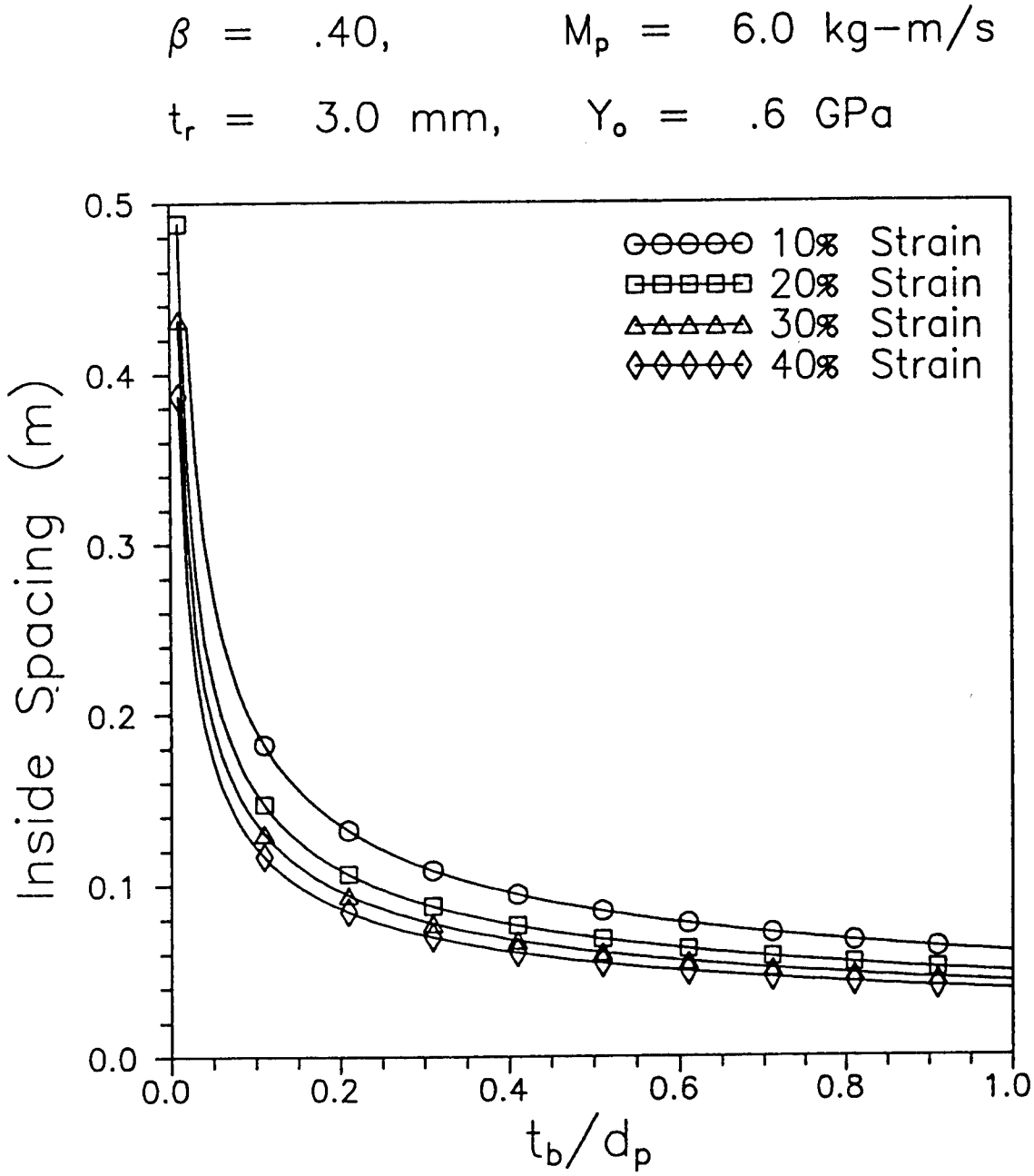


Figure 36. Design Curves for $\beta = 0.4$, $M_p = 6$ kg-m/s, $t_r = 3$ mm, and $Y_r = 0.6$ GPa

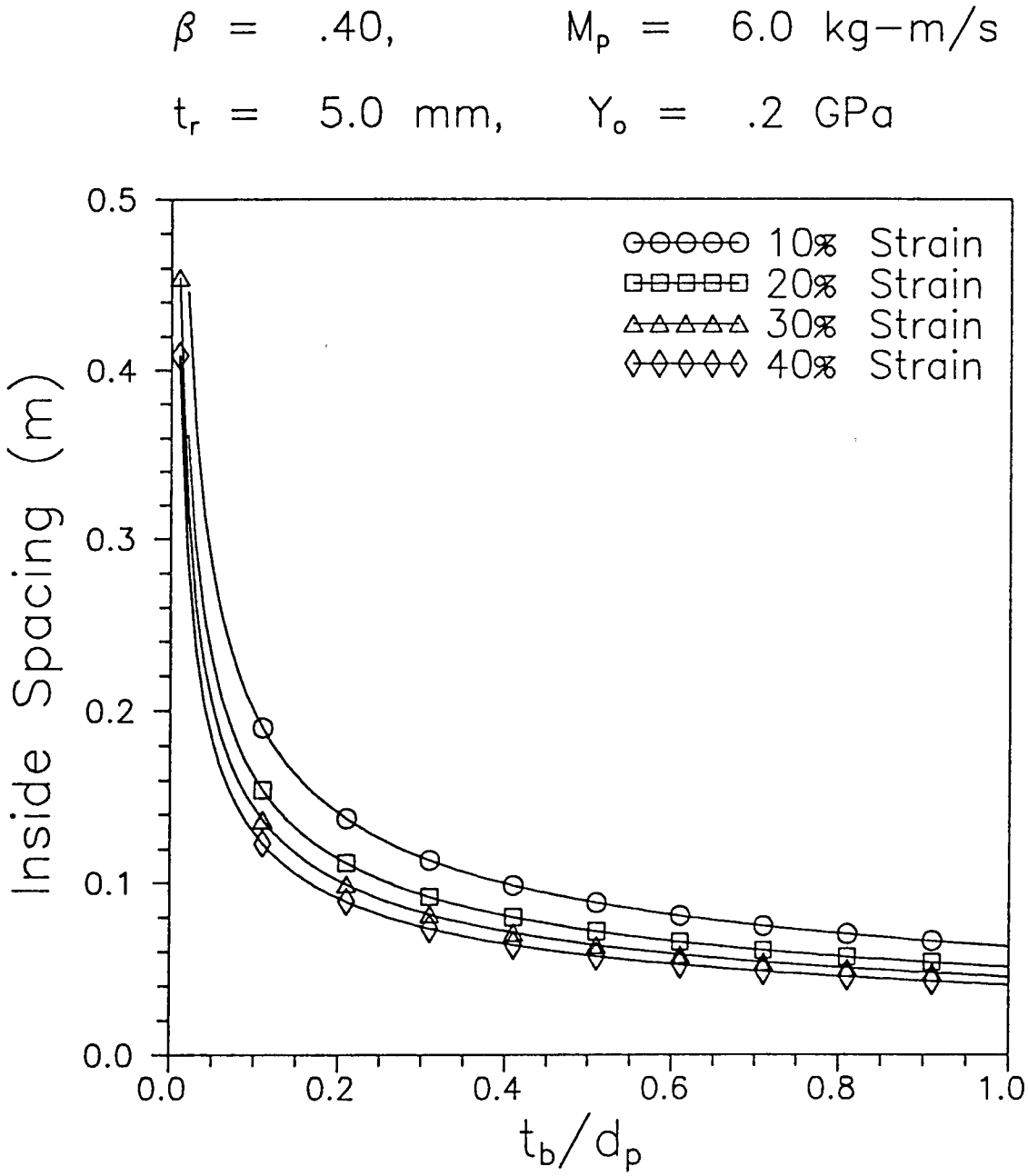


Figure 37. Design Curves for $\beta = 0.4$, $M_p = 6$ kg-m/s, $t_r = 5$ mm, and $Y_r = 0.2$ GPa

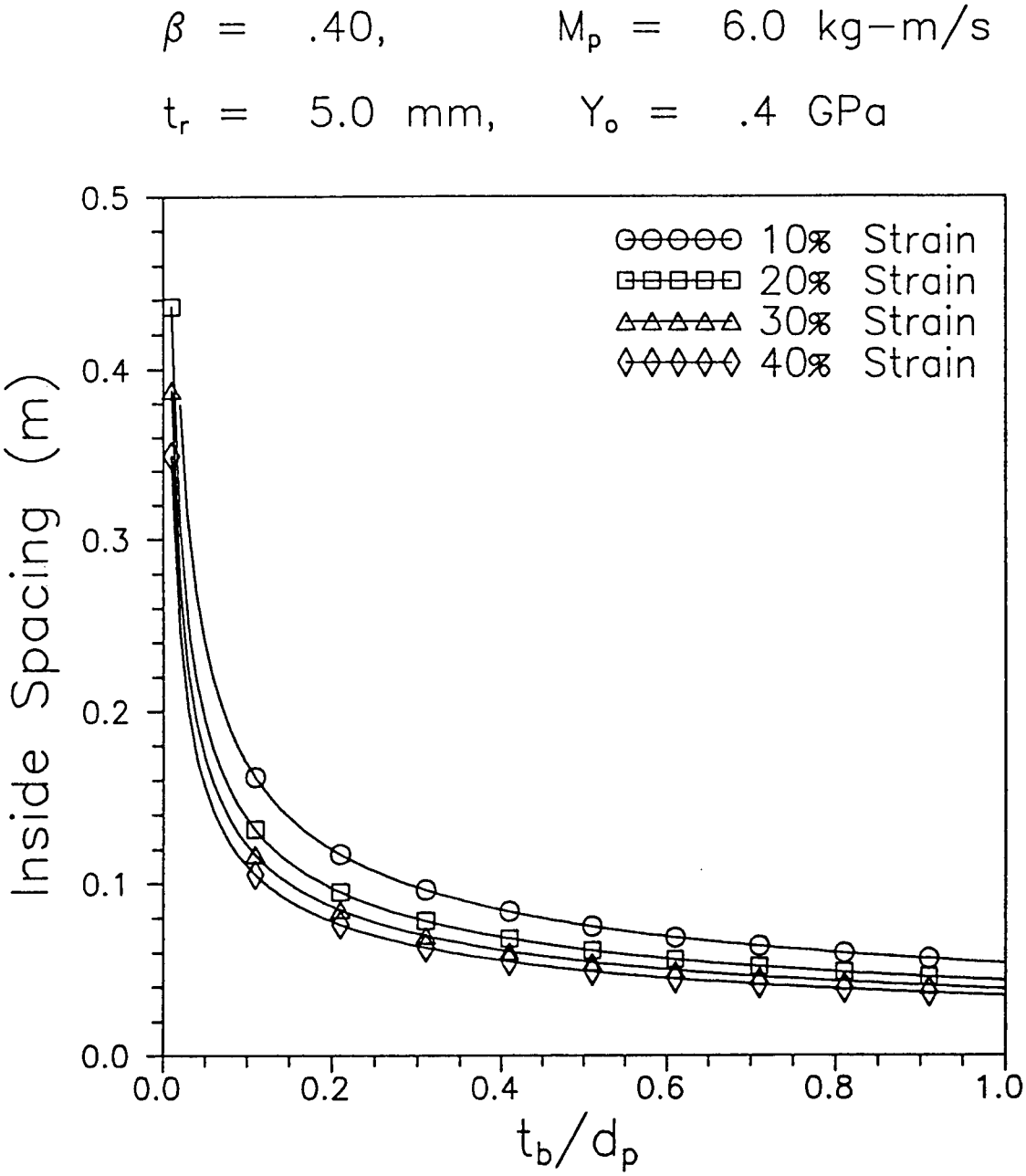


**Figure 38. Design Curves for $\beta = 0.4$, $M_p = 6$ kg-m/s, $t_r = 5$ mm, and $Y_r = 0.4$ GPa**

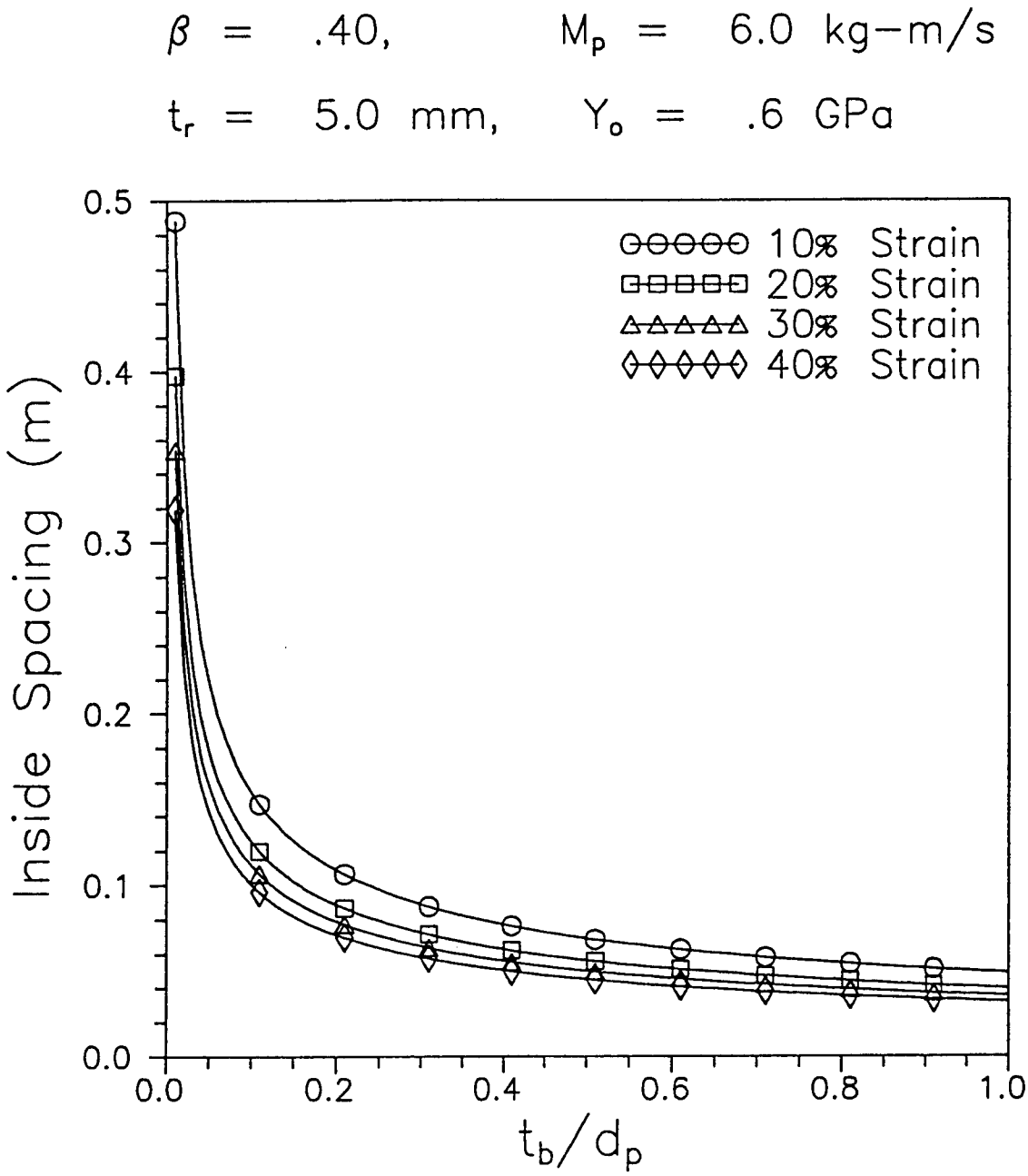


Figure 39. Design Curves for $\beta = 0.4$, $M_p = 6$ kg-m/s, $t_r = 5$ mm, and $Y_r = 0.6$ GPa

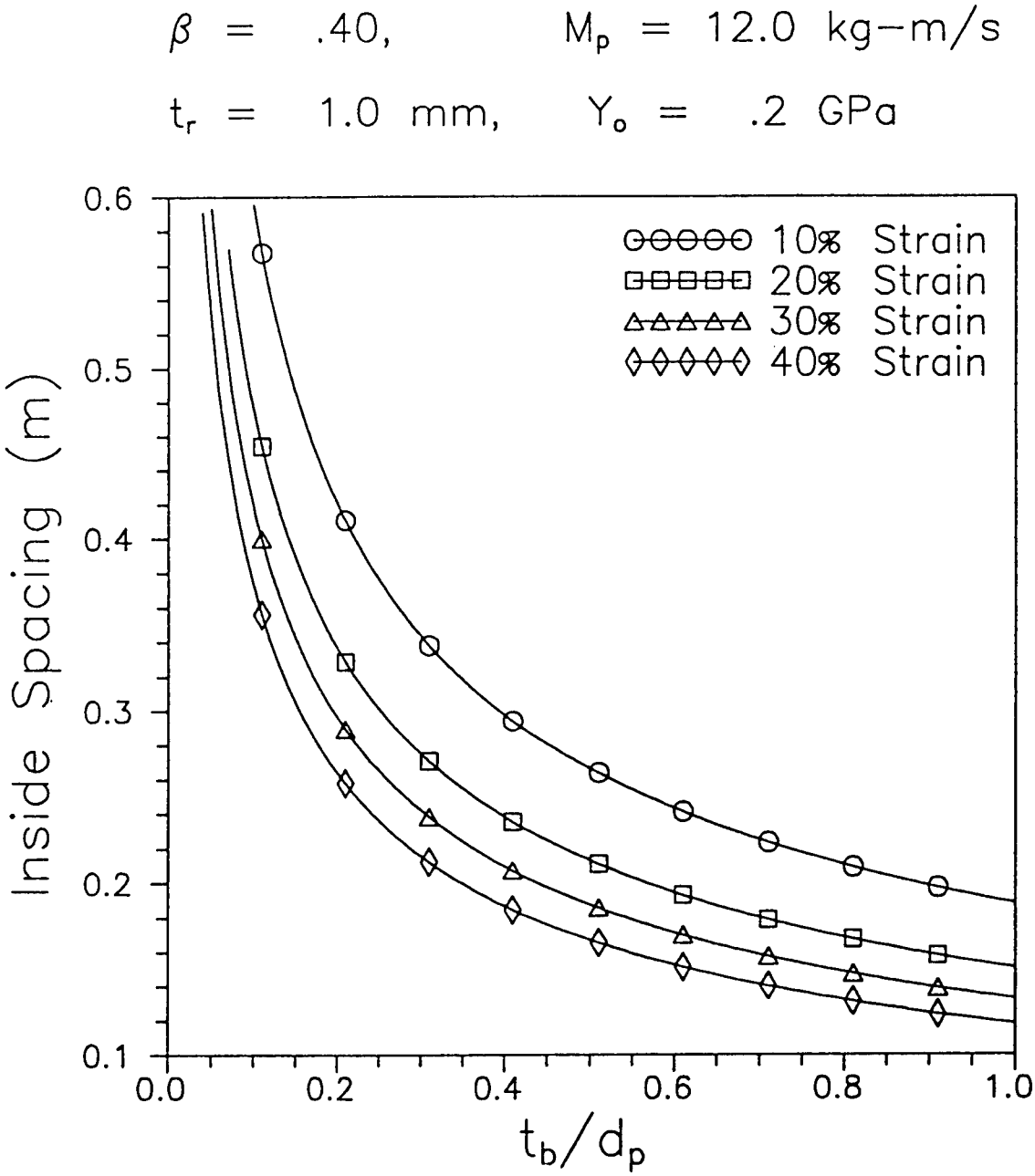


**Figure 40. Design Curves for $\beta$ = 0.4, $M_p$ = 12 kg-m/s, $t_r$ = 1 mm, and $Y_r$ = 0.2 GPa**

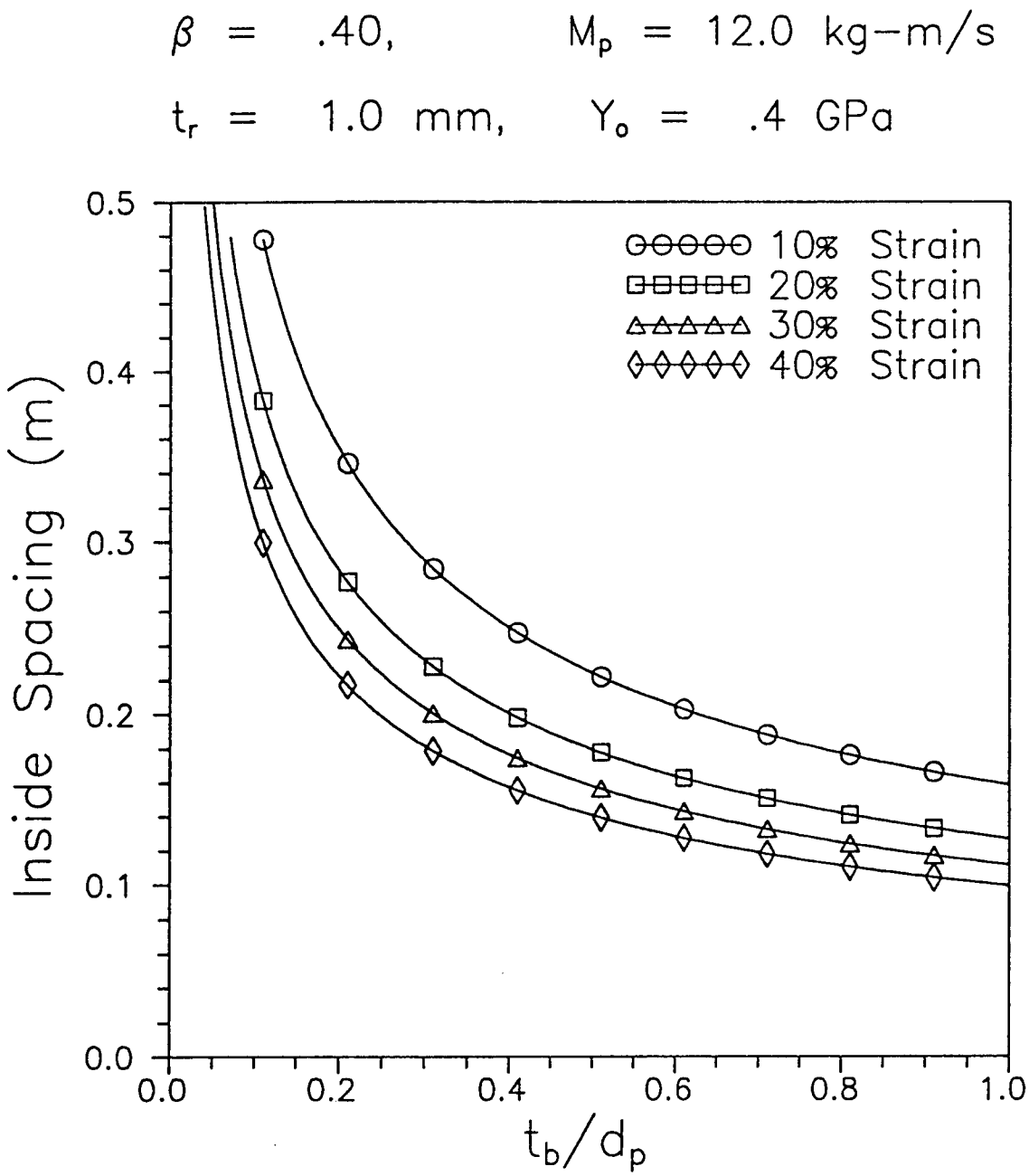


**Figure 41.** Design Curves for $\beta = 0.4$, $M_p = 12$ kg-m/s, $t_r = 1$ mm, and $Y_r = 0.4$ GPa

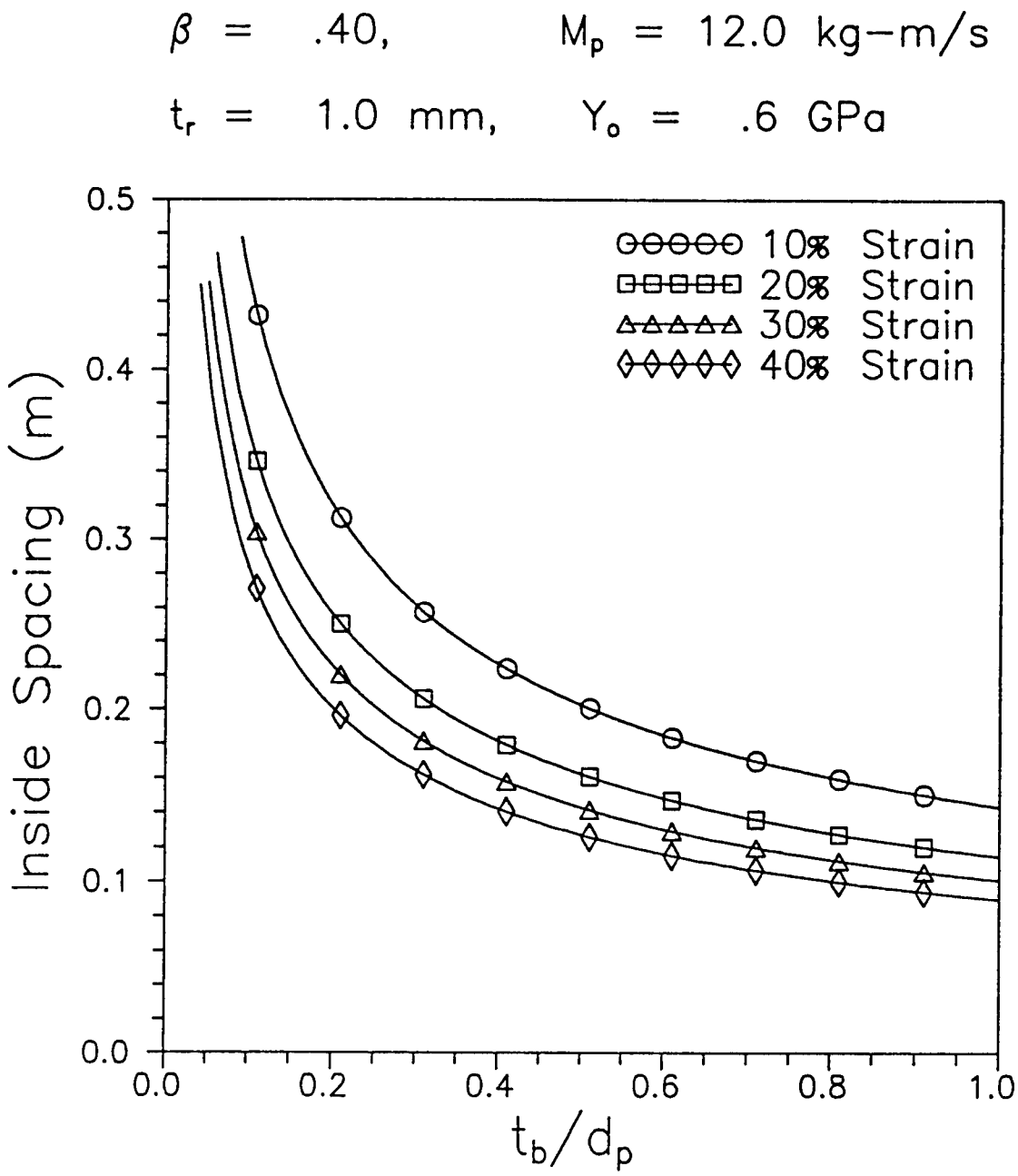


Figure 42. Design Curves for $\beta = 0.4$, $M_p = 12$ kg-m/s, $t_r = 1$ mm, and $Y_r = 0.6$ GPa

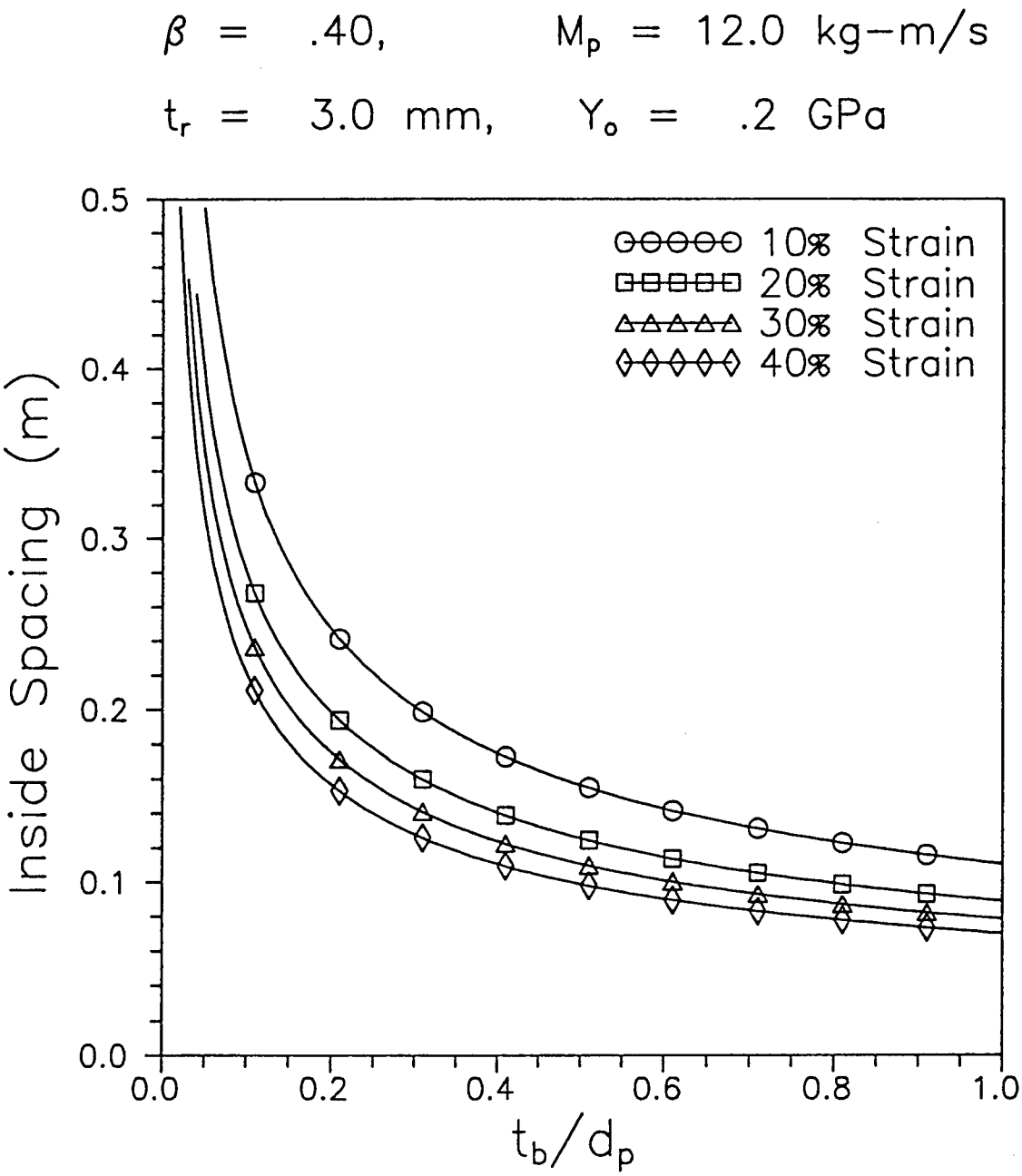


Figure 43. Design Curves for $\beta = 0.4$, $M_p = 12$ kg-m/s, $t_r = 3$ mm, and $Y_r = 0.2$ GPa

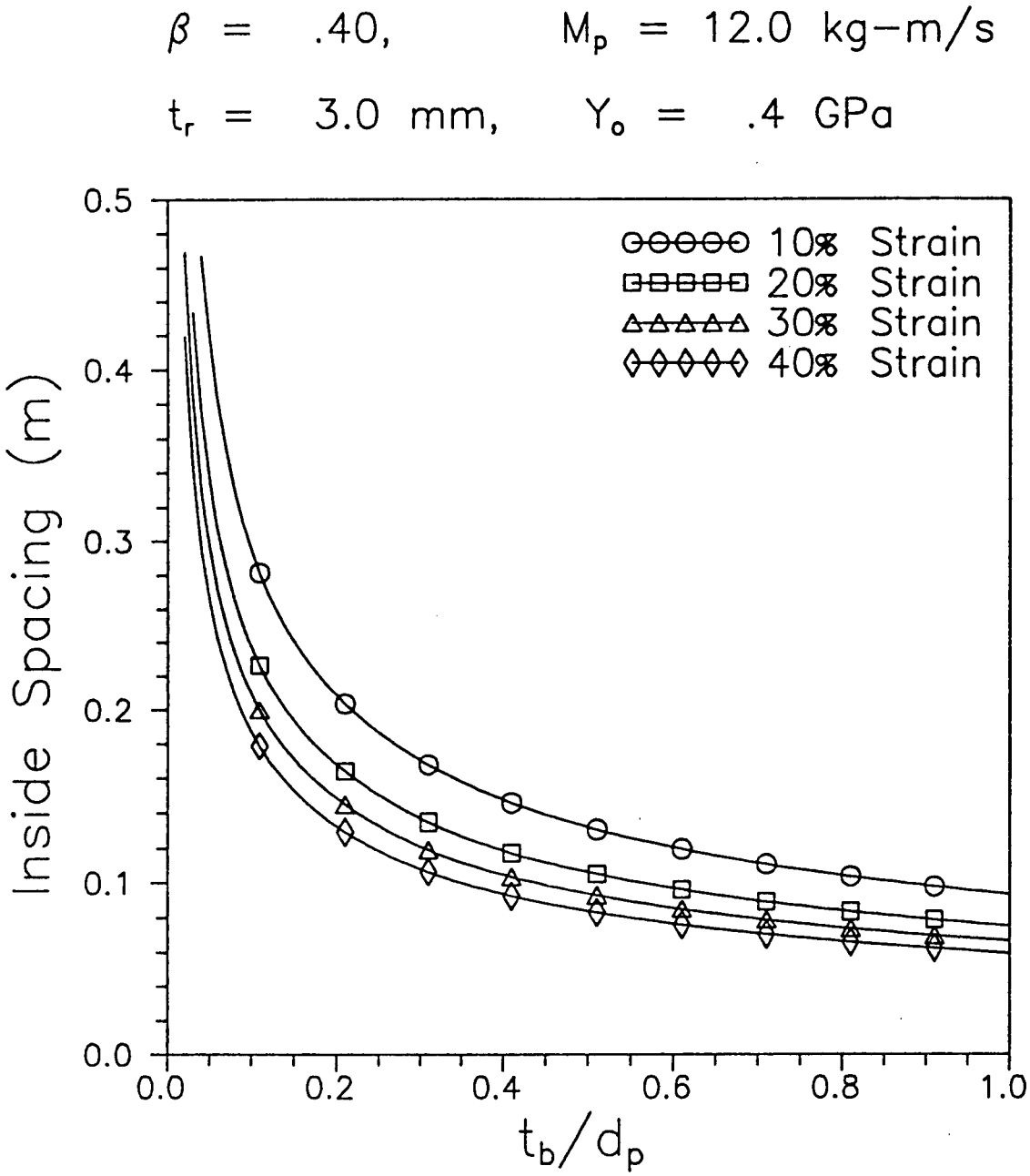


Figure 44. Design Curves for $\beta = 0.4$, $M_p = 12$ kg-m/s, $t_r = 3$ mm, and $Y_r = 0.4$ GPa

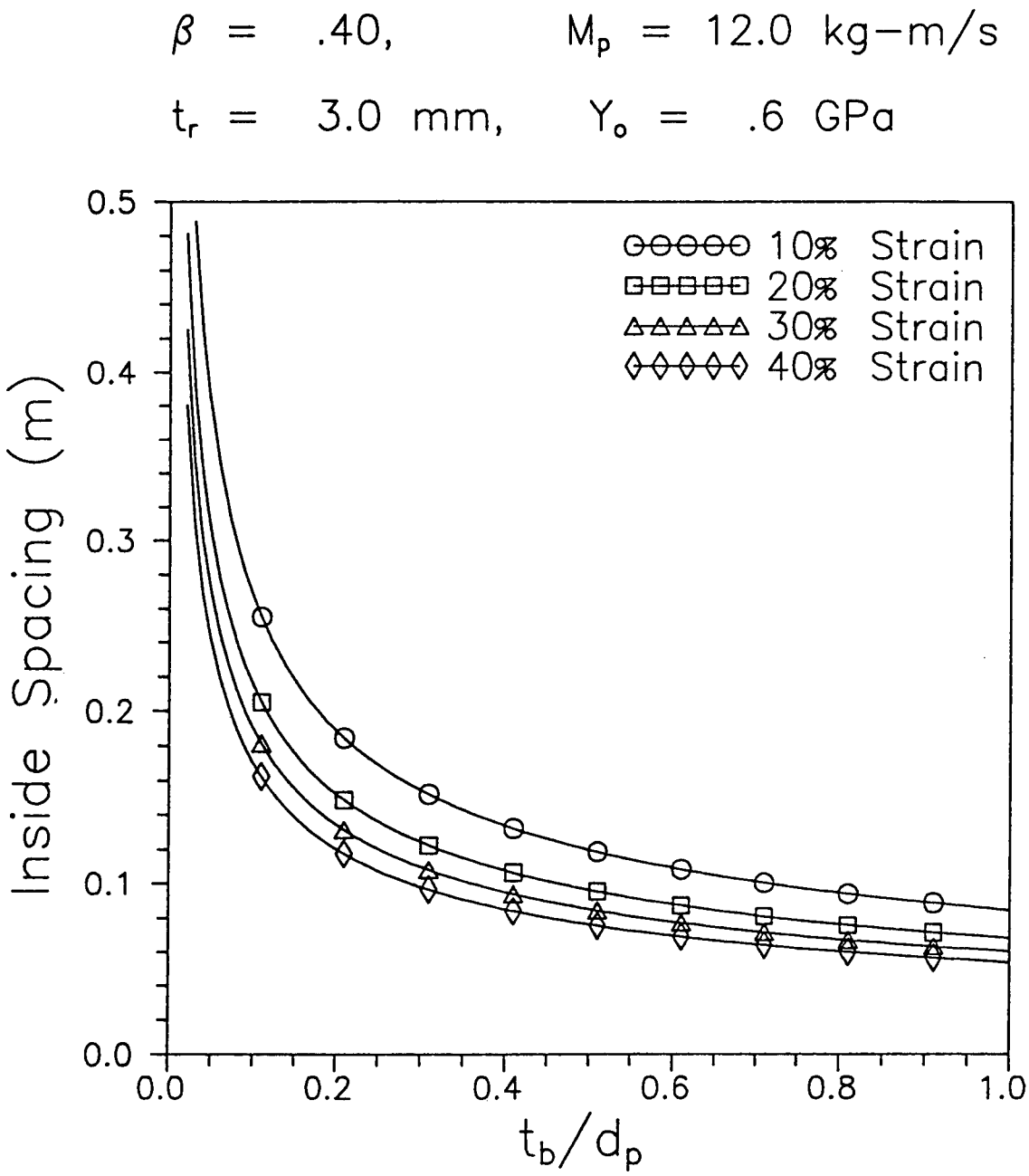


Figure 45. Design Curves for $\beta = 0.4$, $M_p = 12$ kg-m/s, $t_r = 3$ mm, and $Y_r = 0.6$ GPa

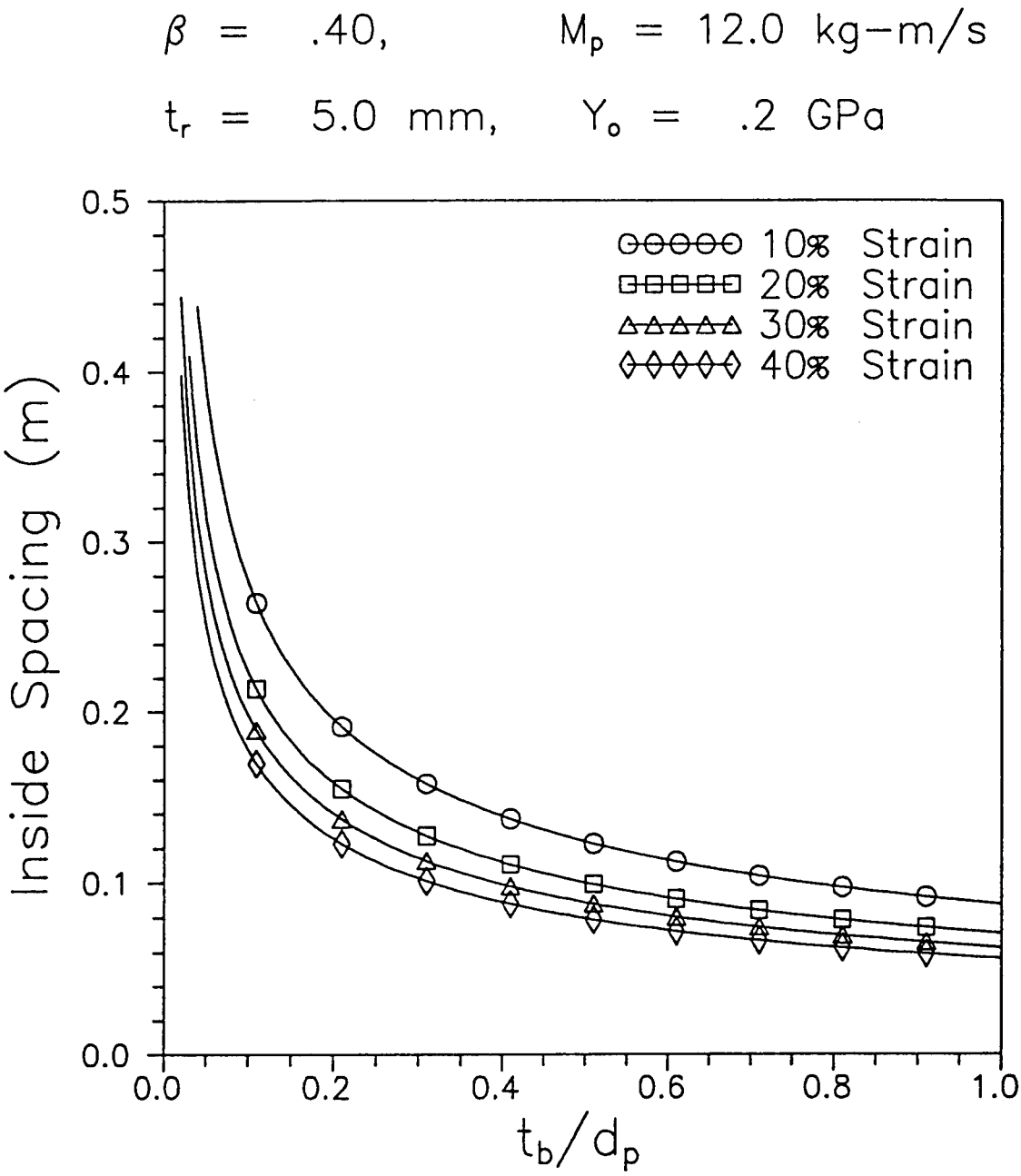


**Figure 46. Design Curves for $\beta$ = 0.4, $M_p$ = 12 kg-m/s, $t_r$ = 5 mm, and $Y_r$ = 0.2 GPa**

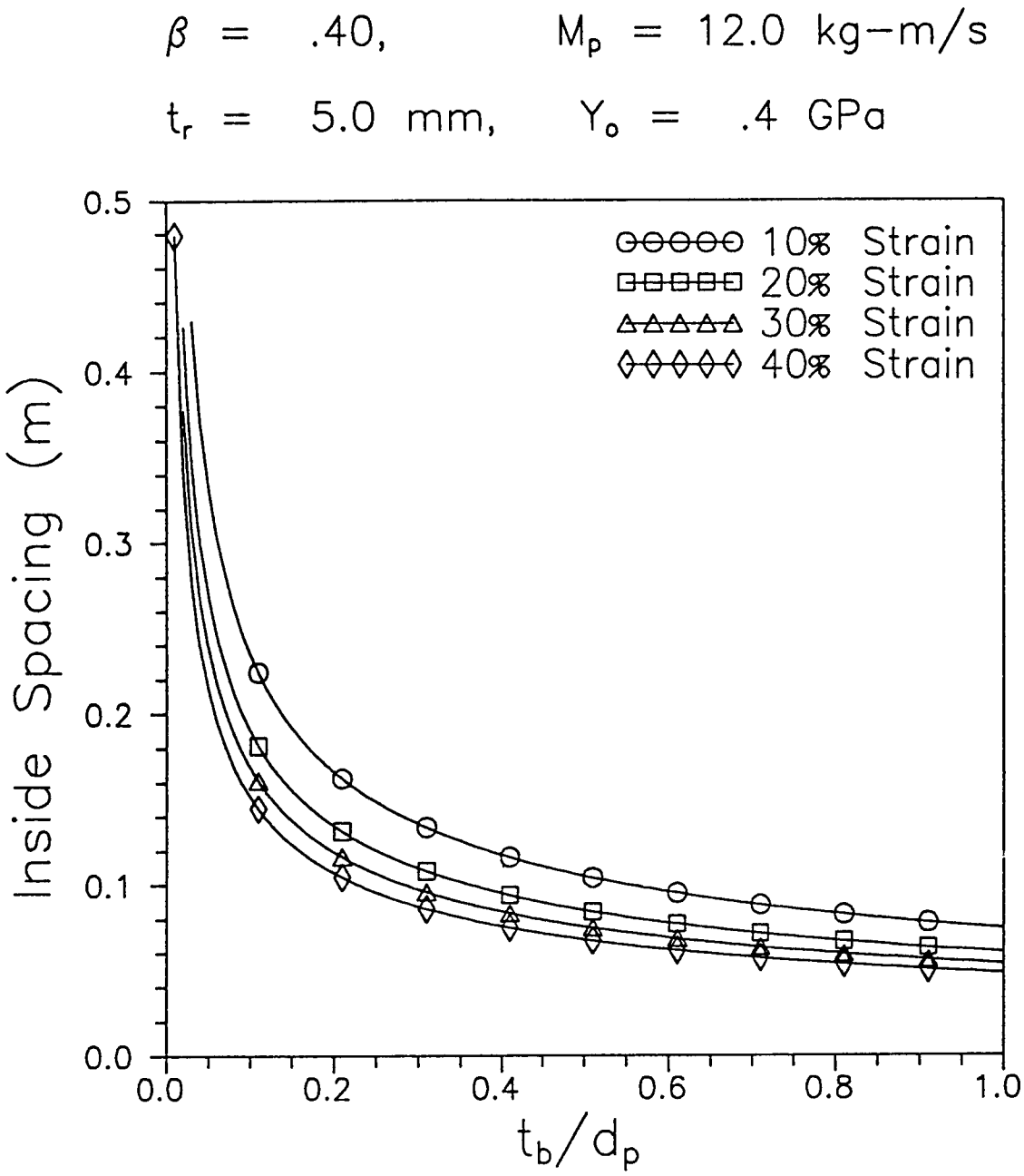


Figure 47. Design Curves for $\beta = 0.4$, $M_p = 12$ kg-m/s, $t_r = 5$ mm, and $Y_r = 0.4$ GPa

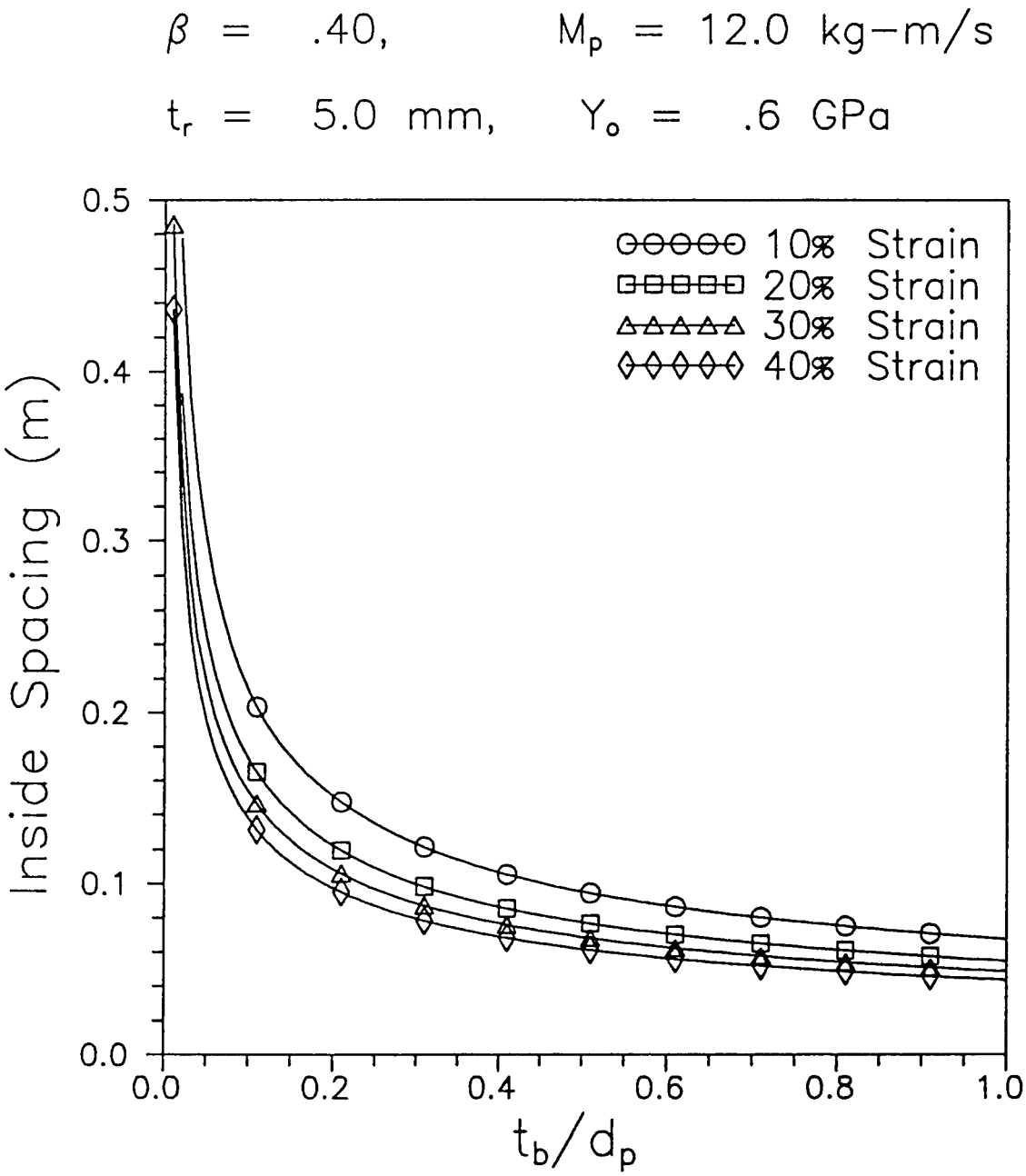


Figure 48. Design Curves for $\beta = 0.4$, $M_p = 12$ kg-m/s, $t_r = 5$ mm, and $Y_r = 0.6$ GPa

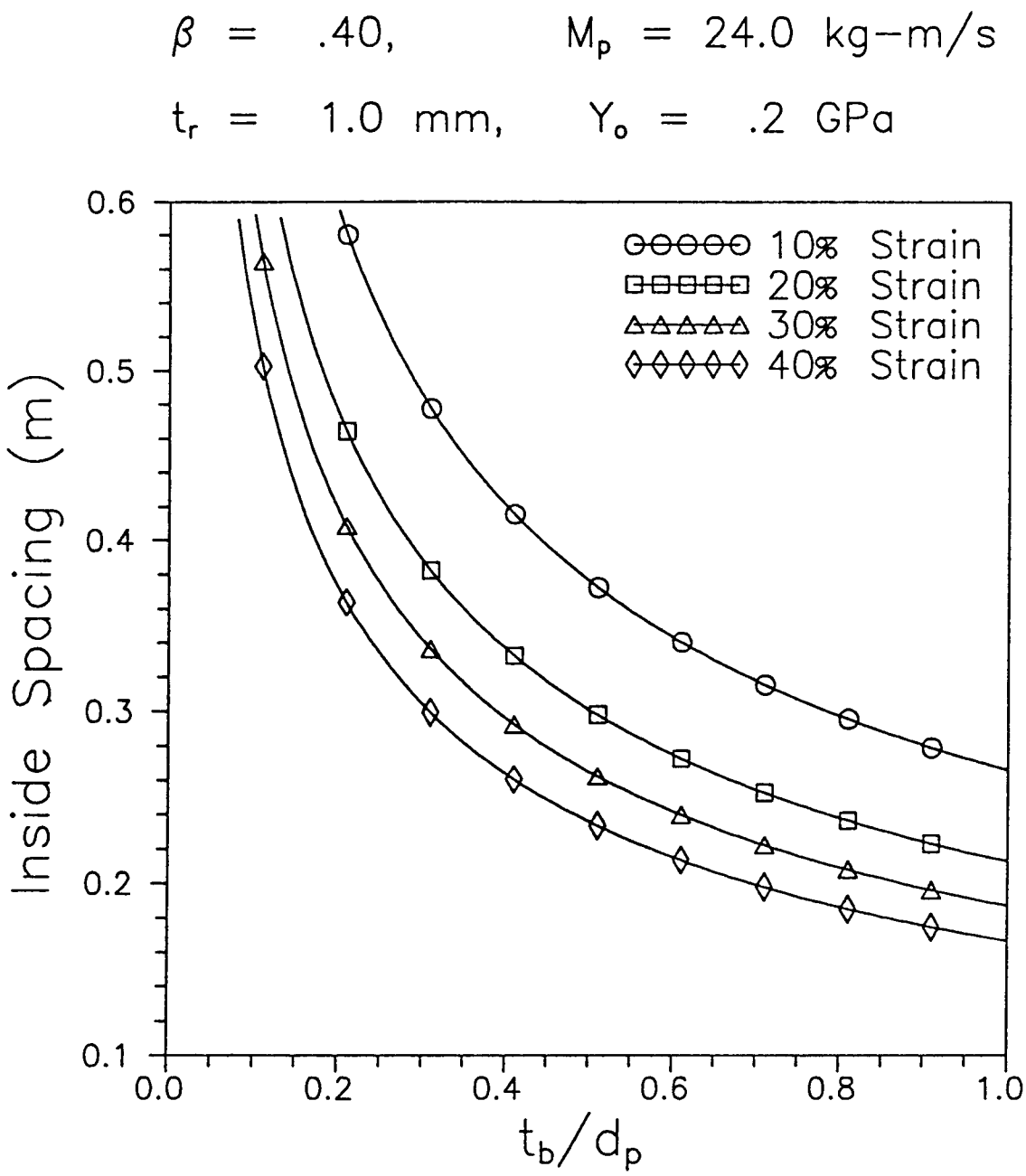


**Figure 49.** Design Curves for $\beta = 0.4$, $M_p = 24$ kg-m/s, $t_r = 1$ mm, and $Y_r = 0.2$ GPa

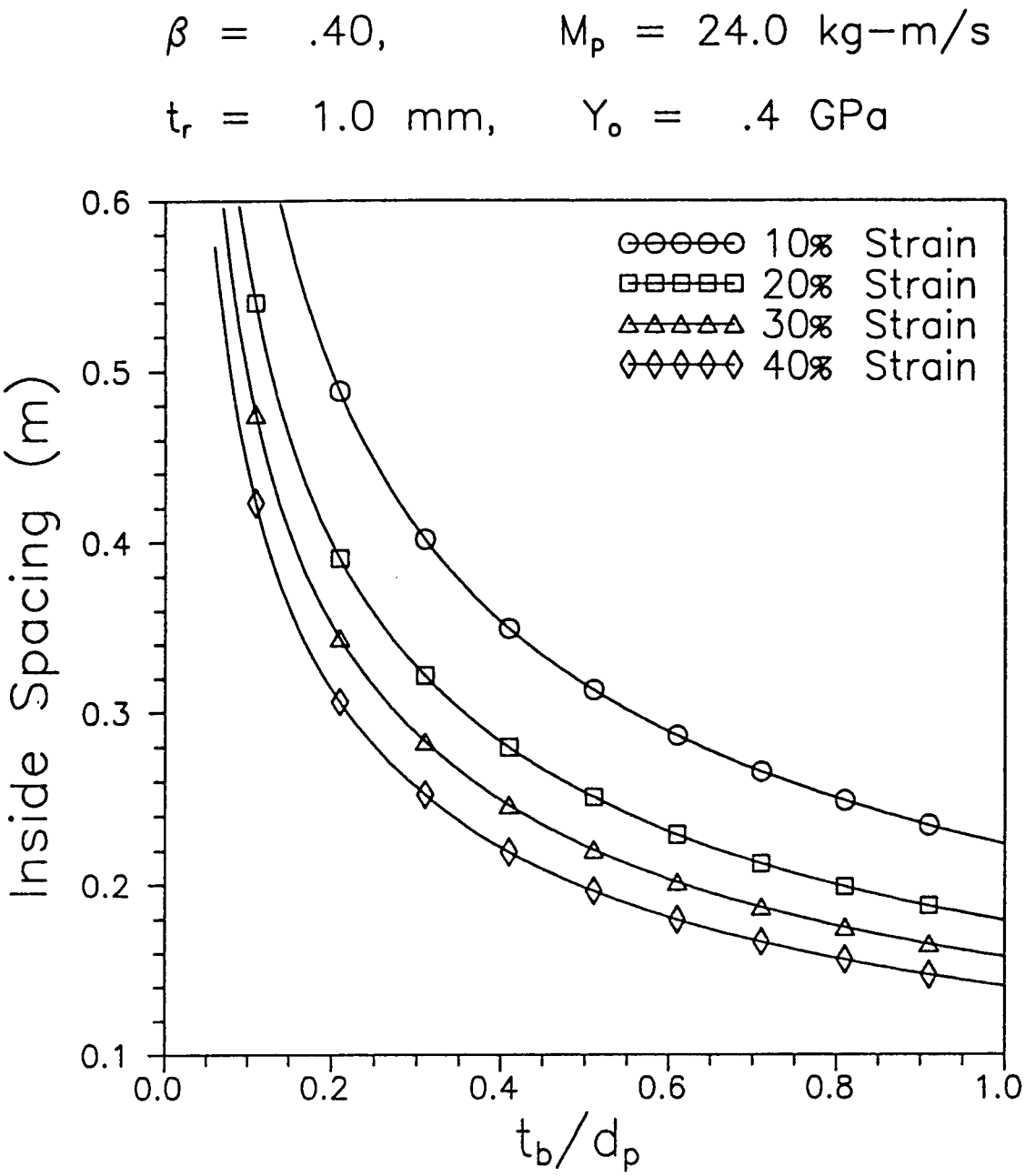


Figure 50. Design Curves for $\beta = 0.4$, $M_p = 24$ kg-m/s, $t_r = 1$ mm, and $Y_r = 0.4$ GPa

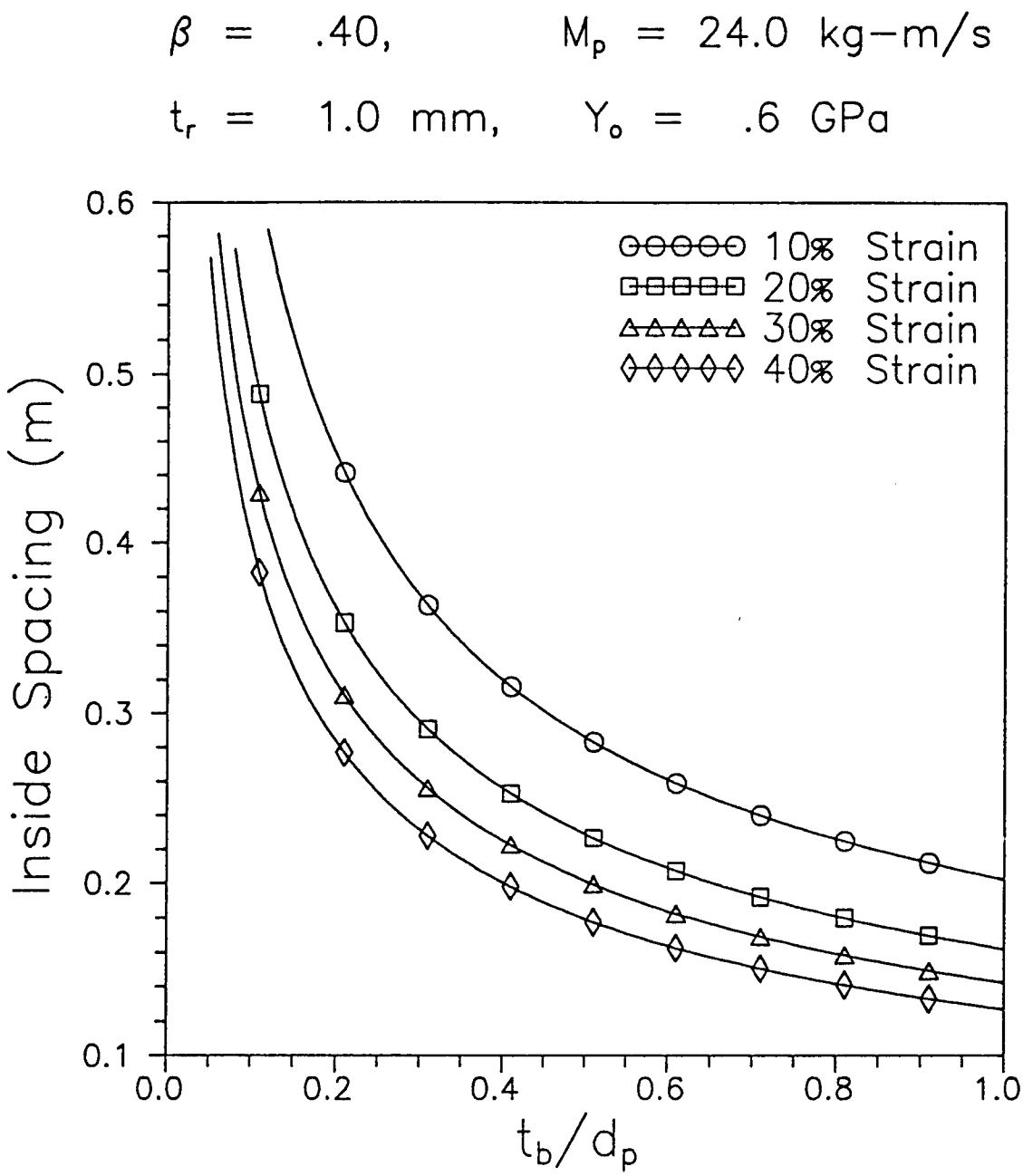


Figure 51. Design Curves for $\beta = 0.4$, $M_p = 24$ kg-m/s, $t_r = 1$ mm, and $Y_r = 0.6$ GPa

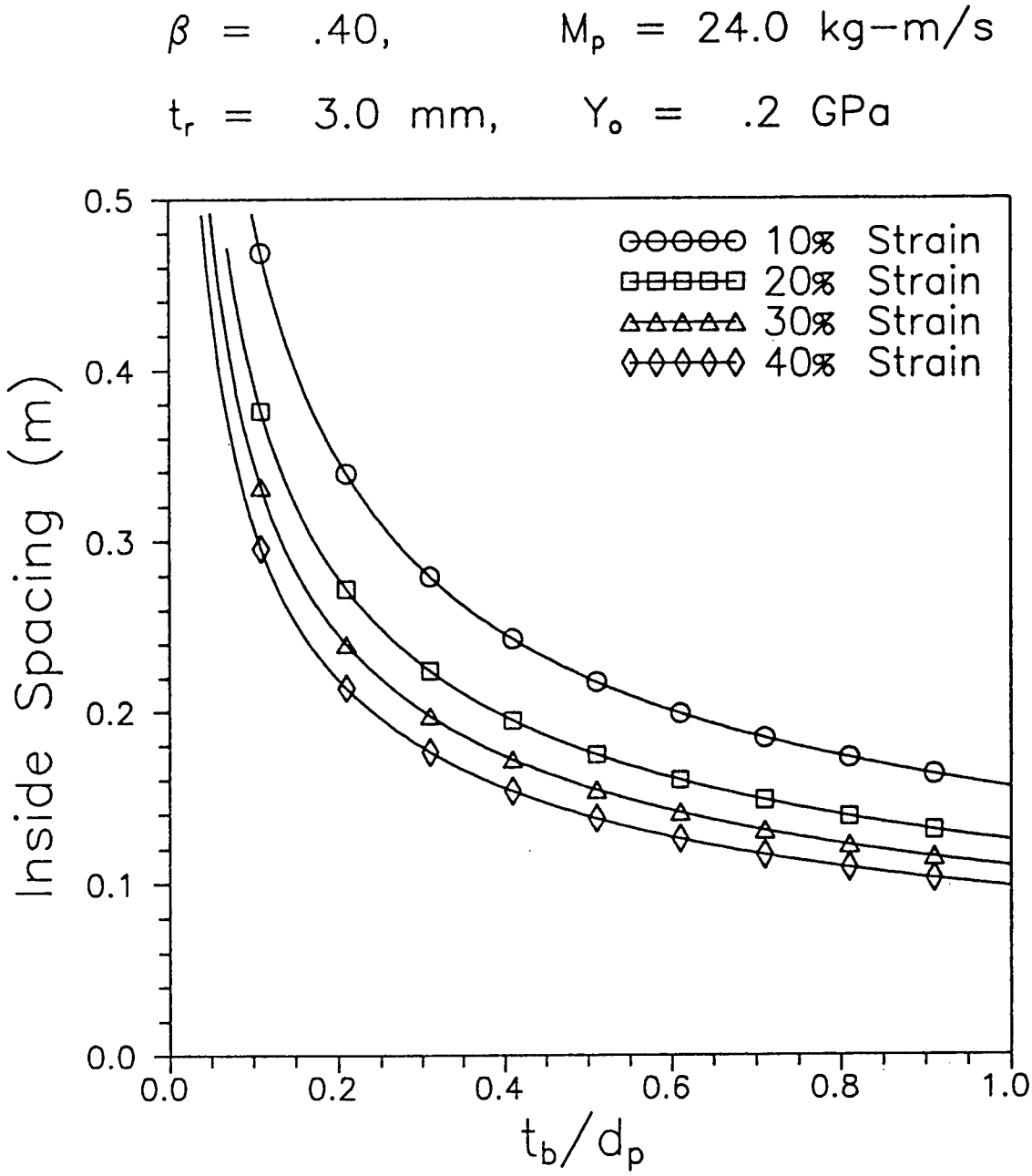


Figure 52. Design Curves for $\beta = 0.4$, $M_p = 24$ kg-m/s, $t_r = 3$ mm, and $Y_r = 0.2$ GPa

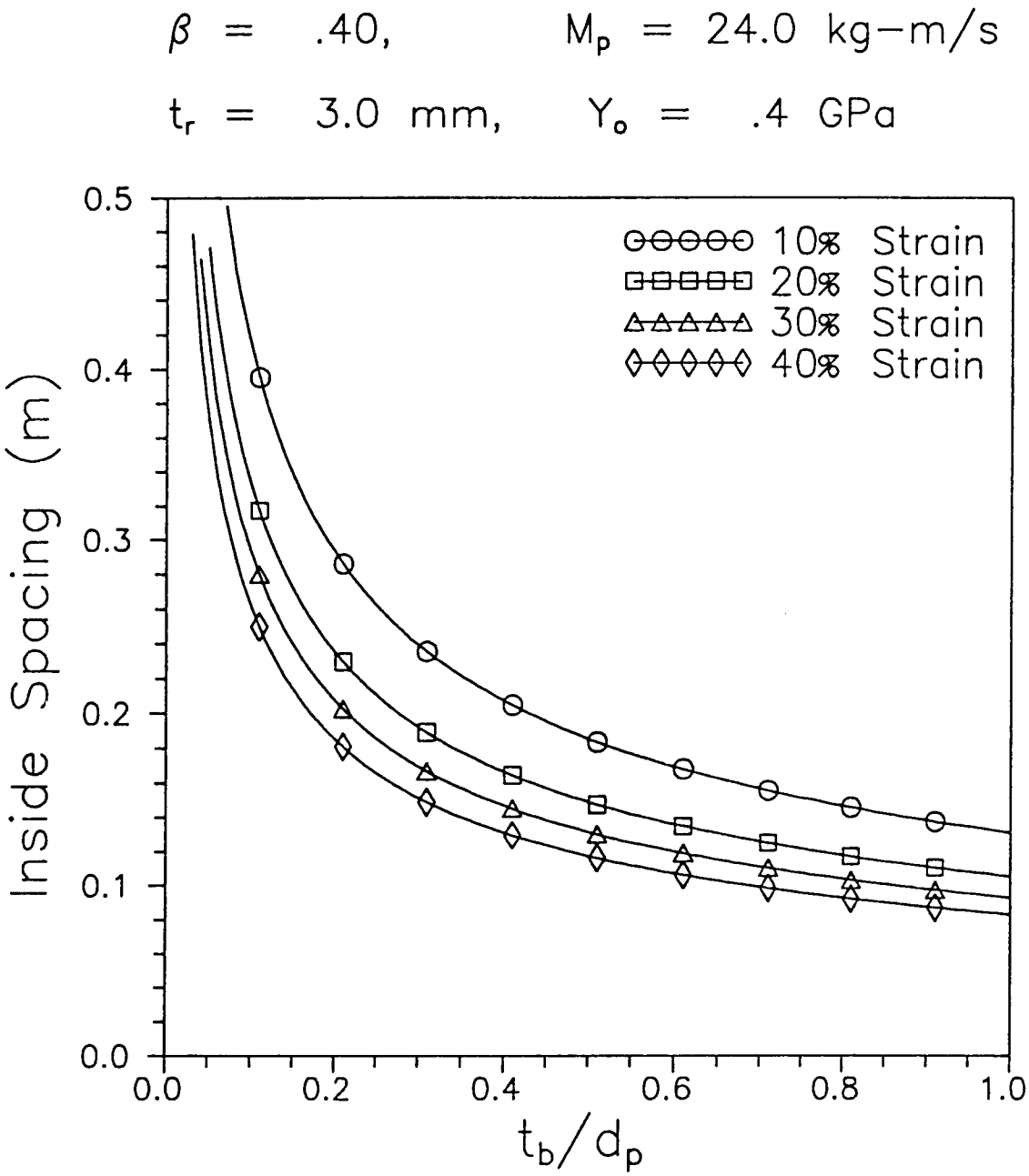


Figure 53. Design Curves for $\beta = 0.4$, $M_p = 24$ kg-m/s, $t_r = 3$ mm, and $Y_r = 0.4$ GPa

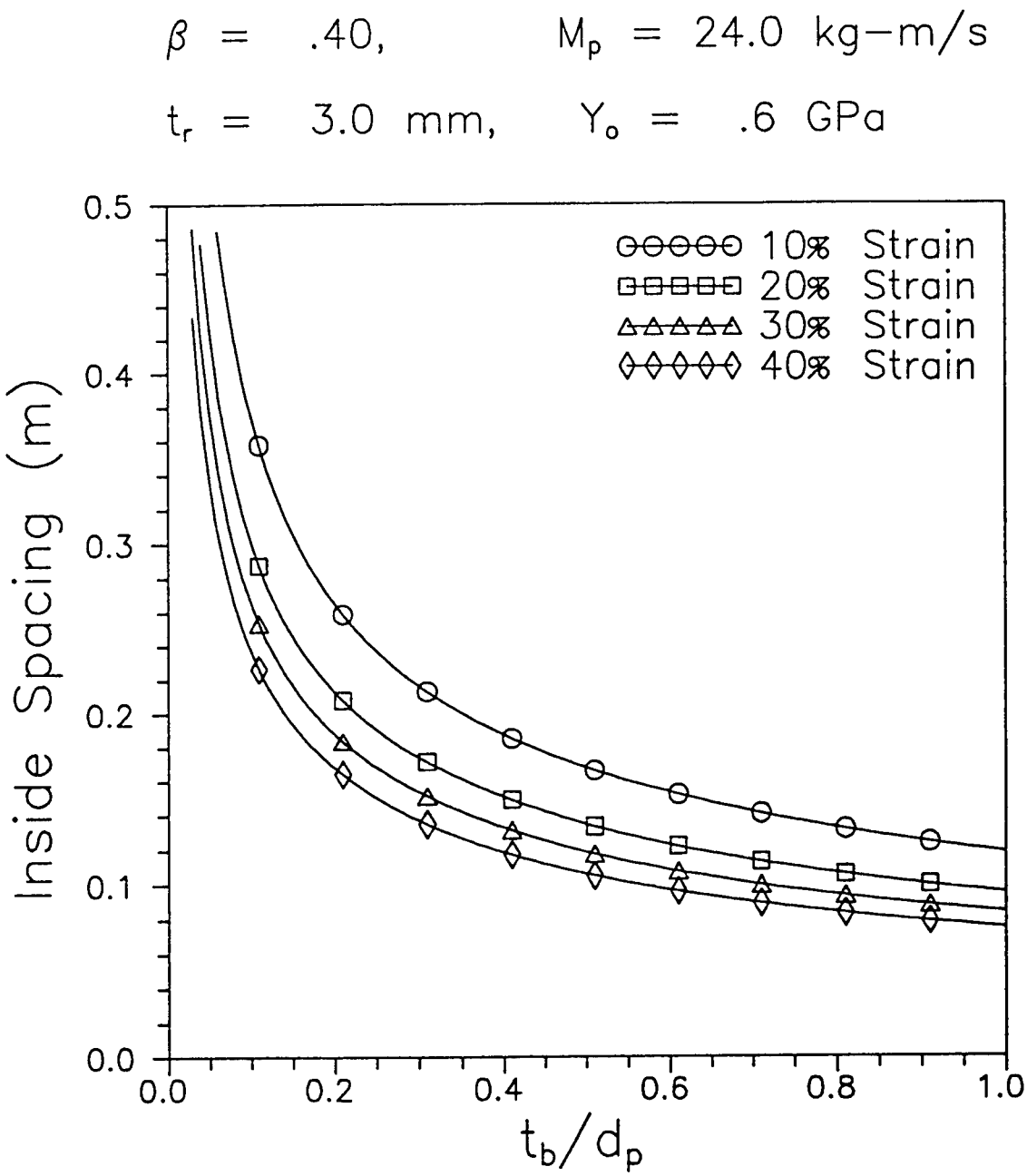


**Figure 54.** Design Curves for $\beta = 0.4$, $M_p = 24$ kg-m/s, $t_r = 3$ mm, and $Y_r = 0.6$ GPa

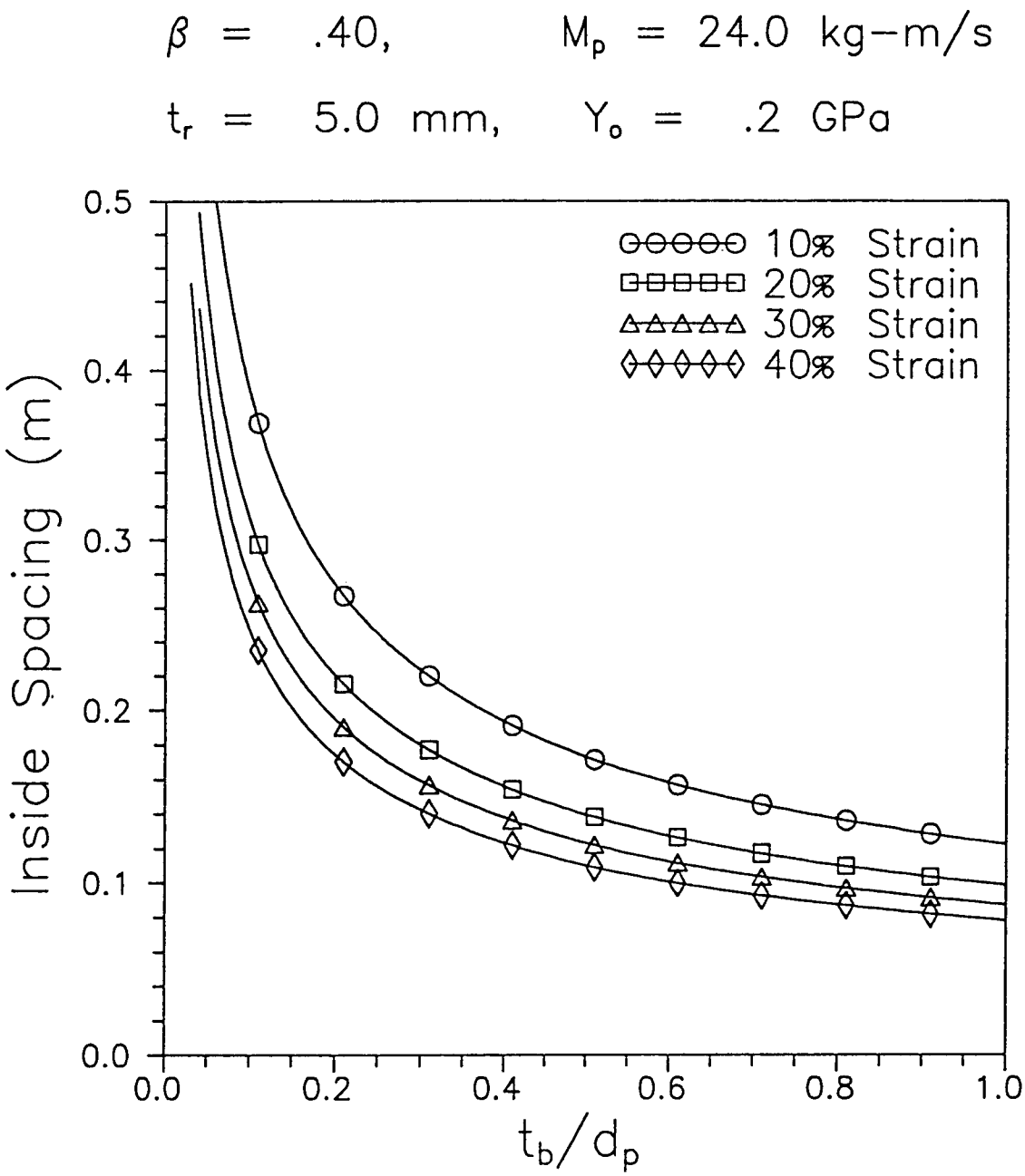


Figure 55. Design Curves for $\beta = 0.4$, $M_p = 24$ kg-m/s, $t_r = 5$ mm, and $Y_r = 0.2$ GPa

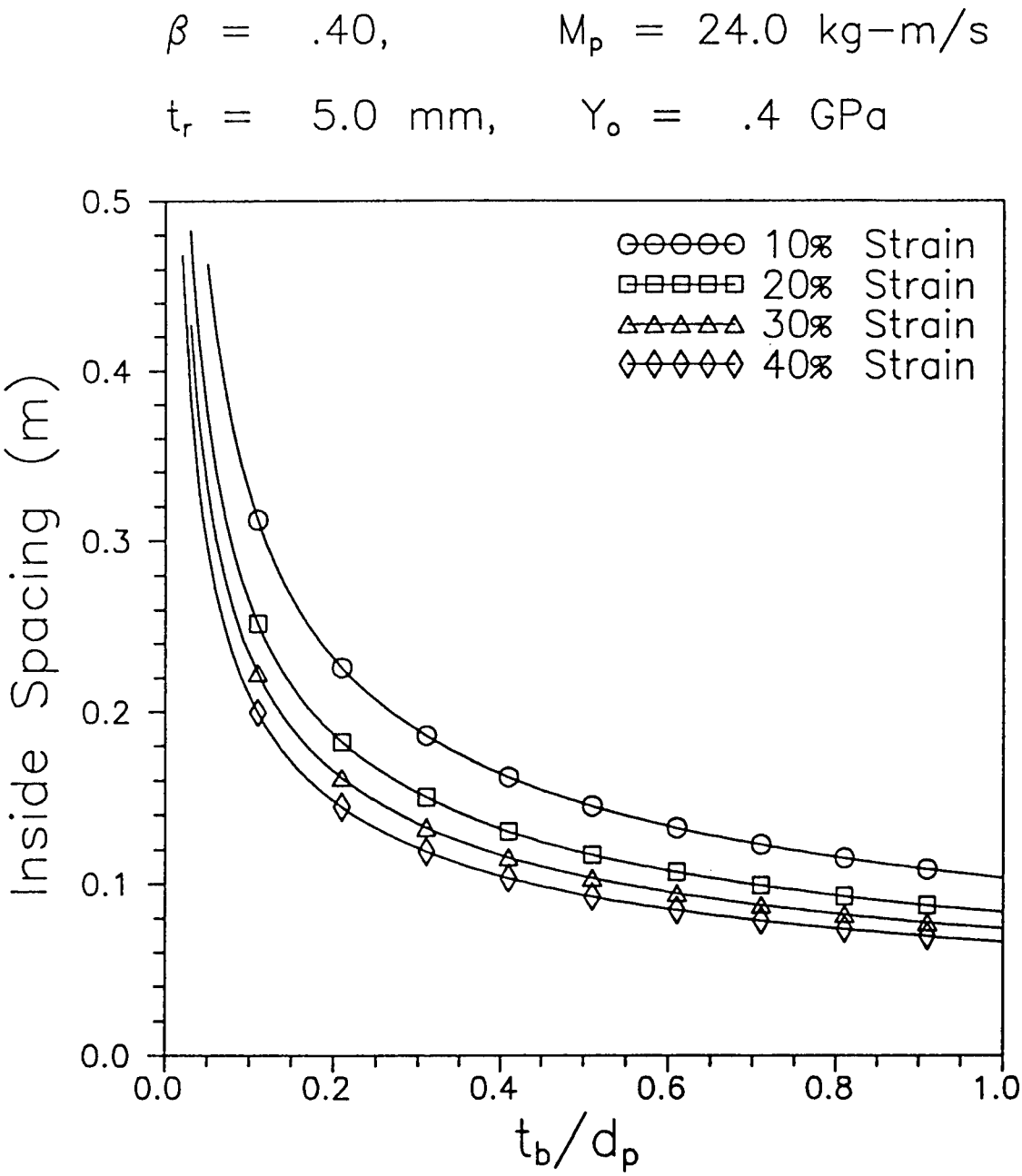


**Figure 56. Design Curves for $\beta$ = 0.4, $M_p$ = 24 kg-m/s, $t_r$ = 5 mm, and $Y_r$ = 0.4 GPa**

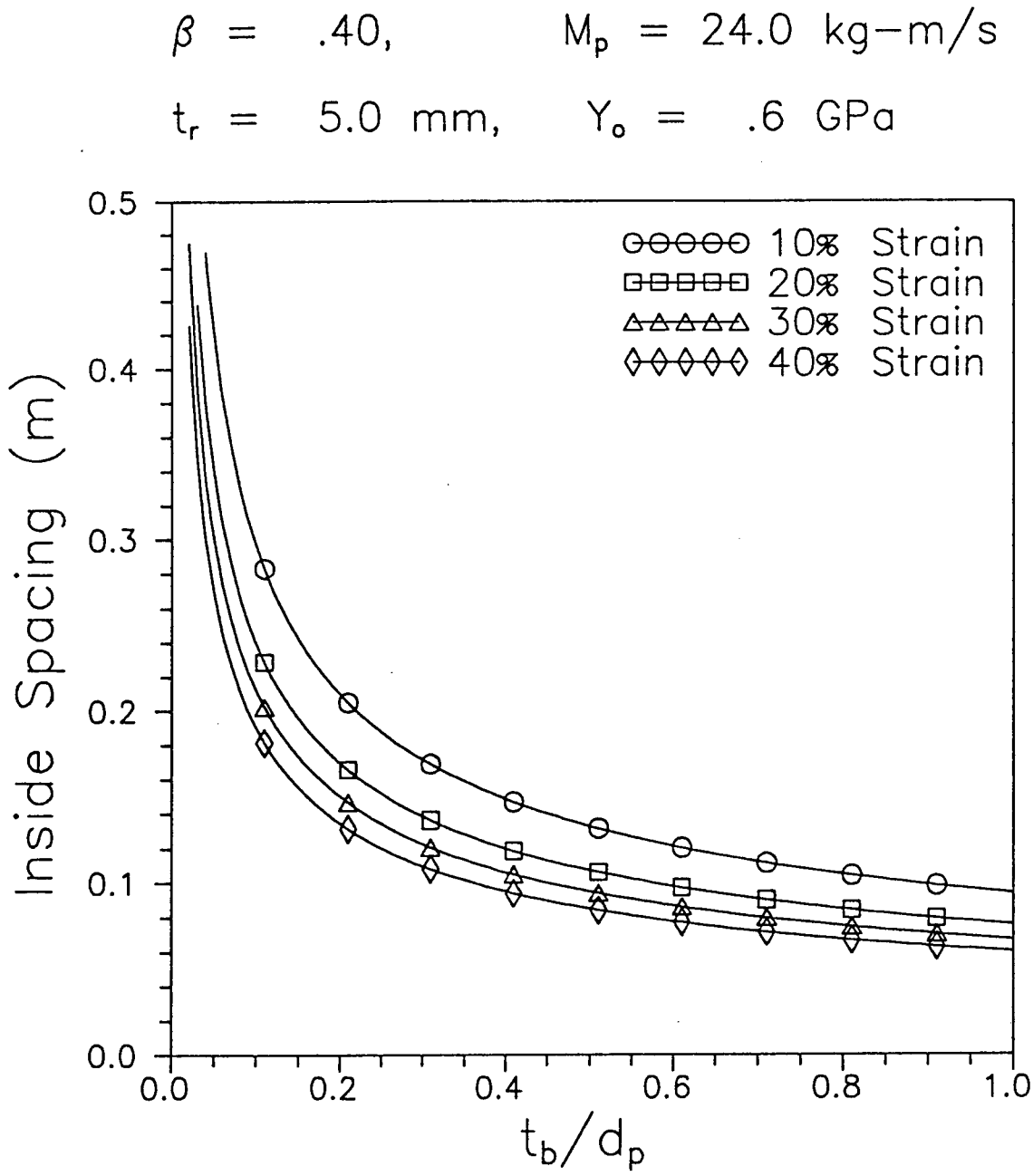


Figure 57. Design Curves for $\beta = 0.4$, $M_p = 24$ kg-m/s, $t_r = 5$ mm, and $Y_r = 0.6$ GPa

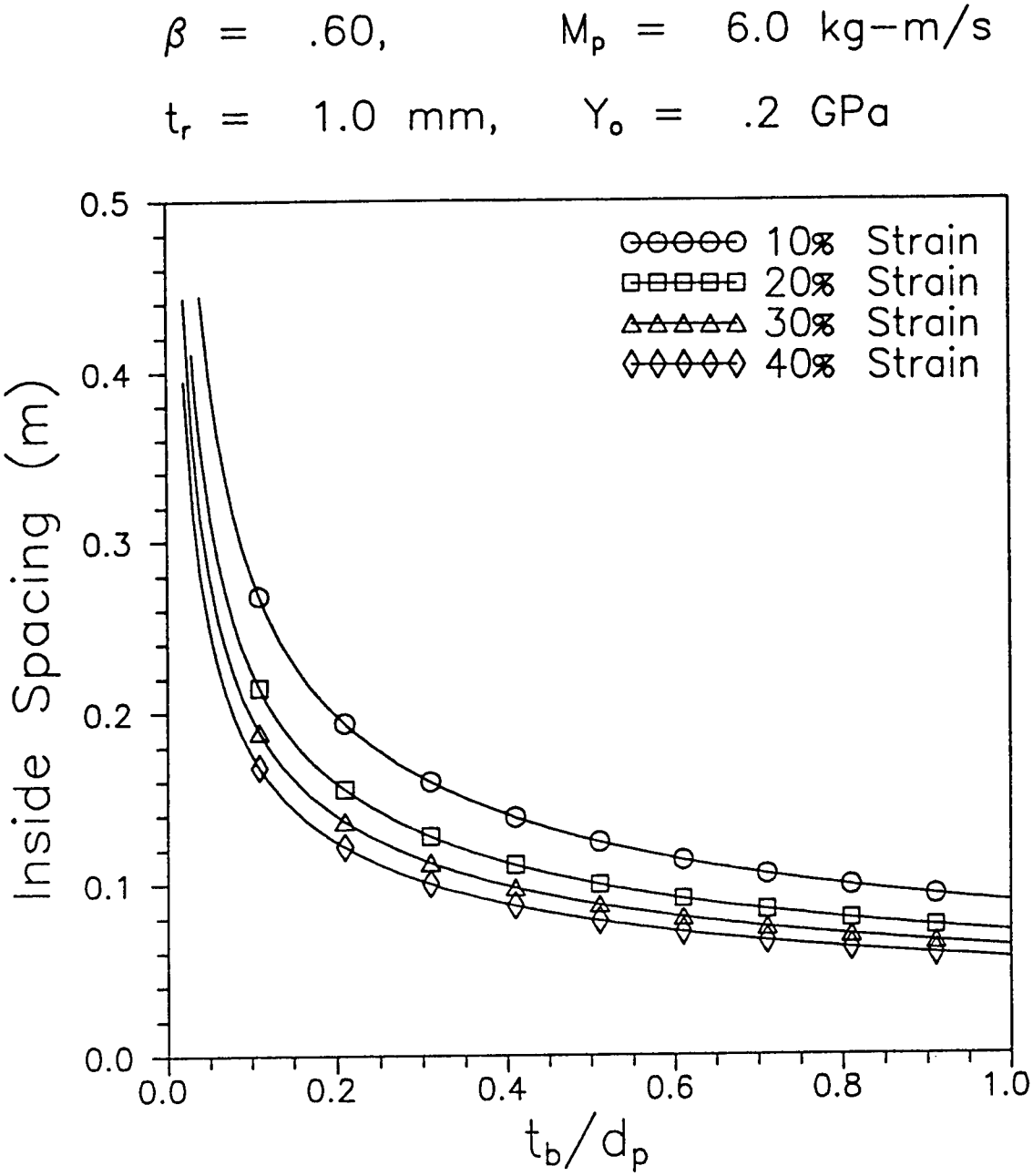


Figure 58. Design Curves for $\beta = 0.6$, $M_p = 6$ kg-m/s, $t_r = 1$ mm, and $Y_r = 0.2$ GPa

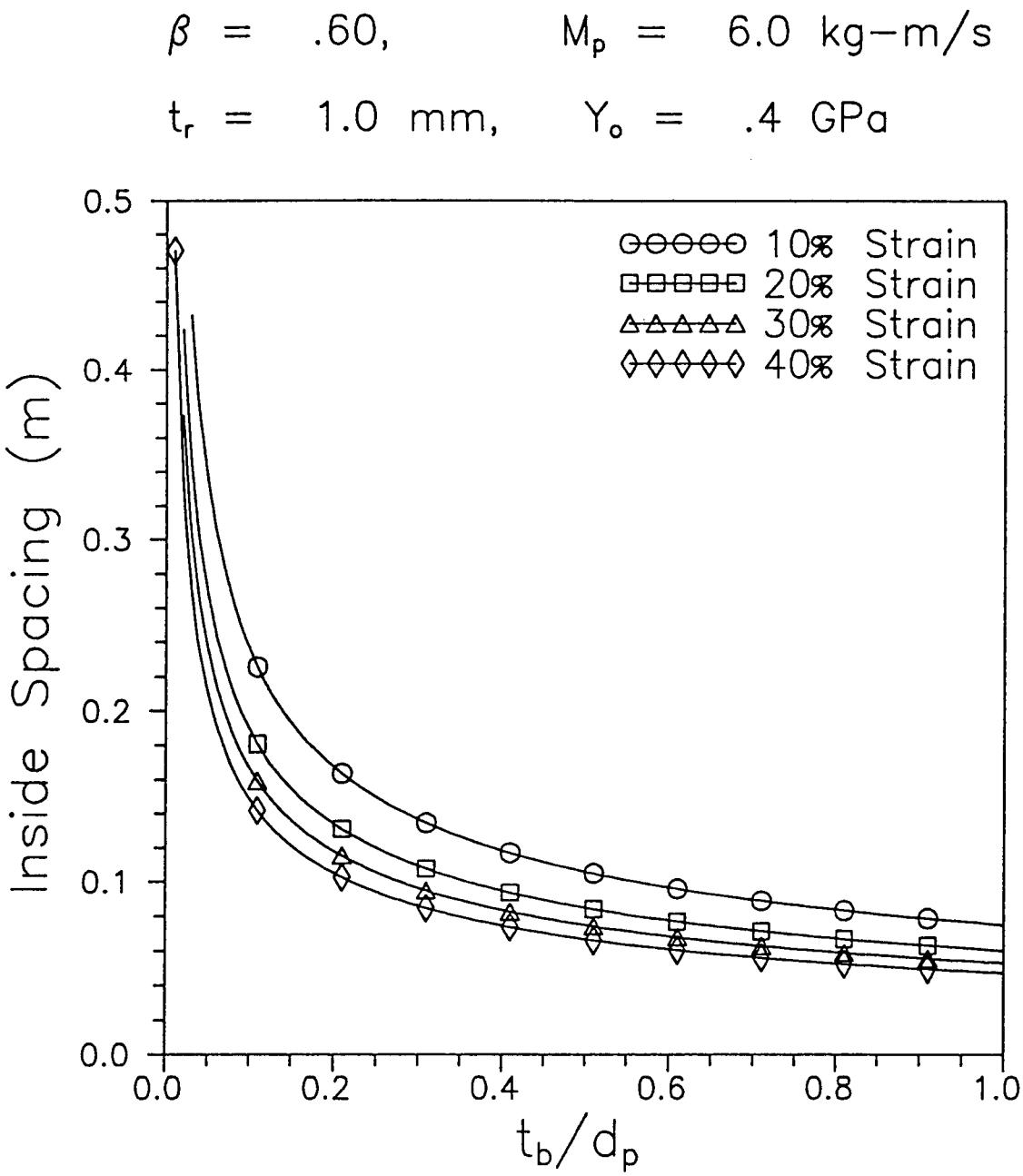


Figure 59. Design Curves for $\beta = 0.6$, $M_p = 6$ kg-m/s, $t_r = 1$ mm, and $Y_r = 0.4$ GPa

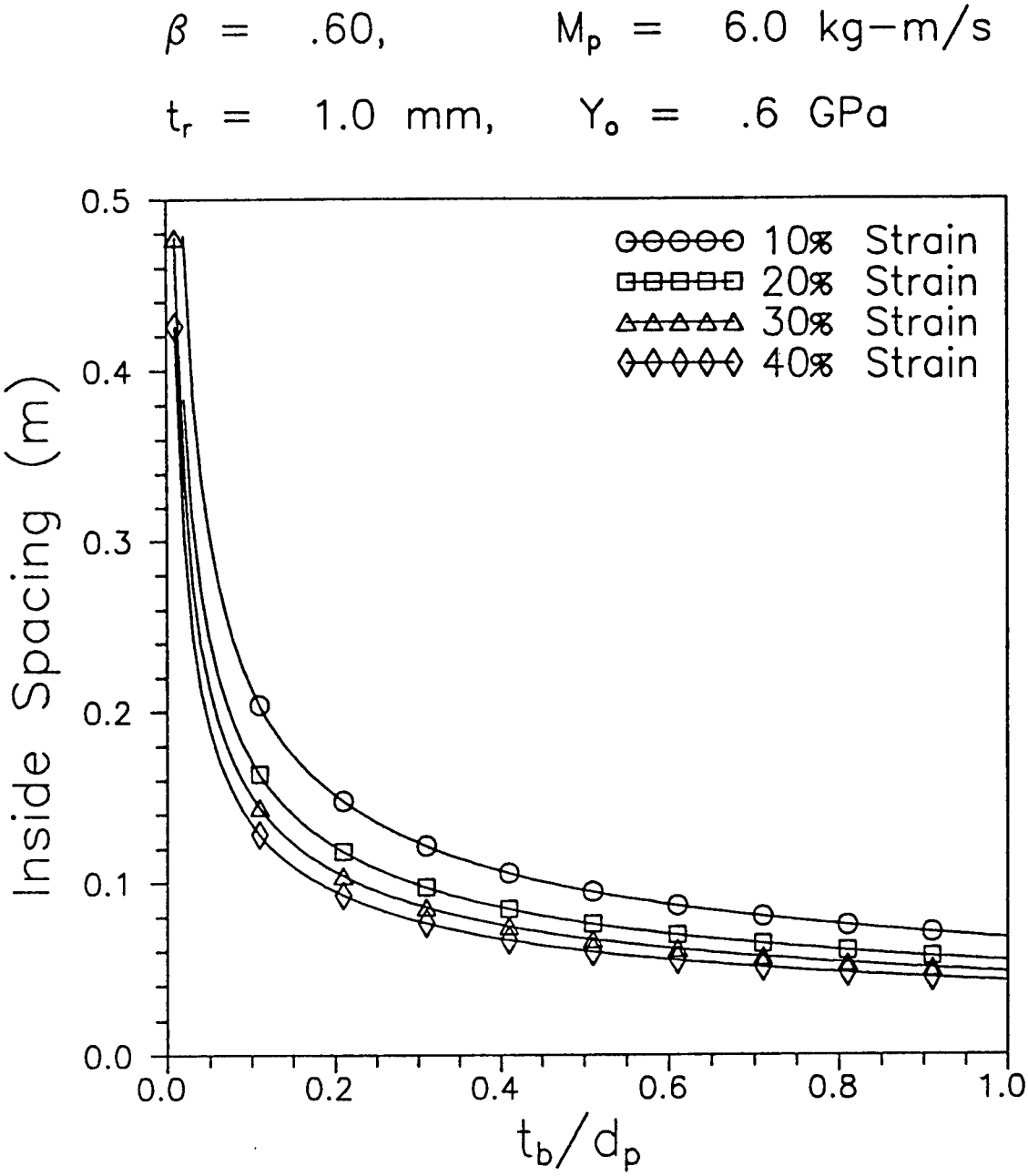


Figure 60. Design Curves for $\beta = 0.6$, $M_p = 6$ kg-m/s, $t_r = 1$ mm, and $Y_r = 0.6$ GPa

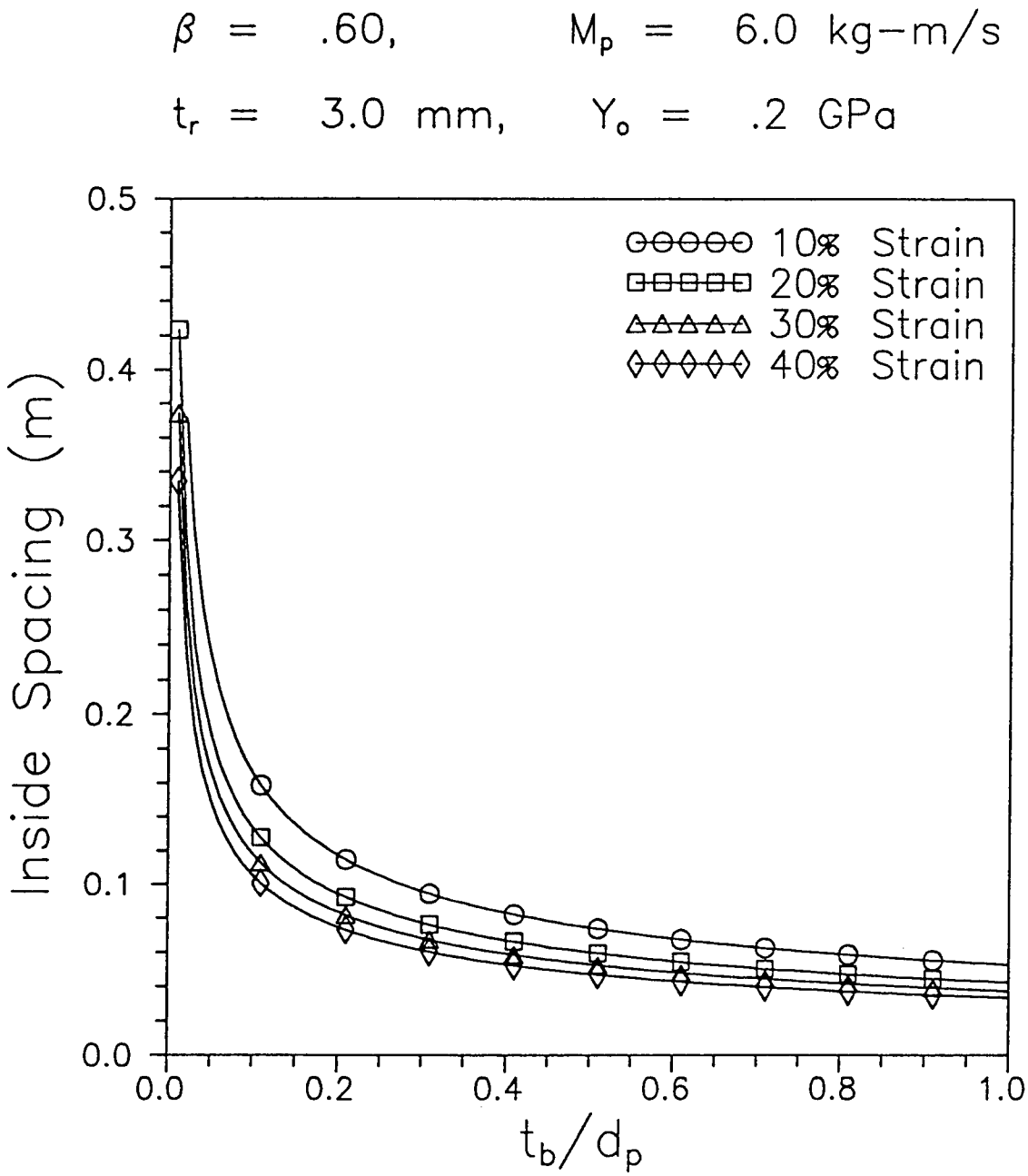


**Figure 61.** Design Curves for $\beta = 0.6$, $M_p = 6$ kg-m/s, $t_r = 3$ mm, and $Y_r = 0.2$ GPa

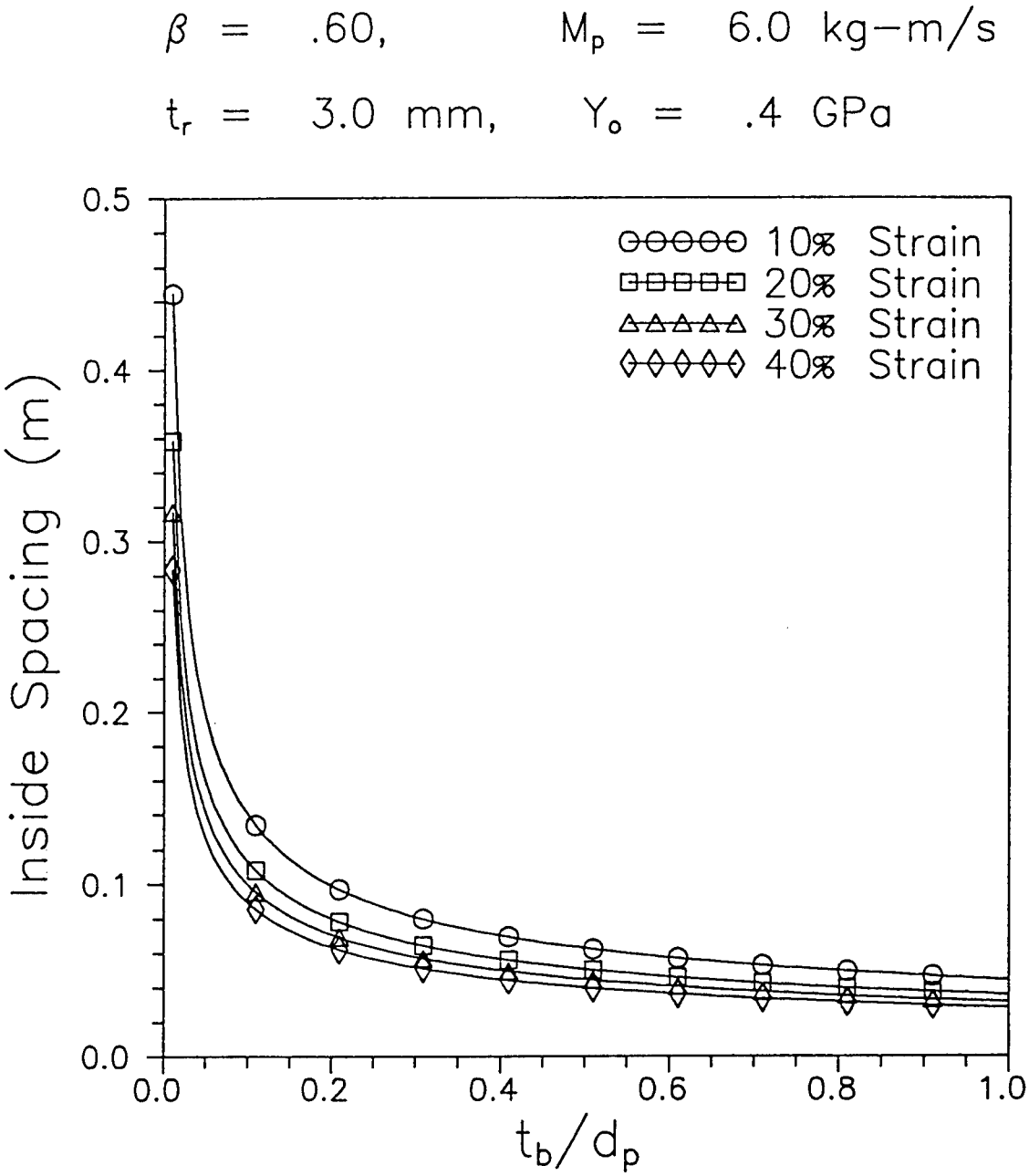


**Figure 62. Design Curves for $\beta = 0.6$, $M_p = 6$ kg-m/s, $t_r = 3$ mm, and $Y_r = 0.4$ GPa**

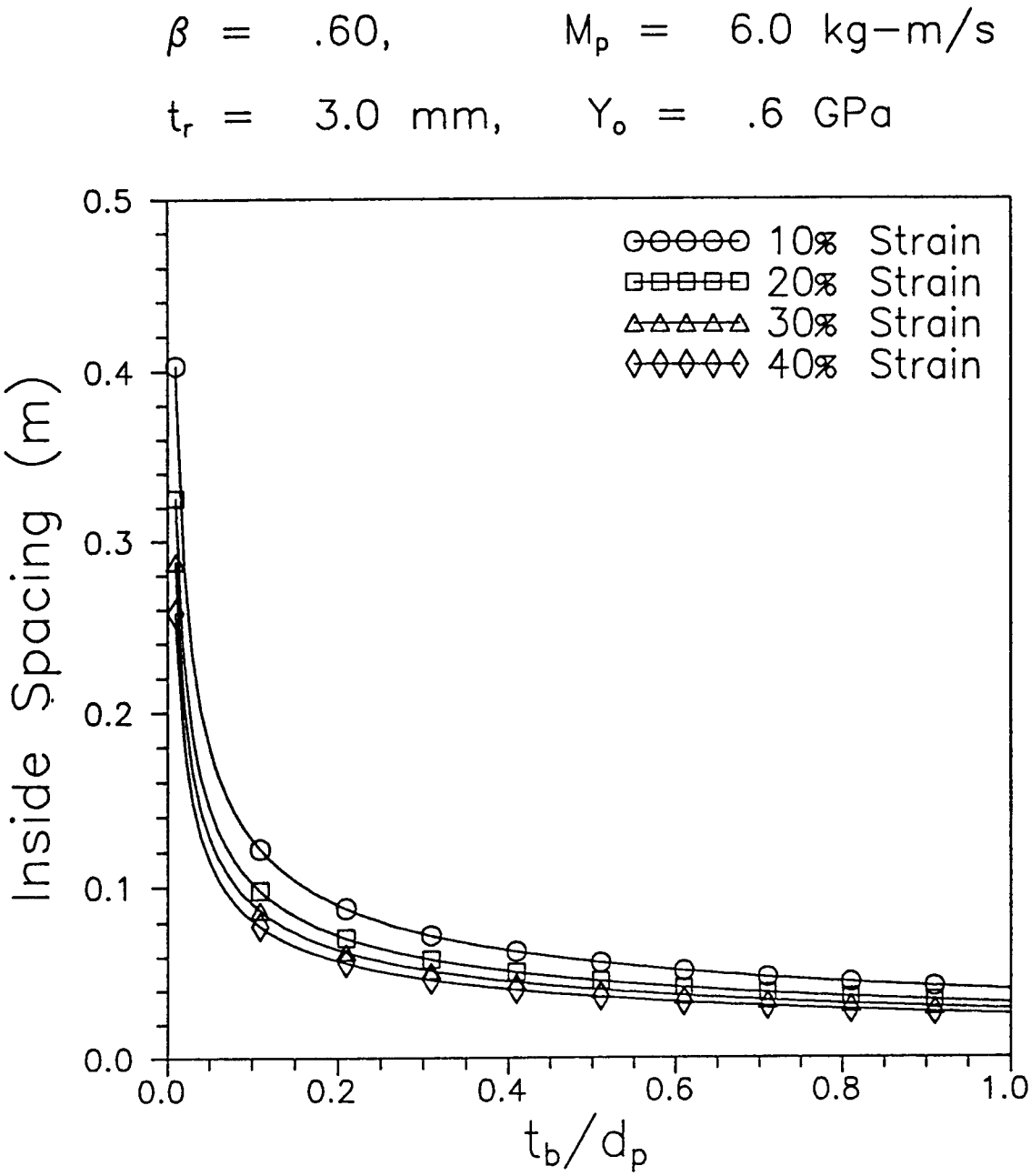


Figure 63. Design Curves for $\beta = 0.6$, $M_p = 6$ kg-m/s, $t_r = 3$ mm, and $Y_r = 0.6$ GPa

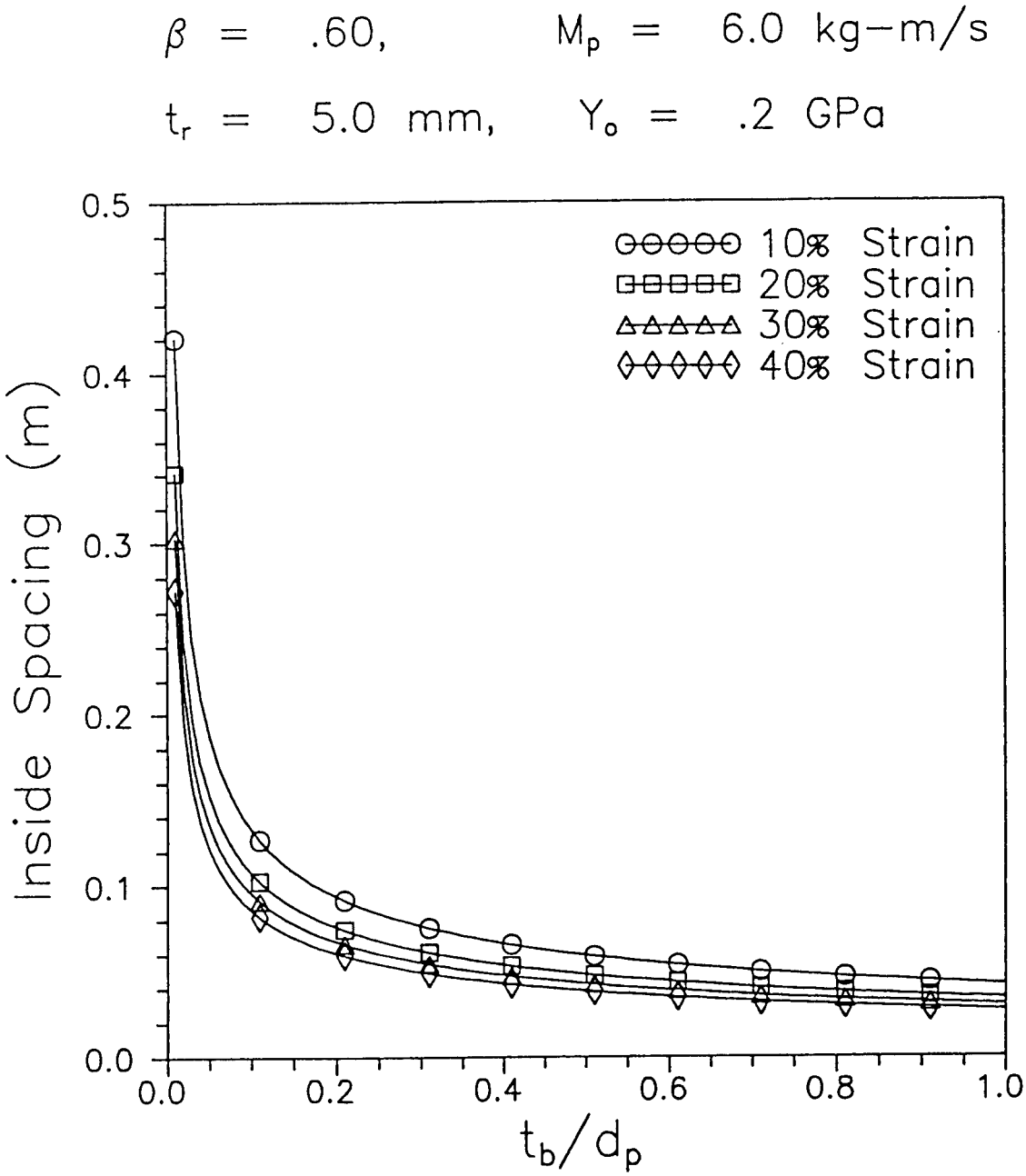


Figure 64. Design Curves for $\beta = 0.6$, $M_p = 6$ kg-m/s, $t_r = 5$ mm, and $Y_r = 0.2$ GPa

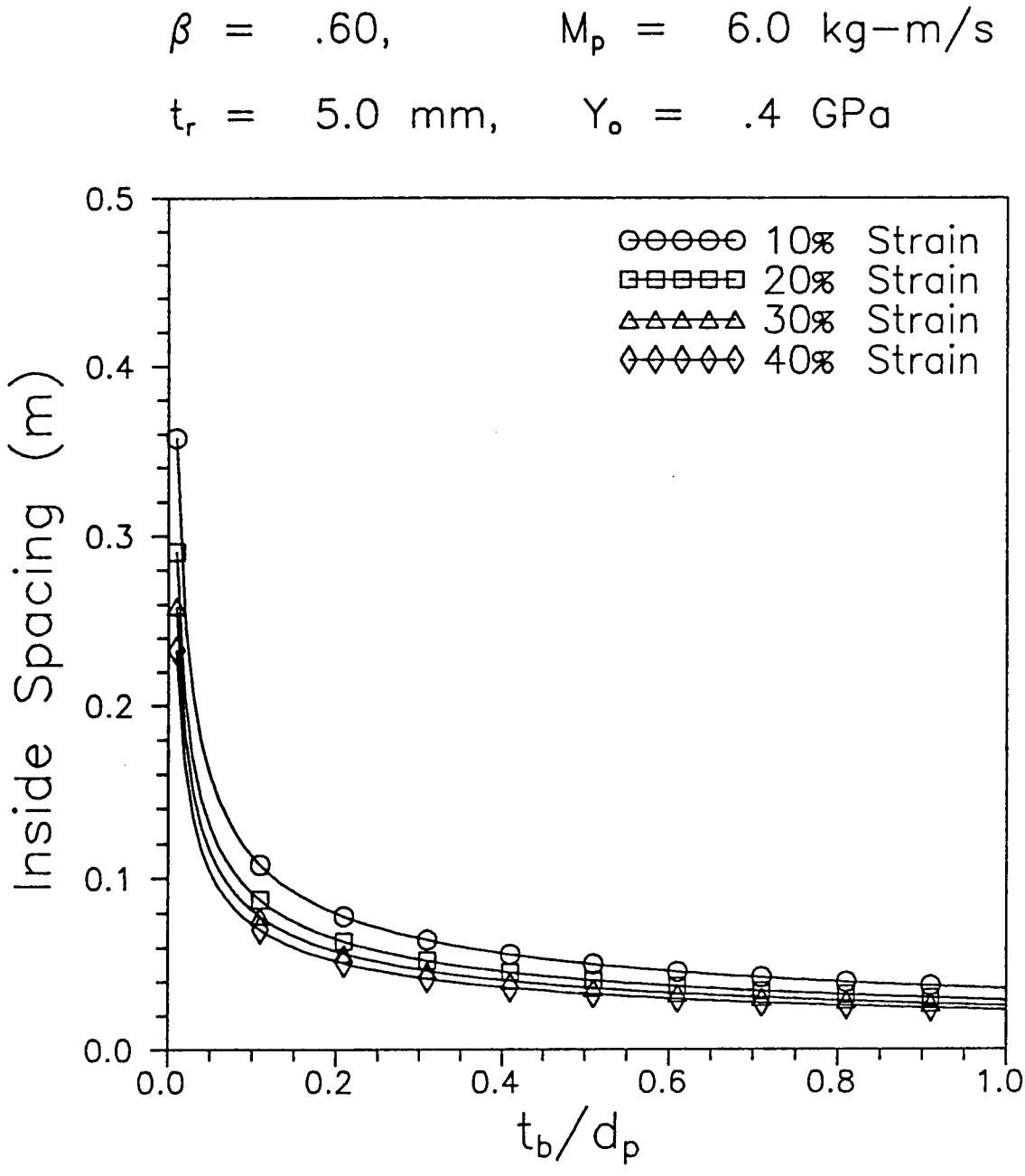


Figure 65. Design Curves for $\beta = 0.6$, $M_p = 6$ kg-m/s, $t_r = 5$ mm, and $Y_r = 0.4$ GPa

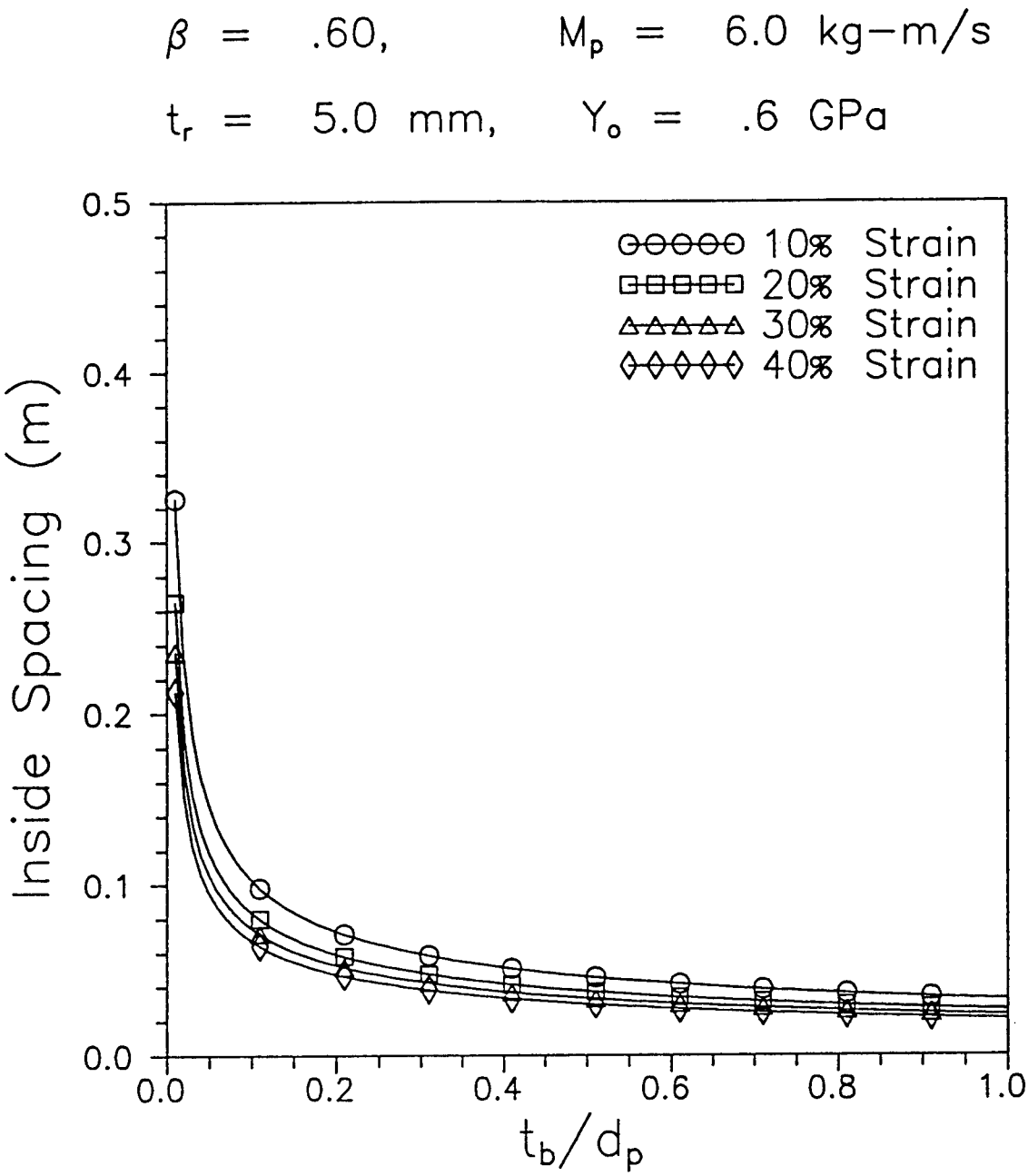


Figure 66. Design Curves for $\beta = 0.6$, $M_p = 6$ kg-m/s, $t_r = 5$ mm, and $Y_r = 0.6$ GPa

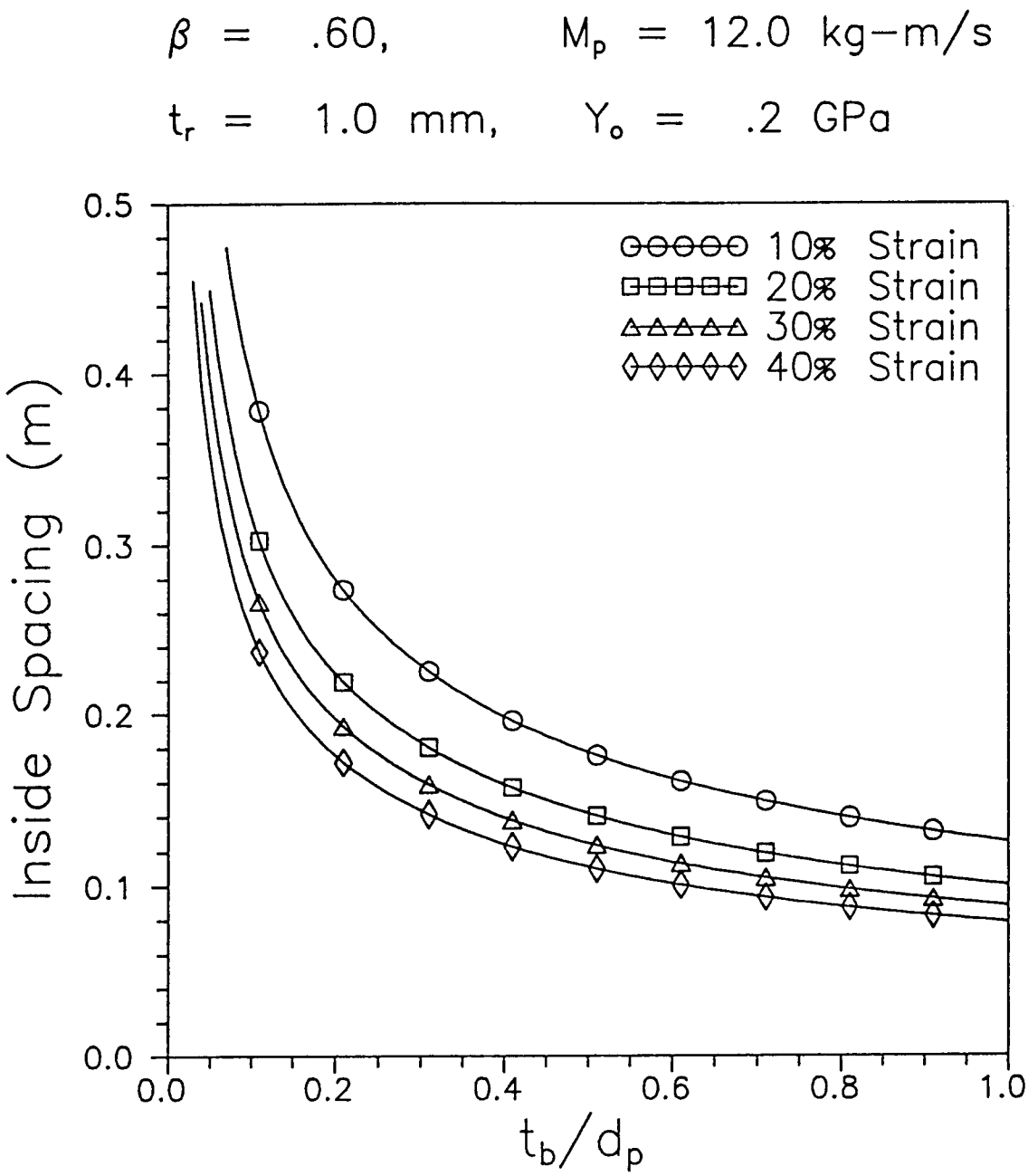


Figure 67. Design Curves for $\beta = 0.6$, $M_p = 12$ kg-m/s, $t_r = 1$ mm, and $Y_r = 0.2$ GPa

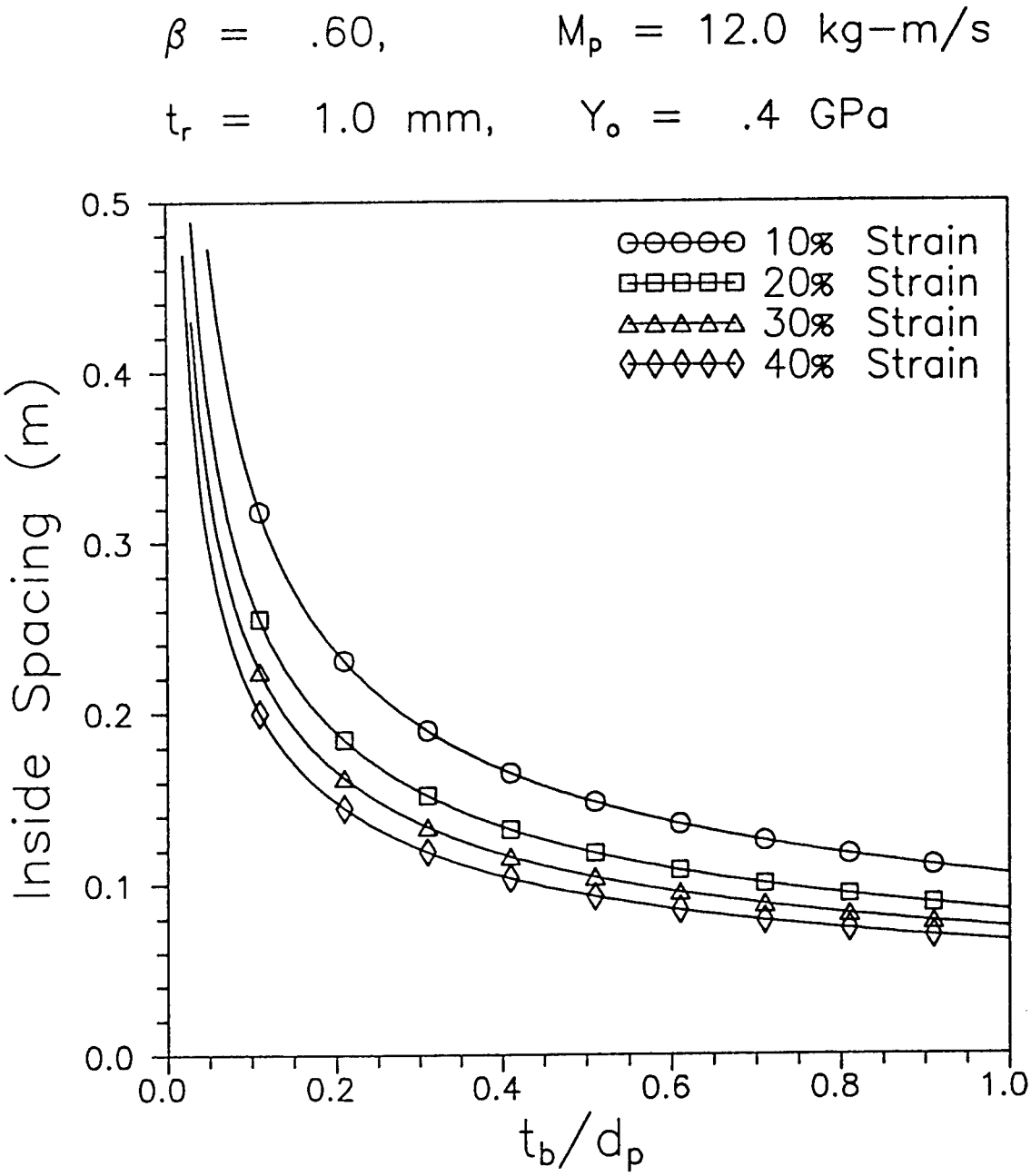


Figure 68. Design Curves for $\beta = 0.6$, $M_p = 12$ kg-m/s, $t_r = 1$ mm, and $Y_r = 0.4$ GPa

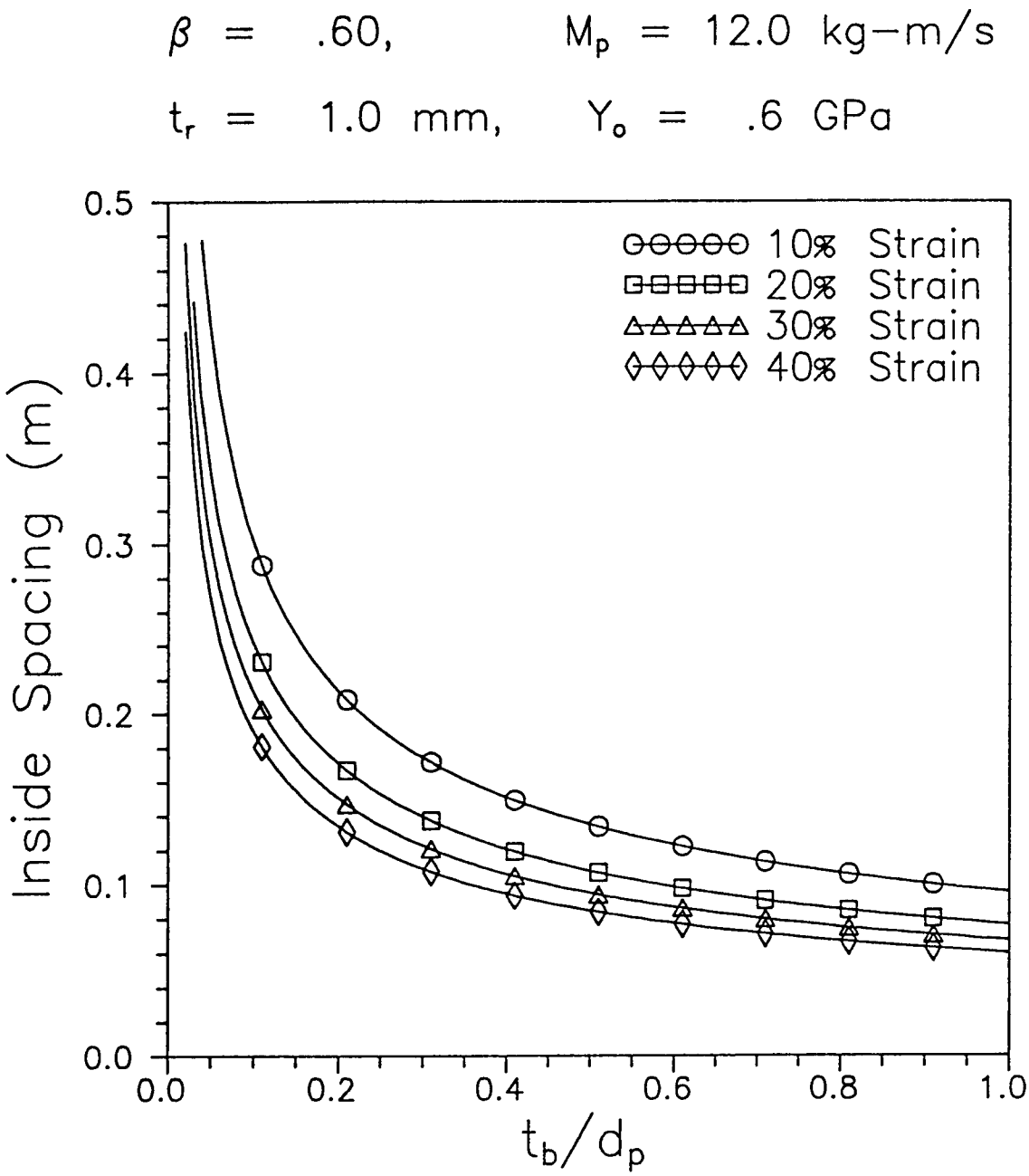


Figure 69. Design Curves for $\beta = 0.6$, $M_p = 12$ kg-m/s, $t_r = 1$ mm, and $Y_r = 0.6$ GPa

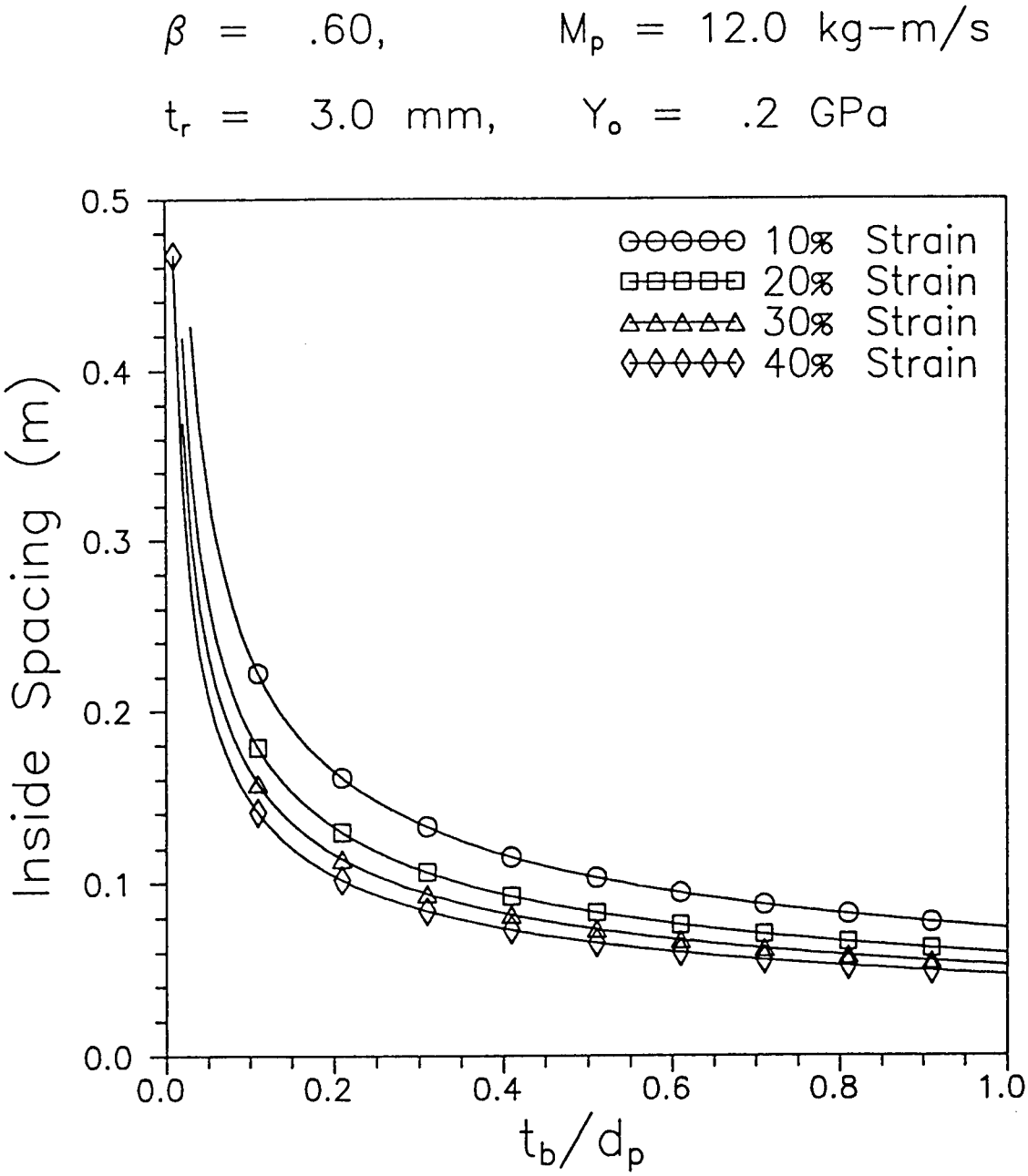


Figure 70. Design Curves for $\beta = 0.6$, $M_p = 12$ kg-m/s, $t_r = 3$ mm, and $Y_r = 0.2$ GPa

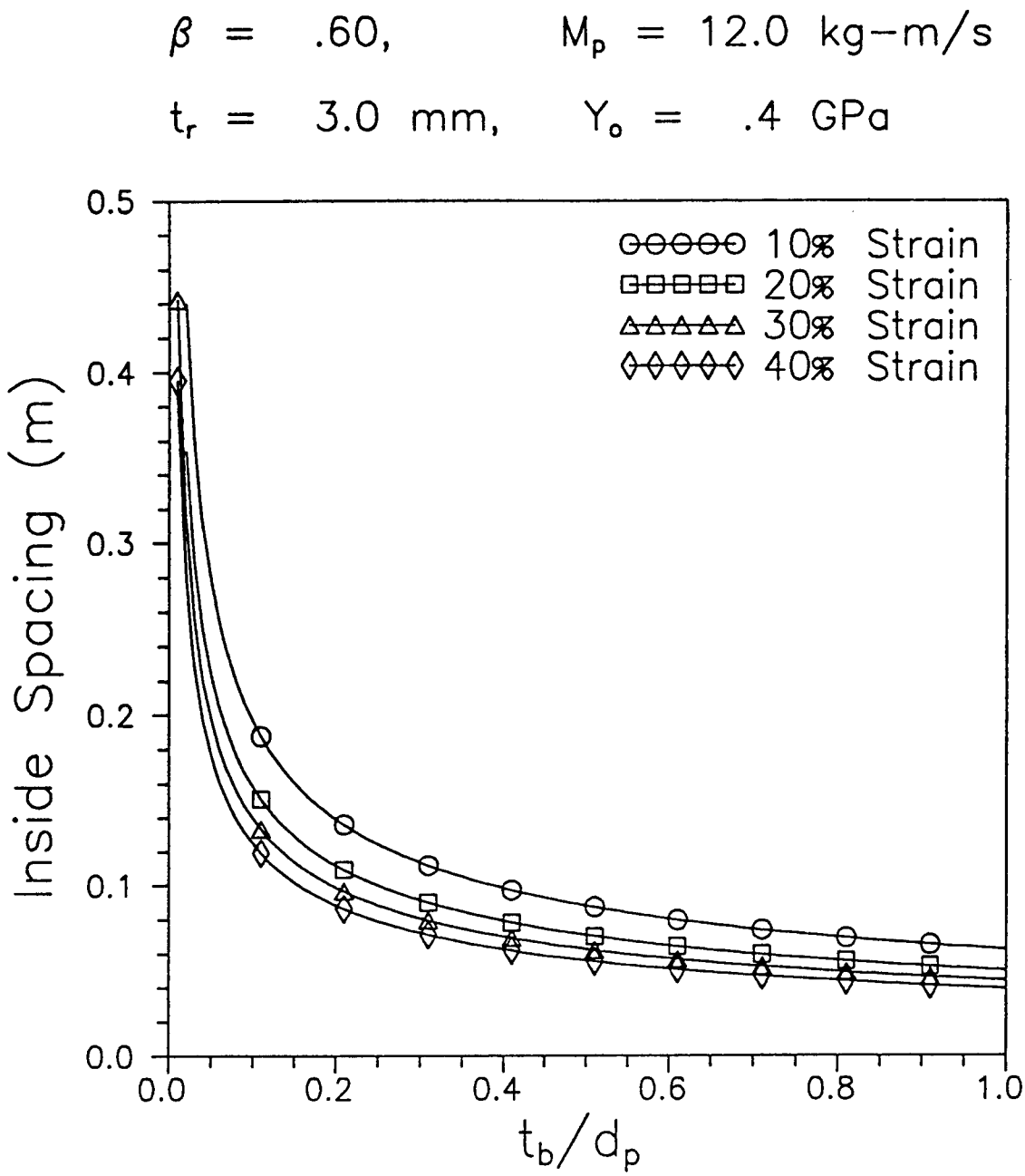


Figure 71. Design Curves for $\beta = 0.6$, $M_p = 12$ kg-m/s, $t_r = 3$ mm, and $Y_r = 0.4$ GPa

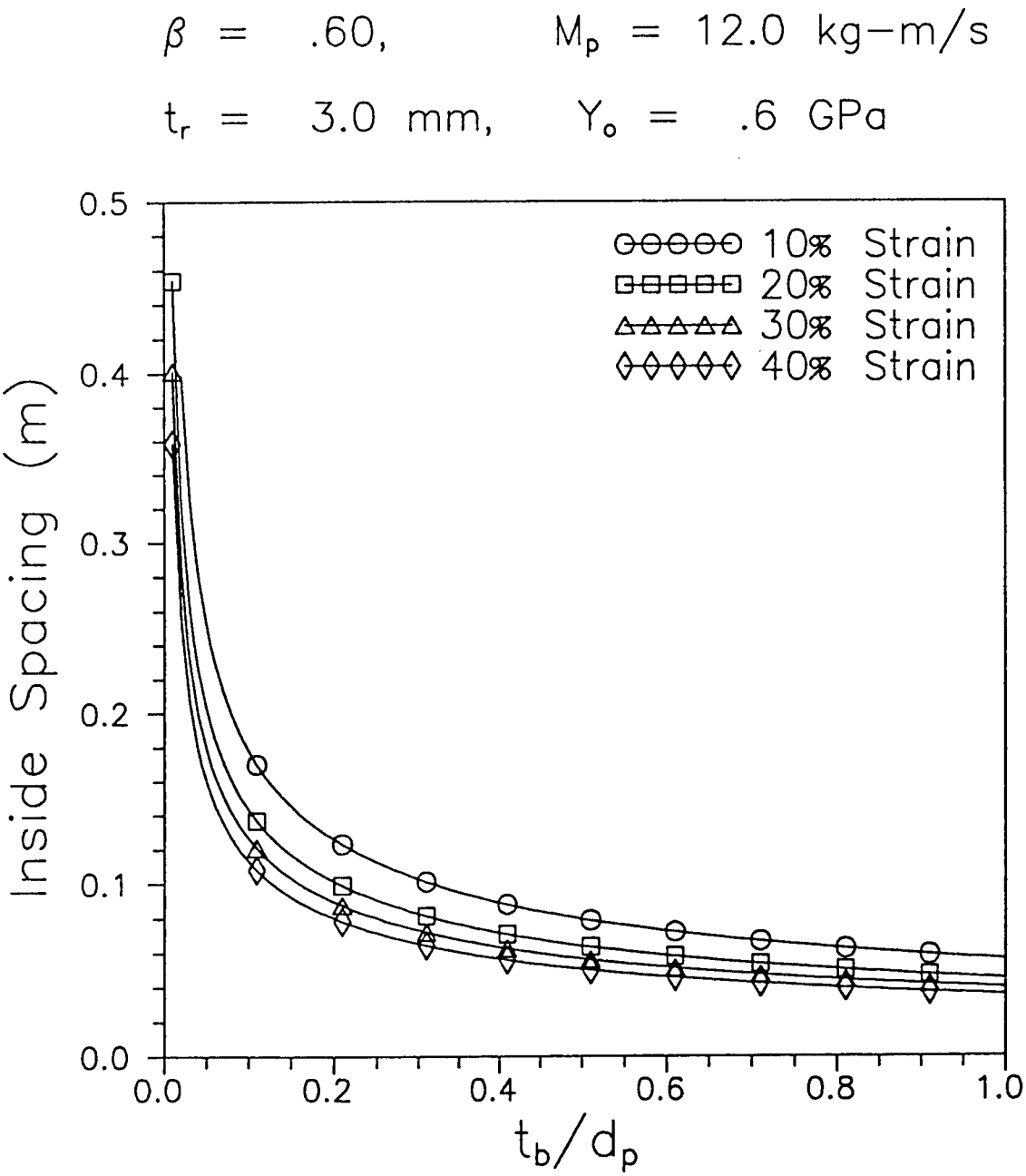


Figure 72. Design Curves for $\beta = 0.6$, $M_p = 12$ kg-m/s, $t_r = 3$ mm, and $Y_r = 0.6$ GPa

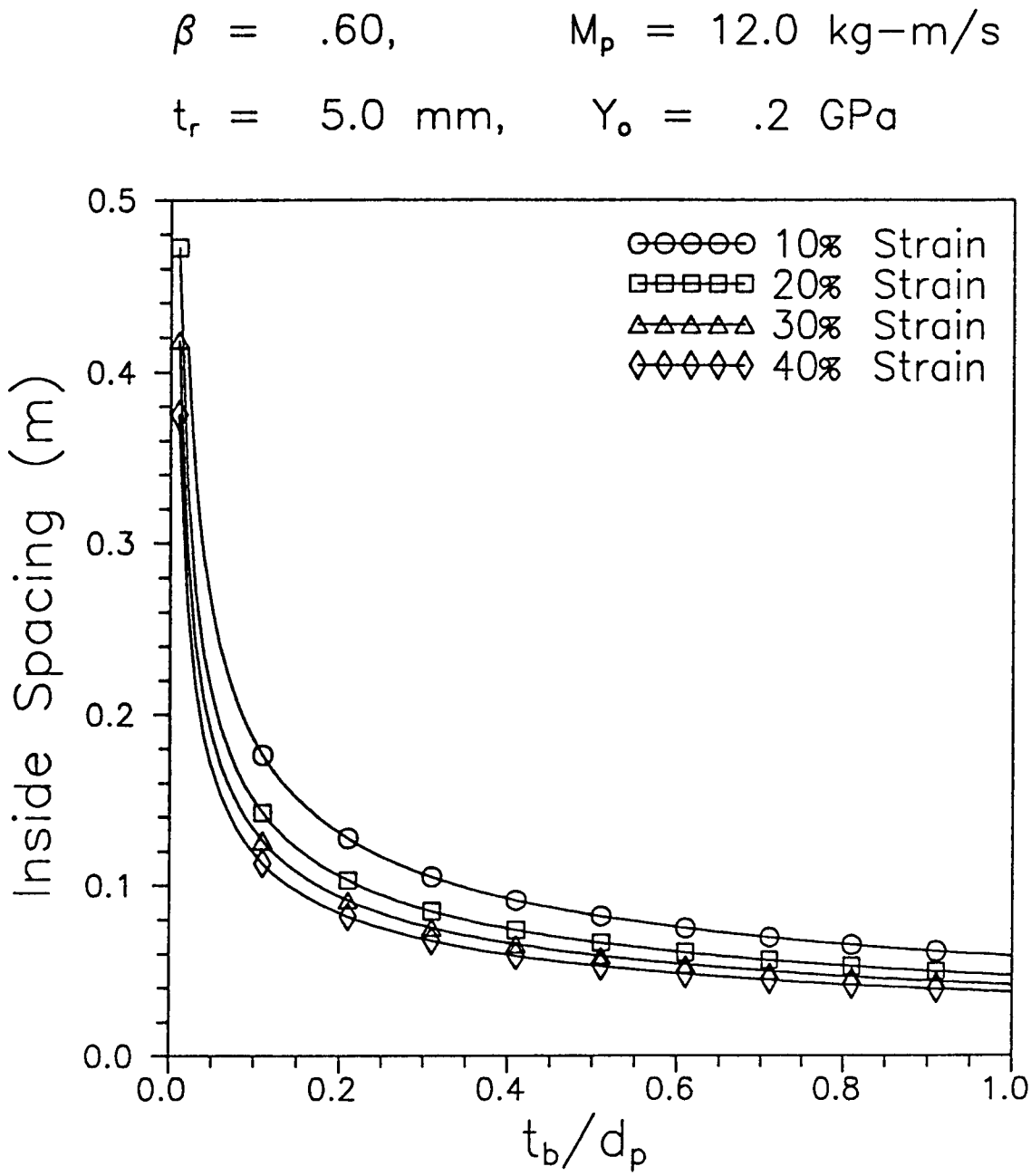


Figure 73. Design Curves for $\beta = 0.6$, $M_p = 12$ kg-m/s, $t_r = 5$ mm, and $Y_r = 0.2$ GPa

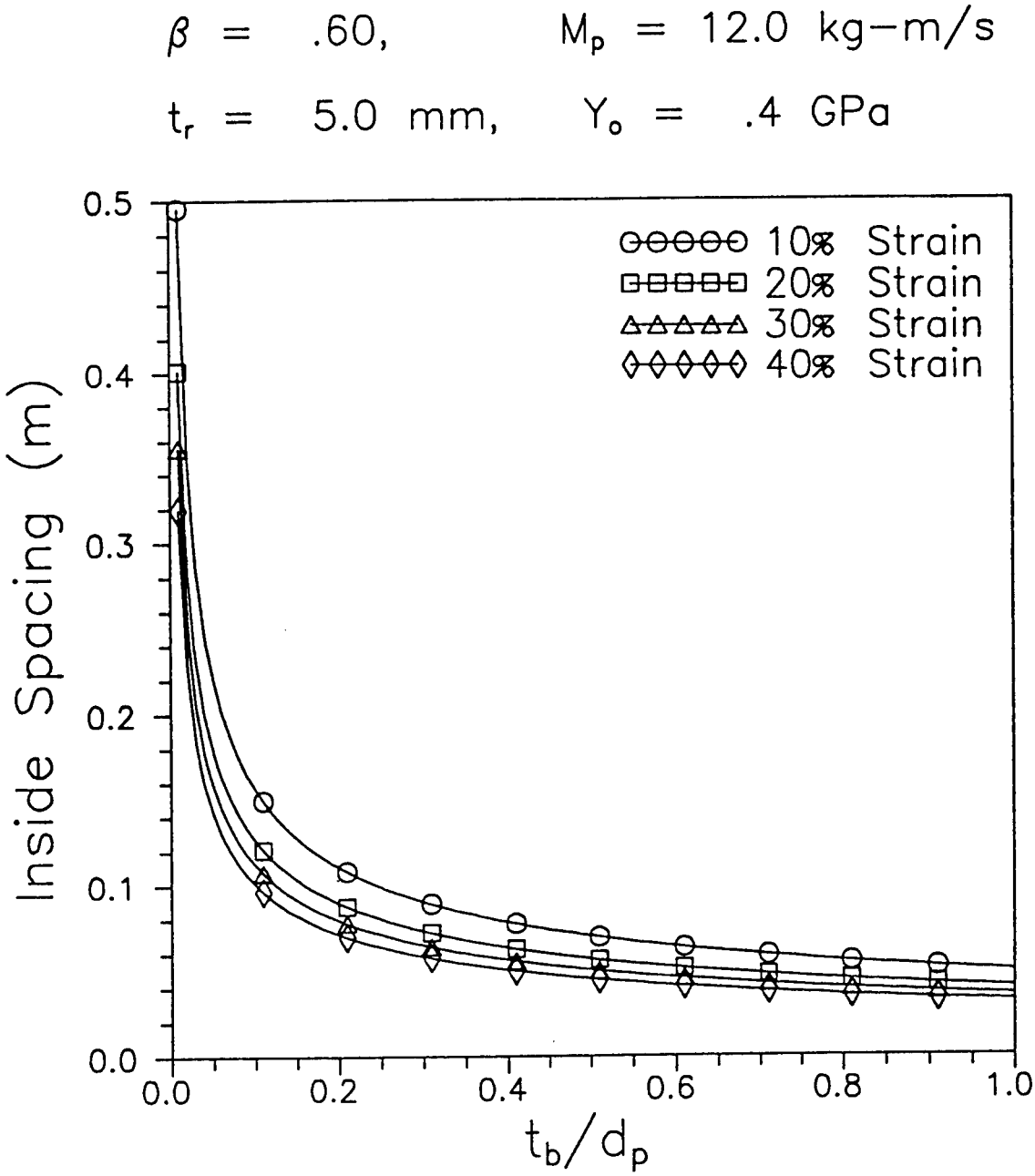


Figure 74. Design Curves for $\beta = 0.6$, $M_p = 12$ kg-m/s, $t_r = 5$ mm, and $Y_r = 0.4$ GPa

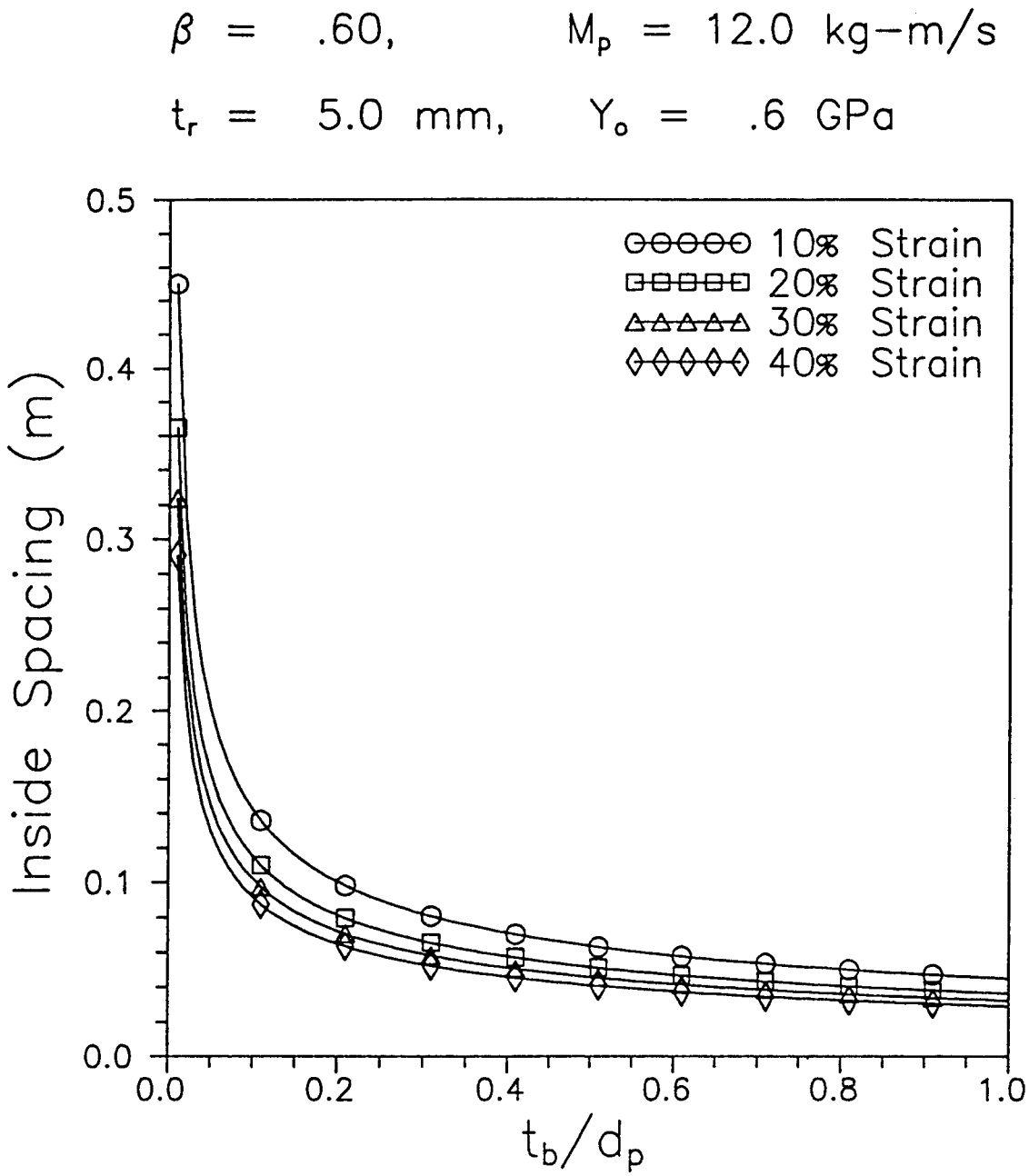


Figure 75. Design Curves for $\beta = 0.6$, $M_p = 12$ kg-m/s, $t_r = 5$ mm, and $Y_r = 0.6$ GPa

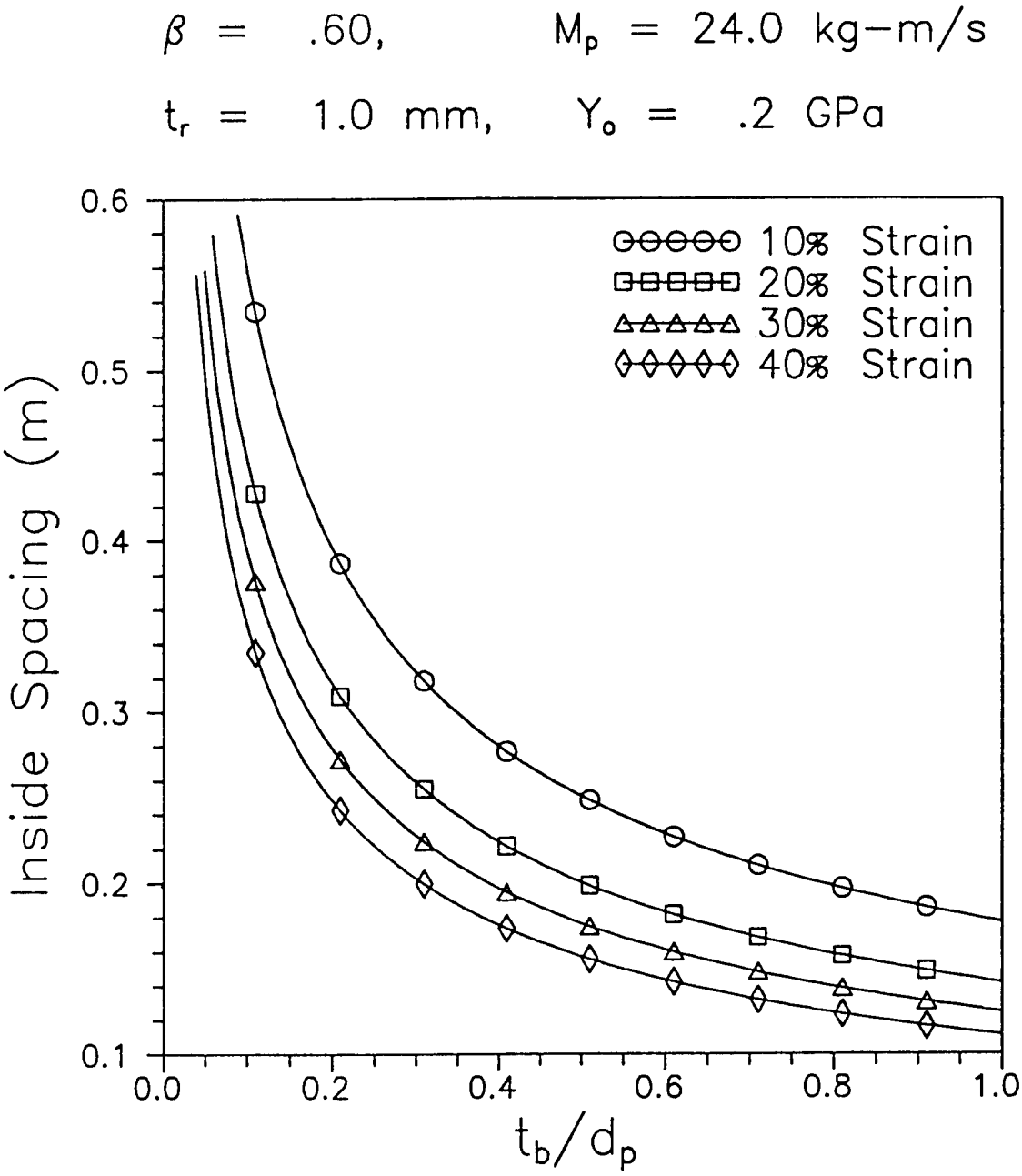


Figure 76. Design Curves for $\beta = 0.6$, $M_p = 24$ kg-m/s, $t_r = 1$ mm, and $Y_r = 0.2$ GPa

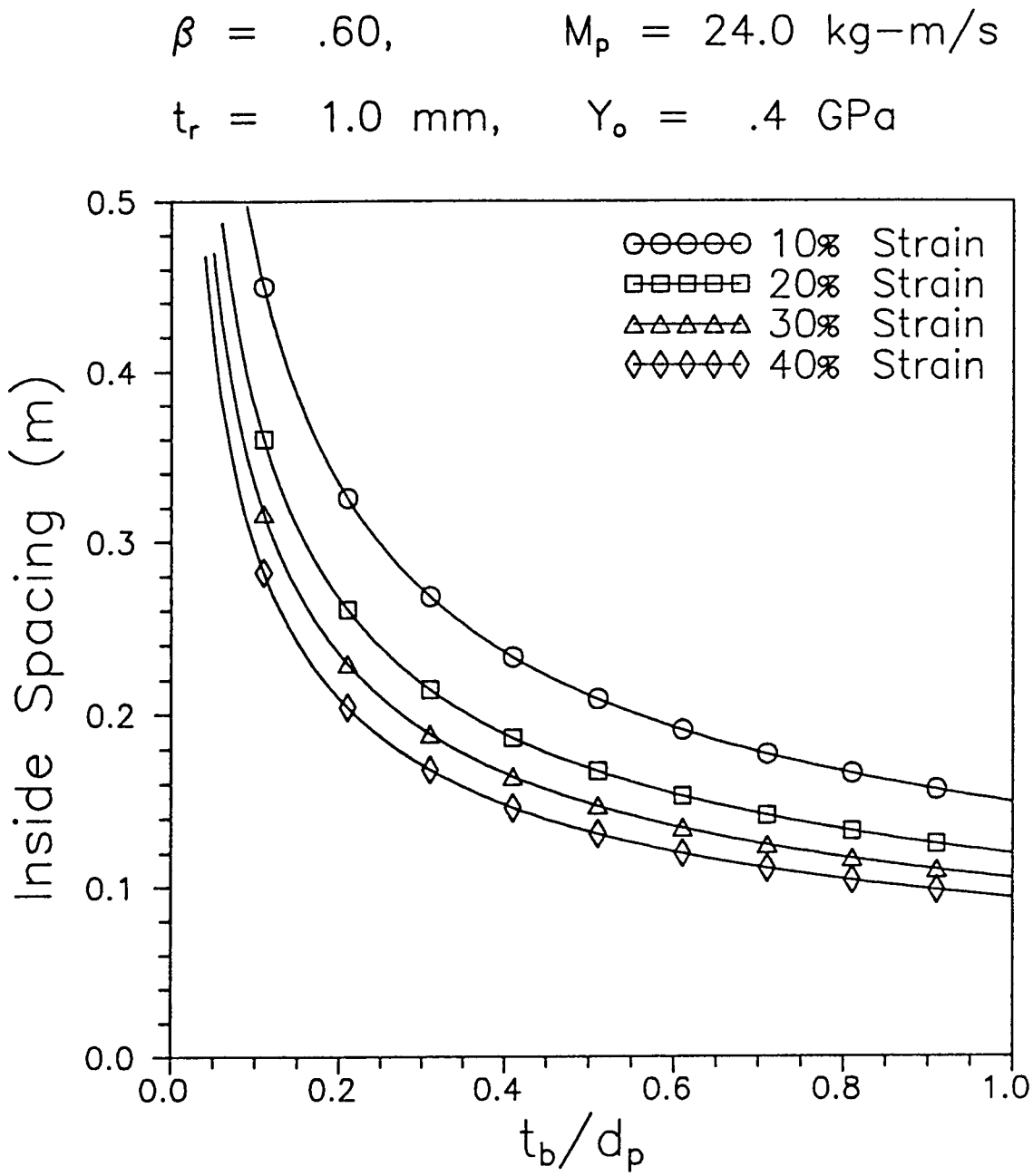


Figure 77. Design Curves for $\beta = 0.6$, $M_p = 24$ kg-m/s, $t_r = 1$ mm, and $Y_r = 0.4$ GPa

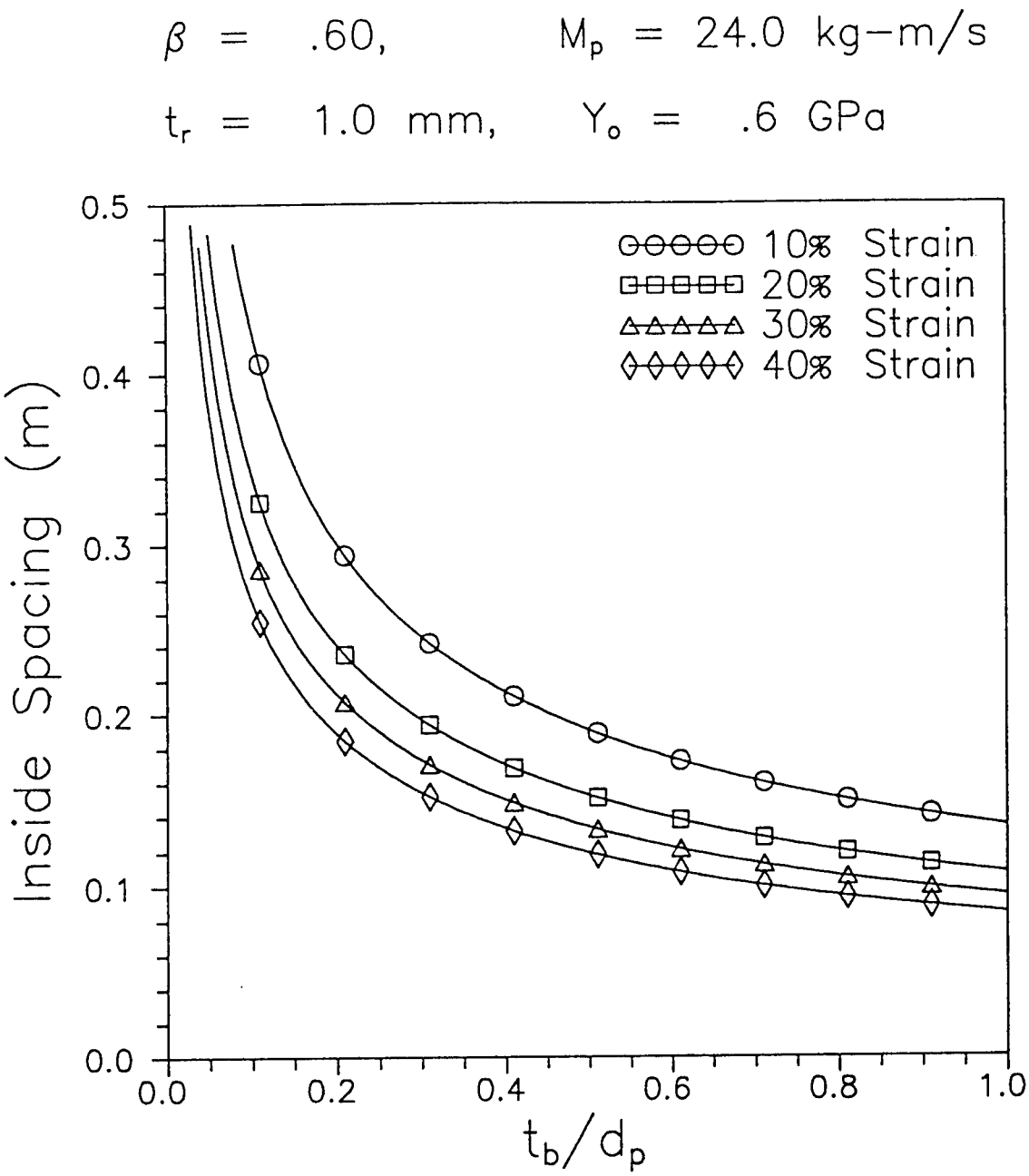


Figure 78. Design Curves for $\beta = 0.6$, $M_p = 24$ kg-m/s, $t_r = 1$ mm, and $Y_r = 0.6$ GPa

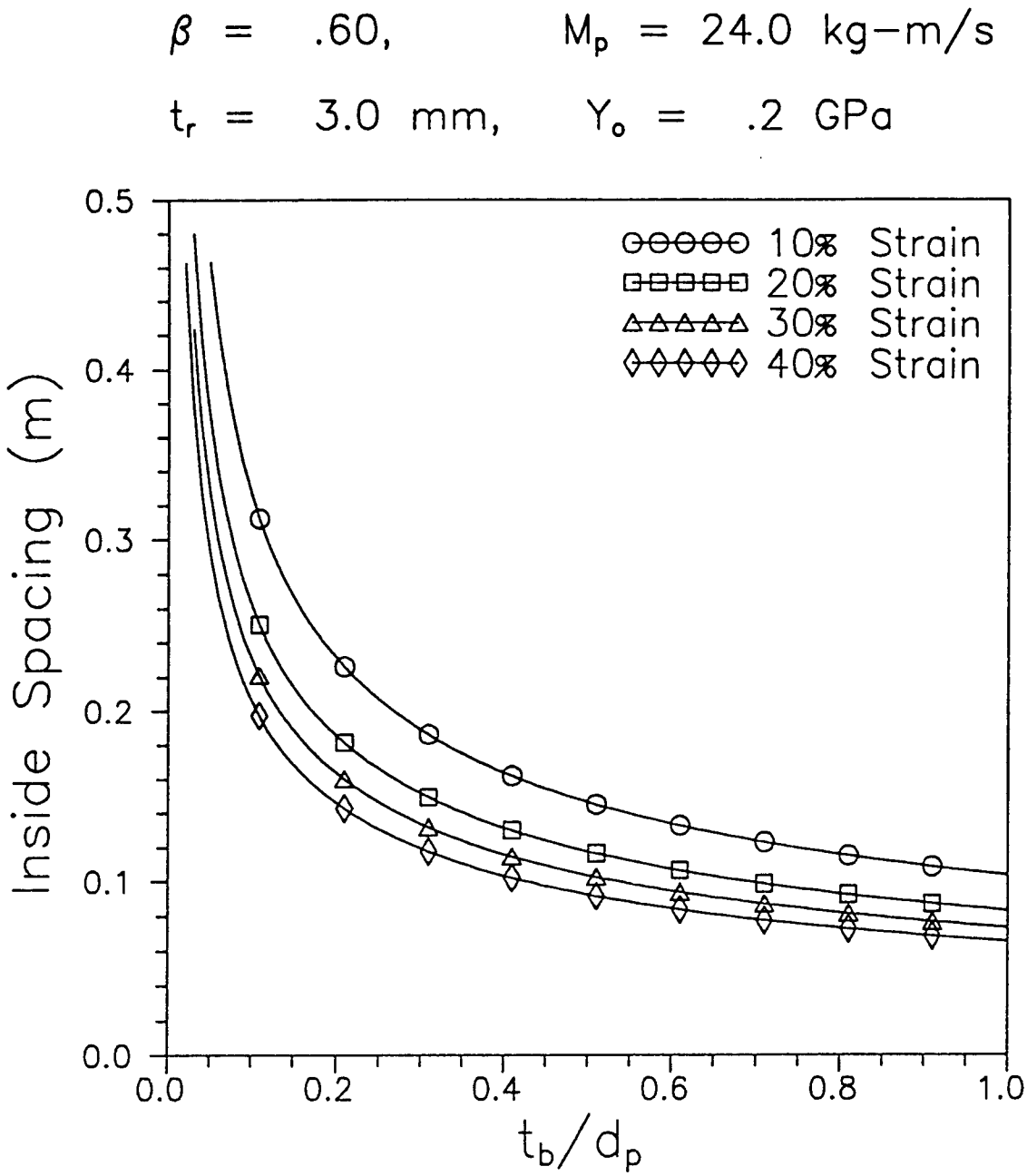


Figure 79. Design Curves for $\beta = 0.6$, $M_p = 24$ kg-m/s, $t_r = 3$ mm, and $Y_r = 0.2$ GPa

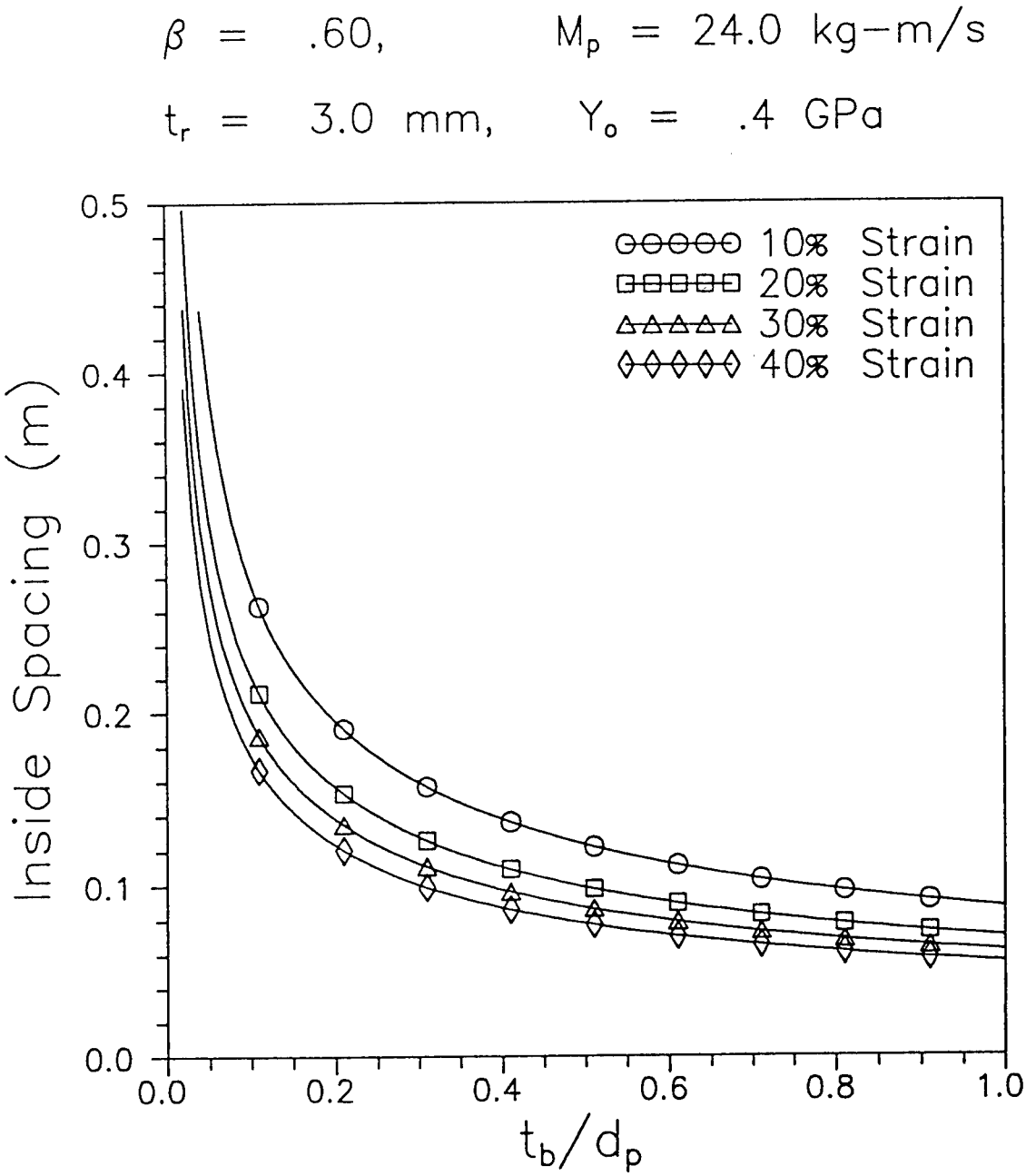


Figure 80. Design Curves for $\beta = 0.6$, $M_p = 24$ kg-m/s, $t_r = 3$ mm, and $Y_r = 0.4$ GPa

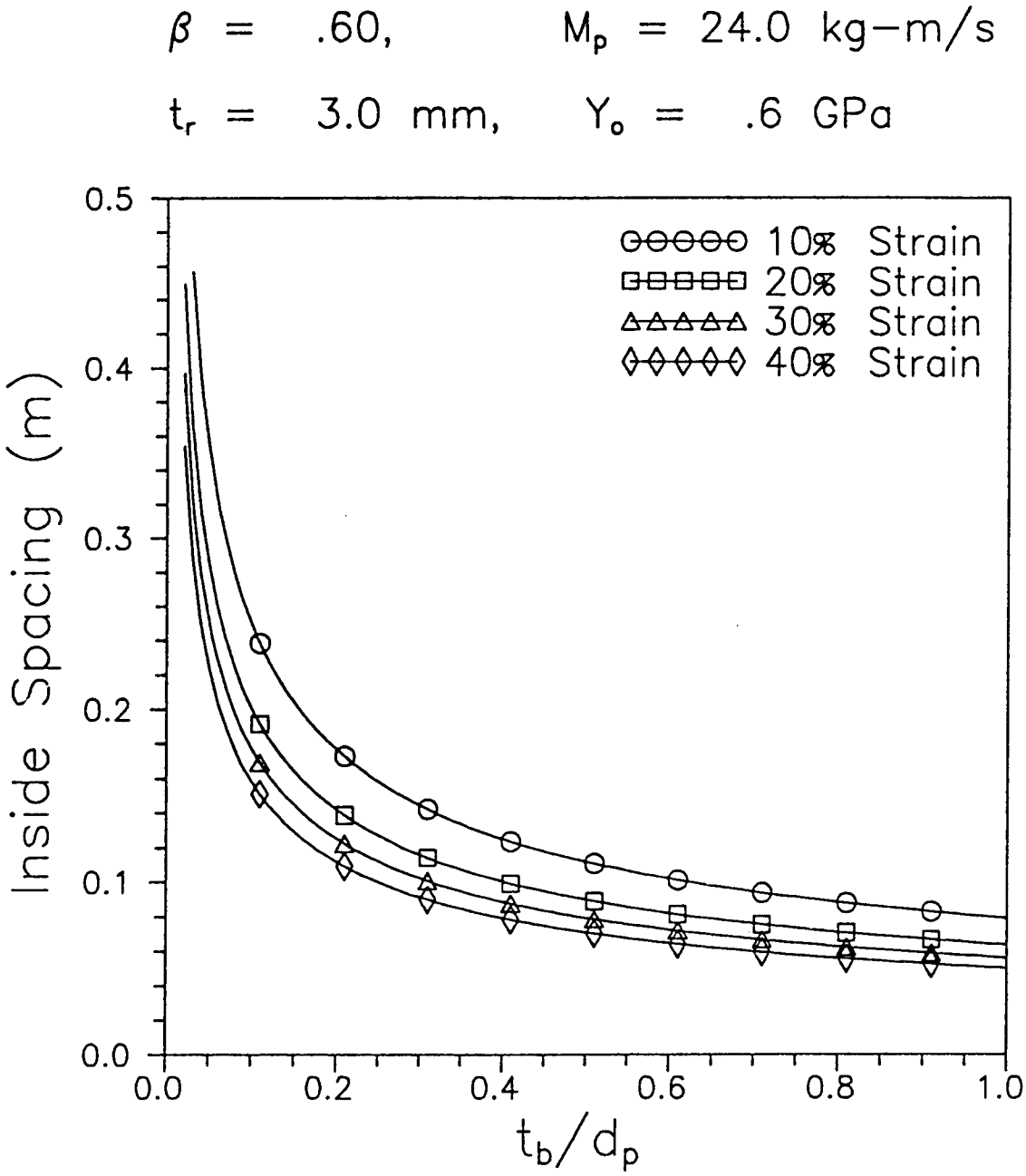


Figure 81. Design Curves for $\beta = 0.6$, $M_p = 24$ kg-m/s, $t_r = 3$ mm, and $Y_r = 0.6$ GPa

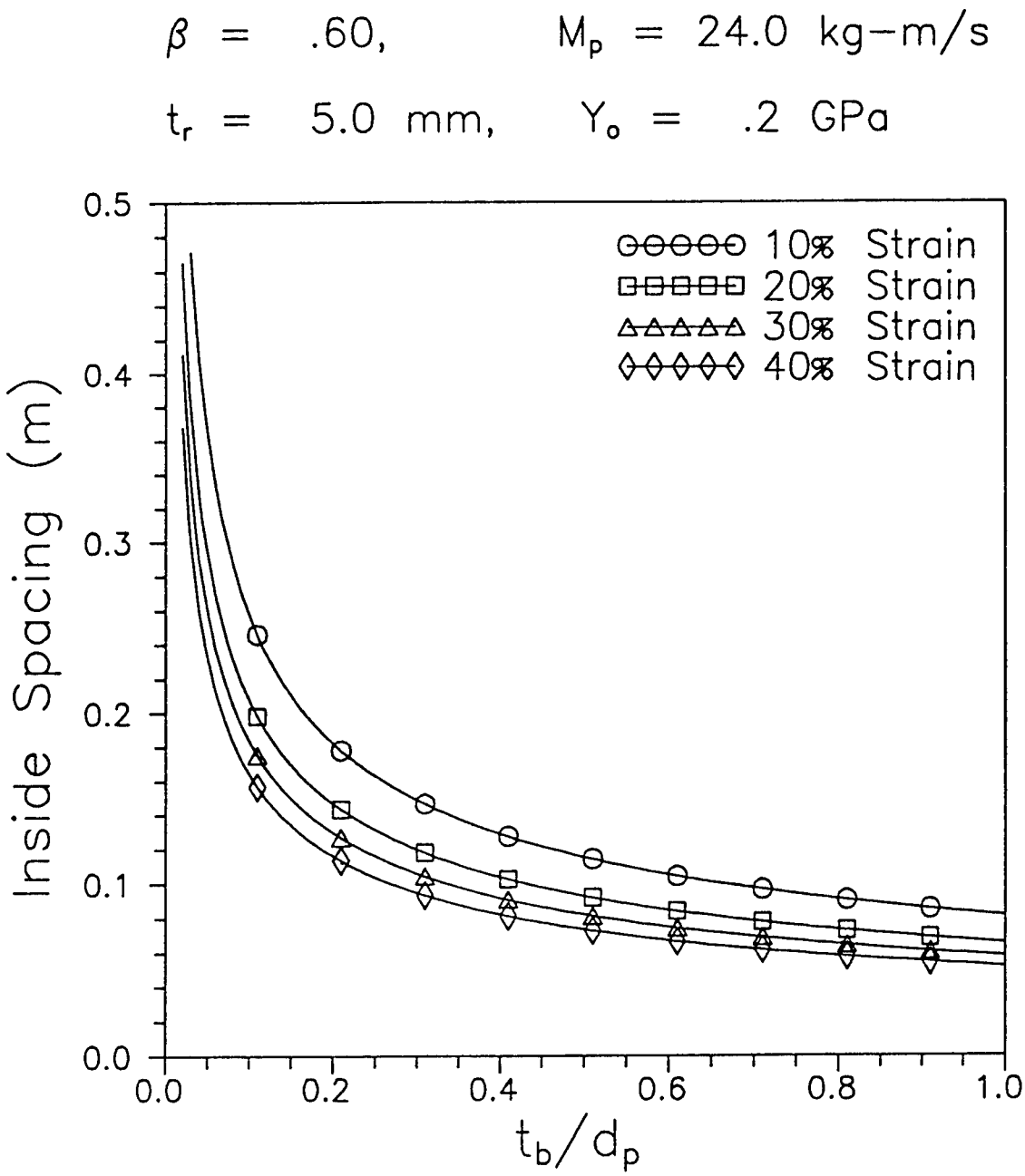


Figure 82. Design Curves for $\beta = 0.6$, $M_p = 24$ kg-m/s, $t_r = 5$ mm, and $Y_r = 0.2$ GPa

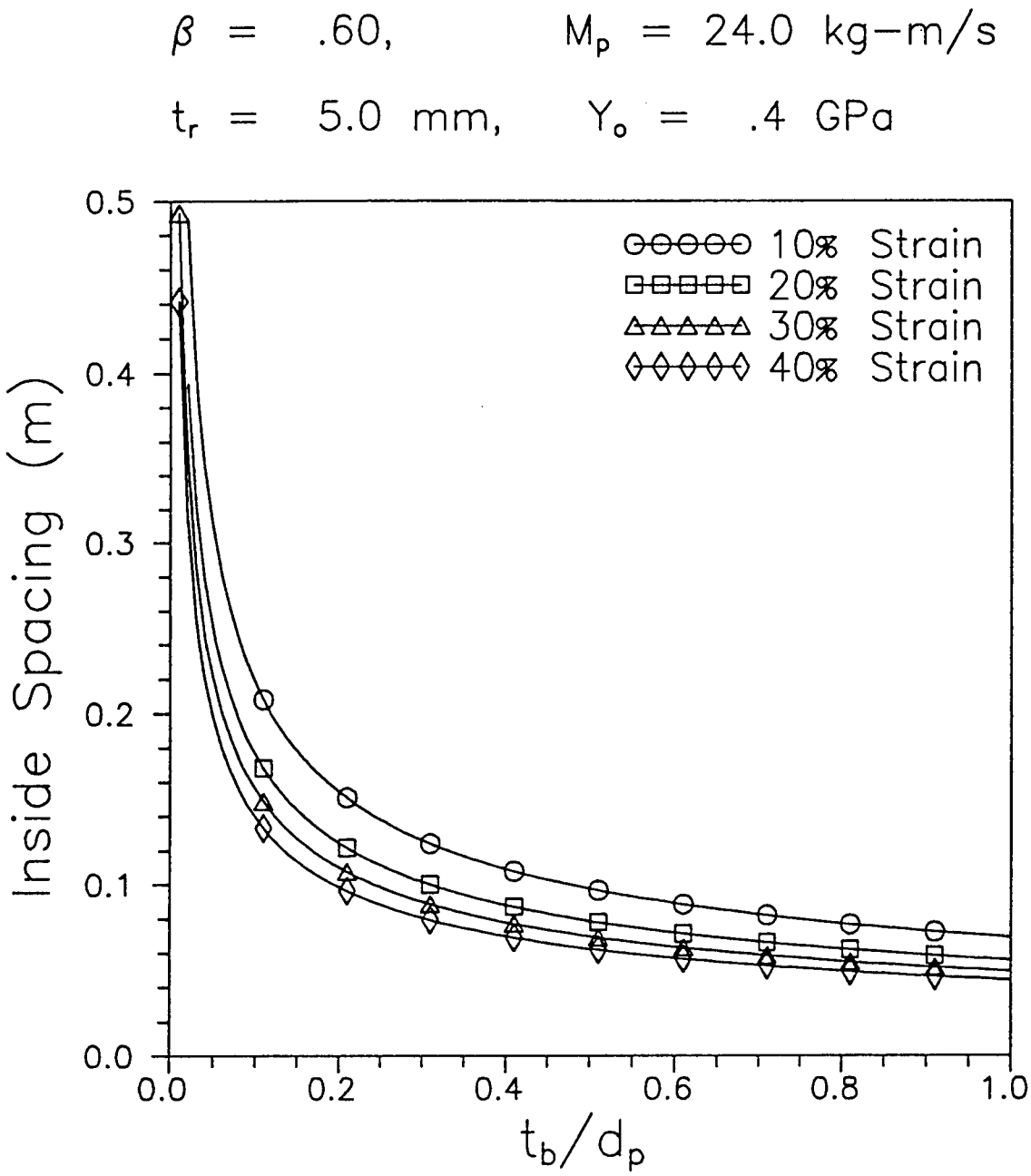


Figure 83. Design Curves for $\beta = 0.6$, $M_p = 24$ kg-m/s, $t_r = 5$ mm, and $Y_r = 0.4$ GPa

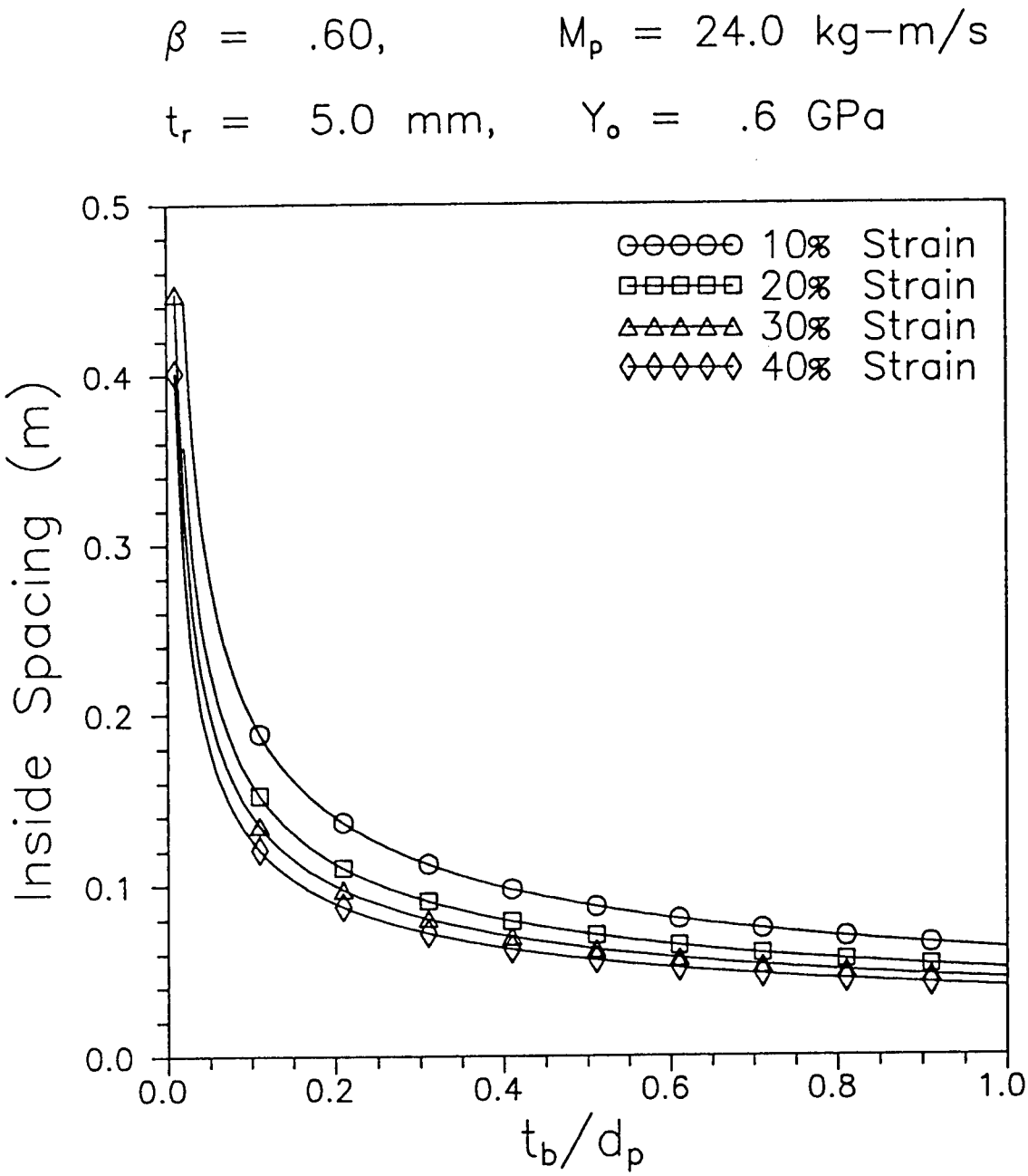


Figure 84. Design Curves for $\beta = 0.6$, $M_p = 24$ kg-m/s, $t_r = 5$ mm, and $Y_r = 0.6$ GPa

## REFERENCES


1. J.P.D. Wilkinson, A penetration criterion for double-walled structures subject to meteoroid impact, AIAA 7 (10) (1969) 1937-1943.

2. A.M. Rajendran and N. Elfer, Debris-impact protection of space structures, Chapter 2, in: Structural Failure, eds. T. Wierzbicki and N. Jones (John-Wiley & Sons, Inc., 1989).

3. R. Hoffman, EPRI, NP-2080, (Nov. 1981).

4. G.R. Johnson and R.A. Stryk, Air Force Report No. AFATL-TR-86-51 (1986).

5. N. Elfer, unpublished works.


☆ U.S. GOVERNMENT PRINTING OFFICE—1996—733-109/40010

# REPORT DOCUMENTATION PAGE

Form Approved
OMB No. 0704-0188

Public reporting burden for this collecton of information is estimated to average 1 hour per response, including the time for reviewing instructions, searching existing data sources, gathering and maintaining the data needed, and completing and reviewing the collection of information. Send comments regarding this burden estimate or any other aspect of this collection of information, including suggestions for reducing this burden, to Washington Headquarters Services, Directorate for Information Operations and Reports, 1215 Jefferson Davis Highway, Suite 1204, Arlington, Va 22202-4302, and to the Office of Management and Budget, Paperwork Reduction Project (0704-0188), Washington, DC 20503.

| 1. AGENCY USE ONLY (Leave Blank) | 2. REPORT DATE | 3. REPORT TYPE AND DATES COVERED |
|---|---|---|
| | February 1996 | Contractor Report (Final) |

**4. TITLE AND SUBTITLE**

Structural Damage Prediction and Analysis for Hypervelocity Impacts - Handbook

**5. FUNDING NUMBERS**

NAS8-38856

**6. AUTHOR(S)**

N. C. Elfer

**7. PERFORMING ORGANIZATION NAME(S) AND ADDRESS(ES)**

Lockheed Martin Marietta Manned Space Systems
P. O. Box 29304
New Orleans, LA 70189

**8. PERFORMING ORGANIZATON REPORT NUMBERS**

M-800

**9. SPONSORING/MONITORING AGENCY NAME(S) AND ADDRESS(ES)**

George C. Marshall Space Flight Center
Marshall Space Flight Center, Alabama 35812

**10. SPONSORING/MONITORING AGENCY REPORT NUMBER**

NASA CR-4706

**11. SUPPLEMENTARY NOTES**

Technical Monitor: Joel Williamsen, Structures and Dynamics Laboratory, Science and Engineering Directorate

**12a. DISTRIBUTION/AVAILABILITY STATEMENT**

Unclassified-Unlimited

Subject Category 18

**12b. DISTRIBUTION CODE**

**13. ABSTRACT** *(Maximum 200 words)*

This handbook reviews the analysis of structural damage on spacecraft due to hypervelocity impacts by meteoroid and space debris. These impacts can potentially cause structural damage to a Space Station module wall. This damage ranges from craters, bulges, minor penetrations, and spall to critical damage associated with a large hole, or even rupture. The analysis of damage depends on a variety of assumptions and the area of most concern is at a velocity beyond well controlled laboratory capability. In the analysis of critical damage, one of the key questions is how much momentum can actually be transfered to the pressure vessel wall. When penetration occurs without maximum bulging at high velocity and obliquities (if less momentum is deposited in the rear wall), then large tears and rupture may be avoided. In analysis of rupture effects of cylindrical geometry, biaxial loading, bending of the crack, a central hole strain rate and R-curve effects are discussed.

**14. SUBJECT TERMS**

aluminum alloys, bumpers, debris shields, fracture mechanics, hypervocity impacts, impact, meteoroids, orbital debris

**15. NUMBER OF PAGES**

320

**16. PRICE CODE**

A14

| 17. SECURITY CLASSIFICATION | 18. SECURITY CLASSIFICATION OF THIS PAGE | 19. SECURITY CLASSIFICATION OF ABSTRACT | 20. LIMITATION OF ABSTRACT |
|---|---|---|---|
| Unclassified | Unclassified | Unclassified | Unlimited |

National Aeronautics and
Space Administration
Code JTT
Washington, DC
20546–0001

*Official Business*
*Penalty for Private Use, $300*

*Postmaster: If Undeliverable (Section 158 Postal Manual), Do Not Return*